Superfluidity, Metastability, and Collective Spin Phenomena in Open Quantum Systems

Igor Timofeev

A dissertation submitted in partial fulfilment
of the requirements for the degree of
Doctor of Philosophy
of
University College London

Department of Physics and Astronomy
University College London

June 3, 2025

I, Igor Timofeev, confirm that the work presented in this thesis is my own. Where information has been derived from other sources, I confirm that this has been indicated in the work.

Parts of this thesis have been published in:
Timofeev, I., Juggins R., Szymanska, M. Geometric and fluctuational divergences in the linear response of coherently driven microcavity polaritons and their relation to superfluidity. Phys. Rev. B 108, 214513 (2023).

Figures in Part Ia are taken from the above paper under CC-BY-4.0[1] with no modifications. Figs 2.1, 4.1, and 4.3 were not produced by me. Much of the text of Part Ia, all written by me, is taken from the same source under the same license, with minor modifications to improve readability and flow with the rest of the thesis.

[1] Creative Commons Attribution 4.0: www.creativecommons.org/licenses/by/4.0/

Abstract

This thesis covers research in three separate but interlinked areas: superfluidity in driven-dissipative polariton systems, path integral methods for the study of metastability in Markovian systems, and phase space methods for spin master equations. The unifying theme of the three works is their non-equilibrium nature, but other overlaps are also present. The first two topics share a primary analytical tool, the Feynman-Vernon path integral, with the first applying it to quantum field theory and the second to quantum mechanics. The first and third both utilise the Truncated Wigner method, albeit for very different purposes and rather different phase spaces, while the second and third illustrate the twin approaches of geometric and deformation quantisation.

The first part is subdivided into three, dealing with different sub-projects undertaken under the broad umbrella of superfluidity. These are, in order, the absence of it in coherently driven polaritons, the application of Truncated Wigner to its study in Markovian polariton systems, and the analysis of whether non-linear dissipation can cause a non-interacting bosonic gas to exhibit it. Non-equilibrium functional integral methods are extensively used for all three but with varying emphasis: the first features extensive diagrammatic calculations, the second focuses on the stochastic semi-classical limit of the integral, while the third foregoes Feynman diagrams for a generating function approach. Conclusive results are obtained in the first project[2], which completes a calculation by a predecessor in the group to show that no regime of coherently driven polaritons exhibits superfluidity; in the second I derive a method to extract the linear response tensor used for identifying superfluid components via the Truncated Wigner method derived from the functional integral, which should allow the numerical study of systems too complicated for the analytical tools employed in the first sub-part; in the final, third part I analyse a non-interacting bosonic system with non-linear dissipation, serving as a minimal model of a dye cavity photon Bose-Einstein condensate, to find that at mean-field level it is predicted to exhibit superfluidity. I then perform a significant portion of the associated fluctuation correction calculation, though difficulties with model regularisation prevent a conclusive answer being given at this time.

[2]Published in Phys. Rev. B 108, 214513 (2023).

Part II is devoted to calculations of Lindbladian spectra via the coherent state path integral, the initial aim of which was the study of metastability of systems governed by such Markovian superoperators. A working perturbation theory based on the exact propagator for a coherently driven-dissipative harmonic oscillator is derived and tested on some toy models. This perturbation theory in principle can be applied to systems not covered by the existing methods of third quantisation[3] and exact expressions for truncated Fock bases. The part also includes a review of the two pre-eminent approaches to the coherent state path integral, emphasizing its links to holomorphic polarisation and highlighting the difficulties associated with it and consequently instanton calculations performed using it.

Finally, moving away from bosonic systems, I develop a stochastic Truncated Wigner approach to spin degrees of freedom of arbitrary magnitude. This builds on earlier work constructing the Stratonovich-Weyl representation of spin as functions on the 2-sphere S^2 by calculating the explicit form of the series expansion of the associated star product to higher order than previously available in the literature. This is then used to study nearest-neighbour and long-range anisotropic XY models in two dimensions, obtaining promising results, in particular the direct observation of vortices associated with the BKT transition that destroy the staggered XY phase in the first model. This method differs from existing discrete Truncated Wigner methods and those specialised to spin-$\frac{1}{2}$, in particular being based around an expansion in a small parameter proportional to $\hbar$. This allows it to be easily integrated with bosonic phase space methods, since a truncation can then be carried out at a consistent order in $\hbar$.

[3]Third quantisation refers to canonical quantisation in the superoperator space.

Impact Statement

In Part I of this thesis I consider models capable of describing systems of driven-dissipative exciton polaritons, an experimental platform that in recent years is finding applications in spintronics, lasing, quantum simulators, and in industry development of optical transistors. A better theoretical and numerical understanding of the behaviour of these systems is of direct relevance to much ongoing work, and I consider approaches of both kinds. In particular I explore aspects of superfluidity, an important physical phenomenon the study of which has previously led directly to two Nobel prizes in physics[4], via an analytical approach and also propose a numerical method for its study. Analytical results were published in Phys. Rev. B 108, 214513 (2023), and it is hoped that the proposed numerical method will lead to further publications for the group at a later time. These methods are also applicable to other experimental platforms, and I use the analytical approach to explore the possibility of superfluidity in a model of non-interacting dye cavity photon Bose-Einstein condensation.

Part II is concerned with the application of coherent state path integrals to the study of metastability in driven-dissipative systems with Markovian dynamics and finite degrees of freedom. Metastability, especially bistability, of this kind may be important for quantum devices, with some previous work relating bistability in circuit-QED to improved qubit readout protocols. While the results in this direction are of a preliminary nature, they provide a theoretical foundation for possible future work in this direction by other members of the research group. A review of the two important approaches to the coherent state path integral, one of them less common in the literature and rarely contrasted against the other but very important for theoretical work, is also provided to assist with this. A manuscript based on this work will be in preparation after submission of this thesis.

In Part III I develop a new stochastic numerical method for the simulation of spin lattice systems. The method, a variant of the Truncated Wigner approach, is very general: it is suitable for arbitrary lattice geometries, both long and short range interactions, and may be easily coupled to existing bosonic Trun-

[4]Half of the 1978 prize was awarded to Pyotr Kapitsa for his discovery of superfluidity in Helium-4, and the 1996 prize went to David Lee, Douglas Osheroff, and Robert Richardson for their discovery of it in Helium-3.

cated Wigner methods to yield a simulation scheme for spin-boson systems. The method may thus find application in a large variety of research. Some new results are obtained for important models, in particular an explicit observation of theoretically predicted BKT vortex proliferation in the nearest neighbour interaction driven-dissipative anisotropic XY model. A manuscript based on this work will be in preparation after submission of this thesis.

Acknowledgements

The completion of this thesis gives me the opportunity to look back on what has been, by any measure, a wonderful intellectual experience. To take the words of Sidney Coleman and analytically continue them from their high energy QFT domain, much of modern physics is nothing short of "a triumph [...], in the old sense of the word: a glorious victory parade, full of wonderful things brought back from far places to make the spectator gasp with awe and laugh with joy". Too few have the opportunity to be that spectator, and I will forever be grateful to have spent some years as a participant.

In this regard I must firstly thank my supervisor, Marzena Szymanska, for the opportunity to conduct the present research and the uncharacteristic freedom granted to me in its pursuit. Our little troupe, the Quantum Collective Dynamics in Light-Matter Systems group, was a place of diverse ideas and occasionally a source of great amusement. To my fellow travellers in it, I express my gratitude for sharing the journey.

Over the course of my work I have also, inevitably, built up a significant tab with those who came before and shared their insight and understanding freely. While their number is far too great to thank individually and many are in no position to collect on this debt, I would nevertheless like to specifically thank Sidney Coleman, Lawrence Schulman, Nicholas Wheeler, and John Klauder: without you shoulders, much of the parade may have remained obscured from view.

A small, special thank you must also be extended to Tom Lehrer. While this thesis may not be entirely what you hoped your music would inspire in people, I hope the abundance of locally Euclidean, metrizable, infinitely differentiable Riemannian manifolds in it balances the scales.

Most importantly, I address those outside the game as I prepare to depart Castalia's borders. My dear friends Katie and Will, this work and I owe much to your friendship, cheer, and occasional song over years prior and present. While I write here one of the final chapters of this manuscript, I deeply hope we are yet in the early ones of ours. And finally, to those who have been with me every step of the way, my earliest friends, best teachers, and finest companions, I dedicate this work to my parents; it was your love and encouragement that made it possible.

Contents

List of Figures

Part I

Superfluidity in Open Quantum Systems

Chapter 1

Superfluidity

We begin our discussion with a review of superfluidity because, for all the details of a given open quantum system or subsequent field-theoretic or stochastic machinery, this is the phenomenon we are actually interested in studying. At the same time it will likely be the most familiar to a reader coming from outside the open quantum systems community and, moreover, is such a broad field in itself that it will be important to establish a shared language and perspective before proceeding with any specifics.

Superfluidity is a well known phenomenon in quantum mechanics. First discovered in 1937 in liquid helium-4 [1], [2], it is characterised by a series of unusual hydrodynamic properties such as vanishingly small viscosity, the inability to rotate except in quantised vortices, and the existence of metastable currents. It has been widely studied and found to occur in a variety of other equilibrium systems including helium-3, ultra-cold bosonic atoms, and charged Cooper pairs in superconductors [3], [4].

Of special note is that, in equilibrium systems, the mechanisms behind superfluidity are well understood and these different hydrodynamic phenomena have generally been observed together, so that the classic notion of superfluidity groups together multiple behaviours into a "complex of phenomena" [5]. Yet when we cross over into the realm of open quantum systems, how superfluidity manifests is less understood and, more importantly, it is unclear whether all the effects seen in equilibrium will continue to manifest together [6]–[8]. If we wish to discuss superfluidity in such systems, then, we must first identify which part of this complex of phenomena we consider as most essential to a superfluid's definition.

In many ways the principal property is that of a persistent flow without viscosity — the prototypical example of a superfluid is liquid helium-4 flowing through a capillary with no dissipation via the capillary walls, as observed by Allen and Misener [2]. It is upon this intuition that perhaps the most famous method of identifying superfluidity, the Landau criterion, is based. Seemingly

requiring only knowledge of the excitation spectrum of a given system and being applicable at both zero and non-zero temperature, it is often the primary tool for identifying superfluid regimes. Were it to also hold for open quantum systems, the majority of the questions in this portion of the thesis would be easily answerable.

Unfortunately, all the more so because a fair number of works in the field have been carried out on the assumption that it holds [6], [9]–[13], the Landau criterion in its conventional form fails in the open system setting. Given that the criterion is such a standard tool , it is important to understand why this occurs. To this end we will explore this question in the subsequent sections, starting with the criterion as it is typically presented. We will then lift the criterion into a field-theoretic setting to better understand its underlying assumptions and demonstrate how these break down in an open system setting.

With this accomplished, the final section will be devoted to a proposed alternative way of characterising superfluidity. Generalised from an equilibrium argument due to Baym [14], this approach defines a superfluid as a system possessing unequal linear responses of its current to longitudinal and transverse current perturbations. This definition, by now standard [15]–[20], relies purely on the properties of the system's linear response and thus transfers easily from closed to open systems.

1.1 The Landau Criterion

To understand the pitfalls of the Landau criterion, we must first recall its typical formulation. Due to and named after Landau [16], the criterion is largely phenomenological, calling for no information about the system other than its excitation energy spectrum $\epsilon(\mathbf{p})$, and is motivated by the following clear physical reasoning (we follow the classical textbooks [21], [22]).

Consider a fluid at zero temperature with total mass M moving with velocity $\mathbf{V}$ relative to a carrying medium (the frame of which we shall refer to as the laboratory frame) such as a capillary or perhaps a semiconductor substrate. Suppose now that, through a dissipative interaction with some external perturbation (e.g. a capillary wall or substrate defect), a quasiparticle with momentum $\mathbf{p}$ is created. In its reference frame, the energy and momentum of the fluid become

$$\boldsymbol{P}_f = \boldsymbol{p}, \tag{1.1}$$

$$E_f = \epsilon(\boldsymbol{p}), \tag{1.2}$$

which, when translated to the laboratory frame, become

$$\boldsymbol{P}_l = \boldsymbol{P}_f + M\boldsymbol{V} = \boldsymbol{p} + M\boldsymbol{V}, \tag{1.3}$$

$$E_l = E_f + \boldsymbol{V}\cdot\boldsymbol{P}_f + \frac{1}{2}MV^2 = \epsilon(\boldsymbol{p}) + \boldsymbol{V}\cdot\boldsymbol{p} + \frac{1}{2}MV^2. \tag{1.4}$$

The last part is simply the energy of the moving fluid without the excitation, and we see that in order for this interaction to have truly been dissipative it must be that

$$\epsilon(\mathbf{p}) + \mathbf{V}\cdot\mathbf{p} < 0. \tag{1.5}$$

Thus, in order for dissipation via interactions with the carrying medium to be possible, the Landau criterion must be satisfied:

$$\min_{\mathbf{p}}[\epsilon(\mathbf{p}) + \mathbf{V}\cdot\mathbf{p}] < 0. \tag{1.6}$$

For an isotropic system this is equivalent to $\min_p[\epsilon(p) - Vp] < 0$, and the largest value of V for which this does not hold $V_{\text{crit}} = \min_p \frac{\epsilon(p)}{p}$ is termed the critical velocity. This is because for fluid velocities not exceeding this value it is energetically unfavourable for the system to generate excitations and thus it cannot dissipate energy via this route — non-dissipative flow characteristic of a superfluid occurs.

That the criterion may be stated in less than a page and with so few equations is no doubt part of its enduring appeal. Moreover, all that is required being the excitation spectrum, superfluidity can be easily tested by an experimentalist capable of measuring it or a theorist in possession of bare or dressed Greens functions. Let us, however, consider what might possibly go wrong with this approach under different circumstances.

Firstly, when deriving the criterion, we have used a change of reference frame. This may cause unease in some when dealing with an optical carrying substrate because the expression for energy in different frames would now be affected by the Fresnel drag effect [23]. It is possible, however, to arrive at the criterion while staying purely in the laboratory frame, thus avoiding this complication.

Next, the above analysis assumed that the fluid was at zero temperature and thus possessed no excitations prior to the interaction with the medium. At finite temperature such excitations will be present and the portion of the fluid associated with them will in fact experience dissipation even when the Landau criterion is satisfied. This too is easily addressed with an approach known as the two-fluid model, and we will briefly outline this in the next section.

A more significant question arises when a system is being externally driven. The Landau criterion argues that an energetic instability of a flow [16] will lead to dissipation via interactions with the medium, which at zero temperature or in

equilibrium will gradually take energy out of the flow and destroy it (manifesting a dynamical instability). It is not immediately obvious, however, whether this is still the case if the flow is being constantly replenished with energy via the external drive — can a flow be dissipative yet still persistent? The answer is yes (see [15] or the mean-field section of Part Ic), but the reason for this is better understood with the criterion embedded in a field-theoretic language.

Finally, the criterion actually only addresses a very small portion of the 'complex of phenomena' that make up superfluidity, namely its ability to maintain a persistent non-dissipative flow. From the above paragraph we already see that, in an open system, 'persistent' and 'non-dissipative' may already not be the same thing, but it is also not immediately clear why a fluid capable of persistent flow should also exhibit properties like irrotationality. We will touch on these matters briefly in our field-theoretic discussion, but more broadly it will be seen in the main body of Part Ia that this indeed need not be the case — coherently driven polaritons may exhibit persistent flow yet still be sensitive to shear forces.

1.2 The Two-Fluid Model

At finite temperature, we consider the excitations already present in the fluid as a gas with energy distribution function $n_r(\epsilon)$ in its rest frame and moving with some velocity $\boldsymbol{v}$. Since

$$n_r(\epsilon) = n_l(\epsilon + \boldsymbol{v}\cdot\boldsymbol{p}) \tag{1.7}$$

we have that the momentum of the gas per unit volume in the laboratory frame is

$$\boldsymbol{P}_l = \frac{1}{(2\pi)^3}\int d^3\boldsymbol{p}\,\boldsymbol{p}\,n_r\left(\epsilon(\boldsymbol{p}) - \boldsymbol{v}\cdot\boldsymbol{p}\right). \tag{1.8}$$

Expanding this for small velocity,

$$\boldsymbol{P}_l = -\frac{1}{(2\pi)^3}\int d^3\boldsymbol{p}\,\boldsymbol{p}(\boldsymbol{v}\cdot\boldsymbol{p})\frac{\partial n_r}{\partial\epsilon} = -\frac{\boldsymbol{v}}{3(2\pi)^3}\int d^3\boldsymbol{p}\,p^2\frac{\partial n_r}{\partial\epsilon}, \tag{1.9}$$

and we can thus associate a density to this gas of excitations:

$$\rho_n = -\frac{1}{3(2\pi)^3}\int d^3\boldsymbol{p}\,p^2\frac{\partial n_r}{\partial\epsilon}. \tag{1.10}$$

This density will not generally equal the total density of the fluid (indeed it is zero at $T = 0$) but will depend on the distribution function. At the same time, since the excitations are already in existence, they will be able to dissipate via interactions with the medium at flow velocities below those stipulated by the Landau criterion. The combined behaviour of a fluid at finite temperature will thus be a 'normal' component of the fluid comprising the above gas of excita-

tions and being at rest with the carrier medium (since its flow is dissipative), and the rest of the fluid exhibiting non-dissipative superfluid flow below the critical velocity.

1.3 Field Theory Model

Let us now construct the Landau criterion in the context of field theory, this being the language of our subsequent work, the prevailing language in the theory of phases of matter, and in general a helpful framework in which to see the subtleties of the criterion. Throughout we shall focus on a toy bosonic model that exhibits superfluidity via a $U(1)$ symmetry breaking transition.

1.3.1 Condensates and Irrotational Flow

The zero-temperature Lagrange density for a system of bosons $H_0 = \bar{\psi}(E_0 - \frac{1}{2m}\nabla^2)\psi$ with a four-body point interaction $H_{\text{int}} = V|\psi|^4$ and chemical potential μ ($\mu' = \mu - E_0$) may be written as[1]

$$S = \bar{\psi}\partial_t\psi + \frac{1}{2m}\bar{\psi}\nabla^2\psi + \mu'|\psi|^2 - V|\psi|^4. \tag{1.11}$$

This action possesses a $U(1)$ symmetry associated with the family of transformations $\psi \to e^{i\alpha}\psi$ which leave it invariant.

Asymptotically in $\hbar$ the possible states of the system will be determined by the solutions of the classical equations of motion of this action. If the state in which the system was being evaluated were known (e.g. the ground state), this would fix the boundary conditions of these equations. We will instead work backwards, searching for time-homogeneous solutions without fixed boundary conditions and then identifying them with possible macroscopic states.

The equations of motion are obtained by searching for the stationary point of the action, yielding

$$\frac{\delta S}{\delta\bar{\psi}} = \partial_t\psi + \frac{1}{2m}\nabla^2\psi + \mu'\psi - 2V|\psi|^2\psi = 0 \tag{1.12}$$

and its complex conjugate (we will not write down conjugate equations in this chapter, since they are trivial in the zero-temperature/equilibrium theory). If spacetime-homogeneous solutions are of interest, this reduces to

$$\mu'\psi = 2V|\psi|^2\psi. \tag{1.13}$$

[1] The present action has been constructed in the coherent state path integral formalism, the details of which may be found in [24] or [25], and we have redefined the fields to turn the condensate oscillation into a $\mu'|\psi|^2$ action term. Chap.3 and Part II of this thesis also cover the construction of such path integrals.

If $\mu' \leq 0$ the only solution is $\psi = 0$ and there is no symmetry breaking. If, however, $\mu' > 0$, there appears a family of solutions characterised by

$$|\psi| = \sqrt{\frac{\mu'}{2V}} \tag{1.14}$$

and arbitrary $\arg\psi$. These states correspond to the occurrence of condensation into a spatially homogeneous state and in finite systems the ground state of the system will be a symmetry-preserving superposition of these. In the thermodynamic limit, however, the system may become pinned in one with no transition rate into the others, leading it to become the effective ground state and causing symmetry breaking.

Relaxing the requirement of spatial homogeneity, we are led to the equation

$$\frac{1}{2m}\nabla^2\psi + \mu'\psi - 2V|\psi|^2\psi = 0. \tag{1.15}$$

Before considering specific solutions, suppose that we decompose an arbitrary solution in polar form as $\psi = \sqrt{\rho}e^{i\theta}$, and use that to write down the mean-field system current:

$$\boldsymbol{j} = \frac{1}{2mi}\left[\bar{\psi}\nabla\psi - \psi\nabla\bar{\psi}\right] = \frac{\rho}{m}\nabla\theta = \rho\boldsymbol{v}. \tag{1.16}$$

We may thus identify $\frac{1}{m}\nabla\theta$ with the flow velocity $\boldsymbol{v}$, which immediately demonstrates that the flow is irrotational: $\nabla\times\boldsymbol{v} \propto \nabla\times\nabla\theta = 0$. Thus any macroscopic flow state that our model supports will be irrotational, just as we would expect of a superfluid.

1.3.2 Energetic Stability: The Landau Criterion in Field Theory

Let us now specialise the discussion to plane wave states $\psi = \sqrt{\rho}e^{i\boldsymbol{q}\cdot\boldsymbol{x}}e^{i\alpha}$, such that the equation of motion becomes (the global phase α is once again arbitrary)

$$\mu' - \frac{|\boldsymbol{q}|^2}{2m} = 2V\rho. \tag{1.17}$$

These states are precisely the sorts of uniform fluid flows that the Landau criterion considers, and so we should be able to apply similar reasoning to them.

In order to do so, let us Fourier-transform our action into ($k = (\omega, \boldsymbol{k})$)

$$S = \sum_k \left[\omega - \frac{|\boldsymbol{k}|^2}{2m} + \mu'\right]|\psi_k|^2 - V\sum_{k,k',p}\bar{\psi}_{k+p}\bar{\psi}_{k'-p}\psi_k\psi_{k'} \tag{1.18}$$

and expand it in small fluctuations around a uniform flow $\psi_k = \psi_{\boldsymbol{q}} = \sqrt{\rho}\delta(\omega)\delta(\boldsymbol{k}-\boldsymbol{q})$ satisfying the equations of motion (we choose the flow to be real for simplicity, using our global phase freedom). This is made simpler by first performing a

transformation $\psi_k \to \psi_{k-(0,\boldsymbol{q})}$ so that the uniform flow state is $\psi_k = \psi_0\delta(k)$ and the action is

$$S = \sum_k [\omega - \epsilon(\boldsymbol{k}) + \mu']|\psi_k|^2 - V\sum_{k,k',p} \bar{\psi}_{k+p}\bar{\psi}_{k'-p}\psi_k\psi_{k'} \tag{1.19}$$

with $\epsilon(\boldsymbol{k}) = \frac{|\boldsymbol{k}+\boldsymbol{q}|^2}{2m}$.

The expansion may be written as

$$S = S_0[\psi_{\boldsymbol{q}}] + \underbrace{\sum_k \frac{\delta S}{\delta\Psi_k^\mu}[\psi_{\boldsymbol{q}}]\delta\Psi_k^\mu}_{=0 \text{ since } \psi_{\boldsymbol{q}} \text{ satisfies the equations of motion}} + \frac{1}{2}\sum_{k,k'} \frac{\delta S}{\delta\bar{\Psi}_k^\mu \delta\Psi_{k'}^\nu}[\psi_{\boldsymbol{q}}]\delta\bar{\Psi}_k^\mu\delta\Psi_{k'}^\nu + \dots \tag{1.20}$$

with the aid of Nambu spinors $\boldsymbol{\Psi}_k = (\psi_k, \bar{\psi}_{-k})$. Setting aside the constant and the zero linear terms, we may examine the quadratic part of this expansion:

$$S_2[\psi_{\boldsymbol{q}}] = \frac{1}{2}\sum_k \delta\bar{\boldsymbol{\Psi}}_k \begin{pmatrix} \omega + \mu' - 4V\psi_0^2 - \epsilon(\boldsymbol{k}) & -2V\psi_0^2 \\ -2V\psi_0^2 & -\omega + \mu' - 4V\psi_0^2 - \epsilon(-\boldsymbol{k}) \end{pmatrix} \delta\boldsymbol{\Psi}_k. \tag{1.21}$$

and calculate the equations of motion corresponding to it, which is equivalent to linearising the original equations around our chosen flow solution:

$$\omega\delta\boldsymbol{\Psi}_k = \begin{pmatrix} \epsilon(\boldsymbol{k}) + 4V\psi_0^2 - \mu' & 2V\psi_0^2 \\ -2V\psi_0^2 & \mu' - 4V\psi_0^2 - \epsilon(-\boldsymbol{k}) \end{pmatrix} \delta\boldsymbol{\Psi}_k. \tag{1.22}$$

Excitations around the uniform flow are thus governed by the above eigenvalue equation. This can be solved [16] via the ansatz

$$\delta\psi_k = u(\boldsymbol{p})\delta(\omega - \omega(\boldsymbol{p}))\delta(\boldsymbol{k} - \boldsymbol{p}) + \bar{v}(\boldsymbol{p})\delta(\omega + \omega(\boldsymbol{p}))\delta(\boldsymbol{k} + \boldsymbol{p}), \tag{1.23}$$

which yields (substituting (1.17))

$$\omega(\boldsymbol{p})\begin{pmatrix} u(\boldsymbol{p}) \\ v(\boldsymbol{p}) \end{pmatrix} = \begin{pmatrix} \epsilon(\boldsymbol{p}) + \mu' - 2\epsilon(\boldsymbol{0}) & \mu' - \epsilon(\boldsymbol{0}) \\ \epsilon(\boldsymbol{0}) - \mu' & 2\epsilon(\boldsymbol{0}) - \mu' - \epsilon(-\boldsymbol{p}) \end{pmatrix}\begin{pmatrix} u(\boldsymbol{p}) \\ v(\boldsymbol{p}) \end{pmatrix}. \tag{1.24}$$

and the corresponding energy fluctuation is

$$\delta E = \omega(\boldsymbol{p})\Big[|u(\boldsymbol{p})|^2 - |v(\boldsymbol{p})|^2\Big], \tag{1.25}$$

which must be positive for any $\boldsymbol{p}$ if the state is to be energetically stable.

Doing the calculation explicitly, we find

$$\omega_\pm(\boldsymbol{p}) = \frac{\boldsymbol{p}\cdot\boldsymbol{q}}{m} \pm \frac{1}{2}\frac{|\boldsymbol{p}|}{\sqrt{m}}\sqrt{\frac{|\boldsymbol{p}|^2}{m} + 4\mu' - 4\epsilon(\boldsymbol{0})}, \tag{1.26}$$

$$\left[|u_{\pm}(\boldsymbol{p})|^2 - |v_{\pm}(\boldsymbol{p})|^2\right] = \left(\frac{|\boldsymbol{p}|^2}{2m} \pm \frac{1}{2}\frac{|\boldsymbol{p}|}{\sqrt{m}}\sqrt{\frac{|\boldsymbol{p}|^2}{m} + 4\mu' - 4\epsilon(\boldsymbol{0})} + \left(\mu' - \epsilon(\boldsymbol{0})\right)\right)^2 - \left(\mu' - \epsilon(\boldsymbol{0})\right)^2. \tag{1.27}$$

Since condensation into the flow state requires $\mu' > \epsilon(\boldsymbol{0})$ (see 1.17),

$$\left[|u_{+}(\boldsymbol{p})|^2 - |v_{+}(\boldsymbol{p})|^2\right] > 0 \text{ and } \left[|u_{-}(\boldsymbol{p})|^2 - |v_{-}(\boldsymbol{p})|^2\right] < 0. \tag{1.28}$$

Moreover, $\omega_+(\boldsymbol{p}) = \omega_-(-\boldsymbol{p})$, so it is sufficient to check energetic stability using $\omega_+(\boldsymbol{p})$ and verifying that it is nowhere negative. This circumstance is common enough that it frequently works to simply consider $\omega_+(\boldsymbol{p})$ from the start, ignoring the negative 'ghost branch'[2] $\omega_-(\boldsymbol{p})$ and the checks on u and v.

Plotting $\omega(\boldsymbol{p})_+$ for $\boldsymbol{q} = 0$ in Fig.1.1, we see the familiar form of the Bogoliubov spectrum with sound velocity $v_s = \frac{d\omega_+}{dp}(0) = \sqrt{\frac{\mu'}{m}}$.

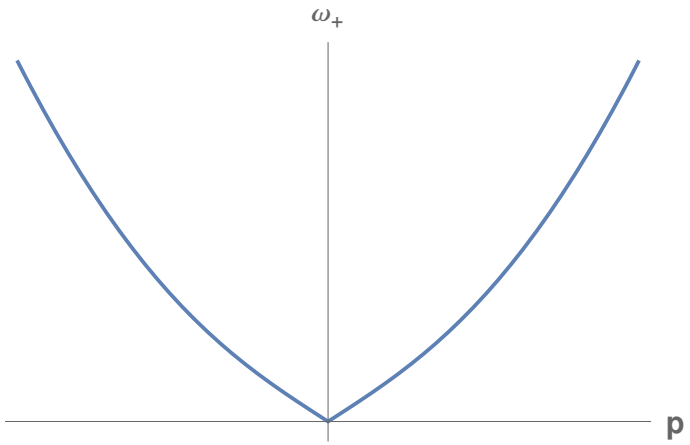

Figure 1.1: Excitation spectrum of a zero temperature weakly interacting Bose gas. The spectrum has the distinctive Bogoliubov form, with a linear dispersion for low momenta and a quadratic one for higher ones.

It is easy to see that in this case the sound velocity is also the critical velocity, with a flow velocity $\left|\frac{\boldsymbol{q}}{m}\right| > v_s$ leading to an energetic instability (see Fig.1.2). Using Landau's logic, interactions with the carrying medium of our Bose gas (which we have not specified) would thus be able to reduce the total energy of the system by creating excitations associated to the portion of the diagram below the horizontal axis and thus dissipate energy. We have thus recovered the Landau criterion in the field-theoretic picture, the same logic as above carrying over to models more complicated than our toy one. With this in hand, we may now consider two situations in which the criterion is not applicable.

Firstly, recall that in this formalism we obtained the excitation spectrum as the eigenvalues of linearised classical equations of motion. Linear stability analysis

[2]The discussion presented here explains why the presence of the negative branch $\omega_-(\boldsymbol{p})$, often confusingly called an energy spectrum, does not immediately imply energetic instability, showing that the real energy fluctuation involves another term $|u_-(\boldsymbol{p})|^2 - |v_-(\boldsymbol{p})|^2$ which typically makes the overall sign positive.

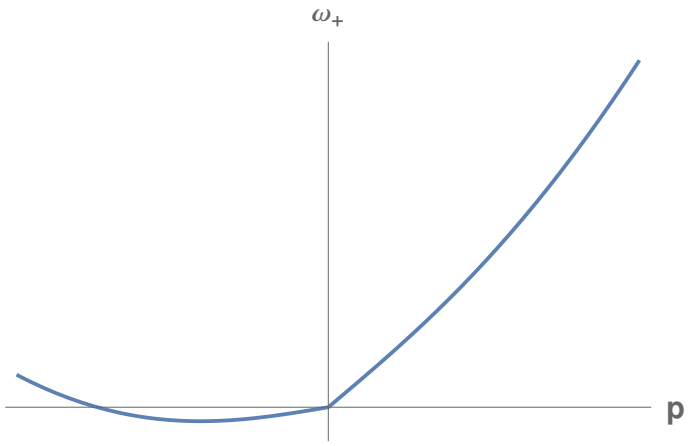

Figure 1.2: Excitation spectrum of a zero temperature weakly interacting Bose gas flowing at velocity $\frac{q}{m}$ exceeding the critical velocity v_s. In this picture the velocity was chosen to be in the 'positive' $\boldsymbol{p}$ direction, so that the instability is driving the fluid back to a lower velocity.

in general yields complex eigenvalues, and the fact that all of ours were real is a feature specific to equilibrium systems — open quantum systems with drive and dissipation typically have complex spectra. Let us thus consider how the analysis is altered if we suppose our tilted Bogoliubov spectrum also has an imaginary component.

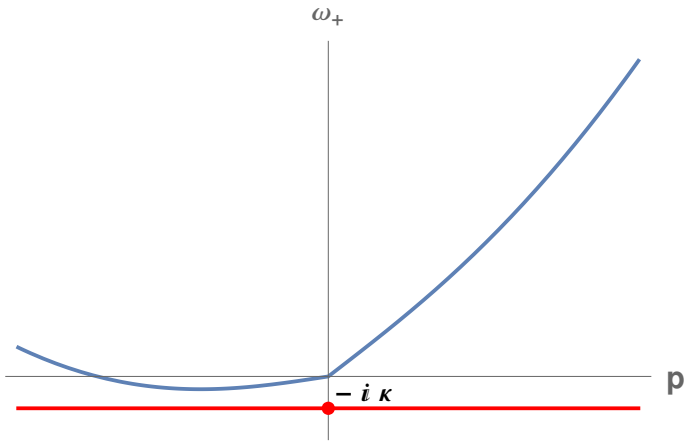

Figure 1.3: Excitation spectrum of a hypothetical dissipative weakly interacting Bose gas flowing at velocity $\frac{q}{m}$ exceeding the critical velocity v_s. The red curve is the imaginary portion of the spectrum, which here has been assumed constant and negative — for real models this will typically not be constant, but the negativity is essential for dynamical stability.

For the system to be dynamically stable, the imaginary portion of the eigenvalues found during stability analysis must be negative. This is distinct from energetic stability since failure of dynamical stability will lead to an immediate 'blow-up' of the system with no need for dissipative interactions with a carrier medium or similar external considerations. Let us thus simply postulate a constant, negative imaginary component of the spectrum $-i\kappa$.

This means that any excitation now has a finite lifetime $\tau = \frac{1}{\kappa}$ and the system thus brings itself back to its original state after being perturbed. Contrast this with the equilibrium case where an excitation, once created by an interaction, was assumed to persist and lead to the eventual collapse of the flow once enough had been created. This important distinction is due to the fact that the spectra of equilibrium systems lie exactly on the boundary of stability and are thus less stable than driven-dissipative systems. Indeed, from the point of view of linear stability analysis, equilibrium systems are the 'odd' ones as their eigenvalues belong to a very restricted class.

When, then, would we expect a flow of a driven-dissipative system that exceeds the Landau critical velocity to be destroyed? A heuristic answer might go as follows: supposing we consider the most energetically unstable excitation and postulate that interactions with the carrier medium generate it at some rate λ independent of the existing number of excitations, we find the following simple rate equation for its occupation n_e:

$$\frac{dn_e}{dt} = \lambda - \kappa n_e. \tag{1.29}$$

This equation can never drive the occupation to above $\frac{\lambda}{\kappa}$ meaning that, unless λ very significantly exceeds κ, interactions with the medium will be unable to generate sufficient excitations to destroy the flow. Whether λ is sufficiently high enough will depend on the nature of interactions with the carrier medium, which were left unstated in the original form of the Landau criterion as there $\kappa = 0$ meant that any rate was sufficient. We see, thus, that in order to apply the Landau criterion to driven-dissipative systems, we would need to specify in detail the form of the dissipative interactions with the carrier, which would complicate its application considerably. It is certainly no longer true that any flow exceeding the Landau critical velocity (as derived from the real part of the spectrum) is unstable.

1.3.3 Sufficiency of the Landau Criterion

From the discussion of the previous section, the reader may get the impression that driven-dissipative systems are in fact even more prone to superfluidity than equilibrium ones. With their more stable spectra it may seem that, while the Landau criterion may no longer be immediately used to prove a flow above a critical velocity is unstable, any flow below the Landau critical velocity must be even more stable than in equilibrium. This would suggest that the Landau criterion in the driven-dissipative setting simply goes from a 'necessary and sufficient' condition to a merely sufficient one for superfluidity.

This is, unfortunately, not the case, because there is at least one other mecha-

nism which undermines its logic. This mechanism is in fact not obviously specific to the open system setting, and it may simply be that it is encountered much less frequently in the equilibrium setting.

Recall our expression (1.17) for the density of the flowing condensate:

$$\mu' - \frac{|\boldsymbol{q}|^2}{2m} = 2V\rho. \tag{1.30}$$

The condensate fraction is thus zero if $\mu' < \frac{|\boldsymbol{q}|^2}{2m}$, or $\frac{|\boldsymbol{q}|}{m} > \sqrt{\frac{2\mu'}{m}} = v_c$. This defines a new critical velocity above which the flowing condensate solution simply does not exist. For our system this velocity is greater than the Landau critical velocity $v_c = \sqrt{2}v_s$ and thus energetic instability sets in first. Were our system's spectrum stabilised by drive and dissipation, however, it would in principle be possible to encounter this vanishing of the flow solution at sufficiently high flow velocity.

More specifically to the work of Part Ia, we will encounter a system for which the classical equation of motion reads[3]

$$\left(i\partial_t + \omega_p + \frac{1}{2m}\nabla^2 + i\kappa\right)\psi - F_p - \frac{V}{2}|\psi|^2\psi = 0. \tag{1.31}$$

We observe that we cannot now simply construct a flow solution via the ansatz $\psi = \psi_0 e^{i\boldsymbol{q}\cdot\boldsymbol{x}}$ because in the resulting equation

$$\left(\omega_p - \frac{q^2}{2m} + i\kappa\right)\psi_0 e^{i\boldsymbol{q}\cdot\boldsymbol{x}} - F_p - \frac{V}{2}|\psi_0|^2\psi_0 e^{i\boldsymbol{q}\cdot\boldsymbol{x}} = 0 \tag{1.32}$$

no $e^{i\boldsymbol{q}\cdot\boldsymbol{x}}$ factor appears on the F_p term and thus it cannot be divided out. This factor, corresponding to a coherent drive of the condensate, in effect locks the condensate to a specific frequency and momentum (here both zero). Taking the spectrum of the stationary condensate and applying the Landau criterion in this case is meaningless, because the flow states which would correspond to the tilted spectrum and give a critical velocity simply do not exist — the condensate is locked to the pump.

An interesting feature of this pumped model is that, if the pump is tilted via $F_p \to F_p e^{i\boldsymbol{q}\cdot\boldsymbol{x}}$, then a flow solution does exist and is stable. Yet the system is still clearly not a superfluid (as will be confirmed by the criterion we introduce in the next section when we apply it in Part Ia). This is because we had to tilt the pump to permit the flow and this is now the only flow that may exist, still being locked to the pump. We thus see here another instance of the Landau criterion coupling the 'complex of phenomena' that is superfluidity too tightly — the existence of persistent flows is a poor indicator of other features of superfluids

[3]We have taken the equation for the classical Keldysh field as this most closely corresponds to an equilibrium equation of motion. The reader unfamiliar with Keldysh may ignore this remark for now and return to it once Keldysh methods have been introduced later in the thesis.

such as insensitivity to shear forces.

The circumstances described in this section, in which the Landau criterion is inapplicable, may be summarized as follows. The Landau criterion assumes that, for any given velocity, it is possible to construct a solution of the system's equations of motion moving with that velocity, and then analyses the linear stability of that solution. This analysis is indirect, however, since as typically used the criterion takes the spectrum of one non-flowing solution and then extrapolates it to flows it supposes exist by linearly tilting that spectrum. If, however, the flows corresponding to a given 'tilted' spectrum are not actual solutions of the equations of motion, then linear stability analysis is meaningless and the criterion is inapplicable.

We see thus that the Landau criterion is generally unreliable in the open quantum system setting. It cannot rule out superfluidity because it does not sufficiently specify the nature of the dissipative interaction with the carrier medium, nor can it confirm superfluidity due to the incomplete way in which it performs linear stability analysis.

1.4 Superfluid Linear Response

With the reader hopefully convinced that the Landau criterion is an unreliable tool for open quantum systems, we now seek to introduce a replacement for it. We will begin by returning to the equilibrium setting for intuition, before extending the result to driven dissipative systems and arguing that it is sufficiently general to still apply.

The criterion we now introduce was first presented in the equilibrium setting by Baym [14] and is covered in great detail in the cited work. Here we will present a highly abridged version, focusing on the most core components of the argument.

To this end, consider a fluid with Hamiltonian H in its rest frame at inverse temperature β in equilibrium. Placing the fluid in a box and taking the box to be moving with velocity $\boldsymbol{v}$, the standard argument about the form of the macrocanonical ensemble given broken global symmetries [26] requires us to write it in a frame in which the walls of the box are stationary. Using our formula for energy in different reference frames once again, we find the ensemble in the box frame to read

$$\frac{1}{Z_{\boldsymbol{v}}} e^{-\beta[H-\boldsymbol{P}\cdot\boldsymbol{v}+\frac{1}{2}Mv^2-\mu N]}, \tag{1.33}$$

$$Z_{\boldsymbol{v}} = \operatorname{Tr} e^{-\beta[H-\boldsymbol{P}\cdot\boldsymbol{v}+\frac{1}{2}Mv^2-\mu N]}, \tag{1.34}$$

where $\boldsymbol{P}$ is the total momentum of the fluid, M its total mass, μ and N the chem-

ical potential and particle number. The core of the argument about to be presented is that by considering different shapes of the box, we can induce either the whole fluid or only its superfluid component to move.

To this end, let us consider the linear (in $\boldsymbol{v}$) response of the system's current $\boldsymbol{j}(\boldsymbol{x})$ to our movement of the box. At linear order in $\boldsymbol{v}$ the term Mv^2 will not appear, and we are thus interested in the response to the term $\boldsymbol{P}\cdot\boldsymbol{v}$. Writing $\boldsymbol{P} = m\int d\boldsymbol{x}\,\boldsymbol{j}(\boldsymbol{x})$, up to the factor m we are seeking the linear response of $\boldsymbol{j}(\boldsymbol{x})$ to $\int d\boldsymbol{x}\,\boldsymbol{j}(\boldsymbol{x})\cdot\boldsymbol{v}$.

In general, when working with linear response of $\boldsymbol{j}(t,\boldsymbol{x})$ to a perturbation $\int d\boldsymbol{x}\,\boldsymbol{j}(t,\boldsymbol{x})\cdot\boldsymbol{v}(t,\boldsymbol{x})$ to the Hamiltonian, the resulting expression will be of the form (we contract on repeated indices throughout this work)

$$\delta j_i(t,\boldsymbol{x}) = \int dt'd\boldsymbol{x}'\,\chi_{ij}(t,\boldsymbol{x};t',\boldsymbol{x}')v_j(t',\boldsymbol{x}') \tag{1.35}$$

where χ_{ij} is some tensor determined by the precise nature of the system. In the zero temperature and driven-dissipative cases it is given by (we typically omit $\hbar$ throughout this work except when it is relevant, here contrasting with β)

$$\chi_{ij}(t,\boldsymbol{x}) = \frac{i}{\hbar}\Theta(t-t')\langle[j_i(t,\boldsymbol{x}),j_j(t',\boldsymbol{x}')]\rangle \tag{1.36}$$

while in the equilibrium setting, because the perturbation also changes the macrocanonical density matrix and there is no t-dependence, the expression is different:

$$\chi^{\mathrm{eq}}_{ij}(t,\boldsymbol{x}) = \beta\Big[\langle j_i(\boldsymbol{x})j_j(\boldsymbol{x}')\rangle - \langle j_i(\boldsymbol{x})\rangle\langle j_j(\boldsymbol{x}')\rangle\Big]. \tag{1.37}$$

The argument about to be made, however, does not depend on either of these specific forms. Rather it will rely on properties that can be ascribed to this tensor on general grounds as follows.

Firstly, we will restrict ourselves to time and space-translationally[4] invariant systems. The former property is obviously true of systems in equilibrium, but is also true of many driven-dissipative systems: dissipation is often time independent, while drive may also either be time-independent or it may be possible to gauge out the dependence. At any rate, we will proceed on the assumption that this is so — a definition of superfluids for systems with explicitly non-stationary dynamics would run into questions like whether the superfluid is always superfluid or only part of the time and is beyond our present scope.

The second property is clearly not always true even in equilibrium, but is a reasonable requirement on similar grounds to our last comment about station-

[4]Here we mean approximate space-translational invariance in the bulk of the box containing the fluid. Such a system's response tensor will be well approximated by a space-translationally invariant form outside boundary regions near the box's walls, and these regions may be neglected when considering the macroscopic properties of a very large system.

arity. A theory of superfluidity without these assumptions would be forced to consider systems that might only be superfluid in certain regions of the system, and would pose problems for the Landau criterion too since the standard spectral representation of Greens functions relies on this invariance (as indeed it also does on the dynamics being stationary).

Given these assumptions, the form of the response tensor is constrained to

$$\chi_{ij}(t-t', \boldsymbol{x}-\boldsymbol{x}'). \tag{1.38}$$

With this, let us rewrite (1.35) using the Fourier transform of our tensor and the fact that our $\boldsymbol{v}(t,\boldsymbol{x})$ is in fact constant, and consider the response of the component of the current $j^{\parallel}$ parallel to $\boldsymbol{v}$:

$$\delta j^{\parallel}(t,\boldsymbol{x}) = \int dt' d\boldsymbol{y} d\omega dk^{\parallel} d\boldsymbol{k}^{\perp} e^{i(k^{\parallel}(x^{\parallel}-y^{\parallel})+\boldsymbol{k}^{\perp}\cdot(\boldsymbol{x}^{\perp}-\boldsymbol{y}^{\perp}))} e^{-i\omega(t-t')} \chi_{ij}(\omega,\boldsymbol{k}) \frac{v_i v_j}{|\boldsymbol{v}|^2}\boldsymbol{v}. \tag{1.39}$$

Taking the box containing the fluid to be of finite extent in all directions, we may still perform the t' and ω integrals between $-\infty$ and ∞ to obtain

$$\delta j^{\parallel}(t,\boldsymbol{x}) = \int d\boldsymbol{y} dk^{\parallel} d\boldsymbol{k}^{\perp} e^{i(k^{\parallel}(x^{\parallel}-y^{\parallel})+\boldsymbol{k}^{\perp}\cdot(\boldsymbol{x}^{\perp}-\boldsymbol{y}^{\perp}))} \chi_{ij}(0,\boldsymbol{k}) \frac{v_i v_j}{|\boldsymbol{v}|^2}\boldsymbol{v}. \tag{1.40}$$

This shows that, for a time-independent $\boldsymbol{v}$, the response will also be static. This is of course generally so in equilibrium since only the change in equilibrium expectation value is taken into account, meaning any transient behaviour of the system is ignored. Since, when studying phases of driven-dissipative matter, we are typically interested in the steady-state behaviour rather than transient effects, it makes sense to focus on the static response in that case also.

Finally, we can consider two situations. First, suppose the box has infinite extent in its direction of motion but finite in the others — this corresponds to the integral in $y^{\parallel}$ being between $-\infty$ and ∞. This integral will yield $\delta(k^{\parallel})$ and set that component of the momentum to zero. In this case, since the walls of the box are now interacting with the fluid only via shear and superfluid is insensitive to shear, only the 'normal' or non-superfluid portion of the fluid should respond. At the end we may also extend the box's walls to spatial infinity, obtaining

$$\delta j_n^{\parallel}(\boldsymbol{x}) = \lim_{\boldsymbol{k}^{\perp}\to 0} \lim_{k^{\parallel}\to 0} \chi_{ij}(0,\boldsymbol{k}) \frac{v_i v_j}{|\boldsymbol{v}|^2}\boldsymbol{v}. \tag{1.41}$$

On the other hand, suppose we first infinitely extend the box in all directions orthogonal to the direction of motion. Now the fluid is being pushed by the rear wall and is expected to move irrespective of whether it is superfluid or not. This situation interchanges the momentum limits and we obtain the response of the

total fluid:

$$\delta j_t^{\parallel}(\boldsymbol{x}) = \lim_{k^{\parallel}\to 0}\lim_{\boldsymbol{k}^{\perp}\to 0} \chi_{ij}(0,\boldsymbol{k})\frac{v_i v_j}{|\boldsymbol{v}|^2}\boldsymbol{v}. \tag{1.42}$$

If these responses are unequal, it stands to reason that a portion of the fluid acts as superfluid in the direction of the $\boldsymbol{v}$ used — by taking $\boldsymbol{v}$ in different directions, one may account for anisotropic systems just as the Landau criterion may yield different critical velocities in different directions. In equilibrium these responses may also be related directly to normal and superfluid densities via identities known as sum rules, but these do not easily generalise to the driven-dissipative case.

While at first it may seem like the line of reasoning above relied on equilibrium considerations (namely the logic about which frame one must write the macrocanonical ensemble in), let us consider the core meaning of the above reasoning. Namely, there exists a general form of static perturbation

$$\int d\boldsymbol{x}\, \boldsymbol{j}(\omega = 0, \boldsymbol{x}) \cdot \boldsymbol{v}(\boldsymbol{x}) \tag{1.43}$$

for a Hamiltonian which can act like a shear in a given direction if $v(k^{\parallel}, \boldsymbol{k}^{\perp}) = v(\boldsymbol{k}^{\perp})$ or a push if $v(k^{\parallel}, \boldsymbol{k}^{\perp}) = v(k^{\parallel})$ independent of the form of the Hamiltonian or the carrying medium (the box can be anything so long as it has spatial extent and confines the fluid).

Nothing about the form of this perturbation restricts it to an equilibrium setting, it captures our intuition about the insensitivity of superfluids to shear (this will be made even more explicit in section 4.3 for an isotropic setting), and every equilibrium superfluid reacts to it as above. The specific form of the response to it outlined above is thus a very strong contender for a generalised definition of superfluid that may be used for open quantum systems, and is the one we will use throughout this work.

Bibliography

[1] P. Kapitza, "Viscosity of liquid helium below the λ-point," *Nature*, vol. 141, no. 3558, pp. 74–74, 1938.

[2] J. F. Allen and A. Misener, "Flow of liquid helium ii," *Nature*, vol. 141, no. 3558, pp. 75–75, 1938.

[3] A. J. Leggett, *Quantum Liquids: Bose Condensation and Cooper Pairing in Condensed-Matter Systems*. Oxford: Oxford University Press, 2006.

[4] J. F. Annett, *Superconductivity, Superfluids and Condensates*. Oxford: Oxford University Press, 2004, vol. 5.

[5] A. J. Leggett, "Superfluidity," *Rev. Mod. Phys.*, vol. 71, S318, 1999.

[6] I. Carusotto and C. Ciuti, "Quantum fluids of light," *Reviews of Modern Physics*, vol. 85, no. 1, p. 299, 2013.

[7] J. Keeling and N. G. Berloff, "Condensed-matter physics: Going with the flow," *Nature*, vol. 457, pp. 273–274, 2009.

[8] E. Cancellieri, F. M. Marchetti, M. H. Szymańska, and C. Tejedor, "Superflow of resonantly driven polaritons against a defect," *Phys. Rev. B*, vol. 82, p. 224 512, 2010.

[9] C. C. I. Carusotto, "Quantum fluid effects and parametric instabilities in microcavities," *physica status solidi (b)*, 2005. DOI: 10.1002/pssb.200560961.

[10] I. Carusotto and C. Ciuti, "Probing microcavity polariton superfluidity through resonant rayleigh scattering," *Physical review letters*, vol. 93, no. 16, p. 166 401, 2004.

[11] P. Stepanov, I. Amelio, J.-G. Rousset, *et al.*, "Dispersion relation of the collective excitations in a resonantly driven polariton fluid," *Nature communications*, vol. 10, no. 1, p. 3869, 2019.

[12] F. Claude, M. J. Jacquet, R. Usciati, *et al.*, "High-resolution coherent probe spectroscopy of a polariton quantum fluid," *Physical Review Letters*, vol. 129, no. 10, p. 103 601, 2022.

[13] F. Claude, M. J. Jacquet, I. Carusotto, Q. Glorieux, E. Giacobino, and A. Bramati, "Spectrum of collective excitations of a quantum fluid of polaritons," *Physical Review B*, vol. 107, no. 17, p. 174 507, 2023.

[14] G. Baym, "The microscopic description of superfluidity," in *Mathematical Methods in Solid State and Superfluid Theory*, R. C. Clark and G. H. Derrick, Eds., Springer, 1968, ch. 3, pp. 121–156.

[15] J. Keeling, "Superfluid density of an open dissipative condensate," *Phys. Rev. Lett.*, vol. 107, p. 080 402, 2011.

[16] L. Pitaevskii and S. Stringari, *Bose-Einstein condensation and superfluidity*. Oxford University Press, 2016, vol. 164.

[17] P. Nozières and D. Pines, *The Theory of Quantum Liquids: Superfluid Bose Liquids*. CRC Press, 2018.

[18] A. Griffin, *Excitations in a Bose-condensed liquid* (Cambridge Studies in Low Temperature Physics 4). Cambridge University Press, 1993.

[19] A. Leggett, "On the superfluid fraction of an arbitrary many-body system at t= 0," *Journal of Statistical Physics*, vol. 93, no. 3, pp. 927–941, 1998.

[20] V. G. Rousseau, "Superfluid density in continuous and discrete spaces: Avoiding misconceptions," *Physical Review B*, vol. 90, no. 13, p. 134 503, 2014.

[21] A. A. Abrikosov, L. P. Gorkov, and I. E. Dzyaloshinski, *Methods of quantum field theory in statistical physics*. Courier Corporation, 2012.

[22] E. M. Lifshitz and L. P. Pitaevskii, *Statistical physics. Part 2. Theory of the condensed state*. Moscow "Nauka", 1976, vol. 9.

[23] I. Amelio, A. Minguzzi, M. Richard, and I. Carusotto, "Galilean boosts and superfluidity of resonantly driven polariton fluids in the presence of an incoherent reservoir," *Physical Review Research*, vol. 2, no. 2, p. 023 158, 2020.

[24] L. S. Schulman, *Techniques and applications of path integration*. Courier Corporation, 2012.

[25] A. Kamenev, *Field theory of non-equilibrium systems*. Cambridge University Press, 2023.

[26] L. D. Landau and E. M. Lifshitz, *Statistical Physics: Volume 5*. Elsevier, 2013, vol. 5.

Part I

Geometric and Fluctuational Divergences in the Linear Response of Coherently Driven Microcavity Polaritons and Their Relation to Superfluidity

Chapter 2

Coherently Driven Microcavity Polaritons

2.1 Microcavity Polaritons and Superfluidity

As was laid out in the previous chapter, research on systems exhibiting superfluidity in thermal equilibrium has been extensive and far-ranging since the phenomenon's discovery. More recently, with the increasing interest in driven-dissipative systems which never thermalise due to constant decay and must be pumped to maintain a steady state, work has begun on identifying whether the same phenomena can occur in these. Examples of such systems are numerous, including Bose-Einstein condensates (BEC) of photons [1], [2], cold atoms coupled to photonic modes in optical cavities [3], and cavity arrays [4]–[6]. Of particular note are microcavity polaritons [7]–[9], which are two-dimensional bosonic quasiparticles made of photons trapped in a cavity strongly coupled to excitons in a quantum well. While we shall focus here on their more fundamental properties, in recent years microcavity polaritons have found many practical applications [10]–[12] including spintronics [13]–[15], lasing [16]–[18], and optical circuits [19], [20].

Polariton experiments have observed a number of effects usually associated with superfluidity, such as the suppression of scattering for flow past a defect [21]–[23], metastable persistent currents [24], and quantised vortices [25]. The question of how superfluidity may occur in these out-of-equilibrium systems has proved contentious [25]–[31], however, and it is unclear whether all the effects seen in equilibrium will continue to occur [7], [32]. The Landau criterion in its usual form is, as we have discussed, no longer applicable to open systems. This opens up space for unusual situations, discussed below, such as persistent currents without suppressed scattering [27] and suppressed scattering without zero viscosity [33].

The properties of microcavity polaritons are heavily dependent on how the system is pumped — that is, on how photons are injected into the cavity. When

this occurs incoherently, meaning photons are injected far off-resonance, then relaxation processes involving excitons and photons will under the right conditions lead to the "condensation" of polaritons into a low energy state [34]. This process involves the spontaneous breaking of the $U(1)$ phase symmetry of the macroscopic wavefunction (very similar to the toy model in the previous chapter), leading to a Goldstone mode in the excitation spectrum of the system [35], [36]. In a theoretical study of the longitudinal and transverse response functions of an incoherently driven system using the Keldysh path integral technique (to be developed in the next chapter) [27], it was found that the driven-dissipative nature of the system allowed superfluidity to survive despite the Landau criterion yielding a zero critical velocity. Crucially, in open quantum systems, it appears that a gapless spectrum is crucial for the phenomenon.

Alternatively, polaritons may be pumped coherently, meaning they are injected at a specific energy and momentum near resonance, and can form a macroscopic state with a phase fixed to that of the external pump [37]. Because of this phase fixing, the excitation spectrum in such a system is typically gapped. Despite this, experiments have observed that coherently pumped polaritons can flow past a defect with vanishing dissipation; this, together with theoretical analysis speculatively applying the Landau criterion to the real part of the polariton spectrum [38], [39], has been claimed as evidence of superfluidity [21]. By applying the Keldysh path integral technique to directly calculate the longitudinal and transverse current-current responses of the system, however, it was found [33] that these responses are equal in all regimes with a gapped excitation spectrum. According to the alternative criterion developed at the end of the last chapter, then, the system is not superfluid in these regimes, in contradiction to the Landau criterion, underscoring the criterion's poor applicability beyond the equilibrium setting.

2.1.1 Summary of Present Work: Absence of Superfluidity in Gapless Regimes of Coherently Driven Polaritons

For special choices of system parameters coherently pumped polaritons may be induced to possess a gapless spectrum and thus possibly exhibit superfluidity. The mean-field[1] responses at such points in parameter space were derived in [40], where it was shown that while an anisotropic[2] pump yields a divergent linear response, an isotropic pump leads to a pure superfluid one. One of the

[1] Strictly speaking, the mean-field of a perturbative calculation corresponds to $O(\hbar^0)$, at which order this response is simply zero. Throughout this part I slightly misuse the term to refer to the lowest order non-zero contribution at $O(\hbar^1)$.

[2] By an anisotropic pump is meant one which injects particles with non-zero momentum in the plane to which the polaritons are confined. Similarly, an isotropic farm injects particles with zero momentum in this plane.

main results of this part of the thesis, though, is that when considered more carefully, coherently driven polaritons do not exhibit superfluidity in any regime. By analysing the system from the point of view of catastrophe theory, it is shown that the anisotropic mean-field divergence of the response is physical and related to bifurcations in the system order parameter. Such bifurcations are also responsible for the gapless mode, which proves to be due to the appearance of a "non-Morse critical point" of the action. Finally, performing perturbative calculations to $O(\hbar^2)$, I demonstrate that higher-order terms of the perturbation expansion in both isotropic and anisotropic cases diverge in the gapless regime due to these points in fact corresponding to phase transitions and the condensate density diverging; this indicates that perturbation theory is not rigorously applicable and that the mean-field superfluidity result is misleading.

The rest of this chapter is devoted to the simple microscopic model of coherently driven microcavity polaritons that is used in this part of the thesis; in Chap.3 this model is rewritten in the language of Keldysh field theory (and Keldysh field theory is introduced). Chap.4 covers earlier work on superfluidity in coherently driven polaritons, explaining the attempted applications of the Landau criterion [38], [39] and the direct calculations of the current responses [33]. This is followed by my catastrophe-theoretic analysis of the anisotropic mean-field behaviour of the system in Chap.5, demonstrating the origin of the mean-field response divergences in bifurcations of the order parameter. Then in Chap.6, quantum fluctuations of the system are taken into account to show that, despite isotropic mean-field calculations yielding a superfluid response, the response in gapless regimes is still divergent. This divergence is analysed both from the perspective of the infinite-dimensional analogue of catastrophe theory, renormalization group theory, and of naive perturbation theory, showing that it originates from the phase transitions in these regimes. In Chap.7 I conclude that, within the bounds of validity of the Keldysh model analysed here, there are no regimes of coherently-driven microcavity polaritons that exhibit superfluidity.

2.2 Strong Coupling of Photons and Excitons: the Coherently Driven Lower Polariton Model

Semiconductor microcavities are typically constructed by placing semiconductor quantum wells supporting Wannier-Mott excitons between Bragg reflectors (layers of alternating refractive index material leading to high quality reflection for wavelengths close to four times the layer widths), typically spaced microns apart (Fig. 2.1 **a**). Semiconductor quantum wells are thin layers of semiconductor with a thickness comparable to the exciton Bohr radius, sandwiched between two barrier layers with a much larger band gap. The exciton centre-of-mass motion is

quantized in the confinement direction, and the wells are typically engineered to support only the lowest of these energy modes at the relevant energies, making the excitons quasi-2D particles [41].

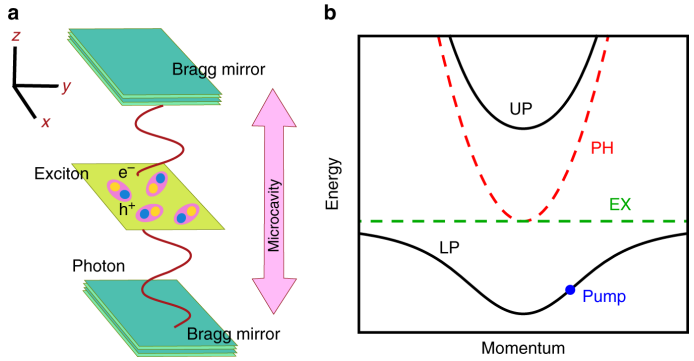

Figure 2.1: Polaritons in semiconductor microcavities. **a** Polaritons are quasiparticles formed when cavity photons, which are massive due to confinement in the z direction between two Bragg mirrors, interact strongly with excitons confined in a quantum well. Polaritons are free to move in the two-dimensional plane perpendicular to their confinement. **b** The excitonic dispersion (dashed green) is approximately constant compared to the photonic (dashed red) due to the much larger exciton mass. Strong coupling leads to anticrossing and the formation of upper and lower polariton branches (solid black). Polaritons interact because of their excitonic component, while their photonic part causes decay and the need for an external drive. A coherent laser pump resonantly tuned to the polariton dispersion is marked by a blue dot.

Photons trapped in the cavity also behave as quasi-2D particles, developing an effective mass related to their quantized mode in the confinement direction. Typically only the lowest mode is considered, and the effective energy spectrum becomes

$$\omega_c(\mathbf{k}) = \frac{c}{n}\sqrt{\left(\frac{2\pi}{L_w}\right)^2 + |\boldsymbol{k}|^2}, \tag{2.1}$$

where n is the refractive index of the quantum well and L_w is the cavity width.

With appropriate tuning, the system can be described by a Jaynes-Cummings interaction[3]:

$$H_0 = \sum_{\mathbf{k}} \omega_c(\mathbf{k}) c_{\mathbf{k}}^\dagger c_{\mathbf{k}} + \sum_{\mathbf{k}} \omega_x(\mathbf{k}) x_{\mathbf{k}}^\dagger x_{\mathbf{k}} + \frac{\Omega_R}{2} \sum_{\mathbf{k}} \left(c_{\mathbf{k}}^\dagger x_{\mathbf{k}} + x_{\mathbf{k}}^\dagger c_{\mathbf{k}} \right) \tag{2.2}$$

with quasi-2D photon annihilation operators $c_{\mathbf{k}}$ and exciton annihilation operators $x_{\mathbf{k}}$, where the Rabi frequency Ω_R acts as the exciton-photon coupling constant. The exciton spectrum $\omega_x(\boldsymbol{k})$ has negligible curvature compared to the

[3]Throughout this part we will perform intermediate calculations as though the system is in a finite volume and thus integrals over momentum are replaced by sums over a momentum lattice. This approach follows [40] and allows us to avoid dealing with expressions involving Dirac deltas of zero, thus acting as a pre-emptive regularisation. Expressions obtained using this approach may safely have the $\boldsymbol{k} \to 0$ limit applied to them as if no lattice had been used (this is demonstrated in Appendix B of [40]).

parabolic cavity photon spectrum $\omega_c(\boldsymbol{k})$ due to the much higher effective mass of the excitons, and may thus be approximated as flat: $\omega_x(\boldsymbol{k}) \approx \omega_x$.

The Hamiltonian may be diagonalized into quasi-particles known as lower and upper polaritons [42]:

$$H_0 \approx \sum_{\mathbf{k}} \omega_{\mathrm{LP}}(\mathbf{k}) a^\dagger_{\mathrm{LP},\mathbf{k}} a_{\mathrm{LP},\mathbf{k}} + \sum_{\mathbf{k}} \omega_{\mathrm{UP}}(\mathbf{k}) a^\dagger_{\mathrm{UP},\mathbf{k}} a_{\mathrm{UP},\mathbf{k}}, \tag{2.3}$$

with ($\omega_{\mathrm{UP/LP}}(\mathbf{k})$ is depicted in Fig. 2.1 **b**)

$$\begin{pmatrix} a_{\mathrm{LP},\boldsymbol{k}} \\ a_{\mathrm{UP},\boldsymbol{k}} \end{pmatrix} = \begin{pmatrix} X_{\boldsymbol{k}} & C_{\boldsymbol{k}} \\ -C_{\boldsymbol{k}} & X_{\boldsymbol{k}} \end{pmatrix} \begin{pmatrix} x_{\boldsymbol{k}} \\ c_{\boldsymbol{k}} \end{pmatrix} \tag{2.4}$$

$$X_{\boldsymbol{k}} = \frac{\omega_c(\boldsymbol{k}) - \omega_{\mathrm{LP}}(\boldsymbol{k})}{\sqrt{(\omega_{\mathrm{LP}}(\boldsymbol{k}) - \omega_c(\boldsymbol{k}))^2 + \Omega_R^2/4}} \tag{2.5}$$

$$C_{\boldsymbol{k}} = -\frac{\Omega_R}{2\sqrt{(\omega_{\mathrm{LP}}(\boldsymbol{k}) - \omega_c(\boldsymbol{k}))^2 + \Omega_R^2/4}} \tag{2.6}$$

$$\omega_{\mathrm{UP/LP}}(\mathbf{k}) = \frac{1}{2}\left(\omega_x + \omega_c(\mathbf{k}) \pm \sqrt{(\omega_x - \omega_c(\mathbf{k}))^2 + \Omega_R^2}\right). \tag{2.7}$$

where $X_{\boldsymbol{k}}$ and $C_{\boldsymbol{k}}$ are known as excitonic and photonic Hopfield coefficients. This change of basis is meaningful if the polaritons can be spectroscopically resolved from the original particles. This may not be the case if, in the region $\omega_c(\boldsymbol{k}) \approx \omega_x$, the energy splitting Ω_R of the polaritons is less than the dissipative linewidth of the excitons or cavity photons [43]. We thus focus on systems in the strong light-matter coupling regime [7], meaning that the exciton-photon coupling Ω_R significantly exceeds the decay and dephasing rates of the excitons and cavity photons and thus their linewidths.

The gap between the lower and upper polariton spectra is typically large enough for the lower polaritons to be considered in isolation (from now on we write $a_{\mathbf{k}}$ for $a_{\mathrm{LP},\mathbf{k}}$) if the relevant energy scales are tuned to them, and excitonic interactions may be modelled as weak contact interactions between polaritons:

$$H_{\mathrm{int}} = \frac{V}{2} \sum_{\mathbf{k},\mathbf{k}',\mathbf{q}} a^\dagger_{\mathbf{k}-\mathbf{q}} a^\dagger_{\mathbf{k}'+\mathbf{q}} a_{\mathbf{k}} a_{\mathbf{k}'}. \tag{2.8}$$

Note that this form for the interaction is only valid so long as we may ignore the spatial extent of the excitons. With a typical exciton Bohr radius as high as 100 Å, we must impose a momentum cut-off on our theory of $k_{\max} = \frac{h}{100\,\text{Å}}$. This will also be relevant to our approximations in Chap.3. Finally, the system is typically driven and subject to dissipation, meaning that it is externally pumped by a laser and is in contact with a photonic decay bath. Denoting the bath photon modes

by $A_{\mathbf{k}}$ and their spectrum by $\omega_A(\mathbf{k})$, the decay term may be written as

$$H_{\text{bath}} = \sum_{\mathbf{k}} \omega_A(\mathbf{k}) A^\dagger_{\mathbf{k}} A_{\mathbf{k}} + \sum_{\mathbf{k},\mathbf{q}} \zeta_{\mathbf{k},\mathbf{q}} (a^\dagger_{\mathbf{k}} A_{\mathbf{q}} + A^\dagger_{\mathbf{q}} a_{\mathbf{k}}). \tag{2.9}$$

The properties of the coupling $\zeta_{\mathbf{k},\mathbf{q}}$ will be explored in Sec.3.2.

The pump laser is typically applied at some angle to the cavity, and the projection of its photons' momenta onto the cavity plane leads to an effective pump wave-vector k_p. A classical coherent pump term, by which we mean resonant or near-resonant with the lower polariton dispersion, may then be represented as

$$H_{\text{pump}} = F_p(t) a^\dagger_{\mathbf{k}_p} + F^*_p(t) a_{\mathbf{k}_p}, \tag{2.10}$$

where $F_p(t) = F_p e^{-i\omega_p t}$, $\omega_p \approx \omega_{\text{LP}}(\boldsymbol{k}_p)$, and the implications of neglecting fluctuations in the pump field are discussed in Sec.6.2. Performing a gauge transformation $a \to a e^{-i\omega_p t}$, resumming relative to the pump $\mathbf{k} \to \mathbf{k} + \mathbf{k}_p$, and writing $a_{\mathbf{k}}$ for $a_{\mathbf{k}+\mathbf{k}_p}$, the complete effective[4] Hamiltonian then reads

$$\begin{aligned} H = &\sum_{\mathbf{k}} (\omega_{\text{LP}}(\mathbf{k}+\mathbf{k}_p) - \omega_p) a^\dagger_{\mathbf{k}} a_{\mathbf{k}} + \frac{V}{2} \sum_{\mathbf{k},\mathbf{k}',\mathbf{q}} a^\dagger_{\mathbf{k}-\mathbf{q}} a^\dagger_{\mathbf{k}'+\mathbf{q}} a_{\mathbf{k}} a_{\mathbf{k}'} + \sum_{\mathbf{k}} \omega_A(\mathbf{p}+\mathbf{k}_p) A^\dagger_{\mathbf{p}} A_{\mathbf{p}} \\ &+ \sum_{\mathbf{k},\mathbf{p}} \zeta_{\mathbf{k},\mathbf{p}} (e^{i\omega_p t} a^\dagger_{\mathbf{k}} A_{\mathbf{p}} + A^\dagger_{\mathbf{p}} a_{\mathbf{k}} e^{-i\omega_p t}) + F_p(a^\dagger_0 + a_0). \end{aligned} \tag{2.11}$$

Note that this is not a closed-system Hamiltonian, since it incorporates a number non-conserving interaction with laser degrees of freedom the dynamics of which we do not incorporate in the model; rather it is the effective Hamiltonian for the polariton and photon bath subsystem.

[4]The extra $-\omega_p a^\dagger_{\boldsymbol{k}} a_{\boldsymbol{k}}$ term is not truly part of the Hamiltonian, but allows for an elegant resolution of the following difficulty that would otherwise be encountered in the next chapter when constructing a functional integral. The gauge-transformed creation and annihilation operators no longer act on field coherent states (to be defined in the next chapter) by $a_{\boldsymbol{k}}|\psi_{\boldsymbol{k}}\rangle = \psi_{\boldsymbol{k}}|\psi_{\boldsymbol{k}}\rangle$, but rather by $a_{\boldsymbol{k}}|\psi_{\boldsymbol{k}}\rangle = e^{i\omega_p t}\psi_{\boldsymbol{k}}|\psi_{\boldsymbol{k}}\rangle$. In order to retain the original relation, one may use gauge-transformed coherent states $|\psi_{\boldsymbol{k}}\rangle_g = |e^{-i\omega_p t}\psi_{\boldsymbol{k}}\rangle$, but these will have a different inner product expression to that of conventional coherent states, complicating the construction of the coherent state functional integral. By adding this effective term to the Hamiltonian, the functional integral in the next chapter may be constructed as if the gauge-transformed coherent states retain the usual coherent state inner product expression: the resulting action is the same as that obtained without the term and taking full account of the more complicated inner product expression.

Chapter 3

Keldysh Field Theory for Polariton Systems

3.1 Non-Equilibrium Field Theory

Zero-temperature perturbative QFT is often concerned with calculating time-ordered (denoted by $\mathcal{T}$, and we assume $t_n > t_{n-1} > \ldots > t_2 > t_1$) expectations of operators in an interacting ground state $|\Omega\rangle$:

$$\langle\Omega|\mathcal{T}\, O_1(t_1)\ldots O_n(t_n)|\Omega\rangle = \frac{\langle 0|U(\infty,t_n)O_n\ldots U(t_2,t_1)O_1U(t_1,-\infty)|0\rangle}{\langle 0|U(\infty,-\infty)|0\rangle}, \tag{3.1}$$

where $|0\rangle$ is the non-interacting ground state. For a Hamiltonian consisting of creation and annihilation operators, the operator $\langle 0|U(\infty,-\infty)|0\rangle$ may be converted to a coherent state path integral expression (up to a phase factor that cancels in the ratio above) of the form

$$\begin{aligned}\langle 0|U(\infty,-\infty)|0\rangle \propto \int_{\psi_{\boldsymbol{k}}(\infty)=\psi_{\boldsymbol{k},\text{out}}} \mathcal{D}[\psi_{\boldsymbol{k},\text{out}},\bar{\psi}_{\boldsymbol{k},\text{out}},\psi_{\boldsymbol{k},\text{in}},\bar{\psi}_{\boldsymbol{k},\text{in}}]\langle 0|\psi_{\boldsymbol{k},\text{out}}\rangle\langle\psi_{\boldsymbol{k},\text{in}}|0\rangle \\ \times \int_{\psi_{\boldsymbol{k}}(-\infty)=\psi_{\boldsymbol{k},\text{in}}} \mathcal{D}[\psi_{\boldsymbol{k}},\bar{\psi}_{\boldsymbol{k}}]\, e^{iS} = G(0),\end{aligned} \tag{3.2}$$

$$S = \int dt \left[-H[\bar{\psi}_{\boldsymbol{k}},\psi_{\boldsymbol{k}},t] + \sum_{\boldsymbol{k}} \bar{\psi}_{\boldsymbol{k}} i\partial_t \psi_{\boldsymbol{k}}\right], \tag{3.3}$$

where the boundary conditions ψ_{in}, ψ_{out} depend on the initial and final states, via Trotter decomposition [44] as described in the next subsection. The numerator in the above ratio may then be calculated (up to the same phase factor) by taking functional derivatives of this object with a modified action:

$$\langle 0|U(\infty,t_n)O_n\ldots U(t_2,t_1)O_1U(t_1,-\infty)|0\rangle \propto \frac{\delta}{\delta i J_1(t_1)}\ldots\frac{\delta}{\delta i J_n(t_n)} G_J(0)\Big|_{J=0}, \tag{3.4}$$

$$G_J(0) = \int \mathcal{D}[\psi_{\boldsymbol{k},\text{out}}, \bar{\psi}_{\boldsymbol{k},\text{out}}, \psi_{\boldsymbol{k},\text{in}}, \bar{\psi}_{\boldsymbol{k},\text{in}}] \langle 0|\psi_{\boldsymbol{k},\text{out}}\rangle\langle\psi_{\boldsymbol{k},\text{in}}|0\rangle \int_{\psi_{\boldsymbol{k}}(-\infty)=\psi_{\boldsymbol{k},\text{in}}}^{\psi_{\boldsymbol{k}}(\infty)=\psi_{\boldsymbol{k},\text{out}}} \mathcal{D}[\psi_{\boldsymbol{k}}, \bar{\psi}_{\boldsymbol{k}}] e^{iS_J}, \tag{3.5}$$

$$S_J = S + \int dt \sum_{\boldsymbol{k}} \sum_{i=1}^{n} J_i(t) O_i(\bar{\psi}_{\boldsymbol{k}}, \psi_{\boldsymbol{k}}). \tag{3.6}$$

The fundamental difference of this approach with that taken in non-equilibrium QFT does not lie in how the coherent state path integral is constructed or how expectations are obtained via a generating function, so we will briefly review where the above expressions come from as a stepping stone in the next section. With these expressions in hand, two of the main constructions of non-equilibrium QFT, the Feynman-Vernon path integral and Keldysh partition function, will be easy to introduce and we shall briefly review some ways they may be used before applying them to our polariton problem. In other parts of this thesis, namely Parts Ib and II, the uses of these objects will be developed further as needed.

3.1.1 Field-Theoretic Coherent State Path Integral

We begin the construction of the above mentioned coherent path integral by writing the unitary time evolution operator in terms of the Hamiltonian via Dyson's formula:

$$U(T,-T) = \mathcal{T} e^{-i\int_{-T}^{T} dt\, H(t)}. \tag{3.7}$$

Splitting the time interval into a large number $N+1$ of segments so that $\epsilon = \frac{2T}{N+1}$ and $t_n = n\epsilon - T$, this expression may be approximately written as

$$U(T,-T) \approx \mathcal{T} \prod_{n=1}^{N+1} e^{-i\epsilon H(t_n)}. \tag{3.8}$$

At this point we introduce what are known as coherent states, which satisfy[1] (ψ is a scalar field while a, $a^\dagger$ are annihilation and creation operators, and $|0\rangle$ is the ground state of the non-interacting QFT)

$$|\psi_{\boldsymbol{k}}\rangle = e^{\sum_k \left[\psi_k a_k^\dagger - \frac{1}{2}|\psi_k|^2\right]}|0\rangle, \tag{3.9}$$

$$a_{\boldsymbol{k}'}|\psi_{\boldsymbol{k}}\rangle = \psi_{\boldsymbol{k}'}|\psi_{\boldsymbol{k}}\rangle, \tag{3.10}$$

$$\langle\phi_{\boldsymbol{k}}|\psi_{\boldsymbol{k}}\rangle = e^{\sum_k \left[\bar{\phi}_k\psi_k - \frac{1}{2}(|\phi_k|^2+|\psi_k|^2)\right]}, \tag{3.11}$$

$$\int \mathcal{D}[\psi_{\boldsymbol{k}}, \bar{\psi}_{\boldsymbol{k}}] |\psi_{\boldsymbol{k}}\rangle\langle\psi_{\boldsymbol{k}}| = \int \prod_{\boldsymbol{k}} \frac{d\,\mathrm{Re}\,\psi_{\boldsymbol{k}}\, d\,\mathrm{Im}\,\psi_{\boldsymbol{k}}}{\pi} |\psi_{\boldsymbol{k}}\rangle\langle\psi_{\boldsymbol{k}}| = I. \tag{3.12}$$

[1] The states being described here are the field-theoretic generalisations of what are typically known as coherent states. The conventional coherent states will play a major role in Part II of this thesis when we consider this construction in the quantum mechanical context.

Inserting the last expression N times into (3.8) and placing the result between two states $\langle\psi_{\boldsymbol{k},\text{out}}| = \langle\psi_{\boldsymbol{k},N+1}|$, $|\psi_{\boldsymbol{k},\text{in}}\rangle = |\psi_{\boldsymbol{k},0}\rangle$, we find

$$\langle\psi_{\boldsymbol{k},\text{out}}|U(T,-T)|\psi_{\boldsymbol{k},\text{in}}\rangle \approx \int \prod_{i=1}^{N} \mathcal{D}[\psi_{\boldsymbol{k},i}, \bar{\psi}_{\boldsymbol{k},i}] \prod_{j=1}^{N+1} \langle\psi_{\boldsymbol{k},j}|e^{-i\epsilon H(t_j)}|\psi_{\boldsymbol{k},j-1}\rangle. \tag{3.13}$$

If the Hamiltonian is normal-ordered, the terms $\langle\psi_{\boldsymbol{k},j}|e^{-i\epsilon H[a^\dagger_{\boldsymbol{k}},a_{\boldsymbol{k}},t_j]}|\psi_{\boldsymbol{k},j-1}\rangle$ may be approximated as (up to terms of order $O(\epsilon^2)$)

$$\begin{aligned}
\langle\psi_{\boldsymbol{k},j}|e^{-i\epsilon H[a^\dagger_{\boldsymbol{k}},a_{\boldsymbol{k}},t_j]}|\psi_{\boldsymbol{k},j-1}\rangle &\approx \langle\psi_{\boldsymbol{k},j}|1 - i\epsilon H[a^\dagger_{\boldsymbol{k}}, a_{\boldsymbol{k}}, t_j]|\psi_{\boldsymbol{k},j-1}\rangle \\
&= \langle\psi_{\boldsymbol{k},j}|\psi_{\boldsymbol{k},j-1}\rangle(1 - i\epsilon H[\bar{\psi}_{\boldsymbol{k},j}, \psi_{\boldsymbol{k},j-1}, t_j]) \\
&\approx e^{-i\epsilon H[\bar{\psi}_{\boldsymbol{k},j},\psi_{\boldsymbol{k},j-1},t_j]+\sum_{\boldsymbol{k}}\left[\bar{\psi}_{\boldsymbol{k},j}\psi_{\boldsymbol{k},j-1}-\frac{1}{2}(|\psi_{\boldsymbol{k},j}|^2+|\psi_{\boldsymbol{k},j-1}|^2)\right]} \\
&= e^{-i\epsilon H[\bar{\psi}_{\boldsymbol{k},j},\psi_{\boldsymbol{k},j-1},t_j]-\frac{\epsilon}{2}\sum_{\boldsymbol{k}}\left[\bar{\psi}_{\boldsymbol{k},j}\frac{\psi_{\boldsymbol{k},j}-\psi_{\boldsymbol{k},j-1}}{\epsilon}-\psi_{\boldsymbol{k},j-1}\frac{\bar{\psi}_{\boldsymbol{k},j}-\bar{\psi}_{\boldsymbol{k},j-1}}{\epsilon}\right]}
\end{aligned} \tag{3.14}$$

where we have written $H[a^\dagger_{\boldsymbol{k}}, a_{\boldsymbol{k}}, t]$ to show that it is a functional of the operators. Putting this expression back into (3.13), we then take $N \to \infty$. Interpreting terms of the form $\frac{\psi_j-\psi_{j-1}}{\epsilon}$ as $\partial_t\psi$ and identifying $H[\bar{\psi}_{\boldsymbol{k},j}, \psi_{\boldsymbol{k},j-1}, t_j] \approx H[\bar{\psi}_{\boldsymbol{k},j}, \psi_{\boldsymbol{k},j}, t_j]$ when $\epsilon \to 0$, we finally obtain (the functional integration measure is now over the field at all continuous moments in time, and the fields are implicitly indexed by time)

$$\langle\psi_{\boldsymbol{k},\text{out}}|U(T,-T)|\psi_{\boldsymbol{k},\text{in}}\rangle \approx \int \mathcal{D}[\psi_{\boldsymbol{k}}, \bar{\psi}_{\boldsymbol{k}}]\, e^{i\int dt\left[-H[\bar{\psi}_{\boldsymbol{k}},\psi_{\boldsymbol{k}},t]+\frac{1}{2}\sum_{\boldsymbol{k}}(\bar{\psi}_{\boldsymbol{k}}i\partial_t\psi_{\boldsymbol{k}}-\psi_{\boldsymbol{k}}i\partial_t\bar{\psi}_{\boldsymbol{k}})\right]}. \tag{3.15}$$

An integration by parts reduces this to

$$\langle\psi_{\boldsymbol{k},\text{out}}|U(T,-T)|\psi_{\boldsymbol{k},\text{in}}\rangle \approx \int \mathcal{D}[\psi_{\boldsymbol{k}}, \bar{\psi}_{\boldsymbol{k}}]\, e^{i\int dt\left[-H[\bar{\psi}_{\boldsymbol{k}},\psi_{\boldsymbol{k}},t]+\sum_{\boldsymbol{k}}\bar{\psi}_{\boldsymbol{k}}i\partial_t\psi_{\boldsymbol{k}}\right]}, \tag{3.16}$$

and noting that

$$\begin{aligned}
\langle 0|U(\infty,-\infty)|0\rangle = \int \mathcal{D}[\psi_{\boldsymbol{k},\text{out}}, \bar{\psi}_{\boldsymbol{k},\text{out}}, \psi_{\boldsymbol{k},\text{in}}, \bar{\psi}_{\boldsymbol{k},\text{in}}]\langle 0|\psi_{\boldsymbol{k},\text{out}}\rangle\langle\psi_{\boldsymbol{k},\text{in}}|0\rangle, \\
\times\langle\psi_{\boldsymbol{k},\text{out}}|U(T,-T)|\psi_{\boldsymbol{k},\text{in}}\rangle,
\end{aligned} \tag{3.17}$$

we recover (3.2). From here it is a short step to (3.4): one sees that, by considering the Hamiltonian

$$H_J(t) = H(t) - \sum_{i=1}^{n} J_i(t)O_i(a^\dagger, a), \tag{3.18}$$

the above construction will yield the action S_J of (3.6). At the same time in the operator picture it is evident that

$$\begin{aligned}\langle 0|U(\infty,t_n)O_n\dots U(t_2,t_1)O_1U(t_1,-\infty)|0\rangle \\ \propto \frac{\delta}{\delta i J_1(t_1)}\dots\frac{\delta}{\delta i J_n(t_n)}\langle 0|\mathcal{T}e^{-i\int_{-T}^{T}dt\,H_J(t)}|0\rangle\Big|_{J=0}.\end{aligned} \tag{3.19}$$

Substituting (3.17) and (3.16) into this expression, we recover (3.4).

3.1.2 The Feynman-Vernon Path Integral and Keldysh Contour

Non-equilibrium theory field theory, like the zero temperature one described above, is often used to calculate certain time-ordered operator expectations. The ordering employed differs, however, from the simpler zero temperature one because the time evolution of a density matrix is more complicated than that of a pure state.

Naively, we may view an expression like

$$\langle 0|U(\infty,t_n)O_n\dots U(t_2,t_1)O_1U(t_1,-\infty)|0\rangle \tag{3.20}$$

as the pure state on the right hand side evolving forwards in time 'to the left', and the operator time ordering $t_1 \leq t_2 \leq \dots \leq t_n$ is dictated by the order in which this time-evolving state temporally reaches each operator.

Considering an analogous expression for the expectation

$$\langle O_1^-(t_1^-)\dots O_m^-(t_m^-)O_n^+(t_n^+)\dots O_1^+(t_1^+)\rangle_{\rho_{-\infty}} \tag{3.21}$$

of a product of operators $O^+_{1\dots n}$, $O^-_{1\dots m}$ with an initial density matrix $\rho_{-\infty}$ and using the cyclicity of the trace to place all operators with a $-$ superscript to the right of the density matrix,

$$\mathrm{Tr}\left[O_n^+U(t_n^+,t_{n-1}^+)\dots O_1^+U(t_1^+,-\infty)\rho_{-\infty}U(-\infty,t_1^-)O_1^-\dots U(t_{m-1}^-,t_m^-)O_m^-\right] \tag{3.22}$$

or, in the Heisenberg picture,

$$\mathrm{Tr}\left[O_n^+(t_n^+)\dots O_1^+(t_1^+)\rho_{-\infty}O_1^-(t_1^-)\dots O_m^-(t_m^-)\right], \tag{3.23}$$

we see that a natural ordering in this case is $t_1^+ \leq t_2^+ \leq \dots \leq t_n^+$ and $t_1^- \leq t_2^- \leq \dots \leq t_n^-$. This 'causal' ordering proves to be the relevant one for most physically observable temporal correlation functions [45].

This ordering is sometimes visualized as a time contour (the "Keldysh contour") consisting of two parts. The first, the "forward contour", runs from $t = -\infty$ to $t = \infty$ while the second, the "backward contour", then runs back from $t = \infty$ to

$t = -\infty$. It is then stated that the operators $O^+_{1\ldots n}$ lie on the forward contour while the operators $O^-_{1\ldots m}$ lie on the backward contour.

The origin of this terminology may be seen by rearranging

$$\mathrm{Tr}\left[O^+_n(t^+_n)\ldots O^+_1(t^+_1)\rho_{-\infty}O^-_1(t^-_1)\ldots O^-_m(t^-_m)\right] \tag{3.24}$$

as

$$\mathrm{Tr}\left[O^-_1(t^-_1)\ldots O^-_m(t^-_m)O^+_n(t^+_n)\ldots O^+_1(t^+_1)\rho_{-\infty}\right]. \tag{3.25}$$

Supposing that the causal ordering holds, we see that this may also be viewed as an ordering along this total contour: starting from the density matrix and going from right to left, the operators $O^+_{1\ldots n}$ always come before $O^-_{1\ldots m}$ since the forward contour comes before the backwards one, and operators on the backwards contour appear in reverse order to the numerical values of their times as this part of the contour runs backwards.

The Keldysh contour picture is frequently referenced in the literature and its power will be seen momentarily when we consider Green's functions. It bears remembering, however, that it does not have a real physical meaning. What is happening is not forwards then backwards evolution in time of a pure state but rather a forward evolution of a density matrix. The physical meaning of O^+ is thus not of an operator existing on a forward-evolving time contour but rather an operator corresponding to one of the Hilbert spaces (the left one) comprising the product Hilbert space in which the density matrix lies. Similarly, O^- corresponds to the degrees of freedom of the right Hilbert space.

Rewriting the density matrix using the Glauber–Sudarshan P representation [46] as

$$\rho_{-\infty} = \int \mathcal{D}[\psi_{\boldsymbol{k},\mathrm{in}}, \bar{\psi}_{\boldsymbol{k},\mathrm{in}}]\,|\psi_{\boldsymbol{k},\mathrm{in}}\rangle P_{-\infty}[\psi_{\boldsymbol{k},\mathrm{in}}]\langle\psi_{\boldsymbol{k},\mathrm{in}}|, \tag{3.26}$$

and using the cyclicity of the trace, the object may be rewritten as

$$\begin{aligned}\int \mathcal{D}[\psi_{\boldsymbol{k},\mathrm{out}}, \bar{\psi}_{\boldsymbol{k},\mathrm{out}}, \psi_{\boldsymbol{k},\mathrm{in}}, \bar{\psi}_{\boldsymbol{k},\mathrm{in}}]\, P_{-\infty}[\psi_{\boldsymbol{k},\mathrm{in}}] \\ \times \langle\psi_{\boldsymbol{k},\mathrm{out}}|U(\infty, t^+_n)O^+_n U(t^+_n, t^+_{n-1})\ldots O^+_1 U(t^+_1, -\infty)|\psi_{\boldsymbol{k},\mathrm{in}}\rangle \\ \times \langle\psi_{\boldsymbol{k},\mathrm{in}}|U(-\infty, t^-_1)O^-_1 \ldots U(t^-_{m-1}, t^-_m)O^-_m U(t^-_m, \infty)|\psi_{\boldsymbol{k},\mathrm{out}}\rangle.\end{aligned} \tag{3.27}$$

We know from (3.4) how to represent the two non-density matrix objects in the integrand as functional integrals: because the ground state is here replaced by purely coherent in and out states, we may omit the leading integral in that ex-

pression to give

$$\langle \psi_{\boldsymbol{k},\mathrm{out}} | U(\infty, t_n^+) O_n^+ U(t_n^+, t_{n-1}^+) \dots O_1^+ U(t_1^+, -\infty) | \psi_{\boldsymbol{k},\mathrm{in}} \rangle \propto \frac{\delta}{\delta i J_1^+(t_1)} \cdots \frac{\delta}{\delta i J_n^+(t_n)} \int_{\substack{\psi_{\boldsymbol{k}}^+(-\infty) = \psi_{\boldsymbol{k},\mathrm{in}} \\ \psi_{\boldsymbol{k}}^+(\infty) = \psi_{\boldsymbol{k},\mathrm{out}}}} \mathcal{D}[\psi_{\boldsymbol{k}}^+, \bar{\psi}_{\boldsymbol{k}}^+] e^{iS_J^+} \Big|_{J=0}, \tag{3.28}$$

$$\langle \psi_{\boldsymbol{k},\mathrm{in}} | U(-\infty, t_1^-) O_1^- \dots U(t_{m-1}^-, t_m^-) O_m^- U(t_m^-, \infty) | \psi_{\boldsymbol{k},\mathrm{out}} \rangle \propto \overline{\left(\frac{\delta}{\delta i J_1^-(t_1)} \cdots \frac{\delta}{\delta i J_m^-(t_m)} \int_{\substack{\psi_{\boldsymbol{k}}^-(-\infty) = \psi_{\boldsymbol{k},\mathrm{in}} \\ \psi_{\boldsymbol{k}}^-(\infty) = \psi_{\boldsymbol{k},\mathrm{out}}}} \mathcal{D}[\psi_{\boldsymbol{k}}^-, \bar{\psi}_{\boldsymbol{k}}^-] e^{iS_J^-} \Big|_{J=0} \right)}, \tag{3.29}$$

$$S_J^+ = S[\bar{\psi}_{\boldsymbol{k}}^+, \psi_{\boldsymbol{k}}^+] + \int dt \sum_{\boldsymbol{k}} \sum_{i=1}^{n} J_i^+(t) O_i^+(\bar{\psi}_{\boldsymbol{k}}^+, \psi_{\boldsymbol{k}}^+), \tag{3.30}$$

$$S_J^- = S[\bar{\psi}_{\boldsymbol{k}}^-, \psi_{\boldsymbol{k}}^-] + \int dt \sum_{\boldsymbol{k}} \sum_{i=1}^{m} J_i^-(t) O_i^-(\bar{\psi}_{\boldsymbol{k}}^-, \psi_{\boldsymbol{k}}^-). \tag{3.31}$$

Here we have annotated the fields ψ^+, ψ^- in the functional integral to indicate whether they lie on the forward or backwards portion of the Keldysh contour. Using the form of the action in (3.16), we may use the above to rewrite (3.23) as

$$\begin{aligned} &\mathrm{Tr}\left[O_n^+(t_n^+) \dots O_1^+(t_1^+) \rho_{-\infty} O_1^-(t_1^-) \dots O_m^-(t_m^-)\right] \\ &\quad = \frac{\delta}{\delta i J_1^+(t_1)} \cdots \frac{\delta}{\delta i J_n^+(t_n)} \frac{\delta}{\delta i J_1^-(t_1)} \cdots \frac{\delta}{\delta i J_m^-(t_m)} \\ &\qquad \int \mathcal{D}[\psi_{\boldsymbol{k},\mathrm{out}}, \bar{\psi}_{\boldsymbol{k},\mathrm{out}}, \psi_{\boldsymbol{k},\mathrm{in}}, \bar{\psi}_{\boldsymbol{k},\mathrm{in}}] P_{-\infty}[\psi_{\boldsymbol{k},\mathrm{in}}] G_J^{+-}[\psi_{\boldsymbol{k},\mathrm{in}}, \psi_{\boldsymbol{k},\mathrm{out}}] \Big|_{J=0}, \end{aligned} \tag{3.32}$$

$$G_J^{+-}[\psi_{\boldsymbol{k},\mathrm{in}}, \psi_{\boldsymbol{k},\mathrm{out}}] = \int_{\substack{\psi_{\boldsymbol{k}}^+(-\infty) = \psi_{\boldsymbol{k},\mathrm{in}} \\ \psi_{\boldsymbol{k}}^-(-\infty) = \psi_{\boldsymbol{k},\mathrm{in}}}}^{\substack{\psi_{\boldsymbol{k}}^+(\infty) = \psi_{\boldsymbol{k},\mathrm{out}} \\ \psi_{\boldsymbol{k}}^-(\infty) = \psi_{\boldsymbol{k},\mathrm{out}}}} \mathcal{D}[\psi_{\boldsymbol{k}}^+, \bar{\psi}_{\boldsymbol{k}}^+, \psi_{\boldsymbol{k}}^-, \bar{\psi}_{\boldsymbol{k}}^-] e^{iS_J^{+-}}, \tag{3.33}$$

$$\begin{aligned} S_J^{+-} = &\int_{-\infty}^{\infty} dt \left[\sum_{\boldsymbol{k}} \bar{\psi}_{\boldsymbol{k}}^+ i \partial_t \psi_{\boldsymbol{k}}^+ - H[\bar{\psi}_{\boldsymbol{k}}^+, \psi_{\boldsymbol{k}}^+, t] \right] - \int_{-\infty}^{\infty} dt \left[\sum_{\boldsymbol{k}} \bar{\psi}_{\boldsymbol{k}}^- i \partial_t \psi_{\boldsymbol{k}}^- - H[\bar{\psi}_{\boldsymbol{k}}^-, \psi_{\boldsymbol{k}}^-, t] \right] \\ &+ \int_{-\infty}^{\infty} dt \sum_{\boldsymbol{k}} \sum_{i=1}^{n} J_i^+(t) O_i^+(\bar{\psi}_{\boldsymbol{k}}^+, \psi_{\boldsymbol{k}}^+) + \int_{-\infty}^{\infty} dt \sum_{\boldsymbol{k}} \sum_{i=1}^{m} J_i^-(t) O_i^-(\bar{\psi}_{\boldsymbol{k}}^-, \psi_{\boldsymbol{k}}^-). \end{aligned} \tag{3.34}$$

Finally, we may discard some of the initial conditions (as encoded in $P_{-\infty}$) and perform a change of variables. The former may be done because we shall be interested in an effective action for the evolution of a driven-dissipative sub-

system of this system. Such systems typically possess a unique steady state [47] independent of the initial conditions, and this is the state we will be calculating correlators in (since we have taken an infinite time interval). However, this must be done with care. The evolution will become driven-dissipative only after some bath is integrated out, and so initial conditions can be discarded only after this step — the initial conditions for the bath may contribute to a correct derivation of an effective action.

The latter is a variable change known as the Keldysh rotation, and allows for the easy calculation of the system's retarded, advanced, and kinetic Green's functions. The transformation is unitary (hence the name "rotation"):

$$\begin{pmatrix}\psi^c\\ \psi^q\end{pmatrix}=\begin{pmatrix}\frac{1}{\sqrt{2}} & \frac{1}{\sqrt{2}}\\ \frac{1}{\sqrt{2}} & -\frac{1}{\sqrt{2}}\end{pmatrix}\begin{pmatrix}\psi^+\\ \psi^-\end{pmatrix}, \tag{3.35}$$

and it may be shown that in these new variables [48]

$$iG_R(\boldsymbol{k},t-t')=\langle\psi^c(\boldsymbol{k},t)\bar{\psi}^q(\boldsymbol{k},t')\rangle, \tag{3.36}$$
$$iG_A(\boldsymbol{k},t-t')=\langle\bar{\psi}^c(\boldsymbol{k},t)\psi^q(\boldsymbol{k},t')\rangle, \tag{3.37}$$
$$iG_K(\boldsymbol{k},t-t')=\langle\psi^c(\boldsymbol{k},t)\bar{\psi}^c(\boldsymbol{k},t')\rangle, \tag{3.38}$$
$$0=\langle\psi^q(\boldsymbol{k},t)\bar{\psi}^q(\boldsymbol{k},t')\rangle. \tag{3.39}$$

That this is the case is precisely because of the forwards-backwards contour structure we have discussed above. Consider, for instance, $\langle\psi^c(\boldsymbol{k},t)\bar{\psi}^q(\boldsymbol{k},t')\rangle$. Writing this in terms of the ψ^+ and ψ^- fields, we find

$$\begin{aligned}\langle\psi^c(\boldsymbol{k},t)\bar{\psi}^q(\boldsymbol{k},t')\rangle=\frac{1}{2}\langle&\psi^+(\boldsymbol{k},t)\bar{\psi}^+(\boldsymbol{k},t')-\psi^+(\boldsymbol{k},t)\bar{\psi}^-(\boldsymbol{k},t')\\&+\psi^-(\boldsymbol{k},t)\bar{\psi}^+(\boldsymbol{k},t')-\psi^-(\boldsymbol{k},t)\bar{\psi}^-(\boldsymbol{k},t')\rangle.\end{aligned} \tag{3.40}$$

Recalling the operator ordering along the Keldysh contour, in terms of operators this is equal to

$$\begin{cases}\frac{1}{2}\langle a_{\boldsymbol{k}}(t)a^\dagger_{\boldsymbol{k}}(t')-a^\dagger_{\boldsymbol{k}}(t')a_{\boldsymbol{k}}(t)+a_{\boldsymbol{k}}(t)a^\dagger_{\boldsymbol{k}}(t')-a^\dagger_{\boldsymbol{k}}(t')a_{\boldsymbol{k}}(t)\rangle=\langle[a_{\boldsymbol{k}}(t),a^\dagger_{\boldsymbol{k}}(t')]\rangle & \text{for } t>t',\\ \frac{1}{2}\langle a^\dagger_{\boldsymbol{k}}(t')a_{\boldsymbol{k}}(t)-a^\dagger_{\boldsymbol{k}}(t')a_{\boldsymbol{k}}(t)+a_{\boldsymbol{k}}(t)a^\dagger_{\boldsymbol{k}}(t')-a_{\boldsymbol{k}}(t)a^\dagger_{\boldsymbol{k}}(t')\rangle=0 & \text{for } t'>t.\end{cases} \tag{3.41}$$

Thus

$$\langle\psi^c(\boldsymbol{k},t)\bar{\psi}^q(\boldsymbol{k},t')\rangle=\theta(t-t')\langle[a_{\boldsymbol{k}}(t),a^\dagger_{\boldsymbol{k}}(t')]\rangle=iG^R(\boldsymbol{k},t-t'), \tag{3.42}$$

with analogous contour reasoning yielding the other Green's function expressions.

The fields ψ^c and ψ^q are known as the classical and quantum fields in Keldysh parlance. While their primary importance in this portion of the thesis will be

their utility for calculating the above Green's functions, it bears to explain their naming and some of their other properties as these will come up in Part Ib. This will hopefully also serve to show the connection between Keldysh theory and driven-dissipative Gross-Pitaevskii equations for those readers more familiar with the latter.

The typical structure of a bosonic Keldysh action is

$$\frac{1}{\hbar}\int dt d^d x \Big[\bar{\psi}^q \cdot \mathrm{CGPE}[\psi^c] + \psi^q \cdot \overline{\mathrm{CGPE}[\psi^c]} + K[\psi^c]|\psi^q|^2 + O(|\psi^q|^3)\Big] \tag{3.43}$$

where we have temporarily re-inserted $\hbar$, CGPE stands for "Complex Gross-Pitaevskii Equation", and $K[\psi^c]$ relates to the dissipation in the problem (we will see how such a term arises upon integrating out the environment in the next section). If we rescale $\psi^q \to \hbar\psi^q$ and $K \to K/\hbar$ (the latter amounting to measuring the dissipation in units of energy [48]), we find the action to now be

$$\int dt d^d x \Big[\bar{\psi}^q \cdot \mathrm{CGPE}[\psi^c] + \psi^q \cdot \overline{\mathrm{CGPE}[\psi^c]} + K[\psi^c]|\psi^q|^2 + O(\hbar^3|\psi^q|^3)\Big]. \tag{3.44}$$

We thus see that in the $\hbar \to 0$ limit, all terms in ψ^q of order higher than quadratic vanish. This is one of the reasons ψ^q is referred to as the quantum field — it is not present beyond quadratic order in the classical limit. Of the remaining terms, if $K[\psi^c] = 0$, the functional integral over ψ^q yields functional Dirac delta functions (via the functional version of the identity $\int dx e^{ixy} = 2\pi\delta(y)$) strictly enforcing the CGPE for the classical field ψ^c. If the dissipative K term is not zero, it can be shown to convert the CGPE to a stochastic CGPE. This term thus introduces classical thermal/driven-dissipative effects into the problem [48].

This brings us to a second reason for the names of these fields. By the symmetry of the problem with respect to the forward and backward contours, it can be shown that $\langle\psi^+\rangle = \langle\psi^-\rangle$ and thus $\langle\psi^c\rangle = \sqrt{2}\langle\psi^+\rangle$, $\langle\psi^q\rangle = 0$. In this way, the classical field ψ^c is what captures the mean field of the problem (as we saw, it is the field that obeys the CGPE in the classical limit) while the quantum field is always zero in the mean field or classical limit.

3.2 Deriving the Action

We are now ready to apply this method to the Hamiltonian of coherently driven polaritons (2.11). Denoting the polariton and bath fields by ψ and b respectively, and grouping them via $\boldsymbol{\Psi} = (\psi^c, \psi^q)$, $\boldsymbol{B} = (b^c, b^q)$, we find the full action to be

$(\omega_b(\boldsymbol{p}) = \omega_A(\boldsymbol{p} + \boldsymbol{k}_p))$

$$
\begin{aligned}
&S[\boldsymbol{\Psi}, \boldsymbol{B}] \\
&= \int dt \Big[\sum_{\mathbf{k}} \bar{\boldsymbol{\Psi}}(t,\mathbf{k})(i\partial_t + \omega_p - \omega_{LP}(\mathbf{k}+\mathbf{k}_p))\sigma_1 \boldsymbol{\Psi}(t,\mathbf{k}) \\
&\qquad - \sqrt{2}F_p(\bar{\psi}^q(t,\mathbf{0}) + \psi^q(t,\mathbf{0})) \\
&\qquad + \sum_{\mathbf{p}} \bar{\boldsymbol{B}}(t,\mathbf{p})(i\partial_t - \omega_b(\mathbf{p}))\sigma_1 \boldsymbol{B}(t,\mathbf{p}) \\
&\qquad - \sum_{\mathbf{k},\mathbf{p}} \zeta_{\mathbf{k},\mathbf{p}} \Big(\bar{\boldsymbol{B}}(t,\mathbf{p})\sigma_1 \boldsymbol{\Psi}(t,\mathbf{k}) e^{-i\omega_p t} \\
&\qquad\qquad + e^{i\omega_p t} \bar{\boldsymbol{\Psi}}(t,\mathbf{k})\sigma_1 \boldsymbol{B}(t,\mathbf{p}) \Big) \\
&\qquad - \sum_{\mathbf{k},\mathbf{k}',\mathbf{q}} \frac{V}{2} \Big(\boldsymbol{\Psi}^T(t,\mathbf{k})\boldsymbol{\Psi}(t,\mathbf{k}') \\
&\qquad\qquad \bar{\psi}^c(t,\mathbf{k}-\mathbf{q})\bar{\psi}^q(t,\mathbf{k}'+\mathbf{q}) + \text{h.c.} \Big) \Big],
\end{aligned}
\tag{3.45}
$$

where σ_i denote the corresponding Pauli matrices acting on the c, q field indices and h.c. stands for Hermitian conjugate. We may split off the part of this action containing the bath fields,

$$
\begin{aligned}
&S_{\text{bath}}[\boldsymbol{\Psi}, \boldsymbol{B}] \\
&\quad = \int dt \Big[\sum_{\mathbf{p}} \bar{\boldsymbol{B}}(t,\mathbf{p})(i\partial_t - \omega_b(\mathbf{p}))\sigma_1 \boldsymbol{B}(t,\mathbf{p}) \\
&\qquad - \sum_{\mathbf{k},\mathbf{p}} \zeta_{\mathbf{k},\mathbf{p}} \Big(\bar{\boldsymbol{B}}(t,\mathbf{p})\sigma_1 \boldsymbol{\Psi}(t,\mathbf{k}) e^{-i\omega_p t} \\
&\qquad\qquad + e^{i\omega_p t} \bar{\boldsymbol{\Psi}}(t,\mathbf{k})\sigma_1 \boldsymbol{B}(t,\mathbf{p}) \Big) \Big],
\end{aligned}
\tag{3.46}
$$

and note that this term is quadratic in them. Performing the corresponding Gaussian integral yields

$$
\begin{aligned}
S_{\text{bath}}[\boldsymbol{\Psi}] = -\int dt dt' \sum_{\mathbf{k},\mathbf{k}',\mathbf{p}} &\bar{\boldsymbol{\Psi}}(t,\mathbf{k})\sigma_1 \zeta_{\mathbf{k},\mathbf{p}} \zeta_{\mathbf{k}',\mathbf{p}} \\
&e^{i\omega_p t} G_b(t-t',\boldsymbol{p}) e^{-i\omega_p t'} \sigma_1 \boldsymbol{\Psi}(t',\mathbf{k}').
\end{aligned}
\tag{3.47}
$$

where $G_b(t-t',\boldsymbol{p}) = \delta(t-t')[(i\partial_{t'} - \omega_b(\mathbf{p}))\sigma_1]^{-1}$. At this stage, we must recall that the initial combined density matrix of the system and reservoir also makes a contribution to the functional integral; the combined system is non-dissipative so there is no unique steady state that would allow us to discard the initial conditions.

The first assumption we will make is that the system begins in a tensor product state of the form

$$\rho_{\text{system}} \otimes \rho_{\text{bath}}.$$

This may be naturally achieved by supposing that we consider the combined sys-

tem from the moment the system and bath first begin interacting[2]. From here, we concentrate on ρ_{bath} since we will eventually be able to disregard ρ_{system}. This is because it will be ρ_{system} evolving in the final driven-dissipative problem, at which point there will be a unique steady state allowing us to disregard the initial density matrix.

The initial bath density matrix enters the problem by amending the term we have written as

$$[(i\partial_t - \omega_b(\mathbf{p}))\sigma_1]^{-1}.$$

With the density matrix accounted for and performing a Fourier transform, $e^{i\omega_p t}G_b(t-t',\boldsymbol{p})e^{-i\omega_p t'}$ instead becomes [48]

$$\tilde{G}_b(\omega+\omega_p,\boldsymbol{p}) = \begin{pmatrix} -2\pi i F(\omega+\omega_p)\delta(\omega+\omega_p-\omega_b) & \frac{1}{\omega+\omega_p-\omega_b(\boldsymbol{p})+i\epsilon} \\ \frac{1}{\omega+\omega_p-\omega_b(\boldsymbol{p})-i\epsilon} & 0 \end{pmatrix} \tag{3.48}$$

where $F(\omega)$ is the "distribution function" corresponding to the bath density matrix. We now seek to show that, for reasonable choices of this initial distribution, the interaction of the polaritons with the reservoir will be Markovian and the resulting action will be time-local.

We can simplify further by assuming the coupling between the bath and the system is independent of the polariton momentum, $\zeta_{\mathbf{k},\mathbf{p}}\zeta_{\mathbf{k}',\mathbf{p}} = \zeta_{\mathbf{p}}^2$, and by suggesting that, if the bath frequencies $\omega_b(\mathbf{p})$ form a dense spectrum and the coupling constants $\zeta_{\mathbf{p}} = \zeta(\omega_b)$ are smooth functions of these, we can replace the sum over bath modes with the integral

$$\sum_{\mathbf{p}} \zeta_{\mathbf{p}}^2 \to \int_0^{\omega_b(k_{\max})} d\omega_b\, \zeta(\omega_b)^2 N(\omega_b), \tag{3.49}$$

where $N(\omega_b)$ is the bath density of states. The action then becomes

$$S_{\text{bath}}[\boldsymbol{\Psi}] = -\int d\omega \sum_{\mathbf{k}} \bar{\boldsymbol{\Psi}}(\omega,\mathbf{k}) \begin{pmatrix} 0 & d^A(\omega) \\ d^R(\omega) & d^K(\omega) \end{pmatrix} \boldsymbol{\Psi}(\omega,\mathbf{k}), \tag{3.50}$$

[2]While this is a common assumption in the theory of open quantum systems and makes subsequent calculations simple, it can reasonably be criticized for being unphysical [49]. Observing, however, that its purpose in our argument is to enable the use of free particle correlators for the reservoir, it may be relaxed to the following more physical one: the reservoir is initially in a thermal state and so large that coupling to the much smaller microcavity does not meaningfully affect its properties. In this case the initial state can be viewed as approximately separable for our purposes [35].

with $d^A(\omega)$, $d^R(\omega)$, and $d^K(\omega)$ obtained via the Sokhotski–Plemelj theorem as

$$d^{R/A}(\omega) = \mathcal{P}\int_0^{\omega_b(k_{\max})} d\omega_b \, \frac{\zeta(\omega_b)^2 N(\omega_b)}{\omega + \omega_p - \omega_b} \mp i\pi\zeta(\omega+\omega_p)^2 N(\omega+\omega_p), \tag{3.51}$$

$$d^K(\omega) = -2\pi i F(\omega+\omega_p)\zeta(\omega+\omega_p)^2 N(\omega+\omega_p). \tag{3.52}$$

In order for the final action to be time-local or "Markovian", the bath must appear to be frequency-independent to the system. To this end, recall that the system's spectrum (that of the interacting lower polaritons) acts like the continuum analogue of the natural frequency of an oscillator — the bath will interact with the system preferentially at these frequencies [48].

Due to our gauge transformation, the spectrum of the interacting polaritons is $\omega_{LP}(\mathbf{k}+\mathbf{k}_p) - \omega_p$. This has also, however, shifted F, ζ, and N in the d functions (3.51, 3.52) via $\omega \to \omega + \omega_p$. Thus we may consider the variation of $N(\omega_{LP}(\mathbf{k}))$, $N(\omega_{LP}(\mathbf{k}))$, and $N(\omega_{LP}(\mathbf{k}))$ over the range of the lower polariton spectrum, assuming that $\mathbf{k}_p$ is negligible relative to our momentum cut-off and that the interacting spectrum has roughly the same range as the bare spectrum (this is true in our weakly interacting case).

For exciton-polaritons, the bottom of the bare spectrum (and ω_p, since we pump resonantly) is typically on the order of 1.5 eV [9] and the spectrum is bounded above by the exciton spectrum, the bottom of which is ~ 10 meV higher. With exciton masses typically being between $0.1m_e$ and $1m_e$, where m_e is the electron mass, we may crudely estimate the variation of the exciton spectrum up to the momentum cut-off of $\frac{h}{100\,\text{Å}}$ as

$$\frac{1}{0.2m_e}\left(\frac{h}{100\,\text{Å}}\right)^2 \approx 0.15\,\text{eV}. \tag{3.53}$$

Together with the ghost branch of the polariton spectrum, this gives an approximate range of variation of 1.5 ± 0.15 eV. We would thus like to argue that the variation of N, ζ, and F is negligible on it.

For a 3D photonic bath, the density of states $N(\omega)$ will be quadratic in ω, and a quick calculation shows that $N_{\max} \approx 1.5 N_{\min}$ on this range. Around the midpoint of these values, $N(\omega_p)$, the variation is on the order of 20% — for our purposes this sufficiently little variation to take this as constant.

We now turn to the frequency-dependence in the bath's distribution function F and decay coupling ζ. This is the point at which assumptions must be made about the initial density matrix. The most natural initial distribution for the bath would be thermal; it is a large reservoir which has equilibrated with its environment before coming into contact with the system. In this case the distribution

function is $F(\omega) = 2n_o(\omega) + 1$, where n_o is the occupation number of the given energy level. If the bath is in thermal equilibrium at an energy scale significantly lower than the range of variation of the polariton spectrum, then at all relevant energies the occupation number n_o will be identically zero and the distribution function will be $F(\omega) = 1$. At the same time, we may expect the decay of the high energy polaritons to not occur preferentially into any of the equally empty photonic modes and thus set $\zeta(\omega) = \zeta_{\text{const}}$. In this case, setting $\kappa = N(\omega_p)\zeta_{\text{const}}$ and $F(\omega) = 1$, we obtain from (3.51, 3.52)[3]:

$$d^{R/A}(\omega) = \mp i\kappa, \tag{3.54}$$

$$d^{K}(\omega) = -2i\kappa. \tag{3.55}$$

We see that stipulating such an initial distribution yields a fully Markovian bath. It remains to check that the thermal distribution is indeed lower energy than the polaritons. With an average thermal photon energy of kT, at room temperature (300 K) this energy is 25 meV, which is significantly lower than the smallest energy in the cut-off polariton spectrum (roughly 1.35 eV). Thus the distribution has negligible occupation at the relevant energy levels as required.

While we have discussed a thermal distribution above, it being a natural experimental distribution, our arguments carry over to any distribution which may be expressed in terms of occupation numbers and which has occupancy only at energies significantly below those of the polaritons.

In this Markovian approximation, the final form of the action is

$$\begin{aligned}\mathcal{S}_{\text{eff}} = \sum_k (\bar{\psi}^c_k \quad \bar{\psi}^q_k) \begin{pmatrix} 0 & g^{-1}(k) \\ (g^{-1})^*(k) & 2i\kappa \end{pmatrix} \begin{pmatrix} \psi^c_k \\ \psi^q_k \end{pmatrix} \\ - \frac{V}{2} \sum_{k,k',q} \left(\bar{\psi}^c_{k-q} \bar{\psi}^q_{k'+q} [\psi^c_k \psi^c_{k'} + \psi^q_k \psi^q_{k'}] + \text{h.c.} \right) - \sqrt{2} F_p (\bar{\psi}^q_0 + \psi^q_0),\end{aligned} \tag{3.56}$$

where $g^{-1}(k) = \omega + \Delta_p - \omega_{LP}(\mathbf{k} + \mathbf{k}_p) - i\kappa$ and h.c. stands for Hermitian conjugate. The perturbative diagrammatics associated with this action are worked out in Appendix A, and will be used extensively throughout the rest of Part Ia.

[3] In principle one could attempt to account for the Cauchy principal value term in (3.51), which will not be exactly zero and will introduce a real 'Lamb shift' [50] to (3.54). Since the numerator is almost constant in the vicinity of the pole, however, the principal value will be heavily suppressed relative to the coefficient of the same term already present in the Hamiltonian and thus may be neglected (the upper bound of the integral for a 3D photonic bath is $\sim 100\,\text{eV} \gg \omega_{\text{LP}}$ so the integral is essentially of an odd function in some symmetric neighbourhood of the pole).

Chapter 4

Previous Results Regarding Coherently Driven Polariton Superfluidity

This chapter summarizes previous results obtained with regards to superfluidity in coherently driven microcavity polaritons. In particular it covers attempts to apply the Landau criterion to this system indicating the presence of superfluid, and the contradictory results in this regard obtained in [40]. It also describes preliminary results obtained by the author of [40] with regards to the gapless regime of this system, which were subsequently published in [51].

The only results in this chapter due to me are the explanation of the structure of the current-current response tensor in terms of the Helmholtz decomposition, the diagrammatic approach to the derivation of this particular mean-field current-current response[1] and, indirectly, the arguments from Chap. 1 for why the Landau criterion is neither necessary nor sufficient for superfluidity in driven-dissipative systems. All non-Feynman diagrams in this chapter are due to Richard Juggins, author of [40].

4.1 Keldysh Effective Action

In the previous chapter we obtained the effective action (3.56) for the coherently driven polaritons in terms of two fields ψ^c, ψ^q. In the absence of the last term, $\sqrt{2}F_p(\bar{\psi}_0^q + \psi_0^q)$, the action possesses a global $U(1)$ symmetry $\psi_k^{c/q} \to \psi_k^{c/q} e^{i\theta}$. Such symmetry in condensed matter systems is often indicative of superfluidity [52] because, as discussed in Chap 1, its spontaneous breaking is a common mechanism by which superfluidity arises; Indeed, incoherently pumped systems, which

[1] Specifically, Fig. 4.2 and equations (4.39), (4.40), and (4.41) as a way to obtain (4.42) are due to me. this quantity was obtained in [40] but via a different method, while the diagrams involved for this general type of system are considered in [27], [31]

do posses this symmetry, can be shown to exhibit superfluidity [27]. The drive term, however, breaks the $U(1)$ symmetry, since the phase of the pump F_p is independent of that of the fields.

The mean-field equations for this action are found by functional differentiation to be

$$\begin{aligned}
\frac{d\mathcal{S}_{\text{eff}}}{d\bar{\psi}^c(k)} =&(\omega+\Delta_p-\epsilon(\mathbf{k})-i\kappa)\psi^q(k)\\
&-\frac{V}{2}\sum_{k',q}\Big(\bar{\psi}^q(k'+q)[\psi^c(k+q)\psi^c(k')+\psi^q(k+q)\psi^q(k')]\\
&\qquad+2\bar{\psi}^c(k'+q)\psi^q(k+q)\psi^c(k')\Big)=0,\\
\frac{d\mathcal{S}_{\text{eff}}}{d\psi^c(-k)} =&(-\omega+\Delta_p-\epsilon(-\mathbf{k})+i\kappa)\bar{\psi}^q(-k)\\
&-\frac{V}{2}\sum_{k',q}\Big(\psi^q(k'+q)[\bar{\psi}^c(-k+q)\bar{\psi}^c(k')+\bar{\psi}^q(-k+q)\bar{\psi}^q(k')]\\
&\qquad+2\psi^c(k'+q)\bar{\psi}^q(-k+q)\bar{\psi}^c(k')\Big)=0,\\
\frac{d\mathcal{S}_{\text{eff}}}{d\bar{\psi}^q(k)} =&(\omega+\Delta_p-\epsilon(\mathbf{k})+i\kappa)\psi^c(k\\
&-\frac{V}{2}\sum_{k',q}\Big(\bar{\psi}^c(k'+q)[\psi^c(k+q)\psi^c(k')+\psi^q(k+q)\psi^q(k')]\\
&\qquad+2\bar{\psi}^q(k'+q)\psi^q(k+q)\psi^c(k')\Big)+2i\kappa\psi^q(k)-\sqrt{2}F_p\delta_{k,0}=0,\\
\frac{d\mathcal{S}_{\text{eff}}}{d\psi^q(-k)} =&(-\omega+\Delta_p-\epsilon(-\mathbf{k})-i\kappa)\bar{\psi}^c(-k)\\
&-\frac{V}{2}\sum_{k',q}\Big(\psi^c(k'+q)[\bar{\psi}^c(-k+q)\bar{\psi}^c(k')+\bar{\psi}^q(-k+q)\bar{\psi}^q(k')]\\
&\qquad+2\psi^q(k'+q)\bar{\psi}^q(-k+q)\bar{\psi}^c(k')\Big)+2i\kappa\bar{\psi}^q(-k)-\sqrt{2}F_p\delta_{-k,0}=0.
\end{aligned}\tag{4.1}$$

Assuming the solution to be space-time homogeneous and classical ($\psi^c(k)=\sqrt{2}\psi_0\delta_{k,0}$, $\psi^q(k)=0$), the equations simplify to

$$(\Delta_p-\epsilon(\mathbf{0})+i\kappa)\psi_0-F_p=V|\psi_0|^2\psi_0, \tag{4.2}$$

$$(\Delta_p-\epsilon(\mathbf{0})-i\kappa)\bar{\psi}_0-F_p=V|\psi_0|^2\bar{\psi}_0. \tag{4.3}$$

Writing $\delta_p=\Delta_p-\epsilon(\mathbf{0})$ for the detuning and taking the squared modulus of the left and right hand sides of one of the above equations yields a cubic equation for the mean-field occupancy of the pump mode $n=|\psi_0|^2$:

$$V^2n^3-2\delta_pVn^2+(\delta_p^2+\kappa^2)n-F_p^2=0. \tag{4.4}$$

Depending on whether $\delta_p>\sqrt{3}\kappa$ or $\delta_p\leq\sqrt{3}\kappa$, the equation may or may not have

multiple (specifically, three) real solutions for certain values of F_p. The former case is referred to as the bistable regime and will be of primary interest to us in this paper.

For a particular value of ψ_0, the action may be rewritten via the background field method in terms of the fields $\psi^c(k) \to \psi^c(k) - \psi_0\delta_{k,0}$, $\psi^q(k) \to \psi^q(k)$. Up to second order in the fields this yields

$$\mathcal{S}_{\text{eff}} = \mathcal{S}_{\text{eff}}\Big|_{\psi=\psi_0} + \frac{1}{2}\sum_{k,k'} \mathbf{\Psi}^\dagger(k)\mathcal{D}^{-1}(k,k')\mathbf{\Psi}(k') + O(\psi^3), \tag{4.5}$$

where

$$\mathcal{D}^{-1}(k,k') = \begin{pmatrix} 0 & 0 & J^*(k) & -V\psi_0^2 \\ 0 & 0 & -V\bar{\psi}_0^2 & J(-k) \\ J(k) & -V\psi_0^2 & 2i\kappa & 0 \\ -V\bar{\psi}_0^2 & J^*(-k) & 0 & 2i\kappa \end{pmatrix}\delta_{k,k'} \tag{4.6}$$

and $J(k) = \omega + \Delta_p - \epsilon(\mathbf{k}) + i\kappa - 2V|\psi_0|^2$. Here we have written the action in terms of the Nambu vector $\mathbf{\Psi}(k) = (\psi^c(k), \bar{\psi}^c(-k), \psi^q(k), \bar{\psi}^q(-k))$, explained in Appendix A. Taking this into account, the bare propagators are given in terms of the block matrix

$$\begin{pmatrix} i\underline{\underline{G}}_K(k,k') & i\underline{\underline{G}}_R(k,k') \\ i\underline{\underline{G}}_A(k,k') & \underline{\underline{0}} \end{pmatrix} = \mathcal{D}(k,k'), \tag{4.7}$$

where the blocks are 2×2 matrices in Nambu space. Each block is named for its corresponding top left entry, so that the conventional Keldysh Green's functions are given by $G_{K/R/A}(k,k') = (\underline{\underline{G}}_{K/R/A}(k,k'))^{11}$. The exact expressions for these are given in Appendix A, and in the next section we will use them to study the system spectrum.

4.2 System Spectrum and the Landau Criterion

In Chap. 1 we discussed in some detail the Landau criterion for superfluidity in equilibrium, which comes down to the condition

$$\min_{\mathbf{p}}[\epsilon(\mathbf{p}) + \mathbf{v}\cdot\mathbf{p}] < 0, \tag{4.8}$$

where $\epsilon(\boldsymbol{p})$ is the excitation spectrum of a fluid in its rest frame, with the largest absolute value of fluid velocity $|\boldsymbol{v}|$ in a given direction for which this does not hold v_{crit} termed the critical velocity in that direction. In equilibrium non-dissipative flow characteristic of a superfluid occurs for velocities below this in said direction.

As we argued in the selfsame chapter, the Landau criterion is not rigorously applicable to driven-dissipative systems. It assumes a real excitation spectrum,

which in such systems is generally complex, and relies on a conservation of energy argument that may be violated by the external drive. Nevertheless, some works have presented results via a heuristic application of it to the real part of the complex spectrum of coherently driven exciton-polaritons in the bistable regime [7], [38], [39].

The excitation spectrum of the system may be obtained from the poles of the retarded Green's function [53], which is given by (see Appendix A):

$$G_R(k) = \frac{J^*(-k)}{J(k)J^*(-k) - V^2|\psi_0|^4}. \tag{4.9}$$

The spectrum $\omega(\mathbf{k})$ is thus given by the solution to

$$J(\omega(\mathbf{k}),\mathbf{k})J^*(-\omega(\mathbf{k}),-\mathbf{k}) - V^2|\psi_0|^4 = 0, \tag{4.10}$$

and is found to be

$$\begin{aligned}\omega^{\pm}(\mathbf{k}) =& \frac{\epsilon(\mathbf{k}) - \epsilon(-\mathbf{k})}{2} - i\kappa \\ &\pm \sqrt{\left(\frac{\epsilon(\mathbf{k}) + \epsilon(-\mathbf{k})}{2} - \Delta_p + 2V|\psi_0|^2\right)^2 - V^2|\psi_0|^4}.\end{aligned} \tag{4.11}$$

For $\mathbf{k}_p = 0$, $\mathrm{Re}\,\omega^+(\mathbf{k}) = -\mathrm{Re}\,\omega^-(\mathbf{k})$, $\mathrm{Im}\,\omega^+(\mathbf{k}) = \mathrm{Im}\,\omega^-(\mathbf{k})$, and the $\omega^-(\mathbf{k})$ negative energy branch corresponds to the same physical excitations as the positive energy one. It may thus be interpreted as the spectrum for "holes", and is sometimes referred to as the ghost branch.

For $\mathbf{k}_p \neq 0$, due to our resummation with respect to the pump momentum in (2.11), we may view the system's action as that for an isotropically pumped (and thus stationary) fluid of polaritons but with a tilted energy spectrum. While similar to a change of reference frame to one in which the polaritons are stationary, we emphasize that this is simply a formal manipulation of the action. Writing $\epsilon(\mathbf{k}) \approx \frac{(\mathbf{k}+\mathbf{k}_p)^2}{2m}$ where m is the effective polariton mass, to linear order one finds that

$$\omega^{\pm}(\mathbf{k}) = \omega^{\pm}(\mathbf{k})\Big|_{\mathbf{k}_p=0} + \frac{\mathbf{k}_p}{m}\cdot\mathbf{k} + O(|\mathbf{k}_p|^2), \tag{4.12}$$

which shows that the tilt is due to the bulk flow of the fluid (induced by the pump) with velocity $\mathbf{v} = \frac{\hbar\mathbf{k}_p}{m}$. From this point of view, superfluidity will be destroyed when the linear tilt becomes so significant as to push $\omega^{\pm}(\mathbf{k})$ for some non-zero k below the energy of the condensed mode $\omega^{\pm}(0)$ so that particles may scatter into this new mode. Comparing with (1.6), it is evident that this is equivalent to applying the Landau criterion to the real part of the spectrum without

this linear correction (here $\delta_p = \Delta_p - \epsilon(\mathbf{0})$):

$$\begin{aligned}&\operatorname{Re}\omega^{+}_{\text{rest}}(\mathbf{k})\\&\quad=\operatorname{Re}\sqrt{\left(\epsilon(\mathbf{k})|_{\mathbf{k}_p=0}-\delta_p+2V|\psi_0|^2\right)^2-V^2|\psi_0|^4}.\end{aligned}\tag{4.13}$$

Here three situations are possible. If $V|\psi_0|^2 < \delta_p$ then, for some value of $|\mathbf{k}_0| \neq 0$,

$$\epsilon(\mathbf{k}_0)|_{\mathbf{k}_p=0}-\delta_p+2V|\psi_0|^2=0\tag{4.14}$$

and $\operatorname{Re}\omega^{+}(\mathbf{k}_0)\Big|_{\mathbf{k}_p=0} = 0$, meaning the critical velocity is zero and there is no superfluid (per the Landau criterion). If $V|\psi_0|^2 > \delta_p$, then the spectrum is gapped and there is a positive critical velocity and associated superfluidity. This velocity is given by

$$V_{\text{crit}}=\sqrt{\frac{-\delta_p+2V|\psi_0|^2-\sqrt{(-\delta_p+2V|\psi_0|^2)^2-V^2|\psi_0|^4}}{m}}.\tag{4.15}$$

Finally, if $V|\psi_0|^2 = \delta_p$, then the real spectrum is gapless at $|\mathbf{k}| = 0$ and its gradient there (the polariton "sound velocity") must be considered. This derivative comes out as

$$V_{\text{crit}}=\frac{d\operatorname{Re}\omega^{+}_{\text{rest}}(|\mathbf{k}|)}{d|\mathbf{k}|}\Big|_{\mathbf{k}=0}=\sqrt{\frac{V|\psi_0|^2}{m}},\tag{4.16}$$

which agrees with the limit of the previous expression in δ_p.

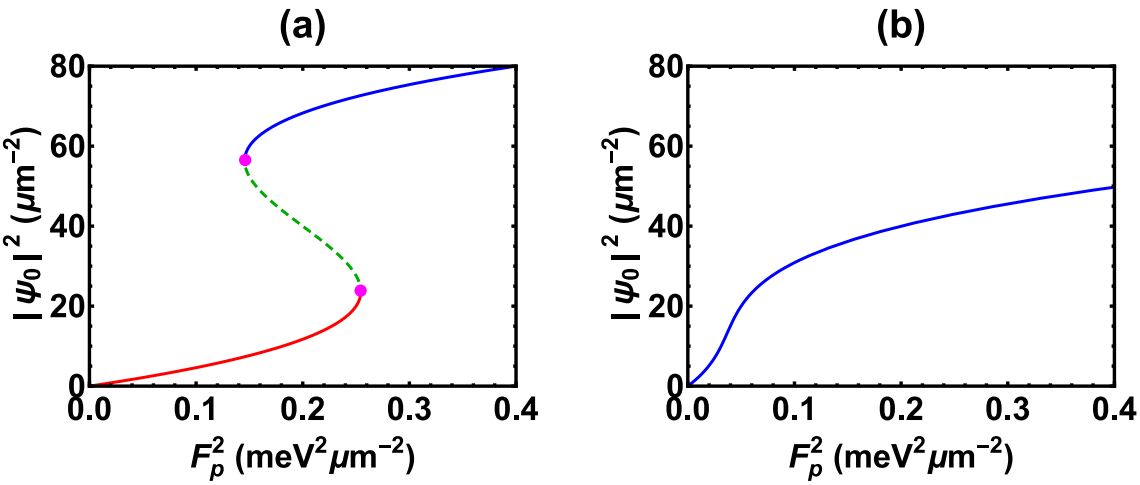

Figure 4.1: Absolute value squared of the homogeneous solution ψ_0 to the mean-field equations for varying values of the pump F_p. The left figure corresponds to the $\delta_p = 3\kappa > \sqrt{3}\kappa$ bistable regime with multivalued solutions and inversion points (marked by fuchsia dots), while the right corresponds to the monostable $\delta_p < \sqrt{3}\kappa$ regime with a single solution for each pump value.

This discussion can be specialised to the case of the bistable regime, where the mean field solution of Eq. (4.4) can be split into three branches (red, green, and blue in Fig. 4.1). These branches are separated by points called "inversion points", which correspond to

$$V|\psi_0|^2 = \frac{1}{3}\left(2\delta_p \pm \sqrt{\delta_p^2 - 3\kappa^2}\right). \tag{4.17}$$

We thus see that $V|\psi_0|^2 < \delta_p$ on the lower red branch, and so superfluidity cannot occur there per the Landau criterion. The middle green branch can be shown to be dynamically unstable since

$$\exists \mathbf{k} \,\text{s.t.}\, \text{Im}\ \omega^{\pm}(\mathbf{k}) > 0 \tag{4.18}$$

for every point on that branch (a simple proof of this is given in Section 5.1), and this is an indication of dynamical instability [53]. Thus, according to the Landau criterion, superfluidity is present on the upper blue branch for every point with $V|\psi_0|^2 \geq \delta_p$. As we are about to see, however, this conclusion is incorrect.

4.3 Current-Current Response and the Rigid State

4.3.1 Linear-Response Superfluid Criterion

The work on which this part of the thesis builds [33] opted to use the linear response-based criterion we introduced in Chap.1 as the correct generalisation of the definition of superfluid to non-equilibrium systems. The results, briefly outlined now, differ from the Landau criterion analysis and highlight its limitations in a driven-dissipative context.

For a system possessing a conserved current $j(\mathbf{x}, t)$, consider a Hamiltonian perturbation of the form

$$-\int d\mathbf{x} dt\, \mathbf{j}(\mathbf{x}, t) \cdot \mathbf{u}(\mathbf{x}, t) \tag{4.19}$$

where $\mathbf{u}(\mathbf{x}, t)$ is an external field. Considering the historical example of fluid in a capillary, this generalises the term $-m\int d\mathbf{x} dt\, \mathbf{j}(\mathbf{x}, t) \cdot \mathbf{u} = -\mathbf{P} \cdot \mathbf{u}$, which appears in the superfluid's rest frame Hamiltonian when the walls are moving with velocity $\mathbf{u}$ (recall the discussion of Chap.1). The Helmholtz decomposition of $\mathbf{u}(\mathbf{x}, t)$,

$$\mathbf{u}(\mathbf{x}, t) = \underbrace{-\nabla\Phi(\mathbf{x}, t)}_{\text{longitudinal}} + \underbrace{\nabla \times \mathbf{A}(\mathbf{x}, t)}_{\text{transverse}}, \tag{4.20}$$

consists of longitudinal and transverse components. Intuitively, the gradient term corresponds to some sort of push, while the curl term introduces shear. The generalisation of the classical superfluid's frictionless flow through a capillary is

the statement that its current does not respond to transverse perturbations, since friction with the walls is a shearing force.

To study this (linear) response, we require the current-current response tensor. By Kubo's formula, this is

$$\chi_{ij}(\mathbf{x}, t, \mathbf{x}', t') = i\theta(t - t')\langle[j_i(\mathbf{x}, t), j_j(\mathbf{x}', t')]\rangle. \tag{4.21}$$

In an isotropic, time and space translation-invariant system, the most general form the static ($\omega = 0$) Fourier transform of this quantity can take is

$$\chi_{ij}(\mathbf{k}) = \frac{\boldsymbol{k}_i \boldsymbol{k}_j}{|\boldsymbol{k}|^2}\chi_L(|\boldsymbol{k}|) + \left(\delta_{ij} - \frac{\boldsymbol{k}_i \boldsymbol{k}_j}{|\boldsymbol{k}|^2}\right)\chi_T(|\boldsymbol{k}|). \tag{4.22}$$

The subscripts indicate that the first term couples to the longitudinal component of the static Helmholtz decomposition, $-\mathbf{k}\Phi(\mathbf{k})$, while the second couples to the transverse component $\mathbf{k} \times \mathbf{A}(\mathbf{k})$. Using the special form of (4.22), we observe that the static limits of the normal and transverse components may be extracted by sequential limits. For example

$$\lim_{k_y \to 0} \lim_{k_x \to 0} \chi_{xx} = \lim_{k \to 0} \chi_T(k), \tag{4.23}$$

$$\lim_{k_x \to 0} \lim_{k_y \to 0} \chi_{xx} = \lim_{k \to 0} \chi_L(k). \tag{4.24}$$

These equations may be understood as special cases of equations (1.41) and (1.42) when $\boldsymbol{u}$ is constant, $|\boldsymbol{u}| = 1$, and $\boldsymbol{u}$ is oriented along the x-direction. While we will use this property later to perform explicit calculations, it is worth highlighting what it suggests about the response tensor. Namely, in order for a system to possess different transverse and longitudinal responses, the response tensor must be discontinuous at zero momentum.

Superfluidity is then defined in the thermodynamic limit as a difference between the static, homogeneous linear and transverse responses:

$$\lim_{k \to 0}(\chi_L(k) - \chi_T(k)) > 0 \implies \text{superfluid}. \tag{4.25}$$

4.3.2 Non-Equilibrium Current

The above definition relies on a conserved system current, but the situation is more complicated for driven-dissipative systems. For such systems, we are interested in the component of the current that is internal to the system as opposed to the component relating to pump and dissipation. This is known as the coherent current [54], and takes the familiar form

$$\mathbf{j}(\mathbf{x}, t) = \frac{1}{2mi}(\bar{\psi}\nabla\psi - \psi\nabla\bar{\psi}). \tag{4.26}$$

In [33], care is taken to normal-order this operator. Normal ordering, however, only affects the expectation of the operator up to a constant. Since we are interested in the linear response of this expectation the constant is irrelevant.

Suppose that we introduce a term of the form

$$-\int d\mathbf{x}dt\,\mathbf{j}(\mathbf{x},t)\cdot\mathbf{u}(\mathbf{x},t) \tag{4.27}$$

to the original Hamiltonian, where $\mathbf{u}$ is a classical field. Writing $\mathbf{j}^+$ for (4.26) written in terms of fields on the forward contour, and similarly $\mathbf{j}^-$ for the backward contour, this will give the following contribution to the overall Keldysh action:

$$\int d\mathbf{x}dt\Big(\mathbf{j}^+(\mathbf{x},t)\cdot\mathbf{u}^+(\mathbf{x},t)-\mathbf{j}^-(\mathbf{x},t)\cdot\mathbf{u}^-(\mathbf{x},t)\Big). \tag{4.28}$$

We may now define, by analogy with the classical and quantum fields, the classical and quantum current operators $\mathbf{j}^c$, $\mathbf{j}^q$ as[2]

$$\mathbf{j}^c=\frac{1}{2}(\mathbf{j}^++\mathbf{j}^-), \tag{4.29}$$

$$\mathbf{j}^q=(\mathbf{j}^+-\mathbf{j}^-). \tag{4.30}$$

Also introducing the "physical" field $\mathbf{f}=\frac{1}{2}(\mathbf{u}^++\mathbf{u}^-)$ and the "unphysical" field $\boldsymbol{\theta}=\mathbf{u}^+-\mathbf{u}^-$, the significance of which will be explained shortly, we may rewrite (4.28) as

$$\int d\mathbf{x}dt\Big(\mathbf{j}^c(\mathbf{x},t)\cdot\boldsymbol{\theta}(\mathbf{x},t)+\mathbf{j}^q(\mathbf{x},t)\cdot\mathbf{f}(\mathbf{x},t)\Big). \tag{4.31}$$

Since the classical field is the same on both contours, $\mathbf{u}^+=\mathbf{u}^-$, we have that the unphysical field $\boldsymbol{\theta}=0$ which motivates its name. On the other hand the physical field is equal to the original field $\mathbf{f}=\mathbf{u}$. The perturbation to the Keldysh action thus takes the form

$$\int d\mathbf{x}dt\,\mathbf{j}^q(\mathbf{x},t)\cdot\mathbf{f}(\mathbf{x},t), \tag{4.32}$$

from which one can see that the first perturbative correction to the expectation of the classical current will be

$$\int d\mathbf{x}'dt'\,i\langle\mathbf{j}^c(\mathbf{x},t)\mathbf{j}^q(\mathbf{x}',t')\rangle\cdot\mathbf{f}(\mathbf{x}',t'). \tag{4.33}$$

Since, up to normal ordering, the expectation value of the classical current is equal to the expectation value of the true current, this shows that the response

[2]The choice of factors $\frac{1}{2}$ and 1 here, contrary to the symmetric choice of $\frac{1}{\sqrt{2}}$ for both classical and quantum fields, ensures that the expectation of the classical current is equal to that of the physical current. This is convenient, since the physical current is the primary observable of interest throughout this part of the thesis.

function we seek is given by

$$\chi_{ij}(\mathbf{x},t,\mathbf{x}',t') = i\langle j_i^c(\mathbf{x},t) j_j^q(\mathbf{x}',t')\rangle, \tag{4.34}$$

and we may view the response we seek as the response of the classical current to the physical field. This result is derived in an alternative way in [54].

In terms of Fourier-transformed fields, (4.32) is

$$\sum_k \mathbf{j}^q(-k)\cdot\mathbf{f}(\mathbf{k}) \tag{4.35}$$

so that the static response in terms of these fields becomes

$$\chi_{ij}(0,\mathbf{q}) = \chi_{ij}(\mathbf{q}) = i\langle j_i^c(0,\mathbf{q}) j_j^q(0,-\mathbf{q})\rangle, \tag{4.36}$$

while the static classical and quantum currents are given by

$$j_i^c(0,\mathbf{q}) = j_i^c(\mathbf{q}) = \frac{1}{2}\sum_{\omega,\mathbf{k}} \gamma_i(2\mathbf{k}+\mathbf{q})[\psi^c(\omega,\mathbf{k}+\mathbf{q})\bar{\psi}^c(\omega,\mathbf{k}) + \psi^q(\omega,\mathbf{k}+\mathbf{q})\bar{\psi}^q(\omega,\mathbf{k})], \tag{4.37}$$

$$j_i^q(0,\mathbf{q}) = j_i^q(\mathbf{q}) = \sum_{\omega,\mathbf{k}} \gamma_i(2\mathbf{k}+\mathbf{q})[\psi^c(\omega,\mathbf{k}+\mathbf{q})\bar{\psi}^q(\omega,\mathbf{k}) + \psi^q(\omega,\mathbf{k}+\mathbf{q})\bar{\psi}^c(\omega,\mathbf{k})], \tag{4.38}$$

where $\gamma(\mathbf{q}) = \frac{\mathbf{q}+\mathbf{k}_p}{2m}$.

4.3.3 The Rigid State

The response tensor may be worked out perturbatively using the diagrammatics of Appendix A. At order $O(\hbar)$ there are six diagrams, presented in Fig. 4.2.

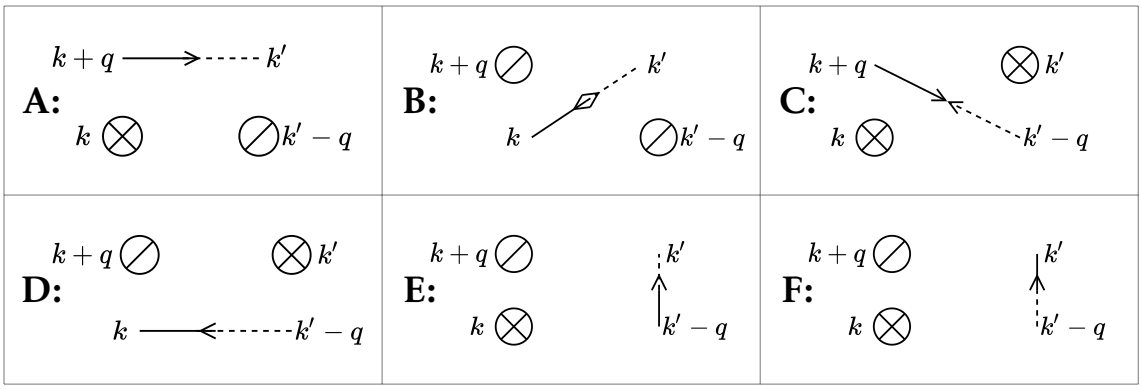

Figure 4.2: Order $O(\hbar)$ diagrams for the current-current response. Circles with a line through them represent the condensate ψ_0 while those with a cross represent $\bar{\psi}_0$. Solid lines with the arrow at their end oriented towards a momentum p represent ψ_p^c, while those with an arrow pointing away from it represent $\bar{\psi}_p^c$. Analogously, such dashed lines represent ψ_p^q and $\bar{\psi}_p^q$. Two such lines, when connected, represent the Green's function equal to the expectation of the product of the associated fields.

Placing one current operator on the left of the diagram and one on the right, the first four of these represent

$$\begin{aligned} &-|\psi_0|^2 G_R^{11}(0,\mathbf{q})\gamma_i(\mathbf{q})\gamma_j(\mathbf{q}) - \psi_0^2 G_R^{21}(0,\mathbf{q})\gamma_i(-\mathbf{q})\gamma_j(\mathbf{q}) \\ &-\bar{\psi}_0^2 G_R^{12}(0,\mathbf{q})\gamma_i(\mathbf{q})\gamma_j(-\mathbf{q}) - |\psi_0|^2 G_R^{22}(0,\mathbf{q})\gamma_i(-\mathbf{q})\gamma_j(-\mathbf{q}), \end{aligned} \tag{4.39}$$

while the last two yield the more complicated term

$$-\gamma_i(0)|\psi_0|^2\delta_{\mathbf{q},0}\sum_{\omega',\mathbf{k}'}[G_R^{11}(\omega',\mathbf{k}') + G_A^{11}(\omega',\mathbf{k}')]\gamma_j(2\mathbf{k}'). \tag{4.40}$$

This term is zero by the Keldysh identity $\sum_\omega[G_R^{11}(\omega,\mathbf{k})+G_A^{11}(\omega,\mathbf{k})] = 0$, so at order $O(\hbar)$ the current-current response is given by

$$\begin{aligned} \chi_{\hbar,ij}(\mathbf{q}) = &-|\psi_0|^2 G_R^{11}(0,\mathbf{q})\gamma_i(\mathbf{q})\gamma_j(\mathbf{q}) - \psi_0^2 G_R^{21}(0,\mathbf{q})\gamma_i(-\mathbf{q})\gamma_j(\mathbf{q}) \\ &-\bar{\psi}_0^2 G_R^{12}(0,\mathbf{q})\gamma_i(\mathbf{q})\gamma_j(-\mathbf{q}) - |\psi_0|^2 G_R^{22}(0,\mathbf{q})\gamma_i(-\mathbf{q})\gamma_j(-\mathbf{q}). \end{aligned} \tag{4.41}$$

We may briefly comment on the physical significance of these diagrams, as related in [27] (the present diagrams correspond to the first diagram in Fig. 1. of that paper). In all (non-zero) of these, each current vertex scatters a particle out of the condensate and thus yields a term of the form $\gamma_i(\mathbf{q})$. All such diagrams thus contribute to the superfluid $q_i q_j$ component of the response tensor.

We may expand this expression out to facilitate taking appropriate limits. Substituting in for the propagators and splitting $\gamma_i(\mathbf{q}) = \frac{1}{2m}(\mathbf{q})_i + \frac{1}{2m}(\mathbf{k}_p)_i$ yields

$$\begin{aligned} \chi_{\hbar,ij}(\mathbf{q}) = &-\frac{|\psi_0|^2}{4m^2(J(\mathbf{q})J^*(-\mathbf{q}) - V^2|\psi_0|^4)} \\ &\Big(\left(J(\mathbf{q}) + J^*(-\mathbf{q}) + 2V|\psi_0|^2\right)(\mathbf{k}_p)_i(\mathbf{k}_p)_j - (J(\mathbf{q}) - J^*(-\mathbf{q}))(\mathbf{q})_i(\mathbf{k}_p)_j \\ &-(J(\mathbf{q}) - J^*(-\mathbf{q}))(\mathbf{k}_p)_i(\mathbf{q})_j + \left(J(\mathbf{q}) + J^*(-\mathbf{q}) - 2V|\psi_0|^2\right)(\mathbf{q})_i(\mathbf{q})_j\Big). \end{aligned} \tag{4.42}$$

So long as $J(\mathbf{0})J^*(-\mathbf{0}) - V^2|\psi_0|^4 \neq 0$ (the condition for the complex spectrum to be gapped), the $\mathbf{q}\to\mathbf{0}$ limit of this quantity is direction-independent and is equal to

$$\chi_{\hbar,ij}(\mathbf{0}) = -\frac{|\psi_0|^2\left(2\delta_p - 2V|\psi_0|^2\right)}{4m^2(3V^2|\psi_0|^4 - 4\delta_p V|\psi_0|^2 + \delta_p^2 + \kappa^2)}(\mathbf{k}_p)_i(\mathbf{k}_p)_j. \tag{4.43}$$

The system (and thus this homogeneous response) is not isotropic unless $\mathbf{k}_p = 0$, so the tensor cannot be decomposed as in (4.22). Note, however, that the direction independence of the limit means that for a perturbation in a given direction $\mathbf{d}$, for $\mathbf{q}\to 0$ the response is $\chi_{\hbar,ij}(\mathbf{0})(\mathbf{d}(\mathbf{0}))_j$ and is thus independent of whether the perturbation was longitudinal or transverse. This absence of a discontinuity at $\mathbf{k} = 0$ means the behaviour is the same in all directions, so we may conclude

that the response is entirely non-superfluid. More specifically, it will be shown in Section 5.2.2 that it can be interpreted as a change in occupation of the macroscopically occupied $\mathbf{q} = \mathbf{k}_p$ pump state (also referred to as the condensate, and corresponding to ψ_0 due to the momentum shift performed earlier), so that the homogeneous component of the non-equilibrium current is rigidly in the $\mathbf{k}_p$ direction. This situation was referred as the system being in a "rigid state" by [33], and corresponds to what was discussed in Chap.1: the system can only support one persistent flow (or none if $\boldsymbol{k}_p = 0$), locked to the pump, and thus does not satisfy the implicit assumptions of the Landau criterion.

A particularly interesting situation occurs when $V|\psi_0|^2 = \delta_p$, as the response then vanishes entirely even at $\mathbf{k}_p \neq 0$. This corresponds to what is sometimes known as the "sonic point", as here the real part of the spectrum becomes gapless and linear (refer to Section 4.2), and has been studied in experiments where the polariton fluid was induced to flow past a defect [21]. Such experiments report significantly reduced scattering of the fluid by the defect (also referred to as frictionless flow) in this regime and interpret this as a sign of superfluidity. It seems, however, that what was actually detected was the vanishing of the linear response in its entirety. This means that, while scattering is indeed expected to be reduced, the transverse and longitudinal responses are equal and both zero so that the system is in the unique rigid state rather than a superfluid state: "frictionless flow in the sonic regime is the only property associated with superfluidity that is exhibited by this rigid state, as vortices and persistent currents cannot form when the phase is externally fixed" (note that recent work has demonstrated that the topological defects associated with coherently driven polaritons are domain walls rather than vortices [55]), "and the superfluid response is zero" [33].

A number of groups have also experimentally measured the spectrum in the sonic regime based on a belief in the importance of the linearisation of the real part of the spectrum (and thus it taking on a Bogoliubov form) to the Landau criterion [56]–[58]. Such interest in this point as a superfluid candidate warrants an explanation for why we detect no superfluid response despite the linearised spectrum (the explanation of Chap.1 continues to apply, this is merely another way of looking at the problem).

Recall that, in order for a superfluid response to be present, there must be a discontinuity in the current-current response at zero momentum. Yet a crucial effect of the excitation spectrum in Bose-condensed systems in the weakly-interacting regime relates to the fact that in such systems the poles of one-particle Green's functions coincide with those of density and current response functions (strictly speaking non-analyticities of the response functions, since a pole of the Green's function may become "smoothed out" in the response function) [59], [60]. This is easily seen to be the case for our system, where the mean-field current-

current response is a linear combination of the retarded Green's functions (see (4.41)). Thus, in order for our static ($\omega = 0$) response to possess a discontinuity at $\mathbf{k} = 0$, the retarded Green's functions must possess a pole at $\omega = 0$, $\mathbf{k} = 0$. This corresponds to a condition that the spectrum be gapless and, in an equilibrium system with a purely real spectrum, the linearised Bogoliubov spectrum would be. In a driven-dissipative system such as ours, however, the spectrum also possesses an imaginary part and this is found to be non-zero in the sonic regime (both analytically and from linewidth measurements in the cited experimental papers). Thus a linearised Bogoliubov form of the real part of the spectrum is not a sufficient condition for superfluidity in such systems: this is an important distinction between equilibrium and driven-dissipative systems due to the possibility of complex dispersion relations for the latter.

Overall, the Landau criterion correctly identifies points at which no superfluid is present; it agrees with the response analysis that no superfluid is present for $V|\psi_0|^2 < \delta_p$. However it also yields false positives since it predicts superfluidity for points with $V|\psi_0|^2 > \delta_p$ (possessing a gapped real spectrum), whereas the linear response at these points is found to be non-superfluid. The Landau criterion does correctly identify the frictionless regime $V|\psi_0|^2 = \delta_p$, but this regime lacks not only a transverse but also a longitudinal response and is thus not a conventional superfluid but rather a special case of the rigid state with vanishing linear response and thus reduced friction.

4.4 Mean-field response in the gapless regime

The above analysis was restricted to the case of $J(\mathbf{0})J^*(-\mathbf{0}) - V^2|\psi_0|^4 \neq 0$, where the complex spectrum is gapped. At the inversion points, however, this condition fails, which can be seen in Fig. 4.3.

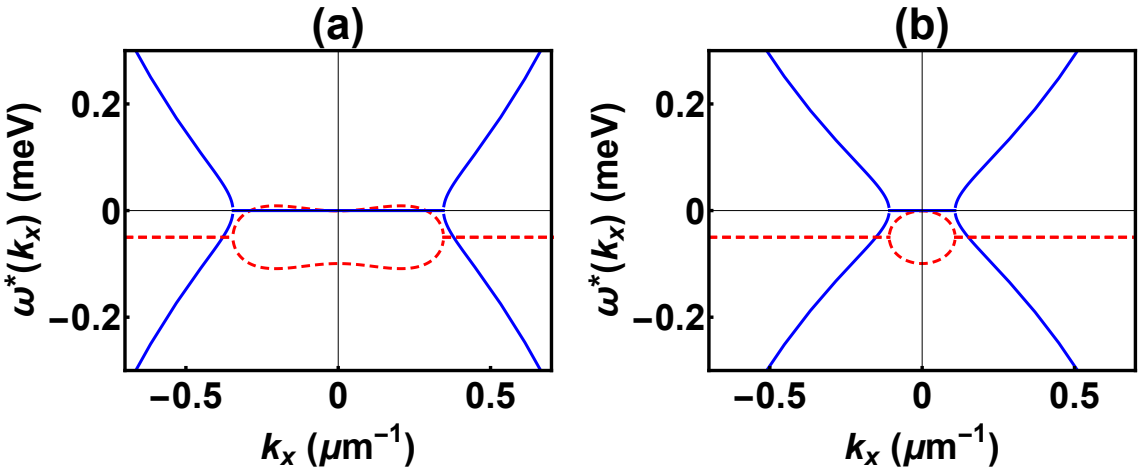

Figure 4.3: Gapless excitation spectra at the bistability inversion points, where blue is the real part and dashed-red imaginary, for the isotropic $k_p = 0$ case. **(a)** The spectrum at the the inversion point on the lower branch in Fig. 4.1(a). **(b)** The spectrum at the the inversion point on the upper branch in Fig. 4.1(a). For the anisotropic case, where $k_p \neq 0$, the real spectra are tilted but still gapless.

To investigate how this change in the spectrum affects the response to perturbations of coherently pumped polaritons, we calculate the homogeneous behaviour of the mean-field response function (Eq. (4.42)) in this regime. Assuming a uniformly oriented perturbing field $\mathbf{u}(\mathbf{q})$, the longitudinal response can be found by taking the momentum to zero along the direction of the perturbation ($\mathbf{u} \perp \mathbf{q} = 0, \mathbf{u} \parallel \mathbf{q} \to 0$), and analogously for the transverse response ($\mathbf{u} \parallel \mathbf{q} = 0, \mathbf{u} \perp \mathbf{q} \to 0$). To do this, we separate the response function into its numerator and denominator,

$$\chi_{\hbar,ij}(\mathbf{q}) = \frac{n_{ij}(q_x, q_y)}{d(q_x, q_y)}, \tag{4.44}$$

where the latter is given by

$$\begin{aligned} d(q_x, q_y) = &\left(\frac{q_x^2 + q_y^2}{2m}\right)^2 - (2\delta_p - 4V\left|\psi_0\right|^2)\frac{q_x^2 + q_y^2}{2m} \\ &- \frac{k_p^2 q_x^2}{m^2} + \frac{2i\kappa k_p q_x}{m} \\ &+ 3V^2\left|\psi_0\right|^4 - 4\delta_p V\left|\psi_0\right|^2 + \delta_p^2 + \kappa^2. \end{aligned} \tag{4.45}$$

The last line above is zero in the regime we are investigating, as that is the condition for a gapless spectrum. Consequently, in the long-range limit, d will go to zero and the response function will exhibit singular behaviour. To discover whether this may be superfluid behaviour, we must look at the limiting behaviour of the numerator.

From Eq. (4.42), the numerator of the $\chi_{\hbar,xx}$ component is given by

$$\begin{aligned} n_{xx}(q_x, q_y) = \frac{\left|\psi_0\right|^2}{2m^2}\Bigg[& \frac{q_x^4}{2m} + \frac{q_x^2 q_y^2}{2m} \\ & - \left(\frac{2k_p^2}{m} + \delta_p - 3V\left|\psi_0\right|^2 \right) q_x^2 \\ & + \frac{2k_p^2}{m} q_y^2 + 4ik_p \kappa q_x - 4k_p^2(\delta_p - V\left|\psi_0\right|^2) \Bigg]. \end{aligned} \tag{4.46}$$

The limits of this expression are different depending on whether $\mathbf{k}_p \neq 0$, the anisotropic case, or whether $\mathbf{k}_p = 0$, the isotropic case. We will deal with each in turn.

4.4.1 Anisotropic case

In the anisotropic case, choosing $\mathbf{k}_p$ in the x-direction without loss of generality, we may study the response to an x-directed perturbation through n_{xx}. Taking the limits of the above expressions in the correct order, one finds the following behaviour for the longitudinal and transverse responses:

$$\lim_{\mathbf{q}\to 0} \chi_{\hbar,xx,L}(\mathbf{q}) = \frac{C_1}{|\mathbf{q}| \to 0}, \tag{4.47}$$

$$\lim_{\mathbf{q}\to 0} \chi_{\hbar,xx,T}(\mathbf{q}) = \frac{C_2}{(|\mathbf{q}| \to 0)^2}, \tag{4.48}$$

for some constants C_1 and C_2. Performing the equivalent calculations, starting again from Eq. (4.42), for the off-diagonal components, $\chi_{\hbar,xy}$ and $\chi_{\hbar,yx}$, we also encounter divergences, and it is tempting to ask whether any physical conclusions can be drawn from any of these cases. The $\chi_{\hbar,yy}$ component of the response function however is equivalent to the isotropic $\chi_{\hbar,xx}$ case (due to our choice of $\mathbf{k}_p$), which we now turn to.

4.4.2 Isotropic case

Taking the correct limits in the isotropic case, it is found that

$$\lim_{\mathbf{q}\to 0} \chi_{\hbar,xx,L}(\mathbf{q}) = \frac{|\psi_0|^2(\delta_p - 3V|\psi_0|^2)}{m(2\delta_p - 4V|\psi_0|^2)}, \tag{4.49}$$

$$\lim_{\mathbf{q}\to 0} \chi_{\hbar,xx,T}(\mathbf{q}) = 0, \tag{4.50}$$

and that $\chi_{\hbar,xy} = \chi_{\hbar,yx} = 0$. This would appear to strongly suggest superfluid behaviour. It is not clear, however, whether this conclusion extends to $O(\hbar^2)$, and

what the mechanism for this superfluidity would be in the absence of a global $U(1)$ symmetry.

In the following two chapters I will answer these questions, starting with the anisotropic, finite $\mathbf{k}_p$ case in Chap.5, and continuing with the isotropic $\mathbf{k}_p = 0$ case in Chap.6.

Chapter 5

Diverging Anisotropic Response

5.1 Catastrophe Structure of the Mean Field Solutions

Before directly tackling the origin of the divergent response, it is helpful to first further analyse the structure of the system's mean-field. Let us thus return to Eq. (4.4) for the homogeneous mean-field solutions

$$V^2 n^3 - 2\delta_p V n^2 + (\delta_p^2 + \kappa^2) n - F_p^2 = 0. \tag{5.1}$$

This equation may be rewritten as

$$\partial_n \left[\frac{1}{4} V^2 n^4 - \frac{2}{3} \delta_p V n^3 + \frac{1}{2} (\delta_p^2 + \kappa^2) n^2 - F_p^2 n \right] = 0, \tag{5.2}$$

indicating that these mean-field solutions correspond to extrema of the effective potential

$$U_{\text{eff}}(n) = \frac{1}{4} V^2 n^4 - \frac{2}{3} \delta_p V n^3 + \frac{1}{2} (\delta_p^2 + \kappa^2) n^2 - F_p^2 n. \tag{5.3}$$

Moreover,

$$\operatorname{Im} \omega^+(\mathbf{0}) = -\kappa + \operatorname{Im} \sqrt{3V^2 n^2 - 4\delta_p V n + \delta_p^2}, \tag{5.4}$$

so a sufficient condition for dynamical instability $\operatorname{Im} \omega^+(\mathbf{0}) > 0$ may be written as

$$3V^2 n^2 - 4\delta_p V n + \delta_p^2 < -\kappa^2, \tag{5.5}$$

or

$$\partial_n^2 U_{\text{eff}} < 0. \tag{5.6}$$

We may reduce U_{eff} to a standard form by eliminating the cubic coefficient via a linear variable change $n = m + \frac{2\delta_p}{3V}$, discarding the constant term (which does not contribute to any derivatives), and subsequently dividing through by the quartic coefficient, yielding

$$U'_{\text{eff}}(m) = m^4 + \frac{2(3\kappa^2 - \delta_p^2)}{3V^2} m^2 + \left(\frac{8\delta_p(\delta_p^2 + 9\kappa^2)}{27V^3} - \frac{4F_p^2}{V^2} \right) m. \tag{5.7}$$

Introducing control parameters $A(\delta_p) = \frac{2(3\kappa^2-\delta_p^2)}{3V^2}$, $B(\delta_p, F_p) = \frac{8\delta_p(\delta_p^2+9\kappa^2)}{27V^3} - \frac{4F_p^2}{V^2}$, this is

$$U'_{\text{eff}}(m) = m^4 + A(\delta_p)m^2 + B(\delta_p, F_p)m. \tag{5.8}$$

The reader familiar with catastrophe theory will recognize this as the universal unfolding of a cusp catastrophe. Catastrophe theory is a branch of bifurcation theory, studying how small changes in an effective potential can yield large changes in the structure of that potential's stationary points. This has clear applications to classical statistical mechanics, where a system's equilibrium state is typically determined by minima of a thermodynamic potential, and extends to mean-field theory when the equations of motion can be reduced to stationarity equations for an effective potential as above. A short mathematical introduction to catastrophe theory is given in Appendix B.

That the potential corresponds to this unfolding globally rather than in a local neighbourhood of a critical point simplifies the analysis. Every possible topological configuration of extrema is given in Fig. 5.1, of which there are seen to be five, and for simplicity we classify points as stable or unstable based on the partial criterion of Eq. (5.5).

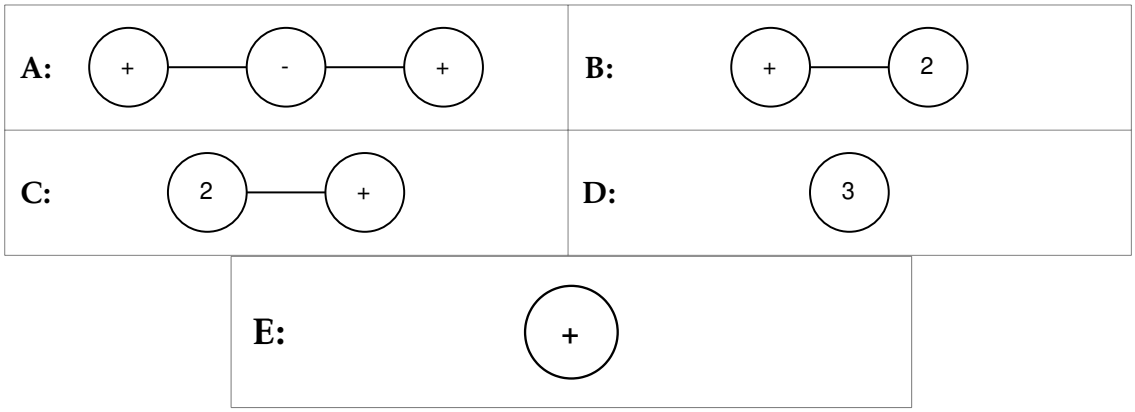

Figure 5.1: Since it is globally expressible as the universal unfolding of a cusp catastrophe, there are five distinct topological configurations for the critical points of the effective potential $U'_{\text{eff}}(m)$. Circles represent critical points, with those containing + denoting local minima and those containing – denoting local maxima. Critical points with zero second derivative resulting from multiple local minima/maxima coalescing into a single point are represented by a circle containing the number of coalesced points.

Non-Morse critical points are points with a vanishing second derivative, or $\partial_m^2 U'_{\text{eff}}(m) = 0$. Since such points are structurally unstable relative to the control parameters A and B, and thus relative to δ_p and F_p, we see that such points correspond to phase transitions [61]. Here these are the coalesced critical points

corresponding to configurations B, C, D in Fig. 5.1. Those of double multiplicity, 5.1.B and 5.1.C, locally correspond to fold bifurcations — an infinitesimal perturbation of the control parameters may split such a point into a stable-unstable pair (case 5.1.A) or eliminate it entirely (case 5.1.E). Such an elimination results in a discontinuous collapse to the remaining stable critical point, meaning these are zero-order phase transition points. The configuration with a point of triple multiplicity 5.1.D, when it is non-Morse (if it is Morse, then we are not in the bistable regime), is just the catastrophe germ[1] for the cusp catastrophe, and thus corresponds to a continuous phase transition. A general infinitesimal perturbation of the control parameters will continuously split it into two stable and one unstable critical point, which is the universal unfolding 5.1.A.

In the rest of this part of the thesis, it will be seen that it is the presence of these structurally unstable non-Morse critical points and their accompanying phase transitions that is the cause of the divergences appearing in the anisotropic current-current linear response. We may note already that the condition for a diverging linear response, a gapless spectrum, corresponds to the inequality in Eqs (5.4) and (5.5) becoming an equality. This is precisely the condition for a non-Morse critical point.

Finally, we may visualise this catastrophe structure by solving $\partial_m U'_{\text{eff}}(m) = 0$ for m in terms of A and B, and plotting the resulting $m_{\text{soln}}(A, B)$. This is seen in Fig. 5.2, where the resulting surface is called the "critical manifold" and the line of non-Morse critical points is termed the "locus of bifurcations". By our stability criterion, the section of the surface inside the locus of bifurcations always corresponds to unstable solutions, while the section outside is generally stable (some of these points are unstable since our criterion only checks dynamical stability at zero momentum, but this will not be relevant).

5.2 The Geometric Origin of the Divergence

5.2.1 Non-Linearity at the Locus of Bifurcations

Having laid the groundwork by identifying the presence of catastrophes and a locus of bifurcations in our system, we may now see how this leads to a diverging anisotropic response.

Consider the static mean-field equations for the anisotropic problem. Recall from section II.D.2 that the current-current response we seek is a response to the physical field $f_i(\mathbf{q})$, so we add the term $\sum_k \mathbf{f}(\mathbf{k}) \cdot \mathbf{j}^q(-k)$ to the action. Moreover, in the absence of an unphysical field, solutions to Keldysh mean-field equations have the quantum fields equal to zero so we pre-emptively set them so. The

[1] Refer to Appendix B for the meaning of this term.

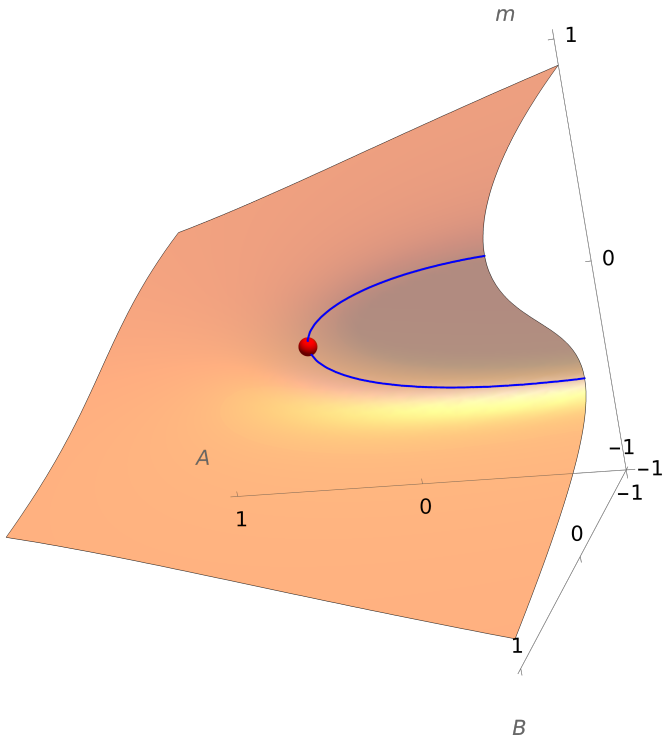

Figure 5.2: Critical manifold of the solution $m_{\text{soln}}(A,B)$ to $\partial_m U'_{\text{eff}}(m) = 0$. Solutions corresponding to non-Morse critical points form a line (blue) on this surface, called the locus of bifurcations — the name is due to infinitesimal perturbations in A and B at these points leading to a change in the number of solutions, i.e. to bifurcations. The critical point on this line corresponding to the cusp catastrophe germ is labelled by a red sphere.

resulting equations are

$$\begin{aligned}&(\Delta_p - \epsilon(\mathbf{k}) + i\kappa)\psi(\mathbf{k}) - F_p\delta_{\mathbf{k},0}\\ &-\frac{V}{2}\sum_{\mathbf{k}',\mathbf{q}}\bar{\psi}(\mathbf{k}'+\mathbf{q})\psi(\mathbf{k}+\mathbf{q})\psi(\mathbf{k}')\\ &+\sum_{\mathbf{q}}\gamma_i(2\mathbf{k}-\mathbf{q})f_i(\mathbf{q})\psi(\mathbf{k}-\mathbf{q}) = 0\end{aligned} \tag{5.9}$$

and its complex conjugate. Splitting $f_i(\mathbf{k})$ as $f_i(\mathbf{k}) = f_i(\mathbf{0})\delta_{\mathbf{k},\mathbf{0}} + f_i(\mathbf{k})(1-\delta_{\mathbf{k},\mathbf{0}})$ and temporarily setting the inhomogeneous components of the force to zero, the equations may be rewritten as

$$\begin{aligned}&(\Delta_p + \gamma_i(2\mathbf{k})f_i(\mathbf{0}) - \epsilon(\mathbf{k}) + i\kappa)\psi(\mathbf{k}) - F_p\delta_{\mathbf{k},0}\\ &-\frac{V}{2}\sum_{\mathbf{k}',\mathbf{q}}\bar{\psi}(\mathbf{k}'+\mathbf{q})\psi(\mathbf{k}+\mathbf{q})\psi(\mathbf{k}') = 0\end{aligned} \tag{5.10}$$

Finally consider homogeneous solutions:

$$((\delta_p + \gamma_i(\mathbf{0})f_i(\mathbf{0})) + i\kappa)\psi_0 - F_p - V\psi_0|\psi_0|^2 = 0 \tag{5.11}$$

We see that the homogeneous component of the force couples into this equation in the same way as the detuning. We can thus absorb this into an effective $\delta_p' = \delta_p + \gamma_i(\mathbf{0})f_i(\mathbf{0})$.

Now, note that the mean-field value of the classical current is given by

$$j_{\mathrm{mf},i}(\mathbf{q}) = \gamma_i(0)|\psi_0|^2\delta_{\mathbf{q},0}, \tag{5.12}$$

so that the mean-field linear response to a homogeneous force can, with some caution, be viewed as

$$\chi_{\mathrm{mf},ij}(0) = \gamma_i(0)\frac{\partial|\psi_0|^2}{\partial f_j(0)} = \gamma_i(0)\frac{\partial|\psi_0|^2}{\partial\delta_p'}\gamma_j(0), \tag{5.13}$$

and herein lies the connection. Looking at the control surface again, we see that along the locus of bifurcations $\frac{\partial m}{\partial A}$ and $\frac{\partial m}{\partial B}$ diverge. This is because, in a neighbourhood of any point on the locus, a fixed-A or B cross-section will possess one of the two forms in Fig. 5.3. Such a divergence of the linear response to control parameters is typical of bifurcation points in catastrophe theory [62].

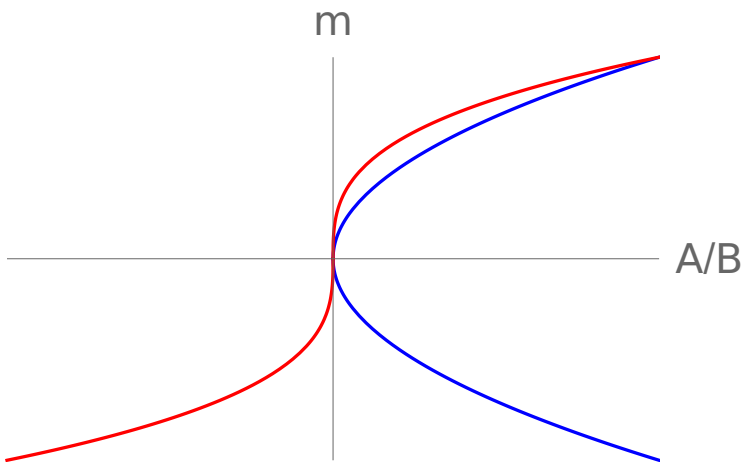

Figure 5.3: A fixed-A or B cross-section of the critical manifold with a point of the locus of bifurcations at the origin will have one of the two general forms shown here. The blue line indicates the case of a two-fold multiplicity point, while the red relates to the point of triple multiplicity. In both cases, derivatives diverge at the origin, i.e. on the locus.

As a result, if we choose F_p and δ_p such that m lies on the locus and m', defined as m but with δ_p' instead of δ_p, is a stable solution, we find

$$\frac{\partial|\psi_0|^2}{\partial\delta_p'} = \frac{2}{3V} + \frac{\partial m'}{\partial A}\frac{\partial A}{\partial\delta_p'} + \frac{\partial m'}{\partial B}\frac{\partial B}{\partial\delta_p'}. \tag{5.14}$$

Thus, as $\mathbf{f}(\mathbf{0}) \to 0$, i.e. $\delta_p' \to \delta_p$, $\frac{\partial|\psi_0|^2}{\partial\delta_p'} \to \infty$. This shows that the divergence in the current-current response in this case is intimately tied to the presence of a bifurcation. Far from being unphysical, the divergence expresses the high degree of non-linearity present in the vicinity of a non-Morse critical point corresponding to a phase transition, and the mechanism just described is typical of the origin of divergent linear responses at phase transitions.

5.2.2 Directional Dependence of the Response

Equation (5.13) is not entirely well-founded. The limit $\lim_{\mathbf{q}\to 0}\chi_{ij}(\mathbf{q})$ is sometimes directional (the definition of superfluid we are using relies on this fact), but the above expression admits no such possibility. In the case that this direction-dependence is absent, however, we may show that the result agrees with a more rigorous treatment using the explicit form of the response tensor. In this case the response is just a measure of the change in occupation $|\psi_0|^2$ of the macroscopically occupied pump state in response to an external static drive $f_j(0)$.

We begin by calculating $\frac{\partial|\psi_0|^2}{\partial\delta_p}$, or $\frac{\partial n}{\partial\delta_p} = \dot{n}$, by starting from the mean-field homogeneous equation:

$$V^2n^3 - 2\delta_p V n^2 + (\delta_p^2 + \kappa^2)n - F_p^2 = 0 \tag{5.15}$$

Differentiating,

$$3V^2n^2\dot{n} - 2Vn^2 - 4\delta_p Vn\dot{n} + 2\delta_p' n + (\delta_p^2 + \kappa^2)\dot{n} = 0 \tag{5.16}$$

and rearranging (provided the denominator is not 0):

$$\dot{n} = \frac{2Vn^2 - 2\delta_p n}{3V^2n^2 - 4\delta_p Vn + \delta_p^2 + \kappa^2}. \tag{5.17}$$

Our expression then yields:

$$\chi_{\text{hom-mf},ij} = -\frac{|\psi_0|^2\left(2\delta_p - 2V|\psi_0|^2\right)}{4m^2(3V^2|\psi_0|^4 - 4\delta_p V|\psi_0|^2 + \delta_p^2 + \kappa^2)}(\mathbf{k}_p)_i(\mathbf{k}_p)_j \tag{5.18}$$

which is identical to our $O(\hbar)$ diagrammatic result in Eq. (4.43). We thus see that, where $3V^2n^2 - 4\delta_p Vn + \delta_p^2 + \kappa^2 \neq 0$, the limit is direction-independent and accurately captured by our formula. Moreover, we know that $\partial_n^2 U_{\text{eff}}(n) = 3V^2n^2 - 4\delta_p Vn + \delta_p^2 + \kappa^2 = 0$ only on the locus of bifurcations, so $\chi_{\text{hom-mf},ij} = \gamma_i(0)\frac{\partial|\psi_0|^2}{\partial f_j(0)}$ is valid as the locus is approached, and the divergence indeed arises from our earlier geometric argument.

Chapter 6

Isotropic Mean-Field Superfluidity

We now turn to the isotropic case. Recalling the discussion of Section 4.4.2, we know that for $\mathbf{k}_p = 0$ the $O(\hbar)$ current-current response is purely superfluid. This mean-field superfluidity has a curious origin as the interplay of two opposing processes; on the one hand, as the point of interest lies on the locus of bifurcations, the response for any non-zero pump momentum diverges for the geometric reasons as discussed in Section 5.2. As $k_p \to 0$, however, the homogeneous component of the force couples increasingly weakly to the mean-field equations (its coupling being $\gamma_i(\mathbf{0}) = \frac{k_p}{2m}$), and in the limit $k_p = 0$ does not appear in them at all. This means that $k_p \to 0$ leads to $\chi_\hbar(\mathbf{0}) \to 0$ off of the locus and the interaction with the divergence at the locus yields a finite, non-zero superfluid response at it.

This elegant picture is unfortunately spoiled by higher-order terms in the perturbation expansion. We will now show that a divergence persists at $O(\hbar^2)$, and is related to the absence of $U(1)$ symmetry in the problem[1].

6.1 One-Loop Keldysh Tadpoles

One-loop tadpoles are truncated Feynman diagrams of the form 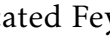 . There are are six such tadpoles with R/A correlators as the loop, presented in Fig. 6.1, and four with a K correlator, presented in Fig. 6.2.

Crucially, the R/A loops are mutually cancelling. To see this, consider the combination of terms coming from tadpoles (A) and (B) in Fig. 6.1 when attached to the same external line on a diagram:

$$-G_X(0)\int dk\left(G_R^{11}(k)+G_A^{11}(k)\right)=0. \tag{6.1}$$

Here $G_X(0)$ is some correlator corresponding to the attachment, while the loops

[1] This divergence was actually also present in the anisotropic case, but there the mean field divergence invalidated the calculation at a lower order of perturbation.

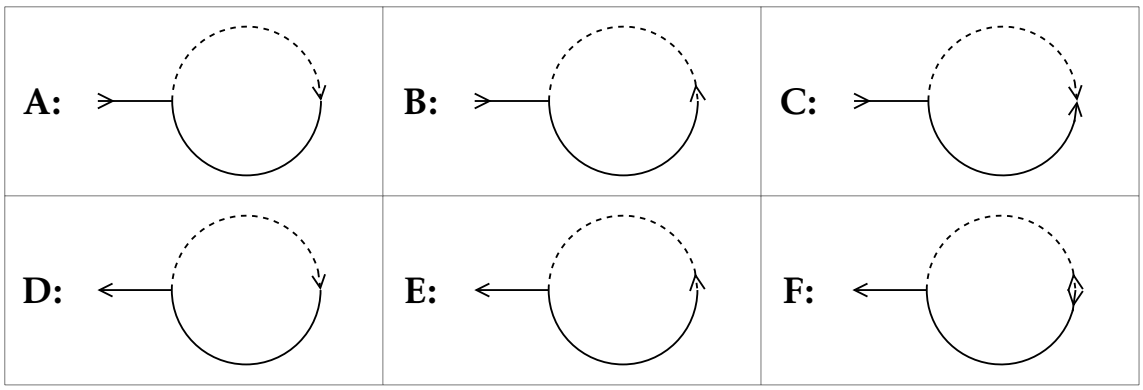

Figure 6.1: R/A-Correlator Tadpoles. Solid lines with the arrow oriented towards the vertex represent $\bar{\psi}^c_p$, while those with an arrow pointing away from it represent ψ^c_p. Analogously, such dashed lines represent $\bar{\psi}^q_p$ and ψ^q_p. Two such lines, when connected, represent the Green's function equal to the expectation of the product of the associated fields.

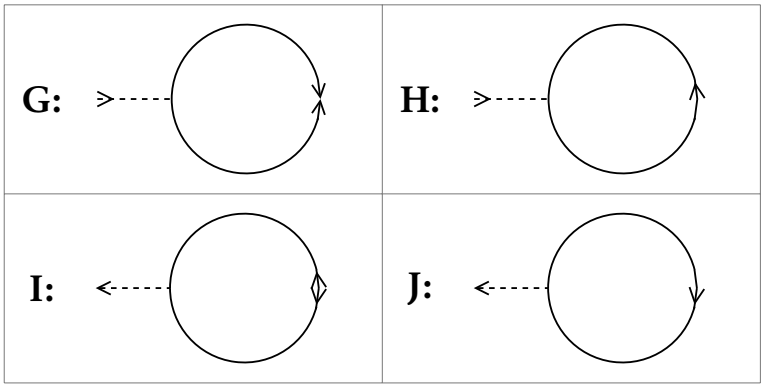

Figure 6.2: K-Correlator Tadpoles. Solid lines with the arrow oriented towards the vertex represent $\bar{\psi}^c_p$, while those with an arrow pointing away from it represent ψ^c_p. Analogously, such dashed lines represent $\bar{\psi}^q_p$ and ψ^q_p. Two such lines, when connected, represent the Green's function equal to the expectation of the product of the associated fields.

themselves are seen to cancel by the Keldysh relation $\int d\omega\,(G_R(\omega) + G_A(\omega)) = 0$ (note that the $\{11\}$ elements of the Keldysh matrices correspond to the true $G_{R/A}$). Tadpoles (D) and (E) cancel in the same manner.

To see that tadpole (C) is zero, we write its attachment out explicitly:

$$\begin{aligned} &-G_X(0)\int dk\, G_R^{12}(k) = \\ &-G_X(0)\int d\mathbf{k}\left(\int d\omega\,\frac{V\psi_0^2}{J(\omega,\mathbf{k})J^*(-\omega,-\mathbf{k}) - V^2|\psi_0|^4}\right). \end{aligned} \tag{6.2}$$

The denominator of the integrand is quadratic in ω, and the pole lies in the lower half-plane (the denominator agrees with that of the true retarded Green's function). Thus, closing the contour in the upper half-plane, the integral is zero. The same reasoning then leads to the vanishing of tadpole (F).

The K-correlator tadpoles, however, do not cancel in this way. Moreover,

when connected to an external line of a diagram, they introduce a term of the form $G_{R/A}(0)$. Such terms become singular in the limit of a gapless spectrum (since in that case the pole is precisely at $\omega = 0$, $\mathbf{k} = 0$) so that, for the perturbation expansion to remain finite, certain diagrams with external legs must vanish. We will now argue that this does not occur.

6.2 Tadpole Diagrams at $\mathbf{O}(\hbar^2)$

Associating the connecting edge to the tadpole rather than to the main diagram, we see that a tadpole contributes $\hbar$ to any diagram to which it is attached. This means that we are interested in cancellation of diagrams with a free leg[2] that are $O(\hbar)$ prior to the attachment of the tadpole.

To understand what kinds of diagrams may appear, we may apply some graph theory, considering diagrams with a free leg as graphs where interaction vertices are the vertices and Green's functions (but not the free leg) are edges. Denote the number of 4-valent vertices by a and 3-valent vertices by b, the number of current fields participating in an edge (as opposed to assuming a mean-field value) by n, and the number of edges and vertices by e and v respectively. Then one finds (we subtract 1 because we do not count the free leg)

$$\frac{4a + 3b - 1 - n}{2} + n = e, \tag{6.3}$$

$$a + b = v, \tag{6.4}$$

$$e - v = 1. \tag{6.5}$$

Here the first condition equates the number of edges to the number of Green's functions connecting two vertices plus the number of Green's functions connecting to at least one current field, the second equates the total number of vertices to the number of interaction vertices, and the last enforces that the diagram is $O(\hbar)$, since each vertex removes a factor of $\hbar$ and each edge adds one. From here a little manipulation yields

$$2a + b = 3 - n, \tag{6.6}$$

which allows us to classify all possible diagrams.

We see that the possible values of n are $n = 1, 2, 3$. We may disregard $n = 1$ because in this case three of the four current fields are set to mean-field values, meaning the remaining field is a quantum field. The attaching field of the K-tadpole is, however, also quantum and the quantum-quantum correlators are all zero, so that such diagrams vanish. For $n = 2$, the only possibility is $b = 1$, while

[2] By this we mean a line coming off of a vertex that has not been paired with another line to form a Green's function. When a tadpole is attached, it is this line that will be paired with the corresponding free leg of the tadpole.

for $n = 3$ we must have $a = b = 0$. These are thus the only types of diagrams that we need consider.

Unfortunately even after discarding those which trivially vanish, this still leaves a comparably large number — 32 diagrams. These diagrams, however, have different asymptotic dependencies on $|\mathbf{q}| \to \infty$ (the momentum variable of the response function)[3]. Because these diagrams must cancel at all momenta for the perturbation theory to be valid, we may group them by this dependence: each group must cancel independently. Each diagram will possess two factors of $\gamma(\pm\mathbf{q})$. Furthermore, *R/A* correlators where the arrows match ($G^{11}_{R/A}$ and $G^{22}_{R/A}$) are $O(|\mathbf{q}^{-2}|)$, while the others ($G^{12}_{R/A}$ and $G^{21}_{R/A}$) are $O(|\mathbf{q}^{-4}|)$. We then have 6 diagrams of $O(|\mathbf{q}|^{-6})$, 12 diagrams of $O(|\mathbf{q}|^{-4})$, 10 diagrams of $O(|\mathbf{q}|^{-2})$, and 4 diagrams of $O(|\mathbf{q}|^{0})$. These are given in Figs. 6.3, 6.4, 6.5, 6.6.

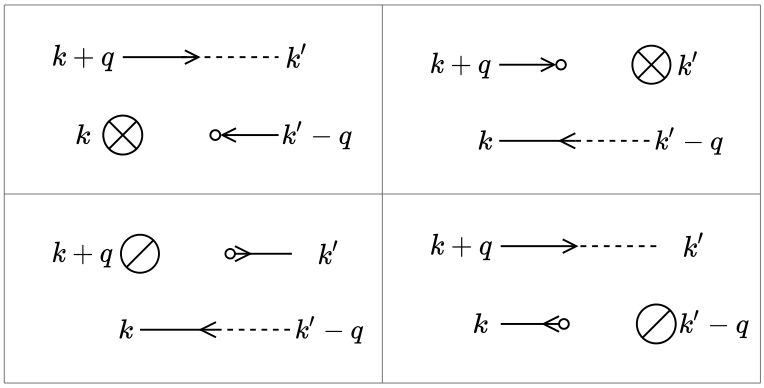

Figure 6.3: $O(|\mathbf{q}|^{0})$ diagrams, with the small circle denoting the tadpole attachment point. Circles with a line through them represent the condensate ψ_0 while those with a cross represent $\bar{\psi}_0$. Solid lines with the arrow at their end oriented towards a momentum p represent ψ^c_p, while those with an arrow pointing away from it represent $\bar{\psi}^c_p$. Analogously, such dashed lines represent ψ^q_p and $\bar{\psi}^q_p$. Two such lines, when connected, represent the Green's function equal to the expectation of the product of the associated fields.

[3]Here we are referring purely to the functional form of this dependence, disregarding the cut-off of the theory.

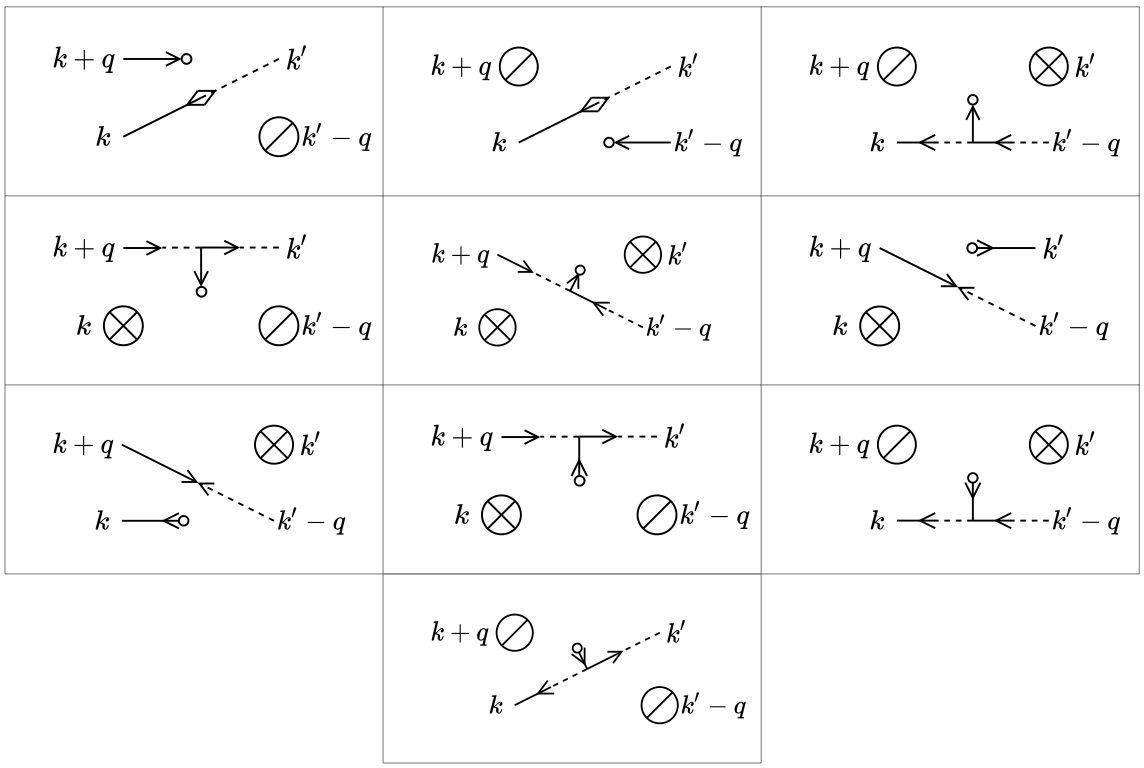

Figure 6.4: $O(|\mathbf{q}|^{-2})$ diagrams, with the small circle denoting the tadpole attachment point. Circles with a line through them represent the condensate ψ_0 while those with a cross represent $\bar{\psi}_0$. Solid lines with the arrow at their end oriented towards a momentum p represent ψ^c_p, while those with an arrow pointing away from it represent $\bar{\psi}^c_p$. Analogously, such dashed lines represent ψ^q_p and $\bar{\psi}^q_p$. Two such lines, when connected, represent the Green's function equal to the expectation of the product of the associated fields.

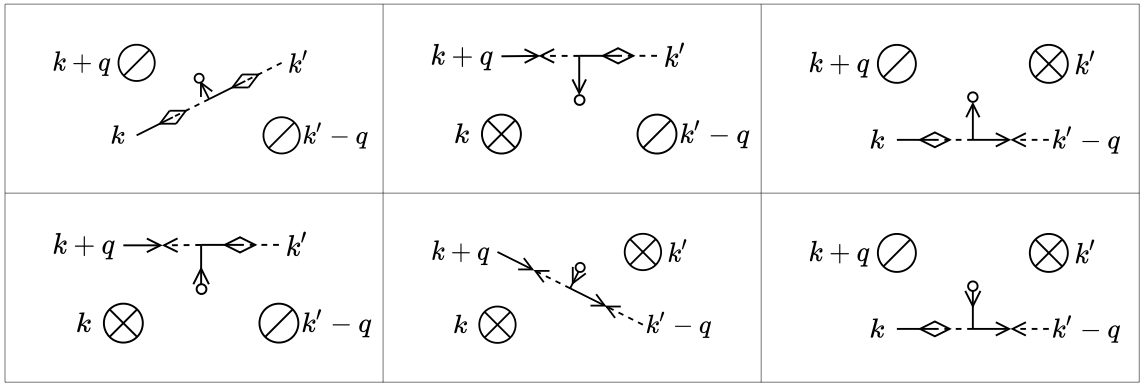

Figure 6.5: $O(|\mathbf{q}|^{-6})$ diagrams, with the small circle denoting the tadpole attachment point. Circles with a line through them represent the condensate ψ_0 while those with a cross represent $\bar{\psi}_0$. Solid lines with the arrow at their end oriented towards a momentum p represent ψ^c_p, while those with an arrow pointing away from it represent $\bar{\psi}^c_p$. Analogously, such dashed lines represent ψ^q_p and $\bar{\psi}^q_p$. Two such lines, when connected, represent the Green's function equal to the expectation of the product of the associated fields.

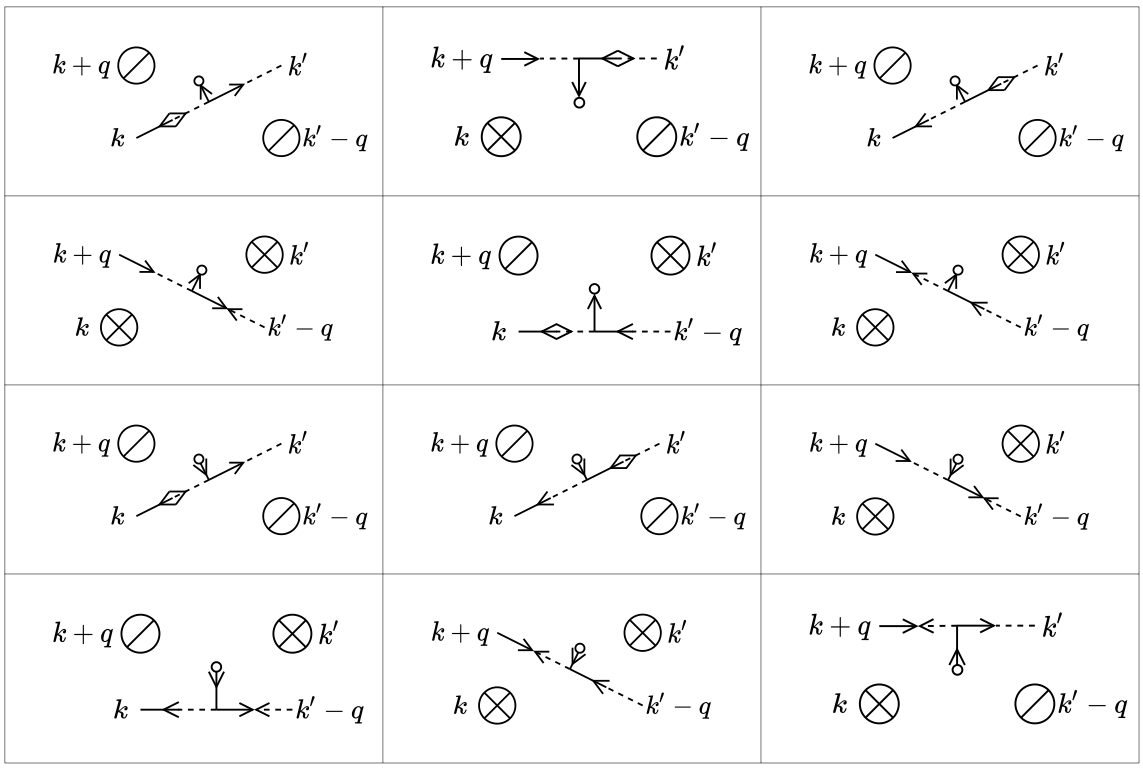

Figure 6.6: $O(|\mathbf{q}|^{-4})$ diagrams, with the small circle denoting the tadpole attachment point. Circles with a line through them represent the condensate ψ_0 while those with a cross represent $\bar{\psi}_0$. Solid lines with the arrow at their end oriented towards a momentum p represent ψ^c_p, while those with an arrow pointing away from it represent $\bar{\psi}^c_p$. Analogously, such dashed lines represent ψ^q_p and $\bar{\psi}^q_p$. Two such lines, when connected, represent the Green's function equal to the expectation of the product of the associated fields.

We begin by considering the four $O(|\mathbf{q}|^0)$ diagrams. The two with a ψ^c connecting field come out to

$$-\frac{1}{\sqrt{2}}(G_R^{11}(\mathbf{q}) + G_R^{22}(\mathbf{q}))\bar{\psi}_0\gamma_i(\mathbf{q})\gamma_j(\mathbf{q}), \tag{6.7}$$

while the other two yield

$$-\frac{1}{\sqrt{2}}(G_R^{11}(\mathbf{q}) + G_R^{22}(\mathbf{q}))\psi_0\gamma_i(\mathbf{q})\gamma_j(\mathbf{q}). \tag{6.8}$$

Considering all possible K-tadpole attachments, we obtain the following expression for the sum of these diagrams:

$$\begin{aligned}-\frac{V}{\sqrt{2}}(G_R^{11}(\mathbf{q}) + G_R^{22}(\mathbf{q}))\gamma_i(\mathbf{q})\gamma_j(\mathbf{q})\Big[&\bar{\psi}_0\Big(G_R^{11}(0)(\frac{1}{2}\bar{\psi}_0\,\mathrm{Tr}[G_K^{12}] + \psi_0\,\mathrm{Tr}[G_K^{11}]) \\ &+ G_R^{12}(0)(\frac{1}{2}\psi_0\,\mathrm{Tr}[G_K^{21}] + \bar{\psi}_0\,\mathrm{Tr}[G_K^{22}])\Big) \\ &+ \psi_0\Big(G_R^{21}(0)(\frac{1}{2}\bar{\psi}_0\,\mathrm{Tr}[G_K^{12}] + \psi_0\,\mathrm{Tr}[G_K^{11}]) \\ &+ G_R^{22}(0)(\frac{1}{2}\psi_0\,\mathrm{Tr}[G_K^{21}] + \bar{\psi}_0\,\mathrm{Tr}[G_K^{22}])\Big)\Big]\end{aligned} \tag{6.9}$$

Denoting

$$a = \frac{1}{2}\bar{\psi}_0 \operatorname{Tr}[G_K^{12}] + \psi_0 \operatorname{Tr}[G_K^{11}], \tag{6.10}$$

$$b = \frac{1}{2}\psi_0 \operatorname{Tr}[G_K^{21}] + \bar{\psi}_0 \operatorname{Tr}[G_K^{22}], \tag{6.11}$$

the condition for this sum to be zero may be written as

$$\underbrace{\bar{\psi}_0 J^*(0)a + \bar{\psi}_0 V \psi_0^2 b}_{A} + \underbrace{\psi_0 V \bar{\psi}_0^2 a + \psi_0 J(0) b}_{-A} = 0. \tag{6.12}$$

Further, recalling that

$$(G_R^{11}(k))^* = G_R^{22}(-k), \tag{6.13}$$

$$(G_R^{12}(k))^* = G_R^{21}(-k), \tag{6.14}$$

$$(G_K^{11}(k))^* = -G_K^{22}(-k), \tag{6.15}$$

$$(G_K^{12}(k))^* = -G_K^{21}(-k), \tag{6.16}$$

we have $a^* = -b$. This means that $A = A^*$ so A is real.

Setting $A' = \frac{A}{|\psi_0|^2}$, another real quantity, this equation may be rewritten as a matrix expression:

$$\begin{pmatrix} J^*(0) & -V\psi_0^2 \\ -V\bar{\psi}_0^2 & J(0) \end{pmatrix} \begin{pmatrix} a \\ a^* \end{pmatrix} = \begin{pmatrix} \psi_0 A' \\ \bar{\psi}_0 A' \end{pmatrix}. \tag{6.17}$$

Since this supposed cancellation is of interest only on the locus of bifurcations, we may specialise ψ_0 to it. From Eq. (4.11) and the fact that the locus of bifurcations corresponds to a gapless complex spectrum, we find the condition ($n = |\psi_0|^2$)

$$3V^2 n^2 - 4\delta_p V n + \delta_p^2 + \kappa^2 = 0 \tag{6.18}$$

This may be combined with Eq. (4.2) to yield

$$\psi_0 = -\sqrt{n}\frac{Vn - \delta_p}{(Vn-\delta_p)^2 + \kappa^2} - i\sqrt{n}\frac{\kappa}{(Vn-\delta_p)^2+\kappa^2}, \tag{6.19}$$

$$V\psi_0^2 = Vn\frac{(Vn-\delta_p)^2 - \kappa^2}{(Vn-\delta_p)^2+\kappa^2} + iVn\frac{2\kappa(Vn-\delta)}{(Vn-\delta_p)^2+\kappa^2}, \tag{6.20}$$

$$V\psi_0^2 = \underbrace{-\frac{2Vn(Vn-\delta_p)}{(Vn-\delta_p)^2+\kappa^2}}_{=-1} J^*(0) = J^*(0). \tag{6.21}$$

From the last equation above we see that the matrix is degenerate, and the existence of a solution to (6.17) is not certain. To check this, we may split the matrix equation into its real and imaginary components via

$$\begin{pmatrix} M_{11}^r + iM_{11}^i & M_{12}^r + iM_{12}^i \\ M_{21}^r + iM_{21}^i & M_{22}^r + iM_{22}^i \end{pmatrix} \begin{pmatrix} x + iy \\ l + im \end{pmatrix} = \begin{pmatrix} v + iw \\ p + iq \end{pmatrix}$$

$$\Downarrow$$

$$\begin{pmatrix} M_{11}^r & -M_{11}^i & M_{12}^r & -M_{12}^i \\ M_{11}^i & M_{11}^r & M_{12}^i & M_{12}^r \\ M_{21}^r & -M_{21}^i & M_{22}^r & -M_{22}^i \\ M_{21}^i & M_{21}^r & M_{22}^i & M_{22}^r \end{pmatrix} \begin{pmatrix} x \\ y \\ l \\ m \end{pmatrix} = \begin{pmatrix} v \\ w \\ p \\ q \end{pmatrix}.$$

Applying this to (6.17) yields

$$2 \begin{pmatrix} \operatorname{Im} J(0) \\ \operatorname{Re} J(0) \\ \operatorname{Im} J(0) \\ -\operatorname{Re} J(0) \end{pmatrix} \operatorname{Im} a = \begin{pmatrix} \operatorname{Re} \psi_0 \\ \operatorname{Im} \psi_0 \\ \operatorname{Re} \psi_0 \\ -\operatorname{Im} \psi_0 \end{pmatrix} A' \tag{6.22}$$

Using (6.21), we must have

$$A' = 2 \frac{\operatorname{Im} J(0)}{\operatorname{Re} \psi_0} \operatorname{Im} a = 4V\sqrt{n}\kappa \operatorname{Im} a, \tag{6.23}$$

$$A' = 2 \frac{\operatorname{Re} J(0)}{\operatorname{Im} \psi_0} \operatorname{Im} a = 2V\sqrt{n}(\kappa - \frac{(Vn - \delta_p)^2}{\kappa}) \operatorname{Im} a. \tag{6.24}$$

Since $\kappa > 0$, $4\kappa \neq 2(\kappa - \frac{(Vn-\delta_p)^2}{\kappa})$ so we must have $\operatorname{Im} a = A' = 0$. Since $\operatorname{Im} a = 0$ implies $A' = 0$, we need only consider this condition:

$$\operatorname{Im}\left(\frac{1}{2} \bar{\psi}_0 \operatorname{Tr}[G_K^{12}] + \psi_0 \operatorname{Tr}[G_K^{11}] \right) = 0. \tag{6.25}$$

Defining

$$\mathfrak{D}(k) = |J(k)J^*(-k) - V^2|\psi_0|^4|^2, \tag{6.26}$$

this is

$$-2i\kappa \int dk \, \frac{1}{\mathfrak{D}(k)} \left(\left[|J(-k)|^2 + V^2|\psi_0|^4 - \epsilon(\mathbf{k})V|\psi_0|^2 \right] \psi_0 + \left[V^2|\psi_0|^2 \right] \psi_0^3 \right) \in \mathbb{R}. \tag{6.27}$$

To proceed, it is helpful to calculate $\int d\omega \, \frac{1}{\mathfrak{D}(\omega,\mathbf{k})}$ and $\int d\omega \, \frac{\omega^2}{\mathfrak{D}(\omega,\mathbf{k})}$ (the denominator here is even in ω so any term of the form $\int d\omega \, \frac{\omega}{\mathfrak{D}(\omega,\mathbf{k})}$ is zero). This may be accomplished by casting $\mathfrak{D}(k)$ in residue form via the equation for the spectrum (4.11):

$$\mathfrak{D}(\omega, \mathbf{k}) = (\omega - \omega_{\mathbf{k}}^-)(\omega - \omega_{\mathbf{k}}^+)(\omega - (\omega_{\mathbf{k}}^-)^*)(\omega - (\omega_{\mathbf{k}}^+)^*). \tag{6.28}$$

At large ω this is $O(\omega^{-4})$, so we may close the contour of integration in the upper

half-plane (we assume for the moment that the complex spectrum is stable and gapped), yielding

$$\begin{aligned}\int d\omega\, \frac{1}{\mathfrak{D}(k)} =& \frac{2\pi i}{((\omega^+_{\mathbf{k}})^* - \omega^-_{\mathbf{k}})((\omega^+_{\mathbf{k}})^* - \omega^+_{\mathbf{k}})((\omega^+_{\mathbf{k}})^* - (\omega^-_{\mathbf{k}})^*)} \\ &+ \frac{2\pi i}{((\omega^-_{\mathbf{k}})^* - \omega^-_{\mathbf{k}})((\omega^-_{\mathbf{k}})^* - \omega^+_{\mathbf{k}})((\omega^-_{\mathbf{k}})^* - (\omega^+_{\mathbf{k}})^*)},\end{aligned} \tag{6.29}$$

$$\begin{aligned}\int d\omega\, \frac{\omega^2}{\mathfrak{D}(k)} =& \frac{2\pi i((\omega^+_{\mathbf{k}})^*)^2}{((\omega^+_{\mathbf{k}})^* - \omega^-_{\mathbf{k}})((\omega^+_{\mathbf{k}})^* - \omega^+_{\mathbf{k}})((\omega^+_{\mathbf{k}})^* - (\omega^-_{\mathbf{k}})^*)} \\ &+ \frac{2\pi i((\omega^-_{\mathbf{k}})^*)^2}{((\omega^-_{\mathbf{k}})^* - \omega^-_{\mathbf{k}})((\omega^-_{\mathbf{k}})^* - \omega^+_{\mathbf{k}})((\omega^-_{\mathbf{k}})^* - (\omega^+_{\mathbf{k}})^*)}.\end{aligned} \tag{6.30}$$

Denoting

$$z = \sqrt{(\epsilon(\mathbf{k}) - \delta_p + 2V|\psi_0|^2)^2 - V^2|\psi_0|^4}, \tag{6.31}$$

$$\omega^{\pm} = -i\kappa \pm z, \tag{6.32}$$

we find

$$\int d\omega\, \frac{1}{\mathfrak{D}(k)} = \frac{8\pi\kappa}{z^4 - 2z^2((z^*)^2 - 4\kappa^2) + ((z^*)^2 + 4\kappa^2)^2}, \tag{6.33}$$

$$\int d\omega\, \frac{\omega^2}{\mathfrak{D}(k)} = \frac{4\pi\kappa(z^2 + (z^*)^2 + 2\kappa^2)}{z^4 - 2z^2((z^*)^2 - 4\kappa^2) + ((z^*)^2 + 4\kappa^2)^2}. \tag{6.34}$$

The above results were worked out on the assumption that the spectrum is stable and gapped. This may be viewed as a regularisation of the gapless case, and we may now study the behaviour of the above expressions for a gapless spectrum and $\mathbf{k} \to 0$. In this case, some algebra yields

$$\int d\omega\, \frac{1}{\mathfrak{D}(k)} \sim \frac{m\pi}{2(2V|\psi_0|^2 - \delta_p)\kappa} \frac{1}{|\mathbf{k}|^2 + \epsilon}, \tag{6.35}$$

$$\int d\omega\, \frac{\omega^2}{\mathfrak{D}(k)} \sim \frac{\pi}{2\kappa}. \tag{6.36}$$

Here ϵ is a quantity that tends to zero as we go from a gapped to a gapless spectrum. The important consequence of this is that for a gapless spectrum, traces over the first of these quantities yield logarithmic divergences (we replace $|\boldsymbol{k}| \to r$

and use rotational symmetry):

$$\begin{aligned}\int dk\,\frac{1}{\mathfrak{D}(k)} &= \int_0^\Lambda dr\,r\int d\omega\,\frac{1}{\mathfrak{D}(\omega,r)}\\ &\sim \frac{m\pi}{2(2V|\psi_0|^2-\delta_p)\kappa}\int_0^{\epsilon'} dr\,\frac{r}{r^2+\epsilon}+\int_{\epsilon'}^\Lambda dr\,r\int d\omega\,\frac{1}{\mathfrak{D}(\omega,r)} \qquad (6.37)\\ &= \frac{m\pi}{4(2V|\psi_0|^2-\delta_p)\kappa}\log\Big(\frac{\epsilon'^2+\epsilon}{\epsilon}\Big)+\int_{\epsilon'}^\Lambda dr\,r\int d\omega\,\frac{1}{\mathfrak{D}(\omega,r)}.\end{aligned}$$

Above ϵ' is some energy scale small enough for our small $|\mathbf{k}|$ approximation to be valid, Λ is the cut-off of the effective field theory, and we have used rotational invariance to write the momentum integral as a one-dimensional integral over $|\mathbf{k}|$. For a fixed κ, ϵ may be shown to be polynomial in δ_p, so that this logarithmic divergence differs from the polynomial divergences of the zero momentum correlators.

Traces over $\frac{\epsilon(\mathbf{k})}{\mathfrak{D}(k)}$ are also seen to be finite (compare (6.35), noting that $\epsilon(\boldsymbol{k})\sim|\boldsymbol{k}|^2$ and the $d\boldsymbol{k}$ integral has a cut-off), so that the logarithmically divergent terms in (6.27) are seen to be

$$-2i\kappa V^2|\psi_0|^2(2|\psi_0|^2\psi_0+\psi_0^3)\int dk\,\frac{1}{\mathfrak{D}(k)}. \qquad (6.38)$$

The gapped-spectrum regularisation of $\int dk\,\frac{1}{\mathfrak{D}(k)}$ is real, so that the only way for the above expression to be real (recall that (6.27) being real is the condition for tadpole cancellation) is for $|\psi_0|^2\psi_0+\psi_0^3$ to be purely imaginary. From (6.19), this is only possible if $Vn-\delta_p=\pm\frac{\kappa}{\sqrt{3}}$. Solving this equation (also recall that Vn is given by (4.17) at the inversion points) yields a single solution of $\delta_p=\sqrt{3}\kappa$ — when the inversion points coincide.

For any other relative magnitudes of δ_p and κ, the condition fails to hold and the tadpole diagrams fail to cancel (moreover, they also possess the additional logarithmic divergences found above). This means that generically, as one approaches a non-Morse critical point of the system, the current-current linear response is perturbatively divergent beyond $O(\hbar)$, nullifying the mean-field result indicative of superfluidity.

The fact that the cancellation occurs at $\delta_p=\sqrt{3}\kappa$, the point corresponding to the monostable to bistable continuous phase transition, may suggest that something interesting may be occurring here. To this end we consider the remaining terms

$$-2i\kappa\int dk\,\frac{1}{\mathfrak{D}(k)}\Big(\omega^2+\epsilon(\mathbf{k})^2+\epsilon(\mathbf{k})(3V|\psi_0|^2-2\delta)\Big)\psi_0. \qquad (6.39)$$

The bracket multiplying $\epsilon(\mathbf{k})$ is zero for $\delta=\sqrt{3}\kappa$ (since $V|\psi_0|^2=\frac{2}{3}\delta$ in this case), so we are left with

$$-2i\kappa\psi_0 \int dk \, \frac{1}{\mathfrak{D}(k)}\Big(\omega^2 + \epsilon(\mathbf{k})^2\Big). \tag{6.40}$$

This is an integral of a real non-negative quantity and thus clearly greater than zero (the integrand is zero only at $\omega = |\mathbf{k}| = 0$). For $\delta_p = \sqrt{3}\kappa$, $\psi_0 \propto 1 - \sqrt{3}i$, so that the above expression cannot be purely real. This means that, even if the logarithmic divergences cancel at $\delta_p = \sqrt{3}\kappa$, the algebraic tadpole divergences do not and so the response still diverges.

Before proceeding, we should comment on our use of a classical drive term F_p despite performing calculations to $O(\hbar^2)$. Because all expectation values we calculate are in terms of the polariton fields only, any connected diagram involving the drive fields would contain either at least two polariton-drive correlators or a drive tadpole. We know that there are no tadpoles at mean-field in the current-current response, so the drive fields would contribute only at $O(\hbar^2)$, namely to the fluctuation calculations above. At that order, the drive tadpoles would replace polariton tadpoles in any diagram in which they appeared. Since these tadpoles would have a significantly different form to the polariton tadpoles, they would fail to cancel the divergences in the latter that we demonstrate, and our analysis would remain unchanged. The presence of two polariton-drive correlators would also not affect the divergences, and thus our analysis above is insensitive to this classical field simplification.

6.3 Perturbative Results and RG at Non-Morse Critical Points

The above perturbative result is sufficient to cast serious doubt on the mean-field assertions of superfluidity we were investigating. That the higher-order fluctuation corrections are divergent is an example of the Ginzburg criterion at a phase transition, and indicates that mean-field and, by extension, perturbation theory are not to be trusted. Mathematically, this is because perturbative results can be highly misleading in the vicinity of non-Morse critical points. Conventional perturbation theory relies on the Morse Lemma to locally approximate the integrand as Gaussian — if the lemma does not apply, integrals over the non-Morse/catastrophe part of the integrand may yield divergences in the perturbative scheme.

For integrals with a finite or countable number of modes such as simple path integral problems in quantum mechanics, the appearance of elementary catastrophes in the action yields certain special functions (e.g. the Airy function above) in an exact evaluation of the propagator or partition function, when a perturbative evaluation would fail [44]. In those simple cases, however, the essential variables/field modes were discrete and the action is purely real. Problems with

a continuum of modes are typically studied via the Renormalization Group (RG), in light of which we may now consider the above result. Since RG is a subject considerably too vast to introduce here in a self-contained manner, it is suggested that the reader interested in this section but unfamiliar with RG first consult [63], which uses the same terminology and notation as we do here.

Consider the continuous phase transition at $\delta_p = \sqrt{3}\kappa$, and the following part of the Keldysh action:

$$\int dt d^2\mathbf{x}\Big(\bar{\psi}^q(i\partial_t + \nabla^2)\psi^c + 2i\kappa|\psi^q|^2\Big). \tag{6.41}$$

With two fields we are free to fix the behaviour of two couplings under the renormalization group (RG) flow, and may also choose the dynamical exponent via anisotropic scaling. Choosing to fix the couplings of $\bar{\psi}^q\nabla^2\psi^c$, $|\psi^q|^2$, and choosing the dynamical exponent to be $z = 2$ yields the following naive scaling dimensions:

$$[\psi^c] = 0, \tag{6.42}$$

$$[\psi^q] = 2. \tag{6.43}$$

If we consider a field coupled to a quantum current, this will add terms to the action of the form

$$\int dt d^2\mathbf{x}\, f^a(\mathbf{x}, t)\bar{\psi}^q\nabla_a\psi^c, \tag{6.44}$$

with $[\psi^q\nabla\psi^c] = 3$. If we consider very long-wavelength fields f^a, such that they may be considered essentially constant, f^a will then correspond to a relevant coupling — the addition of this term to the action at criticality will drive the system to a different RG fixed point, likely altering its behaviour in a non-analytic way. For this reason we expect the long-wavelength linear response to such a coupling to be divergent at the phase transition (in classical statistical mechanics such linear responses are typically second derivatives of an effective energy with names like "heat capacity" and "compressibility", explaining why these transitions are often "second order").

By the above argument, that the low-wavelength current-current response at this phase transition diverged in our perturbative calculation is unsurprising. That it diverged at all wavelengths, however, is of interest. To get a more physical sense of why this occurs, let us focus on the divergent sub-expression of (6.9):

$$\begin{aligned}&\bar{\psi}_0\Big(G_R^{11}(0)(\frac{1}{2}\bar{\psi}_0\,\mathrm{Tr}[G_K^{12}] + \psi_0\,\mathrm{Tr}[G_K^{11}]) + G_R^{12}(0)(\frac{1}{2}\psi_0\,\mathrm{Tr}[G_K^{21}]\bar{\psi}_0\,\mathrm{Tr}[G_K^{22}])\Big)+\\ &+\psi_0\Big(G_R^{21}(0)(\frac{1}{2}\bar{\psi}_0\,\mathrm{Tr}[G_K^{12}] + \psi_0\,\mathrm{Tr}[G_K^{11}]) + G_R^{22}(0)(\frac{1}{2}\psi_0\,\mathrm{Tr}[G_K^{21}] + \bar{\psi}_0\,\mathrm{Tr}[G_K^{22}])\Big).\end{aligned} \tag{6.45}$$

A little inspection shows that this is actually the $O(\hbar)$ correction to $\langle\psi^c(0)\bar{\psi}^c(0)\rangle$,

generated by diagrams of the form (mean-field ψ) $\times$ tadpole, which tells us that $\langle\psi^c(0)\bar{\psi}^c(0)\rangle$ also perturbatively diverges. This is a classic manifestation of the Ginzburg criterion, with the field fluctuations exceeding the mean-field value at the transition. Looking at Figs. 4.2 and 6.3–6.6, we see that to $O(\hbar^2)$ every diagram of the current-current is proportional either $|\psi_0|^2$ or to this $O(\hbar)$ correction. Intuitively this makes sense — the current response is proportional to the amount of condensate "available" to respond. Thus, if $\langle\psi^c(0)\bar{\psi}^c(0)\rangle$ is divergent at a phase transition in a perturbative scheme, so too ought to be the current-current response.

The physical perturbative argument and RG theory argument combined give compelling evidence for the incorrectness of the mean-field superfluid result, and the absence of superfluid at this point. While the RG argument is not directly applicable to the rest of the locus of bifurcations, these points are all dynamically unstable and correspond to first order phase transitions — one would thus a priori expect the linear response at them to also be non-analytic, and the perturbative calculation seems to support this.

6.4 Comparison With Incoherent Drive

It is instructive to contrast the above cancellation failure with the case of isotropic incoherently driven polaritons, for which Ref. [27] established the presence of superfluidity. The Keldysh action of this model may be written as

$$\begin{aligned}\mathcal{S}_{\text{inc}} = &\sum_k (\bar{\psi}^c_k \quad \bar{\psi}^q_k)\begin{pmatrix} 0 & \tilde{g}^{-1}(k) \\ (\tilde{g}^{-1})^*(k) & 2i\kappa \end{pmatrix}\begin{pmatrix} \psi^c_k \\ \psi^q_k \end{pmatrix} \\ &- \frac{V}{2}\sum_{k,k',q}\left(\bar{\psi}^c_{k-q}\bar{\psi}^q_{k'+q}[\psi^c_k\psi^c_{k'} + \psi^q_k\psi^q_{k'}] + \text{h.c.}\right),\end{aligned} \tag{6.46}$$

$$\tilde{g}^{-1} = \omega + \mu - \epsilon(\boldsymbol{k}) - i\kappa + ip(\omega+\mu), \tag{6.47}$$

$$p(\omega) = \gamma - \eta\omega, \quad \mu = \frac{\gamma-\kappa}{\eta}. \tag{6.48}$$

Here the F_p pump term of the coherent model has been replaced by the incoherent $ip(\omega+\mu)$ pump term, where μ is a chemical potential calculated from the condition for the existence of a macroscopically occupied mean-field:

$$\mu + ip(\mu) - i\kappa = V|\psi_0|^2 \implies p(\mu) = \kappa. \tag{6.49}$$

Due to the great similarity of this effective action to that for coherently driven polaritons (3.56), the diagrammatics are identical up to a redefinition of $|\psi_0|^2$

and $J(k)$. For the incoherent model these are given by

$$\tilde{J}(k) = \omega + \mu - \epsilon(\boldsymbol{k}) + i\kappa - ip(\omega + \mu) - 2V|\tilde{\psi}_0|^2, \tag{6.50}$$

$$V|\tilde{\psi}_0|^2 = \mu. \tag{6.51}$$

The condition for tadpole cancellation (6.12) studied in the preceding section carries over to the incoherent model via the $J \to \tilde{J}$, $\psi_0 \to \tilde{\psi}_0$ replacement. Since $\tilde{J}(0) = -V|\tilde{\psi}_0|^2$, the condition is satisfied and the diagrams do not cause a divergence in the gapless regime of the incoherent model. From our above discussion we see that this also means a zero $O(\hbar)$ correction to $\langle \psi^c(0)\bar{\psi}^c(0)\rangle$. Thus there is a well defined value for the condensate, the current-current response is thus finite, and superfluidity is present as expected.

Chapter 7

Conclusion

Early work [38], [39] argued, via an appeal to the Landau criterion for a complex-valued spectrum, that coherently pumped systems below the Optical Parametric Oscillator threshold could display superfluid behaviour in a wide range of pump regimes despite the breaking of $U(1)$ symmetry by the drive. We have reviewed these arguments in the context of subsequent work [33], which focused on a more rigorous definition of superfluidity via a system's current-current response tensor as opposed to the Landau criterion, and showed that the steady states identified by the Landau criterion were not superfluid but rather a kind of rigid state which does not respond to either longitudinal or transverse perturbations (as opposed to a superfluid, which should respond longitudinally but not transversely). The focus of the present part of this thesis is in turn concentrated on a restricted pump regime, namely inversion points of the bistability curve, where the excitation spectrum is gapless and mean-field calculations of the response tensor suggest superfluidity can nevertheless be found.

In the general anisotropic pump regime, we found that such inversion points exhibit diverging current-current responses. While the physical significance of these divergences was initially unclear, we demonstrated that they arise from a cusp-catastrophe structure present in the mean-field values of the system's fields. The inversion points of interest correspond to the cusp's "locus of bifurcations", a line of solutions where small variations in system parameters lead to drastic changes in behaviour due to possible bifurcations of the mean-field solution. It is generically true that at such points the linear response of the variables undergoing the bifurcation, here the system fields, diverges and we show how to relate the divergence of the linear current-current response to this.

Beyond that, in the isotropic case, we found that the mean-field current-current response at an inversion point is indicative of superfluidity. We show, however, that higher-order perturbative corrections at these points are divergent. These divergences may be viewed through either the lens of renormalization, which shows them to be driven by the current being a relevant operator, or via

perturbation theory. In the latter, they arise due to a failure of Keldysh tadpole diagrams to cancel in a consistent manner. This cancellation failure induces a divergence in the condensate magnitude, which then yields a divergence in the current-current response. These divergences indicate that the mean-field superfluid result is not reliable, as is to be expected since the inversion points in fact correspond to phase transitions.

While in both cases the divergences arise from the phase-transition nature of points along the locus of bifurcations, we see that there are two different mechanisms at play — a purely geometric, catastrophe-theoretic mechanism which manifests at the mean-field level in the anisotropic regime, and a fluctuational "Ginzburg criterion" one that appears in both the isotropic and anisotropic regimes.

I have thus shown that initially promising mean-field results indicating superfluidity in the system are invalid, and there remain no known superfluid regimes in coherently driven exciton-polaritons. Nevertheless, there are remaining possible avenues of research. Firstly, we have throughout considered a Markovian photon reservoir for the system, having demonstrated that an experimentally natural thermal reservoir will exhibit this property. Nevertheless, a number of recent works have considered the possibility of non-Markovian reservoir engineering (see [64] and references 50–56 therein) to achieve various desired many-body states. While this seems unlikely to overcome the absence of $U(1)$ symmetry in the system, it may nevertheless be worth investigating. Such an investigation, however, would be significantly more complicated than that in our present manuscript, as the resulting Keldysh action would be non-time local.

Another possible direction would be non-homogeneous systems. For example, Ref. [65] considered scattering against a defect outside a coherently pumped spot, and observed suppressed scattering in the small region around the pump spot where the fluid velocity was below the sound velocity of the sonic regime. Since the $U(1)$ symmetry of the fluid outside the pump region was not directly broken by the pump, there may be a possibility of engineering non-homogeneous systems with regions of the polariton fluid being coherently pumped and others exhibiting superfluidity. While this may prove not to be the case (interactions with fluid flowing out of the pump spot may somehow still break the $U(1)$ symmetry of the fluid outside), it is a possible interesting avenue to explore.

Appendix A

Nambu Diagrammatics for the Keldysh Action

In the main body of Part Ia, a path integral over the action (3.56) is considered. This action may be written in terms of fluctuations $(\delta\psi^c, \delta\psi^q)$ around the mean-field result $(\psi^c, \psi^q) = (\sqrt{2}\psi_0, 0)$ worked out from (4.4). From here on we simply write (ψ^c, ψ^q) for these fluctuations. Such an expansion around the mean-field will, however, contain quadratic fluctuation terms which do not fit the pattern of the quadratic term in the above action. These may be gathered in the following "Nambu" form (see Sec. 4.1 and recall that $J(k) = \omega + \Delta_p - \epsilon(\mathbf{k}) + i\kappa - 2V|\psi_0|^2$),

$$\frac{1}{2}\int dk dk' \begin{pmatrix} \bar{\psi}^c(k') \\ \psi^c(-k') \\ \bar{\psi}^q(k') \\ \psi^q(-k') \end{pmatrix}^T \begin{pmatrix} 0 & 0 & J(k) & -V\psi_0^2 \\ 0 & 0 & -V\bar{\psi}_0^2 & J^*(-k) \\ J^*(k) & -V\psi_0^2 & 2i\kappa & 0 \\ -V\bar{\psi}_0^2 & J(-k) & 0 & 2i\kappa \end{pmatrix} \delta(k-k') \begin{pmatrix} \psi^c(k) \\ \bar{\psi}^c(-k) \\ \psi^q(k) \\ \bar{\psi}^q(-k) \end{pmatrix}, \quad \text{(A.1)}$$

but this introduces a certain redundancy of degrees of freedom. This redundancy arises from the fact that the complex variables in the Nambu vector $\Psi(k) = (\psi^c(k), \bar{\psi}^c(-k), \psi^q(k), \bar{\psi}^q(-k))$ appear on both the left and right-hand sides of the matrix as (k, k') vary. As a result, the Gaussian functional integral cannot be immediately performed via the standard form for $z^\dagger M^{-1} z$ actions. Moreover, the associated measure $\mathcal{D}\Psi(k)\mathcal{D}\bar{\Psi}(k')$ is redundant if a full range is taken for (k, k').

The solution is to note that the action is invariant under the transformation $(k, k') \to (-k', -k)$. This transformation may be used to partition $\mathbb{R}^8$ into two disjoint sets Σ and Σ' such that they transform into each-other under it. There will be some ambiguity for elements of the form $(k, -k)$ since they are invariant under it, but they represent a set of measure 0 and may thus be neglected. With this partition, the action may be rewritten as (note the elimination of the $\frac{1}{2}$ factor to

preserve the action due to the halving of the integration volume)

$$\int_{\Sigma} dkdk' \begin{pmatrix} \bar{\psi}^c(k') \\ \psi^c(-k') \\ \bar{\psi}^q(k') \\ \psi^q(-k') \end{pmatrix}^T \begin{pmatrix} 0 & 0 & J(k) & -V\psi_0^2 \\ 0 & 0 & -V\bar{\psi}_0^2 & J^*(-k) \\ J^*(k) & -V\psi_0^2 & 2i\kappa & 0 \\ -V\bar{\psi}_0^2 & J(-k) & 0 & 2i\kappa \end{pmatrix} \delta(k-k') \begin{pmatrix} \psi^c(k) \\ \bar{\psi}^c(-k) \\ \psi^q(k) \\ \bar{\psi}^q(-k) \end{pmatrix} \tag{A.2}$$

and the functional measure is also taken over Σ, eliminating its redundancy and reproducing the original measure.

It remains to observe that, were we to multiply this functional integral by another where we took Σ' as the integration range, we would again obtain a functional integral with action (A.2) but the integration range unrestricted. Moreover, since in this new integral the field $\psi(-k')$, $(k,k') \in \Sigma$ in the left vector and $\psi(-k')$, $(-k',-k) \in \Sigma'$ in the right vector originate from two separate original integrals and are thus independent, the integral has no redundancy and is simply equal to the functional determinant of

$$\begin{pmatrix} 0 & 0 & J(k) & -V\psi_0^2 \\ 0 & 0 & -V\bar{\psi}_0^2 & J^*(-k) \\ J^*(k) & -V\psi_0^2 & 2i\kappa & 0 \\ -V\bar{\psi}_0^2 & J(-k) & 0 & 2i\kappa \end{pmatrix} \delta(k-k'). \tag{A.3}$$

Since the value of the original integral should not depend on whether Σ or Σ' was used, this means that it is equal to the square root of this functional determinant. We have above that the path integral in this form corresponds to the trace of a time-evolved density matrix, so that this square root should be equal to 1.

From here we may add source terms of the form

$$\begin{pmatrix} J_1(k) \\ J_2(-k) \\ J_3(k) \\ J_4(-k) \end{pmatrix}^T \begin{pmatrix} \psi^c(k) \\ \bar{\psi}^c(-k) \\ \psi^q(k) \\ \bar{\psi}^q(-k) \end{pmatrix} + \begin{pmatrix} \bar{\psi}^c(k) \\ \psi^c(-k) \\ \bar{\psi}^q(k) \\ \psi^q(-k) \end{pmatrix}^T \begin{pmatrix} J_5(k) \\ J_6(-k) \\ J_7(k) \\ J_8(-k) \end{pmatrix} \tag{A.4}$$

to either the Σ or Σ' action, depending on which range of wavevectors we wish to study, and then perform the integral over the sum of the two actions. This will be a standard Gaussian integral with source terms, yielding

$$\begin{aligned} &G[J_1,J_2,J_3,J_4,J_5,J_6,J_7,J_8] \\ &= \exp\left[-i \int_{\tilde{\Sigma}} dkdk' \begin{pmatrix} J_1(k') \\ J_2(-k') \\ J_3(k') \\ J_4(-k') \end{pmatrix}^T \begin{pmatrix} 0 & 0 & J(k) & -V\psi_0^2 \\ 0 & 0 & -V\bar{\psi}_0^2 & J^*(-k) \\ J^*(k) & -V\psi_0^2 & 2i\kappa & 0 \\ -V\bar{\psi}_0^2 & J(-k) & 0 & 2i\kappa \end{pmatrix}^{-1} \begin{pmatrix} J_5(k) \\ J_6(-k) \\ J_7(k) \\ J_8(-k) \end{pmatrix} \right] \end{aligned} \tag{A.5}$$

where we have denoted the integration range of the action to which we added the source terms by $\tilde{\Sigma}$. From here we observe that for $(k,k') \in \tilde{\Sigma}$ (denoting the other integration range by $\tilde{\Sigma}^c$, the corresponding action by $S_{\tilde{\Sigma}^c}$, and the action with source terms and integration range $\tilde{\Sigma}$ by $S_{\tilde{\Sigma},J}$),

$$\begin{aligned}
&\langle(\psi^c_k)^a(\bar{\psi}^c_{-k})^b(\psi^q_k)^c(\bar{\psi}^q_{-k})^d(\bar{\psi}^c_k)^e(\psi^c_{-k})^f(\bar{\psi}^q_k)^g(\psi^q_{-k})^h\rangle \\
&\qquad = \underbrace{\frac{\delta^a}{\delta J_1(k)^a}\frac{\delta^b}{\delta J_2(-k)^b}\frac{\delta^c}{\delta J_3(k)^c}\frac{\delta^d}{\delta J_4(-k)^d}\frac{\delta^e}{\delta J_5(k)^e}\frac{\delta^f}{\delta J_6(-k)^f}\frac{\delta^g}{\delta J_7(k)^g}\frac{\delta^h}{\delta J_8(-k)^h}}_{\partial_J} \\
&\qquad\qquad \int_{\tilde{\Sigma}} \mathcal{D}[\psi^c,\bar{\psi}^c,\psi^q,\bar{\psi}^q]\exp[iS_{\tilde{\Sigma},J}] \\
&\qquad = \partial_J\left(\underbrace{\int_{\tilde{\Sigma}^c}\mathcal{D}[\psi^c,\bar{\psi}^c,\psi^q,\bar{\psi}^q]\exp[iS_{\tilde{\Sigma}^c}]}_{1}\int_{\tilde{\Sigma}}\mathcal{D}[\psi^c,\bar{\psi}^c,\psi^q,\bar{\psi}^q]\exp[iS_{\tilde{\Sigma},J}]\right) \\
&\qquad = \partial_J G[J_1,J_2,J_3,J_4,J_5,J_6,J_7,J_8].
\end{aligned} \tag{A.6}$$

This quadratic generating function structure for expectation values means that Wick's theorem will hold for diagrammatic calculations and, by selectively choosing Σ, Σ', and to which action to add the source terms, we may use the above formula to work out the expectation of the product of any pair of field modes. This yields the following correlators:

$$\begin{aligned}
&\left\langle\begin{pmatrix}\psi^c_k\\ \bar{\psi}^c_{-k}\end{pmatrix}\begin{pmatrix}\bar{\psi}^q_k & \psi^q_{-k}\end{pmatrix}\right\rangle = iG_R(k) = \frac{i}{J(k)J^*(-k)-V^2|\psi_0|^4}\begin{pmatrix}J^*(-k) & V\psi_0^2\\ V\bar{\psi}_0^2 & J(k)\end{pmatrix}, \\
&\left\langle\begin{pmatrix}\psi^q_k\\ \bar{\psi}^q_{-k}\end{pmatrix}\begin{pmatrix}\bar{\psi}^c_k & \psi^c_{-k}\end{pmatrix}\right\rangle = iG_A(k) = \frac{i}{J(-k)J^*(k)-V^2|\psi_0|^4}\begin{pmatrix}J(-k) & V\psi_0^2\\ V\bar{\psi}_0^2 & J^*(k)\end{pmatrix}, \\
&\left\langle\begin{pmatrix}\psi^c_k\\ \bar{\psi}^c_{-k}\end{pmatrix}\begin{pmatrix}\bar{\psi}^c_k & \psi^c_{-k}\end{pmatrix}\right\rangle = iG_K(k) \\
&= \frac{2\kappa}{|J(k)J^*(-k)-V^2|\psi_0|^4|^2}\begin{pmatrix}J^*(-k)J(-k)+V^2|\psi_0|^4 & [J^*(-k)+J^*(k)]V\psi_0^2\\ [J(-k)+J(k)]V\bar{\psi}_0^2 & J^*(k)J(k)+V^2|\psi_0|^4\end{pmatrix}, \\
&\left\langle\begin{pmatrix}\psi^q_k\\ \bar{\psi}^q_{-k}\end{pmatrix}\begin{pmatrix}\bar{\psi}^q_k & \psi^q_{-k}\end{pmatrix}\right\rangle = 0.
\end{aligned} \tag{A.7}$$

Since we expanded around the mean-field, linear terms are removed from the action and quadratic ones have already been included in the matrix above, so it remains to consider the expansion of the quartic term

$$-\frac{V}{2}\int dkdk'dq\left(\bar{\psi}^c_{k-q}\bar{\psi}^q_{k'+q}[\psi^c_k\psi^c_{k'}+\psi^q_k\psi^q_{k'}]+\text{h.c.}\right) \tag{A.8}$$

into trivalent and tetravalent vertices to complete the standard diagrammatics. There are 6 topologically distinct trivalent vertices, and 4 tetravalent vertices, presented in Figs. A.1 and A.2 with their vertex factors. Solid lines with the arrow oriented towards a momentum p represent ψ^c_p, while those with an arrow pointing away from it represent $\bar{\psi}^c_p$. Analogously, such dashed lines represent ψ^q_p and $\bar{\psi}^q_p$. Standard rules for symmetry factors relating to exchange of vertices and edges then apply — symmetry multipliers have been included in the vertex factors, and it remains to divide a given diagram by its symmetry factor. Finally, since the expansion is taken around a non-zero value of ψ^c, diagrams may contain free ψ^c fields, corresponding to a factor of ψ_0, signified by circles with a line through them for ψ_0 and a cross for $\bar{\psi}_0$.

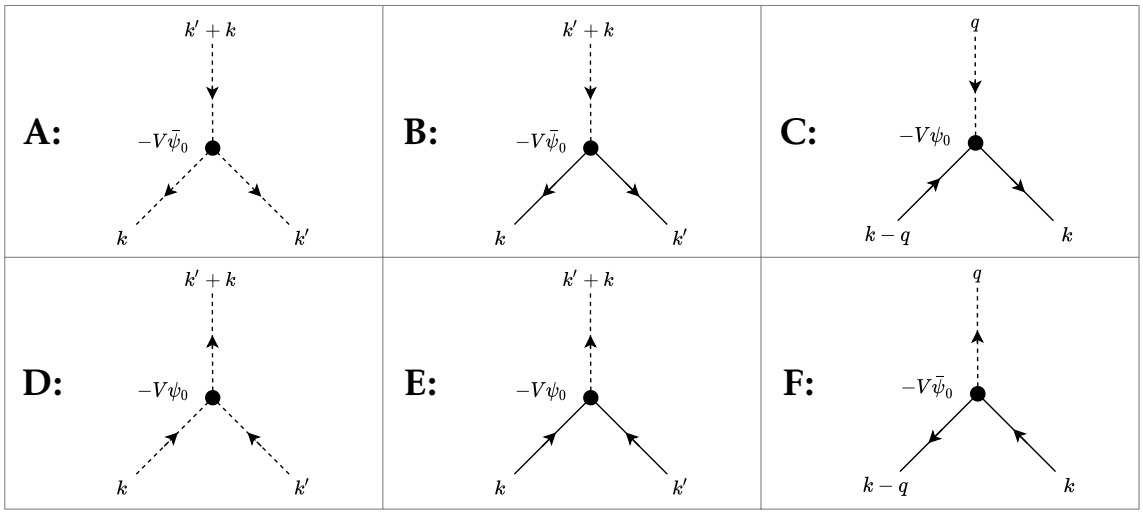

Figure A.1: Trivalent Vertices of the Quartic Interaction.

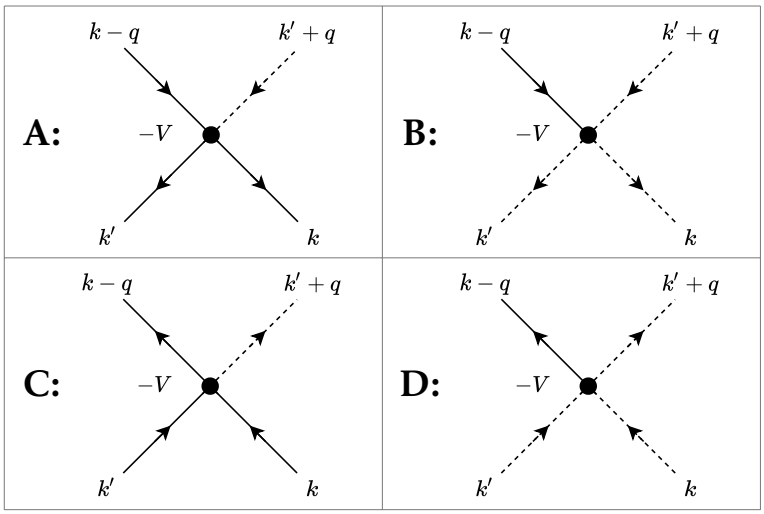

Figure A.2: Tetravalent Vertices of the Quartic Interaction.

Appendix B

Catastrophe Theory

Elementary catastrophe theory studies structurally unstable local behaviour of functions. For systems controlled by the extremization of some effective potential, such local behaviour of the extremum is frequently important [62] — for dynamical systems, the local behaviour of potential minima affects their stability, while in the Landau mean-field theory of phases such behaviour may lead to phase transitions. In the main body of this part of the thesis we find a situation where the steady-state condensate density of a non-equilibrium system is determined by the positions of the minima of a corresponding effective potential, and apply catastrophe theory to understand the resulting phenomena. We thus review catastrophe theory and its applications in this appendix, following the exposition given in [62].

In its most elementary form, catastrophe theory is the extension of two fundamental results on the local behaviour of functions, namely a corollary of the Rectification Theorem for vector fields [66] and the Morse Lemma [61].

Theorem 1 (Rectification Theorem (Corollary))
Let $f(x) = f(x_1, x_2, \ldots, x_n)$ be a smooth function with non-zero gradient at x_0:

$$\nabla f|_{x_0} \neq 0. \tag{B.1}$$

Then there exists a neighbourhood of x_0 and a smooth change of coordinates, $y = (y_1, y_2, \ldots, y_n)$, $y = y(x)$, on this neighbourhood so that

$$f(y) = y_1. \tag{B.2}$$

Theorem 2 (Morse Lemma)
Let $f(x) = f(x_1, x_2, \ldots, x_n)$ be a function with vanishing gradient and non-singular Jacobian matrix at x_0:

$$\nabla f|_{x_0} = 0, \tag{B.3}$$

$$\det[\partial^2 f / \partial x_i \partial x_j]|_{x_0} \neq 0. \tag{B.4}$$

Then there exists a neighbourhood of x_0 and a smooth change of coordinates, $y = (y_1, y_2, \ldots, y_n)$, $y = y(x)$, on this neighbourhood so that

$$f(y) = y_1^2 + y_2^2 + \ldots + y_m^2 - y_{m+1}^2 - \ldots - y_n^2, \tag{B.5}$$

where the number of positive and negative signs matches the Jacobian signature.

The first of these theorems describes the most common situation, away from a function's critical points while the second describes the local behaviour of non-degenerate, or "Morse", critical points. In particular, the Morse Lemma and related family of "Preparation Theorems" facilitate famous integral approximation methods such as Laplace's Method, the Method of Stationary Phase, and the Method of Steepest Descent, which are common in thermodynamic and QFT calculations.

A key feature of non-critical points and Morse critical points is known as "structural stability". Using the above theorems it may be shown that the addition of an infinitesimal perturbation to a function cannot change their nature — if a function $f(x)$ possesses a non-critical or a Morse critical point at x_0, then for sufficiently small ϵ, so will $f(x) + \epsilon g(x)$ (the position of the critical point may shift infinitesimally but it will remain Morse).

Catastrophe theory, then, is concerned with situations where such structural stability is absent and so-called "catastrophes" may occur from infinitesimal perturbations. The bulk of elementary catastrophe theory is contained in two further theorems, the Thom Splitting Lemma and Thom Classification Theorem:

Theorem 3 (Thom Splitting Lemma)
Let $f(x) = f(x_1, x_2, \ldots, x_n)$ be a function with vanishing gradient and singular Jacobian matrix at x_0:

$$\nabla f|_{x_0} = 0, \tag{B.6}$$

$$\det[\partial^2 f / \partial x_i \partial x_j]|_{x_0} = 0. \tag{B.7}$$

If the Jacobian matrix possesses l vanishing eigenvalues, then there exists a neighbourhood of x_0 and a smooth change of coordinates, $y = (y_1, y_2, \ldots, y_n)$, $y = y(x)$, on this neighbourhood so that the function splits as

$$f(y) = f_{NM}(y_1, \ldots, y_l) + M(y_{l+1}, \ldots, y_n), \tag{B.8}$$

$$M(y) = y_{l+1}^2 + y_{l_2}^2 + \ldots + y_{l+m}^2 - y_{l+m+1}^2 - \ldots - y_n^2, \tag{B.9}$$

$$f_{NM} \in O(y^3), \tag{B.10}$$

where $M(y)$ is a structurally stable Morse component (the number of positive and negative signs again matches the signature of the Jacobian's non-zero eigenvalues) while f_{NM} is a structurally unstable non-Morse component.

The coordinates appearing in M are known as "inessential", since they do not participate in the dramatic structural instabilities associated with non-Morse behaviour. Conversely, the coordinates appearing in f_{NM} are known as "essential". The Thom Classification Theorem seeks to classify the possible forms of the non-Morse component in the presence of external "control parameters", namely variables c upon which a function $f(x;c)$ depends but which are not coordinates (e.g. the mean and variance of a normal distribution $\mathrm{Norm}(x;\mu,\sigma)$).

Theorem 4 (Thom Classification Theorem)
Let $f_{NM}(x;c) = f(x_1,\ldots,x_l;c_1,\ldots,c_k)$ be a function of l coordinates and k control parameters, possessing a non-Morse critical point at $\mathbf{x}_0$. Then there exists a neighbourhood of x_0 and a smooth change of coordinates, $y = (y_1,y_2,\ldots,y_n)$, $y = y(x)$, on this neighbourhood so that the function takes the form of an elementary catastrophe function Cat:

$$f_{NM}(y;c) = Cat(y,c), \tag{B.11}$$

$$Cat(y,c) = CG(y) + Pert(y,c). \tag{B.12}$$

Every elementary catastrophe function consists of a catastrophe germ, CG, depending only on the coordinates, and a perturbation Pert, which is linearly dependent on the control parameters.

The possible canonical forms of catastrophe germs and perturbation terms are exhaustively catalogued for small numbers of coordinates and control parameters [62]. The addition of the most general perturbation to a given catastrophe germ is known as its universal unfolding. Structural instability comes from the dramatic effects of infinitesimal variations in the control parameters on the topology of the function's critical points. Such variations may locally create, merge, and annihilate critical points, in stark contrast to the stable regimes around non-critical and Morse critical points.

There exists a simple graphical notation for such topological configurations of critical points in the case of a function of a single coordinate. The idea is to draw a chain of circles corresponding to critical points, connected by lines and ordered from left to right per the ordering of the critical points along the real line. When the maximum possible number of critical points is present, maxima are denoted by a minus inside a circle and minima by a plus. In configurations where two or more critical points have just merged (creating a structurally unstable non-Morse critical point), the plus/minus is replaced by the number of merged critical points. If a critical point is annihilated in a configuration, that circle is removed. An example is given in Fig. B.1. More sophisticated notation exists for the multivariate case [61], but will not be used in this paper.

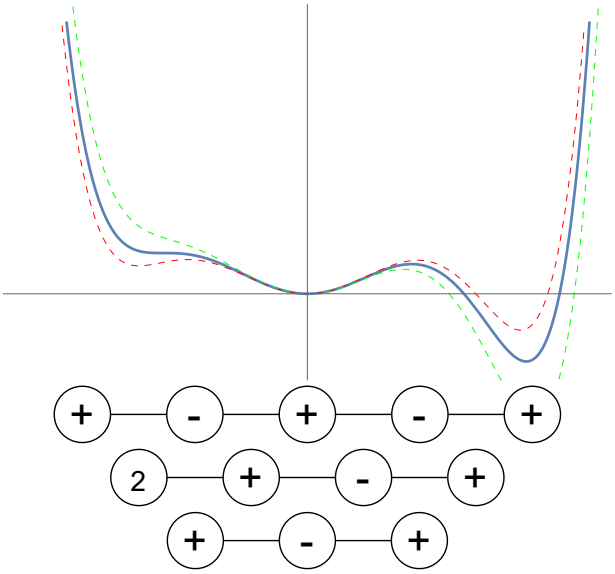

Figure B.1: Plot of a degree six polynomial for various values of its coefficients and the corresponding topological diagrams, showing how the diagrams change as the left-most critical points merge and then annihilate. From top to bottom, the topological diagrams correspond to the red, blue, and green plots respectively.

We conclude this section by proving an important result that is used in the main paper. Suppose that a function $f(x;c)$ possesses a critical point at $x_c(c)$, whose position depends smoothly on c and such that $x_c(c_0) = x_0$. We will now prove that the linear response dx_c/dc diverges if the critical point becomes non-Morse.

Expand $f(x;c)$ in a Taylor series in both coordinates and control variables, taking δx and δc such that $x_c(c_0 + \delta c) = x_0 + \delta x$:

$$\begin{aligned} f(x_0+\delta x; c_0+\delta c) = \Big[& f + \delta x_i \partial_i f + \delta c_a \partial_a f \\ & + \frac{1}{2}\delta x_i \delta x_j \partial_{ij} f + \delta x_i \delta c_a \partial_{ia} f \\ & + \frac{1}{2}\delta c_a \delta c_b f_{ab} + O(3)\Big]\Big|_{x=x_0, c=c_0} \end{aligned} \tag{B.13}$$

From this one obtains an expression for $\frac{d}{dx} f(x_0+\delta x, c_0+\delta c)$, which must be zero due to how we have chosen the increments:

$$\begin{aligned} \frac{d}{dx_i} f(x_0+\delta x, c_0+\delta c) = \Big[& \partial_i f + \delta x_j \partial_{ij} f \\ & + \delta c_a \partial_{ia} f + O(3)\Big]\Big|_{\substack{x=x_0 \\ c=c_0}}. \end{aligned} \tag{B.14}$$

$\partial_i f\Big|_{x=x_0} = 0$ by the condition that x_0 is a critical point, so we find

$$\delta x_j \partial_{ij} f + \delta c_a \partial_{ia} f = 0, \tag{B.15}$$

which yields

$$\frac{dx_{c,i}}{dc_a} = -[\partial^2 f]^{-1}_{ij} \partial_{ja} f. \tag{B.16}$$

If the critical point is non-Morse then $\partial^2 f$ will be degenerate, and its inversion in the above formula will yield a divergent linear response.

Bibliography

[1] J. Klaers, J. Schmitt, F. Vewinger, and M. Weitz, "Bose-Einstein condensation of photons in an optical microcavity," *Nature*, vol. 468, pp. 545–548, 2010.

[2] J. Marelic and R. A. Nyman, "Experimental evidence for inhomogeneous pumping and energy-dependent effects in photon Bose-Einstein condensation," *Phys. Rev. A*, vol. 91, p. 033 813, 2015.

[3] H. Ritsch, P. Domokos, F. Brennecke, and T. Esslinger, "Cold atoms in cavity-generated dynamical optical potentials," *Rev. Mod. Phys.*, vol. 85, p. 553, 2013.

[4] M. J. Hartmann, F. G. S. L. Brandao, and M. B. Plenio, "Quantum many-body phenomena in coupled cavity arrays," *Laser Photonics Rev.*, vol. 2, pp. 527–556, 2008.

[5] I. Carusotto, D. Gerace, H. E. Tureci, S. De Liberato, C. Ciuti, and A. Imamoglu, "Fermionized photons in an array of driven dissipative nonlinear cavities," *Phys. Rev. Lett.*, vol. 103, p. 033 601, 2009.

[6] C. Noh and D. G. Angelakis, "Quantum simulations and many-body physics with light," *Rep. Prog. Phys.*, vol. 80, p. 016 401, 2016.

[7] I. Carusotto and C. Ciuti, "Quantum fluids of light," *Reviews of Modern Physics*, vol. 85, no. 1, p. 299, 2013.

[8] H. Deng, H. Haug, and Y. Yamamoto, "Exciton-polariton Bose-Einstein condensation," *Rev. Mod. Phys.*, vol. 82, p. 1489, 2010.

[9] J. Keeling and N. G. Berloff, "Exciton-polariton condensation," *Contemp. Phys.*, vol. 52, p. 131, 2011.

[10] M. D. Fraser, S. Höfling, and Y. Yamamoto, "Physics and applications of exciton–polariton lasers," *Nature materials*, vol. 15, no. 10, pp. 1049–1052, 2016.

[11] D. Sanvitto, "Shiny condensates," *Nature Materials*, vol. 15, no. 10, pp. 1047–1047, Oct. 2016. DOI: 10.1038/nmat4769.

[12] D. Sanvitto and S. Kéna-Cohen, "The road towards polaritonic devices," *Nature materials*, vol. 15, no. 10, pp. 1061–1073, 2016.

[13] T. Liew, "Electrical spin switching," *Nature Materials*, vol. 15, no. 10, pp. 1053–1054, 2016.

[14] A. Dreismann, H. Ohadi, Y. del Valle-Inclan Redondo, *et al.*, "A sub-femtojoule electrical spin-switch based on optically trapped polariton condensates," *Nature materials*, vol. 15, no. 10, pp. 1074–1078, 2016.

[15] I. Shelykh, R. Johne, D. Solnyshkov, and G. Malpuech, "Optically and electrically controlled polariton spin transistor," *Physical Review B*, vol. 82, no. 15, p. 153 303, 2010.

[16] C. Schneider, A. Rahimi-Iman, N. Y. Kim, *et al.*, "An electrically pumped polariton laser," *Nature*, vol. 497, no. 7449, pp. 348–352, 2013.

[17] P. Bhattacharya, B. Xiao, A. Das, S. Bhowmick, and J. Heo, "Solid state electrically injected exciton-polariton laser," *Physical review letters*, vol. 110, no. 20, p. 206 403, 2013.

[18] A. Imamog, R. Ram, S. Pau, Y. Yamamoto, *et al.*, "Nonequilibrium condensates and lasers without inversion: Exciton-polariton lasers," *Physical Review A*, vol. 53, no. 6, p. 4250, 1996.

[19] T. Liew, A. Kavokin, and I. Shelykh, "Optical circuits based on polariton neurons in semiconductor microcavities," *Physical Review Letters*, vol. 101, no. 1, p. 016 402, 2008.

[20] T. Espinosa-Ortega and T. C. H. Liew, "Complete architecture of integrated photonic circuits based on and and not logic gates of exciton polaritons in semiconductor microcavities," *Physical Review B*, vol. 87, no. 19, p. 195 305, 2013.

[21] A. Amo, J. Lefrère, S. Pigeon, *et al.*, "Superfluidity of polaritons in semiconductor microcavities," *Nat. Phys.*, vol. 5, p. 805, 2009.

[22] A. Amo, D. Sanvitto, F. P. Laussy, *et al.*, "Collective fluid dynamics of a polariton condensate in a semiconductor microcavity," *Nature*, vol. 457, pp. 291–295, 2009.

[23] A. C. Berceanu, L. Dominici, I. Carusotto, *et al.*, "Multicomponent polariton superfluidity in the optical parametric oscillator regime," *Phys. Rev. B*, vol. 92, p. 035 307, 2015.

[24] D. Sanvitto, F. M. Marchetti, M. H. Szymańska, *et al.*, "Persistent currents and quantized vortices in a polariton superfluid," *Nat. Phys.*, vol. 6, pp. 527–533, 2010.

[25] K. G. Lagoudakis, M. Wouters, M. Richard, *et al.*, "Quantized vortices in an exciton-polariton condensate," *Nat. Phys.*, vol. 4, pp. 706–710, 2008.

[26] M. Wouters and I. Carusotto, "Superfluidity and critical velocities in nonequilibrium Bose-Einstein condensates," *Phys. Rev. Lett.*, vol. 105, p. 020 602, 2010.

[27] J. Keeling, "Superfluid density of an open dissipative condensate," *Phys. Rev. Lett.*, vol. 107, p. 080 402, 2011.

[28] A. Janot, T. Hyart, P. R. Eastham, and B. Rosenow, "Superfluid stiffness of a driven dissipative condensate with disorder," *Phys. Rev. Lett.*, vol. 111, p. 230 403, 2013.

[29] V. N. Gladilin and M. Wouters, "Normal and superfluid fractions of inhomogeneous nonequilibrium quantum fluids," *Phys. Rev. B*, vol. 93, p. 134 511, 2016.

[30] G. Wachtel, L. M. Sieberer, S. Diehl, and E. Altman, "Electrodynamic duality and vortex unbinding in driven-dissipative condensates," *Phys. Rev. B*, vol. 94, p. 104 520, 2016.

[31] J. Keeling, L. M. Sieberer, E. Altman, L. Chen, S. Diehl, and J. Toner, "Superfluidity and phase correlations of driven dissipative condensates," in *Universal Themes of Bose-Einstein Condensation*, N. P. Proukakis, D. W. Snoke, and P. B. Littlewood, Eds., Cambridge: Cambridge University Press, 2017, p. 205.

[32] E. Cancellieri, F. M. Marchetti, M. H. Szymańska, and C. Tejedor, "Superflow of resonantly driven polaritons against a defect," *Phys. Rev. B*, vol. 82, p. 224 512, 2010.

[33] R. Juggins, J. Keeling, and M. Szymańska, "Coherently driven microcavity-polaritons and the question of superfluidity," *Nature communications*, vol. 9, no. 1, pp. 1–8, 2018.

[34] J. Kasprzak, M. Richard, S. Kundermann, *et al.*, "Bose-Einstein condensation of exciton polaritons," *Nature*, vol. 443, pp. 409–414, 2006.

[35] M. H. Szymańska, J. Keeling, and P. B. Littlewood, "Mean-field theory and fluctuation spectrum of a pumped decaying bose-fermi system across the quantum condensation transition," *Phys. Rev. B*, vol. 75, p. 195 331, 2007.

[36] M. Wouters and I. Carusotto, "Excitations in a nonequilibrium bose-einstein condensate of exciton polaritons," *Phys. Rev. Lett.*, vol. 99, p. 140 402, 2007.

[37] A. Baas, J.-P. Karr, M. Romanelli, A. Bramati, and E. Giacobino, "Quantum degeneracy of microcavity polaritons," *Phys. Rev. Lett.*, vol. 96, p. 176 401, 2006.

[38] I. Carusotto and C. Ciuti, "Probing microcavity polariton superfluidity through resonant rayleigh scattering," *Physical review letters*, vol. 93, no. 16, p. 166 401, 2004.

[39] C. C. I. Carusotto, "Quantum fluid effects and parametric instabilities in microcavities," *physica status solidi (b)*, 2005. DOI: 10.1002/pssb.200560961.

[40] R. Juggins, "Superfluidity in coherently driven microcavity-polaritons," Ph.D. dissertation, UCL (University College London), 2019.

[41] H. Deng, H. Haug, and Y. Yamamoto, "Exciton-polariton bose-einstein condensation," *Rev. Mod. Phys.*, vol. 82, pp. 1489–1537, 2 May 2010. DOI: 10.1103/RevModPhys.82.1489.

[42] C. Ciuti, P. Schwendimann, and A. Quattropani, "Theory of polariton parametric interactions in semiconductor microcavities," *Semiconductor science and technology*, vol. 18, no. 10, S279, 2003.

[43] M. Hertzog, M. Wang, J. Mony, and K. Börjesson, "Strong light–matter interactions: A new direction within chemistry," *Chemical Society Reviews*, vol. 48, no. 3, pp. 937–961, 2019.

[44] L. S. Schulman, *Techniques and applications of path integration*. Courier Corporation, 2012.

[45] A. Polkovnikov, "Phase space representation of quantum dynamics," *Annals of Physics*, vol. 325, no. 8, pp. 1790–1852, 2010.

[46] R. J. Glauber, "Coherent and incoherent states of the radiation field," *Physical Review*, vol. 131, no. 6, p. 2766, 1963.

[47] D. Nigro, "On the uniqueness of the steady-state solution of the lindblad–gorini–kossakowski–sudarshan equation," *Journal of Statistical Mechanics: Theory and Experiment*, vol. 2019, no. 4, p. 043 202, 2019.

[48] A. Kamenev, *Field theory of non-equilibrium systems*. Cambridge University Press, 2023.

[49] A. Colla, N. Neubrand, and H.-P. Breuer, "Initial correlations in open quantum systems: Constructing linear dynamical maps and master equations," *New Journal of Physics*, vol. 24, no. 12, p. 123 005, 2022.

[50] L. Sieberer, S. D. Huber, E. Altman, and S. Diehl, "Nonequilibrium functional renormalization for driven-dissipative bose-einstein condensation," *Physical Review B*, vol. 89, no. 13, p. 134 310, 2014.

[51] I. Timofeev, R. Juggins, and M. Szymańska, "Geometric and fluctuational divergences in the linear response of coherently driven microcavity polaritons and their relation to superfluidity," *Physical Review B*, vol. 108, no. 21, p. 214 513, 2023.

[52] L. Pitaevskii and S. Stringari, *Bose-Einstein condensation and superfluidity*. Oxford University Press, 2016, vol. 164.

[53] A. A. Abrikosov, L. P. Gorkov, and I. E. Dzyaloshinski, *Methods of quantum field theory in statistical physics*. Courier Corporation, 2012.

[54] L. Sieberer, "Universality in driven-dissipative quantum many-body systems," Ph.D. dissertation, University of Innsbruck (Austria), 2015.

[55] V. Hakim, S. Pigeon, and A. Aftalion, "Metamorphoses of the flow past an obstacle of a resonantly driven bistable polariton fluid," *Physical Review B*, vol. 107, no. 4, p. 045 306, 2023.

[56] P. Stepanov, I. Amelio, J.-G. Rousset, *et al.*, "Dispersion relation of the collective excitations in a resonantly driven polariton fluid," *Nature communications*, vol. 10, no. 1, p. 3869, 2019.

[57] F. Claude, M. J. Jacquet, R. Usciati, *et al.*, "High-resolution coherent probe spectroscopy of a polariton quantum fluid," *Physical Review Letters*, vol. 129, no. 10, p. 103 601, 2022.

[58] F. Claude, M. J. Jacquet, I. Carusotto, Q. Glorieux, E. Giacobino, and A. Bramati, "Spectrum of collective excitations of a quantum fluid of polaritons," *Physical Review B*, vol. 107, no. 17, p. 174 507, 2023.

[59] E. Talbot and A. Griffin, "High-and low-frequency behaviour of response functions in a bose liquid: One-loop approximation," *Annals of Physics*, vol. 151, no. 1, pp. 71–98, 1983.

[60] A. Griffin, *Excitations in a Bose-condensed liquid* (Cambridge Studies in Low Temperature Physics 4). Cambridge University Press, 1993.

[61] K. Okada, *Catastrophe Theory and Phase Transitions*. Trans Tech Publ, 1993.

[62] R. Gilmore, "Catastrophe theory," *Encyclopedia of applied physics*, vol. 3, pp. 85–115, 1992.

[63] L. M. Sieberer, M. Buchhold, and S. Diehl, "Keldysh field theory for driven open quantum systems," *Reports on Progress in Physics*, vol. 79, no. 9, p. 096 001, 2016.

[64] J. Lebreuilly and I. Carusotto, "Quantum simulation of zero-temperature quantum phases and incompressible states of light via non-markovian reservoir engineering techniques," *Comptes Rendus Physique*, vol. 19, no. 6, pp. 433–450, 2018.

[65] I. Amelio and I. Carusotto, "Perspectives in superfluidity in resonantly driven polariton fluids," *Physical Review B*, vol. 101, no. 6, p. 064 505, 2020.

[66] V. Arnold, *Ordinary Differential Equations*. The MIT Press, 1973.

Part II

Keldysh-Derived Truncated Wigner Method in the Study of Superfluidity

Chapter 8

General Markovian Actions

This part of the thesis addresses an alternative approach to studying superfluidity in Markovian driven-dissipative systems. Whereas the previous, significantly longer, part took an analytical Keldysh functional integral approach, here I address the application of the numerical Truncated Wigner technique (to be introduced in Sec. 9.1) to the same problem.

At the same time, the model of a Part Ia was based on a specific microscopic system and the associated Keldysh action was derived by combining two copies of a path integral describing the unitary evolution of the system and its environment, then integrating out the spurious environment variables. If one is in possession of a reasonable model of the environment and its interactions with the system, this is a reasonable way to proceed. It would be somehow inelegant, however, if to produce a description of an open subsystem a full model of a total closed system was always the required starting point. It seems evident that in many situations we would like to speak of just the open system and the properties of its external interactions, yet even simple features such as Markovian evolution may be tedious to engineer starting with a full environment model: we have seen the multi-step reasoning required to show the Markovian nature of the coherently driven polariton system.

Since I will restrict my numerical approach to studying superfluidity in Markovian systems but with a wide range of possible external interactions, we begin with a language in which such models may be specified without the repeated work of specifying (likely unrealistic) environment models. This language will also be used in Parts II and III, making this an especially important introductory chapter[1]. In the following two chapters the numerical method will be introduced and then applied to the specific problem of superfluidity.

[1] This chapter covers standard textbook and literature material rather than my original contributions.

8.1 CPTP Maps

This language is that of the Completely Positive Trace Preserving (CPTP) maps often encountered in quantum information. The full definition of these objects is more involved than is required for our purposes so we will speak of them as maps between operators on Hilbert spaces[2]. These objects physical meaning is that of maps between density matrices corresponding to the time evolution of one matrix into the other, and their properties are precisely those that ensure they do this correctly:

- Positive: The maps must map positive operators to positive operators, since all density matrices are positive semi-definite.

- Completely Positive: The above must still hold true if we tensor the map with the identity map on operators of an arbitrary auxiliary Hilbert space. As will be discussed in the next section, this is not true of every open subsystem and thus CPTP maps do not cover all possible subsystem evolutions. They do, however, to a very large class of these.

- Trace Preserving: Density matrices are trace one and this must be preserved.

- Linear: Unsurprisingly for a quantum evolution operator, the maps must be linear.

The last property is clear when we consider the connection between CPTP maps and our earlier physical construction. Stinespring's dilation theorem [1] says (once again discarding a large amount of mathematical rigour) that any CPTP map may be constructed by attaching an 'ancilla' space to the system (dilation), evolving with a unitary operator, and then tracing out the ancilla. In a condensed matter setting the ancilla is precisely the environment, so that our earlier construction for the polaritons featured an ancilla in the form of the thermal photon bath, and this affirms the obvious physical view that open quantum systems are subsystems of closed systems evolving in a unitary manner. This connection is sometimes known as the 'Church of the Larger Hilbert Space' [2].

CPTP maps $\Phi(\rho)$ of density matrices ρ may be described using what are known

[2]In fact two of the main theorems characterizing representations of CPTP maps, Choi's and Kraus' theorems, assume that the Hilbert spaces are finite-dimensional in their classical forms. This will pose no problem when we later deal with pure spin systems, but is unfortunate in the case of the present field theory considerations. Here we will take the easy way out and implicitly work with finite-dimensional spaces, pointing out later when trouble arises from this assumption.

as Kraus operators B_k so that

$$\Phi(\rho) = \sum_k B_k \rho B_k^\dagger, \tag{8.1}$$

$$\sum_k B_k^\dagger B_k = 1. \tag{8.2}$$

Moreover, if one is content to restrict consideration to Markovian evolution, evolution may be described by what is known as the Lindblad master equation. This equation is specified via a superoperator known as the Lindbladian, and it is precisely the mechanism of constructing this operator that provides the language for describing systems that we are seeking. The rest of this chapter will thus be devoted to the derivation of the Lindblad equation. We follow the compact derivation in Ref. [3], which in turn follows Ref. [4].

8.1.1 Kraus Operators

We begin by demonstrating how the representation of the evolution of a subsystem in terms of Kraus operators comes about. We will start from a closed system with density matrix ρ evolving in the Schrödinger picture via unitary operators $U(t)$ such that

$$\rho(t) = U(t)\rho U^{-1}(t). \tag{8.3}$$

Suppose now that the closed system is partitioned into a subsystem and an environment, with the initial total density matrix separating into subsystem ρ_s and environment ρ_e density matrices as

$$\rho(0) = \rho_s(0) \otimes \rho_e(0). \tag{8.4}$$

This assumption physically corresponds to setting $t = 0$ at the moment the subsystem and environment first come into contact. If one starts in an initially entangled total state violating this construction, the resulting evolution may be non-CPTP — specifically complete positivity may be lost [5]. We will not consider this situation, assuming that we can always start in a completely separable state. The evolution of the subsystem density matrix is then given by

$$\rho_s(t) = \mathrm{Tr}_e\Big[U(t)\rho U^{-1}(t)\Big]. \tag{8.5}$$

Suppose now that we choose an orthonormal eigenbasis $|\psi_\alpha\rangle$ of $\rho_e(0)$ so that

$$\rho_e(0) = \sum_\alpha \lambda_\alpha |\psi_\alpha\rangle\langle\psi_\alpha|, \tag{8.6}$$

$$\sum_\alpha \lambda_\alpha = 1, \tag{8.7}$$

$$\langle\psi_\alpha|\psi_\beta\rangle = \delta_{\alpha,\beta}. \tag{8.8}$$

Then

$$\begin{aligned} \mathrm{Tr}_e\Big[U(t)\rho U^{-1}(t)\Big] &= \sum_{\alpha,\beta}\Big[I_s\otimes\langle\psi_\beta|\Big]U(t)\left[\rho_s(0)\otimes\lambda_\alpha|\psi_\alpha\rangle\langle\psi_\alpha|\right]U^{-1}(t)\Big[I_s\otimes|\psi_\beta\rangle\Big] \\ &= \sum_{\alpha,\beta} B_{\alpha\beta}(t)\rho_s(0)B^\dagger_{\alpha\beta}(t) = \mathcal{V}(t)\rho_s(0), \end{aligned} \tag{8.9}$$

where

$$B_{\alpha\beta} = \Big[I_s\otimes\langle\psi_\beta|\Big]U(t)\Big[I_s\otimes\sqrt{\lambda_\alpha}|\psi_\alpha\rangle\Big] \tag{8.10}$$

and $\mathcal{V}(t)$ is a 'superoperator', meaning it is a linear operator acting on the space of the system's linear operators interpreted as a vector space. We will typically typeset superoperators in calligraphic font.

Verifying that

$$\begin{aligned} \sum_{\alpha,\beta} B^\dagger_{\alpha\beta}B_{\alpha\beta} &= \sum_{\alpha,\beta}\Big[I_s\otimes\sqrt{\lambda_\alpha}\langle\psi_\alpha|\Big]U^{-1}(t)\Big[I_s\otimes|\psi_\beta\rangle\langle\psi_\beta|\Big]U(t)\Big[I_s\otimes\sqrt{\lambda_\alpha}|\psi_\alpha\rangle\Big] \\ &= \sum_\alpha\Big[I_s\otimes\sqrt{\lambda_\alpha}\langle\psi_\alpha|\Big]U^{-1}(t)\left[I_s\otimes I_e\right]U(t)\Big[I_s\otimes\sqrt{\lambda_\alpha}|\psi_\alpha\rangle\Big] \\ &= \sum_\alpha\Big[I_s\otimes\sqrt{\lambda_\alpha}\langle\psi_\alpha|\Big]\Big[I_s\otimes\sqrt{\lambda_\alpha}|\psi_\alpha\rangle\Big] \\ &= \sum_\alpha \lambda_\alpha I_s = I_s, \end{aligned} \tag{8.11}$$

we see that we have reproduced the Kraus operators mentioned in the previous section. The resulting map is positive and trace-preserving by construction, the latter property being easily verified from the above equality and cyclicity of the trace. In finite-dimensional spaces Kraus' theorem [6] allows one to invert this logic, showing that any map written in terms of such operators is CPTP.

8.1.2 Lindblad Master Equation

Our goal now is to move from the general evolution equation

$$\rho_s(t) = \mathcal{V}(t)\rho_s(0) = \sum_{\alpha,\beta} B_{\alpha\beta}(t)\rho_s(0)B^\dagger_{\alpha\beta}(t) \tag{8.12}$$

to a Markovian one of the form

$$\frac{d}{dt}\rho_s(t) = \mathcal{L}(t)\rho_s(t). \tag{8.13}$$

For an open quantum system Markovian evolution means that the states of the system and its environment are always decoupled, i.e. $\rho(t) = \rho_s(t)\otimes\rho_e(t)$, and this assumption will be used to obtain the above form.

Suppose that $\{I, F_i\}$, where I is the identity operator, form a basis for the space of linear system operators. Decomposing the Kraus operators in this basis via the Hilbert-Schmidt inner product $(A, B) = \mathrm{Tr}[A^\dagger B]$, we find

$$B_{\alpha\beta}(t) = I(I, B_{\alpha\beta}(t)) + \sum_i F_i(F_i, B_{\alpha\beta}(t)). \tag{8.14}$$

Denoting

$$a(t) = \sum_{\alpha,\beta}(I, B_{\alpha\beta}(t))(I, B^\dagger_{\alpha\beta}(t)), \tag{8.15}$$

$$b_i(t) = \sum_{\alpha,\beta}(I, B_{\alpha\beta}(t))\overline{(F_i, B_{\alpha\beta}(t))}, \tag{8.16}$$

$$c_{ij}(t) = \sum_{\alpha,\beta}(F_i, B_{\alpha\beta}(t))\overline{(F_j, B_{\alpha\beta}(t))}, \tag{8.17}$$

we may rewrite the evolution equation as

$$\rho_s(t) = a(t)\rho_s(0) + \sum_i \left(\bar{b}_i(t)F_i\rho_s(0) + b_i(t)\rho_s(0)F_i^\dagger\right) + \sum_{i,j} c_{ij}(t)F_i\rho_s(0)F_j^\dagger. \tag{8.18}$$

Consider the rate of change of the density matrix at the initial moment in time:

$$\dot{\rho}_s(0) = \dot{a}(0)\rho_s(0) + \sum_i \left(\dot{\bar{b}}_i(0)F_i\rho_s(0) + \dot{b}_i(0)\rho_s(0)F_i^\dagger\right) + \sum_{i,j} \dot{c}_{ij}(0)F_i\rho_s(0)F_j^\dagger. \tag{8.19}$$

This moment in time was distinguished by being the moment when the total density matrix had the decoupled form, for instance when the system and environment first came into contact. As mentioned above, however, in the Markovian case the density matrix always has this form and thus nothing specific distinguishes one moment in time from another. This leads us to the conclusion that the evolution equation should have the above form at every moment in time, yielding the general form of a Markovian evolution equation

$$\dot{\rho}_s(t) = \alpha(t)\rho_s(t) + \sum_i \left(\bar{\beta}_i(t)F_i\rho_s(t) + \beta_i(t)\rho_s(t)F_i^\dagger\right) + \sum_{i,j} \gamma_{ij}(t)F_i\rho_s(t)F_j^\dagger \tag{8.20}$$

with the functions[3] $\alpha(t)$, $\beta_i(t)$, and $\gamma_{ij}(t)$ inheriting any constraints on $\dot{a}(0)$, $\dot{b}(0)$, $\dot{c}_{ij}(0)$ in (8.19). In particular, $\gamma_{ij}(t)$ is a Hermitian matrix. Moreover, since for any vector v_i it holds that $\sum_{ij} \bar{v}_i c_{ij}(t) v_j = \sum_{\alpha,\beta} \left|(\sum_i \bar{v}_i F_i, B_{\alpha\beta}(t))\right|^2 \geq 0$, $c_{ij}(t)$ must be positive semi-definite. Because $B_{\alpha\beta}(0) = I$ we must have $c_{ij}(0) = 0$, and the previous property thus means that $\dot{c}_{ij}(0)$ must also be positive semi-definite. Therefore $\gamma_{ij}(t)$ must be positive semi-definite.

We may also combine $\sum_i \bar{\beta}_i(t) F_i = F$ to rewrite the above as

$$\dot{\rho}_s(t) = \alpha(t)\rho_s(t) + F\rho_s(t) + \rho_s(t)F^\dagger + \sum_{i,j} \gamma_{ij}(t) F_i \rho_s(t) F_j^\dagger. \tag{8.21}$$

Some further simplifications are possible, and in fact required to enforce trace-preservation. Specifically, we know that the trace of the left hand side of the above is 0:

$$\mathrm{Tr}\,\dot{\rho}_s(t) = 0 = \mathrm{Tr}\left[\alpha(t)\rho_s(t) + F\rho_s(t) + \rho_s(t)F^\dagger + \sum_{i,j} \gamma_{ij}(t) F_i \rho_s(t) F_j^\dagger\right]. \tag{8.22}$$

To explicitly incorporate the above condition into the equation we split the F operator into Hermitian and anti-Hermitian parts (both g and H are Hermitian)

$$F(t) = g(t) - iH(t), \tag{8.23}$$

obtaining

$$\dot{\rho}_s(t) = -i[H(t), \rho_s(t)] + \left\{\frac{\alpha(t)}{2} I + g(t), \rho_s(t)\right\} + \sum_{i,j} \gamma_{ij}(t) F_i \rho_s(t) F_j^\dagger. \tag{8.24}$$

Taking the trace and using its cyclicity (note the trace of a commutator is zero), we find the condition

$$\mathrm{Tr}\left[\left(\alpha(t) I + 2g(t) + \sum_{i,j} \gamma_{ij}(t) F_j^\dagger F_i\right)\rho_s(t)\right] = 0. \tag{8.25}$$

Since the above must hold for any $\rho_s(t)$ and $g(t)$ is arbitrary, we must take the latter to be

$$g(t) = -\frac{1}{2}\left(\alpha(t) I + \sum_{i,j} \gamma_{ij}(t) F_j^\dagger F_i\right), \tag{8.26}$$

[3] The time dependence of these parameters in the non-stationary cases arises because in that case $a(t)$, $b(t)$, $c(t)$, and thus their derivatives depend on the moment in time that is chosen to be $t = 0$. When we use the fact that, for a Markovian system, the always decoupled density matrix means we can choose any time as $t = 0$, we must account for this implicit time dependence.

giving the trace-preserving evolution equation

$$\dot{\rho}_s(t) = -i[H, \rho_s(t)] - \frac{1}{2}\sum_{i,j}\left\{\gamma_{ij}(t)F_j^\dagger F_i, \rho_s(t)\right\} + \sum_{i,j}\gamma_{ij}(t)F_i\rho_s(t)F_j^\dagger. \tag{8.27}$$

This equation is referred to as the 'first standard form' by Breuer and Petruccione [4] and, so long as γ_{ij} is chosen to be Hermitian positive semi-definite, is sufficient to ensure valid evolution of the density matrix. These properties of γ_{ij} may, however, be built explicitly into the equation by diagonalising $\gamma_{ij}(t)$ with unitary matrices $V_{ij}(t)$:

$$\gamma_i(t)\delta_{ij} = \sum_{pq} V_{ip}^\dagger(t)\gamma_{pq}(t)V_{qj}(t), \tag{8.28}$$

$$\gamma_i(t) \geq 0, \tag{8.29}$$

$$L_i(t) = F_j V_{ji}(t), \tag{8.30}$$

$$\dot{\rho}_s(t) = -i[H, \rho_s(t)] + \sum_i \gamma_i(t)\left[L_i(t)\rho_s(t)L_i^\dagger(t) - \frac{1}{2}\left\{L_i^\dagger(t)L_i(t), \rho_s(t)\right\}\right]. \tag{8.31}$$

The last equation above is known as the Lindblad Master Equation, and is the general master equation[4] describing Markovian CPTP maps. If the evolution is stationary, i.e. α, β_i, and γ_{ij} are constant, it takes the particularly simple form

$$\dot{\rho}_s(t) = -i[H, \rho_s(t)] + \sum_i \gamma_i\left[L_i\rho_s(t)L_j^\dagger - \frac{1}{2}\left\{L_j^\dagger L_i, \rho_s(t)\right\}\right]. \tag{8.32}$$

The superoperator associated with this evolution

$$\mathcal{L}(t)\rho = -i[H, \rho] + \sum_i \gamma_i(t)\left[L_i(t)\rho L_j^\dagger(t) - \frac{1}{2}\left\{L_j^\dagger(t)L_i(t), \rho\right\}\right], \tag{8.33}$$

is known as the Lindbladian, the operators L_i are known as jump operators, and the portion of the Lindbladian containing these operators and the $\gamma_i(t)$ terms is known as the dissipator. The Lindbladian assumes a similar role to that of the Hamiltonian in unitary dynamics, it being possible to write the solution to the Lindbladian master equation as

$$\rho_s(t) = \mathcal{V}(t, 0)\rho_s(0), \tag{8.34}$$

$$\mathcal{V}(t, r) = \mathcal{T}\, e^{\int_r^t ds\, \mathcal{L}(s)}, \tag{8.35}$$

$$\mathcal{V}(t, t) = \mathcal{I}. \tag{8.36}$$

[4] We will shortly see that it has close connections with the master equations appearing in the theory of stochastic processes.

When the evolution is stationary, as it will typically be for us, this simplifies to

$$\rho_s(t) = \mathcal{V}(t)\rho_s(0), \tag{8.37}$$

$$\mathcal{V}(t) = e^{t\mathcal{L}}, \tag{8.38}$$

$$\mathcal{V}(0) = \mathcal{I}, \tag{8.39}$$

with the evolution superoperator $\mathcal{V}(t)$ obeying a Markovian Chapman–Kolmogorov equation:

$$\mathcal{V}(t+s) = \mathcal{V}(t)\mathcal{V}(s). \tag{8.40}$$

An important difference with the case of unitary evolution is that the superoperator $\mathcal{V}(t)$ will generally not possess a well-behaved inverse for an infinite-dimensional system. Indeed, much like in the case of the heat equation, running the Lindbladian master equation backwards in time is generally not a well-posed problem for such systems. Driven-dissipative evolution described by this equation is therefore generally 'one-way'. One way of understanding this, related to the spectral properties of $\mathcal{L}$, will be elaborated on further in Part II.

8.2 Keldysh Action from Lindblad Master Equation

Having obtained the general form of the evolution superoperator for Markovian driven-dissipative systems, thus allowing us to easily write down models without worrying about the specifics of the reservoir ancilla, we now require a way to map evolution written in this language into a suitable Keldysh functional integral. We will present here a straightforward mechanism to achieve this, sufficient for our present purposes, due to Ref. [7]. In Part II of this thesis I will provide an alternative construction that rectifies certain deficiencies of the present approach, but doing so now would take us too far afield relative to our present goals.

Similar to the construction of Sec.3.1.1, the starting point is the Trotter decomposition of the evolution superoperator[5] ($\epsilon = \frac{2T}{N+1}$):

$$\rho_T = e^{2T\mathcal{L}}\rho_{-T} = \left[\prod_{n=1}^{N+1} e^{\epsilon\mathcal{L}}\right]\rho_{-T}. \tag{8.41}$$

We may use the coherent state resolution of identity to write an iterative evolu-

[5] We will present the construction, as in [7], for a stationary evolution. Adapting it to a time-dependent $\mathcal{L}(t)$ is not conceptually difficult but adds visual clutter to the presentation, and we will not be considering any non-stationary models.

tion equation for the matrix elements of the density matrix ρ_n at times $t = \epsilon n - T$:

$$\begin{aligned}&\langle\psi^+_{\boldsymbol{k},n+1}|\rho_{n+1}|\psi^-_{\boldsymbol{k},n+1}\rangle = \langle\psi^+_{\boldsymbol{k},n+1}|e^{\epsilon\mathcal{L}}\rho_n|\psi^-_{\boldsymbol{k},n+1}\rangle\\ &= \int \mathcal{D}[\psi^+_{\boldsymbol{k},n},\bar\psi^+_{\boldsymbol{k},n},\psi^-_{\boldsymbol{k},n},\bar\psi^-_{\boldsymbol{k},n}]\langle\psi^+_{\boldsymbol{k},n+1}|e^{\epsilon\mathcal{L}}\Big[|\psi^+_{\boldsymbol{k},n}\rangle\langle\psi^-_{\boldsymbol{k},n}|\Big]|\psi^-_{\boldsymbol{k},n+1}\rangle\langle\psi^+_{\boldsymbol{k},n}|\rho_n|\psi^-_{\boldsymbol{k},n}\rangle.\end{aligned} \tag{8.42}$$

Recursively applying this equation yields

$$\begin{aligned}&\langle\psi^+_{\boldsymbol{k},N+1}|\rho_T|\psi^-_{\boldsymbol{k},N+1}\rangle\\ &= \int\prod_{n=0}^{N}\Big[\mathcal{D}[\psi^+_{\boldsymbol{k},n},\bar\psi^+_{\boldsymbol{k},n},\psi^-_{\boldsymbol{k},n},\bar\psi^-_{\boldsymbol{k},n}]\langle\psi^+_{\boldsymbol{k},n+1}|e^{\epsilon\mathcal{L}}\Big[|\psi^+_{\boldsymbol{k},n}\rangle\langle\psi^-_{\boldsymbol{k},n}|\Big]|\psi^-_{\boldsymbol{k},n+1}\rangle\Big]\langle\psi^+_{\boldsymbol{k},0}|\rho_{-T}|\psi^-_{\boldsymbol{k},0}\rangle,\end{aligned} \tag{8.43}$$

and it is the terms in the product on the right hand side that generate the action of the resulting functional integral.

Taking all operators in $\mathcal{L}$ to be normal ordered[6] we may approximate (again up to $O(\epsilon^2)$ terms)

$$\begin{aligned}&\langle\psi^+_{\boldsymbol{k},n+1}|e^{\epsilon\mathcal{L}}\Big[|\psi^+_{\boldsymbol{k},n}\rangle\langle\psi^-_{\boldsymbol{k},n}|\Big]|\psi^-_{\boldsymbol{k},n+1}\rangle\\ &\qquad\approx \langle\psi^+_{\boldsymbol{k},n+1}|\psi^+_{\boldsymbol{k},n}\rangle\langle\psi^-_{\boldsymbol{k},n}|\psi^-_{\boldsymbol{k},n+1}\rangle + \langle\psi^+_{\boldsymbol{k},n+1}|\epsilon\mathcal{L}\Big[|\psi^+_{\boldsymbol{k},n}\rangle\langle\psi^-_{\boldsymbol{k},n}|\Big]|\psi^-_{\boldsymbol{k},n+1}\rangle\\ &\qquad= \langle\psi^+_{\boldsymbol{k},n+1}|\psi^+_{\boldsymbol{k},n}\rangle\langle\psi^-_{\boldsymbol{k},n}|\psi^-_{\boldsymbol{k},n+1}\rangle\Big(1+\epsilon\mathcal{L}[\psi^+_{\boldsymbol{k},n},\psi^-_{\boldsymbol{k},n},\psi^+_{\boldsymbol{k},n+1},\psi^-_{\boldsymbol{k},n+1}]\Big),\\ &\qquad\approx \langle\psi^+_{\boldsymbol{k},n+1}|\psi^+_{\boldsymbol{k},n}\rangle\langle\psi^-_{\boldsymbol{k},n}|\psi^-_{\boldsymbol{k},n+1}\rangle e^{\epsilon\mathcal{L}[\psi^+_{\boldsymbol{k},n},\psi^-_{\boldsymbol{k},n},\psi^+_{\boldsymbol{k},n+1},\psi^-_{\boldsymbol{k},n+1}]},\end{aligned} \tag{8.44}$$

where

$$\mathcal{L}[\psi^+_{\boldsymbol{k},n},\psi^-_{\boldsymbol{k},n},\psi^+_{\boldsymbol{k},n+1},\psi^-_{\boldsymbol{k},n+1}] = \frac{\langle\psi^+_{\boldsymbol{k},n+1}|\mathcal{L}\Big[|\psi^+_{\boldsymbol{k},n}\rangle\langle\psi^-_{\boldsymbol{k},n}|\Big]|\psi^-_{\boldsymbol{k},n+1}\rangle}{\langle\psi^+_{\boldsymbol{k},n+1}|\psi^+_{\boldsymbol{k},n}\rangle\langle\psi^-_{\boldsymbol{k},n}|\psi^-_{\boldsymbol{k},n+1}\rangle} \tag{8.45}$$

is simply a sum of monomials in the constituent fields when $\mathcal{L}$ is normal ordered.

[6]This is a somewhat delicate point. While requiring the Hamiltonian H to be normal-ordered is fairly customary, difficulties arise in the dissipator for even very simple jump operators L_i. Taking $L = a^\dagger_{\boldsymbol{k}}$ for instance (corresponding to a one-particle incoherent drive), the term $L^\dagger L = a_{\boldsymbol{k}}a^\dagger_{\boldsymbol{k}}$ in the dissipator is clearly not normal-ordered, and the operators must be in this order according to our prescription for the form of the Lindbladian. Attempting to bring the operator to a normal-ordered form by use of the commutation relation for the $a_{\boldsymbol{k}}$, $a^\dagger_{\boldsymbol{k}}$ operators in an infinite-dimensional system will yield a pathological Dirac delta distribution with zero argument, to some extent reflecting the fact that the form of the Lindbladian and many results about it were worked out in the finite-dimensional setting. This difficulty can be ameliorated by starting from a unitary evolution with a specially chosen bath [8] which, upon being integrated out, yields a Feynman-Vernon functional identical (up to Lamb shift terms which we typically neglect) to one which would have been obtained if the Lindbladian had been taken as normal ordered from the start, contrary to its finite-dimensional standard form. This is essentially what was done in Part Ia.

Using (3.11) and (3.14) this becomes

$$\begin{aligned}\langle\psi^+_{\boldsymbol{k},n+1}|e^{\epsilon\mathcal{L}}\Big[|\psi^+_{\boldsymbol{k},n}\rangle\langle\psi^-_{\boldsymbol{k},n}|\Big]|\psi^-_{\boldsymbol{k},n+1}\rangle \\ = \mathrm{Exp}\Bigg[\epsilon\mathcal{L}[\psi^+_{\boldsymbol{k},n},\psi^-_{\boldsymbol{k},n},\psi^+_{\boldsymbol{k},n+1},\psi^-_{\boldsymbol{k},n+1}] \\ -\frac{\epsilon}{2}\sum_{\boldsymbol{k}}\left[\bar\psi^+_{\boldsymbol{k},n+1}\frac{\psi^+_{\boldsymbol{k},n+1}-\psi^+_{\boldsymbol{k},n}}{\epsilon}-\psi^+_{\boldsymbol{k},n}\frac{\bar\psi^+_{\boldsymbol{k},n+1}-\bar\psi^+_{\boldsymbol{k},n}}{\epsilon}\right] \\ -\frac{\epsilon}{2}\sum_{\boldsymbol{k}}\left[\psi^-_{\boldsymbol{k},n+1}\frac{\bar\psi^-_{\boldsymbol{k},n+1}-\bar\psi^-_{\boldsymbol{k},n}}{\epsilon}-\bar\psi^-_{\boldsymbol{k},n}\frac{\psi^-_{\boldsymbol{k},n+1}-\psi^-_{\boldsymbol{k},n}}{\epsilon}\right]\Bigg].\end{aligned} \tag{8.46}$$

and, as $\epsilon\to 0$, we find

$$\prod_{n=0}^{N}\langle\psi^+_{\boldsymbol{k},n+1}|e^{\epsilon\mathcal{L}}\Big[|\psi^+_{\boldsymbol{k},n}\rangle\langle\psi^-_{\boldsymbol{k},n}|\Big]|\psi^-_{\boldsymbol{k},n+1}\rangle\to e^{iS_T[\psi^+_{\boldsymbol{k},t},\psi^-_{\boldsymbol{k},t}]}, \tag{8.47}$$

$$\begin{aligned}S_T[\psi^+_{\boldsymbol{k},t},\psi^-_{\boldsymbol{k},t}] = \int_{-T}^{T}dt\Bigg[-i\mathcal{L}[\psi^+_{\boldsymbol{k},t},\psi^-_{\boldsymbol{k},t}] \\ \frac{i}{2}\sum_{\boldsymbol{k}}\Big(\bar\psi^+_{\boldsymbol{k},t}\partial_t\psi^+_{\boldsymbol{k},t}-\psi^+_{\boldsymbol{k},t}\partial_t\bar\psi^+_{\boldsymbol{k},t}+\psi^-_{\boldsymbol{k},t}\partial_t\bar\psi^-_{\boldsymbol{k},t}-\bar\psi^-_{\boldsymbol{k},t}\partial_t\psi^-_{\boldsymbol{k},t}\Big)\Bigg],\end{aligned} \tag{8.48}$$

or, after integrating by parts,

$$S_T[\psi^+_{\boldsymbol{k},t},\psi^-_{\boldsymbol{k},t}] = \int_{-T}^{T}dt\Bigg[\sum_{\boldsymbol{k}}\Big(i\bar\psi^+_{\boldsymbol{k},t}\partial_t\psi^+_{\boldsymbol{k},t}-i\bar\psi^-_{\boldsymbol{k},t}\partial_t\psi^-_{\boldsymbol{k},t}\Big)-i\mathcal{L}[\psi^+_{\boldsymbol{k},t},\psi^-_{\boldsymbol{k},t}]\Bigg]. \tag{8.49}$$

Performing the Keldysh rotation,

$$S_{cq,T}[\psi^c_{\boldsymbol{k},t},\psi^q_{\boldsymbol{k},t}] = \int_{-T}^{T}dt\Bigg[\sum_{\boldsymbol{k}}\Big(i\bar\psi^c_{\boldsymbol{k},t}\partial_t\psi^q_{\boldsymbol{k},t}+i\bar\psi^q_{\boldsymbol{k},t}\partial_t\psi^c_{\boldsymbol{k},t}\Big)-i\mathcal{L}_{cq}[\psi^c_{\boldsymbol{k},t},\psi^q_{\boldsymbol{k},t}]\Bigg]. \tag{8.50}$$

and we may write

$$\langle\psi^+_{\boldsymbol{k},\mathrm{out}}|\rho_T|\psi^-_{\boldsymbol{k},\mathrm{out}}\rangle = \int_{\substack{\psi^c_{\boldsymbol{k}}(-T)=\sqrt{2}\psi_{\boldsymbol{k},\mathrm{in}}\\ \psi^q_{\boldsymbol{k}}(-T)=0}}^{\substack{\psi^c_{\boldsymbol{k}}(T)=\sqrt{2}\psi_{\boldsymbol{k},\mathrm{out}}\\ \psi^q_{\boldsymbol{k}}(T)=0}}\mathcal{D}[\psi^c_{\boldsymbol{k},t},\bar\psi^c_{\boldsymbol{k},t},\psi^q_{\boldsymbol{k},t},\bar\psi^q_{\boldsymbol{k},t}]\,e^{S_{cq,T}[\psi^c_{\boldsymbol{k},t},\psi^q_{\boldsymbol{k},t}]}\langle\psi^+_{\boldsymbol{k},\mathrm{in}}|\rho_{-T}|\psi^-_{\boldsymbol{k},\mathrm{in}}\rangle. \tag{8.51}$$

For driven-dissipative dynamics with a unique steady state we may discard the initial density matrix so long as we maintain the functional integral's normalisation, and we will generally be interested in traces over the final density matrix (which corresponds to integrating over all final values of field trajectories instead of fixing them at time T) rather than its individual matrix elements. This allows

us to rewrite the foregoing as

$$\mathrm{Tr}\,\rho_T = \int \mathcal{D}[\psi^c_{\boldsymbol{k},t}, \bar{\psi}^c_{\boldsymbol{k},t}, \psi^q_{\boldsymbol{k},t}, \bar{\psi}^q_{\boldsymbol{k},t}]\, e^{S_{cq,T}[\psi^c_{\boldsymbol{k},t}, \psi^q_{\boldsymbol{k},t}]} = 1. \tag{8.52}$$

Finally, just as in Chap.3, by adding terms of the form $J_i(t)O_i$ to the Hamiltonian in $\mathcal{L}$ we may work out expectations of operators via functional differentiation. It is easy to see that, for expectations in the steady state when we may ignore the initial density matrix as above, this amounts to (taking $T = \infty$ to achieve the steady state)

$$\begin{aligned}
&\langle O_1^-(t_1^-)\dots O_m^-(t_m^-) O_n^+(t_n^+)\dots O_1^+(t_1^+)\rangle \\
&= \int \mathcal{D}[\psi^c_{\boldsymbol{k},t}, \bar{\psi}^c_{\boldsymbol{k},t}, \psi^q_{\boldsymbol{k},t}, \bar{\psi}^q_{\boldsymbol{k},t}]\, e^{S_{cq,\infty}[\psi^c_{\boldsymbol{k},t}, \psi^q_{\boldsymbol{k},t}]} \\
&\qquad\qquad O_1^-[\psi^-_{\boldsymbol{k},t_1}]\dots O_m^-[\psi^-_{\boldsymbol{k},t_m}] O_n^+[\psi^+_{\boldsymbol{k},t_n}]\dots O_1^+[\psi^+_{\boldsymbol{k},t_1}] \\
&= \int \mathcal{D}[\psi^c_{\boldsymbol{k},t}, \bar{\psi}^c_{\boldsymbol{k},t}, \psi^q_{\boldsymbol{k},t}, \bar{\psi}^q_{\boldsymbol{k},t}]\, e^{S_{cq,\infty}[\psi^c_{\boldsymbol{k},t}, \psi^q_{\boldsymbol{k},t}]} \\
&\qquad\qquad O_1^-\left[\frac{\psi^c_{\boldsymbol{k},t_1} - \psi^q_{\boldsymbol{k},t_1}}{\sqrt{2}}\right]\dots O_m^-\left[\frac{\psi^c_{\boldsymbol{k},t_m} - \psi^q_{\boldsymbol{k},t_m}}{\sqrt{2}}\right] \\
&\qquad\qquad O_n^+\left[\frac{\psi^c_{\boldsymbol{k},t_n} + \psi^q_{\boldsymbol{k},t_n}}{\sqrt{2}}\right]\dots O_1^+\left[\frac{\psi^c_{\boldsymbol{k},t_1} + \psi^q_{\boldsymbol{k},t_1}}{\sqrt{2}}\right].
\end{aligned} \tag{8.53}$$

We thus possess a way to map Lindbladian master equations to Keldysh path integrals, and a prescription for calculating expectations of operators via the latter in the steady states of the former.

Chapter 9

Stochastic Limit of the Keldysh Path Integral

In Part Ia of this thesis, we saw how the linear current-current response of polariton systems could be calculated via field theoretic perturbation theory. Already at $O(\hbar^2)$ the number of Feynman diagrams involved was very significant and, for more complicated regimes, such analytical calculations become exceedingly impractical. The case of coherently pumped polaritons above the OPO threshold, for instance, is so complicated that the perturbative calculation remains undone [9], [10]. This part of the thesis is thus devoted to exploring the application of alternative, numerical methods to the problem of classifying superfluidity in polariton systems.

A method particularly well suited to the semi-classical phenomena observed in polaritons is the Truncated Wigner Approximation wherein the quantum dynamics reduce to a suitable jump-diffusion process in the semi-classical limit. This method has its roots in the theory of deformation quantisation (which we will explore in the form of the Stratonovich–Weyl correspondence for the 2-sphere in Part III), but may also be derived as a semi-classical limit of the Keldysh functional integral. To set the scene I will present the schematic derivation of the method following Ref. [11] (highlighting some difficulties related to topics addressed in Part II of this thesis) and then work out the concrete stochastic equations for a rather general Lindbladian. The following chapter will cover how the static current-current response may be obtained numerically via this method.

9.1 Truncated Wigner Approximation via Hubbard-Stratonovich

The main idea is that, to order $O(\hbar^2)$, the dynamics of a Markovian open quantum system may be reduced to those of a stochastic differential equation via a

Hubbard-Stratonovich transformation [12] of the associated Keldysh functional integral. To this end, consider a general Keldysh action associated to a Lindbladian $\mathcal{L}$, as constructed in the previous chapter (we have Fourier-transformed to position space):

$$S = \int dtd\boldsymbol{r}\Big(i\bar{\psi}^c_{\boldsymbol{r},t}\dot{\psi}^q_{\boldsymbol{r},t} + i\bar{\psi}^q_{\boldsymbol{r},t}\dot{\psi}^c_{\boldsymbol{r},t} - i\mathcal{L}[\bar{\psi}^c_{\boldsymbol{r},t}, \psi^c_{\boldsymbol{r},t}, \bar{\psi}^q_{\boldsymbol{r},t}, \psi^q_{\boldsymbol{r},t}]\Big). \tag{9.1}$$

With these variables, it is not difficult to show that the $O(\hbar^0)$ expectation of $\psi^q_{\boldsymbol{r},t}$ is 0 — this motivates an expansion fluctuations of $\psi^q_{\boldsymbol{r},t}$, where the redefinition $\psi^q_{\boldsymbol{r},t} \to \hbar\psi^q_{\boldsymbol{r},t}$ then effectively makes this an expansion in $\hbar$ as described in Sec.3.1.2 (though we will omit writing the $\hbar$s explicitly). Truncating this expansion at second order in $\psi^q_{\boldsymbol{r},t}$ is a semi-classical approximation that leads to the Truncated Wigner Approximation [13]:

$$S \approx S[\psi^c_{\boldsymbol{r},t}, 0] + \psi^q_{\boldsymbol{r},t}\frac{\partial S}{\partial \psi^q_{\boldsymbol{r},t}}\Big|_{\psi^q_{\boldsymbol{r},t}=0} + \bar{\psi}^q_{\boldsymbol{r},t}\frac{\partial S}{\partial \bar{\psi}^q_{\boldsymbol{r},t}}\Big|_{\psi^q_{\boldsymbol{r},t}=0} + \psi^q_{\boldsymbol{r},t}\bar{\psi}^q_{\boldsymbol{r},t}\frac{\partial^2 S}{\partial \bar{\psi}^q_{\boldsymbol{r},t}\partial \psi^q_{\boldsymbol{r},t}}\Big|_{\psi^q_{\boldsymbol{r},t}=0} + \dots. \tag{9.2}$$

The first term on the RHS above is zero because $\psi^q_{\boldsymbol{r},t} = 0$ means that the ψ^+ and ψ^- trajectories are equal. For a unitary evolution this means that the actions coming from the ψ^+ and ψ^- fields will cancel perfectly while, if a bath was integrated out, this is the statement that the trace of the bath density matrix is preserved if ψ is treated as a classical external field. Furthermore, for the kinds of actions we typically consider, the above $O(|\psi^q_{\boldsymbol{r},t}|^2)$ term is the only non-zero one at $O(\hbar^2)$. This allows us to utilise a Hubbard-Stratonovich transformation:

$$e^{-\int dtd\boldsymbol{r}\, M_{\boldsymbol{r},t}\bar{\psi}^q_{\boldsymbol{r},t}\psi^q_{\boldsymbol{r},t}} = \int \mathcal{D}[\xi_{\boldsymbol{r},t}, \bar{\xi}_{\boldsymbol{r},t}] e^{\int dtd\boldsymbol{r}\left[-\bar{\xi}_{\boldsymbol{r},t}\xi_{\boldsymbol{r},t} + i\psi^q_{\boldsymbol{r},t}\sqrt{M_{\boldsymbol{r},t}}\bar{\xi}_{\boldsymbol{r},t} + i\bar{\psi}^q_{\boldsymbol{r},t}\sqrt{M_{\boldsymbol{r},t}}\xi_{\boldsymbol{r},t}\right]}, \tag{9.3}$$

$$\int \mathcal{D}[\xi_{\boldsymbol{r},t}, \bar{\xi}_{\boldsymbol{r},t}] e^{-\int dtd\boldsymbol{r}\,\bar{\xi}_{\boldsymbol{r},t}\xi_{\boldsymbol{r},t}} = 1, \tag{9.4}$$

to rewrite the functional integral as (denoting $-i\frac{\partial^2 S}{\partial \bar{\psi}^q_{\boldsymbol{r},t}\partial \psi^q_{\boldsymbol{r},t}}\Big|_{\psi^q_{\boldsymbol{r},t}=0} = M_{\boldsymbol{r},t}$)

$$\begin{aligned}
&\int \mathcal{D}[\bar{\psi}^c_{\boldsymbol{r},t}, \psi^c_{\boldsymbol{r},t}, \bar{\psi}^q_{\boldsymbol{r},t}, \psi^q_{\boldsymbol{r},t}]\, e^{-\int dtd\boldsymbol{r}\left[M_{\boldsymbol{r},t}\psi^q_{\boldsymbol{r},t}\bar{\psi}^q_{\boldsymbol{r},t} - i\psi^q_{\boldsymbol{r},t}\frac{\partial S}{\partial \psi^q_{\boldsymbol{r},t}}\Big|_{\psi^q_{\boldsymbol{r},t}=0} - i\bar{\psi}^q_{\boldsymbol{r},t}\frac{\partial S}{\partial \bar{\psi}^q_{\boldsymbol{r},t}}\Big|_{\psi^q_{\boldsymbol{r},t}=0}\right]} \\
&\quad\approx \int \mathcal{D}[\bar{\psi}^c_{\boldsymbol{r},t}, \psi^c_{\boldsymbol{r},t}, \bar{\psi}^q_{\boldsymbol{r},t}, \psi^q_{\boldsymbol{r},t}, \bar{\xi}^q_{\boldsymbol{r},t}, \xi^q_{\boldsymbol{r},t}] \\
&\qquad e^{\int dtd\boldsymbol{r}\left[-\bar{\xi}_{\boldsymbol{r},t}\xi_{\boldsymbol{r},t} + i\psi^q_{\boldsymbol{r},t}\left(\frac{\partial S}{\partial \psi^q_{\boldsymbol{r},t}}\Big|_{\psi^q_{\boldsymbol{r},t}=0} + \sqrt{M_{\boldsymbol{r},t}}\bar{\xi}_{\boldsymbol{r},t}\right) + i\bar{\psi}^q_{\boldsymbol{r},t}\left(\frac{\partial S}{\partial \bar{\psi}^q_{\boldsymbol{r},t}}\Big|_{\psi^q_{\boldsymbol{r},t}=0} + \sqrt{M_{\boldsymbol{r},t}}\xi_{\boldsymbol{r},t}\right)\right]}
\end{aligned}$$

From here, if one inserts an operator $O[\bar{\psi}^c_{\boldsymbol{r},t}, \psi^c_{\boldsymbol{r},t}]$ dependent only on $\psi^c_{\boldsymbol{r},t}$ and integrates over $\psi^q_{\boldsymbol{r},t}$, one finds that

$$\langle O[\bar{\psi}^c_{\boldsymbol{r},t}, \psi^c_{\boldsymbol{r},t}]\rangle \propto \int \mathcal{D}[\bar{\psi}^c_{\boldsymbol{r},t}, \psi^c_{\boldsymbol{r},t}, \bar{\xi}_{\boldsymbol{r},t}, \xi_{\boldsymbol{r},t}]\, O[\bar{\psi}^c_{\boldsymbol{r},t}, \psi^c_{\boldsymbol{r},t}] e^{-\int dt d\boldsymbol{r}\, \bar{\xi}_{\boldsymbol{r},t}\xi_{\boldsymbol{r},t}} \\ \delta\Big(\frac{\partial S}{\partial \psi^q_{\boldsymbol{r},t}}\Big|_{\psi^q_{\boldsymbol{r},t}=0} + \sqrt{M_{\boldsymbol{r},t}}\bar{\xi}_{\boldsymbol{r},t}\Big)\delta\Big(\frac{\partial S}{\partial \bar{\psi}^q_{\boldsymbol{r},t}}\Big|_{\psi^q_{\boldsymbol{r},t}=0} + \sqrt{M_{\boldsymbol{r},t}}\xi_{\boldsymbol{r},t}\Big). \tag{9.5}$$

At this point [11] argues that such steady-state expectations may thus be calculated by averaging $O[\bar{\psi}^c_{\boldsymbol{r},t}, \psi^c_{\boldsymbol{r},t}]$ over trajectories of the Langevin equation $\frac{\partial S}{\partial \bar{\psi}^q_{\boldsymbol{r},t}}\Big|_{\psi^q_{\boldsymbol{r},t}=0} + \sqrt{M_{\boldsymbol{r},t}}\xi_{\boldsymbol{r},t} = 0$, enforced by the Dirac delta functions, once these have converged to the steady state of their corresponding Fokker-Planck equation. The properties of the Gaussian noise ξ are determined by its expectation $\langle \xi_{\boldsymbol{r},t}\rangle = 0$ and its two-point correlation $\langle \xi_{\boldsymbol{r},t}\xi_{\boldsymbol{r}',t'}\rangle = \delta(\boldsymbol{r}-\boldsymbol{r}')\delta(t-t')$.

There are two points worth considering. The first is that the above prescription only allows the calculation of operators expressible in terms of $\psi^c_{\boldsymbol{r},t}$, while the second concerns the choice of a specific stochastic integral when the Langevin equation contains multiplicative noise. These are addressed in the following two subsections.

9.1.1 Time-Symmetric Ordering of ψ^c Operators

A curious feature of the stochastic formalism developed above, which is shared by other variants of the Truncated Wigner approach, is that it is generally difficult to calculate temporal correlation functions. The reason for this is easier to explain when armed in the Moyal star product (and I will touch on it in Part III), but the heuristic explanation is that this is caused by quantum measurements. Unlike in a classical stochastic theory, where one may sample at different points in time without affecting the evolution of the probability density, 'sampling' (measuring) a quantum operator induces a back action on the density matrix and affects its subsequent evolution. When treated correctly this leads to discontinuous jumps in the otherwise diffusive stochastic dynamics [14] at the times of earlier measurements, so that it is generally invalid to simply average operators at different times over purely diffusive trajectories to obtain their correlation functions.

At the same time, nothing in the reasoning of the previous section appears to forbid us to perform exactly this sort of purely diffusive average on operators at different times so long as they depend only on $\psi^c_{\boldsymbol{r},t}$ and not on $\psi^q_{\boldsymbol{r},t}$. It is thus worth commenting on this, especially for readers more familiar with non-Keldysh approaches to the Truncated Wigner approximation.

Let us denote the quantum operator that generated a field operator by dots on

either side, so that for instance

$$\bullet\psi^c_{\boldsymbol{r}_1,t_1}\bullet = \frac{1}{\sqrt{2}}\bullet\,\psi^+_{\boldsymbol{r}_1,t_1} + \psi^-_{\boldsymbol{r}_1,t_1}\bullet = \frac{1}{\sqrt{2}}\left[a_{\boldsymbol{r}_1,t_1^+} + a_{\boldsymbol{r}_1,t_1^-}\right] \tag{9.6}$$

where, as usual, the plus minus superscripts on times indicate whether the associated quantum operators appears to the left or right of the density matrix in an expectation. Now consider the expectation of a chain of ψ^c fields at different times $t_1 < t_2 < \ldots < t_n$ (some of the fields may be complex conjugated without changing the argument):

$$\langle\psi^c_{\boldsymbol{r}_1,t_1}\psi^c_{\boldsymbol{r}_2,t_2}\ldots\psi^c_{\boldsymbol{r}_n,t_n}\rangle. \tag{9.7}$$

Appealing to the time ordering on the total Keldysh contour introduced in Sec.3.1.2, we know that the earliest time is t_1^+ and the latest is t_1^-. Thus

$$\begin{aligned}\bullet\psi^c_{\boldsymbol{r}_1,t_1}\psi^c_{\boldsymbol{r}_2,t_2}\ldots\psi^c_{\boldsymbol{r}_n,t_n}\bullet &= \frac{1}{\sqrt{2}}\bullet(\psi^+_{\boldsymbol{r}_1,t_1} + \psi^-_{\boldsymbol{r}_1,t_1})\psi^c_{\boldsymbol{r}_2,t_2}\ldots\psi^c_{\boldsymbol{r}_n,t_n}\bullet \\ &\propto a_{\boldsymbol{r}_1,t_1}\bullet\,\psi^c_{\boldsymbol{r}_2,t_2}\ldots\psi^c_{\boldsymbol{r}_n,t_n}\bullet + \bullet\,\psi^c_{\boldsymbol{r}_2,t_2}\ldots\psi^c_{\boldsymbol{r}_n,t_n}\bullet\, a_{\boldsymbol{r}_1,t_1}.\end{aligned} \tag{9.8}$$

This reasoning can be applied recursively to the terms on the right hand side, and we observe that we have obtained the same recursive relation (up to constant factors) as expression (190) in [14]. There it is noted that operators with this ordering, referred to there as time-symmetric ordering, have the special property that they do not generate a back action on the density matrix when measured. They may thus be averaged without introducing jumps to the diffusive stochastic dynamics, which is precisely the claim we are making about operators composed of $\psi^c_{\boldsymbol{r},t}$ fields. Thus operators composed of the classical fields are time-symmetrically ordered, and because of this correspond to those temporal correlation functions that may be calculated using purely diffusive stochastic dynamics.

It is worth noting that most temporal correlation functions of interest (for instance the static current-current response that is key to superfluidity) are not time-symmetrically ordered, and thus do not admit a representation in terms of $\psi^c_{\boldsymbol{r},t}$ fields alone, a difficulty we will face in the next chapter. Moreover, many equal-time operators do not have obvious representations in terms of these fields. Consider for instance $a^\dagger_{\boldsymbol{r}_2,t}a_{\boldsymbol{r}_1,t}$. In order to write this in terms of $\psi^c_{\boldsymbol{r},t}$ we first consider $a^\dagger_{\boldsymbol{r}_2,t_2}a_{\boldsymbol{r}_1,t_1}$, so that

$$a^\dagger_{\boldsymbol{r}_2,t_2}a_{\boldsymbol{r}_1,t_1} = \frac{1}{2}\left(a^\dagger_{\boldsymbol{r}_2,t_2}a_{\boldsymbol{r}_1,t_1} + a_{\boldsymbol{r}_1,t_1}a^\dagger_{\boldsymbol{r}_2,t_2}\right) + \frac{1}{2}\left[a^\dagger_{\boldsymbol{r}_2,t_2}, a_{\boldsymbol{r}_1,t_1}\right]. \tag{9.9}$$

The first term on the right is time-symmetrically ordered, corresponding to $\frac{1}{2}\bar{\psi}^c_{\boldsymbol{r},t_2}\psi^c_{\boldsymbol{r},t_1}$. Now taking $t_2 \to t_1$ and using the equal-time commutation relation for the $a_{\boldsymbol{r},t}$

operators we find

$$a^\dagger_{\boldsymbol{r}_2,t} a_{\boldsymbol{r}_1,t} = \frac{1}{2} \bullet \bar{\psi}^c_{\boldsymbol{r}_2,t} \psi^c_{\boldsymbol{r}_1,t} - \delta(\boldsymbol{r}_2 - \boldsymbol{r}_1) \bullet, \tag{9.10}$$

which differs from the $\bullet \bar{\psi}^c_{\boldsymbol{r}_2,t} \psi^c_{\boldsymbol{r}_1,t} \bullet$ that one might naively expect.

9.1.2 The Ito Convention

The line of reasoning that led to our Langevin equations can be seen to be incomplete because the functional integral contains Dirac delta functions of non-trivial functionals of the fields. This means that, before it is permissible to carry out the integral of the delta functions over the $\psi_{\boldsymbol{r},t}$ field, the formula for composition of a Dirac delta with a functional must be applied. Doing so and denoting $\left.\frac{\partial S}{\partial \bar{\psi}^q_{\boldsymbol{r},t}}\right|_{\substack{\psi^q_{\boldsymbol{r},t}=0 \\ \psi^c_{\boldsymbol{r},t}=\psi_{\boldsymbol{r},t}}} + \sqrt{M_{\boldsymbol{r},t}}\xi_{\boldsymbol{r},t}$ by $f[\bar{\xi}_{\boldsymbol{r},t}, \xi_{\boldsymbol{r},t}, \bar{\psi}_{\boldsymbol{r},t}, \psi_{\boldsymbol{r},t}]$, we may rewrite (9.5) as

$$\begin{aligned}
&\langle O[\bar{\psi}^c_{\boldsymbol{r},t}, \psi^c_{\boldsymbol{r},t}] \rangle \\
&\approx \int \mathcal{D}[\bar{\xi}_{\boldsymbol{r},t}, \xi_{\boldsymbol{r},t}] \exp[-\bar{\xi}_{\boldsymbol{r},t}\xi_{\boldsymbol{r},t}] \left(O[\bar{\psi}_{\boldsymbol{r},t}, \psi_{\boldsymbol{r},t}] \det \begin{pmatrix} \partial_{\psi_{\boldsymbol{r},t}} f & \partial_{\bar{\psi}_{\boldsymbol{r},t}} f \\ \partial_{\psi_{\boldsymbol{r},t}} \bar{f} & \partial_{\bar{\psi}_{\boldsymbol{r},t}} \bar{f} \end{pmatrix}^{-1} \right) \Bigg|_{\psi_{\boldsymbol{r},t} \text{ s.t. } f[\psi_{\boldsymbol{r},t}, \xi_{\boldsymbol{r},t}]=0}.
\end{aligned} \tag{9.11}$$

By correctly treating the delta functions, we have obtained the desired interpretation of the expectation as that of an average over solutions of the $f[\psi_{\boldsymbol{r},t}, \xi_{\boldsymbol{r},t}] = 0$ Langevin equations with noise $\xi_{\boldsymbol{r},t}$. The problem is that, in the process, a functional determinant factor

$$\det \begin{pmatrix} \partial_{\psi_{\boldsymbol{r},t}} f & \partial_{\bar{\psi}_{\boldsymbol{r},t}} f \\ \partial_{\psi_{\boldsymbol{r},t}} \bar{f} & \partial_{\bar{\psi}_{\boldsymbol{r},t}} \bar{f} \end{pmatrix}^{-1} \tag{9.12}$$

has appeared. This factor precisely corresponds to the fact that, when writing down the Langevin equation, we did not stipulate whether the Ito or Stratonovich convention[1] was to be used [12].

The most direct way to remedy this issue, knowing that due to the system's evolution being trace-preserving the expectation of the identity operator should be one ($\langle I \rangle = 1$), is to pick the Ito formalism. In this case the Langevin equation is to be interpreted as the following discretised stochastic differential equation (SDE) (we have multiplied through by the ϵ time factor, an operation that can be easily absorbed into the other spurious constant factors carried around by a functional integral so long as we maintain the normalisation $\langle I \rangle = 1$):

$$f_n[\psi_{\boldsymbol{r},n}, \psi_{\boldsymbol{r},n-1}, \xi_{\boldsymbol{r},n-1}] = \psi_{\boldsymbol{r},n} - \psi_{\boldsymbol{r},n-1} - \epsilon \left(\mu[\psi_{\boldsymbol{r},n-1}] + \sigma[\psi_{\boldsymbol{r},n-1}] \xi_{\boldsymbol{r},n-1} \right) \tag{9.13}$$

[1] Of course other variants of stochastic integral would also be admissible, these being simply the most common ones.

with μ and σ the drift and diffusion coefficients of the Langevin equation taken at the specified discrete moment in time. We find that the discrete form of the Jacobian matrix

$$\begin{pmatrix} \frac{\partial f_i}{\partial \psi_{\boldsymbol{r},j}} & \frac{\partial f_i}{\partial \bar{\psi}_{\boldsymbol{r},j}} \\ \frac{\partial \bar{f}_i}{\partial \psi_{\boldsymbol{r},j}} & \frac{\partial \bar{f}_i}{\partial \bar{\psi}_{\boldsymbol{r},j}} \end{pmatrix}^{-1} \tag{9.14}$$

has

$$\frac{\partial f_i}{\partial \psi_{\boldsymbol{r},i}} = 1, \quad \frac{\partial f_i}{\partial \psi_{\boldsymbol{r},i-1}} \neq 0, \tag{9.15}$$

$$\frac{\partial f_i}{\partial \bar{\psi}_{\boldsymbol{r},i-1}} \neq 0., \tag{9.16}$$

$$\frac{\partial \bar{f}_i}{\partial \psi_{\boldsymbol{r},i-1}} \neq 0, \tag{9.17}$$

$$\frac{\partial \bar{f}_i}{\partial \bar{\psi}_{\boldsymbol{r},i}} = 1, \quad \frac{\partial \bar{f}_i}{\partial \bar{\psi}_{\boldsymbol{r},i-1}} \neq 0, \tag{9.18}$$

with all other elements zero. All four block matrices comprising the Jacobian matrix are lower triangular, so their determinants are the products of their diagonal elements. This means that $\frac{\partial f_i}{\partial \psi_{\boldsymbol{r},j}}$ is invertible (it and $\frac{\partial \bar{f}_i}{\partial \bar{\psi}_{\boldsymbol{r},j}}$ have determinant 1)and the determinant formula for a block matrix

$$M = \begin{pmatrix} A & B \\ C & D \end{pmatrix}, \quad A \text{ invertible}, \tag{9.19}$$

$$\det M = \det A \cdot \det\left(D - CA^{-1}B\right) \tag{9.20}$$

applies. It is easy to see that $\frac{\partial \bar{f}_i}{\partial \psi_{\boldsymbol{r},j}} \left(\frac{\partial f_i}{\partial \psi_{\boldsymbol{r},j}}\right)^{-1} \frac{\partial f_i}{\partial \bar{\psi}_{\boldsymbol{r},j}}$ is lower triangular[2] and has a zero diagonal, so that $\frac{\partial \bar{f}_i}{\partial \bar{\psi}_{\boldsymbol{r},j}} - \frac{\partial \bar{f}_i}{\partial \psi_{\boldsymbol{r},j}} \left(\frac{\partial f_i}{\partial \psi_{\boldsymbol{r},j}}\right)^{-1} \frac{\partial f_i}{\partial \bar{\psi}_{\boldsymbol{r},j}}$ is lower triangular with 1s on the diagonal and thus has determinant 1. Thus

$$\det \begin{pmatrix} \partial_{\psi_{\boldsymbol{r},t}} f & \partial_{\bar{\psi}_{\boldsymbol{r},t}} f \\ \partial_{\psi_{\boldsymbol{r},t}} \bar{f} & \partial_{\bar{\psi}_{\boldsymbol{r},t}} \bar{f} \end{pmatrix}^{-1} = \det \frac{\partial f_i}{\partial \psi_{\boldsymbol{r},j}} \cdot \det\left(\frac{\partial \bar{f}_i}{\partial \bar{\psi}_{\boldsymbol{r},j}} - \frac{\partial \bar{f}_i}{\partial \psi_{\boldsymbol{r},j}} \left(\frac{\partial f_i}{\partial \psi_{\boldsymbol{r},j}}\right)^{-1} \frac{\partial f_i}{\partial \bar{\psi}_{\boldsymbol{r},j}} \right) = 1 \cdot 1 = 1. \tag{9.21}$$

This then ensures that

$$\begin{aligned} &\langle O[\bar{\psi}^c_{\boldsymbol{r},t}, \psi^c_{\boldsymbol{r},t}] \rangle \\ &\approx \int \mathcal{D}[\bar{\xi}_{\boldsymbol{r},t}, \xi_{\boldsymbol{r},t}] \exp[-\bar{\xi}_{\boldsymbol{r},t}\xi_{\boldsymbol{r},t}] \left(O[\bar{\psi}_{\boldsymbol{r},t}, \psi_{\boldsymbol{r},t}] \det \begin{pmatrix} \partial_{\psi_{\boldsymbol{r},t}} f & \partial_{\bar{\psi}_{\boldsymbol{r},t}} f \\ \partial_{\psi_{\boldsymbol{r},t}} \bar{f} & \partial_{\bar{\psi}_{\boldsymbol{r},t}} \bar{f} \end{pmatrix}^{-1} \right) \Bigg|_{\psi_{\boldsymbol{r},t} \text{ s.t. } f[\psi_{\boldsymbol{r},t}, \xi_{\boldsymbol{r},t}]=0} \\ &= \int \mathcal{D}[\bar{\xi}_{\boldsymbol{r},t}, \xi_{\boldsymbol{r},t}] \exp[-\bar{\xi}_{\boldsymbol{r},t}\xi_{\boldsymbol{r},t}] \, O[\bar{\psi}_{\boldsymbol{r},t}, \psi_{\boldsymbol{r},t}] \big|_{\psi_{\boldsymbol{r},t} \text{ s.t. } f[\psi_{\boldsymbol{r},t}, \xi_{\boldsymbol{r},t}]=0}, \end{aligned} \tag{9.22}$$

[2]The inverses and products of lower triangular matrices are also lower triangular.

which ensures $\langle I \rangle = 1$ due to the normalisation of the $\xi_{\boldsymbol{r},t}$ Gaussian integral and gives the desired interpretation of an average over stochastic trajectories with no extra determinant factor.

It must be noted that, while likely sufficient for our applications, this line of reasoning is not entirely satisfying. In particular the choice of discretisation convention is made very late in the process, based almost purely on the desire to achieve $\langle I \rangle = 1$, and in fact disagrees with the discretisation that was used when initially constructing the path integral. That discretisation of the action, as described in Sec.8.2, does not actually admit the Hubbard-Stratonovich transformation used to obtain the Langevin equation because of how the quantum fields are offset in time. To perform the transformation one thus has to first pass to the continuous form, discarding discretisation information, obtain a Langevin equation, and then select a new discretisation convention based on some other principle (here the normalisation requirement).

My suspicion is that this is closely related to the general difficulties with discretisation choice when handling coherent state path integrals, some of which are addressed in Part II. In particular, from the point of view of the Klauder-Daubechies construction [15] of the coherent path integral, the passage from the discrete to the continuous form of the action we used in Sec.8.2 (specifically the implicit discarding of the time offset of fields in the Lindbladian term before passing to the continuous form), while conventional, actually corresponds to an incorrect operator ordering and would not satisfy $\langle I \rangle = 1$. It is thus unsurprising that a post-hoc correction is required at a later stage to achieve this desired normalisation.

9.2 General Lindbladian Model

In this section I construct the Keldysh action and associated Truncated Wigner equations for a general Lindbladian with many-particle gain and loss. This model generalises that found in Ref. [16] for incoherently driven polaritons.
Denoting the individual dissipator operators $D[o,\rho] = \int d\boldsymbol{r}\,[o\rho o^\dagger - \frac{1}{2}\{o^\dagger o, \rho\}]$,

$$\mathcal{L}[\rho] = -i[H,\rho] + \mathscr{D}[\rho], \tag{9.23}$$

$$H = \int d\boldsymbol{r}\Big[a^\dagger_{\boldsymbol{r}}(\omega_0 - K\nabla^2)a_{\boldsymbol{r}} + \sum_{n=2}^{M} u_n (a^\dagger_{\boldsymbol{r}})^n a^n_{\boldsymbol{r}}\Big], \tag{9.24}$$

$$\mathscr{D}[\rho] = \sum_{n=1}^{N} \gamma_{p,n} D[(a^\dagger_{\boldsymbol{r}})^n, \rho] + \sum_{n=1}^{L} \gamma_{l,n} D[a^n_{\boldsymbol{r}}, \rho]. \tag{9.25}$$

The pumping terms $D[(a^\dagger_{\boldsymbol{r}})^n, \rho]$ pose a difficulty for constructing a corresponding Keldysh functional integral since, as discussed before, they are not normal-

ordered. Moreover, the approach taken in [8] and Part Ia to circumvent this problem generates Lamb shift terms that affect the coefficients of terms $u_n(a_{\boldsymbol{r}}^\dagger)^n a_{\boldsymbol{r}}^n$ in the Hamiltonian. In order to neglect these terms the Hamiltonian coefficients should be significantly larger, which means that the Hamiltonian must possess such terms in the first place. We thus require that $M \geq N$.

With this in mind, we may now proceed using the method of Sec. 8.2 as if all terms are normal-ordered. We undertake this in the following subsections.

9.2.1 Dissipation Contribution

Starting with the dissipation contributions $\gamma_{l,n} D[a_{\boldsymbol{r}}^n, \rho]$, we find

$$
\begin{aligned}
&\frac{\mathrm{Tr}[|\psi^-_{\boldsymbol{r},j}\rangle\langle\psi^+_{\boldsymbol{r},j}| D\left[a_{\boldsymbol{r}}^n, |\psi^+_{\boldsymbol{r},j-1}\rangle\langle\psi^-_{\boldsymbol{r},j-1}|\right]]}{\mathrm{Tr}[|\psi^-_{\boldsymbol{r},j}\rangle\langle\psi^+_{\boldsymbol{r},j}|\psi^+_{\boldsymbol{r},j-1}\rangle\langle\psi^-_{\boldsymbol{r},j-1}|]} \\
&= \int d\boldsymbol{r}\, \frac{\gamma_{l,n}}{\langle\psi^-_{\boldsymbol{r},j-1}|\psi^-_{\boldsymbol{r},j}\rangle\langle\psi^+_{\boldsymbol{r},j}|\psi^+_{\boldsymbol{r},j-1}\rangle}\Big[\langle\psi^+_{\boldsymbol{r},j}|a_{\boldsymbol{r}}^n|\psi^+_{\boldsymbol{r},j-1}\rangle\langle\psi^-_{\boldsymbol{r},j-1}|(a_{\boldsymbol{r}}^\dagger)^n|\psi^-_{\boldsymbol{r},j}\rangle \\
&\qquad\qquad - \frac{1}{2}\Big(\langle\psi^+_{\boldsymbol{r},j}|(a_{\boldsymbol{r}}^\dagger)^n a_{\boldsymbol{r}}^n|\psi^+_{\boldsymbol{r},j-1}\rangle\langle\psi^-_{\boldsymbol{r},j-1}|\psi^-_{\boldsymbol{r},j}\rangle \\
&\qquad\qquad + \langle\psi^+_{\boldsymbol{r},j}|\psi^+_{\boldsymbol{r},j-1}\rangle\langle\psi^-_{\boldsymbol{r},j-1}|(a_{\boldsymbol{r}}^\dagger)^n a_{\boldsymbol{r}}^n|\psi^-_{\boldsymbol{r},j}\rangle\Big)\Big] \qquad (9.26) \\
&\xrightarrow[\epsilon\to 0]{} \int d\boldsymbol{r}\, \gamma_{l,n}\Big[(\psi^+_{\boldsymbol{r},t})^n(\bar\psi^-_{\boldsymbol{r},t})^n - \frac{1}{2}((\psi^+_{\boldsymbol{r},t})^n(\bar\psi^+_{\boldsymbol{r},t})^n + (\psi^-_{\boldsymbol{r},t})^n(\bar\psi^-_{\boldsymbol{r},t})^n\Big] \\
&= \int d\boldsymbol{r}\, \frac{\gamma_{l,n}}{2^n}\Big[(\psi^c_{\boldsymbol{r},t} + \psi^q_{\boldsymbol{r},t})^n(\bar\psi^c_{\boldsymbol{r},t} - \bar\psi^q_{\boldsymbol{r},t})^n \\
&\qquad\qquad - \frac{1}{2}\Big((\psi^c_{\boldsymbol{r},t} + \psi^q_{\boldsymbol{r},t})^n(\bar\psi^c_{\boldsymbol{r},t} + \bar\psi^q_{\boldsymbol{r},t})^n + (\psi^c_{\boldsymbol{r},t} - \psi^q_{\boldsymbol{r},t})^n(\bar\psi^c_{\boldsymbol{r},t} - \bar\psi^q_{\boldsymbol{r},t})^n\Big)\Big].
\end{aligned}
$$

Anticipating our use of the Truncated Wigner approximation, we may expand this to second order in $\psi^q_{\boldsymbol{r},t}$ to obtain

$$
\int d\boldsymbol{r}\, \frac{n\gamma_{l,n}|\psi^c_{\boldsymbol{r},t}|^{2(n-1)}}{2^{n-1}}\left[\frac{1}{2}\psi^q_{\boldsymbol{r},t}\bar\psi^c_{\boldsymbol{r},t} - \frac{1}{2}\bar\psi^q_{\boldsymbol{r},t}\psi^c_{\boldsymbol{r},t} - n|\psi^q_{\boldsymbol{r},t}|^2\right]. \qquad (9.27)
$$

9.2.2 Drive Contribution

Moving onto the drive terms $\gamma_{p,n} D[(a_{\boldsymbol{r}}^\dagger)^n, \rho]$ and recalling that we may treat them as normal ordered up to Lamb shifts, the process is very similar:

$$\begin{aligned}
&\frac{\mathrm{Tr}[|\psi^-_{\boldsymbol{r},j}\rangle\langle\psi^+_{\boldsymbol{r},j}| D\left[(a_{\boldsymbol{r}}^\dagger)^n, |\psi^+_{\boldsymbol{r},j-1}\rangle\langle\psi^-_{\boldsymbol{r},j-1}|\right]]}{\mathrm{Tr}[|\psi^-_{\boldsymbol{r},j}\rangle\langle\psi^+_{\boldsymbol{r},j}|\psi^+_{\boldsymbol{r},j-1}\rangle\langle\psi^-_{\boldsymbol{r},j-1}|]} \\
&= \int d\boldsymbol{r}\, \frac{\gamma_{p,n}}{\langle\psi^-_{\boldsymbol{r},j-1}|\psi^-_{\boldsymbol{r},j}\rangle\langle\psi^+_{\boldsymbol{r},j}|\psi^+_{\boldsymbol{r},j-1}\rangle} \Big[\langle\psi^+_{\boldsymbol{r},j}|(a_{\boldsymbol{r}}^\dagger)^n|\psi^+_{\boldsymbol{r},j-1}\rangle\langle\psi^-_{\boldsymbol{r},j-1}|a_{\boldsymbol{r}}^n|\psi^-_{\boldsymbol{r},j}\rangle \\
&\qquad - \frac{1}{2}\Big(\langle\psi^+_{\boldsymbol{r},j}|(a_{\boldsymbol{r}}^\dagger)^n a_{\boldsymbol{r}}^n|\psi^+_{\boldsymbol{r},j-1}\rangle\langle\psi^-_{\boldsymbol{r},j-1}|\psi^-_{\boldsymbol{r},j}\rangle \\
&\qquad + \langle\psi^+_{\boldsymbol{r},j}|\psi^+_{\boldsymbol{r},j-1}\rangle\langle\psi^-_{\boldsymbol{r},j-1}|(a_{\boldsymbol{r}}^\dagger)^n a_{\boldsymbol{r}}^n|\psi^-_{\boldsymbol{r},j}\rangle\Big)\Big] \\
&\xrightarrow[\epsilon\to 0]{} \int d\boldsymbol{r}\, \gamma_{p,n}\left[(\bar\psi^+_{\boldsymbol{r},t})^n(\psi^-_{\boldsymbol{r},t})^n - \frac{1}{2}((\psi^+_{\boldsymbol{r},t})^n(\bar\psi^+_{\boldsymbol{r},t})^n + (\psi^-_{\boldsymbol{r},t})^n(\bar\psi^-_{\boldsymbol{r},t})^n\right] \\
&= \int d\boldsymbol{r}\, \frac{\gamma_{p,n}}{2^n}\Big[(\bar\psi^c_{\boldsymbol{r},t} + \bar\psi^q_{\boldsymbol{r},t})^n(\psi^c_{\boldsymbol{r},t} - \psi^q_{\boldsymbol{r},t})^n \\
&\qquad - \frac{1}{2}\left((\psi^c_{\boldsymbol{r},t} + \psi^q_{\boldsymbol{r},t})^n(\bar\psi^c_{\boldsymbol{r},t} + \bar\psi^q_{\boldsymbol{r},t})^n + (\psi^c_{\boldsymbol{r},t} - \psi^q_{\boldsymbol{r},t})^n(\bar\psi^c_{\boldsymbol{r},t} - \bar\psi^q_{\boldsymbol{r},t})^n\right)\Big].
\end{aligned} \tag{9.28}$$

Again anticipating Truncated Wigner, to second order in $\psi^q_{\boldsymbol{r},t}$ this is

$$\int d\boldsymbol{r}\, \frac{n\gamma_{p,n}|\psi^c_{\boldsymbol{r},t}|^{2(n-1)}}{2^{n-1}}\left[\frac{1}{2}\bar\psi^q_{\boldsymbol{r},t}\psi^c_{\boldsymbol{r},t} - \frac{1}{2}\psi^q_{\boldsymbol{r},t}\bar\psi^c_{\boldsymbol{r},t} - n|\psi^q_{\boldsymbol{r},t}|^2\right]. \tag{9.29}$$

9.2.3 Hamiltonian Contribution

Finally we consider the contribution to the action from the Hamiltonian

$$H = \int d\boldsymbol{r}\left[a_{\boldsymbol{r}}^\dagger(\omega_0 - K\nabla^2)a_{\boldsymbol{r}} + \sum_{n=2}^{M} u_n (a_{\boldsymbol{r}}^\dagger)^n a_{\boldsymbol{r}}^n\right]. \tag{9.30}$$

This is clearly

$$\begin{aligned}
-\int dt d\boldsymbol{r}\Big[&\bar\psi^+_{\boldsymbol{r},t}(\omega_0 - K\nabla^2)\psi^+_{\boldsymbol{r},t} + \sum_{n=2}^{M} u_n(\bar\psi^+_{\boldsymbol{r},t})^n(\psi^+_{\boldsymbol{r},t})^n \\
&- \bar\psi^-_{\boldsymbol{r},t}(\omega_0 - K\nabla^2)\psi^-_{\boldsymbol{r},t} - \sum_{n=2}^{M} u_n(\bar\psi^-_{\boldsymbol{r},t})^n(\psi^-_{\boldsymbol{r},t})^n\Big]
\end{aligned} \tag{9.31}$$

which, when rewritten in terms of Keldysh fields, yields to second order $\psi^q_{\boldsymbol{r},t}$:

$$\int dtd\boldsymbol{r}\Bigg[\begin{pmatrix}\psi^c_{\boldsymbol{r},t}\\ \psi^q_{\boldsymbol{r},t}\end{pmatrix}^\dagger\begin{pmatrix}0 & -\omega_0+K\nabla^2\\ -\omega_0+K\nabla^2 & 0\end{pmatrix}\begin{pmatrix}\psi^c_{\boldsymbol{r},t}\\ \psi^q_{\boldsymbol{r},t}\end{pmatrix} - \sum_{n=2}^{M}\frac{nu_n|\psi^c_{\boldsymbol{r},t}|^{2(n-1)}}{2^{n-1}}\left(\bar\psi^c_{\boldsymbol{r},t}\psi^q_{\boldsymbol{r},t}+\psi^c_{\boldsymbol{r},t}\bar\psi^q_{\boldsymbol{r},t}\right)\Bigg] \tag{9.32}$$

9.2.4 Truncated Wigner Equations

Taking into account the dynamical terms, the overall action to second order in the ψ^q fields comes out to be

$$\begin{aligned}S=\int dtd\boldsymbol{r}\Bigg[&\begin{pmatrix}\psi^c_{\boldsymbol{r},t}\\ \psi^q_{\boldsymbol{r},t}\end{pmatrix}^\dagger\begin{pmatrix}0 & i\partial_t-\omega_0+K\nabla^2\\ i\partial_t-\omega_0+K\nabla^2 & 0\end{pmatrix}\begin{pmatrix}\psi^c_{\boldsymbol{r},t}\\ \psi^q_{\boldsymbol{r},t}\end{pmatrix}\\ &-\sum_{n=2}^{M}\frac{nu_n|\psi^c_{\boldsymbol{r},t}|^{2(n-1)}}{2^{n-1}}\left(\bar\psi^c_{\boldsymbol{r},t}\psi^q_{\boldsymbol{r},t}+\psi^c_{\boldsymbol{r},t}\bar\psi^q_{\boldsymbol{r},t}\right)\\ &-i\sum_{n=1}^{N}\frac{n\gamma_{p,n}|\psi^c_{\boldsymbol{r},t}|^{2(n-1)}}{2^{n-1}}\left(\frac{1}{2}\bar\psi^q_{\boldsymbol{r},t}\psi^c_{\boldsymbol{r},t}-\frac{1}{2}\psi^q_{\boldsymbol{r},t}\bar\psi^c_{\boldsymbol{r},t}-n|\psi^q_{\boldsymbol{r},t}|^2\right)\\ &-i\sum_{n=1}^{L}\frac{n\gamma_{l,n}|\psi^c_{\boldsymbol{r},t}|^{2(n-1)}}{2^{n-1}}\left(\frac{1}{2}\psi^q_{\boldsymbol{r},t}\bar\psi^c_{\boldsymbol{r},t}-\frac{1}{2}\bar\psi^q_{\boldsymbol{r},t}\psi^c_{\boldsymbol{r},t}-n|\psi^q_{\boldsymbol{r},t}|^2\right)\Bigg].\end{aligned} \tag{9.33}$$

This may be rewritten in a more familiar form by writing $\gamma_{p,1}-\gamma_{l,1}=\delta_\gamma$, $\gamma_{p,1}+\gamma_{l,1}=\sigma_\gamma$, and moving the $n=1$ terms from the dissipator contributions into the quadratic matrix contribution, yielding

$$\begin{aligned}S=\int dtd\boldsymbol{r}\Bigg[&\begin{pmatrix}\psi^c_{\boldsymbol{r},t}\\ \psi^q_{\boldsymbol{r},t}\end{pmatrix}^\dagger\begin{pmatrix}0 & i\partial_t-\omega_0+K\nabla^2+\frac{i}{2}\delta_\gamma\\ i\partial_t-\omega_0+K\nabla^2-\frac{i}{2}\delta_\gamma & i\sigma_\gamma\end{pmatrix}\begin{pmatrix}\psi^c_{\boldsymbol{r},t}\\ \psi^q_{\boldsymbol{r},t}\end{pmatrix}\\ &-\sum_{n=2}^{M}\frac{nu_n|\psi^c_{\boldsymbol{r},t}|^{2(n-1)}}{2^{n-1}}\left(\bar\psi^c_{\boldsymbol{r},t}\psi^q_{\boldsymbol{r},t}+\psi^c_{\boldsymbol{r},t}\bar\psi^q_{\boldsymbol{r},t}\right)\\ &-i\sum_{n=2}^{N}\frac{n\gamma_{p,n}|\psi^c_{\boldsymbol{r},t}|^{2(n-1)}}{2^{n-1}}\left(\frac{1}{2}\bar\psi^q_{\boldsymbol{r},t}\psi^c_{\boldsymbol{r},t}-\frac{1}{2}\psi^q_{\boldsymbol{r},t}\bar\psi^c_{\boldsymbol{r},t}-n|\psi^q_{\boldsymbol{r},t}|^2\right)\\ &-i\sum_{n=2}^{L}\frac{n\gamma_{l,n}|\psi^c_{\boldsymbol{r},t}|^{2(n-1)}}{2^{n-1}}\left(\frac{1}{2}\psi^q_{\boldsymbol{r},t}\bar\psi^c_{\boldsymbol{r},t}-\frac{1}{2}\bar\psi^q_{\boldsymbol{r},t}\psi^c_{\boldsymbol{r},t}-n|\psi^q_{\boldsymbol{r},t}|^2\right)\Bigg].\end{aligned} \tag{9.34}$$

Finally, we may add external classical scalar and vector fields $h_{\boldsymbol{r},t}$, $f^j_{\boldsymbol{r},t}$ coupled to the system's quantum field and quantum current (as defined in Sec. 4.3.2) to the action. These contributions have the form

$$\bar h_{\boldsymbol{r},t}\psi^q_{\boldsymbol{r},t}+h_{\boldsymbol{r},t}\bar\psi^q_{\boldsymbol{r},t}, \tag{9.35}$$

$$\underbrace{f^j_{\boldsymbol{r},t}\frac{K}{i}\left(\bar{\psi}^c_{\boldsymbol{r},t}\nabla_j\psi^q_{\boldsymbol{r},t}+\bar{\psi}^q_{\boldsymbol{r},t}\nabla_j\psi^c_{\boldsymbol{r},t}-\psi^c_{\boldsymbol{r},t}\nabla_j\bar{\psi}^q_{\boldsymbol{r},t}-\psi^q_{\boldsymbol{r},t}\nabla_j\bar{\psi}^c_{\boldsymbol{r},t}\right)}_{j_q}, \tag{9.36}$$

and will allow us, in the next chapter, to calculate response functions (we will not actually make use of the $h_{\boldsymbol{r},t}$ field, but add it for completeness).

With these in place we are ready to derive the Truncated Wigner equations for the total action.

$$\begin{aligned}
S_{hf}=\int dtd\boldsymbol{r}\Bigg[&\begin{pmatrix}\psi^c_{\boldsymbol{r},t}\\ \psi^q_{\boldsymbol{r},t}\end{pmatrix}^\dagger\begin{pmatrix}0 & i\partial_t-\omega_0+K\nabla^2+\frac{i}{2}\delta_\gamma\\ i\partial_t-\omega_0+K\nabla^2-\frac{i}{2}\delta_\gamma & i\sigma_\gamma\end{pmatrix}\begin{pmatrix}\psi^c_{\boldsymbol{r},t}\\ \psi^q_{\boldsymbol{r},t}\end{pmatrix}\\
&-\sum_{n=2}^{M}\frac{nu_n|\psi^c_{\boldsymbol{r},t}|^{2(n-1)}}{2^{n-1}}\left(\bar{\psi}^c_{\boldsymbol{r},t}\psi^q_{\boldsymbol{r},t}+\psi^c_{\boldsymbol{r},t}\bar{\psi}^q_{\boldsymbol{r},t}\right)\\
&-i\sum_{n=2}^{N}\frac{n\gamma_{p,n}|\psi^c_{\boldsymbol{r},t}|^{2(n-1)}}{2^{n-1}}\left(\frac{1}{2}\bar{\psi}^q_{\boldsymbol{r},t}\psi^c_{\boldsymbol{r},t}-\frac{1}{2}\psi^q_{\boldsymbol{r},t}\bar{\psi}^c_{\boldsymbol{r},t}-n|\psi^q_{\boldsymbol{r},t}|^2\right)\\
&-i\sum_{n=2}^{L}\frac{n\gamma_{l,n}|\psi^c_{\boldsymbol{r},t}|^{2(n-1)}}{2^{n-1}}\left(\frac{1}{2}\psi^q_{\boldsymbol{r},t}\bar{\psi}^c_{\boldsymbol{r},t}-\frac{1}{2}\bar{\psi}^q_{\boldsymbol{r},t}\psi^c_{\boldsymbol{r},t}-n|\psi^q_{\boldsymbol{r},t}|^2\right)\\
&+\bar{h}_{\boldsymbol{r},t}\psi^q_{\boldsymbol{r},t}+h_{\boldsymbol{r},t}\bar{\psi}^q_{\boldsymbol{r},t}\\
&-if^j_{\boldsymbol{r},t}K\left(\bar{\psi}^c_{\boldsymbol{r},t}\nabla_j\psi^q_{\boldsymbol{r},t}+\bar{\psi}^q_{\boldsymbol{r},t}\nabla_j\psi^c_{\boldsymbol{r},t}-\psi^c_{\boldsymbol{r},t}\nabla_j\bar{\psi}^q_{\boldsymbol{r},t}-\psi^q_{\boldsymbol{r},t}\nabla_j\bar{\psi}^c_{\boldsymbol{r},t}\right)\Bigg].
\end{aligned} \tag{9.37}$$

We know from Sec 9.1 that these take the form

$$\frac{\partial S}{\partial\bar{\psi}^q_{\boldsymbol{r},t}}\Big|_{\psi^q_{\boldsymbol{r},t}=0}+\sqrt{M_{\boldsymbol{r},t}}\xi_{\boldsymbol{r},t}=0, \tag{9.38}$$

$$M_{\boldsymbol{r},t}=-i\frac{\partial^2 S}{\partial\bar{\psi}^q_{\boldsymbol{r},t}\partial\psi^q_{\boldsymbol{r},t}}\Big|_{\psi^q_{\boldsymbol{r},t}=0}, \tag{9.39}$$

so all that is required is to calculate $\frac{\partial S}{\partial\bar{\psi}^q_{\boldsymbol{r},t}}\Big|_{\psi^q_{\boldsymbol{r},t}=0}$, $\frac{\partial^2 S}{\partial\bar{\psi}^q_{\boldsymbol{r},t}\partial\psi^q_{\boldsymbol{r},t}}\Big|_{\psi^q_{\boldsymbol{r},t}=0}$. This is easily achieved, giving[3]

$$\frac{\partial^2 S}{\partial\bar{\psi}^q_{\boldsymbol{r},t}\partial\psi^q_{\boldsymbol{r},t}}\Big|_{\psi^q_{\boldsymbol{r},t}=0}=i\sigma_\gamma+i\sum_{n=2}^{N}\frac{n^2\gamma_{p,n}|\psi^c_{\boldsymbol{r},t}|^{2(n-1)}}{2^{n-1}}+i\sum_{n=2}^{L}\frac{n^2\gamma_{l,n}|\psi^c_{\boldsymbol{r},t}|^{2(n-1)}}{2^{n-1}}, \tag{9.40}$$

[3]We will consider the dynamical and external classical fields to be cyclic on their domains, meaning no boundary terms are generated during required integrations by parts. For the dynamical fields this can be argued on the grounds that the domain is meant to represent the bulk of a driven dissipative system and so spatial cyclic boundary conditions are appropriate, while the smoothing nature of dissipative dynamics means that the initial conditions may be ignored and thus freely set equal to the final ones. The external fields will generally be used in the static limit (cyclic in time), and no difficulties arise from choosing them to be cyclic in space.

$$\begin{aligned}\frac{\partial S}{\partial \bar{\psi}^q_{\boldsymbol{r},t}}\Big|_{\psi^q_{\boldsymbol{r},t}=0} = \Bigg(& i\partial_t - \omega_0 + K\nabla^2 - \frac{i}{2}\delta_\gamma - \sum_{n=2}^{M} \frac{n u_n |\psi^c_{\boldsymbol{r},t}|^{2(n-1)}}{2^{n-1}} \\ & - i\sum_{n=2}^{N} \frac{n\gamma_{p,n}|\psi^c_{\boldsymbol{r},t}|^{2(n-1)}}{2^n} + i\sum_{n=2}^{L} \frac{n\gamma_{l,n}|\psi^c_{\boldsymbol{r},t}|^{2(n-1)}}{2^n} \\ & - 2iKf^j\nabla_j - iK(\nabla_j f^j)\Bigg)\psi^c_{\boldsymbol{r},t} + h_{\boldsymbol{r},t}.\end{aligned} \tag{9.41}$$

The overall Langevin equation, over the trajectories of which we may average observables dependent on ψ^c to find their expectation values, is thus

$$\begin{aligned}& \Bigg(i\partial_t - \omega_0 + K\nabla^2 - \frac{i}{2}\delta_\gamma - \sum_{n=2}^{M} \frac{n u_n |\psi^c_{\boldsymbol{r},t}|^{2(n-1)}}{2^{n-1}} \\ & \quad - i\sum_{n=2}^{N} \frac{n\gamma_{p,n}|\psi^c_{\boldsymbol{r},t}|^{2(n-1)}}{2^n} + i\sum_{n=2}^{L} \frac{n\gamma_{l,n}|\psi^c_{\boldsymbol{r},t}|^{2(n-1)}}{2^n} \\ & \quad - 2iKf^j\nabla_j - iK(\nabla_j f^j)\Bigg)\psi^c_{\boldsymbol{r},t} \\ & + h_{\boldsymbol{r},t} \\ & + \xi_{\boldsymbol{r},t}\sqrt{\sigma_\gamma + \sum_{n=2}^{N} \frac{n^2\gamma_{p,n}|\psi^c_{\boldsymbol{r},t}|^{2(n-1)}}{2^{n-1}} + \sum_{n=2}^{L} \frac{n^2\gamma_{l,n}|\psi^c_{\boldsymbol{r},t}|^{2(n-1)}}{2^{n-1}}} = 0.\end{aligned} \tag{9.42}$$

To finish, let us specialise this expression to a Lindbladian plausibly describing a polariton system (one which we will consider in Part Ic), namely one with a quartic interaction in the Hamiltonian $M = 2$, single-particle incoherent gain $N = 1 < M$, and single and two-particle loss $L = 2$. In this case the Langevin equation simplifies considerably, yielding

$$\begin{aligned}\Big(i\partial_t - \omega_0 + K\nabla^2 - \frac{i}{2}\delta_\gamma + \Big(\frac{i}{2}\gamma_{l,2} - u_n\Big)|\psi^c_{\boldsymbol{r},t}|^2 - 2iKf^j\nabla_j - iK(\nabla_j f^j)\Big)\psi^c_{\boldsymbol{r},t} \\ + h_{\boldsymbol{r},t} + \sqrt{\sigma_\gamma + 2\gamma_{l,2}|\psi^c_{\boldsymbol{r},t}|^2}\,\xi_{\boldsymbol{r},t} = 0.\end{aligned} \tag{9.43}$$

In the next chapter I will consider how this equation (or the more general equation if a more exotic system is considered) may be used to calculate a system's current-current response and thus analyse whether it can sustain a superfluid phase.

Chapter 10

Truncated Wigner Approximation for Superfluidity

With the Truncated Wigner equations in hand, we are now ready to consider how they may be used to calculate the superfluid fraction of the system they describe. As in Part Ia we will use the definition of superfluid based on the system's current-current response, and once again consider its directional static limits. Unlike in the Keldysh formalism where operators could depend on both classical and quantum fields with no difficulty, however, with the Truncated Wigner approximation we are constrained to calculating expectations of time-symmetrically ordered operators depending only on the classical fields. Since the current-current response does not fit this description, we will have to take a more indirect approach to its calculation.

10.1 Current-Current Response

As discussed in Chap. 4, in studying superfluidity we typically seek the static current-current response tensor

$$\chi_{ij}(\mathbf{q}) = i\langle j_i^c(\omega = 0, \mathbf{q}) j_j^q(\omega = 0, -\mathbf{q})\rangle, \tag{10.1}$$

$$j_i^c(0, \mathbf{q}) = j_i^c(\mathbf{q}) = \frac{1}{2}\sum_{\omega,\mathbf{k}} \gamma_i(2\mathbf{k} + \mathbf{q})[\psi^c(\omega, \mathbf{k} + \mathbf{q})\bar{\psi}^c(\omega, \mathbf{k}) + \psi^q(\omega, \mathbf{k} + \mathbf{q})\bar{\psi}^q(\omega, \mathbf{k})], \tag{10.2}$$

$$j_i^q(0, \mathbf{q}) = j_i^q(\mathbf{q}) = \sum_{\omega,\mathbf{k}} \gamma_i(2\mathbf{k} + \mathbf{q})[\psi^c(\omega, \mathbf{k} + \mathbf{q})\bar{\psi}^q(\omega, \mathbf{k}) + \psi^q(\omega, \mathbf{k} + \mathbf{q})\bar{\psi}^c(\omega, \mathbf{k})], \tag{10.3}$$

$$\gamma_i(\boldsymbol{k}) = K(\boldsymbol{k})_i, \tag{10.4}$$

which encodes the response of the classical static current $j_i^c(\mathbf{q})$ to the static component of the external classical field $f^i(\boldsymbol{q}) = f^i(0,\mathbf{q})$:

$$\langle \delta j_i^c(\mathbf{q})\rangle = \chi_{ij}(\mathbf{q}) f^j(\mathbf{q}). \tag{10.5}$$

As mentioned in the first paragraph, we cannot directly calculate $\chi_{ij}(\boldsymbol{q})$ with the Truncated Wigner method because it is an expectation of an operator dependent on both the quantum and classical fields. We may notice, however, that $j_i^c(\boldsymbol{q})$ splits into terms individually consisting of either only classical or quantum fields. Since the correlator of two quantum fields is 0 in the Keldysh formalism [12], we see that

$$\langle j_i^c(\mathbf{q})\rangle = \sum_{\omega,\mathbf{k}} \gamma_i(2\mathbf{k}+\mathbf{q})\langle \psi^c(\omega,\mathbf{k}+\mathbf{q})\bar{\psi}^c(\omega,\mathbf{k})\rangle. \tag{10.6}$$

This now depends only on classical fields, and may be calculated in our formalism. A possible approach to calculating $\chi_{ij}(\boldsymbol{q})$ is thus to work backwards from (10.5). By measuring the response of the current to appropriately chosen external fields, the response tensor may be recovered from this equation.

Considering all averages in the remainder of this section to be over realisations of the stochastic trajectories of the system's Langevin equation, we wish to calculate $\langle \delta j_c^a(\boldsymbol{q})\rangle$ as the difference between $\langle j_c^a(\mathbf{q})\rangle_f$ and $\langle j_c^a(\mathbf{q})\rangle_0$. The subscript denotes whether the field $\boldsymbol{f}$ is present in the action, and we have set $h = 0$ since we are not calculating responses associated to it here. Assuming a bounded, cyclic domain of temporal extent T and spatial extent L with Fourier conventions

$$k_n = 2\pi n/T, \tag{10.7}$$

$$f(t) = \sum_{n=-\infty}^{\infty} f_n e^{ik_n t}, \tag{10.8}$$

$$f_n = \frac{1}{T}\int_{-T/2}^{T/2} dt\, f(t) e^{-ik_n t}, \tag{10.9}$$

we have, for the static current:

$$j_i^c(0,\mathbf{x}) = \frac{1}{T}\int_{-T/2}^{T/2} dt\, j_i^c(t,\mathbf{x}) = \frac{2K}{T}\int_{-T/2}^{T/2} dt\, \mathrm{Im}\Big[\bar{\psi}(t,\mathbf{x})\nabla_a\psi(t,\mathbf{x})\Big], \tag{10.10}$$

$$j_i^c(0,\mathbf{k}) = \frac{1}{T}\sum_{\mathbf{q}}\int_{-T/2}^{T/2} dt\, \gamma_i(2\mathbf{q}+\mathbf{k})\psi(\mathbf{q}+\mathbf{k})\bar{\psi}(\mathbf{q}). \tag{10.11}$$

The stochastic average commutes with integration, summation, and differentiation, so it is sufficient to calculate either $\langle \bar{\psi}(t,\mathbf{x})\psi(t,\mathbf{y})\rangle$ or $\langle \bar{\psi}(t,\mathbf{q})\psi(t,\mathbf{k})\rangle$. The

current average can then be obtained by post-processing this expectation according to the preceding formulas.

One way to extract the response would be to select a sequence $\epsilon_n \to 0$ as $n \to \infty$ and, for each ϵ_m, calculate the response for two different perturbing fields

$$\mathbf{f}_1(\mathbf{x}) = \epsilon_m \begin{pmatrix} g(\mathbf{x}) \\ 0 \end{pmatrix}, \tag{10.12}$$

$$\mathbf{f}_2(\mathbf{x}) = \epsilon_m \begin{pmatrix} 0 \\ g(\mathbf{x}) \end{pmatrix}, \tag{10.13}$$

where $g(\mathbf{x})$ is a function containing all Fourier basis functions (or at least all those in some neighbourhood of $\boldsymbol{k} = 0$, since that is the region of the response we are most interested in). This means that the response equation in two spatial dimensions (we take $i = x, y$) will take the form ($j_{i,n}$ represents the i-th coordinate of the current in the presence of the n-th external field $\boldsymbol{f}_n$).

$$\left\langle \delta \begin{pmatrix} j_{x,1}(\mathbf{k}_n) & j_{x,2}(\mathbf{k}_n) \\ j_{y,1}(\mathbf{k}_n) & j_{y,2}(\mathbf{k}_n) \end{pmatrix} \right\rangle = \epsilon_m g(\mathbf{k}_n) \begin{pmatrix} \chi_{11}(\mathbf{k}_n) & \chi_{12}(\mathbf{k}_n) \\ \chi_{21}(\mathbf{k}_n) & \chi_{22}(\mathbf{k}_n) \end{pmatrix} \begin{pmatrix} 1 & 0 \\ 0 & 1 \end{pmatrix}, \tag{22}$$

i.e.

$$\begin{pmatrix} \chi_{11}(\mathbf{k}_n) & \chi_{12}(\mathbf{k}_n) \\ \chi_{21}(\mathbf{k}_n) & \chi_{22}(\mathbf{k}_n) \end{pmatrix} = \lim_{m\to\infty} \frac{1}{\epsilon_m g(\mathbf{k}_n)} \left(\left\langle \begin{pmatrix} j_{x,1}(\mathbf{k}_n) & j_{x,2}(\mathbf{k}_n) \\ j_{y,1}(\mathbf{k}_n) & j_{y,2}(\mathbf{k}_n) \end{pmatrix} \right\rangle_{\epsilon_m} - \left\langle \begin{pmatrix} j_{x,1}(\mathbf{k}_n) & j_{x,2}(\mathbf{k}_n) \\ j_{y,1}(\mathbf{k}_n) & j_{y,2}(\mathbf{k}_n) \end{pmatrix} \right\rangle_0 \right). \tag{23}$$

If the sequence on the RHS converges, one obtains a good estimate for the response tensor in Fourier components. This can then be analysed analytically to study superfluidity. Note that this approach does not require the separate use of longitudinal and transverse forces.

10.1.1 Isotropic Simplification

In the isotropic case this simplifies considerably. The most general form of a rotationally invariant matrix in momentum space is

$$\chi_{ij}(\mathbf{q}) = \frac{q_i q_j}{|\mathbf{q}|^2} \chi_S(|\mathbf{q}|) + \delta_{ij} \chi_N(|\mathbf{q}|). \tag{10.14}$$

Here χ_S encodes the superfluid response in the $|\mathbf{q}| \to 0$ limit, and likewise χ_N the normal response in that same limit. Comparing to expression (4.22) in Chap. 4, we have put $\chi_S = \chi_L - \chi_T$ and $\chi_N = \chi_T$ since a superfluid responds only to longitudinal perturbations.

This means that if we consider the χ^{xx} component:

$$\chi_{xx}(\mathbf{q}) = \frac{(q_x)^2}{(q_x)^2 + (q_y)^2}\chi_S(|\mathbf{q}|) + \chi_N(\mathbf{q}) \tag{10.15}$$

$$\lim_{q_x\to 0}\chi_{xx}(\mathbf{q}) = \chi_N(|q_y|) \tag{10.16}$$

$$\lim_{q_y\to 0}\lim_{q_x\to 0}\chi_{xx}(\mathbf{q}) = \lim_{|\mathbf{q}|\to 0}\chi_N(|\mathbf{q}|) = N \tag{10.17}$$

$$\lim_{q_y\to 0}\chi_{xx}(\mathbf{q}) = \chi_S(|q_x|) + \chi_N(|q_x|) \tag{10.18}$$

$$\lim_{q_x\to 0}\lim_{q_y\to 0}\chi_{xx}(\mathbf{q}) = \lim_{|\mathbf{q}|\to 0}\Big(\chi_S(|\mathbf{q}|) + \chi_N(|\mathbf{q}|)\Big) = T \tag{10.19}$$

We thus see that we can obtain all information about the superfluid fraction from just the χ_{xx} component as:

$$\mathrm{f}_S = \frac{T-N}{N}. \tag{10.20}$$

In light of this, it is sufficient to calculate $\chi_{xx}(\mathbf{q})$. We may now choose a convenient magnitude function $g(\mathbf{x})$ for our source field:

$$f_x(\mathbf{x}) = \epsilon_m g(\mathbf{x}) \tag{10.21}$$

$$f_y(\mathbf{x}) = 0. \tag{10.22}$$

Given we are typically working in the bulk of the condensate (our justification for cyclic boundary conditions earlier), it would be conceptually elegant to consider a field that is strongly localised to this bulk. If the external field has a minimal effect near our boundaries, we may imagine that beyond the boundaries the field is not applied while keeping cyclic boundary conditions.

To this end, we will consider the "finite box" analogue of a sharply peaked Gaussian. This is the Jacobi Theta Function, or third Elliptic Theta Function. For our purposes what matters is its Fourier decomposition which, taking $\theta(\boldsymbol{x}) = \prod_i \theta_3(\frac{x_i}{L}; \frac{4i\pi}{L^2})$ for time and likewise for the spatial variables, is

$$\theta(\boldsymbol{q}) = e^{-|\boldsymbol{q}|^2}. \tag{10.23}$$

We then have the relation

$$\delta\langle j_x(\mathbf{q})\rangle = \chi_{xx}(\mathbf{q}) f_x(\mathbf{q}) = \epsilon_m e^{-|\mathbf{q}|^2}\chi_{xx}(\mathbf{q}), \tag{10.24}$$

and we have an expression for $\chi_{xx}(\mathbf{q})$:

$$\chi_{xx}(\mathbf{q}) = \lim_{\epsilon_m\to 0}\frac{e^{|\mathbf{q}|^2}}{\epsilon_m}\Big(\langle j_x(\mathbf{q})\rangle_{\epsilon_m} - \langle j_x(\mathbf{q})\rangle_0\Big). \tag{10.25}$$

If it were possible to calculate the right hand side for all momenta in some neighbourhood of $\boldsymbol{q} = 0$ this would, as we established earlier, be sufficient to find the effective superfluid fraction of the system. In practice, one will run into the problem that due to the finite box/grid size of the simulation the available momenta will form a non-dense grid $\mathcal{Q}_L$ with spacing $\frac{2\pi}{L}$ and it will be possible to calculate $\chi_{xx}(\mathbf{q})$ only for $\boldsymbol{q} \in \mathcal{Q}_L$. This will pose an obstacle to taking the $\mathbf{q} \to 0$ limits, since the smallest non-zero available momenta values will be off-set by $\frac{2\pi}{L}$ from zero. This means that L must be big enough to see convergence in these limits. It is thus likely that, in practice, the application of this method would amount to taking a double limit of the sought quantity

$$\chi_{xx}(\mathbf{q}) = \lim_{\substack{L\to\infty \\ \epsilon_m\to 0}} \frac{e^{|\mathbf{q}|^2}}{\epsilon_m} \Big(\langle j_x(\mathbf{q}) \rangle_{\epsilon_m} - \langle j_x(\mathbf{q}) \rangle_0 \Big). \tag{10.26}$$

and observing whether convergence is obtained for numerically viable grid sizes and perturbations.

10.2 Conclusion

In the preceding two chapters we introduced the language of Lindbladian superoperators to describe general Markovian driven-dissipative systems and introduced the mappings from a Lindbladian to a Keldysh action and from the latter to a stochastic process via Truncated Wigner. Having then worked out the form of the stochastic process for a general Lindbladian with non-linear drive and dissipation and presented its simplification in the case of a Lindbladian appropriate to some polariton systems, this concluding chapter has been devoted to how this may be employed to calculate a driven-dissipative system's superfluid fraction.

In the process we have highlighted some difficulties such as:

1. normal-ordering problems associated with Lindbladians of infinite-dimensional systems;

2. the fact that only time-symmetrically ordered the finite strength of any perturbing external field;

3. disagreement between the Ito discretisation used for defining the stochastic process and the original discretisation of the Keldysh action; and

4. the need to numerically take a double limit in external field magnitude and system size.

The first three of these are essentially theoretical in nature, with the first two already possessing standard solutions in the literature. The third is somewhat

unsatisfactory and likely related to the material in Part II, but is not expected to pose any difficulties in practice. On the last point, it remains to be seen whether the double limit is numerically feasible.

During the course of my PhD I did not have the opportunity to apply this method to any problems, only derive it. The next steps for this project would entail the use of the XMDS software package [17] to run the associated stochastic simulations for the polariton model described in the previous chapter and to compare the results to known analytical ones [16]. This is likely to be undertaken by a different member of the group in the near future.

Bibliography

[1] W. F. Stinespring, "Positive functions on c*-algebras," *Proceedings of the American Mathematical Society*, vol. 6, no. 2, pp. 211–216, 1955.

[2] D. Gottesman and H.-K. Lo, "From quantum cheating to quantum security," *Physics Today*, vol. 53, no. 11, pp. 22–27, 2000.

[3] N. Wheeler, *Motion of the reduced density operator*, Reed College, 2009.

[4] H.-P. Breuer and F. Petruccione, *The theory of open quantum systems*. Oxford University Press, USA, 2002.

[5] C. J. Wood, "Non-completely positive maps: Properties and applications," *arXiv preprint arXiv:0911.3199*, 2009.

[6] M. A. Nielsen and I. L. Chuang, *Quantum computation and quantum information*. Cambridge university press Cambridge, 2001, vol. 2.

[7] L. M. Sieberer, M. Buchhold, and S. Diehl, "Keldysh field theory for driven open quantum systems," *Reports on Progress in Physics*, vol. 79, no. 9, p. 096 001, 2016.

[8] L. Sieberer, S. D. Huber, E. Altman, and S. Diehl, "Nonequilibrium functional renormalization for driven-dissipative bose-einstein condensation," *Physical Review B*, vol. 89, no. 13, p. 134 310, 2014.

[9] D. Whittaker, "Effects of polariton-energy renormalization in the microcavity optical parametric oscillator," *Physical Review B*, vol. 71, no. 11, p. 115 301, 2005.

[10] R. Juggins, "Superfluidity in coherently driven microcavity-polaritons," Ph.D. dissertation, UCL (University College London), 2019.

[11] L. M. Sieberer, M. Buchhold, and S. Diehl, "Keldysh field theory for driven open quantum systems," *Reports on Progress in Physics*, vol. 79, no. 9, p. 096 001, Aug. 2016. DOI: 10.1088/0034-4885/79/9/096001.

[12] A. Kamenev, *Field theory of non-equilibrium systems*. Cambridge University Press, 2023.

[13] A. Polkovnikov, "Quantum corrections to the dynamics of interacting bosons: Beyond the truncated wigner approximation," *Physical Review A*, vol. 68, no. 5, p. 053 604, 2003.

[14] A. Polkovnikov, "Phase space representation of quantum dynamics," *Annals of Physics*, vol. 325, no. 8, pp. 1790–1852, 2010.

[15] I. Daubechies and J. R. Klauder, "Quantum-mechanical path integrals with wiener measure for all polynomial hamiltonians. ii," *Journal of mathematical physics*, vol. 26, no. 9, pp. 2239–2256, 1985.

[16] N. P. Proukakis, D. W. Snoke, and P. B. Littlewood, *Universal themes of Bose-Einstein condensation*. Cambridge university press, 2017.

[17] G. R. Dennis, J. J. Hope, and M. T. Johnsson, "Xmds2: Fast, scalable simulation of coupled stochastic partial differential equations," *Computer Physics Communications*, vol. 184, no. 1, pp. 201–208, 2013.

Part III

Superfluidity in Non-Interacting Photon BEC

Chapter 11

The Model and its Mean Field

Aside from polaritons, photons in a dye cavity are another light-matter system capable of exhibiting Bose-Einstein condensation [1], [2]. Compared to the former, however, such photons have significantly weaker particle-particle interactions[1], which has motivated the study of how condensation can take place in this system via incoherent drive and dissipation rather than particle-particle interactions [4].

Given the possibility of condensation, a related question is whether a system with no particle-particle interactions can also exhibit superfluidity. A typical model for such dye cavity photons in the absence of a trapping potential and neglecting the particle-particle interactions is given by the following Lindbladian[2] [3], [5], [6]:

$$\mathscr{L}[\rho] = -i[H,\rho] + \mathscr{D}[\rho], \tag{11.1}$$

$$H = \int d\boldsymbol{r} \left[\psi^\dagger_{\boldsymbol{r}}(\omega_0 - K\nabla^2)\psi_{\boldsymbol{r}}\right], \tag{11.2}$$

$$\mathscr{D}[\rho] = \int d\boldsymbol{r} \left[\gamma_{p,1} D[\psi^\dagger_{\boldsymbol{r}},\rho] + \gamma_{l,1} D[\psi_{\boldsymbol{r}},\rho] + \gamma_{l,2} D[\psi^2_{\boldsymbol{r}},\rho]\right], \tag{11.3}$$

$$D[O,\rho] = O\rho O^\dagger - \frac{1}{2}\{O^\dagger O,\rho\}. \tag{11.4}$$

This model is an ideal Bose gas subject to one-particle gain $\gamma_{p,1}$ from stimulated scattering of photons into the condensate and one-particle loss $\gamma_{l,1}$ through the cavity mirrors. There is also effective two-particle loss $\gamma_{l,2}$, modelling the fact that gain in such systems is typically saturable: the condensate does not grow indefinitely if one-particle gain exceeds one-particle loss [7]. As is well known [8], though the ideal Bose gas is capable of condensation, it does not exhibit superfluidity in equilibrium due to the absence of interactions. Goldstone modes and superfluidity are instead found in the weakly interacting Bose gas, with the prototypical interaction being of the form $V|\psi|^4$. We shall refer to this as the unitary

[1] There are at least two possible mechanisms for this interaction [3], with the Kerr mechanism that is more likely to be observed on experimental time-scales being particularly weak.

[2] This Lindbladian agrees with the Gross-Pitaevskii equations used in the cited works.

two-particle contact interaction.

Nevertheless, the above driven-dissipative version of the ideal Bose gas has been proposed as a model of vortex formation in trapped dye cavity photon Bose-Einstein condensates; numerical simulation of the associated mean field Gross-Pitaevskii equation demonstrates vortex lattice formation [6] analogous to the exciton-polariton case [7]. Since vortices are a topological defect frequently associated with superfluidity, this raises the question of whether this system can support the latter phenomenon in the absence of a trapping potential (when the steady state should be stable against vortex formation), i.e. whether an ideal Bose gas can exhibit superfluidity via non-linear dissipation rather than unitary interactions. This interpretation of vortex formation as indicative of superfluidity was argued against in [4] due to the dye photon model's Landau criterion critical velocity being zero. As I have emphasized throughout this part, however, the Landau criterion is unreliable in the driven-dissipative setting. Thus, while I agree with [4] that vortices are not synonymous with superfluidity, it does not appear possible to rule it out so simply.

An important and promising distinction between this and the equilibrium model is that the non-linear loss terms of the Lindbladian generate what look like two-particle contact interactions in the associated Keldysh action. These are not the unitary interactions mentioned above, as their coupling constants are now imaginary, but could still be sufficient for superfluidity to manifest. Thus, in this sub-part I will use the Keldysh formalism and the current-current response superfluidity criterion to analyse the effect of these incoherent particle-particle pseudo-interactions.

To begin, we write out the Keldysh action associated to the Lindbladian. Via the mapping presented in Chap. 9, in the Fourier domain we find this to be (we perform a change of variables $\psi(\omega,\boldsymbol{k}) \to \psi(\omega-\omega_0,\boldsymbol{k})$ to eliminate ω_0, and denote $k=(\omega,\boldsymbol{k})$, $\epsilon(\boldsymbol{k}) = K|\boldsymbol{k}|^2$, $\gamma_{p,1}-\gamma_{l,1}=\delta_\gamma$, $\gamma_{p,1}+\gamma_{l,1}=\sigma_\gamma$):

$$
\begin{aligned}
S = \int dk \Bigg[\begin{pmatrix} \psi^c_k \\ \psi^q_k \end{pmatrix}^\dagger \begin{pmatrix} 0 & \omega-\epsilon(\boldsymbol{k})+\frac{i}{2}\delta_\gamma \\ \omega-\epsilon(\boldsymbol{k})-\frac{i}{2}\delta_\gamma & i\sigma_\gamma \end{pmatrix} \begin{pmatrix} \psi^c_k \\ \psi^q_k \end{pmatrix} \\
\int dk' dq \Bigg[-\frac{i}{2}\gamma_{l,2}\bar{\psi}^c_{k-q}\bar{\psi}^c_{k'+q}\psi^c_k\psi^q_{k'} + \frac{i}{2}\gamma_{l,2}\bar{\psi}^c_{k-q}\bar{\psi}^q_{k'+q}\psi^c_k\psi^c_{k'} \\
+\frac{i}{2}\gamma_{l,2}\bar{\psi}^c_{k-q}\bar{\psi}^q_{k'+q}\psi^q_k\psi^q_{k'} - \frac{i}{2}\gamma_{l,2}\bar{\psi}^q_{k-q}\bar{\psi}^q_{k'+q}\psi^c_k\psi^q_{k'} \\
+2i\gamma_{l,2}\bar{\psi}^c_{k-q}\bar{\psi}^q_{k'+q}\psi^c_k\psi^q_{k'} \Bigg] \Bigg].
\end{aligned}
\tag{11.5}
$$

The mean-field equations for a spacetime-homogeneous condensate are then

$$\left.\frac{\delta S}{\delta \bar{\psi}_0^q}\right|_{\psi^q=\bar{\psi}^q=0} = -\frac{i}{2}\delta_\gamma \psi_0^c + \frac{i}{2}\gamma_{l,2}|\psi_0^c|^2\psi_0^c = 0, \tag{11.6}$$

$$\left.\frac{\delta S}{\delta \psi_0^q}\right|_{\psi^q=\bar{\psi}^q=0} = \frac{i}{2}\delta_\gamma \bar{\psi}_0^c - \frac{i}{2}\gamma_{l,2}|\psi_0^c|^2\bar{\psi}_0^c = 0. \tag{11.7}$$

which yields the two possible solutions

$$\psi_0^c = 0 \quad \text{or} \quad |\psi_0^c|^2 = |\psi_0|^2 = \frac{\delta_\gamma}{\gamma_{l,2}}. \tag{11.8}$$

The second of these corresponds to condensation, with the density of the condensate controlled by the constant pumping term. The fact that such a constant pump can achieve saturation is an important difference with the open dissipative condensate considered in [9], and is due to the quartic coupling being imaginary rather than real (i.e. to the presence of two-body decay rather than unitary interactions).

The excitation spectrum for the condensate is calculated in [10] (in fact they consider the more general model containing both two-particle loss and unitary interactions), and is found to be dynamically stable. I briefly present the calculation, since we shall need the system's Greens functions for subsequent calculations anyway.

Expanding our action around the condensate (which we choose to be real $\psi_0 = \bar{\psi}_0$ via our system's $U(1)$ symmetry and associated phase freedom of the symmetry broken condensate) to second order, we may write the resulting expression in terms of Nambu spinors $\Psi_k = (\psi_k^c, \bar{\psi}_{-k}^c, \psi_k^q, \bar{\psi}_{-k}^q)^T$:

$$S_2 = \frac{1}{2}\int dk dk' \Psi_k^\dagger \frac{\delta^2 S}{\delta\bar{\Psi}_k \delta\Psi_{k'}}\Psi_{k'} \tag{11.9}$$

$$\frac{\delta^2 S}{\delta\bar{\Psi}_k \delta\Psi_{k'}} = \begin{pmatrix} 0 & [G^{-1}]^A(k) \\ [G^{-1}]^R(k) & [G^{-1}]^K(k) \end{pmatrix}\delta(k-k') \tag{11.10}$$

$$\begin{aligned}[G^{-1}]^R(k) &= \begin{pmatrix} \omega - \epsilon(\boldsymbol{k}) - \frac{i}{2}\delta_\gamma + i\gamma_{l,2}|\psi_0|^2 & \frac{i}{2}\gamma_{l,2}\psi_0^2 \\ -\frac{i}{2}\gamma_{l,2}\bar{\psi}_0^2 & -\omega - \epsilon(-\boldsymbol{k}) + \frac{i}{2}\delta_\gamma - i\gamma_{l,2}|\psi_0|^2 \end{pmatrix} \\ &= \begin{pmatrix} \omega - \epsilon(\boldsymbol{k}) + \frac{i}{2}\delta_\gamma & \frac{i}{2}\delta_\gamma \\ -\frac{i}{2}\delta_\gamma & -\omega - \epsilon(\boldsymbol{k}) - \frac{i}{2}\delta_\gamma \end{pmatrix}\end{aligned} \tag{11.11}$$

$$
\begin{aligned}
[G^{-1}]^A(k) &= \begin{pmatrix} \omega - \epsilon(\boldsymbol{k}) + \frac{i}{2}\delta_\gamma - i\gamma_{l,2}|\psi_0|^2 & \frac{i}{2}\gamma_{l,2}\psi_0^2 \\ -\frac{i}{2}\gamma_{l,2}\bar{\psi}_0^2 & -\omega - \epsilon(-\boldsymbol{k}) - \frac{i}{2}\delta_\gamma + i\gamma_{l,2}|\psi_0|^2 \end{pmatrix} \\
&= \begin{pmatrix} \omega - \epsilon(\boldsymbol{k}) - \frac{i}{2}\delta_\gamma & \frac{i}{2}\delta_\gamma \\ -\frac{i}{2}\delta_\gamma & -\omega - \epsilon(\boldsymbol{k}) + \frac{i}{2}\delta_\gamma \end{pmatrix}
\end{aligned} \tag{11.12}
$$

$$
\begin{aligned}
[G^{-1}]^K(k) &= \begin{pmatrix} i\sigma_\gamma + 2i\gamma_{l,2}|\psi_0|^2 & 0 \\ 0 & i\sigma_\gamma + 2i\gamma_{l,2}|\psi_0|^2 \end{pmatrix} \\
&= \begin{pmatrix} i\sigma_\gamma + 2i\delta_\gamma & 0 \\ 0 & i\sigma_\gamma + 2i\delta_\gamma \end{pmatrix}
\end{aligned} \tag{11.13}
$$

$$
\begin{aligned}
iG^R(k) &= i\Big([G^{-1}]^R(k)\Big)^{-1} \\
&= \frac{i}{\epsilon(\boldsymbol{k})^2 - i\omega\delta_\gamma - \omega^2} \begin{pmatrix} -\omega - \epsilon(\boldsymbol{k}) - \frac{i}{2}\delta_\gamma & -\frac{i}{2}\delta_\gamma \\ \frac{i}{2}\delta_\gamma & \omega - \epsilon(\boldsymbol{k}) + \frac{i}{2}\delta_\gamma \end{pmatrix}
\end{aligned} \tag{11.14}
$$

$$
\begin{aligned}
iG^A(k) &= i\Big([G^{-1}]^R(k)\Big)^{-1} \\
&= \frac{i}{\epsilon(\boldsymbol{k})^2 + i\omega\delta_\gamma - \omega^2} \begin{pmatrix} -\omega - \epsilon(\boldsymbol{k}) + \frac{i}{2}\delta_\gamma & -\frac{i}{2}\delta_\gamma \\ \frac{i}{2}\delta_\gamma & \omega - \epsilon(\boldsymbol{k}) - \frac{i}{2}\delta_\gamma \end{pmatrix}
\end{aligned} \tag{11.15}
$$

$$
\begin{aligned}
iG^K(k) &= -iG^R(k)[G^{-1}]^K(k)G^A(k) \\
&= \frac{\sigma_\gamma + 2\delta_\gamma}{(\epsilon(\boldsymbol{k})^2 - \omega^2)^2 + \omega^2\delta_\gamma^2} \begin{pmatrix} (\omega + \epsilon(\boldsymbol{k}))^2 + \frac{1}{2}\delta_\gamma^2 & i\delta_\gamma(\frac{i}{2}\delta_\gamma + \epsilon(\boldsymbol{k})) \\ i\delta_\gamma(\frac{i}{2}\delta_\gamma - \epsilon(\boldsymbol{k})) & (\omega - \epsilon(\boldsymbol{k}))^2 + \frac{1}{2}\delta_\gamma^2 \end{pmatrix}
\end{aligned} \tag{11.16}
$$

The excitation spectrum of the system is given by the poles of the retarded Greens function, namely by

$$\epsilon(\boldsymbol{k})^2 - i\omega\delta_\gamma - \omega^2 = 0. \tag{11.17}$$

This is easily solved to give

$$\omega = -\frac{i}{2}\delta_\gamma \pm \sqrt{\epsilon(\boldsymbol{k})^2 - \frac{\delta_\gamma^2}{4}}. \tag{11.18}$$

This is gapless and, if plotted for simple values of the constants and a quadratic $\epsilon(\boldsymbol{k})$, looks like

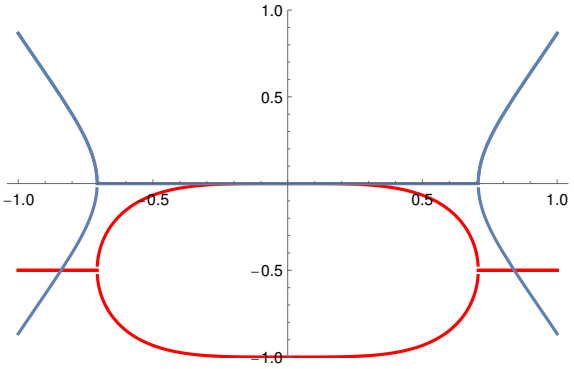

Figure 11.1: The excitation spectrum around the condensate of the ideal dissipative Bose gas. The real part of the spectrum is in blue, the imaginary part in red.

This spectrum clearly fails the Landau criterion/gives a superfluid velocity of 0. The calculation of the current-current response at order $O(\hbar)$ goes through essentially unchanged from Sec. 4.3.3, however, and is given by (we choose the mean-field ψ_0 to be real and $\gamma_i(\boldsymbol{q}) = Kq_i$):

$$\begin{aligned}\chi_{\hbar,ij}(\mathbf{q}) = &-\psi_0^2 G_R^{11}(0,\mathbf{q})\gamma_i(\mathbf{q})\gamma_j(\mathbf{q}) \\ &-\psi_0^2 G_R^{21}(0,\mathbf{q})\gamma_i(-\mathbf{q})\gamma_j(\mathbf{q}) \\ &-\psi_0^2 G_R^{12}(0,\mathbf{q})\gamma_i(\mathbf{q})\gamma_j(-\mathbf{q}) \\ &-\psi_0^2 G_R^{22}(0,\mathbf{q})\gamma_i(-\mathbf{q})\gamma_j(-\mathbf{q}),\end{aligned} \tag{11.19}$$

which comes out simply to

$$\chi^0_{ij}(\boldsymbol{q}) = \frac{2\delta_\gamma}{\gamma_{l,2}}\frac{\gamma_i(\boldsymbol{q})\gamma_j(\boldsymbol{q})}{\epsilon(\boldsymbol{q})} \tag{11.20}$$

and thus exhibits pure superfluid behaviour. While the current-current response approach is more reliable than the Landau criterion, the question arises whether this is conclusion modified by fluctuations. Generally this is expected to be the case [11], and I undertake the calculation in the next chapter.

Chapter 12

Fluctuations

12.1 Current Generating Function

In Part Ia I used Feynman diagrams, calculated by hand, to analyse fluctuation corrections to the mean field. When one is interested in only a specific class of diagrams, such as those exhibiting tadpoles, this allows you to effectively focus on them. Here, however, we are after all the fluctuation diagrams, the number of which is quite considerable and would be cumbersome to tabulate. Instead, it is better to use a generating function approach [9], [12], [13].

To this end, we may insert source fields $f_i(\boldsymbol{q})$, $\theta_i(\boldsymbol{q})$ coupled to the classical and quantum currents $j^c(-\boldsymbol{q})$, $j^q(-\boldsymbol{q})$ into the Keldysh action (we omit the factor of $\frac{1}{2}$ in the classical current and instead add it when taking functional derivatives below):

$$S_J = S + \sum_{\omega,\boldsymbol{k},\boldsymbol{q}} \gamma_i(2\boldsymbol{k}+\boldsymbol{q}) \begin{pmatrix} \psi^c \\ \psi^q \end{pmatrix}^\dagger_{\omega,\boldsymbol{k}+\boldsymbol{q}} \begin{pmatrix} \theta_i & f_i \\ f_i & \theta_i \end{pmatrix}_{\boldsymbol{q}} \begin{pmatrix} \psi^c \\ \psi^q \end{pmatrix}_{\omega,\boldsymbol{k}} . \tag{12.1}$$

Then, defining the $T = \infty$ functional integral with this new action by $\mathcal{Z}[\boldsymbol{f},\boldsymbol{\theta}]$ (recall that $\mathcal{Z}[\boldsymbol{f},0]$ = since it is simply the trace of the steady state density matrix), we have[1]

$$\chi_{ij}(\mathbf{q}) = i\langle j_i^c(0,\mathbf{q}) j_j^q(0,-\mathbf{q})\rangle = -\frac{i}{2}\left[\frac{\delta^2 Z[\boldsymbol{f},\boldsymbol{\theta}]}{\delta f_i(\boldsymbol{q})\delta\theta_j(-\boldsymbol{q})}\right]_{\substack{f=0\\ \boldsymbol{\theta}=0}} . \tag{12.2}$$

$\mathcal{Z}[\boldsymbol{f},\boldsymbol{\theta}]$ may be approximated by the method of steepest descent. This requires us to expand the action around a solution of the mean field equations to second order, with the latter now also dependent on $\boldsymbol{f},\boldsymbol{\theta}$. Writing the Nambu field vector as $\Psi_k = (\psi_k^c, \bar{\psi}_{-k}^c, \psi_k^q, \bar{\psi}_{-k}^q)^T$, the path integral at this order may be schematically

[1] Strictly speaking i and j in the last expression should be switched, but because the system is isotropic the tensor is symmetric. For historical reasons the calculation was done with the indices in the order displayed.

represented as

$$Z[\boldsymbol{f},\boldsymbol{\theta}] = \int \mathcal{D}[\delta\Psi_k, \delta\bar{\Psi}_k] \exp\left(iS_0[\boldsymbol{f},\boldsymbol{\theta}] + i\sum_k \delta\bar{\psi}_k (G^{-1} + A[\boldsymbol{f},\boldsymbol{\theta}])\delta\Psi_k \right) \tag{12.3}$$

where G is the matrix of bare Green's functions for $\boldsymbol{f} = \boldsymbol{\theta} = 0$ and S_0 is the action evaluated on the solution of the mean field equations. This Gaussian integral is easy to carry out (see Part Ia Appendix A, in particular the redundancy in the Nambu vector leading to the functional derivative appearing under a square root):

$$\begin{aligned} Z[\boldsymbol{f},\boldsymbol{\theta}] &= \int \mathcal{D}[\delta\Psi_k, \delta\bar{\Psi}_k] \exp\left(iS_0[\boldsymbol{f},\boldsymbol{\theta}] + i\sum_k \delta\bar{\psi}_k (G^{-1} + A[\boldsymbol{f},\boldsymbol{\theta}])\delta\Psi_k \right) \\ &= \exp\left(iS_0[\boldsymbol{f},\boldsymbol{\theta}]\right) \left(\det i(G^{-1} + A[\boldsymbol{f},\boldsymbol{\theta}])\right)^{-\frac{1}{2}} \\ &= \Big(\underbrace{\det iG^{-1}}_{=1}\Big)^{-\frac{1}{2}} \exp(iS_0[\boldsymbol{f},\boldsymbol{\theta}]) \exp\left(-\frac{1}{2}\operatorname{Tr}\log\left(I + GA[\boldsymbol{f},\boldsymbol{\theta}]\right)\right) \\ &= \exp\left(iS_0[\boldsymbol{f},\boldsymbol{\theta}] - \frac{1}{2}\operatorname{Tr}\left(GA[\boldsymbol{f},\boldsymbol{\theta}]\right) + \frac{1}{4}\operatorname{Tr}\left(GA[\boldsymbol{f},\boldsymbol{\theta}]GA[\boldsymbol{f},\boldsymbol{\theta}]\right) + \ldots \right) \end{aligned} \tag{12.4}$$

where we have used the fact that $Z[\boldsymbol{f},0] = 1$ to set the term in the third line to 1 and also disregarded terms higher than quadratic in source fields in the last line: since at most two source fields will be removed by the functional derivatives, all terms of higher order will vanish when the source terms are set to zero.

A final simplification is achieved by carrying out the $\boldsymbol{\theta}$ functional derivative first (if no functional derivatives are applied to A, it vanishes when the source fields are taken to zero):

$$\begin{aligned} &\left[\frac{\delta^2 Z[\boldsymbol{f},\boldsymbol{\theta}]}{\delta f_i(\boldsymbol{q})\delta\theta_j(-\boldsymbol{q})}\right]_{\substack{\boldsymbol{f}=0\\ \boldsymbol{\theta}=0}} \\ &= \left(i\frac{\delta^2 S_0[\boldsymbol{f},\boldsymbol{\theta}]}{\delta f_i(\boldsymbol{q})\delta\theta_j(-\boldsymbol{q})} - \frac{1}{2}\operatorname{Tr}\left(G\frac{\delta^2 A[\boldsymbol{f},\boldsymbol{\theta}]}{\delta f_i(\boldsymbol{q})\delta\theta_j(-\boldsymbol{q})}\right) + \frac{1}{2}\operatorname{Tr}\left(G\frac{\delta A[\boldsymbol{f},\boldsymbol{\theta}]}{\delta f_i(\boldsymbol{q})}G\frac{\delta A[\boldsymbol{f},\boldsymbol{\theta}]}{\delta\theta_j(-\boldsymbol{q})}\right)\right)_{\substack{\boldsymbol{f}=0\\ \boldsymbol{\theta}=0}} \\ &\quad + \left(i\frac{\delta S_0[\boldsymbol{f},\boldsymbol{\theta}]}{\delta\theta_j(-\boldsymbol{q})} - \frac{1}{2}\operatorname{Tr}\left(G\frac{\delta A[\boldsymbol{f},\boldsymbol{\theta}]}{\delta\theta_j(-\boldsymbol{q})}\right)\right)_{\substack{\boldsymbol{f}=0\\ \boldsymbol{\theta}=0}} \left[\frac{\delta Z[\boldsymbol{f},\boldsymbol{\theta}]}{\delta f_i(\boldsymbol{q})}\right]_{\substack{\boldsymbol{f}=0\\ \boldsymbol{\theta}=0}}. \end{aligned} \tag{12.5}$$

Since $Z[\boldsymbol{f},0]=1$, $\left[\frac{\delta Z[\boldsymbol{f},\boldsymbol{\theta}]}{\delta f_i(\boldsymbol{q})}\right]_{\substack{\boldsymbol{f}=0\\ \boldsymbol{\theta}=0}}=0$ and so we have

$$\begin{aligned}
&\chi_{ij}(\mathbf{q})\\
&=-\frac{i}{2}\left[\frac{\delta^2 Z[\boldsymbol{f},\boldsymbol{\theta}]}{\delta f_i(\boldsymbol{q})\delta\theta_j(-\boldsymbol{q})}\right]_{\substack{\boldsymbol{f}=0\\ \boldsymbol{\theta}=0}}\\
&=-\frac{i}{2}\left(i\frac{\delta^2 S_0[\boldsymbol{f},\boldsymbol{\theta}]}{\delta f_i(\boldsymbol{q})\delta\theta_j(-\boldsymbol{q})}-\frac{1}{2}\mathrm{Tr}\left(G\frac{\delta^2 A[\boldsymbol{f},\boldsymbol{\theta}]}{\delta f_i(\boldsymbol{q})\delta\theta_j(-\boldsymbol{q})}\right)+\frac{1}{2}\mathrm{Tr}\left(G\frac{\delta A[\boldsymbol{f},\boldsymbol{\theta}]}{\delta f_i(\boldsymbol{q})}G\frac{\delta A[\boldsymbol{f},\boldsymbol{\theta}]}{\delta\theta_j(-\boldsymbol{q})}\right)\right)_{\substack{\boldsymbol{f}=0\\ \boldsymbol{\theta}=0}}.
\end{aligned}\tag{12.6}$$

Thinking perturbatively, every functional derivative brings down a factor of $\hbar^{-1}$ so there is an omitted $\hbar^2$ factor in front of the whole expression to counteract this. Then S_0 and A each contribute a factor of $\hbar^{-1}$ while G contributes $\hbar$, so the first term inside the brackets is of order $\hbar$ and thus the mean field contribution we have already calculated in the previous chapter. The other two terms are of order $\hbar^2$, and are the fluctuation contributions we aim to calculate. I undertake this calculation in the rest of this chapter.

12.2 Fluctuation Calculation

Expanding the Nambu vector as

$$\begin{pmatrix}\psi^c_k\\ \bar\psi^c_{-k}\\ \psi^q_k\\ \bar\psi^q_{-k}\end{pmatrix}=\delta(\omega)\left[\begin{pmatrix}\psi_0\\ \bar\psi_0\\ 0\\ 0\end{pmatrix}\delta(\boldsymbol{k})+\begin{pmatrix}X^{(1)}_{\boldsymbol{k}}\\ \bar X^{(1)}_{-\boldsymbol{k}}\\ Y^{(1)}_{\boldsymbol{k}}\\ \bar Y^{(1)}_{-\boldsymbol{k}}\end{pmatrix}+\begin{pmatrix}X^{(2)}_{\boldsymbol{k}}\\ \bar X^{(2)}_{-\boldsymbol{k}}\\ Y^{(2)}_{\boldsymbol{k}}\\ \bar Y^{(2)}_{-\boldsymbol{k}}\end{pmatrix}\right]\tag{12.7}$$

where the (1) expressions are first-order in the source fields while the (2) expressions are second order, and writing

$$\frac{\delta^2 S}{\delta\bar\Phi_k\delta\Phi_{k'}}=\begin{pmatrix}S_{\bar c c} & S_{\bar c\bar c} & S_{\bar c q} & S_{\bar c\bar q}\\ S_{cc} & S_{c\bar c} & S_{cq} & S_{c\bar q}\\ S_{\bar q c} & S_{\bar q\bar c} & S_{\bar q q} & S_{\bar q\bar q}\\ S_{qc} & S_{q\bar c} & S_{qq} & S_{q\bar q}\end{pmatrix}\delta_{\omega,\omega'}\tag{12.8}$$

one finds to second order ($J(k)=\omega+\frac{i}{2}\delta_\gamma-K\epsilon(\boldsymbol{k})$):

$$S_{\bar c c}=\gamma_i(\boldsymbol{k}+\boldsymbol{k}')\theta_i(\boldsymbol{k}-\boldsymbol{k}')+2i\gamma_{l,2}\sum_{\boldsymbol{q}}Y^{(1)}_{\boldsymbol{k}+\boldsymbol{q}}\bar Y^{(1)}_{\boldsymbol{k}'+\boldsymbol{q}}$$

$$- i\gamma_{l,2}\left[\bar{\psi}_0(Y^{(1)}_{\boldsymbol{k}-\boldsymbol{k}'} + Y^{(2)}_{\boldsymbol{k}-\boldsymbol{k}'}) - \psi_0(\bar{Y}^{(1)}_{\boldsymbol{k}'-\boldsymbol{k}} + \bar{Y}^{(2)}_{\boldsymbol{k}'-\boldsymbol{k}}) + \sum_{\boldsymbol{q}}\left[\bar{X}^{(1)}_{\boldsymbol{k}'+\boldsymbol{q}}Y^{(1)}_{\boldsymbol{k}+\boldsymbol{q}} - X^{(1)}_{\boldsymbol{k}+\boldsymbol{q}}\bar{Y}^{(1)}_{\boldsymbol{k}'+\boldsymbol{q}}\right]\right]$$

$$S_{\bar{c}\bar{c}} = - i\gamma_{l,2}\left[\psi_0(Y^{(1)}_{\boldsymbol{k}-\boldsymbol{k}'} + Y^{(2)}_{\boldsymbol{k}-\boldsymbol{k}'}) + \sum_{\boldsymbol{q}} X^{(1)}_{\boldsymbol{k}-\boldsymbol{q}}Y^{(1)}_{\boldsymbol{q}-\boldsymbol{k}'}\right]$$

$$S_{\bar{c}q} = \bar{J}(k)\delta_{\boldsymbol{k},\boldsymbol{k}'} + \gamma_i(\boldsymbol{k}+\boldsymbol{k}')f_i(\boldsymbol{k}-\boldsymbol{k}')$$
$$- i\gamma_{l,2}\left[\bar{\psi}_0(X^{(1)}_{\boldsymbol{k}-\boldsymbol{k}'} + X^{(2)}_{\boldsymbol{k}-\boldsymbol{k}'}) + \psi_0(\bar{X}^{(1)}_{\boldsymbol{k}'-\boldsymbol{k}} + \bar{X}^{(2)}_{\boldsymbol{k}'-\boldsymbol{k}}) + \sum_{\boldsymbol{q}}\left[X^{(1)}_{\boldsymbol{k}+\boldsymbol{q}}\bar{X}^{(1)}_{\boldsymbol{k}'+\boldsymbol{q}} - Y^{(1)}_{\boldsymbol{k}+\boldsymbol{q}}\bar{Y}^{(1)}_{\boldsymbol{k}'+\boldsymbol{q}}\right]\right]$$
$$+ 2i\gamma_{l,2}\left[\psi_0(\bar{Y}^{(1)}_{\boldsymbol{k}'-\boldsymbol{k}} + \bar{Y}^{(2)}_{\boldsymbol{k}'-\boldsymbol{k}}) + \sum_{\boldsymbol{q}} X^{(1)}_{\boldsymbol{k}+\boldsymbol{q}}\bar{Y}^{(1)}_{\boldsymbol{k}'+\boldsymbol{q}}\right]$$

$$S_{\bar{c}\bar{q}} = \frac{i}{2}\gamma_{l,2}\left[\psi_0^2\delta_{\boldsymbol{k},\boldsymbol{k}'} + \sum_{\boldsymbol{q}}\left[X^{(1)}_{\boldsymbol{k}-\boldsymbol{q}}X^{(1)}_{\boldsymbol{q}-\boldsymbol{k}'} + Y^{(1)}_{\boldsymbol{k}-\boldsymbol{q}}Y^{(1)}_{\boldsymbol{q}-\boldsymbol{k}'}\right]\right]$$
$$+ i\gamma_{l,2}\psi_0(X^{(1)}_{\boldsymbol{k}-\boldsymbol{k}'} + X^{(2)}_{\boldsymbol{k}-\boldsymbol{k}'})$$
$$+ 2i\gamma_{l,2}\left[\psi_0(Y^{(1)}_{\boldsymbol{k}-\boldsymbol{k}'} + Y^{(2)}_{\boldsymbol{k}-\boldsymbol{k}'}) + \sum_{\boldsymbol{q}} X^{(1)}_{\boldsymbol{k}-\boldsymbol{q}}Y^{(1)}_{\boldsymbol{q}-\boldsymbol{k}'}\right]$$

$$S_{cc} = i\gamma_{l,2}\left[\bar{\psi}_0(\bar{Y}^{(1)}_{\boldsymbol{k}'-\boldsymbol{k}} + \bar{Y}^{(2)}_{\boldsymbol{k}'-\boldsymbol{k}}) + \sum_{\boldsymbol{q}}\bar{X}^{(1)}_{\boldsymbol{k}'-\boldsymbol{q}}\bar{Y}^{(1)}_{\boldsymbol{q}-\boldsymbol{k}}\right]$$

$$S_{c\bar{c}} = \gamma_i(-\boldsymbol{k}-\boldsymbol{k}')\theta_i(\boldsymbol{k}-\boldsymbol{k}') + 2i\gamma_{l,2}\sum_{\boldsymbol{q}} Y^{(1)}_{\boldsymbol{k}+\boldsymbol{q}}\bar{Y}^{(1)}_{\boldsymbol{k}'+\boldsymbol{q}}$$
$$- i\gamma_{l,2}\left[\bar{\psi}_0(Y^{(1)}_{\boldsymbol{k}-\boldsymbol{k}'} + Y^{(2)}_{\boldsymbol{k}-\boldsymbol{k}'}) - \psi_0(\bar{Y}^{(1)}_{\boldsymbol{k}'-\boldsymbol{k}} + \bar{Y}^{(2)}_{\boldsymbol{k}'-\boldsymbol{k}}) + \sum_{\boldsymbol{q}}\left[\bar{X}^{(1)}_{\boldsymbol{k}'+\boldsymbol{q}}Y^{(1)}_{\boldsymbol{k}+\boldsymbol{q}} - X^{(1)}_{\boldsymbol{k}+\boldsymbol{q}}\bar{Y}^{(1)}_{\boldsymbol{k}'+\boldsymbol{q}}\right]\right]$$

$$S_{cq} = - \frac{i}{2}\gamma_{l,2}\left[\bar{\psi}_0^2\delta_{\boldsymbol{k},\boldsymbol{k}'} + \sum_{\boldsymbol{q}}\left[\bar{X}^{(1)}_{\boldsymbol{k}'-\boldsymbol{q}}\bar{X}^{(1)}_{\boldsymbol{q}-\boldsymbol{k}} + \bar{Y}^{(1)}_{\boldsymbol{k}'-\boldsymbol{q}}\bar{Y}^{(1)}_{\boldsymbol{q}-\boldsymbol{k}}\right]\right]$$
$$- i\gamma_{l,2}\bar{\psi}_0(\bar{X}^{(1)}_{\boldsymbol{k}'-\boldsymbol{k}} + \bar{X}^{(2)}_{\boldsymbol{k}'-\boldsymbol{k}})$$
$$+ 2i\gamma_{l,2}\left[\psi_0(\bar{Y}^{(1)}_{\boldsymbol{k}'-\boldsymbol{k}} + \bar{Y}^{(2)}_{\boldsymbol{k}'-\boldsymbol{k}}) + \sum_{\boldsymbol{q}}\bar{X}^{(1)}_{\boldsymbol{k}'-\boldsymbol{q}}\bar{Y}^{(1)}_{\boldsymbol{q}-\boldsymbol{k}}\right]$$

$$S_{c\bar{q}} = J(-k)\delta_{\boldsymbol{k},\boldsymbol{k}'} + \gamma_i(-\boldsymbol{k}-\boldsymbol{k}')f_i(\boldsymbol{k}-\boldsymbol{k}')$$
$$+ i\gamma_{l,2}\left[\psi_0(\bar{X}^{(1)}_{\boldsymbol{k}'-\boldsymbol{k}} + \bar{X}^{(2)}_{\boldsymbol{k}'-\boldsymbol{k}}) + \bar{\psi}_0(X^{(1)}_{\boldsymbol{k}-\boldsymbol{k}'} + X^{(2)}_{\boldsymbol{k}-\boldsymbol{k}'}) + \sum_{\boldsymbol{q}}\left[X^{(1)}_{\boldsymbol{k}+\boldsymbol{q}}\bar{X}^{(1)}_{\boldsymbol{k}'+\boldsymbol{q}} - Y^{(1)}_{\boldsymbol{k}+\boldsymbol{q}}\bar{Y}^{(1)}_{\boldsymbol{k}'+\boldsymbol{q}}\right]\right]$$
$$+ 2i\gamma_{l,2}\left[\bar{\psi}_0(Y^{(1)}_{\boldsymbol{k}-\boldsymbol{k}'} + Y^{(2)}_{\boldsymbol{k}-\boldsymbol{k}'}) + \sum_{\boldsymbol{q}}\bar{X}^{(1)}_{\boldsymbol{k}'+\boldsymbol{q}}Y^{(1)}_{\boldsymbol{k}+\boldsymbol{q}}\right]$$

$$S_{\bar{q}c} = J(k)\delta_{\boldsymbol{k},\boldsymbol{k}'} + \gamma_i(\boldsymbol{k}+\boldsymbol{k}')f_i(\boldsymbol{k}-\boldsymbol{k}')$$

$$+ i\gamma_{l,2}\left[\psi_0(\bar{X}^{(1)}_{\boldsymbol{k}'-\boldsymbol{k}} + \bar{X}^{(2)}_{\boldsymbol{k}'-\boldsymbol{k}}) + \bar{\psi}_0(X^{(1)}_{\boldsymbol{k}-\boldsymbol{k}'} + X^{(2)}_{\boldsymbol{k}-\boldsymbol{k}'}) + \sum_{\boldsymbol{q}}\left[X^{(1)}_{\boldsymbol{k}+\boldsymbol{q}}\bar{X}^{(1)}_{\boldsymbol{k}'+\boldsymbol{q}} - Y^{(1)}_{\boldsymbol{k}+\boldsymbol{q}}\bar{Y}^{(1)}_{\boldsymbol{k}'+\boldsymbol{q}}\right]\right]$$

$$+ 2i\gamma_{l,2}\left[\bar{\psi}_0(Y^{(1)}_{\boldsymbol{k}-\boldsymbol{k}'} + Y^{(2)}_{\boldsymbol{k}-\boldsymbol{k}'}) + \sum_{\boldsymbol{q}}\bar{X}^{(1)}_{\boldsymbol{k}'+\boldsymbol{q}}Y^{(1)}_{\boldsymbol{k}+\boldsymbol{q}}\right]$$

$$S_{\bar{q}\bar{c}} = \frac{i}{2}\gamma_{l,2}\left[\psi_0^2\delta_{\boldsymbol{k},\boldsymbol{k}'} + \sum_{\boldsymbol{q}}\left[X^{(1)}_{\boldsymbol{k}-\boldsymbol{q}}X^{(1)}_{\boldsymbol{q}-\boldsymbol{k}'} + Y^{(1)}_{\boldsymbol{k}-\boldsymbol{q}}Y^{(1)}_{\boldsymbol{q}-\boldsymbol{k}'}\right]\right]$$

$$+ i\gamma_{l,2}\psi_0(X^{(1)}_{\boldsymbol{k}-\boldsymbol{k}'} + X^{(2)}_{\boldsymbol{k}-\boldsymbol{k}'})$$

$$+ 2i\gamma_{l,2}\left[\psi_0(Y^{(1)}_{\boldsymbol{k}-\boldsymbol{k}'} + Y^{(2)}_{\boldsymbol{k}-\boldsymbol{k}'}) + \sum_{\boldsymbol{q}}X^{(1)}_{\boldsymbol{k}-\boldsymbol{q}}Y^{(1)}_{\boldsymbol{q}-\boldsymbol{k}'}\right]$$

$$S_{\bar{q}q} = i\sigma_\gamma\delta_{\boldsymbol{k},\boldsymbol{k}'} + \gamma_i(\boldsymbol{k}+\boldsymbol{k}')\theta_i(\boldsymbol{k}-\boldsymbol{k}')$$

$$- i\gamma_{l,2}\left[\psi_0(\bar{Y}^{(1)}_{\boldsymbol{k}'-\boldsymbol{k}} + \bar{Y}^{(2)}_{\boldsymbol{k}'-\boldsymbol{k}}) - \bar{\psi}_0(Y^{(1)}_{\boldsymbol{k}-\boldsymbol{k}'} + Y^{(2)}_{\boldsymbol{k}-\boldsymbol{k}'}) + \sum_{\boldsymbol{q}}\left[X^{(1)}_{\boldsymbol{k}+\boldsymbol{q}}\bar{Y}^{(1)}_{\boldsymbol{k}'+\boldsymbol{q}} - \bar{X}^{(1)}_{\boldsymbol{k}'+\boldsymbol{q}}Y^{(1)}_{\boldsymbol{k}+\boldsymbol{q}}\right]\right]$$

$$+ 2i\gamma_{l,2}\left[\psi_0(\bar{X}^{(1)}_{\boldsymbol{k}'-\boldsymbol{k}} + \bar{X}^{(2)}_{\boldsymbol{k}'-\boldsymbol{k}}) + \bar{\psi}_0(X^{(1)}_{\boldsymbol{k}-\boldsymbol{k}'} + X^{(2)}_{\boldsymbol{k}-\boldsymbol{k}'}) + \sum_{\boldsymbol{q}}X^{(1)}_{\boldsymbol{k}+\boldsymbol{q}}\bar{X}^{(1)}_{\boldsymbol{k}'+\boldsymbol{q}}\right]$$

$$S_{\bar{q}\bar{q}} = -i\gamma_{l,2}\left[\psi_0(Y^{(1)}_{\boldsymbol{k}-\boldsymbol{k}'} + Y^{(2)}_{\boldsymbol{k}-\boldsymbol{k}'}) + \sum_{\boldsymbol{q}}X^{(1)}_{\boldsymbol{k}-\boldsymbol{q}}Y^{(1)}_{\boldsymbol{q}-\boldsymbol{k}'}\right]$$

$$S_{qc} = -\frac{i}{2}\gamma_{l,2}\left[\bar{\psi}_0^2\delta_{\boldsymbol{k},\boldsymbol{k}'} + \sum_{\boldsymbol{q}}\left[\bar{X}^{(1)}_{\boldsymbol{k}'-\boldsymbol{q}}\bar{X}^{(1)}_{\boldsymbol{q}-\boldsymbol{k}} + \bar{Y}^{(1)}_{\boldsymbol{k}'-\boldsymbol{q}}\bar{Y}^{(1)}_{\boldsymbol{q}-\boldsymbol{k}}\right]\right]$$

$$- i\gamma_{l,2}\bar{\psi}_0(\bar{X}^{(1)}_{\boldsymbol{k}'-\boldsymbol{k}} + \bar{X}^{(2)}_{\boldsymbol{k}'-\boldsymbol{k}})$$

$$+ 2i\gamma_{l,2}\left[\psi_0(\bar{Y}^{(1)}_{\boldsymbol{k}'-\boldsymbol{k}} + \bar{Y}^{(2)}_{\boldsymbol{k}'-\boldsymbol{k}}) + \sum_{\boldsymbol{q}}\bar{X}^{(1)}_{\boldsymbol{k}'-\boldsymbol{q}}\bar{Y}^{(1)}_{\boldsymbol{q}-\boldsymbol{k}}\right]$$

$$S_{q\bar{c}} = \bar{J}(-k)\delta_{\boldsymbol{k},\boldsymbol{k}'} + \gamma_i(-\boldsymbol{k}-\boldsymbol{k}')f_i(\boldsymbol{k}-\boldsymbol{k}')$$

$$- i\gamma_{l,2}\left[\bar{\psi}_0(X^{(1)}_{\boldsymbol{k}-\boldsymbol{k}'} + X^{(2)}_{\boldsymbol{k}-\boldsymbol{k}'}) + \psi_0(\bar{X}^{(1)}_{\boldsymbol{k}'-\boldsymbol{k}} + \bar{X}^{(2)}_{\boldsymbol{k}'-\boldsymbol{k}}) + \sum_{\boldsymbol{q}}\left[X^{(1)}_{\boldsymbol{k}+\boldsymbol{q}}\bar{X}^{(1)}_{\boldsymbol{k}'+\boldsymbol{q}} - Y^{(1)}_{\boldsymbol{k}+\boldsymbol{q}}\bar{Y}^{(1)}_{\boldsymbol{k}'+\boldsymbol{q}}\right]\right]$$

$$+ 2i\gamma_{l,2}\left[\psi_0(\bar{Y}^{(1)}_{\boldsymbol{k}'-\boldsymbol{k}} + \bar{Y}^{(2)}_{\boldsymbol{k}'-\boldsymbol{k}}) + \sum_{\boldsymbol{q}}X^{(1)}_{\boldsymbol{k}+\boldsymbol{q}}\bar{Y}^{(1)}_{\boldsymbol{k}'+\boldsymbol{q}}\right]$$

$$S_{qq} = i\gamma_{l,2}\left[\bar{\psi}_0(\bar{Y}^{(1)}_{\boldsymbol{k}'-\boldsymbol{k}} + \bar{Y}^{(2)}_{\boldsymbol{k}'-\boldsymbol{k}}) + \sum_{\boldsymbol{q}}\bar{X}^{(1)}_{\boldsymbol{k}'-\boldsymbol{q}}\bar{Y}^{(1)}_{\boldsymbol{q}-\boldsymbol{k}}\right]$$

$$S_{q\bar{q}} = i\sigma_\gamma\delta_{\boldsymbol{k},\boldsymbol{k}'} + \gamma_i(-\boldsymbol{k}-\boldsymbol{k}')\theta_i(\boldsymbol{k}-\boldsymbol{k}')$$

$$- i\gamma_{l,2}\left[\psi_0(\bar{Y}^{(1)}_{\boldsymbol{k}'-\boldsymbol{k}} + \bar{Y}^{(2)}_{\boldsymbol{k}'-\boldsymbol{k}}) - \bar{\psi}_0(Y^{(1)}_{\boldsymbol{k}-\boldsymbol{k}'} + Y^{(2)}_{\boldsymbol{k}-\boldsymbol{k}'}) + \sum_{\boldsymbol{q}}\left[X^{(1)}_{\boldsymbol{k}+\boldsymbol{q}}\bar{Y}^{(1)}_{\boldsymbol{k}'+\boldsymbol{q}} - \bar{X}^{(1)}_{\boldsymbol{k}'+\boldsymbol{q}}Y^{(1)}_{\boldsymbol{k}+\boldsymbol{q}}\right]\right]$$

$$+ 2i\gamma_{l,2}\left[\psi_0(\bar{X}^{(1)}_{\boldsymbol{k}'-\boldsymbol{k}} + \bar{X}^{(2)}_{\boldsymbol{k}'-\boldsymbol{k}}) + \bar{\psi}_0(X^{(1)}_{\boldsymbol{k}-\boldsymbol{k}'} + X^{(2)}_{\boldsymbol{k}-\boldsymbol{k}'}) + \sum_{\boldsymbol{q}} X^{(1)}_{\boldsymbol{k}+\boldsymbol{q}}\bar{X}^{(1)}_{\boldsymbol{k}'+\boldsymbol{q}}\right] \tag{12.9}$$

As before $\gamma_{l,2}|\psi_0|^2 = \delta_\gamma$, while the Xs and Ys are given by solving (we have set $\omega = 0$ throughout since this is the form of our ansatz)

$$\begin{aligned}\frac{\delta S}{\delta\bar{\psi}^q_{\boldsymbol{k}}} =&(-K\epsilon(\boldsymbol{k}) - \frac{i}{2}\delta_\gamma)\psi^c_{\boldsymbol{k}} + i\sigma_\gamma\psi^q_{\boldsymbol{k}} + \sum_{\boldsymbol{q}}\gamma_i(2\boldsymbol{k}-\boldsymbol{q})\left[f_i(\boldsymbol{q})\psi^c_{\boldsymbol{k}-\boldsymbol{q}} + \theta_i(\boldsymbol{q})\psi^q_{\boldsymbol{k}-\boldsymbol{q}}\right]\\ &+ \frac{i}{2}\gamma_{l,2}\sum_{\boldsymbol{q},\boldsymbol{k}'}\left[\bar{\psi}^c_{\boldsymbol{q}+\boldsymbol{k}'}(\psi^c_{\boldsymbol{k}+\boldsymbol{q}}\psi^c_{\boldsymbol{k}'} + \psi^q_{\boldsymbol{k}+\boldsymbol{q}}\psi^q_{\boldsymbol{k}'}) - 2\bar{\psi}^q_{\boldsymbol{q}+\boldsymbol{k}'}\psi^c_{\boldsymbol{k}+\boldsymbol{q}}\psi^q_{\boldsymbol{k}'} + 4\bar{\psi}^c_{\boldsymbol{q}+\boldsymbol{k}'}\psi^c_{\boldsymbol{k}+\boldsymbol{q}}\psi^q_{\boldsymbol{k}'}\right] = 0,\end{aligned} \tag{12.10}$$

$$\begin{aligned}\frac{\delta S}{\delta\psi^q_{\boldsymbol{k}}} =&(-K\epsilon(\boldsymbol{k}) + \frac{i}{2}\delta_\gamma)\bar{\psi}^c_{\boldsymbol{k}} + i\sigma_\gamma\bar{\psi}^q_{\boldsymbol{k}} + \sum_{\boldsymbol{q}}\gamma_i(2\boldsymbol{k}+\boldsymbol{q})\left[f_i(\boldsymbol{q})\bar{\psi}^c_{\boldsymbol{k}+\boldsymbol{q}} + \theta_i(\boldsymbol{q})\bar{\psi}^q_{\boldsymbol{k}+\boldsymbol{q}}\right]\\ &- \frac{i}{2}\gamma_{l,2}\sum_{\boldsymbol{q},\boldsymbol{k}'}\left[\psi^c_{\boldsymbol{q}+\boldsymbol{k}'}(\bar{\psi}^c_{\boldsymbol{k}+\boldsymbol{q}}\bar{\psi}^c_{\boldsymbol{k}'} + \bar{\psi}^q_{\boldsymbol{k}+\boldsymbol{q}}\bar{\psi}^q_{\boldsymbol{k}'}) - 2\psi^q_{\boldsymbol{q}+\boldsymbol{k}'}\bar{\psi}^c_{\boldsymbol{k}+\boldsymbol{q}}\bar{\psi}^q_{\boldsymbol{k}'} - 4\psi^c_{\boldsymbol{q}+\boldsymbol{k}'}\bar{\psi}^c_{\boldsymbol{k}+\boldsymbol{q}}\bar{\psi}^q_{\boldsymbol{k}'}\right] = 0,\end{aligned} \tag{12.11}$$

$$\begin{aligned}\frac{\delta S}{\delta\bar{\psi}^c_{\boldsymbol{k}}} =&(-K\epsilon(\boldsymbol{k}) + \frac{i}{2}\delta_\gamma)\psi^q_{\boldsymbol{k}} + \sum_{\boldsymbol{q}}\gamma_i(2\boldsymbol{k}-\boldsymbol{q})\left[f_i(\boldsymbol{q})\psi^q_{\boldsymbol{k}-\boldsymbol{q}} + \theta_i(\boldsymbol{q})\psi^c_{\boldsymbol{k}-\boldsymbol{q}}\right]\\ &+ \frac{i}{2}\gamma_{l,2}\sum_{\boldsymbol{q},\boldsymbol{k}'}\left[\bar{\psi}^q_{\boldsymbol{q}+\boldsymbol{k}'}(\psi^c_{\boldsymbol{k}+\boldsymbol{q}}\psi^c_{\boldsymbol{k}'} + \psi^q_{\boldsymbol{k}+\boldsymbol{q}}\psi^q_{\boldsymbol{k}'}) - 2\bar{\psi}^c_{\boldsymbol{q}+\boldsymbol{k}'}\psi^c_{\boldsymbol{k}+\boldsymbol{q}}\psi^q_{\boldsymbol{k}'} + 4\bar{\psi}^q_{\boldsymbol{q}+\boldsymbol{k}'}\psi^c_{\boldsymbol{k}+\boldsymbol{q}}\psi^q_{\boldsymbol{k}'}\right] = 0,\end{aligned} \tag{12.12}$$

$$\begin{aligned}\frac{\delta S}{\delta\psi^c_{\boldsymbol{k}}} =&(-K\epsilon(\boldsymbol{k}) - \frac{i}{2}\delta_\gamma)\bar{\psi}^q_{\boldsymbol{k}} + \sum_{\boldsymbol{q}}\gamma_i(2\boldsymbol{k}+\boldsymbol{q})\left[f_i(\boldsymbol{q})\bar{\psi}^q_{\boldsymbol{k}+\boldsymbol{q}} + \theta_i(\boldsymbol{q})\bar{\psi}^c_{\boldsymbol{k}+\boldsymbol{q}}\right]\\ &- \frac{i}{2}\gamma_{l,2}\sum_{\boldsymbol{q},\boldsymbol{k}'}\left[\psi^q_{\boldsymbol{q}+\boldsymbol{k}'}(\bar{\psi}^c_{\boldsymbol{k}+\boldsymbol{q}}\bar{\psi}^c_{\boldsymbol{k}'} + \bar{\psi}^q_{\boldsymbol{k}+\boldsymbol{q}}\bar{\psi}^q_{\boldsymbol{k}'}) - 2\psi^c_{\boldsymbol{q}+\boldsymbol{k}'}\bar{\psi}^c_{\boldsymbol{k}+\boldsymbol{q}}\bar{\psi}^q_{\boldsymbol{k}'} - 4\psi^q_{\boldsymbol{q}+\boldsymbol{k}'}\bar{\psi}^c_{\boldsymbol{k}+\boldsymbol{q}}\bar{\psi}^q_{\boldsymbol{k}'}\right] = 0,\end{aligned} \tag{12.13}$$

which translate into (recall we have chosen $\epsilon(-\boldsymbol{k}) = \epsilon(\boldsymbol{k})$, $\psi_0 = \bar{\psi}_0$, and $\gamma_{l,2}|\psi_0|^2 = \delta_\gamma$) for $X^{(1)}_{\boldsymbol{k}}$, $Y^{(1)}_{\boldsymbol{k}}$, $\bar{X}^{(1)}_{\boldsymbol{k}}$, $\bar{Y}^{(1)}_{\boldsymbol{k}}$:

$$\underbrace{\begin{pmatrix} -K\epsilon(\boldsymbol{k}) + \frac{i}{2}\delta_\gamma & \frac{i}{2}\delta_\gamma \\ -\frac{i}{2}\delta_\gamma & -K\epsilon(\boldsymbol{k}) - \frac{i}{2}\delta_\gamma \end{pmatrix}}_{[G^{-1}]^R(0,\boldsymbol{k})} \begin{pmatrix} X^{(1)}_{\boldsymbol{k}} \\ \bar{X}^{(1)}_{-\boldsymbol{k}} \end{pmatrix} =$$

$$- \underbrace{\begin{pmatrix} i\sigma_\gamma + 2i\delta_\gamma & 0 \\ 0 & i\sigma_\gamma + 2i\delta_\gamma \end{pmatrix}}_{[G^{-1}]^K(0,\boldsymbol{k})} \begin{pmatrix} Y^{(1)}_{\boldsymbol{k}} \\ \bar{Y}^{(1)}_{-\boldsymbol{k}} \end{pmatrix} - \begin{pmatrix} \psi_0\gamma_i(\boldsymbol{k}) \\ \bar{\psi}_0\gamma_i(-\boldsymbol{k}) \end{pmatrix} f_i(\boldsymbol{k}) \tag{12.14}$$

$$\underbrace{\begin{pmatrix} -K\epsilon(\boldsymbol{k}) - \frac{i}{2}\delta_\gamma & \frac{i}{2}\delta_\gamma \\ -\frac{i}{2}\delta_\gamma & -K\epsilon(\boldsymbol{k}) + \frac{i}{2}\delta_\gamma \end{pmatrix}}_{[G^{-1}]^A(0,\boldsymbol{k})} \begin{pmatrix} Y^{(1)}_{\boldsymbol{k}} \\ \bar{Y}^{(1)}_{-\boldsymbol{k}} \end{pmatrix} = - \begin{pmatrix} \psi_0\gamma_i(\boldsymbol{k}) \\ \bar{\psi}_0\gamma_i(-\boldsymbol{k}) \end{pmatrix} \theta_i(\boldsymbol{k}) \tag{12.15}$$

Observing that $\gamma_i(-\boldsymbol{k}) = -\gamma_i(\boldsymbol{k})$ and identity (11.16), this may be succinctly rewritten as

$$\Gamma_i(\boldsymbol{k}) = \begin{pmatrix} \psi_0\gamma_i(\boldsymbol{k}) \\ -\psi_0\gamma_i(\boldsymbol{k}) \end{pmatrix}, \tag{12.16}$$

$$\begin{pmatrix} X^{(1)}_{\boldsymbol{k}} \\ \bar{X}^{(1)}_{-\boldsymbol{k}} \end{pmatrix} = -G^K(0,\boldsymbol{k})\Gamma_i(\boldsymbol{k})\theta_i(\boldsymbol{k}) - G^R(0,\boldsymbol{k})\Gamma_i(\boldsymbol{k})f_i(\boldsymbol{k}), \tag{12.17}$$

$$\begin{pmatrix} Y^{(1)}_{\boldsymbol{k}} \\ \bar{Y}^{(1)}_{-\boldsymbol{k}} \end{pmatrix} = -G^A(0,\boldsymbol{k})\Gamma_i(\boldsymbol{k})\theta_i(\boldsymbol{k}). \tag{12.18}$$

This begins to reveal the fundamentally diagrammatic nature of the technique, as we see the components of the final expression being built up from Greens functions connecting to external source terms. We can now calculate the first-order derivatives of our action Hessian ($G^X(\boldsymbol{k}) = G^X(0,\boldsymbol{k})$):

$$\hat{\Gamma}_1 = \begin{pmatrix} i\gamma_{l,2}\psi_0 \\ i\gamma_{l,2}\psi_0 \end{pmatrix}^T, \quad \hat{\Gamma}_2 = \begin{pmatrix} -i\gamma_{l,2}\psi_0 \\ 0 \end{pmatrix}^T, \quad \hat{\Gamma}_3 = \begin{pmatrix} 0 \\ i\gamma_{l,2}\psi_0 \end{pmatrix}^T \tag{12.19}$$

$$\left(\frac{\delta A^{(1)}}{\delta f_i(\boldsymbol{q})}\right)_{k,k'} = \begin{pmatrix} 0 & a_i^A \\ a_i^R & a_i^K \end{pmatrix}_{\boldsymbol{k},\boldsymbol{k'}} \delta_{\omega,\omega'}\delta_{\boldsymbol{k},\boldsymbol{q}+\boldsymbol{k'}} \tag{12.20}$$

$$a_i^A(\boldsymbol{k},\boldsymbol{k'}) = \begin{pmatrix} \gamma_i(\boldsymbol{k}+\boldsymbol{k'}) & 0 \\ 0 & \gamma_i(-\boldsymbol{k}-\boldsymbol{k'}) \end{pmatrix} + \begin{pmatrix} \hat{\Gamma}_1 G^R \Gamma_i & \hat{\Gamma}_2 G^R \Gamma_i \\ \hat{\Gamma}_3 G^R \Gamma_i & -\hat{\Gamma}_1 G^R \Gamma_i \end{pmatrix}_{\boldsymbol{k}-\boldsymbol{k'}} \tag{12.21}$$

$$a_i^R(\boldsymbol{k},\boldsymbol{k'}) = \begin{pmatrix} \gamma_i(\boldsymbol{k}+\boldsymbol{k'}) & 0 \\ 0 & \gamma_i(-\boldsymbol{k}-\boldsymbol{k'}) \end{pmatrix} + \begin{pmatrix} -\hat{\Gamma}_1 G^R \Gamma_i & \hat{\Gamma}_2 G^R \Gamma_i \\ \hat{\Gamma}_3 G^R \Gamma_i & \hat{\Gamma}_1 G^R \Gamma_i \end{pmatrix}_{\boldsymbol{k}-\boldsymbol{k'}} \tag{12.22}$$

$$a_i^K(\boldsymbol{k},\boldsymbol{k'}) = \begin{pmatrix} -2\hat{\Gamma}_1 G^R \Gamma_i & 0 \\ 0 & -2\hat{\Gamma}_1 G^R \Gamma_i \end{pmatrix}_{\boldsymbol{k}-\boldsymbol{k'}} \tag{12.23}$$

$$\left(\frac{\delta A^{(1)}}{\delta \theta_i(-\boldsymbol{q})}\right) = \begin{pmatrix} b_i^Q & b_i^A \\ b_i^R & b_i^K \end{pmatrix}_{\boldsymbol{k},\boldsymbol{k'}} \delta_{\omega,\omega'}\delta_{\boldsymbol{k}+\boldsymbol{q},\boldsymbol{k'}} \tag{12.24}$$

$$b_i^Q(\boldsymbol{k},\boldsymbol{k'}) = \begin{pmatrix} \gamma_i(\boldsymbol{k}+\boldsymbol{k'}) & 0 \\ 0 & \gamma_i(-\boldsymbol{k}-\boldsymbol{k'}) \end{pmatrix} + \begin{pmatrix} \hat{\Gamma}_1 \sigma_3 G^A \Gamma_i & -\hat{\Gamma}_2 G^A \Gamma_i \\ -\hat{\Gamma}_3 G^A \Gamma_i & \hat{\Gamma}_1 \sigma_3 G^A \Gamma_i \end{pmatrix}_{\boldsymbol{k}-\boldsymbol{k'}} \tag{12.25}$$

$$b_i^A(\boldsymbol{k},\boldsymbol{k'}) = \begin{pmatrix} \hat{\Gamma}_1 G^K \Gamma_i - 2\hat{\Gamma}_3 G^A \Gamma_i & \hat{\Gamma}_2 G^K \Gamma_i + 2\hat{\Gamma}_2 G^A \Gamma_i \\ \hat{\Gamma}_3 G^K \Gamma_i - 2\hat{\Gamma}_3 G^A \Gamma_i & -\hat{\Gamma}_1 G^K \Gamma_i + 2\hat{\Gamma}_2 G^A \Gamma_i \end{pmatrix}_{\boldsymbol{k}-\boldsymbol{k'}} \tag{12.26}$$

$$b_i^R(\boldsymbol{k},\boldsymbol{k'}) = \begin{pmatrix} -\hat{\Gamma}_1 G^K \Gamma_i + 2\hat{\Gamma}_2 G^A \Gamma_i & \hat{\Gamma}_2 G^K \Gamma_i + 2\hat{\Gamma}_2 G^A \Gamma_i \\ \hat{\Gamma}_3 G^K \Gamma_i - 2\hat{\Gamma}_3 G^A \Gamma_i & \hat{\Gamma}_1 G^K \Gamma_i - 2\hat{\Gamma}_3 G^A \Gamma_i \end{pmatrix}_{\boldsymbol{k}-\boldsymbol{k'}} \tag{12.27}$$

$$\begin{aligned} b_i^K(\boldsymbol{k},\boldsymbol{k'}) = &\begin{pmatrix} \gamma_i(\boldsymbol{k}+\boldsymbol{k'}) & 0 \\ 0 & \gamma_i(-\boldsymbol{k}-\boldsymbol{k'}) \end{pmatrix} \\ &+ \begin{pmatrix} -\hat{\Gamma}_1 \sigma_3 G^A \Gamma_i - 2\hat{\Gamma}_1 G^K \Gamma_i & -\hat{\Gamma}_2 G^A \Gamma_i \\ -\hat{\Gamma}_3 G^A \Gamma_i & -\hat{\Gamma}_1 \sigma_3 G^A \Gamma_i - 2\hat{\Gamma}_1 G^K \Gamma_i \end{pmatrix}_{\boldsymbol{k}-\boldsymbol{k'}} \end{aligned} \tag{12.28}$$

Proceeding to the expression for the first part of the $O(\hbar^2)$ corrections to the response tensor, we find (any terms of the form $\delta(0)$ which may arise are due to us not being careful with length/time factors in taking the continuum limit — they are spurious and may be ignored, as explained in Appendix B of [13])

$$\begin{aligned} \chi_{ij}^{(1)}(\boldsymbol{q}) &= -\frac{i}{4}\int dk dk' d\hat{k} d\tilde{k}\ \mathrm{Tr}\left[[G]_{k,k'}\left(\frac{\delta A^{(1)}}{\delta f_i(\boldsymbol{q})}\right)_{k',\hat{k}}[G]_{\hat{k},\tilde{k}}\left(\frac{\delta A^{(1)}}{\delta \theta_i(-\boldsymbol{q})}\right)_{\tilde{k},k}\right] \\ &= -\frac{i}{4}\int d\omega d\boldsymbol{k}\ \mathrm{Tr}\left[\begin{pmatrix} G^K & G^R \\ G^A & 0 \end{pmatrix}_{\omega,\boldsymbol{k}+\boldsymbol{q}}\begin{pmatrix} 0 & a_i^A \\ a_i^R & a_i^K \end{pmatrix}_{\boldsymbol{k}+\boldsymbol{q},\boldsymbol{k}}\begin{pmatrix} G^K & G^R \\ G^A & 0 \end{pmatrix}_{\omega,\boldsymbol{k}}\begin{pmatrix} b_j^Q & b_j^A \\ b_j^R & b_j^K \end{pmatrix}_{\boldsymbol{k},\boldsymbol{k}+\boldsymbol{q}}\right] \\ &= -\frac{i}{4}\int d\omega d\boldsymbol{k}\ \mathrm{Tr}\Big[\Big(G^K(\omega,\boldsymbol{k}+\boldsymbol{q})a_i^A(\boldsymbol{k}+\boldsymbol{q},\boldsymbol{k})G^A(\omega,\boldsymbol{k}) \\ &\qquad + G^R(\omega,\boldsymbol{k}+\boldsymbol{q})a_i^R(\boldsymbol{k}+\boldsymbol{q},\boldsymbol{k})G^K(\omega,\boldsymbol{k}) \\ &\qquad + G^R(\omega,\boldsymbol{k}+\boldsymbol{q})a_i^K(\boldsymbol{k}+\boldsymbol{q},\boldsymbol{k})G^A(\omega,\boldsymbol{k})\Big)b_j^Q(\boldsymbol{k},\boldsymbol{k}+\boldsymbol{q})\Big]. \end{aligned} \tag{12.29}$$

Here we have discarded any terms with two G^Rs or two G^As, as such terms have all their frequency domain poles in the same half-plane and are thus annihilated by the frequency integral when it is performed via contour integration. Proceeding to $X_{\boldsymbol{k}}^{(2)}$, $Y_{\boldsymbol{k}}^{(2)}$, $\bar{X}_{\boldsymbol{k}}^{(2)}$, $\bar{Y}_{\boldsymbol{k}}^{(2)}$, we find

$$\begin{aligned}
&\underbrace{\begin{pmatrix} -K\epsilon(\boldsymbol{k})+\frac{i}{2}\delta_\gamma & \frac{i}{2}\delta_\gamma \\ -\frac{i}{2}\delta_\gamma & -K\epsilon(\boldsymbol{k})-\frac{i}{2}\delta_\gamma \end{pmatrix}}_{[G^{-1}]^R(0,\boldsymbol{k})} \begin{pmatrix} X_{\boldsymbol{k}}^{(2)} \\ \bar{X}_{-\boldsymbol{k}}^{(2)} \end{pmatrix} = -\underbrace{\begin{pmatrix} i\sigma_\gamma+2i\delta_\gamma & 0 \\ 0 & i\sigma_\gamma+2i\delta_\gamma \end{pmatrix}}_{[G^{-1}]^K(0,\boldsymbol{k})} \begin{pmatrix} Y_{\boldsymbol{k}}^{(2)} \\ \bar{Y}_{-\boldsymbol{k}}^{(2)} \end{pmatrix} \\
&-\sum_q \begin{pmatrix} \left(f_i(\boldsymbol{q})X_{\boldsymbol{k}-\boldsymbol{q}}^{(1)}+\theta_i(\boldsymbol{q})Y_{\boldsymbol{k}-\boldsymbol{q}}^{(1)}\right)\gamma_i(2\boldsymbol{k}-\boldsymbol{q})) \\ \left(f_i(\boldsymbol{q})\bar{X}_{\boldsymbol{q}-\boldsymbol{k}}^{(1)}+\theta_i(\boldsymbol{q})\bar{Y}_{\boldsymbol{q}-\boldsymbol{k}}^{(1)}\right)\gamma_i(\boldsymbol{q}-2\boldsymbol{k})) \end{pmatrix} \\
&-\frac{i}{2}\gamma_{l,2}\sum_q \begin{pmatrix} \begin{pmatrix} \bar{X}_{-\boldsymbol{q}}^{(1)} \\ \bar{Y}_{-\boldsymbol{q}}^{(1)} \end{pmatrix}^T \begin{pmatrix} 2\psi_0 & 4\psi_0 \\ 0 & -2\psi_0 \end{pmatrix} \begin{pmatrix} X_{\boldsymbol{k}-\boldsymbol{q}}^{(1)} \\ Y_{\boldsymbol{k}-\boldsymbol{q}}^{(1)} \end{pmatrix} + \begin{pmatrix} X_{\boldsymbol{q}}^{(1)} \\ Y_{\boldsymbol{q}}^{(1)} \end{pmatrix}^T \begin{pmatrix} \psi_0 & 2\psi_0 \\ 2\psi_0 & \psi_0 \end{pmatrix} \begin{pmatrix} X_{\boldsymbol{k}-\boldsymbol{q}}^{(1)} \\ Y_{\boldsymbol{k}-\boldsymbol{q}}^{(1)} \end{pmatrix} \\ \begin{pmatrix} \bar{X}_{-\boldsymbol{q}}^{(1)} \\ \bar{Y}_{-\boldsymbol{q}}^{(1)} \end{pmatrix}^T \begin{pmatrix} -2\psi_0 & 0 \\ 4\psi_0 & 2\psi_0 \end{pmatrix} \begin{pmatrix} X_{\boldsymbol{k}-\boldsymbol{q}}^{(1)} \\ Y_{\boldsymbol{k}-\boldsymbol{q}}^{(1)} \end{pmatrix} + \begin{pmatrix} \bar{X}_{-\boldsymbol{q}}^{(1)} \\ \bar{Y}_{-\boldsymbol{q}}^{(1)} \end{pmatrix}^T \begin{pmatrix} -\psi_0 & 2\psi_0 \\ 2\psi_0 & -\psi_0 \end{pmatrix} \begin{pmatrix} \bar{X}_{\boldsymbol{q}-\boldsymbol{k}}^{(1)} \\ \bar{Y}_{\boldsymbol{q}-\boldsymbol{k}}^{(1)} \end{pmatrix} \end{pmatrix}
\end{aligned} \tag{12.30}$$

$$\begin{aligned}
&\underbrace{\begin{pmatrix} -K\epsilon(\boldsymbol{k})-\frac{i}{2}\delta_\gamma & \frac{i}{2}\delta_\gamma \\ -\frac{i}{2}\delta_\gamma & -K\epsilon(\boldsymbol{k})+\frac{i}{2}\delta_\gamma \end{pmatrix}}_{[G^{-1}]^A(0,\boldsymbol{k})} \begin{pmatrix} Y_{\boldsymbol{k}}^{(2)} \\ \bar{Y}_{-\boldsymbol{k}}^{(2)} \end{pmatrix} = -\sum_q \begin{pmatrix} \left(\theta_i(\boldsymbol{q})X_{\boldsymbol{k}-\boldsymbol{q}}^{(1)}+f_i(\boldsymbol{q})Y_{\boldsymbol{k}-\boldsymbol{q}}^{(1)}\right)\gamma_i(2\boldsymbol{k}-\boldsymbol{q})) \\ \left(\theta_i(\boldsymbol{q})\bar{X}_{\boldsymbol{q}-\boldsymbol{k}}^{(1)}+f_i(\boldsymbol{q})\bar{Y}_{\boldsymbol{q}-\boldsymbol{k}}^{(1)}\right)\gamma_i(\boldsymbol{q}-2\boldsymbol{k})) \end{pmatrix} \\
&-\frac{i}{2}\gamma_{l,2}\sum_q \begin{pmatrix} \begin{pmatrix} \bar{X}_{-\boldsymbol{q}}^{(1)} \\ \bar{Y}_{-\boldsymbol{q}}^{(1)} \end{pmatrix}^T \begin{pmatrix} 0 & -2\psi_0 \\ 2\psi_0 & 4\psi_0 \end{pmatrix} \begin{pmatrix} X_{\boldsymbol{k}-\boldsymbol{q}}^{(1)} \\ Y_{\boldsymbol{k}-\boldsymbol{q}}^{(1)} \end{pmatrix} + \begin{pmatrix} X_{\boldsymbol{q}}^{(1)} \\ Y_{\boldsymbol{q}}^{(1)} \end{pmatrix}^T \begin{pmatrix} 0 & -\psi_0 \\ -\psi_0 & 0 \end{pmatrix} \begin{pmatrix} X_{\boldsymbol{k}-\boldsymbol{q}}^{(1)} \\ Y_{\boldsymbol{k}-\boldsymbol{q}}^{(1)} \end{pmatrix} \\ \begin{pmatrix} \bar{X}_{-\boldsymbol{q}}^{(1)} \\ \bar{Y}_{-\boldsymbol{q}}^{(1)} \end{pmatrix}^T \begin{pmatrix} 0 & -2\psi_0 \\ 2\psi_0 & 4\psi_0 \end{pmatrix} \begin{pmatrix} X_{\boldsymbol{k}-\boldsymbol{q}}^{(1)} \\ Y_{\boldsymbol{k}-\boldsymbol{q}}^{(1)} \end{pmatrix} + \begin{pmatrix} \bar{X}_{-\boldsymbol{q}}^{(1)} \\ \bar{Y}_{-\boldsymbol{q}}^{(1)} \end{pmatrix}^T \begin{pmatrix} 0 & \psi_0 \\ \psi_0 & 0 \end{pmatrix} \begin{pmatrix} \bar{X}_{\boldsymbol{q}-\boldsymbol{k}}^{(1)} \\ \bar{Y}_{\boldsymbol{q}-\boldsymbol{k}}^{(1)} \end{pmatrix} \end{pmatrix}
\end{aligned} \tag{12.31}$$

These may again be rewritten so as to make clearer the diagrammatic structure via the identity (11.16):

$$\begin{pmatrix} Y^{(2)}_{\boldsymbol{k}} \\ \bar{Y}^{(2)}_{-\boldsymbol{k}} \end{pmatrix} = -G^A(0,\boldsymbol{k}) \sum_q \begin{pmatrix} \left(\theta_i(\boldsymbol{q}) X^{(1)}_{\boldsymbol{k}-\boldsymbol{q}} + f_i(\boldsymbol{q}) Y^{(1)}_{\boldsymbol{k}-\boldsymbol{q}}\right)\gamma_i(2\boldsymbol{k}-\boldsymbol{q})) \\ \left(\theta_i(\boldsymbol{q}) \bar{X}^{(1)}_{\boldsymbol{q}-\boldsymbol{k}} + f_i(\boldsymbol{q}) \bar{Y}^{(1)}_{\boldsymbol{q}-\boldsymbol{k}}\right)\gamma_i(\boldsymbol{q}-2\boldsymbol{k})) \end{pmatrix}$$
$$-\frac{i}{2}\gamma_{l,2} G^A(0,\boldsymbol{k}) \sum_q \begin{pmatrix} \begin{pmatrix} \bar{X}^{(1)}_{-\boldsymbol{q}} \\ \bar{Y}^{(1)}_{-\boldsymbol{q}} \end{pmatrix}^T \begin{pmatrix} 0 & -2\psi_0 \\ 2\psi_0 & 4\psi_0 \end{pmatrix} \begin{pmatrix} X^{(1)}_{\boldsymbol{k}-\boldsymbol{q}} \\ Y^{(1)}_{\boldsymbol{k}-\boldsymbol{q}} \end{pmatrix} + \begin{pmatrix} X^{(1)}_{\boldsymbol{q}} \\ Y^{(1)}_{\boldsymbol{q}} \end{pmatrix}^T \begin{pmatrix} 0 & -\psi_0 \\ -\psi_0 & 0 \end{pmatrix} \begin{pmatrix} X^{(1)}_{\boldsymbol{k}-\boldsymbol{q}} \\ Y^{(1)}_{\boldsymbol{k}-\boldsymbol{q}} \end{pmatrix} \\ \begin{pmatrix} \bar{X}^{(1)}_{-\boldsymbol{q}} \\ \bar{Y}^{(1)}_{-\boldsymbol{q}} \end{pmatrix}^T \begin{pmatrix} 0 & -2\psi_0 \\ 2\psi_0 & 4\psi_0 \end{pmatrix} \begin{pmatrix} X^{(1)}_{\boldsymbol{k}-\boldsymbol{q}} \\ Y^{(1)}_{\boldsymbol{k}-\boldsymbol{q}} \end{pmatrix} + \begin{pmatrix} \bar{X}^{(1)}_{-\boldsymbol{q}} \\ \bar{Y}^{(1)}_{-\boldsymbol{q}} \end{pmatrix}^T \begin{pmatrix} 0 & \psi_0 \\ \psi_0 & 0 \end{pmatrix} \begin{pmatrix} \bar{X}^{(1)}_{\boldsymbol{q}-\boldsymbol{k}} \\ \bar{Y}^{(1)}_{\boldsymbol{q}-\boldsymbol{k}} \end{pmatrix} \end{pmatrix}, \tag{12.32}$$

$$\begin{pmatrix} X^{(2)}_{\boldsymbol{k}} \\ \bar{X}^{(2)}_{-\boldsymbol{k}} \end{pmatrix} = -G^K(0,\boldsymbol{k}) \sum_q \begin{pmatrix} \left(\theta_i(\boldsymbol{q}) X^{(1)}_{\boldsymbol{k}-\boldsymbol{q}} + f_i(\boldsymbol{q}) Y^{(1)}_{\boldsymbol{k}-\boldsymbol{q}}\right)\gamma_i(2\boldsymbol{k}-\boldsymbol{q})) \\ \left(\theta_i(\boldsymbol{q}) \bar{X}^{(1)}_{\boldsymbol{q}-\boldsymbol{k}} + f_i(\boldsymbol{q}) \bar{Y}^{(1)}_{\boldsymbol{q}-\boldsymbol{k}}\right)\gamma_i(\boldsymbol{q}-2\boldsymbol{k})) \end{pmatrix}$$
$$-\frac{i}{2}\gamma_{l,2} G^K(0,\boldsymbol{k}) \sum_q \begin{pmatrix} \begin{pmatrix} \bar{X}^{(1)}_{-\boldsymbol{q}} \\ \bar{Y}^{(1)}_{-\boldsymbol{q}} \end{pmatrix}^T \begin{pmatrix} 0 & -2\psi_0 \\ 2\psi_0 & 4\psi_0 \end{pmatrix} \begin{pmatrix} X^{(1)}_{\boldsymbol{k}-\boldsymbol{q}} \\ Y^{(1)}_{\boldsymbol{k}-\boldsymbol{q}} \end{pmatrix} + \begin{pmatrix} X^{(1)}_{\boldsymbol{q}} \\ Y^{(1)}_{\boldsymbol{q}} \end{pmatrix}^T \begin{pmatrix} 0 & -\psi_0 \\ -\psi_0 & 0 \end{pmatrix} \begin{pmatrix} X^{(1)}_{\boldsymbol{k}-\boldsymbol{q}} \\ Y^{(1)}_{\boldsymbol{k}-\boldsymbol{q}} \end{pmatrix} \\ \begin{pmatrix} \bar{X}^{(1)}_{-\boldsymbol{q}} \\ \bar{Y}^{(1)}_{-\boldsymbol{q}} \end{pmatrix}^T \begin{pmatrix} 0 & -2\psi_0 \\ 2\psi_0 & 4\psi_0 \end{pmatrix} \begin{pmatrix} X^{(1)}_{\boldsymbol{k}-\boldsymbol{q}} \\ Y^{(1)}_{\boldsymbol{k}-\boldsymbol{q}} \end{pmatrix} + \begin{pmatrix} \bar{X}^{(1)}_{-\boldsymbol{q}} \\ \bar{Y}^{(1)}_{-\boldsymbol{q}} \end{pmatrix}^T \begin{pmatrix} 0 & \psi_0 \\ \psi_0 & 0 \end{pmatrix} \begin{pmatrix} \bar{X}^{(1)}_{\boldsymbol{q}-\boldsymbol{k}} \\ \bar{Y}^{(1)}_{\boldsymbol{q}-\boldsymbol{k}} \end{pmatrix} \end{pmatrix}$$
$$- G^R(0,\boldsymbol{k}) \sum_q \begin{pmatrix} \left(f_i(\boldsymbol{q}) X^{(1)}_{\boldsymbol{k}-\boldsymbol{q}} + \theta_i(\boldsymbol{q}) Y^{(1)}_{\boldsymbol{k}-\boldsymbol{q}}\right)\gamma_i(2\boldsymbol{k}-\boldsymbol{q})) \\ \left(f_i(\boldsymbol{q}) \bar{X}^{(1)}_{\boldsymbol{q}-\boldsymbol{k}} + \theta_i(\boldsymbol{q}) \bar{Y}^{(1)}_{\boldsymbol{q}-\boldsymbol{k}}\right)\gamma_i(\boldsymbol{q}-2\boldsymbol{k})) \end{pmatrix}$$
$$-\frac{i}{2}\gamma_{l,2} G^R(0,\boldsymbol{k}) \sum_q \begin{pmatrix} \begin{pmatrix} \bar{X}^{(1)}_{-\boldsymbol{q}} \\ \bar{Y}^{(1)}_{-\boldsymbol{q}} \end{pmatrix}^T \begin{pmatrix} 2\psi_0 & 4\psi_0 \\ 0 & -2\psi_0 \end{pmatrix} \begin{pmatrix} X^{(1)}_{\boldsymbol{k}-\boldsymbol{q}} \\ Y^{(1)}_{\boldsymbol{k}-\boldsymbol{q}} \end{pmatrix} + \begin{pmatrix} X^{(1)}_{\boldsymbol{q}} \\ Y^{(1)}_{\boldsymbol{q}} \end{pmatrix}^T \begin{pmatrix} \psi_0 & 2\psi_0 \\ 2\psi_0 & \psi_0 \end{pmatrix} \begin{pmatrix} X^{(1)}_{\boldsymbol{k}-\boldsymbol{q}} \\ Y^{(1)}_{\boldsymbol{k}-\boldsymbol{q}} \end{pmatrix} \\ \begin{pmatrix} \bar{X}^{(1)}_{-\boldsymbol{q}} \\ \bar{Y}^{(1)}_{-\boldsymbol{q}} \end{pmatrix}^T \begin{pmatrix} -2\psi_0 & 0 \\ 4\psi_0 & 2\psi_0 \end{pmatrix} \begin{pmatrix} X^{(1)}_{\boldsymbol{k}-\boldsymbol{q}} \\ Y^{(1)}_{\boldsymbol{k}-\boldsymbol{q}} \end{pmatrix} + \begin{pmatrix} \bar{X}^{(1)}_{-\boldsymbol{q}} \\ \bar{Y}^{(1)}_{-\boldsymbol{q}} \end{pmatrix}^T \begin{pmatrix} -\psi_0 & 2\psi_0 \\ 2\psi_0 & -\psi_0 \end{pmatrix} \begin{pmatrix} \bar{X}^{(1)}_{\boldsymbol{q}-\boldsymbol{k}} \\ \bar{Y}^{(1)}_{\boldsymbol{q}-\boldsymbol{k}} \end{pmatrix} \end{pmatrix}. \tag{12.33}$$

Given the unwieldy nature of these expressions, some simplifications to the expression we intend to plug them into are in order. At second order in the source

fields, the Hessian has only 8 distinct elements:

$$A^{(2)}_{k,k'} = \underbrace{\begin{pmatrix} A^{(2)}_1 & A^{(2)}_2 & A^{(2)}_3 & A^{(2)}_4 \\ A^{(2)}_5 & A^{(2)}_1 & A^{(2)}_6 & A^{(2)}_7 \\ A^{(2)}_7 & A^{(2)}_4 & A^{(2)}_8 & A^{(2)}_2 \\ A^{(2)}_6 & A^{(2)}_3 & A^{(2)}_5 & A^{(2)}_8 \end{pmatrix}}_{A^{(2)}_{\boldsymbol{k},\boldsymbol{k}'}} \delta_{\omega,\omega'} \tag{12.34}$$

We can block-multiply with the Greens function matrix and consider

$$\mathrm{Tr}[[G]_k A^{(2)}_{\boldsymbol{k},\boldsymbol{k}}] = \mathrm{Tr}\left[G^K(k) \begin{pmatrix} A^{(2)}_1 & A^{(2)}_2 \\ A^{(2)}_5 & A^{(2)}_1 \end{pmatrix}_{\boldsymbol{k},\boldsymbol{k}} + G^R(k) \begin{pmatrix} A^{(2)}_7 & A^{(2)}_4 \\ A^{(2)}_6 & A^{(2)}_3 \end{pmatrix}_{\boldsymbol{k},\boldsymbol{k}} + G^A(k) \begin{pmatrix} A^{(2)}_3 & A^{(2)}_4 \\ A^{(2)}_6 & A^{(2)}_7 \end{pmatrix}_{\boldsymbol{k},\boldsymbol{k}} \right] \tag{12.35}$$

Focusing on and expanding the G^R and G^A portions of this expression, we obtain

$$\begin{aligned} &G^R_{11}(k)A^{(2)}_7(\boldsymbol{k}) + G^R_{12}(k)A^{(2)}_6(\boldsymbol{k}) + G^R_{21}(k)A^{(2)}_4(\boldsymbol{k}) + G^R_{22}(k)A^{(2)}_3(\boldsymbol{k}) \\ &+ G^A_{11}(k)A^{(2)}_3(\boldsymbol{k}) + G^A_{12}(k)A^{(2)}_6(\boldsymbol{k}) + G^A_{21}(k)A^{(2)}_4(\boldsymbol{k}) + G^A_{22}(k)A^{(2)}_7(\boldsymbol{k}). \end{aligned} \tag{12.36}$$

If we consider the eventual integral over frequency, all the terms with indices 12 or 21 vanish via the estimation lemma and contour integration. Using the fact that $G^A_{22}(-\omega,\boldsymbol{k}) = G^R_{11}(\omega,\boldsymbol{k})$, $G^R_{22}(-\omega,\boldsymbol{k}) = G^A_{11}(\omega,\boldsymbol{k})$, we may write the remaining integral as

$$\int d\omega \left[(G^R_{11}(k) + G^A_{11}(k))(A^{(2)}_7(\boldsymbol{k}) + A^{(2)}_3(\boldsymbol{k})) + (G^R_{11}(k) - G^A_{11}(k))(A^{(2)}_7(\boldsymbol{k}) - A^{(2)}_3(\boldsymbol{k})) \right]. \tag{12.37}$$

The first term vanishes by the Keldysh identity $\int d\omega\, [G^R(\omega) + G^A(\omega)] = 0$ while the second is simplified via the identity $\int d\omega\, [G^R(\omega) - G^A(\omega)] = -2\pi i$, and we are left with

$$\int dk\, \mathrm{Tr}[[G]_k A^{(2)}_{\boldsymbol{k},\boldsymbol{k}}] = \mathrm{Tr}\left[\int dk\, G^K(k) \begin{pmatrix} A^{(2)}_1 & A^{(2)}_2 \\ A^{(2)}_5 & A^{(2)}_1 \end{pmatrix}_{\boldsymbol{k},\boldsymbol{k}} \right] - 2\pi i \int d\boldsymbol{k} \left[(A^{(2)}_7(\boldsymbol{k}) - A^{(2)}_3(\boldsymbol{k})) \right]. \tag{12.38}$$

In the coherently driven polariton model considered in the main body of this part, only the first trace on the right above was present. This is partly due to the universal cancellation of G^R/G^A tadpoles in that model, which does not occur so trivially here.

$$A^{(2)}_7(\boldsymbol{k}) = i\gamma_{l,2} \left[\psi_0 \bar{X}^{(2)}_{\boldsymbol{0}} + \bar{\psi}_0 X^{(2)}_{\boldsymbol{0}} + 2\bar{\psi}_0 Y^{(2)}_{\boldsymbol{0}} + \sum_{\boldsymbol{q}} \left[X^{(1)}_{\boldsymbol{q}} \bar{X}^{(1)}_{\boldsymbol{q}} - Y^{(1)}_{\boldsymbol{q}} \bar{Y}^{(1)}_{\boldsymbol{q}} + 2\bar{X}^{(1)}_{\boldsymbol{q}} Y^{(1)}_{\boldsymbol{q}} \right] \right] \tag{12.39}$$

$$A_3^{(2)}(\boldsymbol{k}) = -i\gamma_{l,2}\left[\bar{\psi}_0 X_{\mathbf{0}}^{(2)} + \psi_0 \bar{X}_{\mathbf{0}}^{(2)} - 2\psi_0 \bar{Y}_{\mathbf{0}}^{(2)} + \sum_{\boldsymbol{q}}\left[X_{\boldsymbol{q}}^{(1)}\bar{X}_{\boldsymbol{q}}^{(1)} - Y_{\boldsymbol{q}}^{(1)}\bar{Y}_{\boldsymbol{q}}^{(1)} - 2X_{\boldsymbol{q}}^{(1)}\bar{Y}_{\boldsymbol{q}}^{(1)}\right]\right] \tag{12.40}$$

The first three terms in each expression are tadpoles, while the rest are those originating from 4-valent vertices forming a loop (but without a connecting leg, thus making them not tadpoles). The total tadpole contribution from the second term on the right of (12.38) is thus

$$4\pi\gamma_{l,2}\psi_0 \int d\boldsymbol{k}\, \frac{\delta^2}{\delta f_i(\boldsymbol{q})\theta_i(-\boldsymbol{q})}\left[X_{\mathbf{0}}^{(2)} + \bar{X}_{\mathbf{0}}^{(2)} + Y_{\mathbf{0}}^{(2)} - \bar{Y}_{\mathbf{0}}^{(2)}\right] \tag{12.41}$$

and the integrand must evidently cancel if this term is to be well-behaved.

Here we may perform an elegant trick. Observe that the equations for $X_{\mathbf{0}}^{(2)}$, $\bar{X}_{\mathbf{0}}^{(2)}$, $Y_{\mathbf{0}}^{(2)}$, $\bar{Y}_{\mathbf{0}}^{(2)}$ are of the form

$$\begin{pmatrix} X_{\mathbf{0}}^{(2)} \\ \bar{X}_{\mathbf{0}}^{(2)} \end{pmatrix} = -G^K(\mathbf{0})V_1 - G^R(\mathbf{0})V_2, \tag{12.42}$$

$$\begin{pmatrix} Y_{\mathbf{0}}^{(2)} \\ \bar{Y}_{\mathbf{0}}^{(2)} \end{pmatrix} = -G^A(\mathbf{0})V_3. \tag{12.43}$$

The pathology here lies in the denominators of the Greens matrices, which we can label $\mathfrak{D}^{K/G/A}(\boldsymbol{k})$ and assume temporarily regularised, making these expressions

$$\begin{pmatrix} X_{\mathbf{0}}^{(2)} \\ \bar{X}_{\mathbf{0}}^{(2)} \end{pmatrix} = -\frac{1}{\mathfrak{D}^K(\mathbf{0})}\begin{pmatrix} \frac{1}{2}\delta_\gamma^2 & -\frac{1}{2}\delta_\gamma^2 \\ -\frac{1}{2}\delta_\gamma^2 & \frac{1}{2}\delta_\gamma^2 \end{pmatrix} V_1 - \frac{1}{\mathfrak{D}^R(\mathbf{0})}\begin{pmatrix} -\frac{i}{2}\delta_\gamma & -\frac{i}{2}\delta_\gamma \\ \frac{i}{2}\delta_\gamma & \frac{i}{2}\delta_\gamma \end{pmatrix} V_2, \tag{12.44}$$

$$\begin{pmatrix} Y_{\mathbf{0}}^{(2)} \\ \bar{Y}_{\mathbf{0}}^{(2)} \end{pmatrix} = -\frac{1}{\mathfrak{D}^A(\mathbf{0})}\begin{pmatrix} \frac{i}{2}\delta_\gamma & -\frac{i}{2}\delta_\gamma \\ \frac{i}{2}\delta_\gamma & -\frac{i}{2}\delta_\gamma \end{pmatrix} V_3. \tag{12.45}$$

Now observe that the integrand in question has the form

$$\begin{pmatrix} 1 & 1 \end{pmatrix}\begin{pmatrix} X_{\mathbf{0}}^{(2)} \\ \bar{X}_{\mathbf{0}}^{(2)} \end{pmatrix} + \begin{pmatrix} 1 & -1 \end{pmatrix}\begin{pmatrix} Y_{\mathbf{0}}^{(2)} \\ \bar{Y}_{\mathbf{0}}^{(2)} \end{pmatrix} \tag{12.46}$$

and that $\begin{pmatrix} 1 & 1 \end{pmatrix}$ is in the left null-space of the two matrices in (12.44) while $\begin{pmatrix} 1 & -1 \end{pmatrix}$ is in the left null-space of the matrix in (12.45). Thus the integrand is zero and the pathological tadpole diagrams cancel.

We are thus left with (terms containing two Ys do not survive the mixed func-

tional derivative)

$$4\pi\gamma_{l,2}\int d\boldsymbol{k}\,\frac{\delta^2}{\delta f_i(\boldsymbol{q})\delta\theta_j(-\boldsymbol{q})}\left[\sum_{\boldsymbol{q}}\left[X^{(1)}_{\boldsymbol{q}}\bar{X}^{(1)}_{\boldsymbol{q}}+\bar{X}^{(1)}_{\boldsymbol{q}}Y^{(1)}_{\boldsymbol{q}}-X^{(1)}_{\boldsymbol{q}}\bar{Y}^{(1)}_{\boldsymbol{q}}\right]\right]. \tag{12.47}$$

Denoting

$$U=\begin{pmatrix}1 & 0\end{pmatrix},\quad D=\begin{pmatrix}0 & 1\end{pmatrix}, \tag{12.48}$$

this may be rewritten in matrix form as

$$-4\pi\gamma_{l,2}\int d\boldsymbol{k}\,\mathrm{Tr}\left[\begin{pmatrix}UG^R(\boldsymbol{q})\Gamma_i(\boldsymbol{q}) & DG^R(\boldsymbol{q})\Gamma_i(\boldsymbol{q})\\ DG^R(\boldsymbol{q})\Gamma_i(\boldsymbol{q}) & -UG^R(\boldsymbol{q})\Gamma_i(\boldsymbol{q})\end{pmatrix}\begin{pmatrix}DG^K(\boldsymbol{q})\Gamma_j(\boldsymbol{q}) & UG^A(\boldsymbol{q})\Gamma_j(\boldsymbol{q})\\ UG^K(\boldsymbol{q})\Gamma_j(\boldsymbol{q}) & DG^A(\boldsymbol{q})\Gamma_j(\boldsymbol{q})\end{pmatrix}\right]. \tag{12.49}$$

We may now turn our attention back to the term

$$\int d\omega d\boldsymbol{k}\,\mathrm{Tr}\left[G^K(k)\begin{pmatrix}A^{(2)}_1 & A^{(2)}_2\\ A^{(2)}_5 & A^{(2)}_1\end{pmatrix}_{\boldsymbol{k},\boldsymbol{k}}\right]. \tag{12.50}$$

Per the argument in [13], this should be corrected to

$$\begin{aligned}\int d\boldsymbol{k}\,\frac{i}{2}\,\mathrm{Tr}\left[\begin{pmatrix}A^{(2)}_1 & A^{(2)}_2\\ A^{(2)}_5 & A^{(2)}_1\end{pmatrix}_{\boldsymbol{k},\boldsymbol{k}}\right]&+\int d\omega d\boldsymbol{k}\,\mathrm{Tr}\left[G^K(k)\begin{pmatrix}A^{(2)}_1 & A^{(2)}_2\\ A^{(2)}_5 & A^{(2)}_1\end{pmatrix}_{\boldsymbol{k},\boldsymbol{k}}\right]\\ &=\int d\boldsymbol{k}\,iA^{(2)}_1(\boldsymbol{k})\\ &+\int d\omega d\boldsymbol{k}\left[G^K_{11}(k)A^{(2)}_1(\boldsymbol{k})+G^K_{12}(k)A^{(2)}_5(\boldsymbol{k})+G^K_{21}(k)A^{(2)}_2(\boldsymbol{k})+G^K_{22}(k)A^{(2)}_1(\boldsymbol{k})\right],\end{aligned} \tag{12.51}$$

and we have the following expressions for $A^{(2)}_1$, $A^{(2)}_2$, $A^{(2)}_5$:

$$A^{(2)}_1=-i\gamma_{l,2}\psi_0\underbrace{[Y^{(2)}_{\boldsymbol{0}}-\bar{Y}^{(2)}_{\boldsymbol{0}}]}_{0}+i\gamma_{l,2}\sum_{\boldsymbol{q}}\left[2Y^{(1)}_{\boldsymbol{q}}\bar{Y}^{(1)}_{\boldsymbol{q}}+X^{(1)}_{\boldsymbol{q}}\bar{Y}^{(1)}_{\boldsymbol{q}}-\bar{X}^{(1)}_{\boldsymbol{q}}Y^{(1)}_{\boldsymbol{q}}\right], \tag{12.52}$$

$$A^{(2)}_2=-i\gamma_{l,2}\psi_0Y^{(2)}_{\boldsymbol{0}}-i\gamma_{l,2}\sum_{\boldsymbol{q}}X^{(1)}_{\boldsymbol{q}}Y^{(1)}_{-\boldsymbol{q}}, \tag{12.53}$$

$$A^{(2)}_5=i\gamma_{l,2}\psi_0\bar{Y}^{(2)}_{\boldsymbol{0}}+i\gamma_{l,2}\sum_{\boldsymbol{q}}\bar{X}^{(1)}_{\boldsymbol{q}}\bar{Y}^{(1)}_{-\boldsymbol{q}}. \tag{12.54}$$

By our earlier argument, the combination $Y^{(2)}_{\boldsymbol{0}}-\bar{Y}^{(2)}_{\boldsymbol{0}}$ vanishes, so that the only remaining tadpole diagrams arise from

$$-i\gamma_{l,2}\psi_0[G^K_{21}(k)Y^{(2)}_{\boldsymbol{0}}-G^K_{12}(k)\bar{Y}^{(2)}_{\boldsymbol{0}}]. \tag{12.55}$$

Unfortunately $G^K_{21}(k)\neq G^K_{12}(k)$ and this remains true after integration over fre-

quency and momentum, so the simple argument about $Y^{(2)}_{\mathbf{0}} - \bar{Y}^{(2)}_{\mathbf{0}}$ is inapplicable. Instead, the term may be rewritten as (recall (12.45))

$$-i\gamma_{l,2}\psi_0\begin{pmatrix} G^K_{21}(k) & -G^K_{12}(k)\end{pmatrix}\begin{pmatrix} Y^{(2)}_{\mathbf{0}} \\ \bar{Y}^{(2)}_{\mathbf{0}}\end{pmatrix} = \frac{i\gamma_{l,2}\psi_0}{\mathcal{D}^A(\mathbf{0})}\begin{pmatrix} G^K_{21}(k) & -G^K_{12}(k)\end{pmatrix}\begin{pmatrix} \frac{i}{2}\delta_\gamma & -\frac{i}{2}\delta_\gamma \\ \frac{i}{2}\delta_\gamma & -\frac{i}{2}\delta_\gamma\end{pmatrix} V_3 \tag{12.56}$$

and we must consider $\frac{\delta^2 V_3}{\delta f_i(\boldsymbol{q})\delta\theta_j(-\boldsymbol{q})}$. With some effort this can be calculated to be

$$\begin{aligned}(V_3)_1 =& -UG^R(\boldsymbol{q})\Gamma_i(\boldsymbol{q})\gamma_j(\boldsymbol{q}) - UG^A(\boldsymbol{q})\Gamma_j(\boldsymbol{q})\gamma_i(\boldsymbol{q}) \\ &+\frac{i}{2}\gamma_{l,2}\Big[-2\psi_0\Big(UG^R(\boldsymbol{q})\Gamma_i(\boldsymbol{q})\Big)\Big(DG^A(\boldsymbol{q})\Gamma_j(\boldsymbol{q})\Big) \\ &\qquad + 2\psi_0\Big(UG^A(\boldsymbol{q})\Gamma_j(\boldsymbol{q})\Big)\Big(DG^R(\boldsymbol{q})\Gamma_i(\boldsymbol{q})\Big) \\ &\qquad + 2\psi\Big(UG^R(\boldsymbol{q})\Gamma_i(\boldsymbol{q})\Big)\Big(UG^A(\boldsymbol{q})\Gamma_j(\boldsymbol{q})\Big)\Big],\end{aligned} \tag{12.57}$$

$$\begin{aligned}(V_3)_2 =& DG^R(\boldsymbol{q})\Gamma_i(\boldsymbol{q})\gamma_j(\boldsymbol{q}) + DG^A(\boldsymbol{q})\Gamma_j(\boldsymbol{q})\gamma_i(\boldsymbol{q}) \\ &+\frac{i}{2}\gamma_{l,2}\Big[-2\psi_0\Big(UG^R(\boldsymbol{q})\Gamma_i(\boldsymbol{q})\Big)\Big(DG^A(\boldsymbol{q})\Gamma_j(\boldsymbol{q})\Big) \\ &\qquad + 2\psi_0\Big(UG^A(\boldsymbol{q})\Gamma_j(\boldsymbol{q})\Big)\Big(DG^R(\boldsymbol{q})\Gamma_i(\boldsymbol{q})\Big) \\ &\qquad - 2\psi\Big(DG^R(\boldsymbol{q})\Gamma_i(\boldsymbol{q})\Big)\Big(DG^A(\boldsymbol{q})\Gamma_j(\boldsymbol{q})\Big)\Big],\end{aligned} \tag{12.58}$$

which, upon substituting concrete expressions for all the terms, simplifies drastically to

$$V_3 = \frac{\gamma_i(\boldsymbol{q})\gamma_j(\boldsymbol{q})}{K^3\epsilon(\boldsymbol{q})^3}\begin{pmatrix}\psi_0(2K^2\epsilon(\boldsymbol{q})^2 - \delta_\gamma^2) \\ \psi_0(2K^2\epsilon(\boldsymbol{q})^2 - \delta_\gamma^2)\end{pmatrix} \propto \begin{pmatrix}1\\1\end{pmatrix}. \tag{12.59}$$

This lies in the right null-space of the matrix in (12.56) and thus the remaining tadpoles all cancel.

This leaves just (we again discard terms containing two Ys)

$$\begin{aligned}&-\gamma_{l,2}\int d\boldsymbol{k}\sum_{\boldsymbol{q}}\Big[X^{(1)}_{\boldsymbol{q}}\bar{Y}^{(1)}_{\boldsymbol{q}} - \bar{X}^{(1)}_{\boldsymbol{q}}Y^{(1)}_{\boldsymbol{q}}\Big] \\ &+\int d\omega d\boldsymbol{k}\Big[i\gamma_{l,2}\Big(G^K_{11}(k)+G^K_{22}(k)\Big)\sum_{\boldsymbol{q}}\Big[X^{(1)}_{\boldsymbol{q}}\bar{Y}^{(1)}_{\boldsymbol{q}} - \bar{X}^{(1)}_{\boldsymbol{q}}Y^{(1)}_{\boldsymbol{q}}\Big] \\ &-i\gamma_{l,2}G^K_{21}(k)\sum_{\boldsymbol{q}}X^{(1)}_{\boldsymbol{q}}Y^{(1)}_{-\boldsymbol{q}} \\ &+i\gamma_{l,2}G^K_{12}(k)\sum_{\boldsymbol{q}}\bar{X}^{(1)}_{\boldsymbol{q}}\bar{Y}^{(1)}_{-\boldsymbol{q}}\Big]\end{aligned} \tag{12.60}$$

which, upon functional differentiation, yields

$$\gamma_{l,2}\int d\boldsymbol{k}\begin{pmatrix}UG^R(\boldsymbol{q})\Gamma_i(\boldsymbol{q})\\DG^R(\boldsymbol{q})\Gamma_i(\boldsymbol{q})\end{pmatrix}^T\sigma_3\begin{pmatrix}DG^A(\boldsymbol{q})\Gamma_j(\boldsymbol{q})\\UG^A(\boldsymbol{q})\Gamma_j(\boldsymbol{q})\end{pmatrix}$$
$$-i\gamma_{l,2}\int d\omega d\boldsymbol{k}\begin{pmatrix}UG^R(\boldsymbol{q})\Gamma_i(\boldsymbol{q})\\DG^R(\boldsymbol{q})\Gamma_i(\boldsymbol{q})\end{pmatrix}^T\begin{pmatrix}G^K_{11}(k)+G^K_{22}(k) & -G^K_{21}(k)\\ G^K_{12}(k) & -G^K_{11}(k)-G^K_{22}(k)\end{pmatrix}\begin{pmatrix}DG^A(\boldsymbol{q})\Gamma_j(\boldsymbol{q})\\UG^A(\boldsymbol{q})\Gamma_j(\boldsymbol{q})\end{pmatrix}. \tag{12.61}$$

Thus, defining

$$\begin{pmatrix}c^Q(k) & c^A(k)\\ c^R(k) & c^K(k)\end{pmatrix}=\begin{pmatrix}G^K_{11}(k)+G^K_{22}(k) & -G^K_{21}(k)\\ G^K_{12}(k) & -G^K_{11}(k)-G^K_{22}(k)\end{pmatrix} \tag{12.62}$$

we have

$$\begin{aligned}\chi^{(2)}_{ij}(\boldsymbol{q}) &= \frac{i}{4}\int dk\ \mathrm{Tr}[[G]_k A^{(2)}_{\boldsymbol{k},\boldsymbol{k}}]\\ &=\frac{i\gamma_{l,2}}{4}\int d\boldsymbol{k}\begin{pmatrix}UG^R(\boldsymbol{q})\Gamma_i(\boldsymbol{q})\\DG^R(\boldsymbol{q})\Gamma_i(\boldsymbol{q})\end{pmatrix}^T\sigma_3\begin{pmatrix}DG^A(\boldsymbol{q})\Gamma_j(\boldsymbol{q})\\UG^A(\boldsymbol{q})\Gamma_j(\boldsymbol{q})\end{pmatrix}\\ &+\frac{\gamma_{l,2}}{4}\int dk\begin{pmatrix}UG^R(\boldsymbol{q})\Gamma_i(\boldsymbol{q})\\DG^R(\boldsymbol{q})\Gamma_i(\boldsymbol{q})\end{pmatrix}^T\begin{pmatrix}c^Q(k) & c^A(k)\\ c^R(k) & c^K(k)\end{pmatrix}\begin{pmatrix}DG^A(\boldsymbol{q})\Gamma_j(\boldsymbol{q})\\UG^A(\boldsymbol{q})\Gamma_j(\boldsymbol{q})\end{pmatrix}\\ &-i\pi\gamma_{l,2}\int d\boldsymbol{k}\ \mathrm{Tr}\left[\begin{pmatrix}UG^R(\boldsymbol{q})\Gamma_i(\boldsymbol{q}) & DG^R(\boldsymbol{q})\Gamma_i(\boldsymbol{q})\\ DG^R(\boldsymbol{q})\Gamma_i(\boldsymbol{q}) & -UG^R(\boldsymbol{q})\Gamma_i(\boldsymbol{q})\end{pmatrix}\begin{pmatrix}DG^K(\boldsymbol{q})\Gamma_j(\boldsymbol{q}) & UG^A(\boldsymbol{q})\Gamma_j(\boldsymbol{q})\\ UG^K(\boldsymbol{q})\Gamma_j(\boldsymbol{q}) & DG^A(\boldsymbol{q})\Gamma_j(\boldsymbol{q})\end{pmatrix}\right]\end{aligned} \tag{12.63}$$

With this, all the pieces are in place to write down the current-current response tensor to $O(\hbar^2)$. This will be done in the next chapter, and the resulting expression and its implications for whether the system exhibits superfluidity will be discussed.

Chapter 13

Conclusion

Finally putting all the pieces together, this yields the following expression for the current-current response tensor:

$$
\begin{aligned}
\chi_{ij}(\boldsymbol{q}) &= \frac{2\delta_\gamma}{\gamma_{l,2}} \frac{\gamma_i(\boldsymbol{q})\gamma_j(\boldsymbol{q})}{\epsilon(\boldsymbol{q})} \\
&-\frac{i}{4}\int d\omega d\boldsymbol{k}\, \mathrm{Tr}\Big[\Big(G^K(\omega,\boldsymbol{k}+\boldsymbol{q})a_i^A(\boldsymbol{k}+\boldsymbol{q},\boldsymbol{k})G^A(\omega,\boldsymbol{k}) \\
&\qquad + G^R(\omega,\boldsymbol{k}+\boldsymbol{q})a_i^R(\boldsymbol{k}+\boldsymbol{q},\boldsymbol{k})G^K(\omega,\boldsymbol{k}) \\
&\qquad + G^R(\omega,\boldsymbol{k}+\boldsymbol{q})a_i^K(\boldsymbol{k}+\boldsymbol{q},\boldsymbol{k})G^A(\omega,\boldsymbol{k})\Big)b_j^Q(\boldsymbol{k},\boldsymbol{k}+\boldsymbol{q})\Big]. \\
&+\frac{\gamma_{l,2}}{4}\int dk \begin{pmatrix} UG^R(\boldsymbol{q})\Gamma_i(\boldsymbol{q}) \\ DG^R(\boldsymbol{q})\Gamma_i(\boldsymbol{q}) \end{pmatrix}^T \begin{pmatrix} c^Q(k) & c^A(k) \\ c^R(k) & c^K(k) \end{pmatrix} \begin{pmatrix} DG^A(\boldsymbol{q})\Gamma_j(\boldsymbol{q}) \\ UG^A(\boldsymbol{q})\Gamma_j(\boldsymbol{q}) \end{pmatrix} \\
&+\frac{i\gamma_{l,2}}{4}\int d\boldsymbol{k} \begin{pmatrix} UG^R(\boldsymbol{q})\Gamma_i(\boldsymbol{q}) \\ DG^R(\boldsymbol{q})\Gamma_i(\boldsymbol{q}) \end{pmatrix}^T \sigma_3 \begin{pmatrix} DG^A(\boldsymbol{q})\Gamma_j(\boldsymbol{q}) \\ UG^A(\boldsymbol{q})\Gamma_j(\boldsymbol{q}) \end{pmatrix} \\
&-i\pi\gamma_{l,2}\int d\boldsymbol{k}\, \mathrm{Tr}\left[\begin{pmatrix} UG^R(\boldsymbol{q})\Gamma_i(\boldsymbol{q}) & DG^R(\boldsymbol{q})\Gamma_i(\boldsymbol{q}) \\ DG^R(\boldsymbol{q})\Gamma_i(\boldsymbol{q}) & -UG^R(\boldsymbol{q})\Gamma_i(\boldsymbol{q}) \end{pmatrix}\begin{pmatrix} DG^K(\boldsymbol{q})\Gamma_j(\boldsymbol{q}) & UG^A(\boldsymbol{q})\Gamma_j(\boldsymbol{q}) \\ UG^K(\boldsymbol{q})\Gamma_j(\boldsymbol{q}) & DG^A(\boldsymbol{q})\Gamma_j(\boldsymbol{q}) \end{pmatrix}\right]
\end{aligned}
\tag{13.1}
$$

$$
U = \begin{pmatrix} 1 \\ 0 \end{pmatrix}^T, \quad D = \begin{pmatrix} 0 \\ 1 \end{pmatrix}^T, \tag{13.2}
$$

$$
\Gamma_i(\boldsymbol{k}) = \begin{pmatrix} \psi_0\gamma_i(\boldsymbol{k}) \\ -\psi_0\gamma_i(\boldsymbol{k}) \end{pmatrix}^T, \quad \hat{\Gamma}_1 = \begin{pmatrix} i\gamma_{l,2}\psi_0 \\ i\gamma_{l,2}\psi_0 \end{pmatrix}^T, \quad \hat{\Gamma}_2 = \begin{pmatrix} -i\gamma_{l,2}\psi_0 \\ 0 \end{pmatrix}^T, \quad \hat{\Gamma}_3 = \begin{pmatrix} 0 \\ i\gamma_{l,2}\psi_0 \end{pmatrix}^T \tag{13.3}
$$

$$
a_i^A(\boldsymbol{k},\boldsymbol{k}') = \begin{pmatrix} \gamma_i(\boldsymbol{k}+\boldsymbol{k}') & 0 \\ 0 & \gamma_i(-\boldsymbol{k}-\boldsymbol{k}') \end{pmatrix} + \begin{pmatrix} \hat{\Gamma}_1 G^R\Gamma_i & \hat{\Gamma}_2 G^R\Gamma_i \\ \hat{\Gamma}_3 G^R\Gamma_i & -\hat{\Gamma}_1 G^R\Gamma_i \end{pmatrix}_{\boldsymbol{k}-\boldsymbol{k}'} \tag{13.4}
$$

$$
a_i^R(\boldsymbol{k},\boldsymbol{k}') = \begin{pmatrix} \gamma_i(\boldsymbol{k}+\boldsymbol{k}') & 0 \\ 0 & \gamma_i(-\boldsymbol{k}-\boldsymbol{k}') \end{pmatrix} + \begin{pmatrix} -\hat{\Gamma}_1 G^R\Gamma_i & \hat{\Gamma}_2 G^R\Gamma_i \\ \hat{\Gamma}_3 G^R\Gamma_i & \hat{\Gamma}_1 G^R\Gamma_i \end{pmatrix}_{\boldsymbol{k}-\boldsymbol{k}'} \tag{13.5}
$$

$$
a_i^K(\boldsymbol{k},\boldsymbol{k}') = \begin{pmatrix} -2\hat{\Gamma}_1 G^R\Gamma_i & 0 \\ 0 & -2\hat{\Gamma}_1 G^R\Gamma_i \end{pmatrix}_{\boldsymbol{k}-\boldsymbol{k}'} \tag{13.6}
$$

$$b_i^Q(\boldsymbol{k},\boldsymbol{k}') = \begin{pmatrix} \gamma_i(\boldsymbol{k}+\boldsymbol{k}') & 0 \\ 0 & \gamma_i(-\boldsymbol{k}-\boldsymbol{k}') \end{pmatrix} + \begin{pmatrix} \hat{\Gamma}_1\sigma_3 G^A\Gamma_i & -\hat{\Gamma}_2 G^A\Gamma_i \\ -\hat{\Gamma}_3 G^A\Gamma_i & \hat{\Gamma}_1\sigma_3 G^A\Gamma_i \end{pmatrix}_{\boldsymbol{k}-\boldsymbol{k}'} \tag{13.7}$$

$$\begin{pmatrix} c^Q(k) & c^A(k) \\ c^R(k) & c^K(k) \end{pmatrix} = \begin{pmatrix} G^K_{11}(k)+G^K_{22}(k) & -G^K_{21}(k) \\ G^K_{12}(k) & -G^K_{11}(k)-G^K_{22}(k) \end{pmatrix} \tag{13.8}$$

This expression may be compared with the diagrams in Figure 1 of [9] (also reprinted as Figure 11.4 of [11]). It is not hard to see that the class of diagrams stated there to be responsible for the normal fluid response corresponds to the first integral term in my expression

$$\begin{aligned} -\frac{i}{4}\int d\omega d\boldsymbol{k}\,\mathrm{Tr}\Big[\Big(&G^K(\omega,\boldsymbol{k}+\boldsymbol{q})a_i^A(\boldsymbol{k}+\boldsymbol{q},\boldsymbol{k})G^A(\omega,\boldsymbol{k}) \\ &+ G^R(\omega,\boldsymbol{k}+\boldsymbol{q})a_i^R(\boldsymbol{k}+\boldsymbol{q},\boldsymbol{k})G^K(\omega,\boldsymbol{k}) \\ &+ G^R(\omega,\boldsymbol{k}+\boldsymbol{q})a_i^K(\boldsymbol{k}+\boldsymbol{q},\boldsymbol{k})G^A(\omega,\boldsymbol{k})\Big)b_j^Q(\boldsymbol{k},\boldsymbol{k}+\boldsymbol{q})\Big], \end{aligned} \tag{13.9}$$

and it is thus this term that should be studied to see if there is a fluctuation correction to the mean field pure superfluid response.

Before this can be done, however, a number of other difficulties must be addressed. Firstly, in its present form, (13.1) contains many terms that are divergent in the $|\boldsymbol{q}| \to 0$ limit. These are terms of the form

$$\frac{q_i q_j}{|\boldsymbol{q}|^n} \tag{13.10}$$

for $n > 2$, and must be shown to cancel if the fluctuation corrections to the response in this limit are to be well-defined. This cancellation occurs in [9], but expression (13.1) exhibits significant structural differences with the analogous one therein and so the result does not easily transfer.

Moreover, difficulties are present with the integrals involving $c^{Q/A/R/K}(k)$ and thus $G^K(k)$. Considering the integral

$$\int dk\, c^R(k), \tag{13.11}$$

performing the frequency integral first, and replacing $k_x^2 + k_y^2 \to r^2$, we are left with

$$\int dk\, c^R(k) = -\int dr\, r\left[\frac{\pi\delta_\gamma(2\delta_\gamma+\sigma_\gamma)}{2K^4 r^4} + O(r^{-2})\right]. \tag{13.12}$$

The right hand side is clearly divergent, and it thus appears that infrared sector of the model as written is not correct. It is possible that the culprits are the frequency-independent drive and dissipation terms, but I did not have time to explore this. Adding a frequency dependence to $\delta_\gamma(\omega)$ and $\sigma_\gamma(\omega)$ would not alter the final expression for the response tensor since it is written entirely in terms

of Green's functions, and would not affect any tadpole cancellations since those occur at $\omega = 0$. The only changes required would be to use the forms of the Green's functions prior to substituting $\gamma_{l,2}\psi_0^2 \to \delta_\gamma$ and instead use $\gamma_{l,2}\psi_0^2 \to \delta_\gamma(0)$ (or $\delta_\gamma(\omega_0)$ if using the non-frequency shifted quantity). More generally, it is possible that a derivation of the Keldysh action directly from a microscopic dye molecule and photon model such as those used in [14], [15] is required to identify the needed corrections to the minimal Lindbladian model I have used.

As such, while the bulk of the fluctuation calculation has been performed and an analytical expression for the current-current response tensor at this order has been derived, work remains to ensure that required cancellations of terms occur and that the model is well-behaved in the infrared sector. Until this is done, little can be said about the superfluid behaviour at this order.

Bibliography

[1] J. Klaers, J. Schmitt, F. Vewinger, and M. Weitz, "Bose-Einstein condensation of photons in an optical microcavity," *Nature*, vol. 468, pp. 545–548, 2010.

[2] J. Marelic and R. A. Nyman, "Experimental evidence for inhomogeneous pumping and energy-dependent effects in photon Bose-Einstein condensation," *Phys. Rev. A*, vol. 91, p. 033 813, 2015.

[3] R. Nyman and M. Szymańska, "Interactions in dye-microcavity photon condensates and the prospects for their observation," *Physical Review A*, vol. 89, no. 3, p. 033 844, 2014.

[4] D. Snoke and S. Girvin, "Dynamics of phase coherence onset in bose condensates of photons by incoherent phonon emission," *Journal of Low Temperature Physics*, vol. 171, pp. 1–12, 2013.

[5] R. A. Nyman and B. T. Walker, "Bose-einstein condensation of photons from the thermodynamic limit to small photon numbers," *Journal of Modern Optics*, vol. 65, no. 5-6, pp. 754–766, 2018.

[6] E. Stein, "Dimensional crossover and thermo-optic interaction in photon bose-einstein condensates," 2022.

[7] J. Keeling and N. G. Berloff, "Spontaneous rotating vortex lattices in a pumped decaying condensate," *Physical review letters*, vol. 100, no. 25, p. 250 401, 2008.

[8] L. Pitaevskii and S. Stringari, *Bose-Einstein condensation and superfluidity*. Oxford University Press, 2016, vol. 164.

[9] J. Keeling, "Superfluid density of an open dissipative condensate," *Phys. Rev. Lett.*, vol. 107, p. 080 402, 2011.

[10] L. M. Sieberer, M. Buchhold, and S. Diehl, "Keldysh field theory for driven open quantum systems," *Reports on Progress in Physics*, vol. 79, no. 9, p. 096 001, 2016.

[11] J. Keeling, L. M. Sieberer, E. Altman, L. Chen, S. Diehl, and J. Toner, "Superfluidity and phase correlations of driven dissipative condensates," in *Universal Themes of Bose-Einstein Condensation*, N. P. Proukakis, D. W. Snoke, and P. B. Littlewood, Eds., Cambridge: Cambridge University Press, 2017, p. 205.

[12] R. Juggins, J. Keeling, and M. Szymańska, "Coherently driven microcavity-polaritons and the question of superfluidity," *Nature communications*, vol. 9, no. 1, pp. 1–8, 2018.

[13] R. Juggins, "Superfluidity in coherently driven microcavity-polaritons," Ph.D. dissertation, UCL (University College London), 2019.

[14] V. N. Gladilin and M. Wouters, "Classical field model for arrays of photon condensates," *Physical Review A*, vol. 101, no. 4, p. 043 814, 2020.

[15] P. Kirton and J. Keeling, "Nonequilibrium model of photon condensation," *Physical review letters*, vol. 111, no. 10, p. 100 404, 2013.

Part II

Some Results on Path Integral Calculation of Lindbladian Spectra for the Study of Classical Metastability

Chapter 14

Introduction

The original motivation for the work presented in this part was the desire to study metastability in quantum mechanical Lindbladian systems via the Feynman-Vernon path integral. Due to difficulties encountered with the coherent state path integral, however, only very partial results in this direction were achieved, namely the construction of a suitably regularised path integral for Lindbladians[1] and a perturbation theory for the calculation of Lindbladian spectra. While the developed perturbative approach may be of some interest on its own, more broadly these results can be viewed as initial steps in the more ambitious general direction of the projects initial goal.

To set the scene, note that the real parts of a Lindbladian's eigenvalues are always non-positive [3]. This is, as was mentioned in Part Ib, the reason why evolving a system backwards in time with a Lindbladian is not a well-posed problem: the forward dynamics converge to a steady state, while the backward dynamics become extremely sensitive to initial conditions. For our purposes Lindbladian metastability will refer to the opening of a gap in its spectrum between the first n largest real part eigenvalue pairs and the rest of the spectrum such that $\mathrm{Re}\,\lambda_{n-1} \ll \mathrm{Re}\,\lambda_n$ (we take $\lambda_0 = 0$ as the steady state eigenvalue corresponding to right eigenvector ρ_{ss}) [4]. In this case any initial state ρ_{in} will decay on a timescale $(\mathrm{Re}\,\lambda_n)^{-1}$ to a state spanned by the first n eigenvectors[2] R_i:

$$\rho_{\mathrm{in}} \xrightarrow[t\sim(\mathrm{Re}\,\lambda_n)^{-1}]{} \rho_{ss} + \sum_{i=0}^{n} c_i R_i. \tag{14.1}$$

At the same time, on this time-scale there will be effectively no evolution in the subspace spanned by these eigenvectors so, denoting the projection operator onto

[1] Specifically the generalisation of the Klauder-Daubechies path integral [1], [2] from Hamiltonian to Lindbladian dynamics.

[2] We denote the right eigenvectors of the Lindbladian by R_i and the left by L_i.

this subspace by $\mathcal{P}_n$, we have approximately

$$\rho_{\text{in}} \xrightarrow[t\sim(\text{Re}\,\lambda_n)^{-1}]{} \mathcal{P}_n\rho_{\text{in}} \tag{14.2}$$

and the long-time evolution of the system is thus governed by effective dynamics in this subspace.

In the case of 'classical' metastability, the shape of this subspace (the 'metastable manifold' or MM) will be approximated by an n-vertex simplex, whose vertices are known as 'extreme metastable states' or 'eMS' [4]. These extremal states will be approximately disjoint, states in the MM will be representable as probability mixtures of them, and the effective dynamics in the MM will be approximated by classical stochastic transitions between them [5]. The system thus acts much like a classical system with disjoint basins of attraction and stochastic dynamics. A typical example is the bistability manifested by a driven-dissipative Kerr non-linearity $Va^\dagger a^\dagger aa$. We saw the field-theoretic version of this in Part Ia, where a mean-field bistability curve was identified: the states on the bistable section of the curve correspond to the two bounding eMSes of a two-dimensional simplex, and we may infer that the Lindbladian associated to that field theory has a gap between its first two eigenvalues and the rest of its spectrum in the bistable regime.

In the case of such classical metastability, it is meaningful to talk about 'switching rates' between the eMSes. There are at least two obvious ways to analytically study these in the Truncated Wigner approximation (see Part Ib): firstly, one could formulate a generalised Kramers problem for each eMS basin of attraction and solve it via the adjoint of the relevant Fokker-Planck operator [6]. Alternatively, it is possible to represent the stochastic dynamics as a path integral over the noise (much like we did in Part Ib) and calculate a probability per unit time to escape the basin by considering the most likely (optimal) escape trajectory (e.g. [7], [8]). From a numerical perspective, the problem is evidently susceptible to Monte Carlo simulation to simply observe the switching rates.

Without invoking the stochastic limit of the quantum process, one approach to calculating such rates would be to attempt to generalise the concept of an optimal escape trajectory to the original Feynman-Vernon path integral. Recall from Part Ib the expression (in this part we will be interested in quantum mechanics rather than quantum field theory, but the expression is still relevant up to the presence of the mode label $\boldsymbol{k}$)

$$\langle\psi^+_{\boldsymbol{k},\text{out}}|\rho_T|\psi^-_{\boldsymbol{k},\text{out}}\rangle = \int_{\substack{\psi^c_{\boldsymbol{k}}(-T)=\sqrt{2}\psi_{\boldsymbol{k},\text{in}}\\ \psi^q_{\boldsymbol{k}}(-T)=0}}^{\substack{\psi^c_{\boldsymbol{k}}(T)=\sqrt{2}\psi_{\boldsymbol{k},\text{out}}\\ \psi^q_{\boldsymbol{k}}(T)=0}} \mathcal{D}[\psi^c_{\boldsymbol{k},t},\bar{\psi}^c_{\boldsymbol{k},t},\psi^q_{\boldsymbol{k},t},\bar{\psi}^q_{\boldsymbol{k},t}]\, e^{S_{cq,T}[\psi^c_{\boldsymbol{k},t},\psi^q_{\boldsymbol{k},t}]}\langle\psi^+_{\boldsymbol{k},\text{in}}|\rho_{-T}|\psi^-_{\boldsymbol{k},\text{in}}\rangle. \tag{14.3}$$

Throughout Part I we have always integrated out $\psi_{\boldsymbol{k},\text{out}}$ as we were aiming to take the trace. If this is not done, however, we see that the Feynman-Vernon path integral gives the projection of some initial density matrix onto some pure state after the former has been evolved by the Lindbladian dynamics for time $2T$, giving something analogous to a transition probability. If an initial eMS and either a final eMS or some state on the boundary between them are in some sense well represented by coherent states (perhaps with ψ given by its mean-field value), the classical path with largest contribution to the steepest descent approximation of the path integral could act as an analogue of the stochastic optimal escape path. Some work by other members of my group has been in this direction [9].

In a sense, however, the application of path integral methods to Lindbladian metastability would be more interesting when it is not classical, if nothing else because of the abundance of stochastic methods already in existence for such problems. In this case the concept of a switching rate is not necessarily meaningful (one no longer has the eMS 'macro-states' to switch between and the effective dynamics in the MM may not be of a stochastic nature) so it is helpful to decompose them into the two more fundamental pieces of information contained in them. Specifically, switching rates give information both about the steady state and the rate at which dynamics in the MM converge to it, via the eigenvectors and eigenvalues respectively of their associated stochastic matrix. When these two aspects of the problem are no longer tied together by switching rates, it is valuable to consider them in isolation.

Focusing on the rates, these are given by the real parts of the eigenvalues lying below the gap (and thus associated with the eigenvectors spanning the MM). The primary way spectra of operators are studied via the path integral in quantum mechanics is by considering the spectral decomposition of the propagator associated to that operator[10], [11], since the latter is a natural object to calculate with the path integral and contains the relevant information. For a Euclidean path integral, for instance, the propagator for the Hamiltonian may be expanded as

$$\langle x'|e^{-\beta H}|x\rangle = \sum_n \langle x'|n\rangle e^{-\beta E_n}\langle n|x\rangle \tag{14.4}$$

and so encodes the entire spectrum. Indeed, if one is able to calculate the exact propagator for arbitrary initial and final states, information about all the eigenvectors of the Hamiltonian is also present in the decomposition, even if more difficult to extract analytically.

Outside of quadratic operators or those possessing some special symmetries, however, the exact propagator is typically not available. Some progress may be made via perturbation theory relative to a known simple propagator, but this will fail to pick up many interesting non-perturbative corrections such as the

eigenvalue splitting of the double well potential. One way to recover the latter, at least for the slowest decaying eigenvalues, is to consider 'instanton' paths in the long time limit. This term has, at this point, acquired a wide range of meanings: to be concrete, we are referring to classical paths (approximately, exactly in the $T \to \infty$ limit) connecting some preferred points in phase space that have finite action as $T \to \infty$. Such paths will yield the leading order contribution to the propagator in this limit and, by summing over such paths (for instance the gas of instantons and anti-instantons of the double well potential) it is possible to obtain corrections to the smallest real part eigenvalues (the corresponding terms in the propagator vanish last in the $T \to \infty$ limit) that would not have been picked up by perturbation theory.

My initial aim, then, was to investigate perturbative and instanton approaches to calculating at least the largest real part portions of Lindbladian spectra for the purpose of understanding the time-scales of the dynamics in the MM manifold. While I was somewhat successful in developing a perturbation theory for such spectra, as will be seen in the relevant Chap. 18 the appearance of the gap in the spectrum of the driven-dissipative Kerr oscillator in its bistable regime appears to be non-perturbative. Given this is one of the simplest models of bistability available, this suggests that the study of metastable spectra will often necessitate the calculation of non-perturbative corrections to capture the appearance of the gap. There does not appear be much existing work in this direction. An instanton calculation of a Lindbladian eigenvalue correction appeared in [12] for a system possessing high degrees of symmetry allowing the instantons to be found analytically, while [9] calculates instanton paths numerically for the Kerr oscillator but does not sum them into an eigenvalue correction. There thus appears room for further development of these methods.

Unfortunately, there appears to be some difficulties with the use of the coherent state path integral for the calculation of instantons. There are two main ways to interpret such integrals (what I will call the Berezin and Klauder-Daubechies formalisms, to be discussed in detail in the next chapter) and, while both agree on how to calculate the classical paths[3] and this appears generally well-known, the same is not true for the corrections from fluctuations around these paths. Indeed, the main work I am aware of that covers this calculation for the Berezin formalism is [16], appearing some twenty years after the results for classical paths, which I have not seen cited in any mainstream textbook, and which does not frame the calculation as that of a functional determinant[4]. The Klauder-Daubechies formalism disagrees with the foregoing and does reduce the calcu-

[3]Though they disagree on why they are calculated this way. [13], [14] are the relevant works for the Berezin formalism, while [15] covers the Klauder-Daubechies formalism.

[4]This complicates the analysis of zero modes, which we will see is crucial for instanton calculations.

lation to that of a functional determinant (albeit a very cumbersome one), but this prescription appears even less well known: the only literature reference I am aware of is Ref. [17], a masters thesis with three citations.

At the same time, the rigorous use of instantons requires the ability to calculate this contribution. The reason for this is that the differential operator will typically have a zero mode in the $T \to \infty$ limit which will contribute a factor of T to the fluctuation contribution. For the configuration space path integral a rule of thumb is that each path connecting to stationary points contributes a single factor of T [11], but it appears this need not always be true: while Ref. [9] obtain results following this rule (they consider the fluctuation contribution of such a path divided by T to be an 'escape attempt frequency'), Ref. [12] assigns a factor of T to paths connecting both two and four stationary points (the latter should have a factor of T^3 by the rule of thumb) and obtains correct results. Both works are unable to calculate the fluctuation contribution precisely, being forced to infer the factors of T by other means and then numerically fit.

The situation thus appears to be that the method of primary interest to us crucially relies on the ability to calculate and analyse the zero modes of fluctuation contributions, which is something uniquely difficult and not extensively studied for the coherent state path integral. Because of this unfortunate circumstance, prior to performing any calculations a significant portion of my time was diverted to reviewing the literature on the coherent state path integral, as a deep understanding of it appears crucial to making real progress: indeed, we shall see that there are many non-trivial aspects, with even the method of calculating classical paths being unusual[5]. The next chapter summarizes this exercise, providing much more detailed coverage of the nature of this integral than was given in Part I. In particular I compare the Berezin and Klauder-Daubechies approaches and attempt to emphasize some links between them.

In subsequent chapters I extend the Klauder-Daubechies formalism, originally formulated for Hamiltonian systems, to Lindbladian path integrals and use it to calculate an exact propagator for the coherent driven-dissipative harmonic oscillator. This is then used to formulate a perturbation theory for more complicated Lindbladian propagators and their associated spectra. Unfortunately, due to the aforementioned difficulties and the requirement of my time for other projects, I do not attempt any instanton calculations.

[5]It is possible that this is somehow responsible for the failure of the rule of thumb for T factors, but this is purely a hypothesis.

Chapter 15

The Coherent State Path Integral: A Phase-Space Path Integral with Holomorphic Polarization

As we have already covered the construction of this integral in Part Ia Chap. 3, it may seem odd to devote another chapter to it here. Unfortunately, the coherent path integral is a much more complicated object than our prior exposition made it seem. In so far as it is used as a convenient shorthand for perturbative calculations (the diagrammatics of Part I could have equally well been performed using canonical quantisation as in [18]) or as compact notation for its discrete form (correctly emphasized in [19] and responsible for the corrections to the G^K traces in [20] and our Part I) there is generally no issue. Attempting to treat it as a bona fide continuous-time path integral, however, will quickly run into problems if one is not careful. Since we are interested in calculating continuous-time classical paths and, equally importantly, fluctuations around these paths as functional determinants of continuous-time differential operators, it is important that we define the integral carefully.

A closely related issue is that there are now what appear to be two very different characterisations of the coherent state path integral in the literature. The one most frequently quoted in condensed matter (indeed the one our exposition in Part I essentially follows) is due to Berezin [13]: in this approach operators appear as their Wick symbols[1], the action is first-order in time derivatives, the paths entering the integral may be discontinuous, and in order to calculate (continuous) classical paths one typically has to deform the real contour of integration into the complex plane. If the reader was introduced to the coherent path integral via any of [10], [19], [22]–[29], this is the formalism they will have encountered.

Unfortunately this formalism appears not entirely mathematically rigorous

[1] The Wick symbol $Q_O(z)$ (also sometimes known as a Q-symbol or Q-function due to its connection to the Husimi Q Representation [21]) of an operator $\hat{O}$ is a function equal to its expectation in a coherent state: $Q_O(z) = \langle z|\hat{O}|z\rangle$.

upon closer inspection. I will go through the difficulties in some detail later when we examine the structure of phase-space path integrals and construct the alternative formalism, but will give here a brief summary. Firstly, that the underlying paths are discontinuous[2] is a significant obstacle. While most of the above cited works either omit this fact entirely or briefly mention that the paths are 'jagged' [27], this family of paths (which, to be precise, are the square integrable functions $L^2([0,T])$ on a finite time interval $[0,T]$) clearly cannot respect Dirichlet boundary conditions.

Next, the use of Wick symbols introduces an error into the action that it is commonly claimed (except, to its credit, in [10]) will vanish in the continuum limit: this is incorrect. This error would vanish if all the paths involved were continuous but, as they are not, it may not be rightfully discarded. This error term is, in fact, fundamental for understanding the correspondence of the coherent state path integral to operator ordering, as will be demonstrated later.

Lastly, that the action contains time derivatives only to first order means that the resulting differential operator together with the combined Dirichlet boundary conditions for both position and momentum at both ends of the interval is not elliptic [30]; there are twice the allowed number of boundary conditions for ellipticity. It is thus likely that its eigenfunctions fail to be complete, which brings into question the connection between its functional determinant and the sum over fluctuations around the classical trajectory. While there exist alternative boundary conditions that may be used to find classical paths[3] and of which there is the correct number for ellipticity, attempting to use them appears to give incorrect results.

I have seen no examples in this formalism of a sum over fluctuations being successfully performed by appealing to functional determinant of the continuous time differential operator. The results in [16] come closest in that they resemble the final expression one obtains from a functional determinant calculation of the above first order differential operator, but that is not how they are obtained (rather they are derived directly from the discrete representation of the action, allowing them to correctly incorporate the error term mentioned above) and it is not clear what boundary conditions would reproduce them[4]. More frequently the

[2]This is somewhat an abuse of notation. The argument by Berezin attempts to generalise a construction that demonstrates the concentration of a measure on a set to the setting of a phase-space path integral where no bona fide measure is available (the argument will be presented in Sec. 15.2). As such, while we will use this nomenclature, it is important to understand that this is a much weaker statement than the analogous one that the paths of a Euclidean configuration space path integral are Wiener.

[3]As we will see later, these are not the true boundary conditions of the path integral regardless but rather a convenient computational tool for classical paths specifically. As such, the functional determinant should really be restricted to the full Dirichlet boundary conditions.

[4]Per [30], the calculation of this functional determinant would also require a choice of 'ray of minimal growth' for the differential operator: these results resemble those one obtains for a specific such choice, but it is a mystery as to why this would be the correct one.

calculation is either avoided via other considerations (in the Keldysh formalism the relevant quantity can often be argued to be 1 as we did in Part Ia Chap. 3, in equilibrium it is divided out with the bubble diagrams in the partition function, while in toy quantum mechanical models the answer can be extrapolated from known results) or performed by returning to the discrete action and computing a matrix determinant. The latter approach is entirely justified, but untenable when one is dealing with a complicated classical path unless one switches to the approach of Ref. [16] and also calls into question the integral's claim of being continuous time. Incidentally, this is also the reason why the aforementioned error due to Wick symbols typically goes unnoticed — it appears in the functional determinant, which is never explicitly calculated in continuous time.

Overall, I will argue that the Berezin conception of the coherent state path integral is not entirely well defined mathematically, making it difficult to reason rigorously about. Nevertheless, convenient prescriptions exist for semiclassical calculations using it: [13], [14] and an interesting but non-standard approach by [31] for finding classical paths, and [16], resorting to the discrete form of the action, or finding a way to neglect them for the fluctuation corrections. When not dealing with instantons, therefore, it is a reliable computational workhorse, which likely explains its continued prevalence in the literature, particularly in the condensed matter community.

There is, however, another formalism due to Ingrid Daubechies and John Klauder [1], [2], [32], which was subsequently significantly extended by the latter [33]–[36]. While it appears to have generated some interest in those working on topological field theories [37], [38] (albeit for more exotic coherent states than the bosonic ones we will treat) and in the wider HEP community [39], [40], it does not seem to have been embraced by the condensed matter community. As a mathematical object, however, the Klauder-Daubechies (KD) path integral is much better controlled than the Berezin one: the integral is over continuous paths, the action is second-order in time and the use of operator P-symbols avoids the error term associated with Wick symbols.

Overall, however, the approach is more complicated: the path integral is defined by a limiting procedure of well-defined configuration space-like path integrals, which makes direct calculation using it difficult (though eminently possible: indeed, I will demonstrate two examples of an exact functional determinant calculation of fluctuation corrections using this approach). A useful application of this method outside of direct computation, however, is that it can be used to rigorously justify some of the computationally convenient but ad-hoc prescriptions of the Berezin approach, such as the way classical paths are calculated. If one is able to show that the latter are a simplification of a more laborious but rigorous KD calculation, this places them on a rigorous footing. With regards to

fluctuation corrections, a very desirable similar result would be the reframing of the calculation in Ref. [16] as a simplification of the much more involved functional derivative calculation prescribed by KD. Unfortunately, at present this is not available.

The most direct way to the KD path integral goes through the deep but rarely mentioned connection between the coherent state path integral and the more conventional 'phase space path integral' (which uses a very similar action but different boundary conditions): they correspond to different polarisations of the underlying phase space. Since the idea of polarization may not be familiar to a reader without prior interest in quantisation procedures, yet in some sense motivates the whole formalism, we will begin by describing its manifestation for the simple bosonic particles we will treat, before proceeding to show how it can be used to understand phase space path integrals. Thereafter we will be in a position to introduce and compare the Berezin and KD approaches.

15.1 Polarisations: Decomposing the Phase Space

This section is devoted to introducing the step of geometric quantisation known as selection of a polarisation. A much more detailed reference for this and other aspects of the geometric quantisation procedure may be found in Ref. [41] if required.

Consider the classical phase space Γ of a single particle in one dimension, corresponding simply to $\mathbb{R}^2$ endowed with the symplectic form $\omega = dx \wedge dp$. We know that the wave functions of our theory are $L^2(\mathbb{R})$ functions defined on position or momentum, represented by $\mathbb{R} \subset \mathbb{R}^2$, and so in some sense our phase space is larger than the space needed to define the Hilbert space of the theory: we can choose functions depending only on x to construct our position wave functions $\psi_{\text{pos}}(x,p) = \psi(x)$, and functions depending only on p to construct the momentum ones $\psi_{\text{mom}}(x,p) = \tilde{\psi}(p)$. This could also obviously be characterised as $\partial_p \psi_{\text{pos}}(x,p) = 0$, $\partial_x \psi_{\text{mom}}(x,p) = 0$.

That we must restrict our wave functions to a single coordinate is a consequence of the fact that the representation of the Heisenberg group $H_3(\mathbb{R})$ (the Lie algebra of which corresponds to our observables) on $L^2(\mathbb{R}^2)$ will fail to be irreducible, meaning that the Hilbert space $L^2(\mathbb{R}^2)$ contains a subspace already suitable for fully describing the system[5]. Fortunately, as seen above, this is easily achieved for $\mathbb{R}^2$ on account of its extreme simplicity as a phase space. Not only

[5]More precisely, the reducibility of the representation will imply the existence of a projection operator that commutes with any operator constructed from the Lie algebra of the group, which will generally be true of the Hamiltonian. This means that its eigenvalues are constant in time and, once measured, will yield a superselection rule that permits the restriction of the dynamics to the relevant eigenspace.

is it a cotangent bundle, but in fact may be viewed as a simple product of a base manifold $\mathbb{R}$ and its single cotangent space $T^*_x(\mathbb{R}) \cong \mathbb{R}$. When viewing a cotangent bundle as a phase space $\Gamma_{\mathcal{M}}$, the base manifold $\mathcal{M}$ is often associated with position while the cotangent spaces represent (local) momentum — this trivial decomposition of $\mathbb{R}^2$ into a product is what allows the global decoupling of position and momentum that we are accustomed to.

Things become rather more difficult when one attempts to define a position-space wave function on something as seemingly simple as a 2-sphere $\Gamma = S^2$. S^2 is the classical phase space of a spin degree of freedom[6] with associated Lie group SU(2) and admits an exact deformation quantisation (as we will see in Part III), so ought to be quantizable. Because it is not a cotangent bundle[7], however, it does not admit an obvious decomposition into a position space and associated momentum cotangent spaces. Yet this decomposition is needed if we are to achieve an irreducible representation of SU(2) (we will not go further into this as the geometric quantisation of S^2 is too involved to justify the detour — the reader is directed to Ref. [43]). The concept of polarisation arose as a way to 'carve up' such unwieldy manifolds into spaces that can be understood as position and momentum.

We will present a very simplified view of polarisation that captures its core intuition and is sufficient for what we intend to discuss on $\Gamma = \mathbb{R}^2$. To this end we will introduce the intuitive concept of a real polarisation, ignoring considerations such as integrability conditions, before making a somewhat unjustified jump to the holomorphic polarisation. It will be seen, however, that the holomorphic polarisation gives reasonable results.

To begin, let us suppose that our manifold $\Gamma \ni q$ is $2n$-dimensional, real, and symplectic. We are thus equipped with a symplectic form ω_q and $T_q(\Gamma) \cong \mathbb{R}^{2n}$. Thinking back to the case of $\Gamma = \mathbb{R}^2$, we recall that a wave function being a function of position was equivalent to the condition $\partial_p \psi(x,p) = 0$. From a geometrically local point of view at point q this means that it is annihilated by the tangent vector $\partial_p \in T_q(\mathbb{R}^2)$ while from a global one it is constant on the streamlines of the associated vector field. The same reasoning can be applied to wave functions depending on momentum, now with vector field ∂_x. Note also that the restriction of the symplectic form $dx \wedge dp$ to a streamline of either vector field gives zero.

The generalisation of the concept of position that we may lift from the above considerations then goes as follows. Select a subbundle V of the tangent bun-

[6] This can be understood via the orbit method as the co-adjoint orbits of SU(2) being either a point (too small for a phase space) or 2-spheres. Alternatively, via the orbit-stabilizer theorem, one obtains S^2 as the quotient of SU(2) by the stabilizer $U(1)$ of its co-adjoint action: $S^2 = \mathrm{SU}(2)/U(1)$ (there are elements of the dual of the Lie algebra for which the stabilizer will be SU(2) and yield a point, which we again ignore).

[7] This may be seen directly from the fact that S^2 is compact, cotangent spaces are non-compact, and no fibre bundle with non-compact fibres may compact [42]

dle $T(\Gamma)$ such that the associated vector spaces are half the dimension of the original bundle's and the restriction of the symplectic form to this subbundle vanishes. This amounts to locally choosing n momentum directions (with the n position directions corresponding to the complement of the subbundle) — the vanishing of the symplectic form ensures we have correctly separated position and momentum rather than mixing them together. Under suitable conditions [41] there will exist a family of integral manifolds of V, namely submanifolds (which we can imagine are indexed by an n-dimensional index x) $\mathcal{X}_x \subset \Gamma$ such that $\forall q \in \mathcal{X}_x$, $T_q(\mathcal{X}_x) = V_q$, that foliate the original manifold Γ[8]. Now if we select wave functions $\psi(q \in \Gamma)$ such that $V\psi = 0$, these functions will be constant on the submanifolds $\mathcal{X}_x$ and thus essentially functions of their labels: $\psi(q) = \psi(x)$. These are the position space wave functions of the theory, and repeating the construction with the complement of the subbundle will yield the momentum space ones.

The procedure described above is the construction of a real polarisation. Unfortunately this fails on the aforementioned S^2 because on a two-dimensional surface the selection of the subbundle amounts to choosing a nowhere-vanishing vector field. By the hairy ball theorem these do not exist on S^2 and so the procedure fails. Thus, when constructing a general polarisation, one uses the complexification of the tangent bundle $T(\Gamma)$ in the above. This loses a good deal of the physical intuition of real polarisations but nevertheless successfully generalises the construction and, as we are about to see, gives a familiar construction on $\mathbb{R}^2$.

15.1.1 Position, Momentum, and Bargmann-Segal Spaces

Let us rewrite the symplectic form on $\mathbb{R}^2$ as $\frac{i}{2} dz \wedge d\bar{z}$ with $z = x + ip$. Following the procedure of the previous section we can choose the following polarisation:

$$\partial_{\bar{z}} \psi = 0. \tag{15.1}$$

Evidently this selects the family holomorphic functions on $\mathbb{R}^2 \cong \mathbb{C}$, and is thus known as the holomorphic polarisation.

Unfortunately this is not quite the Hilbert space we are actually after — there are more steps to geometric quantisation, which in its whole runs roughly in three stages

$$\text{Prequantisation} \to \text{Polarisation} \to \text{Quantization}. \tag{15.2}$$

We have entirely ignored prequantisation since it is not central to the presentation, but now hit an obstacle in the quantisation stage. Recall that our concept of

[8] These submanifolds will also possess the property that the symplectic form vanishes on them and that they are of maximum dimension for this property. This makes them Lagrangian submanifolds, which is a key definition for the general definition of polarisation.

a real polarisation suggests a possible choice of position space wavefunctions via

$$\partial_p \psi(x,p) = 0. \tag{15.3}$$

The problem is that these functions will evidently not be in $L^2(\mathbb{R}^2)$, whereas the point was to cut down that Hilbert space to a sufficiently small subspace. Machinery to deal with this during the quantisation stage for general manifolds is available [41], but on flat phase spaces we know from basic quantum mechanics that it is sufficient to forget about L^2 integrability on the full phase space $\mathbb{R}^2$ and instead take $L^2(\mathbb{R})$ (this is a special case of a convenient metric existing on the space of leaves of the polarisation foliation). Unfortunately there is no equally obvious trick for the holomorphic polarisation, and some work is required: we will skip all of it and present the conclusion. The Hilbert space constructed during quantisation from the holomorphic polarisation on $\mathbb{R}^2$ is the Bargmann-Segal space $\mathcal{F}(\mathbb{C})$ of holomorphic functions square integrable with respect to a Gaussian measure:

$$\partial_{\bar{z}} \psi = 0, \tag{15.4}$$

$$\int dz d\bar{z} |\psi|^2 e^{-|z|^2} < \infty. \tag{15.5}$$

There are thus at least three possible polarisations of the phase space of a bosonic particle:

$$\text{Position:} \quad \partial_p \psi(x,p) = 0 \to \psi(x), \tag{15.6}$$

$$\text{Momentum:} \quad \partial_x \psi(x,p) = 0 \to \tilde{\psi}(p), \tag{15.7}$$

$$\text{Holomorphic:} \quad \partial_{\bar{z}} \psi(z,\bar{z}) = 0 \to \psi(z), \tag{15.8}$$

with each constructing a different Hilbert space. By the Stone–von Neumann theorem [44] the representations of the Heisenberg group acting on them will be unitarily equivalent and thus essentially the same, so we need not worry about obtaining the 'wrong' irreducible representation (this is in contrast to the situation on S^2, where one obtains different representations for different spin numbers). Nevertheless the constructions lead to different Hilbert spaces, and thus in order to quantize $\mathbb{R}^2$ (or any other manifold) one must first select a polarisation.

Looking ahead, we will find that each of these polarisations corresponds to a different phase space path integral. Moreover, while the conventional phase space path integrals (those that propagate position and momentum wave functions) restrict the Hilbert space they act on to the right one for their given polarisation via boundary conditions (and an implicit choice of family of trajectories), the Berezin formulation of the coherent state path integral (which we argue corresponds to the holomorphic polarisation) fails to do so. It is in repairing this

failure to select a polarisation that most of the ills of the coherent state path integral are cured.

15.1.2 Ladder of Coherent State Hilbert Spaces

Before moving on, we briefly demonstrate how a generalisation of coherent states can be used to decompose $L^2(\mathbb{R}^2)$ into a countable set of copies of the Bargmann-Segal space. Repairing the coherent state path integral requires a way to restrict it to acting on only a single one of these copies.

As we recall from Part Ia Sec. 3.1.1, a coherent state in a Hilbert space (which for simplicity we will take to be the position space $L^2(\mathbb{R})$) may be written as

$$|\alpha\rangle = e^{\alpha\hat{a}^\dagger} e^{-\frac{1}{2}|\alpha|^2}|0\rangle \tag{15.9}$$

with $|0\rangle$ the harmonic oscillator ground state. Thinking in terms of the more familiar real variables x and p this may be rewritten as (we will use hats to denote operators in this section, as it is easier to get operators and numbers confused than usual)

$$\begin{aligned}|\alpha\rangle &= e^{\alpha\hat{a}^\dagger} e^{-\frac{1}{2}|\alpha|^2}|0\rangle = e^{\alpha\hat{a}^\dagger} e^{\bar{\alpha}\hat{a}} e^{-\frac{1}{2}|\alpha|^2}|0\rangle = e^{\alpha\hat{a}^\dagger - \bar{\alpha}\hat{a}}|0\rangle \\ &= e^{\frac{\alpha-\bar{\alpha}}{\sqrt{2}}\hat{x} - i\frac{\alpha+\bar{\alpha}}{\sqrt{2}}\hat{p}}|0\rangle = e^{i(p\hat{x}-x\hat{p})}|0\rangle = e^{ip\hat{x}} e^{-ix\hat{p}} e^{-\frac{i}{2}xp}|0\rangle = |x,p\rangle.\end{aligned} \tag{15.10}$$

The object $E(x,p) = e^{i(p\hat{x}-x\hat{p})}$ (or equivalently $e^{\alpha\hat{a}^\dagger - \bar{\alpha}\hat{a}}$) is an element of the irreducible representation of the Heisenberg Lie group [44], with the properties [45]

$$\begin{aligned}E(x,p)E^\dagger(x',p') &= e^{ip\hat{x}} e^{-i(x-x')\hat{p}} e^{-ip'\hat{x}} e^{-\frac{i}{2}(xp-x'p')} \\ &= e^{i(p-p')\hat{x}} e^{-i(x-x')\hat{p}} e^{i(x-x')p' - \frac{i}{2}(xp-x'p')} \\ &= E(x-x',p-p') e^{\frac{i}{2}(x-x')(p-p') + i(x-x')p' - \frac{i}{2}(xp-x'p')} \\ &= E(x-x',p-p') e^{\frac{i}{2}(xp'-px')},\end{aligned} \tag{15.11}$$

$$\begin{aligned}\operatorname{Tr} E(x,p) &= \sum_n \langle n|E(x,p)|n\rangle \\ &= \sum_n \int dy \left[\bar{\psi}_n(y) e^{\frac{i}{2}p\hat{x}} e^{-ix\hat{p}} e^{\frac{i}{2}p\hat{x}} \psi_n(y)\right] \\ &= \sum_n \int dy \left[\bar{\psi}_n(y) e^{\frac{i}{2}py} e^{-x\partial_y} e^{\frac{i}{2}py} \psi_n(y)\right] \\ &= \sum_n \int dy \left[\bar{\psi}_n(y) e^{\frac{i}{2}py} e^{\frac{i}{2}p(y-x)} \psi_n(y-x)\right] \\ &= \int du\, e^{ipu} \sum_n \left[\bar{\psi}_n(u+\frac{x}{2}) \psi_n(u-\frac{x}{2})\right] \\ &= 2\pi\delta(p)\delta(x)\end{aligned} \tag{15.12}$$

where in the last line we have used the completeness of the states $|n\rangle$ we used to take the trace and thus of their $L^2(\mathbb{R})$ representations $\psi_n(x) = \langle x|n\rangle$. We will make use of these presently.

First, we notice that the coherent states furnish a mapping from our Hilbert space $\mathcal{H}$ into $L^2(\mathbb{R}^2)$:

$$\forall|\psi\rangle \in \mathcal{H}.\, f_\psi(x,p) = \langle\psi|x,p\rangle = \langle\psi|\alpha\rangle = f_\psi(\alpha), \tag{15.13}$$

$$\int dxdp\, \bar{f}_\psi(x,p) f_\psi(x,p) = \int dxdp\, \langle\psi|x,p\rangle\langle x,p|\psi\rangle = \langle\psi|\psi\rangle < \infty. \tag{15.14}$$

where we have used the real form of the completeness relation for coherent states and that our original $|\psi\rangle \in \mathcal{H}$ had finite norm in $\mathcal{H}$. At the same time, if we split $E(x,p)$ into $e^{\alpha\hat{a}^\dagger} e^{\bar{\alpha}\hat{a}}$ and $e^{-\frac{1}{2}|\alpha|^2}$, we find that

$$\partial_{\bar{\alpha}} \langle\psi|e^{\alpha\hat{a}^\dagger} e^{\bar{\alpha}\hat{a}}|0\rangle = \langle\psi|e^{\alpha\hat{a}^\dagger} e^{\bar{\alpha}\hat{a}}\hat{a}|0\rangle = 0. \tag{15.15}$$

This means that $f_\psi(\alpha)$ is the product of a holomorphic function $h(\alpha)$ and a Gaussian weight $e^{-|\alpha|^2}$ or, equivalently, that our coherent state mapping sends elements of $\mathcal{H}$ to holomorphic functions that are square-integrable with Gaussian measure $e^{-|\alpha|^2} d\alpha d\bar{\alpha}$. But this is precisely the Bargmann-Segal space of the previous section, and the mapping we have found is the unitary equivalence between irreducible representations of the Heisenberg group guaranteed by the Stone–von Neumann theorem (this is known as the Bargmann-Segal transform) [43]. We have thus succeeded in embedding an equivalent copy of our Hilbert space into $L^2(\mathbb{R}^2)$.

At the same time, we are far from exhausting the 'capacity' of $L^2(\mathbb{R}^2)$. While the coherent states are usually defined with respect to the ground state of the harmonic oscillator, this is not mandatory [46]. In fact, labelling the complete set of eigenstates of the harmonic oscillator by $|n\rangle$, we can define generalised coherent states (sometimes known as 'displaced number states')

$$|x,p,n\rangle = E(x,p)|n\rangle \tag{15.16}$$

which also possess a completeness relation[9] [2]

$$\int dxdp\, |x,p,n\rangle\langle x,p,m| = \delta_{m,n} I. \tag{15.17}$$

Moreover, these states provide variations of the Bargmann-Segal transform for

[9] For a finite-dimensional Hilbert space and Lie group with finite Haar volume, an identity of this form is easily proven by arguing that the left hand side is an intertwiner for an irreducible representation of the group and thus proportional to the identity, with the proportionality constant found by taking the trace. In this case the proof is more difficult: the identity can be seen to be a consequence of equation (4.6) in Ref. [47], which is proven in Appendix 2 of that work.

each eigenstate

$$f_{\psi,n}(x,p) = \langle \psi | x,p,n \rangle \tag{15.18}$$

with mutually orthogonal ranges $\mathcal{F}_n(\mathbb{C})$:

$$f_{\psi,n} \in \mathcal{F}_n(\mathbb{C}),\ f_{\phi,m} \in \mathcal{F}_m(\mathbb{C}),\ m \neq n, \tag{15.19}$$

$$\int dxdp\, \bar{f}_{\psi,n}(x,p) f_{\phi,m}(x,p) = \int dxdp\, \langle \phi | x,p,m \rangle \langle x,p,n | \psi \rangle = \delta_{m,n} \langle \phi | \psi \rangle = 0. \tag{15.20}$$

Each of the resulting copies $\mathcal{F}_n(\mathbb{C})$ of the Bargmann-Segal space can be viewed as the closure of the span of the mapped states $|n\rangle$:

$$\mathcal{F}_n(\mathbb{C}) = \overline{\text{span}\{\langle m|x,p,n\rangle \,|\, m \in \mathbb{N}_0\}}. \tag{15.21}$$

At the same time, the total set of functions $\{\langle m|x,p,n\rangle \,|\, m \in \mathbb{N}_0,\ n \in \mathbb{N}_0\}$ forms an overcomplete basis for $L^2(\mathbb{R}^2)$:

$$\begin{aligned} \sum_{n,m} \langle x,p,n|m\rangle\langle m|x',p',n\rangle &= \sum_n \langle x,p,n|x',p',n\rangle \\ &= \sum_n \langle n|E^\dagger(x,p)E(x',p')|n\rangle \\ &= e^{\frac{i}{2}(x'p-p'x)} \operatorname{Tr} E(x'-x,p'-p) \\ &= 2\pi\delta(x-x')\delta(p-p'). \end{aligned} \tag{15.22}$$

Thus

$$\bigoplus_{n\in\mathbb{N}_0} \mathcal{F}_n(\mathbb{C}) = L^2(\mathbb{R}^2) \tag{15.23}$$

and $L^2(\mathbb{R}^2)$ will carry a reducible representation of the Heisenberg group[10] that decomposes as a direct sum of irreducible ones on the spaces $\mathcal{F}_n(\mathbb{C})$.

When constructing a coherent path integral using some family of states $|x,p,n\rangle$ (we will generally use $n = 0$, namely the typical coherent states), we will thus require some way to encode the restriction to the appropriate subspace $\mathcal{F}_n(\mathbb{C})$ into it. In the next section we shall see how Berezin [13] suggested that real polarisations could be encoded into the conventional phase space path integral[11]. I will then argue that his extension of that procedure to the coherent state path integral is incorrect, and present the alternative approach of Daubechies and Klauder to encoding the holomorphic polarisation explicitly [1], [2].

[10] Here we are referring to $H_3(\mathbb{R})$, the three dimensional Heisenberg group over the reals that is appropriate for a one dimensional particle. Since $\mathbb{R}^2$ is the configuration space of a two dimensional particle, there will evidently be an irreducible representation of $H_5(\mathbb{R})$ on $L^2(\mathbb{R}^2)$, but that is not the Heisenberg group we are after.

[11] Berezin does not use the language of polarisations, but it will fairly clear that this is what his procedure indirectly accomplishes.

15.2 Phase Space Path Integrals

We begin by writing down the prototypical action for a phase-space path integral ($\psi = \frac{1}{\sqrt{2}}(x + ip)$):

$$S_p = \int [pdx - H(x,p)dt] = \int [-xdp - H(x,p)dt] = \int \left[i\bar{\psi}\partial_t\psi - H(\psi,\bar{\psi})\right]dt. \tag{15.24}$$

The first form is typically used for phase space path integrals with fixed initial and final particle positions, which in the case of a Hamiltonian quadratic in momentum can be reduced down to the conventional configuration space path integral and are perhaps the most familiar type. The second may be taken to describe phase space path integrals with fixed initial and final momenta, while the third is usually used for coherent state path integrals. Up to integration by parts, however, all three forms of the action are equivalent and thus the three types of integrals must have other distinguishing features. Importantly, the components required to construct these actions are the tautological one-form pdx and the Hamiltonian, both of which are just classical objects associated with the appropriate symplectic manifold. This action alone, thus, contains no information about polarisation.

The first two types of integral are fairly clearly delineated by their boundary conditions. Position boundary conditions mark the integral out as acting on position space wavefunctions and corresponding to the real position polarisation, while momentum ones analogously correspond to the momentum polarisation. This simplicity again owes itself to the trivial nature of $\mathbb{R}^2$ as a phase space. Nevertheless, even in this simple case, the different boundary conditions are not enough. Berezin argued that the two integrals should be taken over trajectories belonging to different function families, so that polarisation is encoded in the path integral as a combination of boundary conditions and an associated set of trajectories.

The problem with the coherent state path integral is that, to be meaningful, it must possess both position and momentum boundary conditions, something which runs into direct conflict with the acceptable sets of trajectories identified by Berezin. At the same time, while it is easy to restrict a boundary condition to a position or momentum polarisation by fixing only the appropriate variable, there is no obvious way to encode the holomorphic polarisation in this way. To enforce this polarisation, therefore, one is forced to explicitly build projection onto it into the path integral. This proves to modify the action, which in turn significantly changes the acceptable set of trajectories relative to Berezin's suggestion.

Below, I first present Berezin's argument for the correct set of paths of a phase space path integral: this argument covers all three types of integral and may

thus be presented in one go. Following a discussion of how the resulting paths plausibly encode the two real polarisations, I then argue that they are unsuitable for the holomorphic one and discuss some other difficulties associated with the conventional form of the action, namely the lack of clarity with regards to the boundary conditions and other aspects of the associated differential operator. This then motivates the construction of the coherent path integral as one explicitly corresponding to the holomorphic polarisation, greatly improving the properties of the associated paths and modifying the action to contain a more amenable differential operator. With all this material presented, the next chapter is then devoted to my extension of the Klauder-Daubechies path integral to a path integral for Lindbladian evolution, which is my original contribution to the theory of coherent state path integrals.

15.3 Berezin Approach

Berezin's approach to understanding phase space path integrals relies on assuming there exists something akin to a measure, what we will call the symplectic pseudomeasure, on the space of paths over which the integral is to be performed. Choosing some property he wishes the paths to have, he then demonstrates that this property holds on a set of pseudomeasure equal to the pseudomeasure of the total space of paths, and refers to this as the integral being concentrated on this set. In the absence of a true measure this approach is not entirely legitimate but nevertheless provides some interesting insights and contradictions, so is worth reviewing. At the same time the thrust of the argument may be unclear if the reader has not seen a similar approach before. Thus, before tackling Berezin's calculation, I will very briefly present Coleman's classic argument [11] about the measure of paths of finite action which has precisely this structure.

15.3.1 Finite Action is Zero Measure

Consider a Euclidean path integral on a time interval $[0, T]$ with action

$$S[x(t)] = \int_0^T dt \left[\frac{1}{2} \left(\frac{dx(t)}{dt} \right)^2 + V[x(t)] \right]. \tag{15.25}$$

and boundary conditions $x(0) = x(T) = 0$. Coleman asks the question whether the most important paths for this path integral are those on which this action is finite or positive infinite (since we assume $V[x(t)]$ bounded from below). At first glance, given the integral is usually written as

$$\int \mathcal{D}x(t)\, e^{-S[x(t)]}, \tag{15.26}$$

it may appear obvious that any path for which the action is infinite will zero out the integrand and have no contribution to the path integral.

The problem with this argument is that $\mathcal{D}x(t)$ is not a measure: there is no non–trivial Lebesgue measure on an infinite dimensional vector space [48], [49]. What may be regarded as a measure is rather the combination

$$\mu_W = \mathcal{D}x(t) e^{-\int_0^T dt \, \frac{1}{2}\left(\frac{dx(t)}{dt}\right)^2} \tag{15.27}$$

which yields the Wiener measure on continuous paths (essentially the probability distribution of Brownian motion trajectories). Writing $x(t)$ as a sine series[12]

$$x(t) = \sqrt{2T} \sum_{n=1}^{\infty} \frac{X_n}{\pi n} \sin\left(\frac{\pi n t}{T}\right), \tag{15.28}$$

the above measure may be rewritten as[13]

$$\mu_W = \frac{1}{\sqrt{2\pi T}} \prod_{n=1}^{\infty} \int_{-\infty}^{\infty} dX_n \, \frac{1}{\sqrt{2\pi}} e^{-\frac{1}{2}\sum_{n=1}^{\infty} X_n^2}, \tag{15.29}$$

which is an infinite-dimensional Gaussian measure. Incidentally, this gives the almost surely uniformly convergent Fourier representation of a Wiener process [50], [51]

$$x(t) = \sqrt{2T} \sum_{n=1}^{\infty} \frac{X_n}{\pi n} \sin\left(\frac{\pi n t}{T}\right) \tag{15.30}$$

where all the X_n are independent and identically distributed (i.i.d.) $\mathcal{N}(0,1)$ random variables, though proving this rigorously requires more work.

With a convenient representation of the measure in hand, we may consider sets on which the original action is finite. The portion of the action corresponding to $V[x(t)]$ will be finite for any continuous $x(t)$ as long as $V[x(t)]$ is itself a continuous function of $x(t)$, so we may restrict our attention to the kinetic energy term. Using our Fourier representation this is simply

$$\int_0^T dt \, \frac{1}{2}\left(\frac{dx(t)}{dt}\right)^2 = \frac{1}{2}\sum_{n=1}^{\infty} X_n^2, \tag{15.31}$$

so for this to be finite the terms of the series must at a minimum be bounded: $\exists C. \forall n. X_n < C$. We may thus consider an increasing sequence of sets such that

[12] For simplicity we will consider a Wiener process pinned to $x(T) = 0$ at the terminal time, also known as a Brownian bridge. Because of this the term $\frac{X_0}{\sqrt{T}} t$ that would otherwise be present in the below equation is absent.

[13] The extra factor in the front matches the total measure of the space to the correct result for the Wick-rotated free particle propagator. The total measure of the space is thus not 1 like it would be in probability.

any trajectory with finite action must be in one of these sets:

$$A_k = \{x(t) | \forall n. X_n < k\}, \quad k \in \mathbb{N}, \tag{15.32}$$

$$A_k \subset A_{k+1}, \tag{15.33}$$

$$x_{\text{finite } S}(t) \in \bigcup_{k \in \mathbb{N}} A_k. \tag{15.34}$$

At the same time, the measure of each of these sets is zero:

$$\mu_W(A_k) = \frac{1}{\sqrt{2\pi T}} \prod_{n=1}^{\infty} \int_{-k}^{k} dX_n \, e^{-\frac{1}{2}\sum_{n=1}^{\infty} X_n^2} = \frac{1}{\sqrt{2\pi T}} \prod_{n=1}^{\infty} \operatorname{erf} \frac{k}{\sqrt{2}} = 0 \tag{15.35}$$

since $\operatorname{erf} \frac{k}{\sqrt{2}} < 1$ for $k \in \mathbb{N}$. Thus, because measures are continuous from below,

$$\mu_W \left(\bigcup_{k \in \mathbb{N}} A_k \right) = \lim_{k \to \infty} \mu_W(A_k) = 0, \tag{15.36}$$

and we have that the measure of the set of paths with finite action is zero. This is of course not a problem because in this form of the integral the integrand no longer contains the full action, but only the potential term:

$$\int \mathcal{D}x(t) \, e^{-S[x(t)]} = \int d\mu_W \, e^{-V[x(t)]} \tag{15.37}$$

and the latter is finite on all the Wiener paths. This result amounts to the fact that Wiener processes are almost surely nowhere differentiable, which is why the kinetic part of the action with derivatives diverges almost surely, and also points to the rightful place of that kinetic term as a component of the measure rather than as part of the integrand.

15.3.2 Space of Paths for the Symplectic Pseudomeasure

Having seen how one may study the space of paths of a configuration space path integral via Fourier analysis, we may now tackle Berezin's analogous argument for the phase space ones [13]. The first immediate difference is that such integrals do not contain a kinetic action term and thus no Wiener measure is immediately available. The closest term available, the one analogously corresponding to the kinematics rather than the dynamics of the problem, is the symplectic term pdx. This does not, however, yield a bona fide measure in the way that the configuration kinetic term did; indeed, to pass from the phase space path integral to the configuration one, one also requires a term quadratic in momentum in the Hamiltonian. Nevertheless, we are about to see that the structure of the above argument (if not entirely the meaning) may be carried through in just the same way

while replacing the measure μ_W with the symplectic pseudomeasure (invariant under Wick rotation)

$$\mathcal{D}x(t)\mathcal{D}p(t)e^{i\int pdx}. \tag{15.38}$$

Representing the trajectories $x(t)$, $p(t)$ by complex Fourier series[14] (no boundary conditions are being applied, unlike in the Coleman argument)

$$x(t) = \sum_{n=-\infty}^{\infty} \beta_{2n+1} e^{(2n+1)\frac{i\pi}{T}t}, \tag{15.39}$$

$$p(t) = \sum_{n=-\infty}^{\infty} \alpha_{2n+1} e^{(2n+1)\frac{i\pi}{T}t}, \tag{15.40}$$

the symplectic pseudomeasure takes the form $\mu_p(\infty)$, where[15]

$$\mu_p(N) = d[\boldsymbol{\alpha}, \bar{\boldsymbol{\alpha}}]d[\boldsymbol{\beta}, \bar{\boldsymbol{\beta}}] \exp\left[-\frac{\pi}{2}\sum_{|n|=0}^{N}(2n+1)(\bar{\alpha}_{2n+1}\beta_{2n+1} - \bar{\beta}_{2n+1}\alpha_{2n+1})\right]. \tag{15.41}$$

Here $\mu_p(N)$ may be interpreted as the restriction[16] of the pseudomeasure to the set of functions in a Fourier subspace. These sets are increasing with N so, if we assume the pseudomeasure behaves like a true measure and because Lebesgue integrals are continuous from below in their domain, we have

$$\lim_{N\to\infty}\int d\mu_p(N)\circ = \int d\mu_p(\infty)\circ. \tag{15.42}$$

with $\circ$ a placeholder for some function.

Berezin considers trajectories with finite weighted norm in Fourier space:

$$\sqrt{\sum_{n=-\infty}^{\infty}[\sigma(2n+1)|\alpha_{2n+1}|^2 + \tau(2n+1)|\beta_{2n+1}|^2]}. \tag{15.43}$$

Varying the weights $\sigma(n)$, $\tau(n)$ changes the decay rates required of the Fourier coefficients α_{2n+1}, β_{2n+1} to maintain the finiteness of this norm and thus the smoothness conditions of the associated functions. To this end, define the func-

[14] I denote Fourier coefficients consistently with Berezin, who has α and β this way round because he defines a vector $\boldsymbol{x} = (p, q)$ with momentum as the first variable. Berezin also argues earlier in the paper that the space of paths may be restricted to those with anti-periodic boundary values, an argument we will not consider but which explains the anti-periodic Fourier series used.

[15] $\boldsymbol{\alpha}$ and $\boldsymbol{\beta}$ are vectors of the Fourier coefficients, and the sum over $|n|$ includes both positive and negative n with $|n| \leq$ the upper bound.

[16] We take the measure to assign zero measure to the complement of the set to which it is restricted.

tion

$$J_N(r) = \int \mu_p(N) \int_{-r^2}^{r^2} ds\, \delta\left(s - \sum_{|n|=0}^{N} \left[\sigma(2n+1)|\alpha_{2n+1}|^2 + \tau(2n+1)|\beta_{2n+1}|^2 \right] \right), \quad (15.44)$$

This is the restricted pseudomeasure of the set of weighted norm $\leq r$. Then, removing the restriction by taking $N \to \infty$, Berezin tries to show that the pseudomeasure is concentrated on the union of these increasing sets for $r \to \infty$. The argument goes that this is so if

$$\lim_{r\to\infty} \frac{J_N(r)}{J_N(\infty)} = 1, \quad \lim_{r\to\infty} \lim_{N\to\infty} \frac{J_N(r)}{J_N(\infty)} = 1. \quad (15.45)$$

I will argue in a moment that this way of defining pseudomeasure concentration leads to some unintuitive properties, but for now we continue with Berezin's argument.

Evaluating $J_N(r)$ comes down to a sequence of Gaussian integrals:

$$\begin{aligned}
&J_N(r) \\
&= \int d[\boldsymbol{\alpha}, \bar{\boldsymbol{\alpha}}] d[\boldsymbol{\beta}, \bar{\boldsymbol{\beta}}] \int_{-r^2}^{r^2} ds \exp\left[-\frac{\pi}{2} \sum_{|n|=0}^{N} (2n+1)(\bar{\alpha}_{2n+1}\beta_{2n+1} - \bar{\beta}_{2n+1}\alpha_{2n+1}) \right] \\
&\qquad \cdot \delta\left(s - \sum_{|n|=0}^{N} \left[\sigma(2n+1)|\alpha_{2n+1}|^2 + \tau(2n+1)|\beta_{2n+1}|^2 \right] \right) \\
&= \int d[\boldsymbol{\alpha}, \bar{\boldsymbol{\alpha}}] d[\boldsymbol{\beta}, \bar{\boldsymbol{\beta}}] \int_{-r^2}^{r^2} ds \int \frac{dp}{2\pi} \exp\left[-\frac{\pi}{2} \sum_{|n|=0}^{N} (2n+1)(\bar{\alpha}_{2n+1}\beta_{2n+1} - \bar{\beta}_{2n+1}\alpha_{2n+1}) \right] \\
&\qquad \cdot \exp\left[ip \left(s - \sum_{|n|=0}^{N} \left[\sigma(2n+1)|\alpha_{2n+1}|^2 + \tau(2n+1)|\beta_{2n+1}|^2 \right] \right) \right] \\
&= \int d[\boldsymbol{\beta}, \bar{\boldsymbol{\beta}}] \int \frac{dp}{2\pi} \frac{e^{ipr^2} - e^{-ipr^2}}{ip} \\
&\qquad \cdot \exp\left[-\sum_{|n|=0}^{N} \left(ip\tau(2n+1) + \frac{(2n+1)^2\pi^2}{4ip\sigma(2n+1)} \right) |\beta_{2n+1}|^2 \right] \prod_{|n|=0}^{N} \frac{1}{ip\sigma(2n+1)} \\
&= \int \frac{dp}{2\pi} \frac{e^{ipr^2} - e^{-ipr^2}}{ip} \prod_{|n|=0}^{N} \frac{1}{\frac{(2n+1)^2\pi^2}{4ip\sigma(2n+1)} + ip\tau_{2n+1}} \frac{1}{ip\sigma(2n+1)} \\
&= \int \frac{dp}{\pi} \frac{\sin(pr^2)}{p} \left(\frac{4}{\pi^2} \right)^{2N+1} \frac{1}{((2N+1)!!)^4} \prod_{|n|=0}^{N} \frac{1}{1 - \frac{4p^2\sigma(2n+1)\tau(2n+1)}{(2n+1)^2\pi^2}}.
\end{aligned} \quad (15.46)$$

Since $\lim_{r\to 0}\frac{\sin(pr^2)}{p} = \pi\delta(p)$, we have

$$J_N(\infty) = \left(\frac{4}{\pi^2}\right)^{2N+1}\frac{1}{((2N+1)!!)^4} \tag{15.47}$$

and thus

$$\frac{J_N(r)}{J_N(\infty)} = \int\frac{dp}{\pi}\frac{\sin(pr^2)}{p}\prod_{|n|=0}^{N}\frac{1}{1-\frac{4p^2\sigma(2n+1)\tau(2n+1)}{(2n+1)^2\pi^2}}. \tag{15.48}$$

If the weights σ, τ are positive, which we will assume since we are not considering seminorms, then the product

$$F(p) = \prod_{|n|=0}^{\infty}\left(1-\frac{4p^2\sigma(2n+1)\tau(2n+1)}{(2n+1)^2\pi^2}\right) \tag{15.49}$$

is absolutely convergent iff

$$\sum_{|n|=0}^{\infty}\frac{4p^2\sigma(2n+1)\tau(2n+1)}{(2n+1)^2\pi^2} \tag{15.50}$$

converges [52]. Assuming this is the case, it is clear that $F(0) = 1$, and we find

$$\lim_{r\to\infty}\lim_{N\to\infty}\frac{J_N(r)}{J_N(\infty)} = \lim_{r\to\infty}\int\frac{dp}{\pi}\frac{\sin(pr^2)}{p}F^{-1}(p) = \int dp\,\delta(p)F^{-1}(p) = 1. \tag{15.51}$$

The question of whether the pseudomeasure is concentrated on a set of finite weighted norm thus reduces to whether the sum

$$\sum_{|n|=0}^{\infty}\frac{\sigma(2n+1)\tau(2n+1)}{(2n+1)^2} \tag{15.52}$$

converges for that norm's weights.

It is worth pausing here to consider a strange property of this procedure: take a norm for which the above limit is 1, so that the measure is considered concentrated on the union $\bigcup_{r\to\infty}V_r$ of sets V_r with that norm bounded by r. Now consider those same sets also projected onto the subspace of the first M Fourier modes, giving new sets $U_{r,M}$. Clearly $\bigcup_{r\to\infty}V_r = \bigcup_{r,M\to\infty}U_{r,M}$ so that the pseudomeasure should also be concentrated on the second union. If we construct a J for this second type of set, it is easy to see that $J_N(r,M) = J_M(r)$. But then

$$\lim_{N\to\infty}\frac{J_N(r,M)}{J_N(\infty)} = \lim_{N\to\infty}\frac{J_M(r)}{J_N(\infty)} = \infty, \tag{15.53}$$

so

$$\lim_{r\to\infty}\lim_{N\to\infty}\frac{J_N(r)}{J_N(\infty)} = 1, \quad \lim_{r,M\to\infty}\lim_{N\to\infty}\frac{J_N(r,M)}{J_N(\infty)} = \infty, \tag{15.54}$$

which suggests the procedure is dependent on how we choose the sets from which we construct the union. The infinities appear to be a consequence of the rather odd fact that the total mass of the pseudomeasure is zero:

$$\lim_{N\to\infty} J_N(\infty) = \lim_{N\to\infty} \left(\frac{4}{\pi^2}\right)^{2N+1} \frac{1}{((2N+1)!!)^4} = 0, \tag{15.55}$$

but were this mass infinite they would be replaced by zeroes and we would have the same difficulty. In general the limiting procedure presented here only works correctly for measures of finite positive mass, and thus its application to this pseudomeasure should not be trusted (setting aside that the pseudomeasure itself is not a well-behaved object).

Returning to the sum

$$\sum_{|n|=0}^{\infty} \frac{\sigma(2n+1)\tau(2n+1)}{(2n+1)^2} \tag{15.56}$$

consider the choices

1. $\sigma(2n+1) = (2n+1)^{1+\epsilon}, \quad \tau(2n+1) = (2n+1)^{-2\epsilon}$;
2. $\sigma(2n+1) = (2n+1)^{-2\epsilon}, \quad \tau(2n+1) = (2n+1)^{1+\epsilon}$;
3. $\sigma(2n+1) = (2n+1)^{(1-\epsilon)/2}, \quad \tau(2n+1) = (2n+1)^{(1-\epsilon)/2}$.

For the first, finite norm implies

$$|\alpha_{2n+1}| \in o((2n+1)^{-(2+\epsilon)/2}), \quad |\beta_{2n+1}| \in o((2n+1)^{-(1-2\epsilon)/2}). \tag{15.57}$$

This scaling of the Fourier coefficients implies that the momentum is continuous, while position is not necessarily in $L^2(\mathbb{R})$. The second choice gives the reverse of this, while the third symmetric choice gives

$$|\alpha_{2n+1}| \in o((2n+1)^{-(3-\epsilon)/4}), \quad |\beta_{2n+1}| \in o((2n+1)^{-(3-\epsilon)/4}). \tag{15.58}$$

which suggests both position and momentum are $L^2(\mathbb{R})$ but neither is necessarily continuous: indeed, there is no choice one can make that would make both continuous. This completes Berezin's analysis of the paths on which phase space path integrals are concentrated.

15.3.3 Boundary Conditions

Continuing to take the pseudomeasure result at face value, two of the permissible sets of paths are clearly suitable for two variants of the phase space path integral. Specifically, if one is considering the position space polarisation path integral,

it would be natural to take position as continuous since one could then impose Dirichlet boundary conditions on it. Similarly, continuous momentum enables sensible boundary conditions for the momentum polarisation path integral.

When confronted with the coherent state path integral, however, we face a problem. The integral calls for boundary conditions on both position and momentum but, as we have seen, the pseudomeasure is not concentrated on the set where both of these are continuous. One thus cannot meaningfully impose the necessary Dirichlet boundary conditions, and it becomes unclear what the integral is to mean.

There are also downstream difficulties with boundary conditions when one considers the semiclassical approximation. The differential equations resulting from the action are first order in time, which generally cannot be solved for Dirichlet boundary conditions on all variables at both the initial and final times. For the position and momentum polarisations the conditions are relaxed on either momentum or position respectively, and there is no issue, but the coherent state path integral calls for the full set of conditions. A way out of this predicament is offered in [13], [14] as follows. Consider the discrete form of the coherent state path integral action for a normal-ordered Hamiltonian ($\psi_0 = \psi_i$, $\psi_{N+1} = \psi_f$, and compare (3.14)):

$$S = \sum_{n=0}^{N} \epsilon \left[\frac{i}{2} \bar{\psi}_{n+1} \frac{\psi_{n+1} - \psi_n}{\epsilon} - \frac{i}{2} \psi_n \frac{\bar{\psi}_{n+1} - \bar{\psi}_n}{\epsilon} - H(\bar{\psi}_{n+1}, \psi_n) \right]. \tag{15.59}$$

Here $H(\bar{\psi}_{n+1}, \psi_n)$ is the Wick symbol $\langle \psi_{n+1} | H | \psi_n \rangle$ of the Hamiltonian, which is why it contains the field at different times. Note that ψ_{N+1} and $\bar{\psi}_0$ do not appear outside of the time-derivative terms. The argument then goes that if one searches for stationary points of this action in the complexified space of real parts of the fields (see Appendix D), one can effectively treat ψ and $\bar{\psi}$ as independent and thus only impose the boundary conditions $\psi_0 = \psi_i$, $\bar{\psi}_T = \bar{\psi}_f$. With the field and its complex conjugate decouples, this is now the right number of boundary conditions for the first order equations of motion.

This prescription for finding classical paths is correct (we will see in the next chapter that it can be derived rigorously from the KD approach) but this way of arriving at it is flawed because the paths are still not smooth enough to impose even these boundary conditions. This approach, however, reveals something of the correct way to regularise the integral. Consider again the above discrete action as a function of a large number of real variables (the real and imaginary parts of the various fields), which we will denote by $\boldsymbol{x}$. Complexifying these to $\boldsymbol{z}$, the equations of motion in effect become

$$\nabla_{\boldsymbol{z}} S(\boldsymbol{z}) = 0. \tag{15.60}$$

Choosing a solution z_s of the above, we now observe the following: if the original action $S(\boldsymbol{x})$ was real and $S(\boldsymbol{z})$ is holomorphic, $\bar{\boldsymbol{z}}_s$ is also a solution:

$$\nabla_{\boldsymbol{z}} S(\bar{\boldsymbol{z}}_s) = \overline{\nabla_{\boldsymbol{z}} S(\boldsymbol{z}_s)} = 0 \tag{15.61}$$

The continuous version of the coherent state action is certainly real, and one thus might expect a second conjugated solution for each complex classical path. The above prescription, however, frequently gives only a single classical path. The reason is that the discrete action is in fact not real, breaking the above construction. Indeed this is why ψ_{N+1} and $\bar{\psi}_0$ do not appear, so the prescription is crucially dependent on a feature of the discrete rather than the continuous action. Isolating the imaginary part of the discrete action in fact leads to the correction term that we will see in the KD approach [17], though it is not the best way to arrive at it.

Finally, a comment is in order on the fluctuation corrections of the path integral. The closest thing to a continuous-time approach to this is presented in [16], which gives them as

$$\sqrt{\frac{\delta\bar{\psi}_0}{\delta\bar{\psi}_T}} \exp\left(\frac{i}{2} \int_0^T dt \left[\frac{\partial^2 H(\bar{\psi}_t, \psi_t)}{\partial\psi_t \partial\bar{\psi}_t} \right]_{\substack{\psi_t = \delta\psi_t, \\ \bar{\psi}_t = \delta\bar{\psi}_t}} \right) \tag{15.62}$$

where $\delta\psi_t$ and $\delta\bar{\psi}_t$ are treated as independent and solve

$$\partial_t \delta\psi_t = -i \left[\frac{\partial^2 H(\bar{\psi}_t, \psi_t)}{\partial\psi_t \partial\bar{\psi}_t} \right]_{\substack{\psi_t = \delta\psi_t, \\ \bar{\psi}_t = \delta\bar{\psi}_t}} \delta\psi_t - i \left[\frac{\partial^2 H(\bar{\psi}_t, \psi_t)}{\partial\bar{\psi}_t \partial\bar{\psi}_t} \right]_{\substack{\psi_t = \delta\psi_t, \\ \bar{\psi}_t = \delta\bar{\psi}_t}} \delta\bar{\psi}_t, \tag{15.63}$$

$$\partial_t \delta\bar{\psi}_t = i \left[\frac{\partial^2 H(\bar{\psi}_t, \psi_t)}{\partial\psi_t \partial\psi_t} \right]_{\substack{\psi_t = \delta\psi_t, \\ \bar{\psi}_t = \delta\bar{\psi}_t}} \delta\psi_t + i \left[\frac{\partial^2 H(\bar{\psi}_t, \psi_t)}{\partial\psi_t \partial\bar{\psi}_t} \right]_{\substack{\psi_t = \delta\psi_t, \\ \bar{\psi}_t = \delta\bar{\psi}_t}} \delta\bar{\psi}_t, \tag{15.64}$$

with initial conditions $\delta\psi_t(0) = 0$ and $\delta\bar{\psi}_t(0)$ arbitrary. This prescription is derived entirely from the discrete form of the action, and so is not really 'continuous time' in the sense of being the result of a manipulation on a continuous time path integral. Since it is not presented as the determinant of a differential operator, it is also difficult to analyse the appearance of zero modes in the operator governing the action. Interestingly, however, it is possibly not far off from being such an object. Specifically, if one were to interpret this as the result of Gaussian integration, it would need to be the inverse square root of the functional determinant

$$\frac{\delta\bar{\psi}_T}{\delta\bar{\psi}_0} \exp\left(-i \int_0^T dt \left[\frac{\partial^2 H(\bar{\psi}_t, \psi_t)}{\partial\psi_t \partial\bar{\psi}_t} \right]_{\substack{\psi_t = \delta\psi_t, \\ \bar{\psi}_t = \delta\bar{\psi}_t}} \right) \tag{15.65}$$

If one applies Forman's theorem (for first-order differential operators, which I

do not cover in the appendix but may be found in [30]), the term in the exponent is precisely what the continuous time differential operator would give for a specific choice of ray of minimal growth[17]. The pre-exponential factor also depends on the boundary values as expected, but I have not been able to work out which boundary conditions would give this result. As such, it seems possible to derive from the discrete action an object that greatly resembles the functional determinant of a first order differential operator, but it is unclear how to motivate the required boundary conditions (or even establish what they are) and ray of minimal growth choice outside of appealing directly to the discretisation. Nevertheless, this is an interesting avenue of inquiry that I hope is pursued further in the future: it would be particularly interesting to have a derivation of an effective first order differential operator from the KD second order operator we are about to see in the next section.

With this, we come to the end of our review of the Berezin continuous time path integral and its semiclassical prescriptions, moving now onto the Klauder-Daubechies path integral.

15.4 Klauder-Daubechies Approach

The most direct way to arrive at the KD path integral is, as promised, via the concept of holomorphic polarisation. Recall that the latter is characterized by holomorphic functions that are square-integrable with respect to a Gaussian measure on the complex plane, which from (15.15) may arise as (here the complex variable is α, corresponding to a coherent state, and ψ is an arbitrary state)

$$\langle 0|e^{\alpha\hat{a}^\dagger}e^{\bar{\alpha}\hat{a}}|\psi\rangle = e^{|\alpha|^2/2}\langle\alpha|\psi\rangle. \tag{15.66}$$

A better function space to work with is such functions with half of the Gaussian measure absorbed into them so that they are square integrable with respect to the plain Lebesgue measure: evidently functions $\langle\alpha|\psi\rangle$ are of this form, and they comprise one of the many Hilbert spaces that we saw[18] make up the larger space $L^2(\mathbb{R}^2)$.

Since, as we argued earlier, we are interested only in this single Hilbert space rather than all of $L^2(\mathbb{R}^2)$, we require a way to restrict the path integral to it. To achieve this, we may roughly follow the procedure suggested in [36] and define an operator that is zero on this space:

$$\mathcal{P}_{\mathrm{SB}}\circ = \partial_\alpha\left[e^{|\alpha|^2/2}\circ\right]. \tag{15.67}$$

[17] Specifically, $\pi_x = \frac{1}{2}\begin{pmatrix}1 & -i\\ i & 1\end{pmatrix}$.

[18] The construction in Chap. 15 technically used the complex conjugates of such functions, but would go through just as well with these.

It will be helpful to work with a positive semi-definite operator, so we will also define its adjoint. Since this operator maps functions square-integrable with respect to a Lebesgue measure into ones square-integrable with respect to a Gaussian measure $e^{-|\alpha|^2} d[\alpha, \bar{\alpha}]$, this difference in spaces needs to be accounted for when defining the adjoint. Thus

$$\mathcal{P}_{\mathrm{SB}}^{\dagger} \circ = -e^{|\alpha|^2/2} \partial_{\bar{\alpha}} \left[e^{-|\alpha|^2} \circ \right] \tag{15.68}$$

and we have the positive semi-definite operator

$$\mathcal{P}_{\mathrm{SB}}^{\dagger} \mathcal{P}_{\mathrm{SB}} \circ = -e^{|\alpha|^2/2} \partial_{\bar{\alpha}} \left[e^{-|\alpha|^2} \partial_{\alpha} \left[e^{|\alpha|^2/2} \circ \right] \right]. \tag{15.69}$$

Using these operators one may define a projector onto the desired Hilbert space as

$$\lim_{\epsilon \to 0} e^{-\frac{1}{2\epsilon} \mathcal{P}_{\mathrm{SB}}^{\dagger} \mathcal{P}_{\mathrm{SB}}}. \tag{15.70}$$

Since the operator is positive semi-definite, the exponent will always be negative or zero. As $\epsilon \to 0$, only functions on which the exponent is zero will survive, which is precisely functions from the desired Hilbert space.

It is possible to obtain an integral kernel representation by applying the operator to a Dirac delta function. The latter has the complex form ($z = x + iy$)

$$\begin{aligned} \delta(\alpha) &= \delta(\mathrm{Re}\,\alpha)\delta(\mathrm{Im}\,\alpha) = 4\delta(\mathrm{Re}\,2\alpha)\delta(\mathrm{Im}\,2\alpha) \\ &= \frac{1}{\pi^2} \int dx dy\, e^{2ix\,\mathrm{Re}\,\alpha + 2iy\,\mathrm{Im}\,\alpha} = \frac{1}{\pi} \int d[z, \bar{z}]\, e^{iz\bar{\alpha} + i\bar{z}\alpha}, \end{aligned} \tag{15.71}$$

so

$$\begin{aligned} e^{-\frac{1}{2\epsilon} \mathcal{P}_{\mathrm{SB}}^{\dagger} \mathcal{P}_{\mathrm{SB}}} \delta(\alpha - \beta) &= \frac{1}{\pi} \int d[z, \bar{z}] \exp\left[\frac{1}{4\epsilon} - \frac{|\alpha|^2}{8\epsilon} - \frac{|z|^2}{2\epsilon} \right. \\ &\qquad \left. + i\bar{z}\left(\alpha - \beta - \frac{\alpha}{4\epsilon} \right) + iz\left(\bar{\alpha} - \bar{\beta} + \frac{\bar{\alpha}}{4\epsilon} \right) \right] \\ &= \frac{2\epsilon}{\pi} \exp\left[\frac{1}{4\epsilon} - \frac{|\alpha|^2}{8\epsilon} - \frac{1}{2\epsilon}\left(\alpha - \beta - \frac{\alpha}{4\epsilon} \right)\left(\bar{\alpha} - \bar{\beta} + \frac{\bar{\alpha}}{4\epsilon} \right) \right] \\ &= \frac{2\epsilon}{\pi} e^{1/4\epsilon} \exp\left[-2\epsilon|\alpha - \beta|^2 + \frac{1}{2}\alpha(\bar{\alpha} - \bar{\beta}) - \frac{1}{2}\bar{\alpha}(\alpha - \beta) \right]. \end{aligned} \tag{15.72}$$

At this point we make the redefinition $2\epsilon \to \frac{\epsilon}{\delta t}$, giving a final expression for the projector:

$$\lim_{\epsilon \to 0} \frac{\epsilon}{\pi \delta t} e^{\delta t/2\epsilon} \exp\left[i\delta t \left(-i\epsilon \frac{|\alpha - \beta|^2}{\delta t^2} + \frac{i}{2}\bar{\alpha}\frac{\alpha - \beta}{\delta t} - \frac{i}{2}\alpha\frac{\bar{\alpha} - \bar{\beta}}{\delta t} \right) \right]. \tag{15.73}$$

However, there is another representation for this projector, namely $\langle\alpha|\beta\rangle$ since (recall from Chap. 15 that $\langle\beta, n|m\rangle$ span $L^2(\mathbb{R}^2)$[19]):

$$\int d[\beta,\bar{\beta}]\langle\alpha|\beta\rangle\left[\sum_{m,n}\langle\beta,n|m\rangle\langle m|\psi\rangle\right] = \sum_{m,n}\delta_{n,0}\langle\alpha|m\rangle\langle m|\psi\rangle = \langle\alpha|\psi\rangle. \tag{15.74}$$

Thus

$$\langle\alpha|\beta\rangle = \lim_{\epsilon\to 0}\frac{\epsilon}{\pi\delta t}e^{\delta t/2\epsilon}\exp\left[i\delta t\left(-i\epsilon\frac{|\alpha-\beta|^2}{\delta t^2}+\frac{i}{2}\bar{\alpha}\frac{\alpha-\beta}{\delta t}-\frac{i}{2}\alpha\frac{\bar{\alpha}-\bar{\beta}}{\delta t}\right)\right]. \tag{15.75}$$

In a sense this is the main result of the KD approach[20]. Notice that the term in the exponent is very similar to a portion of the discrete coherent state action but with a new ϵ term. This term is in fact very similar to what one would obtain as the small imaginary portion of the action [17] (recall that, while the continuous action is real, the discrete action is not) which is typically discarded because it appears to be $O(\delta t^2)$, but with ϵ now replacing one of the δt factors. Using this relation in place of the usual one for the inner product on the left, one can construct the discrete form of the path integral as usual and then take the continuum limit (absorbing the exponential prefactor into the normalisation). This yields the following continuous time action:

$$S_\epsilon = \frac{i}{2}\bar{\psi}_t\partial_t\psi_t - \frac{i}{2}\psi_t\partial_t\bar{\psi}_t - i\epsilon|\partial_t\psi_t|^2, \tag{15.76}$$

which in fact resolves basically every conceptual difficulty with the path integral.

To wit, the ϵ term together with the prefactors in the normalisation is enough to construct a Wiener measure over the paths entering the integral [36]. This means that for every positive ϵ we are now dealing with a path integral over entirely continuous paths, on which the appropriate Dirichlet boundary conditions may be validly imposed. Furthermore, the differential operator in the action is now second order, meaning that the standard Dirichlet boundary conditions are now correct in number for solutions of the equations of motion to exist: no changes to the boundary conditions as in the Berezin approach are required (though we will see in the next chapter that the Berezin approach can be derived as a simplification of this). This also means that the differential operator with these Dirichlet boundary conditions is elliptic and thus subject to Forman's theorem [30], meaning fluctuation corrections can now be calculated as a functional determinant of a well-defined operator which may be analysed directly without reverting to the discrete action. The procedure for any calculation is thus to per-

[19] Again, the construction in Chap. 15 was for the complex conjugates of these functions, but the idea is exactly the same. Also there $|\beta, n\rangle$ was written as $|x, p, n\rangle$.

[20] The actual results of [1], [2] are significantly more rigorous, but most of the 'idea' is encompassed in this result [36].

form it with an $\epsilon > 0$ for which the integral is very well-defined, and then take the $\epsilon \to 0$ limit of the result. In a heuristic way this acts somewhat like a Wick rotation, allowing one to improve the properties of the integral and perform calculations before then 'rotating back' by setting $\epsilon \to 0$.

The main difficulties with this approach are that the limit may be difficult to perform and that the action is now complex. The first difficulty may be quite serious both analytically (an explosion of ϵ factors may make even problems that should be exactly solvable intractable) and numerically (the equations of motion may become very stiff in this limit), so often one seeks to derive a way to avoid taking the limit explicitly. The second leads to the method of steepest descent being necessary, which introduces problems not faced with the method of stationary phase as described in Appendix D. Since the Feynman-Vernon action is complex regardless, however, in the non-equilibrium setting this is the case regardless so extra complexity arises only in the zero temperature and equilibrium settings.

Before concluding, it is also important to consider how a Hamiltonian (or other operator like a Lindbladian) enters in this picture. This will be addressed in the next section.

15.4.1 Wick Symbol versus P-Symbol

Consider the conventional discrete action corresponding to the very simple Hamiltonian $\omega a^\dagger a$, whose Wick symbol at time n is $\omega \bar{\psi}_{n+1}\psi_n$:

$$S_N = \sum_{n=0}^{N} \delta t \left[\frac{i}{2}\bar{\psi}_{n+1}\frac{\psi_{n+1}-\psi_n}{\delta t} - \frac{i}{2}\psi_n \frac{\bar{\psi}_{n+1}-\bar{\psi}_n}{\delta t} - \omega \bar{\psi}_{n+1}\psi_n \right]. \tag{15.77}$$

We may rewrite this in matrix form by introducing

$$-M^{-1} = \begin{pmatrix} -1 & & & & & \\ 1-i\omega\delta t & -1 & & & & \\ & 1-i\omega\delta t & -1 & & & \\ & & 1-i\omega\delta t & -1 & & \\ & & & 1-i\omega\delta t & -1 & \\ & & & & 1-i\omega\delta t & -1 \end{pmatrix} \Bigg\} N, \tag{15.78}$$

$$\boldsymbol{\Psi} = \begin{pmatrix} \psi_1 & \dots & \psi_N \end{pmatrix}^T, \tag{15.79}$$

in terms of which it becomes

$$iS_N = -\boldsymbol{\Psi}^\dagger M^{-1}\boldsymbol{\Psi} + \boldsymbol{\Psi}^\dagger \begin{pmatrix} \psi_0 \\ \vdots \\ 0 \end{pmatrix} + \begin{pmatrix} 0 \\ \vdots \\ \bar{\psi}_{N+1}(1-i\omega\delta t) \end{pmatrix}^T \boldsymbol{\Psi} - \frac{|\psi_{N+1}|^2}{2} - \frac{|\psi_0|^2}{2}. \tag{15.80}$$

It is easy to show that $\det M^{-1} = 1$, and from here a simple Gaussian integral yields

$$\int d\mathbf{\Psi} d\bar{\mathbf{\Psi}}\, e^{iS[\mathbf{\Psi},\bar{\mathbf{\Psi}}]} = e^{-\frac{1}{2}(|\psi_0|^2+|\psi_{N+1}|^2)} \det M = e^{-\frac{1}{2}(|\psi_0|^2+|\psi_{N+1}|^2)} e^{\psi_0 \bar{\psi}_N (1-i\omega\frac{T}{N+1})^N}. \tag{15.81}$$

In the limit of $N \to \infty$ this becomes ($\psi_0 = \psi_i$, $\psi_{N+1} = \psi_f$)

$$\lim_{N\to\infty} e^{-\frac{1}{2}(|\psi_0|^2+|\psi_{N+1}|^2)} e^{\psi_0 \bar{\psi}_{N+1} (1-i\omega\frac{T}{N+1})^N} = e^{-\frac{1}{2}(|\psi_i|^2+|\psi_f|^2)+\bar{\psi}_f \psi_i e^{-i\omega T}}. \tag{15.82}$$

which is the known correct result for $\langle \phi_f | e^{-iH_0 T} | \phi_i \rangle$ [10]. At this stage we may observe that it is crucial for this result that the $-i\omega\delta t$ term be off of the main diagonal. Moving it to said diagonal, as the usual continuous time notation suggests, alters the determinant of M^{-1} to $\det M^{-1}_{\text{diag}} = e^{i\omega T}$ which is incorrect.

What this example demonstrates is that the error incurred by replacing the Wick symbol $H(\bar{\psi}_{n+1}, \psi_n)$ by $H(\bar{\psi}_t, \psi_t)$ in the continuous time limit is in fact meaningful for the fluctuational determinant. Repeating the above calculation using Forman's theorem for the continuous version of the action with the KD ϵ term gives the same erroneous result, but the correct result may be obtained by observing that

$$\delta t \omega \bar{\psi}_{n+1} \psi_n = \delta t \omega \bar{\psi}_n \psi_n + \delta t^2 \omega \frac{\bar{\psi}_{n+1} - \bar{\psi}_n}{\delta t} \psi_n \tag{15.83}$$

and rather than discarding the second term, replacing it by $\epsilon \omega \psi_t \partial_t \bar{\psi}_t$ in the continuous time limit. The correctness of this procedure could be heuristically argued on the grounds that when we performed the substitution $2\epsilon \to \frac{\epsilon}{\delta t}$, we ensured that ϵ goes to 0 faster than δt and so one cannot discard dt^2 terms so long as the $dt\, \epsilon |\partial_t \psi_t|^2$ term is present. This would lead, however, to delicate question about the order of the $\delta t \to 0$ and $\epsilon \to 0$ limits which it would be best to avoid as the rigour of such manipulations would be in question. An alternative way of avoiding this difficulty is thus desirable.

The answer comes in the form of observing that the $\det M^{-1}_{\text{diag}} = e^{i\omega T}$ functional determinant result would in fact be correct for the anti-normal ordered Hamiltonian $\omega a a^\dagger$. Anti-normal ordered Hamiltonians do not have simple Wick symbols, but often have an alternative symbol known as the Glauber-Sudarshan P-Symbol. If this is the case, then the Hamiltonian (or other operator) may be represented as

$$\int d[\psi, \bar{\psi}] |\psi\rangle P_H(\psi, \bar{\psi}) \langle \psi| \tag{15.84}$$

with P_H the P-symbol of the Hamiltonian.

While essentially every operator has a Wick symbol (referred to as the T-representation by Glauber), the same is not true of the P-symbol [53]. Any anti-normal ordered operator that is polynomial in the a, $a^\dagger$ operators does have such

a symbol however, which is why the main KD results [1], [2] specifically refer to polynomial Hamiltonians.

To use the P-symbol in construction of the path integral for such an operator, one inserts the coherent state resolution of identity between the a and $a^\dagger$ operators, so that for instance if $H = \omega a a^\dagger$, we have

$$\omega a a^\dagger = \int d[\psi_n, \bar{\psi}_n]\, a|\psi_n\rangle\langle\psi_n|a^\dagger = \int d[\psi_n, \bar{\psi}_n]|\psi_n\rangle(\omega|\psi_n|^2)\langle\psi_n| \tag{15.85}$$

and $P_H = \omega|\psi_n|^2$. One then Trotterizes e^{-iHT} and represents $e^{-iH\delta t}$ by

$$e^{-iH\delta t} \approx I - iH\delta t = \int d[\psi, \bar{\psi}]|\psi\rangle\Big(1 - iP_H(\psi, \bar{\psi})\delta t\Big)\langle\psi| \approx \int d[\psi, \bar{\psi}]|\psi\rangle e^{-iP_H(\psi,\bar{\psi})\delta t}\langle\psi| \tag{15.86}$$

which may be justified rigorously. These are then stacked together in the usual way, using the projector integral kernel expression for the overlap of coherent states to obtain the kinematic part of the action. Notice that the P-symbol contains the fields at equal times and thus does not introduce the δt error when passing to the continuous time limit, so it makes sense that the continuous time action with fields at equal times would correspond to it and give the correct answer for an anti-normal rather than normal ordered operator. As such, the Hamiltonian in a continuous time KD action should be interpreted as the P-symbol of an anti-normal ordered polynomial operator. If the original operator was normal ordered, it should first be brought to anti-normal form via commutation relations prior to constructing the integral.

In the next chapter I will use the ideas of KD for Hamiltonian path integrals to construct an analogous path integral for Lindbladians, which so far as I am aware has not appeared in the literature. The key ingredients will be the integral kernel for the projector on the appropriate Hilbert space defined above, and an appropriate operator kernel for constructing what are essentially P-symbols of superoperators.

Chapter 16

P-Symbol Coherent State Path Integral for Lindbladian Operators

16.1 Alternative construction: The Superoperator Antinormal Kernel

An alternative to [24] construction of the path integral for a Lindbladian stems from representing the superoperator via the antinormal kernel

$$\mathcal{I} = \int d[\psi^+, \bar{\psi}^+] d[\psi^-, \bar{\psi}^-] \Big(|\psi^+\rangle\langle\psi^-| \Big) \otimes \Big(|\psi^-\rangle\langle\psi^+| \Big) \tag{16.1}$$

This approach follows the lessons learned from the Klauder-Daubechies formalism, allowing us to avoid error terms in the action and have better control over the operator ordering.

Applying this superoperator to an operator involves tracing that operator against the right hand side term in the integrand tensor product, after which it is clear from the coherent state resolution of identity that the above is the identity superoperator.

A typical Lindbladian constructed from the $a^\dagger$, a ladder operators[1] can be recast as an antinormal-ordered non-Hermitian Hamiltonian, an antinormal-ordered recycling term, and a constant resulting from the antinormal-ordering:

$$H = \sum_j Q_j R_j(a) S_j(a^\dagger),\ Q_j \in \mathbb{C}, \tag{16.2}$$

$$\mathcal{R} = \sum_k Y_k \overrightarrow{T}_k(a) \overrightarrow{U}_k(a^\dagger) \overleftarrow{V}_k(a^\dagger) \overleftarrow{W}_k(a), \tag{16.3}$$

$$\mathcal{L} = -i\overrightarrow{H} + i\overleftarrow{H^\dagger} + \mathcal{R} + C(\mathbf{Q}, \mathbf{Y}). \tag{16.4}$$

[1] Everything in this section easily generalises to multiple creating and annihilation operators, so long as their number is finite. Evidently in the case of field theories there are complications with naively commuting the operators [54].

Here an arrow over a normal operator denotes a superoperator corresponding to application from the appropriate side:

$$\vec{O}[\rho] = O\rho, \quad \overleftarrow{O}[\rho] = \rho O, \tag{16.5}$$

and it is notable that operators with arrows pointing in different directions commute.

When interacting with the superoperator kernel, superoperators coming to the right (before) the kernel will apply to the right hand side tensor product term from the opposite side to what their arrow suggests. This is because in the trace against this term they initially apply to the other operator being traced over, and then in the process of moving over by trace cyclicity change side. When applying to the left (after) the kernel, they apply to the left hand side tensor product term from the side one would expect from their arrow since this is just a direct application.

We may now write

$$\begin{aligned}
\vec{H} &= \sum_j Q_j \vec{R}_j(a) \mathcal{I} \vec{S}_j(a^\dagger) \\
&= \sum_j Q_j \vec{R}_j(a) \left(\int d[\psi^+, \bar{\psi}^+] d[\psi^-, \bar{\psi}^-] \left(|\psi^+\rangle\langle\psi^-| \right) \otimes \left(|\psi^-\rangle\langle\psi^+| \right) \right) \vec{S}_j(a^\dagger) \\
&= \int d[\psi^+, \bar{\psi}^+] d[\psi^-, \bar{\psi}^-] \sum_j Q_j R_j(\psi^+) S_j(\bar{\psi}^+) \left(|\psi^+\rangle\langle\psi^-| \right) \otimes \left(|\psi^-\rangle\langle\psi^+| \right),
\end{aligned} \tag{16.6}$$

$$\begin{aligned}
\overleftarrow{H^\dagger} &= \sum_j \bar{Q}_j \overleftarrow{R}_j(a^\dagger) \mathcal{I} \overleftarrow{S}_j(a) \\
&= \sum_j \bar{Q}_j \overleftarrow{R}_j(a^\dagger) \left(\int d[\psi^+, \bar{\psi}^+] d[\psi^-, \bar{\psi}^-] \left(|\psi^+\rangle\langle\psi^-| \right) \otimes \left(|\psi^-\rangle\langle\psi^+| \right) \right) \overleftarrow{S}_j(a) \\
&= \int d[\psi^+, \bar{\psi}^+] d[\psi^-, \bar{\psi}^-] \sum_j \bar{Q}_j R_j(\bar{\psi}^-) S_j(\psi^-) \left(|\psi^+\rangle\langle\psi^-| \right) \otimes \left(|\psi^-\rangle\langle\psi^+| \right),
\end{aligned} \tag{16.7}$$

$$\begin{aligned}
\mathcal{R} &= \sum_k Y_k \vec{T}_k(a) \vec{U}_k(a^\dagger) \overleftarrow{V}_k(a^\dagger) \overleftarrow{W}_k(a) = \sum_k Y_k \vec{T}_k(a) \overleftarrow{V}_k(a^\dagger) \mathcal{I} \vec{U}_k(a^\dagger) \overleftarrow{W}_k(a) \\
&= \sum_k Y_k \vec{T}_k(a) \overleftarrow{V}_k(a^\dagger) \left(\int d[\psi^+, \bar{\psi}^+] d[\psi^-, \bar{\psi}^-] \left(|\psi^+\rangle\langle\psi^-| \right) \otimes \left(|\psi^-\rangle\langle\psi^+| \right) \right) \vec{U}_k(a^\dagger) \overleftarrow{W}_k(a) \\
&= \int d[\psi^+, \bar{\psi}^+] d[\psi^-, \bar{\psi}^-] \sum_k Y_k T_k(\psi^+) V_k(\bar{\psi}^-) U_k(\bar{\psi}^+) W_k(\psi^-) \left(|\psi^+\rangle\langle\psi^-| \right) \otimes \left(|\psi^-\rangle\langle\psi^+| \right),
\end{aligned} \tag{16.8}$$

which permits us to represent the infinitesimal time evolution operator as

$$\begin{aligned}
e^{\mathcal{L}\delta t} &\approx e^{C(\mathbf{Q},\mathbf{Y})\delta t}\left(\mathcal{I}+\left[-i\overrightarrow{H}+i\overleftarrow{H^{\dagger}}+\mathcal{R}\right]\delta t\right)\\
&= e^{C(\mathbf{Q},\mathbf{Y})\delta t}\int d[\psi^{+},\bar{\psi}^{+}]d[\psi^{-},\bar{\psi}^{-}]\Big(|\psi^{+}\rangle\langle\psi^{-}|\Big)\otimes\Big(|\psi^{-}\rangle\langle\psi^{+}|\Big)\\
&\qquad\cdot\Bigg(1+\Bigg[\sum_{j}i\Big(\bar{Q}_{j}R_{j}(\bar{\psi}^{-})S_{j}(\psi^{-})-Q_{j}R_{j}(\psi^{+})S_{j}(\bar{\psi}^{+})\Big)\\
&\qquad\qquad+\sum_{k}Y_{k}T_{k}(\psi^{+})V_{k}(\bar{\psi}^{-})U_{k}(\bar{\psi}^{+})W_{k}(\psi^{-})\Bigg]\delta t\Bigg)\\
&\approx e^{C(\mathbf{Q},\mathbf{Y})\delta t}\int d[\psi^{+},\bar{\psi}^{+}]d[\psi^{-},\bar{\psi}^{-}]\Big(|\psi^{+}\rangle\langle\psi^{-}|\Big)\otimes\Big(|\psi^{-}\rangle\langle\psi^{+}|\Big)\\
&\qquad\cdot\exp\Bigg(\Bigg[\sum_{j}i\Big(\bar{Q}_{j}R_{j}(\bar{\psi}^{-})S_{j}(\psi^{-})-Q_{j}R_{j}(\psi^{+})S_{j}(\bar{\psi}^{+})\Big)\\
&\qquad\qquad+\sum_{k}Y_{k}T_{k}(\psi^{+})V_{k}(\bar{\psi}^{-})U_{k}(\bar{\psi}^{+})W_{k}(\psi^{-})\Bigg]\delta t\Bigg).
\end{aligned}\tag{16.9}$$

From here we simply need to evaluate the geometric part of the action, which originates from the interaction of two kernel superoperators at adjacent moments in time:

$$\begin{aligned}
&\Big[\Big(|\psi^{+}_{n+1}\rangle\langle\psi^{-}_{n+1}|\Big)\otimes\Big(|\psi^{-}_{n+1}\rangle\langle\psi^{+}_{n+1}|\Big)\Big]\Big[\Big(|\psi^{+}_{n}\rangle\langle\psi^{-}_{n}\Big)\otimes\Big(|\psi^{-}_{n}\rangle\langle\psi^{+}_{n}|\Big)\Big]\\
&=\langle\psi^{+}_{n+1}|\psi^{+}_{n}\rangle\langle\psi^{-}_{n}|\psi^{-}_{n+1}\rangle\Big[\Big(|\psi^{+}_{n+1}\rangle\langle\psi^{-}_{n+1}|\Big)\otimes\Big(|\psi^{-}_{n}\rangle\langle\psi^{+}_{n}|\Big)\Big]\\
&\sim\exp\left[-\delta t\epsilon\left(\left|\frac{\psi^{+}_{n+1}-\psi^{+}_{n}}{\delta t}\right|^{2}+\left|\frac{\psi^{-}_{n+1}-\psi^{-}_{n}}{\delta t}\right|^{2}\right)\right]\\
&\cdot\exp\left[\frac{\delta t}{2}\left(\psi^{+}_{n+1}\frac{\bar{\psi}^{+}_{n+1}-\bar{\psi}^{+}_{n}}{\delta t}-\bar{\psi}^{+}_{n+1}\frac{\psi^{+}_{n+1}-\psi^{+}_{n}}{\delta t}-\psi^{-}_{n+1}\frac{\tilde{\psi}^{-}_{n+1}-\tilde{\psi}^{-}_{n}}{\delta t}+\bar{\psi}^{-}_{n+1}\frac{\psi^{-}_{n+1}-\psi^{-}_{n}}{\delta t}\right)\right]\\
&\cdot\Big[\Big(|\psi^{+}_{n+1}\rangle\langle\psi^{-}_{n+1}|\Big)\otimes\Big(|\psi^{-}_{n}\rangle\langle\psi^{+}_{n}|\Big)\Big].
\end{aligned}\tag{16.10}$$

where I have used $\sim$ to denote the omission of normalising factors associated with the holomorphic polarisation projection operator. As discussed in the last chapter, these are independent of the dynamics of the integral and thus may be neglected so long as the integral is normalised against a known one[2].

[2]In so far as we use Forman's Theorem (see Appendix C), we will always do this to regularise our functional determinants. As ever, a more rigorous discussion is present in [1], [2].

Setting $\delta t = \frac{T}{N}$, by Trotterization we obtain

$$\begin{aligned} e^{T\mathcal{L}} &= \underbrace{e^{\delta t\mathcal{L}} \dots e^{\delta t\mathcal{L}}}_{N} \\ &= \int \prod_{m=1}^{N} d[\psi_m^+, \bar{\psi}_m^+] d[\psi_m^-, \bar{\psi}_m^-]\, e^{iS_{1,N-1}[\{\psi_n, \bar{\psi}_n\}]} \Big(|\psi_N^+\rangle\langle\psi_N^-| \Big) \otimes \Big(|\psi_1^-\rangle\langle\psi_1^+| \Big), \end{aligned} \tag{16.11}$$

$$\begin{aligned} S_{p,q} =& i \sum_{n=p}^{q} \delta t \epsilon \left(\left| \frac{\psi_{n+1}^+ - \psi_n^+}{\delta t} \right|^2 + \left| \frac{\psi_{n+1}^- - \psi_n^-}{\delta t} \right|^2 \right) \\ & - i \sum_{n=p}^{q} \frac{\delta t}{2} \Bigg(\psi_{n+1}^+ \frac{\bar{\psi}_{n+1}^+ - \bar{\psi}_n^+}{\delta t} - \bar{\psi}_{n+1}^+ \frac{\psi_{n+1}^+ - \psi_n^+}{\delta t} \\ & \qquad - \psi_{n+1}^- \frac{\tilde{\psi}_{n+1}^- - \tilde{\psi}_n^-}{\delta t} + \bar{\psi}_{n+1}^- \frac{\psi_{n+1}^- - \psi_n^-}{\delta t} \Bigg) \\ & + \sum_{n=1}^{N} \delta t \Bigg(\sum_j \Big(\bar{Q}_j R_j(\bar{\psi}_n^-) S_j(\psi_n^-) - Q_j R_j(\psi_n^+) S_j(\bar{\psi}_n^+) \Big) \\ & \qquad - i \sum_k Y_k T_k(\psi_n^+) V_k(\bar{\psi}_n^-) U_k(\bar{\psi}_n^+) W_k(\psi_n^-) \Bigg) \\ & - i \sum_{n=1}^{N} \delta t\, C(\mathbf{Q}, \mathbf{Y}). \end{aligned} \tag{16.12}$$

This representation can be used to obtain matrix elements of the time evolution operator in various bases. The most straightforward expression is obtained for the coherent states basis, yielding

$$\begin{aligned} & \Big(|\psi_f^-\rangle\langle\psi_f^+| \Big) e^{T\mathcal{L}} \Big(|\psi_i^+\rangle\langle\psi_i^-| \Big) \\ &= \int \prod_{m=1}^{N} d[\psi_m^+, \bar{\psi}_m^+] d[\psi_m^-, \bar{\psi}_m^-]\, e^{iS_{0,N-1}[\{\psi_n, \bar{\psi}_n\}]} \cdot \langle \psi_f^+ + \phi_f^+ | \psi_N^+ \rangle \langle \psi_N^- + \phi_N^- | \psi_f^- \rangle \\ &= \int \prod_{m=1}^{N} d[\psi_m^+, \bar{\psi}_m^+] d[\psi_m^-, \bar{\psi}_m^-]\, e^{iS_{0,N}[\{\psi_n, \bar{\psi}_n\}]} \end{aligned} \tag{16.13}$$

where $\psi_i = \psi_0$, $\psi_f = \psi_{N+1}$.

The continuum limit of the action $S_{0,N}$ as $N \to \infty$ comes out to

$$\begin{aligned} S_c = \int dt \Bigg[& i\epsilon \left(|\partial_t \psi_t^+|^2 + |\partial_t \psi_t^-|^2 \right) + \frac{i}{2} \left(\bar{\psi}_t^+ \partial_t \psi_t^+ - \psi_t^+ \partial_t \bar{\psi}_t^+ - \bar{\psi}_t^- \partial_t \psi_t^- + \psi_t^- \partial_t \bar{\psi}_t^- \right) \\ & + \sum_j \left(\bar{Q}_j R_j(\bar{\psi}_t^-) S_j(\psi_t^-) - Q_j R_j(\psi_t^+) S_j(\bar{\psi}_t^+) \right) \\ & - i \sum_k Y_k T_k(\psi_t^+) V_k(\bar{\psi}_t^-) U_k(\bar{\psi}_t^+) W_k(\psi_t^-) \Bigg] \end{aligned} \tag{16.14}$$

and a final integration by parts yields, with $\psi_T^+ = \psi_f^+$, $\psi_T^- = \psi_f^-$, $\psi_0^+ = \psi_i^+$, $\psi_0^- = \psi_i^-$, the form of the propagator that we will use for the remainder of this part:

$$\left(|\psi_f^-\rangle\langle\psi_f^+| \right) e^{T\mathcal{L}} \left(|\psi_i^+\rangle\langle\psi_i^-| \right) = \int d[\psi_t^+, \bar{\psi}_t^+] d[\psi_t^-, \bar{\psi}_t^-] \, e^{iS}, \tag{16.15}$$

$$\begin{aligned} S = & \frac{i}{2} \left(|\psi_i^+|^2 + |\psi_f^-|^2 - |\psi_f^+|^2 - |\psi_i^-|^2 \right) \\ & + \int dt \Bigg[i\epsilon \left(|\partial_t \psi_t^+|^2 + |\partial_t \psi_t^-|^2 \right) + i \left(\bar{\psi}_t^+ \partial_t \psi_t^+ - \bar{\psi}_t^- \partial_t \psi_t^- \right) \\ & \quad + \sum_j \left(\bar{Q}_j R_j(\bar{\psi}_t^-) S_j(\psi_t^-) - Q_j R_j(\psi_t^+) S_j(\bar{\psi}_t^+) \right) \\ & \quad - i \sum_k Y_k T_k(\psi_t^+) V_k(\bar{\psi}_t^-) U_k(\bar{\psi}_t^+) W_k(\psi_t^-) \Bigg]. \end{aligned} \tag{16.16}$$

Before moving on to concrete calculations, in the next section we will consider a simplification that allows us to find 'effective' classical trajectories of this action without an explicit $\epsilon \to 0$ limit.

16.2 Equivalence of Berezin and Daubechies-Klauder Equations of Motion

Denoting the portion of the action coming from the Lindbladian by $-i\mathcal{L}[\psi_t^+, \bar{\psi}_t^+, \psi_t^-, \bar{\psi}_t^-]$, the equations of motion for our action are[3]

$$2\partial_t \operatorname{Im}\psi_t^+ + i\frac{\delta\mathcal{L}}{\delta \operatorname{Re}\psi_t^+} = -2i\epsilon\partial_t^2 \operatorname{Re}\psi_t^+, \tag{16.17}$$

$$2\partial_t \operatorname{Re}\psi_t^+ - i\frac{\delta\mathcal{L}}{\delta \operatorname{Im}\psi_t^+} = 2i\epsilon\partial_t^2 \operatorname{Im}\psi_t^+, \tag{16.18}$$

$$2\partial_t \operatorname{Im}\psi_t^- - i\frac{\delta\mathcal{L}}{\delta \operatorname{Re}\psi_t^-} = 2i\epsilon\partial_t^2 \operatorname{Re}\psi_t^-, \tag{16.19}$$

$$2\partial_t \operatorname{Re}\psi_t^- + i\frac{\delta\mathcal{L}}{\delta \operatorname{Im}\psi_t^-} = -2i\epsilon\partial_t^2 \operatorname{Im}\psi_t^-, \tag{16.20}$$

where we have had to write them in terms of the real fields because the action is complex[4]. These equations are correct, but difficult to use. Solving them analytically for systems where closed-form solutions are available often yields unwieldy expressions in ϵ, the limits of which as $\epsilon \to 0$ are difficult to find, while numerically they are liable to become very stiff as $\epsilon \to 0$. It would be favourable, therefore, to obtain a way of solving them without explicitly taking that limit.

How to do this for purely Hamiltonian systems is known [15], and I now extend this method to the Lindbladian setting. The resulting method closely resembles Berezin's approach, but with a different justification. We start with the ansatz

$$\operatorname{Re}\psi_t^+ = q_t^+ + (\operatorname{Re}\psi_i^+ - q_0^+)e^{-t/\epsilon} + (\operatorname{Re}\psi_f^+ - q_T^+)e^{-(T-t)/\epsilon}, \tag{16.21}$$

$$\operatorname{Im}\psi_t^+ = r_t^+ + (\operatorname{Im}\psi_i^+ - r_0^+)e^{-t/\epsilon} + (\operatorname{Im}\psi_f^+ - r_T^+)e^{-(T-t)/\epsilon}, \tag{16.22}$$

$$\operatorname{Re}\psi_t^- = q_t^- + (\operatorname{Re}\psi_i^- - q_0^-)e^{-t/\epsilon} + (\operatorname{Re}\psi_f^- - q_T^-)e^{-(T-t)/\epsilon}, \tag{16.23}$$

$$\operatorname{Im}\psi_t^- = r_t^- + (\operatorname{Im}\psi_i^- - r_0^-)e^{-t/\epsilon} + (\operatorname{Im}\psi_f^- - r_T^-)e^{-(T-t)/\epsilon}, \tag{16.24}$$

where $\tilde{\psi}^\pm$ are not restricted to being real. This represents the bulk of the motion occurring as q_t, r_t, with a short time period on the order of ϵ at either end during which the solution corrects to satisfy the boundary conditions. Substituting this into the real and imaginary parts of each equation[5] and taking the $\epsilon \to 0$ limit,

[3] Recall that the fields are fixed at both initial and final times, so the functional derivatives used to obtain these equations yield no boundary constraint equations.

[4] This and why we are permitted to complexify real variables when searching for solutions when applying the method of steepest descent is covered in Appendix D.

[5] It is important to do it this way to correctly account for the deformed contour, because the real and imaginary parts of each equation must be satisfied individually. Substituting the ansatz directly into the complex forms of the equations does not correctly enforce this.

we obtain the following constraints:

$$q_0^+ + ir_0^+ = \operatorname{Re}\psi_i^+ + i\operatorname{Im}\psi_i^+, \quad q_T^+ - ir_T^+ = \operatorname{Re}\psi_f^+ - i\operatorname{Im}\psi_f^+, \tag{16.25}$$

$$q_0^- - ir_0^- = \operatorname{Re}\psi_i^- - i\operatorname{Im}\psi_i^-, \quad q_T^- + ir_T^- = \operatorname{Re}\psi_f^- + i\operatorname{Im}\psi_f^-, \tag{16.26}$$

$$2\partial_t r_t^+ + i\frac{\delta\mathcal{L}}{\delta\operatorname{Re}\psi_t^+}\bigg|_{\psi\to q,r} = 0, \tag{16.27}$$

$$2\partial_t q_t^+ - i\frac{\delta\mathcal{L}}{\delta\operatorname{Im}\psi_t^+}\bigg|_{\psi\to q,r} = 0, \tag{16.28}$$

$$2\partial_t r_t^- - i\frac{\delta\mathcal{L}}{\delta\operatorname{Re}\psi_t^-}\bigg|_{\psi\to q,r} = 0, \tag{16.29}$$

$$2\partial_t q_t^- + i\frac{\delta\mathcal{L}}{\delta\operatorname{Im}\psi_t^-}\bigg|_{\psi\to q,r} = 0, \tag{16.30}$$

where $\psi \to q, r$ indicates that q_t^+, r_t^+, q_T^-, r_t^- are substituted for $\operatorname{Re}\psi_t^+$, $\operatorname{Im}\psi_t^+$, $\operatorname{Re}\psi_t^-$, $\operatorname{Im}\psi_t^-$. Defining

$$\phi_t^+ = q_t^+ + ir_t^+, \quad \tilde{\phi}_t^+ = q_t^+ - ir_t^+, \quad \phi_t^- = q_t^- + ir_t^-, \quad \tilde{\phi}_t^- = q_t^- - ir_t^-, \tag{16.31}$$

and taking account of the definition of Wirtinger derivatives[6], these may be rewritten as

$$\phi_0^+ = \psi_i^+, \quad \tilde{\phi}_T^+ = \bar{\psi}_f^+, \tag{16.32}$$

$$\tilde{\phi}_0^- = \bar{\psi}_i^-, \quad \phi_T^- = \psi_f^-, \tag{16.33}$$

$$\partial_t\phi_t^+ - i\frac{\delta\mathcal{L}}{\delta\bar{\psi}_t^+}\bigg|_{\psi\to\phi} = 0, \tag{16.34}$$

$$\partial_t\tilde{\phi}_t^+ + i\frac{\delta\mathcal{L}}{\delta\psi_t^+}\bigg|_{\psi\to\phi} = 0, \tag{16.35}$$

$$\partial_t\phi_t^- + i\frac{\delta\mathcal{L}}{\delta\bar{\psi}_t^-}\bigg|_{\psi\to\phi} = 0, \tag{16.36}$$

$$\partial_t\tilde{\phi}_t^- - i\frac{\delta\mathcal{L}}{\delta\bar{\psi}_t^-}\bigg|_{\psi\to\phi} = 0, \tag{16.37}$$

where now $\psi \to \phi$ indicates that ϕ_t^+, $\tilde{\phi}_t^+$, ϕ_T^-, $\tilde{\phi}_t^-$ are substituted for ψ_t^+, $\bar{\psi}_t^+$, ψ_t^-,

[6] $\frac{\partial}{\partial\psi} = \frac{1}{2}\left(\frac{\partial}{\partial\operatorname{Re}\psi} - i\frac{\partial}{\partial\operatorname{Im}\psi}\right)$, $\frac{\partial}{\partial\bar{\psi}} = \frac{1}{2}\left(\frac{\partial}{\partial\operatorname{Re}\psi} + i\frac{\partial}{\partial\operatorname{Im}\psi}\right)$.

$\bar{\psi}_t^-$.

These equations and the halved set of boundary conditions look exactly like those stipulated in the Berezin approach if it was extended to Lindbladian functional integrals. Observe that ϕ_t^+ is fixed at $t = 0$ but ϕ_t^- is fixed at $t = T$, and vice versa for their conjugates: this agrees with Berezin's reasoning that there are no ψ_{N+1}^+, ψ_0^-, $\bar{\psi}_0^+$, $\bar{\psi}_T^-$ in the discrete action when constructed the conventional way (see Sec 8.2). Our action does contain these terms, however, and we have arrived at these equations not as the true equations of motion but as the effective equations for the bulk of the motion as $\epsilon \to 0$. It remains to understand how to substitute them back into the action

$$\begin{aligned} S =& \frac{i}{2}\left(|\psi_i^+|^2 + |\psi_f^-|^2 - |\psi_f^+|^2 - |\psi_i^-|^2\right) \\ &+ \int dt \left[i\epsilon\left(|\partial_t \psi_t^+|^2 + |\partial_t \psi_t^-|^2\right) + i\left(\bar{\psi}_t^+ \partial_t \psi_t^+ - \bar{\psi}_t^- \partial_t \psi_t^-\right) - i\mathcal{L}[\psi_t^+, \bar{\psi}_t^+, \psi_t^-, \bar{\psi}_t^-] \right]. \end{aligned} \tag{16.38}$$

Substituting our ansatz (and taking account of the boundary conditions for ϕ) from earlier corresponds to substituting

$$\psi_t^+ \to \phi_t^+ + (\psi_f^+ - \phi_T^+)e^{-(T-t)/\epsilon}, \tag{16.39}$$

$$\bar{\psi}_t^+ \to \tilde{\phi}_t^+ + (\bar{\psi}_i^+ - \tilde{\phi}_0^+)e^{-t/\epsilon}, \tag{16.40}$$

$$\psi_t^- \to \phi_t^- + (\psi_i^- - \phi_0^-)e^{-t/\epsilon}, \tag{16.41}$$

$$\bar{\psi}_t^- \to \tilde{\phi}_t^- + (\bar{\psi}_f^- - \tilde{\phi}_T^-)e^{-(T-t)/\epsilon}. \tag{16.42}$$

Upon substitution it can be shown that the $i\epsilon\left(|\partial_t \psi_t^+|^2 + |\partial_t \psi_t^-|^2\right)$ terms in the action vanish because they decay to 0 as $\epsilon \to 0$ on $(0, T)$ while at $t = 0, T$ they are annihilated by the boundary conditions. Similarly, because the $i\mathcal{L}[\psi_t^+, \bar{\psi}_t^+, \psi_t^-, \bar{\psi}_t^-]$ term contains no time derivatives, as $\epsilon \to 0$ all the exponential terms inside it decay to 0 on $(0, T)$ while their values do not matter on the boundary as it is a set of measure 0, effectively leaving $i\mathcal{L}[\phi_t^+, \tilde{\phi}_t^+, \phi_t^-, \tilde{\phi}_t^-]$.

The terms $i\left(\bar{\psi}_t^+ \partial_t \psi_t^+ - \bar{\psi}_t^- \partial_t \psi_t^-\right)$, however, do interact with the exponential terms when a single exponential term is present . If the exponential term is not affected by a derivative, it decays point-wise to zero and there is no contribution. If it is differentiated with respect to time, however, the extra factor of ϵ^{-1} means there is a small contribution from near one of the boundaries of the interval. Thus, via integration by parts, it can be shown that

$$i \lim_{\epsilon \to 0} \int_0^T dt\, \tilde{\phi}_t^+ \partial_t (\psi_f^+ - \phi_T^+) e^{-(T-t)/\epsilon} = i\tilde{\phi}_T^+(\psi_f^+ - \phi_T^+) = i\bar{\psi}_f^+(\psi_f^+ - \phi_T^+), \tag{16.43}$$

$$-i \lim_{\epsilon \to 0} i \int_0^T dt\, \tilde{\phi}_t^- \partial_t (\psi_i^- - \phi_0^-) e^{-t/\epsilon} = i\tilde{\phi}_0^-(\psi_i^- - \phi_0^-) = i\bar{\psi}_i^-(\psi_i^- - \phi_0^-), \tag{16.44}$$

so that after substitution the action becomes

$$\begin{aligned} S =& \frac{i}{2}\left(|\psi_i^+|^2 + |\psi_f^-|^2 + |\psi_f^+|^2 + |\psi_i^-|^2 - 2\phi_T^+\bar{\psi}_f^+ - 2\phi_0^-\bar{\psi}_i^-\right) \\ &+ \int dt\left[i\left(\tilde{\phi}_t^+\partial_t\phi_t^+ - \tilde{\phi}_t^-\partial_t\phi_t^-\right) - i\mathcal{L}[\phi_t^+, \tilde{\phi}_t^+, \phi_t^-, \tilde{\phi}_t^-]\right]. \end{aligned} \tag{16.45}$$

Note that varying this action with respect to ϕ yields (16.34)–(16.37) so long as one disregards the boundary terms outside the integral. As such, when we refer to varying this action, we will mean a formal manipulation involving only the integral portion.

This way of finding the leading contribution in the method of steepest descent is very convenient. Though we will not consider any such examples in this part, when calculating functional determinants that depend on the classical path it should be possible to find the effective path ϕ via this method and then substitute the full ansatz before taking the $\epsilon \to 0$ limit. At present, unfortunately, I do not know of an analogous approach that would allow one to not take the $\epsilon \to 0$ limit of the functional determinant: the present approach relies greatly on the action depending only on the integral of the path, while Forman's theorem depends specifically on path boundary values. Finding such an approach would likely constitute the next meaningful step in this development.

Chapter 17

Exact Result for the Coherently Driven Harmonic Oscillator

17.1 Coherently Driven-Dissipative Harmonic Oscillator

The Hamiltonian of the system which we refer to as the Coherently Driven Harmonic Oscillator (the F and E terms may be viewed as a classical coherent drive) is

$$H_{\text{CDHO}} = \delta a^\dagger a + iE(a^\dagger - a) + F(a^\dagger + a). \tag{17.1}$$

Setting the Lindbladian jump operator as $L = a$, we first write the Lindbladian

$$\mathcal{L}\rho = -i[H_{\text{CDHO}}, \rho] + 2\kappa\left(a\rho a^\dagger - \frac{1}{2}\left(a^\dagger a\rho + \rho a^\dagger a\right)\right) \tag{17.2}$$

in our standard form[1]:

$$\mathcal{L} = -i\overrightarrow{H} + i\overleftarrow{H^\dagger} + \mathcal{R} + C, \tag{17.3}$$

$$H = (F + iE)a^\dagger + (F - iE)a + (\delta - i\kappa)aa^\dagger, \quad \mathcal{R} = 2\kappa\overrightarrow{a}\overleftarrow{a^\dagger}, \quad C = 2\kappa. \tag{17.4}$$

Setting $\omega = \delta + i\kappa$, $\Phi = F + iE$ and mapping $\langle\langle\psi_f|e^{T\mathcal{L}}|\psi_i\rangle\rangle$ into a path integral via our kernel, we obtain

$$\begin{aligned} S =& \frac{i}{2}\left(|\psi_i^+|^2 + |\psi_f^-|^2 - |\psi_f^+|^2 - |\psi_i^-|^2\right) \\ &+ \int dt \Bigg[i\epsilon\left(|\partial_t\psi_t^+|^2 + |\partial_t\psi_t^-|^2\right) + i\left(\bar{\psi}_t^+\partial_t\psi_t^+ - \bar{\psi}_t^-\partial_t\psi_t^-\right) \\ &\qquad - \bar{\omega}\bar{\psi}_t^+\psi_t^+ - \bar{\Phi}\psi_t^+ - \Phi\bar{\psi}_t^+ + \omega\bar{\psi}_t^-\psi_t^- + \Phi\bar{\psi}_t^- + \bar{\Phi}\psi_t^- - 2i\kappa\psi_t^+\bar{\psi}_t^- - 2i\kappa \Bigg]. \end{aligned} \tag{17.5}$$

[1] Recall the superoperator arrow notation of Sec.16.1.

For the purposes of finding the effective classical paths described in the last section, our effective action becomes

$$\begin{aligned} S =& \frac{i}{2}\left(|\psi_i^+|^2+|\psi_f^-|^2+|\psi_f^+|^2+|\psi_i^-|^2-2\phi_T^+\bar{\psi}_f^+-2\phi_0^-\bar{\psi}_i^-\right) \\ &+\int dt\Bigg[i\left(\tilde{\phi}_t^+\partial_t\phi_t^+-\tilde{\phi}_t^-\partial_t\phi_t^-\right) \\ &\qquad -\bar{\omega}\tilde{\phi}_t^+\phi_t^+-\bar{\Phi}\phi_t^+-\Phi\tilde{\phi}_t^++\omega\tilde{\phi}_t^-\phi_t^-+\Phi\tilde{\phi}_t^-+\bar{\Phi}\phi_t^--2i\kappa\phi_t^+\tilde{\phi}_t^--2i\kappa\Bigg]. \end{aligned} \tag{17.6}$$

Varying it with respect to ϕ_t yields[2] equations of motion

$$i\partial_t\phi_t^+-\bar{\omega}\phi_t^+-\Phi=0, \tag{17.7}$$

$$i\partial_t\tilde{\phi}_t^++\bar{\omega}\tilde{\phi}_t^++\bar{\Phi}+2i\kappa\tilde{\phi}_t^-=0, \tag{17.8}$$

$$i\partial_t\phi_t^--\omega\phi_t^--\Phi+2i\kappa\phi_t^+=0, \tag{17.9}$$

$$i\partial_t\tilde{\phi}_t^-+\omega\tilde{\phi}_t^-+\bar{\Phi}=0, \tag{17.10}$$

with $\phi_0^+=\psi_i^+$, $\tilde{\phi}_T^+=\bar{\psi}_f^+$, $\tilde{\phi}_0^-=\bar{\psi}_i^-$, $\phi_T^-=\psi_f^-$. Rewriting the action as

$$\begin{aligned} S =& \frac{i}{2}\left(|\psi_i^+|^2+|\psi_f^-|^2+|\psi_f^+|^2+|\psi_i^-|^2-\phi_T^+\bar{\psi}_f^+-\tilde{\phi}_0^+\psi_i^+-\phi_0^-\bar{\psi}_i^--\tilde{\phi}_T^-\psi_f^-\right) \\ &+\int dt\Bigg[\frac{i}{2}\left(\tilde{\phi}_t^+\partial_t\phi_t^+-\phi_t^+\partial_t\tilde{\phi}_t^+-\tilde{\phi}_t^-\partial_t\phi_t^-+\phi_t^-\partial_t\tilde{\phi}_t^-\right) \\ &\qquad -\bar{\omega}\tilde{\phi}_t^+\phi_t^+-\bar{\Phi}\phi_t^+-\Phi\tilde{\phi}_t^++\omega\tilde{\phi}_t^-\phi_t^-+\Phi\tilde{\phi}_t^-+\bar{\Phi}\phi_t^--2i\kappa\phi_t^+\tilde{\phi}_t^--2i\kappa\Bigg]. \end{aligned} \tag{17.11}$$

and substituting the effective classical solutions of the above equations yields

$$\begin{aligned} \langle\langle\psi_f|e^{T\mathcal{L}}|\psi_i\rangle\rangle =& e^{\frac{1}{2}\left(\phi_T^+\bar{\psi}_f^++\tilde{\phi}_0^+\psi_i^++\phi_0^-\bar{\psi}_i^-+\tilde{\phi}_T^-\psi_f^--|\psi_i^+|^2-|\psi_f^-|^2-|\psi_f^+|^2-|\psi_i^-|^2\right)} \\ &\cdot e^{\frac{i}{2}\int_0^T dt\left(\Phi\tilde{\phi}_t^-+\bar{\Phi}\phi_t^--\Phi\tilde{\phi}_t^+-\bar{\Phi}\phi_t^+\right)} \\ &\cdot e^{2\kappa T}\int\mathcal{D}[\delta\psi_t^+,\delta\bar{\psi}_t^+,\delta\psi_t^-,\delta\bar{\psi}_t^-]\,e^{iS_f[\{\delta\psi_t,\delta\bar{\psi}_t\}]} \end{aligned} \tag{17.12}$$

[2] Recall that this is a formal manipulation and we vary only the integral portion of the action.

where the last term is the quadratic fluctuation integral with

$$\begin{aligned} iS_f = \int dt \Big[& -\epsilon\left(|\partial_t \delta\psi_t^+|^2 + |\partial_t \delta\psi_t^-|^2\right) - \left(\delta\bar{\psi}_t^+ \partial_t \delta\psi_t^+ - \delta\bar{\psi}_t^- \partial_t \delta\psi_t^-\right) \\ & - i\bar{\omega}\delta\bar{\psi}_t^+ \delta\psi_t^+ + i\omega\delta\bar{\psi}_t^- \delta\psi_t^- + 2\kappa\delta\psi_t^+ \delta\bar{\psi}_t^- \Big] \\ = & -\int_0^T dt \begin{pmatrix} \delta\psi_r^+ \\ \delta\psi_i^+ \\ \delta\psi_r^- \\ \delta\psi_i^- \end{pmatrix}^T M \begin{pmatrix} \delta\psi_r^+ \\ \delta\psi_i^+ \\ \delta\psi_r^- \\ \delta\psi_i^- \end{pmatrix}, \end{aligned} \tag{17.13}$$

$$M = \Bigg[\underbrace{-\frac{\epsilon}{2}\begin{pmatrix} 1 & 0 & 0 & 0 \\ 0 & 1 & 0 & 0 \\ 0 & 0 & 1 & 0 \\ 0 & 0 & 0 & 1 \end{pmatrix}}_{P_0} \frac{d^2}{dt^2} + \underbrace{\begin{pmatrix} 0 & i & 0 & 0 \\ -i & 0 & 0 & 0 \\ 0 & 0 & 0 & -i \\ 0 & 0 & i & 0 \end{pmatrix}}_{P_1} \frac{d}{dt} + \underbrace{\begin{pmatrix} i\bar{\omega} & 0 & -\kappa & i\kappa \\ 0 & i\bar{\omega} & -i\kappa & -\kappa \\ -\kappa & -i\kappa & -i\omega & 0 \\ i\kappa & -\kappa & 0 & -i\omega \end{pmatrix}}_{P_1} \Bigg]. \tag{17.14}$$

The fluctuational integral thus comes down to evaluating the functional determinant of the operator M. Since $\det P_0 \neq 0$ and the boundary conditions are homogeneous Dirichlet, M is an elliptic operator and thus subject to Forman's theorem. Applying it (see Appendix C), the determinant is found to be $\det M = e^{4\kappa T}$, so that $(\det M)^{-\frac{1}{2}} = e^{-2\kappa T}$ perfectly cancels the factor that arose from the antinormal-ordering. We once again see that the quadratic fluctuations are critical for correctly taking account of the operator ordering.

The contribution from the classical path, which may be calculated exactly for this linear boundary problem, comes out to be

$$\begin{aligned} \langle\langle \psi_f | e^{T\mathcal{L}} | \psi_i \rangle\rangle = \exp\Bigg[& -\frac{1}{2}\left(|\psi_i^+|^2 + |\psi_f^+|^2 + |\psi_i^-|^2 + |\psi_f^-|^2\right) \\ & + \underbrace{e^{i(\omega-\bar{\omega})T}(e^{-i\omega T}-1)\frac{\bar{\Phi}}{\omega}}_{A(T)}\psi_i^+ + \underbrace{e^{i(\omega-\bar{\omega})T}(e^{i\bar{\omega}T}-1)\frac{\Phi}{\bar{\omega}}}_{B(T)}\bar{\psi}_i^- \\ & + \underbrace{(e^{-i\bar{\omega}T}-1)\frac{\Phi}{\bar{\omega}}}_{C(T)}\bar{\psi}_f^+ + \underbrace{(e^{i\omega T}-1)\frac{\bar{\Phi}}{\omega}}_{D(T)}\psi_f^- \\ & + \psi_i^+\bar{\psi}_f^+ e^{-i\bar{\omega}T} + \psi_f^-\bar{\psi}_i^- e^{i\omega T} + \psi_i^+\bar{\psi}_i^-(1-e^{i(\omega-\bar{\omega})T}) \\ & - C(T)D(T)\Bigg]. \end{aligned} \tag{17.15}$$

Here we have introduced the functions $A(t)$, $B(t)$, $C(t)$, $D(t)$ for convenience in

later perturbative treatments.

17.1.1 Spectrum of the Coherently Driven Harmonic Oscillator

The spectrum of the operator in this case may easily be extracted from the trace, since we know the propagator is exact. Noting that the trace has to be taken over all basis elements, not only diagonal ones, we must consider a double integral for $z = \psi_f^+ = \psi_i^+$, $u = \psi_f^- = \psi_i^-$:

$$\begin{aligned}
&\mathrm{Tr}\langle\langle\psi_f|e^{T\mathcal{L}}|\psi_i\rangle\rangle = \int d\psi\,\langle\langle\psi_f|e^{T\mathcal{L}}|\psi_i\rangle\rangle \\
&= \int d[\bar{z},z]d[\bar{u},u]\exp\Bigg[-\begin{pmatrix}z\\u\end{pmatrix}^\dagger\begin{pmatrix}1-e^{-i\bar{\omega}T} & 0\\ -1+e^{i(\omega-\bar{\omega})T} & 1-e^{i\omega T}\end{pmatrix}\begin{pmatrix}z\\u\end{pmatrix} \\
&\qquad\qquad + \begin{pmatrix}A(T)\\D(T)\end{pmatrix}^T\begin{pmatrix}z\\u\end{pmatrix} + \begin{pmatrix}z\\u\end{pmatrix}^\dagger\begin{pmatrix}C(T)\\B(T)\end{pmatrix} - C(T)D(T)\Bigg] \qquad (17.16)\\
&= \frac{1}{(1-e^{-i\bar{\omega}T})(1-e^{i\omega T})} \\
&= \frac{1}{(e^{i\delta T}-e^{-\kappa T})(e^{-i\delta T}-e^{-\kappa T})}.
\end{aligned}$$

Expanding this in a suitable series yields the sum of exponents of eigenvalues:

$$\begin{aligned}
\mathrm{Tr}\langle\langle\psi_f|e^{T\mathcal{L}}|\psi_i\rangle\rangle &= (1-e^{-\kappa T-i\delta T})^{-1}(1-e^{-\kappa T+i\delta T})^{-1} \\
&= \Big(\sum_{n=0}^{\infty}e^{-n(\kappa+i\delta)T}\Big)\Big(\sum_{m=0}^{\infty}e^{-m(\kappa-i\delta)T}\Big) \qquad (17.17)
\end{aligned}$$

from which we can read off the eigenvalues

$$\lambda_{m,n} = -n(\kappa+i\delta) - m(\kappa-i\delta) \quad \forall n,m\in\mathbb{N}_0. \qquad (17.18)$$

Checking this against the method of bosonic third quantisation [55] confirms that we have found the correct spectrum (the explicit final result in the cited paper appears to be missing $\lambda_{0,1}$ and $\lambda_{1,0}$, but the actual algebra in the paper and the fact our expression reduces to the known correct expression for $\kappa \to 0$ means they must be there). While we will not go to the effort of working out all the eigenvectors, we can easily identify the stationary state by taking $T \to \infty$. This

yields

$$\begin{aligned}\lim_{T\to\infty}\langle\langle\psi_f|e^{T\mathcal{L}}|\psi_i\rangle\rangle &= \exp\left[-\frac{1}{2}\left(|\psi_f^+|^2+|\psi_f^-|^2\right)-\frac{\Phi}{\bar\omega}\bar\psi_f^+-\frac{\bar\Phi}{\omega}\psi_f^- -\frac{|\Phi|^2}{|\omega|^2}\right]\\ &= \exp\left[-\frac{1}{2}\left(|\psi_f^+|^2+\frac{|\Phi|^2}{|\omega|^2}\right)-\frac{\Phi}{\bar\omega}\bar\psi_f^+\right]\exp\left[-\frac{1}{2}\left(\frac{|\Phi|^2}{|\omega|^2}+|\psi_f^-|^2\right)-\frac{\bar\Phi}{\omega}\psi_f^-\right]\\ &= \left\langle -\frac{\Phi}{\bar\omega}\middle|\psi_f^-\right\rangle\left\langle\psi_f^+\middle|-\frac{\Phi}{\bar\omega}\right\rangle.\end{aligned} \tag{17.19}$$

The steady state is thus

$$\left|-\frac{\Phi}{\bar\omega}\right\rangle\!\!\right\rangle = \left|-\frac{\Phi}{\bar\omega}\right\rangle\left\langle -\frac{\Phi}{\bar\omega}\right|. \tag{17.20}$$

This makes sense for the following reason. Our Lindbladian is invariant under the following inhomogeneous transformation [56]:

$$L \to L+\frac{\Phi}{\bar\omega}, \tag{17.21}$$

$$H_{\text{CDHO}} \to H_{\text{CDHO}} + i\kappa\frac{\Phi}{\bar\omega}a^\dagger - i\kappa\frac{\bar\Phi}{\omega}a. \tag{17.22}$$

Introducing $b = a+\frac{\Phi}{\bar\omega}$, our Lindbladian may be rewritten as (we can discard any real constants appearing in the Hamiltonian since they do not affect the resulting Lindbladian)

$$H = \delta b^\dagger b, \tag{17.23}$$

$$\mathcal{L}\rho = -i[H,\rho]+2\kappa\left(b\rho b^\dagger-\frac{1}{2}\left(b^\dagger b\rho+\rho b^\dagger b\right)\right). \tag{17.24}$$

Since $\|b^\dagger b\|\geq 0$, the zero energy ground state of the new Hamiltonian is the state annihilated by b, which is precisely $\left|-\frac{\Phi}{\bar\omega}\right\rangle$. At the same time, $\left|-\frac{\Phi}{\bar\omega}\right\rangle\left\langle-\frac{\Phi}{\bar\omega}\right|$ is clearly annihilated by the dissipative part of the Lindbladian, and these facts together mean $\mathcal{L}\left|-\frac{\Phi}{\bar\omega}\right\rangle\left\langle-\frac{\Phi}{\bar\omega}\right| = 0$ and thus it is the steady state.

While these spectral results are not new, with [55] providing a way to solve essentially any quadratic Lindbladian via a method known as 'third quantisation' and giving fairly general results, they demonstrate that the Lindbladian path integral propagator formalism is capable of correctly replicating them. Moreover, the process of obtaining them has highlighted how the Klauder-Daubechies formalism allows for full control of the operator ordering and the exact calculation of the associated functional determinant, showing that the resulting coherent state path integral is a well-behaved and controlled object. Finally, as far as I know the expression for the propagator itself is novel and in the next chapter we will put it to use to derive a path integral perturbative approach to finding spectra.

17.2 Incoherent and Parametric Drive

Having obtained an expression for the coherently driven harmonic oscillator, a reasonable next step would be to consider oscillators with incoherent (possessing an $L = a^\dagger$ jump operator) and parametric (possessing a Hamiltonian term $H_p = \lambda((a^\dagger)^2 + a^2)$) drive. Being able to derive the propagator for either one would yield an approximate propagator for the other, as they are connected by a Bogoliubov transformation up to terms that vanish in the rotating wave approximation [19].

In the time devoted to this project, unfortunately, I was not able to obtain tractable expression for the propagator of either oscillator. With the aid of Mathematica [57] formal expressions were obtainable for both the classical path contribution and fluctuational derivative, but were colossal in size and failed to simplify even with computer algebra. Moreover, taking the $\epsilon \to 0$ limit of the fluctuational determinant expression was infeasible under these circumstances. Thus, while these systems are in principle solvable exactly via the path integral, obtaining a useful expression this way seems difficult. In the next chapter we will obtain some perturbative results for the spectrum of both oscillators augmented with a further coherent drive.

Chapter 18

Perturbation Theory

18.1 Perturbative Evaluation of the Propagator

It is possible to obtain perturbative corrections to spectra of Lindbladians by perturbatively evaluating their associated propagator. This may be done knowing only the propagator for the coherently driven harmonic oscillator. For any perturbation of that oscillator's Lindbladian (recall it must be anti-normal ordered)

$$\mathcal{L}_{\text{pert}} = \mathcal{L}_{\text{CDHO}} + \chi l(a, a^\dagger), \tag{18.1}$$

the real part of the coherent state action for the associated Lindbladian will take the form

$$S = S_{\text{CDHO}} + \chi \int_0^T dt\, l(\psi_t^+, \bar{\psi}_t^+, \psi_t^-, \bar{\psi}_t^-). \tag{18.2}$$

Performing a perturbative expansion in χ of the propagator [10] amounts to taking the functional integral representation of it and Taylor-expanding the portion of the integrand exponential containing the perturbation to the action. Schematically ($t_0 = T$, $\psi(T) = \psi_f$)

$$\begin{aligned}
\langle\langle \psi_f | e^{T\mathcal{L}_{\text{pert}}} | \psi_i \rangle\rangle &= \int_{\psi_i}^{\psi_f} \mathcal{D}\psi\, e^{iS_{\text{CDHO}} + \chi \int dt\, l(\psi(t))} \\
&\sim \sum_{n=0}^{\infty} \chi^n \int_0^T dt_1 \ldots \int_0^{t_{n-1}} dt_n \int_{\psi_i}^{\psi_f} \mathcal{D}\psi\, e^{iS_{\text{CDHO}}} \prod_{j=1}^{n} l(\psi(t_j)) \\
&\sim \sum_{n=0}^{\infty} \chi^n \int_0^T dt_1 \int d\psi(t_1) \ldots \int_0^{t_{n-1}} dt_n \int d\psi(t_n) \\
&\qquad \cdot \langle\langle \psi(t_n) | e^{t_n \mathcal{L}_{\text{CDHO}}} | \psi_i \rangle\rangle \\
&\qquad \cdot \prod_{j=0}^{n-1} \langle\langle \psi(t_{n-j-1}) | e^{(t_{n-j-1} - t_{n-j})\mathcal{L}_{\text{CDHO}}} | \psi(t_{n-j}) \rangle\rangle l(\psi(t_{n-j})).
\end{aligned} \tag{18.3}$$

where I have omitted most indices and details of the notation to make clear the skeleton of the calculation. The final line is obtained by performing the unperturbed path integrals between the times at which the perturbing terms $f(\psi(t_j))$ appear to obtain unperturbed propagators, leaving integration only over the dynamical variables at those times. It is also important to keep in mind that this series will generally be asymptotic rather than convergent.

We may define the terms in this series recursively by the following scheme:

$$\langle\langle \psi_f | e^{T\mathcal{L}_{\text{pert}}} | \psi_i \rangle\rangle = \sum_{n=0}^{\infty} X_n[\psi_f; T], \tag{18.4}$$

$$X_0[\psi; t] = \langle\langle \psi | e^{t\mathcal{L}_{\text{CDHO}}} | \psi_i \rangle\rangle, \tag{18.5}$$

$$X_n[\psi; t] = \chi \int_0^t dt' \int d\psi' \langle\langle \psi | e^{(t-t')\mathcal{L}_{\text{CDHO}}} | \psi' \rangle\rangle l(\psi', \bar{\psi}') X_{n-1}[\psi'; t']. \tag{18.6}$$

This recursive structure will significantly simply some of our calculations.

Returning the forwards/backwards contour indices to our notation, the first order perturbation is

$$\chi \int_0^T dt \int \mathcal{D}[u, \bar{u}]\mathcal{D}[v, \bar{v}] \langle\langle \psi_f^+, \psi_f^- | e^{(T-t)\mathcal{L}_{\text{CDHO}}} | u, v \rangle\rangle l(u, \bar{u}, v, \bar{v}) \langle\langle u, v | e^{t\mathcal{L}_{\text{CDHO}}} | \psi_i^+, \psi_i^- \rangle\rangle, \tag{18.7}$$

while the second is given by

$$\begin{aligned} \chi^2 \int_0^T dt \int_0^t dt' \int & \mathcal{D}[u, \bar{u}]\mathcal{D}[v, \bar{v}]\mathcal{D}[w, \bar{w}]\mathcal{D}[x, \bar{x}] \\ & \cdot \langle\langle \psi_f^+, \psi_f^- | e^{(T-t)\mathcal{L}_{\text{CDHO}}} | w, x \rangle\rangle l(w, \bar{w}, x, \bar{x}) \\ & \cdot \langle\langle w, x | e^{(t-t')\mathcal{L}_{\text{CDHO}}} | u, v \rangle\rangle l(u, \bar{u}, v, \bar{v}) \\ & \cdot \langle\langle u, v | e^{t'\mathcal{L}_{\text{CDHO}}} | \psi_i^+, \psi_i^- \rangle\rangle. \end{aligned} \tag{18.8}$$

I will restrict the calculations in this chapter to the first two perturbative orders, though I will provide a general expression for a generating function for arbitrary order.

Begin by defining the auxiliary functions

$$A'_u(t) = A(t) + \bar{u} e^{-i\bar{\omega}t}, \tag{18.9}$$

$$B'_v(t) = B(t) + v e^{i\omega t}, \tag{18.10}$$

$$C'_w(t) = C(t) + w e^{-i\bar{\omega}t}, \tag{18.11}$$

$$D'_x(t) = D(t) + \bar{x} e^{i\omega t}. \tag{18.12}$$

This allows us to write

$$\begin{aligned}\langle\langle u,v|e^{(t-t')\mathcal{L}_{\mathrm{CDHO}}}|w,x\rangle\rangle = \exp\Bigg[\\ -\frac{1}{2}\begin{pmatrix}w\\x\end{pmatrix}^\dagger\begin{pmatrix}1 & 0\\ 2(e^{i(\omega-\bar\omega)(t-t')}-1) & 1\end{pmatrix}\begin{pmatrix}w\\x\end{pmatrix}+\begin{pmatrix}A'_u(t-t')\\0\end{pmatrix}^T\begin{pmatrix}w\\x\end{pmatrix}+\begin{pmatrix}w\\x\end{pmatrix}^\dagger\begin{pmatrix}0\\B'_v(t-t')\end{pmatrix} \\ -\frac{1}{2}\begin{pmatrix}u\\v\end{pmatrix}^\dagger\begin{pmatrix}1&0\\0&1\end{pmatrix}\begin{pmatrix}u\\v\end{pmatrix}+\begin{pmatrix}u\\v\end{pmatrix}^\dagger\begin{pmatrix}C(t-t')\\0\end{pmatrix}+\begin{pmatrix}0\\D(t-t')\end{pmatrix}\begin{pmatrix}u\\v\end{pmatrix}-C(t-t')D(t-t')\Bigg].\end{aligned} \tag{18.13}$$

Since the integrals over u, v, w, x here will be of the form of Gaussian moments, it is useful to combine terms of the above form in at each perturbation order into a single exponent. For first order perturbations we may then add source terms J_1, J_2, J_3, J_4 for u, $\bar u$, v, $\bar v$ to obtain the generating function $F_1(J_1,J_2,J_3,J_4)$, while for second order the additional source terms J_5, J_6, J_7, J_8 for w, $\bar w$, x, $\bar x$ are required to obtain $F_2(J_1,J_2,J_3,J_4,J_5,J_6,J_7,J_8)$. In general, at nth order there will be $4n$ source terms, with J_{1+4j}, J_{2+4j}, J_{3+4j}, J_{4+4j}, $1\le j\le n-1$, corresponding to $\psi^+(t_{n-j})$, $\bar\psi^+(t_{n-j})$, $\psi^-(t_{n-j})$, $\bar\psi^-(t_{n-j})$ respectively. Differentiation with respect to the source terms will then bring down the appropriate variables into the integral.

Because of the recursive structure outlined above, the most prudent way to do this is to define a helper kernel (compare to $\langle\langle u,v|e^{(t-t')\mathcal{L}_{\mathrm{CDHO}}}|w,x\rangle\rangle$)

$$\begin{aligned}K(J_1,J_2,J_3,J_4)[u,v,w,x;t,t'] = \exp\Bigg[\\ -\frac{1}{2}\begin{pmatrix}w\\x\end{pmatrix}^\dagger\begin{pmatrix}1 & 0\\ 2(e^{i(\omega-\bar\omega)(t-t')}-1) & 1\end{pmatrix}\begin{pmatrix}w\\x\end{pmatrix}+\begin{pmatrix}A'_u(t-t')+J_1\\J_3\end{pmatrix}^T\begin{pmatrix}w\\x\end{pmatrix}+\begin{pmatrix}w\\x\end{pmatrix}^\dagger\begin{pmatrix}J_2\\B'_v(t-t')+J_4\end{pmatrix} \\ -\frac{1}{2}\begin{pmatrix}u\\v\end{pmatrix}^\dagger\begin{pmatrix}1&0\\0&1\end{pmatrix}\begin{pmatrix}u\\v\end{pmatrix}+\begin{pmatrix}u\\v\end{pmatrix}^\dagger\begin{pmatrix}C(t-t')\\0\end{pmatrix}+\begin{pmatrix}0\\D(t-t')\end{pmatrix}\begin{pmatrix}u\\v\end{pmatrix}-C(t-t')D(t-t')\Bigg],\end{aligned} \tag{18.14}$$

in terms of which we may write (compare to the recursive structure for the perturbation series terms)

$$F_0()[u,v,w,x;t_1] = \langle\langle u,v|e^{t_1\mathcal{L}_{\mathrm{CDHO}}}|w,x\rangle\rangle, \tag{18.15}$$

$$\begin{aligned}&F_n(J_1\dots J_{4n})[u,v,w,x;t_1,\dots,t_{n+1}]\Big|_{J=0} \\ &= \int d[y,\bar y]d[z,\bar z]\,K(J_{4n-3},J_{4n-2},J_{4n-1},J_{4n})[u,v,y,z;t_1,t_2] \\ &\qquad\qquad \cdot F_{n-1}(J_1\dots J_{4(n-1)})[y,z,w,x;t_2,\dots,t_{n+1}].\end{aligned} \tag{18.16}$$

Then

$$\int d[u,\bar{u}]d[v,\bar{v}]\langle\langle\psi_f^+,\psi_f^-|e^{(T-t)\mathcal{L}_{\mathrm{CDHO}}}|u,v\rangle\rangle u^a\bar{u}^b v^c\bar{v}^d\langle\langle u,v|e^{t\mathcal{L}_{\mathrm{CDHO}}}|\psi_i^+,\psi_i^-\rangle\rangle \quad (18.17)$$

may be obtained from the first generating function as

$$\partial^a_{J_1}\partial^b_{J_2}\partial^c_{J_3}\partial^d_{J_4}F_1(J_1,J_2,J_3,J_4)[\psi_f^+,\psi_f^-,\psi_i^+,\psi_i^-;T,t]\Big|_{J=0}, \quad (18.18)$$

while

$$\begin{aligned}\int d[u,\bar{u}]d[v,\bar{v}]d[w,\bar{w}]d[x,\bar{x}]\langle\langle\psi_f^+,\psi_f^-|e^{(T-t)\mathcal{L}_{\mathrm{CDHO}}}|w,x\rangle\rangle w^e\bar{w}^f x^g\bar{x}^h \\ \cdot\langle\langle w,x|e^{(t-t')\mathcal{L}_{\mathrm{CDHO}}}|u,v\rangle\rangle u^a\bar{u}^b v^c\bar{v}^d\langle\langle u,v|e^{t'\mathcal{L}_{\mathrm{CDHO}}}|\psi_i^+,\psi_i^-\rangle\rangle\end{aligned} \quad (18.19)$$

is given by

$$\partial^a_{J_1}\partial^b_{J_2}\partial^c_{J_3}\partial^d_{J_4}\partial^e_{J_5}\partial^f_{J_6}\partial^g_{J_7}\partial^h_{J_8}F_2(J_1,J_2,J_3,J_4,J_5,J_6,J_7,J_8)[\psi_f^+,\psi_f^-,\psi_i^+,\psi_i^-;T,t,t']\Big|_{J=0}. \quad (18.20)$$

The Gaussian integrals involved are comparatively simple, and we may avoid work by first calculating the first order generating function

$$\begin{aligned}&F_1(J_1,J_2,J_3,J_4)[\psi_f^+,\psi_f^-,\psi_i^+,\psi_i^-;T,t]\\
&=\int d[u,\bar{u}]d[v,\bar{v}]\,K(J_1,J_2,J_3,J_4)[\psi_f^+,\psi_f^-,u,v;T,t]\langle\langle u,v|e^{t\mathcal{L}_{\mathrm{CDHO}}}|\psi_i^+,\psi_i^-\rangle\rangle\\
&=\int d[u,\bar{u}]d[v,\bar{v}]\exp\Bigg[-C(t)D(t)-C(T-t)D(T-t)\\
&-\begin{pmatrix}u\\v\end{pmatrix}^\dagger\begin{pmatrix}1 & 0\\(e^{i(\omega-\bar{\omega})(T-t)}-1) & 1\end{pmatrix}\begin{pmatrix}u\\v\end{pmatrix}+\begin{pmatrix}A'(T-t)+J_1\\D'(t)+J_3\end{pmatrix}^T\begin{pmatrix}u\\v\end{pmatrix}+\begin{pmatrix}u\\v\end{pmatrix}^\dagger\begin{pmatrix}C'(t)+J_2\\B'(T-t)+J_4\end{pmatrix}\\
&-\frac{1}{2}\begin{pmatrix}\psi_f^+\\\psi_f^-\end{pmatrix}^\dagger\begin{pmatrix}1 & 0\\0 & 1\end{pmatrix}\begin{pmatrix}\psi_f^+\\\psi_f^-\end{pmatrix}+\begin{pmatrix}\psi_f^+\\\psi_f^-\end{pmatrix}^\dagger\begin{pmatrix}C(T-t)\\0\end{pmatrix}+\begin{pmatrix}0\\D(T-t)\end{pmatrix}\begin{pmatrix}\psi_f^+\\\psi_f^-\end{pmatrix}\\
&-\frac{1}{2}\begin{pmatrix}\psi_i^+\\\psi_i^-\end{pmatrix}^\dagger\begin{pmatrix}1 & 0\\2(e^{i(\omega-\bar{\omega})t}-1) & 1\end{pmatrix}\begin{pmatrix}\psi_i^+\\\psi_i^-\end{pmatrix}+\begin{pmatrix}\psi_i^+\\\psi_i^-\end{pmatrix}^\dagger\begin{pmatrix}0\\B(t)\end{pmatrix}+\begin{pmatrix}A(t)\\0\end{pmatrix}\begin{pmatrix}\psi_i^+\\\psi_i^-\end{pmatrix}\Bigg]\end{aligned} \quad (18.21)$$

which comes out to

$$\begin{aligned}\exp\Bigg[&\begin{pmatrix} A'_{\psi_f^+}(T-t)+J_1 \\ D'_{\psi_i^-}(t)+J_3 \end{pmatrix}^T \begin{pmatrix} 1 & 0 \\ (1-e^{i(\omega-\bar\omega)(T-t)}) & 1 \end{pmatrix}\begin{pmatrix} C'_{\psi_i^+}(t)+J_2 \\ B'_{\psi_f^-}(T-t)+J_4 \end{pmatrix}+ \\ &-\frac{1}{2}\begin{pmatrix}\psi_f^+\\ \psi_f^-\end{pmatrix}^\dagger\begin{pmatrix}1&0\\0&1\end{pmatrix}\begin{pmatrix}\psi_f^+\\ \psi_f^-\end{pmatrix}+\begin{pmatrix}\psi_f^+\\ \psi_f^-\end{pmatrix}^\dagger\begin{pmatrix}C(T-t)\\0\end{pmatrix}+\begin{pmatrix}0\\D(T-t)\end{pmatrix}\begin{pmatrix}\psi_f^+\\ \psi_f^-\end{pmatrix} \\ &-\frac{1}{2}\begin{pmatrix}\psi_i^+\\ \psi_i^-\end{pmatrix}^\dagger\begin{pmatrix}1&0\\2(e^{i(\omega-\bar\omega)t}-1)&1\end{pmatrix}\begin{pmatrix}\psi_i^+\\ \psi_i^-\end{pmatrix}+\begin{pmatrix}\psi_i^+\\ \psi_i^-\end{pmatrix}^\dagger\begin{pmatrix}0\\B(t)\end{pmatrix}+\begin{pmatrix}A(t)\\0\end{pmatrix}\begin{pmatrix}\psi_i^+\\ \psi_i^-\end{pmatrix} \\ &-C(t)D(t)-C(T-t)D(T-t)\Bigg].\end{aligned} \tag{18.22}$$

It is clear that for all Js equal to zero this reduces to the CDHO propagator, so we may write

$$\begin{aligned}F_1(J_1,J_2,J_3,J_4)[\psi_f^+,\psi_f^-,\psi_i^+,\psi_i^-;T,t] =&\langle\langle\psi_f^+,\psi_f^-|e^{T\mathcal{L}_{\text{CDHO}}}|\psi_i^+,\psi_i^-\rangle\rangle\Lambda(J_1,J_2,J_3,J_4)[T,t] \\ &\cdot H(J_2,J_3)[\psi_f^+,\psi_f^-;T,t] \\ &\cdot C(J_1,J_2,J_3,J_4)[\psi_i^+,\psi_i^-;T,t].\end{aligned} \tag{18.23}$$

$$f(t,t') = (1-e^{i(\omega-\bar\omega)(t-t')})e^{-i\bar\omega t'}, \tag{18.24}$$

$$g(t,t') = (1-e^{i(\omega-\bar\omega)(t-t')})e^{i\omega t'}, \tag{18.25}$$

$$H(J_a,J_b)[u,v;t,t'] = \exp\left[\bar u e^{-i\bar\omega(t-t')}J_a + v e^{i\omega(t-t')}J_b\right], \tag{18.26}$$

$$C(J_a,J_b,J_c,J_d)[u,v;t,t'] = \exp\left[u(J_a e^{-i\bar\omega t'} + f(t,t')J_c) + \bar v(e^{i\omega t'}J_d + g(t,t')J_b)\right] \tag{18.27}$$

$$\begin{aligned}\Lambda(J_a,J_b,J_c,J_d)[t,t'] = \exp\Big[&A(t-t')J_b + C(t')J_a + J_aJ_b \\ &+(1-e^{i(\omega-\bar\omega)(t-t')})(C(t')J_c + D(t')J_b + J_bJ_c) \\ &+B(t-t')J_c + D(t')J_d + J_cJ_d\Big].\end{aligned} \tag{18.28}$$

More generally, the above result is easily extrapolated[1] to

$$\begin{aligned}
&\int d[u,\bar{u}]d[v,\bar{v}]\,K(J_a,J_b,J_c,J_d)[u,v,y,z;t_{n-1},t_n] \\
&\qquad\qquad \cdot\langle\langle y,z|e^{t_n\mathcal{L}_{\mathrm{CDHO}}}|\psi_i^+,\psi_i^-\rangle\rangle H(J_e,J_f)[y,z;t_n,t_{n+1}] \\
&=\Lambda(J_a,J_b',J_c',J_d)[t_{n-1},t_n]C(J_a,J_b',J_c',J_d)[\psi_i^+,\psi_i^-;t_{n-1},t_n] \\
&\quad\langle\langle u,v|e^{t_{n-1}\mathcal{L}_{\mathrm{CDHO}}}|\psi_i^+,\psi_i^-\rangle\rangle H(J_b',J_c')[u,v;t_{n-1},t_n],
\end{aligned} \tag{18.29}$$

$$J_b' = J_b + e^{-i\bar{\omega}(t_n-t_{n+1})}J_e, \quad J_c' = J_c + e^{i\omega(t_n-t_{n+1})}J_f, \tag{18.30}$$

which means that, by repeatedly applying (18.16) starting from F_1, we find that ($t_0 = T$):

$$\begin{aligned}
&F_n(J_1\ldots J_{4n})[\psi_f^+,\psi_f^-,\psi_i^+,\psi_i^-;T,t_1,\ldots,t_n]\Big|_{J=0} \\
&=\langle\langle\psi_f^+,\psi_f^-|e^{T\mathcal{L}_{\mathrm{CDHO}}}|\psi_i^+,\psi_i^-\rangle\rangle H(M_{n,4n-2},M_{n,4n-1})[\psi_f^+,\psi_f^-;T,t1] \\
&\quad\cdot\prod_{i=0}^{n-1}\Lambda(J_{1+4i},M_{n,2+4i},M_{n,3+4i},J_{4+4i})[t_{n-i-1},t_{n-i}] \\
&\qquad\cdot C(J_{1+4i},M_{n,2+4i},M_{n,3+4i},J_{4+4i})[\psi_i^+,\psi_i^-;t_{n-i-1},t_{n-i}],
\end{aligned} \tag{18.31}$$

where, for $j \geq 1$,

$$M_{n,4j-2} = J_{4j-2} + e^{-i\bar{\omega}(t_{n-j+1}-t_{n-j+2})}M_{4(j-1)-2}, \tag{18.32}$$

$$M_{n,4j-1} = J_{4j-1} + e^{i\omega(t_{n-j+1}-t_{n-j+2})}M_{4(j-1)-1}, \tag{18.33}$$

$$M_{n,2} = J_2, \tag{18.34}$$

$$M_{n,3} = J_3. \tag{18.35}$$

Armed with this expression and a symbolic computation tool like [57] it is possible to perform perturbative calculations to fairly high orders if desired.

To calculate the spectrum of a Lindbladian, our usual approach is to take the trace of its associated propagator. The generating functions for the asymptotic series terms of this trace are simply the traces of the generating functions for the

[1] Replacing T, t by t_{n-1}, t_n, ψ_f^+, ψ_f^- by u, v, and redefining Js by absorbing the H term yields this result from the one above it.

propagator series:

$$
\begin{aligned}
&T_n(J_1 \dots J_{4n})[T, t_1, \dots, t_n] = \mathrm{Tr}\Big[F_n(J_1 \dots J_{4n})[\psi_f^+, \psi_f^-, \psi_i^+, \psi_i^-; T, t_1, \dots, t_n]\Big] \\
&= \mathrm{Tr}\Bigg[\langle\langle \psi_f^+, \psi_f^- | e^{T\mathcal{L}_{\mathrm{CDHO}}} | \psi_i^+, \psi_i^- \rangle\rangle H(M_{n,4n-2}, M_{n,4n-1})[\psi_f^+, \psi_f^-; T, t1] \\
&\quad \cdot \prod_{i=0}^{n-1} C(J_{1+4i}, M_{n,2+4i}, M_{n,3+4i}, J_{4+4i})[\psi_i^+, \psi_i^-; t_{n-i-1}, t_{n-i}]\Bigg] \\
&\quad \cdot \prod_{i=0}^{n-1} \Lambda(J_{1+4i}, M_{n,2+4i}, M_{n,3+4i}, J_{4+4i})[t_{n-i-1}, t_{n-i}]. \\
&= \int d[\psi, \bar{\psi}] d[\phi, \bar{\phi}] \Bigg[\langle\langle \psi, \phi | e^{T\mathcal{L}_{\mathrm{CDHO}}} | \psi, \phi \rangle\rangle \\
&\quad \cdot \exp\left(\begin{pmatrix} \psi \\ \phi \end{pmatrix}^\dagger \begin{pmatrix} e^{-i\bar{\omega}(T-t_1)} M_{n,4n-2} \\ \sum_{i=0}^{n-1} \left[J_{4+4i} e^{i\omega t_{n-i}} + g(t_{n-i-1}, t_{n-i}) M_{2+4i}\right] \end{pmatrix}\right) \\
&\quad \cdot \exp\left(\begin{pmatrix} \sum_{i=0}^{n-1} J_{1+4i} e^{-i\bar{\omega} t_{n-i}} + f(t_{n-i-1}, t_{n-i}) M_{3+4i} \\ e^{i\omega(T-t_1)} M_{n,4n-1} \end{pmatrix}^T \begin{pmatrix} \psi \\ \phi \end{pmatrix}\right)\Bigg] \\
&\quad \cdot \prod_{i=0}^{n-1} \Lambda(J_{1+4i}, M_{n,2+4i}, M_{n,3+4i}, J_{4+4i})[t_{n-i-1}, t_{n-i}]
\end{aligned}
\tag{18.36}
$$

This final trace integral is Gaussian and may be done exactly. Denoting

$$W_n = e^{-i\bar{\omega}(T-t_1)} M_{n,4n-2}, \tag{18.37}$$

$$X_n = e^{i\omega(T-t_1)} M_{n,4n-1}, \tag{18.38}$$

$$Y_n = \sum_{i=0}^{n-1} J_{1+4i} e^{-i\bar{\omega} t_{n-i}} + f(t_{n-i-1}, t_{n-i}) M_{n,3+4i}, \tag{18.39}$$

$$Z_n = \sum_{i=0}^{n-1} J_{4+4i} e^{i\omega t_{n-i}} + g(t_{n-i-1}, t_{n-i}) M_{n,2+4i}, \tag{18.40}$$

$$\mathcal{M} = \begin{pmatrix} 1 + \frac{1}{-1+e^{iT\bar{\omega}}} & 0 \\ \frac{i}{2}\left(\cot\left(\frac{\omega T}{2}\right) - \cot\left(\frac{\bar{\omega} T}{2}\right)\right) & \frac{1}{1-e^{i\omega T}} \end{pmatrix} \tag{18.41}$$

we finally have

$$
\begin{aligned}
&T_n(J_1 \dots J_{4n})[T, t_1, \dots, t_n] = \\
&\frac{1}{(1 - e^{-i\bar{\omega}T})(1 - e^{i\omega T})} \exp\left(\begin{pmatrix} Y_n + A(T) \\ X_n + D(T) \end{pmatrix} \mathcal{M} \begin{pmatrix} W_n + C(T) \\ Z_n + B(T) \end{pmatrix} - C(T)D(T)\right) \\
&\cdot \prod_{i=0}^{n-1} \Lambda(J_{1+4i}, M_{n,2+4i}, M_{n,3+4i}, J_{4+4i})[t_{n-i-1}, t_{n-i}].
\end{aligned}
\tag{18.42}
$$

To extract the eigenvalue correction from this, we consider the symbolic expression for the traced propagator in terms of its spectrum (we assume a unique

steady state):

$$\int d[u,\bar{u}]d[v,\bar{v}]\langle\langle u,v|e^{T\mathcal{L}_\chi}|u,v\rangle\rangle = 1+\sum_{n=1}^{\infty}(e^{\lambda_n(\chi)T}+e^{\bar{\lambda}_n(\chi)T}). \tag{18.43}$$

Were we to assume that this expression is analytic in χ, the linear change would be

$$\begin{aligned}&\chi\cdot\partial_\chi\left[\int d[u,\bar{u}]d[v,\bar{v}]\langle\langle u,v|e^{T\mathcal{L}_\chi}|u,v\rangle\rangle\right]_{\chi=0}\\&=T\chi\cdot\sum_{n=1}^{\infty}\left(\left[\frac{\partial\lambda_n(\chi)}{\partial\chi}\right]_{\chi=0}e^{\lambda_n(0)T}+\left[\frac{\partial\bar{\lambda}_n(\chi)}{\partial\chi}\right]_{\chi=0}e^{\bar{\lambda}_n(0)T}\right).\end{aligned} \tag{18.44}$$

We can rewrite this in terms of the real and imaginary parts of the eigenvalues as

$$\begin{aligned}T\chi\cdot\sum_{n=1}^{\infty}2e^{\mathrm{Re}[\lambda_n(0)]T}\Bigg(&\cos(T\,\mathrm{Im}[\lambda_n(0)])\,\mathrm{Re}\left[\frac{\partial\lambda_n(\chi)}{\partial\chi}\right]_{\chi=0}\\&-\sin(T\,\mathrm{Im}[\lambda_n(0)])\,\mathrm{Im}\left[\frac{\partial\lambda_n(\chi)}{\partial\chi}\right]_{\chi=0}\Bigg).\end{aligned} \tag{18.45}$$

Taking λ_1 to have the largest real part, for $T\to\infty$ this expression will tend to just

$$\begin{aligned}T\chi\cdot 2e^{\mathrm{Re}[\lambda_1(0)]T}\Bigg(&\cos(T\,\mathrm{Im}[\lambda_1(0)])\,\mathrm{Re}\left[\frac{\partial\lambda_1(\chi)}{\partial\chi}\right]_{\chi=0}\\&-\sin(T\,\mathrm{Im}[\lambda_1(0)])\,\mathrm{Im}\left[\frac{\partial\lambda_1(\chi)}{\partial\chi}\right]_{\chi=0}\Bigg).\end{aligned} \tag{18.46}$$

The quadratic change, meanwhile, comes out to

$$\begin{aligned}&\frac{\chi^2}{2}\cdot\partial_\chi^2\left[\int d[u,\bar{u}]d[v,\bar{v}]\langle\langle u,v|e^{T\mathcal{L}_\chi}|u,v\rangle\rangle\right]_{\chi=0}\\&=T\frac{\chi^2}{2}\cdot\sum_{n=1}^{\infty}\left(\left[\frac{\partial^2\lambda_n(\chi)}{\partial\chi^2}\right]_{\chi=0}e^{\lambda_n(0)T}+\left[\frac{\partial^2\bar{\lambda}_n(\chi)}{\partial\chi^2}\right]_{\chi=0}e^{\bar{\lambda}_n(0)T}\right)\\&\quad+T^2\frac{\chi^2}{2}\cdot\sum_{n=1}^{\infty}\left(\left[\frac{\partial\lambda_n(\chi)}{\partial\chi}\right]^2_{\chi=0}e^{\lambda_n(0)T}+\left[\frac{\partial\bar{\lambda}_n(\chi)}{\partial\chi}\right]^2_{\chi=0}e^{\bar{\lambda}_n(0)T}\right),\end{aligned} \tag{18.47}$$

which again may be rewritten in terms of the real and imaginary parts of the

eigenvalues:

$$\begin{aligned} T\chi^2 \cdot \sum_{n=1}^{\infty} e^{\mathrm{Re}[\lambda_n(0)]T} \Bigg(& \cos(T\,\mathrm{Im}[\lambda_n(0)])\,\mathrm{Re}\left[\frac{\partial^2 \lambda_n(\chi)}{\partial \chi^2}\right]_{\chi=0} \\ & -\sin(T\,\mathrm{Im}[\lambda_n(0)])\,\mathrm{Im}\left[\frac{\partial^2 \lambda_n(\chi)}{\partial \chi^2}\right]_{\chi=0}\Bigg) \\ +T^2\chi^2 \cdot \sum_{n=1}^{\infty} e^{\mathrm{Re}[\lambda_n(0)]T} \Bigg(& \cos(T\,\mathrm{Im}[\lambda_n(0)])\,\mathrm{Re}\left[\left(\frac{\partial \lambda_n(\chi)}{\partial \chi}\right)^2\right]_{\chi=0} \\ & -\sin(T\,\mathrm{Im}[\lambda_n(0)])\,\mathrm{Im}\left[\left(\frac{\partial \lambda_n(\chi)}{\partial \chi}\right)^2\right]_{\chi=0}\Bigg). \end{aligned} \tag{18.48}$$

With λ_1 having the largest real part, for $T \to \infty$ this expression will tend to

$$\begin{aligned} T\chi^2 e^{\mathrm{Re}[\lambda_1(0)]T} \Bigg(& \cos(T\,\mathrm{Im}[\lambda_1(0)])\,\mathrm{Re}\left[\frac{\partial^2 \lambda_1(\chi)}{\partial \chi^2}\right]_{\chi=0} \\ & -\sin(T\,\mathrm{Im}[\lambda_1(0)])\,\mathrm{Im}\left[\frac{\partial^2 \lambda_1(\chi)}{\partial \chi^2}\right]_{\chi=0}\Bigg) \\ +T^2\chi^2 e^{\mathrm{Re}[\lambda_1(0)]T} \Bigg(& \cos(T\,\mathrm{Im}[\lambda_1(0)])\,\mathrm{Re}\left[\left(\frac{\partial \lambda_1(\chi)}{\partial \chi}\right)^2\right]_{\chi=0} \\ & -\sin(T\,\mathrm{Im}[\lambda_1(0)])\,\mathrm{Im}\left[\left(\frac{\partial \lambda_1(\chi)}{\partial \chi}\right)^2\right]_{\chi=0}\Bigg). \end{aligned} \tag{18.49}$$

By matching these results against terms in our perturbation series, we should be able to extract derivatives of the eigenvalues with respect to χ. Note that, since we are using the coherently driven harmonic oscillator as the basis for our perturbation method, we have $\mathfrak{Re}[\lambda_1(0)] = -\kappa$ and $\mathfrak{Im}[\lambda_1(0)] = i\delta$. We may now consider the linear and quadratic corrections to the spectra of some systems.

18.2 Spectra Calculations

We will consider four systems, namely the parametrically driven oscillator, an anti-normal ordered Kerr oscillator, an incoherently driven oscillator, and an oscillator with ternary dissipation. The first of these are Hamiltonian systems with linear dissipation of strength 2κ, so we may compare our results against those obtained for linear dissipation systems with a truncated Fock basis in [58]. Specifically, it was found there that if the Hamiltonian has spectrum E_n, the spectrum of the corresponding truncated Lindbladian with our linear dissipation strength should be

$$\lambda_{n,m} = -i(E_n - E_m) - \kappa(n+m), \quad n, m \in \mathcal{N}_0. \tag{18.50}$$

We will find that our results agree with this result, suggesting that our perturbation theory captures a similar portion of the true result to truncating the Fock basis.

18.2.1 Parametrically Driven Harmonic Oscillator

We will take the parametrically driven harmonic oscillator to be the coherently driven harmonic oscillator with a Hamiltonian perturbed by

$$H_{CDHO} \to H_{CDHO} + \chi((a^\dagger)^2 + a^2). \tag{18.51}$$

This corresponds to the following perturbation to the action (from now on we absorb the perturbation coefficient into l):

$$\delta S = \int_0^T dt\, l(\psi_t^+, \bar{\psi}_t^+, \psi_t^-, \bar{\psi}_t^-), \tag{18.52}$$

$$l(\psi_t^+, \bar{\psi}_t^+, \psi_t^-, \bar{\psi}_t^-) = i\chi\left[(\psi_t^-)^2 + (\bar{\psi}_t^-)^2 - (\psi_t^+)^2 - (\bar{\psi}_t^+)^2\right]. \tag{18.53}$$

Applying the theory from the previous section, we find the following first and second order perturbations to the trace of the propagator:

$$\chi : i\chi \int_0^T dt \left(\partial_{J_3}^2 + \partial_{J_4}^2 - \partial_{J_1}^2 - \partial_{J_2}^2\right) T_1(J_1, \ldots, J_4)[T, t] = 0, \tag{18.54}$$

$$\begin{aligned}\chi^2 : -\chi^2 \int_0^T dt_1 \int_0^{t_1} dt_2 \left(\partial_{J_7}^2 + \partial_{J_8}^2 - \partial_{J_5}^2 - \partial_{J_6}^2\right)\left(\partial_{J_3}^2 + \partial_{J_4}^2 - \partial_{J_3}^2 - \partial_{J_4}^2\right) \\ \cdot T_2(J_1, \ldots, J_8)[T, t_1, t_2] \\ = \frac{\chi^2 T e^{\kappa T} \sin(\delta T)}{\delta\left(\cos(\delta T) - \cosh(\kappa T)\right)^2}.\end{aligned} \tag{18.55}$$

There is thus no linear correction to any of the eigenvalues, while taking $T \to \infty$ and using (18.49) suggests that the quadratic corrections to the non-zero eigenvalues with largest real part are

$$\lambda_1 \to \lambda_1 - \frac{2i\chi^2}{\delta} = -\kappa + i\left(\delta - \frac{2\chi^2}{\delta}\right), \tag{18.56}$$

$$\bar{\lambda}_1 \to \bar{\lambda}_1 - \frac{2i\chi^2}{\delta} = -\kappa - i\left(\delta - \frac{2\chi^2}{\delta}\right). \tag{18.57}$$

When the parametrically driven oscillator is stable, the spectrum for $\Phi = 0$ is easily found by a Bogoliubov transformation [19] to be $E_n = n\sqrt{\delta^2 - 4\chi^2}$, so for a truncated Fock basis the expected spectrum would be

$$\lambda_{n,m} = -i(n-m)\sqrt{\delta^2 - 4\chi^2} - \kappa(n+m). \tag{18.58}$$

The two non-zero eigenvalues with largest real part would be $\lambda_{1,0} = -i\sqrt{\delta^2 - 4\chi^2} - \kappa$ and $\lambda_{0,1} = i\sqrt{\delta^2 - 4\chi^2} - \kappa$, and it is easy to check that their series expansions in χ match our result. Based on the perturbative result, the Φ terms appear to again not affect the spectrum.

18.2.2 Antinormal Kerr Oscillator

We will consider an antinormal-ordered Kerr perturbation of the Hamiltonian $\chi a^2 (a^\dagger)^2$. This is partly because it is neater for our antinormal formalism, but also because unlike its normal-ordered counterpart it generates non-zero corrections to the leading eigenvalues. Thus

$$\delta S = \int_0^T dt\, l(\psi_t^+, \bar{\psi}_t^+, \psi_t^-, \bar{\psi}_t^-), \tag{18.59}$$

$$l(\psi_t^+, \bar{\psi}_t^+, \psi_t^-, \bar{\psi}_t^-) = i\chi\left[(\psi_t^-)^2(\bar{\psi}_t^-)^2 - (\psi_t^+)^2(\bar{\psi}_t^+)^2\right], \tag{18.60}$$

and first order correction is given by

$$\begin{aligned} &i\chi \int_0^T dt\, (\partial_{J_3}^2 \partial_{J_4}^2 - \partial_{J_1}^2 \partial_{J_2}^2) T(J_1, \ldots, J_4)[T, t] \\ &= \frac{T\chi e^{\kappa T} \sin(\delta T)\left(\left(\delta^2 + \kappa^2\right)\sinh(\kappa T) - \left(\delta^2 + 2F^2 + \kappa^2 + 2E^2\right)(\cos(\delta T) - \cosh(\kappa T))\right)}{(\delta^2 + \kappa^2)(\cos(\delta T) - \cosh(\kappa T))^3}. \end{aligned} \tag{18.61}$$

while the second order one is too cumbersome to fruitfully write down.

Once again matching this against our expression for the series expansion of the trace in χ, we obtain

$$\mathfrak{Re}\left[\frac{\partial \lambda_1(\chi)}{\partial \chi}\right]_{\chi=0} = 0, \tag{18.62}$$

$$\mathfrak{Im}\left[\frac{\partial \lambda_1(\chi)}{\partial \chi}\right]_{\chi=0} = \frac{4\left(\delta^2 + F^2 + \kappa^2 + E^2\right)}{\delta^2 + \kappa^2}, \tag{18.63}$$

$$\mathfrak{Re}\left[\frac{\partial^2 \lambda_1(\chi)}{\partial \chi^2}\right]_{\chi=0} = -\frac{16\kappa\left(F^2 + E^2\right)}{\left(\delta^2 + \kappa^2\right)^2}, \tag{18.64}$$

$$\mathfrak{Im}\left[\frac{\partial^2 \lambda_1(\chi)}{\partial \chi^2}\right]_{\chi=0} = -\frac{4\left(F^2 + E^2\right)\left(20\delta^4 + \delta^2\left(20\kappa^2 + 9E^2\right) + F^2\left(9\delta^2 + \kappa^2\right) + \kappa^2 E^2\right)}{\delta\left(\delta^2 + \kappa^2\right)^3}. \tag{18.65}$$

Thus our perturbative analysis suggests that:

$$\begin{aligned}\lambda_1 =& -\kappa\left(1+\chi^2\frac{8\left(F^2+E^2\right)}{\left(\delta^2+\ \kappa^2\right)^2}\right)\\ &+i\Bigg(\delta+\chi\frac{4\left(\delta^2+F^2+\kappa^2+E^2\right)}{\delta^2+\kappa^2}\\ &\quad-\chi^2\frac{2\left(F^2+E^2\right)\left(20\delta^4+\delta^2\ \left(20\kappa^2+9E^2\right)+F^2\left(9\delta^2+\kappa^2\right)+\kappa^2E^2\right)}{\delta\left(\delta^2+\kappa^2\right)^3}\Bigg).\end{aligned} \tag{18.66}$$

We see that in this case the $\Phi = F + iE$ terms do affect the spectrum. We may once again check whether the result is reasonable by considering the spectrum predicted in the absence of the Φ terms by the truncated Fock basis method. The Hamiltonian

$$\delta a^\dagger a + \chi a^2 (a^\dagger)^2 \tag{18.67}$$

may be rearranged via commutation into (I drop constant terms as these cancel out in the Lindbladian, and define $n = a^\dagger a$)

$$\delta n + 3\chi n + \chi n^2. \tag{18.68}$$

The first non-zero eigenvalue of this is $\delta + 4\chi$, so that the truncated method predicts the non-zero eigenvalues of the Lindbladian with the largest real part to be $\lambda_1 = -\kappa + i(\delta + 4\chi)$, $\bar{\lambda}_1 = -\kappa - i(\delta + 4\chi)$. This matches the perturbative result when $\Phi = 0$, though unlike in the previous two examples Φ now affects the spectrum.

Unfortunately, the result fails to pick up the appearance of bistability in the Kerr oscillator. As seen in Figure 3 of [59], the real part of λ_1 does initially decrease with F but after a certain critical value of the latter reverses and approaches 0. This corresponds to the beginning of the bistable region. The absence of this effect from our approach despite the fact that it should be present for even small non-linearity suggests it is non-perturbative/non-smooth in χ at $\chi = 0$. This is unfortunate, since it suggests the perturbative approach may be a poor fit for the study of metastability even in very simple models like the the Kerr oscillator that exhibit classical metastability.

18.2.3 Incoherently Driven Oscillator

For an oscillator interacting with a bath of oscillators in thermal equilibrium at a positive temperature, the total dissipator may be represented [19], [58] through an average thermal occupation number $\bar{n}_{\text{th}}$ as

$$2\kappa(\bar{n}_{\text{th}}+1)\left[a\rho a^\dagger - \frac{1}{2}\left(a^\dagger a\rho + \rho a^\dagger a\right)\right] + 2\kappa\bar{n}_{\text{th}}\left[a^\dagger\rho a - \frac{1}{2}\left(aa^\dagger\rho + \rho aa^\dagger\right)\right]. \tag{18.69}$$

This is essentially an incoherently driven oscillator, but with a restriction on the magnitude of the drive relative to the dissipation. Since we were unable to obtain an exact expression for this oscillator in the last chapter and because there is generally no simple truncated Fock basis formula for systems with such a bath [58] (though the present quadratic case is covered by [55] and so our result may be checked), it is a good example to consider.

Replacing the coefficients by arbitrary α, β, this constitutes a perturbation

$$\begin{aligned}\delta\mathcal{L} &= \alpha\left[a\rho a^\dagger - \frac{1}{2}\left(a^\dagger a\rho + \rho a^\dagger a\right)\right] + \beta\left[a^\dagger\rho a - \frac{1}{2}\left(aa^\dagger\rho + \rho aa^\dagger\right)\right] \\ &= \alpha\left[a\rho a^\dagger - \frac{1}{2}\left(aa^\dagger\rho + \rho aa^\dagger\right)\right] + \beta\left[a^\dagger\rho a - \frac{1}{2}\left(aa^\dagger\rho + \rho aa^\dagger\right)\right] + \alpha\rho.\end{aligned} \tag{18.70}$$

Mapping them to fields gives

$$\delta S = \int_0^T dt\, l(\psi_t^+, \bar{\psi}_t^+, \psi_t^-, \bar{\psi}_t^-), \tag{18.71}$$

$$l(\psi_t^+, \bar{\psi}_t^+, \psi_t^-, \bar{\psi}_t^-) = \alpha\psi_t^+\bar{\psi}_t^- + \beta\bar{\psi}_t^+\psi_t^- - \frac{\alpha+\beta}{2}\bar{\psi}_t^+\psi_t^+ - \frac{\alpha+\beta}{2}\bar{\psi}_t^-\psi_t^- + \alpha, \tag{18.72}$$

to which we now apply our perturbation expressions. The first order correction is given by

$$\begin{aligned}&\int_0^T dt\,(\alpha\partial_{J_1}\partial_{J_4} + \beta\partial_{J_2}\partial_{J_3} - \frac{\alpha+\beta}{2}\partial_{J_1}\partial_{J_2} - \frac{\alpha+\beta}{2}\partial_{J_3}\partial_{J_4} + \alpha)T(J_1,\ldots,J_4)[T,t] \\ &= \frac{T(\alpha-\beta)\left(2 - 2e^{\kappa T}\cos(\delta T)\right)}{8(\cos(\delta T) - \cosh(\kappa T))^2}.\end{aligned} \tag{18.73}$$

Adjusting our method in turn to α and β instead of χ, we obtain

$$\mathfrak{Re}\left[\frac{\partial\lambda_1(\alpha,\beta)}{\partial\alpha}\right]_{\alpha,\beta=0} = -\frac{1}{2}, \quad \mathfrak{Im}\left[\frac{\partial\lambda_1(\alpha,\beta)}{\partial\alpha}\right]_{\alpha,\beta=0} = 0, \tag{18.74}$$

$$\mathfrak{Re}\left[\frac{\partial\lambda_1(\alpha,\beta)}{\partial\beta}\right]_{\alpha,\beta=0} = \frac{1}{2}, \quad \mathfrak{Im}\left[\frac{\partial\lambda_1(\alpha,\beta)}{\partial\beta}\right]_{\alpha,\beta=0} = 0. \tag{18.75}$$

Since there are no terms linear in T, the second derivatives are zero, and so to quadratic order we have

$$\lambda_1 = -\left(\kappa + \frac{\alpha-\beta}{2}\right) + i\delta \tag{18.76}$$

This agrees with [55], indeed being the exact result. As stated there, we can see that a sufficiently large incoherent drive β can destabilize the system. For the thermal bath, however, $\alpha = 2\kappa\bar{n}_{\text{th}} = \beta$ so there is no correction to the lowest non-zero eigenvalue.

Overall, we see that the perturbative approach can correctly calculate corrections to eigenvalues of various Lindbladians for which exact propagators are not

available. As the Kerr oscillator example demonstrates, however, the appearance of a gap in the spectrum in a system's metastable regime may be (and likely generally is) a non-perturbative phenomena.

Chapter 19

Conclusion

While the lofty ambitions of studying metastability in Lindbladian systems that motivated this work have not been realised, some interesting results have nevertheless been obtained. This includes a path integral-based perturbation theory for Lindbladian systems and their spectra, offering a simple way to calculate corrections to eigenvalues of systems not covered by the method of third quantisation [55] or standard formula from the truncated Fock space approach [58].

The perturbative result for the driven-dissipative Kerr oscillator also confirms that the bistability it exhibits is non-perturbative, highlighting the need for the development of such methods for the analytical study of metastable systems. A significant portion of this part is devoted to a review of the difficulties encountered with one main-stream approach to this problem, namely the instantonic one [10], [27], due to the limitations of the coherent state path integral typically employed in condensed matter and quantum optics.

The primary issue is found to be that the conventional formulation of the path integral [13] lacks a way to represent the fluctuation corrections of the integral as a property of a well-defined continuous time operator, complicating the analysis of zero modes associated to instantons. I review this approach alongside the competing approach of Klauder and Daubechies (KD) [1], [2], highlighting the relationship between them and the more rigorous nature of the latter. While the latter approach does allow for the study of fluctuation contributions as a functional determinant of a continuous time operator, the latter is extremely difficult to analyse for all but the simplest paths, and I express hope that it may be linked to the more manageable method derived in [16] directly from the discrete form of the integral.

The KD approach for Hamiltonian dynamics leads to the possibility of defining an analogous path integral for Lindbladian systems, which I carry out. This in turn allows for the exact calculation of the propagator for a coherently driven-dissipative harmonic oscillator, which forms the basis for the aforementioned perturbation theory. It is hoped that in future exact propagators could be ob-

tained for more complicated systems, improving the properties of the perturbation theory.

Overall, this part constitutes some preliminary steps towards the study of Lindbladian spectra via the coherent state path integral. With a perturbation theory now available, the next step lies in overcoming the challenges associated with instantons in the coherent state driven dissipative setting. It is hoped that the review of coherent state theory presented herein will be of value to future workers pursuing this direction.

Appendix C

Forman's Theorem

The method we will use to calculate functional determinants is known as Forman's Theorem, and is a generalisation of the Gelfand-Yaglom (G-Y) Theorem [60]. The latter is a well-known method in quantum mechanics and relates the functional determinant of a Schrödinger-type differential operator

$$\begin{aligned} \mathcal{O} &= -\partial_t^2 + V(t), \\ \psi(0) &= \psi(T) = 0 \end{aligned} \tag{C.1}$$

to an initial value problem associated to this operator:

$$\begin{aligned} \mathcal{O}\psi &= 0, \\ \psi(0) = 0, \quad \psi'(0) &= 1, \\ \mathrm{Det}[\mathcal{O}] &\doteq \psi(T). \end{aligned} \tag{C.2}$$

Here $\doteq$ signifies 'formal' equality. In general functional determinants are naively divergent, and must be regularised. The G-Y Theorem (and Forman's Theorem) perform this regularisation by dividing the formal expression for the required determinant by the formal expression for a simpler determinant, which has a known value via other means. Thus, the formal equality becomes a true equality when a ratio is taken:

$$\begin{aligned} \mathrm{Det}[\mathcal{O}] \doteq \psi(T), \quad \mathrm{Det}[\mathcal{O}_{\mathrm{simple}}] &\doteq \psi_{\mathrm{simple}}(T), \\ \frac{\mathrm{Det}[\mathcal{O}]}{\mathrm{Det}[\mathcal{O}_{\mathrm{simple}}]} &= \frac{\psi(T)}{\psi_{\mathrm{simple}}(T)}. \end{aligned} \tag{C.3}$$

Forman's Theorem extends this to matrix elliptic differential operators of arbitrary order[1], though for our purposes we shall present the second-order case with

[1] The result is more general than this, but we will only require this portion of it.

Dirichlet conditions. For a differential operator

$$\begin{aligned} \Omega &= P_0(t)\partial_t^2 + P_1(t)\partial_t + P_2(t), \\ \boldsymbol{\psi}(a) &= \mathbf{0}, \quad \boldsymbol{\psi}(b) = \mathbf{0}, \end{aligned} \tag{C.4}$$

where P_0, P_1, and P_2 are complex $r \times r$ matrices, Forman's theorem states that

$$\mathrm{Det}[\Omega] \doteq \frac{\det[MH_\Omega(a) + NH_\Omega(b)]}{\sqrt{\det[H_\Omega(a)]\det[H_\Omega(b)]}} \tag{C.5}$$

where H_Ω is a matrix with columns $\begin{pmatrix} \boldsymbol{\psi}_i \\ \dot{\boldsymbol{\psi}}_i \end{pmatrix}$, $\boldsymbol{\psi}_i$ are $2r$ linearly independent solutions for $\Omega\boldsymbol{\psi} = 0$, M is the square block matrix $\begin{pmatrix} I_{r\times r} & 0 \\ 0 & 0 \end{pmatrix}$, and N is $\begin{pmatrix} 0 & 0 \\ I_{r\times r} & 0 \end{pmatrix}$.

There exist some generalisations of Forman's theorem to field theories [61], [62], though I am not aware of an equally general result in that case.

Appendix D

Method of Steepest Descent

The method of steepest descent is a generalisation of both the Laplace method and the method of stationary phase, applicable when the exponent is neither purely real nor purely imaginary. Its essence lies in the deformation of the contour of integration to one possessing a constant imaginary part in the vicinity of select stationary points and thus admitting a local Laplace approximation. This requires us to consider our initial integration contour as a half-dimensional manifold in a space formed by complexifying all of our real variables of integration, and to deform it through suitable stationary points in this complexified space.

In functional integral literature the method of steepest descent is sometimes referred to as "Picard-Lefschetz theory", possibly due to the term being used in [63], and represents a flavour of it that relies on results from homology theory. We will not consider these aspects of it in any detail.

Before considering its applications to functional integration, we shall review steepest descent for conventional integrals. We will particularly wish to highlight the complexities related to choosing a suitable complex integration cycle, which are not specific to functional integration and thus best presented in isolation.

The method of steepest descent consists of two parts [64]:

1. Topological aspect: deformation of the integration contour γ into a contour γ^* that is most convenient for obtaining an asymptotic approximation;

2. Analytical aspect: Calculation of the asymptotic approximation from the contour γ^*.

The second aspect is the more familiar, and is what we shall briefly review first. This is the "local" part of the method, as it consists of calculating local approximations to the integral in the vicinity of stationary points — this can generally be accomplished by means of a standard formula, and then the contributions are summed for all the stationary points on the contour.

Local Steepest Descent Approximation

Consider an integral over a half-dimensional integration cycle γ in an n-dimensional complex space $\mathbb{C}^n$ (a line contour in the complex plane for $n = 1$) of the following form

$$\int_\gamma d^n\mathbf{z}\, e^{\lambda\mathcal{I}(\mathbf{z})}, \tag{D.1}$$

where $\mathcal{I}$ is a holomorphic function. We wish to approximate this integral in the vicinity of a non-degenerate stationary point $\mathbf{z}_0$ of $\mathcal{I}$, which we assume lies on γ. By the complex Morse lemma, there exists a local holomorphic variable change $\boldsymbol{\omega} = \boldsymbol{\phi}(\mathbf{z})$ such that

$$\mathcal{I}(\boldsymbol{\omega}) = \mathcal{I} \circ \boldsymbol{\phi}^{-1}(\boldsymbol{\omega}) = \mathcal{I}(\boldsymbol{\omega}_0) - \sum_{i=1}^{n} \omega_i^2. \tag{D.2}$$

If $\omega_i = x_i + iy_i$, this means that ($\boldsymbol{\omega}_0 = \boldsymbol{\phi}(\mathbf{z}_0)$)

$$\mathrm{Re}\,\mathcal{I}(\boldsymbol{\omega}) = \mathrm{Re}\,\mathcal{I}'(\boldsymbol{\omega}_0) - \sum_{i=1}^{n} (x_i^2 - y_i^2), \tag{D.3}$$

$$\mathrm{Im}\,\mathcal{I}(\boldsymbol{\omega}) = \mathrm{Im}\,\mathcal{I}'(\boldsymbol{\omega}_0) - \sum_{i=1}^{n} 2x_i y_i, \tag{D.4}$$

from which we see that non-degenerate stationary points of holomorphic functions are always saddle-points of the real part.

Now assume that the cycle γ was chosen such that in the vicinity of $\mathbf{z}_0$, it is given by $y_i = 0$; This defines a half-dimensional manifold of constant $\mathrm{Im}\,\mathcal{I}$ and fastest decreasing $\mathrm{Re}\,\mathcal{I}$, making it suitable for the application of Laplace's method. In a neighbourhood γ_0 of $\mathbf{z}_0$ on which our coordinate transformation is defined, we may rewrite

$$\begin{aligned}\int_{\gamma_0} d^n\mathbf{z}\, e^{\lambda\mathcal{I}(\mathbf{z})} &= \left|\frac{\partial\mathbf{z}}{\partial\boldsymbol{\omega}}\right| e^{\lambda\mathcal{I}(\mathbf{z}_0)} \int_{\gamma_0} d^n\boldsymbol{x}\, e^{-\lambda\sum_{i=1}^{n} x_i^2} \\ &\approx \left(\frac{\pi}{\lambda}\right)^{n/2} \left|\frac{\partial\mathbf{z}}{\partial\boldsymbol{\omega}}\right| e^{\lambda\mathcal{I}(\mathbf{z}_0)}\end{aligned} \tag{D.5}$$

where we have employed the real Laplace approximation to approximate the local integral. It remains to observe that

$$\left(\frac{\partial\mathbf{z}}{\partial\boldsymbol{\omega}}\right)^T \cdot \left(\frac{\partial^2\mathcal{I}}{\partial\mathbf{z}^2}\right) \cdot \left(\frac{\partial\mathbf{z}}{\partial\boldsymbol{\omega}}\right) = \left(\frac{\partial^2\mathcal{I}}{\partial\boldsymbol{\omega}^2}\right) = -2I, \tag{D.6}$$

$$\left|\frac{\partial\mathbf{z}}{\partial\boldsymbol{\omega}}\right| = (\sqrt{2}i)^n \left(\frac{\partial^2\mathcal{I}}{\partial\mathbf{z}^2}\right)^{-1/2}, \tag{D.7}$$

so that (denoting $\frac{\partial^2 \mathcal{I}}{\partial \mathbf{z}^2} = \mathcal{I}''(\mathbf{z})$)

$$\int_{\gamma_0} d^n\mathbf{z}\, e^{\lambda \mathcal{I}(\mathbf{z})} \approx \left| -\frac{\lambda \mathcal{I}''(\mathbf{z}_0)}{2\pi} \right|^{-1/2} e^{\lambda \mathcal{I}(\mathbf{z}_0)}. \tag{D.8}$$

Thus, for a cycle γ passing through stationary points $\mathbf{z}_0^i$ in an appropriate local manner, the approximation states

$$\int_{\gamma} d^n\mathbf{z}\, e^{\lambda \mathcal{I}(\mathbf{z})} \approx \sum_i \left| -\frac{\lambda \mathcal{I}''(\mathbf{z}_0^i)}{2\pi} \right|^{-1/2} e^{\lambda \mathcal{I}(\mathbf{z}_0^i)}. \tag{D.9}$$

Some care ought to be exercised with respect to which branch of the square root is taken. Splitting $\left|-\mathcal{I}''(\boldsymbol{z}_0^i)\right|$ into a product of its eigenvalues $\prod_j \mu_j$, more careful considerations than those we have provided [64] indicate that the determinant should be taken as $\prod_j \sqrt{\mu_j}$, $\arg(\sqrt{\mu_j}) \leq \frac{\pi}{4}$. Since Forman's theorem does not give the individual eigenvalues, we will thus generally have a phase ambiguity in our results obtained with it. For a single classical path this poses no difficulty since this phase is constant and can be easily worked out by considering limiting behaviour such as $T \to 0$. For multiple paths, however, this could lead to interference effects between them that we will be unable to resolve without explicitly finding the spectrum of the Hessian. In this part we will only ever deal with a single path, and so will not run into these difficulties.

Global Problem: Contour Selection

The far more difficult problem, when applying steepest descent, is the selection of a suitable contour γ. For the approximation to be valid the stationary points must be the "most important" parts of the cycle, with the integrand negligible outside their neighbourhoods, and the imaginary part of the integrand should be locally constant on the contour in their vicinity.

A simple example of how a naive choice of contour (attempting to include all existing stationary points) may fail is provided in [63] via the Airy function integral ($\lambda \in \mathbb{R}$)

$$2\pi\lambda^{-1/3} Ai(\lambda^{2/3}) = \int_{-\infty}^{\infty} dx\, e^{i\lambda(x^3/3+x)}. \tag{D.10}$$

Complexifying the exponent yields

$$\mathcal{I}(z) = i(z^3/3 + z), \tag{D.11}$$

which possess two stationary points:

$$\partial_z \mathcal{I}(z) = i(z^2+1) = 0 \tag{D.12}$$

$$\Downarrow$$

$$z = \pm i. \tag{D.13}$$

Including both points would yield the approximation

$$2\pi\lambda^{-1/3} Ai(\lambda^{2/3}) \approx \sqrt{\frac{\pi}{\lambda}} e^{-\frac{2}{3}\lambda} \pm i\sqrt{\frac{\pi}{\lambda}} e^{\frac{2}{3}\lambda}, \tag{D.14}$$

where the second term ($z_0 = -i$) is incorrect: the Airy function of a real variable is real, and its $\lambda \to \infty$ behaviour scales as $e^{-\frac{2}{3}\lambda}$, which is the contribution of the first term ($z_0 = i$).

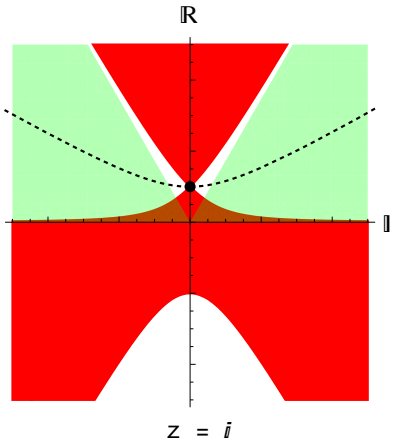

Figure D.1: (Left) One may see that it is easy to draw a non-self intersecting line through the black point ($z = i$) which is locally tangent to its dashed surface of steepest descent, begins and ends in the appropriate green asymptotic regions ($0 \leq \mathrm{Arg}\, z < \pi/3$ and $2\pi/3 < \mathrm{Arg}\, z \leq \pi$), and stays outside the red forbidden region.

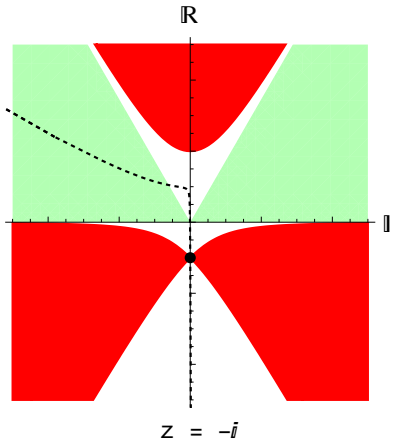

Figure D.2: (Right) It is impossible to draw an analogous non-self intersecting line through the black point ($z = -i$).

To understand the problem, it is instructive to plot[1] the region of $\mathbb{C}$ on which $\mathrm{Re}\,\mathcal{I}(z)$ is greater than $\mathcal{I}(i)$, and similarly for $\mathcal{I}(-i)$. A contour passing through one of these two stationary points should not pass through the corresponding region if that point is to have the largest contribution on the contour.

At the same time, we may plot the lines of constant $\mathrm{Im}\,\mathcal{I}$ and fastest decreasing $\mathrm{Re}\,\mathcal{I}$ (from now we will refer to these as surfaces of steepest descent) passing through the stationary points: a valid contour should be locally tangent to these lines at the stationary points, as described in the last section.

[1] We plot using $\lambda = 1 - 0.01i$. The small imaginary part of λ avoids a surface of steepest descent connecting the stationary points, which is a complication we will not discuss. More details may be found in [63].

Finally, any valid contour must have its ends in the appropriate asymptotic regions: regions at infinity at which $\mathrm{Re}\,\mathcal{I}(z) \to -\infty$ such that the integral converges, and which are "connected" to the original contour ends at $\pm\infty$. For the Airy integral these are $0 \leq \mathrm{Arg}\, z < \pi/3$ for ∞ and $2\pi/3 < \mathrm{Arg}\, z \leq \pi$ for $-\infty$. Looking at Figures D.1 and D.2, one may see that a non-self intersecting contour (self intersection implies a closed loop, along which the integral is trivially zero and should be discarded) passing through $z = i$ and locally tangent to its surface of steepest descent may be drawn that remains in the region where $\mathrm{Re}\,\mathcal{I}(z) < \mathrm{Re}\,\mathcal{I}(i)$, so that $z = i$ is indeed the most significant contribution on such a contour. For $z = -i$, however, it is easy to see that an analogous contour does not exist. Thus this point cannot be included on any contour suitable for an asymptotic approximation, and must be discarded. Doing so yields

$$2\pi\lambda^{-1/3} Ai(\lambda^{2/3}) \approx \sqrt{\frac{\pi}{\lambda}} e^{-\frac{2}{3}\lambda}, \tag{D.15}$$

which is the correct result.

Obviously the kind of graphic analysis performed above is entirely unsuitable for higher-dimensional integrals. Fortunately, there is a more systematic way to construct a suitable contour, though it is by no means simple to implement. We address this in the following section.

Steepest Descent Surfaces

Let us consider the following gradient system in the complexified space ($\boldsymbol{z} = \boldsymbol{x} + i\boldsymbol{y}$):

$$\partial_s \boldsymbol{x}(s) = -\nabla_{\boldsymbol{x}} \mathrm{Re}\,\mathcal{I}(\boldsymbol{x}(s), \boldsymbol{y}(s)), \tag{D.16}$$

$$\partial_s \boldsymbol{y}(s) = -\nabla_{\boldsymbol{y}} \mathrm{Re}\,\mathcal{I}(\boldsymbol{x}(s), \boldsymbol{y}(s)). \tag{D.17}$$

This system, which for holomorphic $\mathcal{I}$ may be rewritten as (and thus shares the stationary points of the action)

$$\partial_s \mathbf{z}(s) = -\overline{\partial_{\mathbf{z}} \mathcal{I}(\boldsymbol{z}(s))}, \tag{D.18}$$

generates trajectories along which the magnitude of the integrand monotonically decreases and locally does so the fastest. At the same time, it can be shown that $\mathrm{Im}\,\mathcal{I}$ is a conserved quantity. Indeed, the surface of steepest descent for the stationary point $\boldsymbol{z}_i$ may be characterised as the set [63]

$$\mathcal{J}_i = \{\mathbf{z} = \mathbf{z}(0) : \partial_s \mathbf{z}(s) = -\overline{\partial_{\mathbf{z}} \mathcal{I}(\boldsymbol{z}(s))}, \mathbf{z}(-\infty) = \mathbf{z}_i\} \tag{D.19}$$

of points reachable from the stationary point by such trajectories.

Consider now what happens if we evolve the original contour of integration using this gradient system (the essence of this explanation is due to [65]). Since the magnitude of the integrand will decrease at every point along the evolved contour, the convergence of the integral must improve: this means that the ends of the contour remain in valid asymptotic regions throughout. At the same time, due to a corollary of Lojasiewicz's inequality [66], [67], for a real analytic $\mathrm{Re}\,\mathcal{I}$ the trajectories of this system will either converge to its stationary points or diverge to infinity. Thus, as the contour evolves, portions of it will either move off to infinity in the valid asymptotic regions (with correspondingly negligible value of the integrand on them) or become 'pinned' on stationary points (and locally assume the shape of the point's surface of steepest descent, since the equations characterising the latter are the same as of the system). A plot of this is provided for the Airy function:

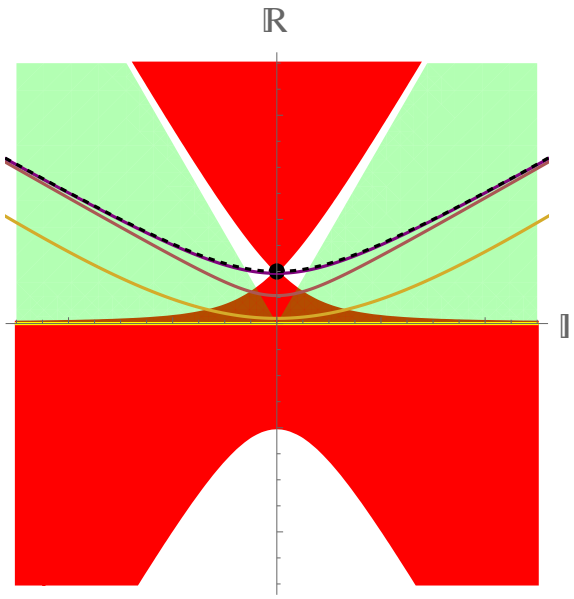

Figure D.3: The original contour (yellow) for the Airy function evolving (colour shifting to purple as it evolves) into the dashed black steepest descent surface of the $z = i$ stationary point according to the gradient system $\partial_s \mathbf{z}(s) = -\overline{\partial_{\mathbf{z}} \mathcal{I}(\mathbf{z}(s))}$. The ends of the contour remain within the valid asymptotic regions throughout the evolution and the final contour lies outside the forbidden red region.

The question of whether the original contour may be validly deformed through a stationary point thus becomes one of whether the point is reachable from some point on the original contour via a trajectory of this system: if so, we can evolve the contour as above and the neighbourhood of this point on it will become pinned on the corresponding stationary point. There are, however, further complications. Specifically, the neighbourhood may arrive at the stationary point with different orientations [63], [65], so its contribution is determined only up to a sign unless the orientation is known. Furthermore, multiple regions of the original contour may arrive at the same stationary point (possibly with differ-

ent orientations), and their number must somehow be calculated. A theoretical answer to these problems is provided in [63], but there is no easy practical way to implement it. Indeed, even the question of whether a given stationary point is reachable from the original contour appears intractable in the infinite-dimensional setting of path integration [68].

Some simplifications are possible. An argument in [63] shows that for a purely imaginary $\mathcal{I}$, as in zero-temperature quantum mechanics, the dominant stationary points appearing on the original contour will contribute a single time with positive orientation and be dominant over any points not on the contour. The same reasoning may be used to argue the same for a purely real $\mathcal{I}$, explaining why these difficulties are not encountered in Laplace's method and the method of stationary phase. Furthermore, if only a single stationary point is present, arguments ibidem show that it will necessarily contribute to the integral. The multiplicity and orientation of its contribution, however, will not necessarily be single and positive[2]. This will not generally be a problem for us, however, as with all functional integrals we perform the correct value of a limiting case will be known (this is also essentially necessary to calculate functional determinants via Forman's theorem). Thus, like the phase ambiguity discussed in the previous section, the multiplicity/orientation ambiguity for a single stationary point is easily resolved by comparing to a known limiting case.

Finding Stationary Points, Phases, and Intersection Numbers

The preceding theory is well-known, and a desire to apply it to functional integration had been expressed as far back as 1983 [69]. This has been hindered, however, by the complexity associated with calculating contributing stationary points, their orientations, and multiplicities [68]. In infinite dimensions this appears computationally intractable.

The state of affairs is thus roughly as follows. Finding the stationary points of a given complexified action is by far the simplest part of the theory: in quantum mechanics this amounts to solving a system of ODEs with appropriate boundary conditions, while in QFTs these are elevated to PDEs. So long as these can be solved, the goal is achievable.

Next, how hard it is to calculate the phase associated with the branch of the square root of the functional determinant varies. If the non-complexified action is purely real, as it is in Euclidean path integrals, the phase is always zero. In the case of a purely imaginary action of zero temperature quantum mechanics, this phase is related to the Maslov index [10] of the trajectory and there is possibly a similar result for QFT. For a general complex action, such as arises in Feynman-Vernon path integrals, however, no method appears to exist other than

[2] If there is a stronger result in this direction, I am unfortunately unaware of it.

the explicit computation of the spectrum of the associated Hessian. This may be tractable for some simple differential operators (and in the case of only a single path may be worked out by other means), but is likely to be very hard in general.

Finally, as mentioned at the start, there is the essentially intractable problem of identifying which stationary points should contribute, and with what orientations and multiplicities. So far as only a single path is involved, this is not a problem since it is guaranteed to contribute and the multiplicity/orientation may be fixed by other means; thus many problems in driven-dissipative quantum mechanics (ones for which the equations of motion and their boundary conditions ensure unique solutions) should be solvable while disregarding this difficulty. Otherwise, however, there does not appear to be a rigorous way to identifying contributing points.

Bibliography

[1] J. R. Klauder and I. Daubechies, "Quantum mechanical path integrals with wiener measures for all polynomial hamiltonians," *Physical review letters*, vol. 52, no. 14, p. 1161, 1984.

[2] I. Daubechies and J. R. Klauder, "Quantum-mechanical path integrals with wiener measure for all polynomial hamiltonians. ii," *Journal of mathematical physics*, vol. 26, no. 9, pp. 2239–2256, 1985.

[3] N. (https://physics.stackexchange.com/users/60644/noiralef), *Negativity of the real part of eigenvalues of lindblad operators*, Physics Stack Exchange, URL:https://physics.stackexchange.com/q/755225 (version: 2023-04-03).

[4] K. Macieszczak, M. Guţă, I. Lesanovsky, and J. P. Garrahan, "Towards a theory of metastability in open quantum dynamics," *Physical review letters*, vol. 116, no. 24, p. 240 404, 2016.

[5] K. Macieszczak, D. C. Rose, I. Lesanovsky, and J. P. Garrahan, "Theory of classical metastability in open quantum systems," *Physical Review Research*, vol. 3, no. 3, p. 033 047, 2021.

[6] S. M. Rytov, Y. A. Kravtsov, and V. I. Tatarskii, *Principles of statistical radiophysics 1. Elements of random process theory.* 1987.

[7] M. Dykman and M. Krivoglaz, "Theory of fluctuational transitions between stable states of a nonlinear oscillator," *Sov. Phys. JETP*, vol. 50, no. 1, pp. 30–37, 1979.

[8] M. Dykman, "Large fluctuations and fluctuational transitions in systems driven by colored gaussian noise: A high-frequency noise," *Physical Review A*, vol. 42, no. 4, p. 2020, 1990.

[9] C.-W. Lee, P. Brookes, K.-S. Park, M. H. Szymańska, and E. Ginossar, "A real-time instanton approach to quantum activation," *arXiv preprint arXiv:2409.00681*, 2024.

[10] L. S. Schulman, *Techniques and applications of path integration*. Courier Corporation, 2012.

[11] S. Coleman, *Aspects of symmetry: selected Erice lectures*. Cambridge University Press, 1988.

[12] F. Thompson and A. Kamenev, "Qubit decoherence and symmetry restoration through real-time instantons," *Physical Review Research*, vol. 4, no. 2, p. 023 020, 2022.

[13] F. A. Berezin, "Feynman path integrals in a phase space," *Soviet Physics Uspekhi*, vol. 23, no. 11, p. 763, 1980.

[14] Y. Weissman, "On the stationary phase evaluation of path integrals in the coherent states representation," *Journal of Physics A: Mathematical and General*, vol. 16, no. 12, p. 2693, 1983.

[15] J. R. Klauder, "Path integrals and stationary-phase approximations," *Physical Review D*, vol. 19, no. 8, p. 2349, 1979.

[16] M. Baranger, M. A. de Aguiar, F. Keck, H.-J. Korsch, and B. Schellhaaß, "Semiclassical approximations in phase space with coherent states," *Journal of Physics A: Mathematical and General*, vol. 34, no. 36, p. 7227, 2001.

[17] L. C. L. Y. Voon, "An investigation of coherent state path integrals as applied to a harmonic oscillator and a single spin," Ph.D. dissertation, University of British Columbia, 1989.

[18] J. Rammer, "Quantum field theory of non-equilibrium states," *Quantum Field Theory of Non-equilibrium States*, 2011.

[19] A. Kamenev, *Field theory of non-equilibrium systems*. Cambridge University Press, 2023.

[20] J. Keeling, "Superfluid density of an open dissipative condensate," *Phys. Rev. Lett.*, vol. 107, p. 080 402, 2011.

[21] K. Husimi, "Some formal properties of the density matrix," *Proceedings of the Physico-Mathematical Society of Japan. 3rd Series*, vol. 22, no. 4, pp. 264–314, 1940.

[22] A. Altland and B. D. Simons, *Condensed matter field theory*. Cambridge university press, 2010.

[23] J. Zinn-Justin, *Quantum field theory and critical phenomena*. Oxford university press, 2021, vol. 171.

[24] L. M. Sieberer, M. Buchhold, and S. Diehl, "Keldysh field theory for driven open quantum systems," *Reports on Progress in Physics*, vol. 79, no. 9, p. 096 001, 2016.

[25] X.-G. Wen, *Quantum field theory of many-body systems: From the origin of sound to an origin of light and electrons*. Oxford university press, 2004.

[26] U. C. Täuber, *Critical dynamics: a field theory approach to equilibrium and non-equilibrium scaling behavior*. Cambridge University Press, 2014.

[27] P. Coleman, *Introduction to many-body physics*. Cambridge University Press, 2015.

[28] R. Shankar, *Quantum field theory and condensed matter: an introduction*. Cambridge University Press, 2017.

[29] H. Kleinert, *Path integrals in quantum mechanics, statistics, polymer physics, and financial markets*. World Scientific Publishing Company, 2006.

[30] R. Forman, "Functional determinants and geometry," *Inventiones mathematicae*, vol. 88, no. 3, pp. 447–493, 1987.

[31] H. G. Solari, "Glauber's coherent states and the semiclassical propagator," *Journal of mathematical physics*, vol. 27, no. 5, pp. 1351–1357, 1986.

[32] I. Daubechies, J. R. Klauder, and T. Paul, "Wiener measures for path integrals with affine kinematic variables," *Journal of mathematical physics*, vol. 28, no. 1, pp. 85–102, 1987.

[33] J. R. Klauder, "Quantization is geometry, after all," *Annals of Physics*, vol. 188, no. 1, pp. 120–141, 1988.

[34] J. R. Klauder, "Understanding quantization," *Foundations of Physics*, vol. 27, no. 11, pp. 1467–1483, 1997.

[35] J. R. Klauder, "Coherent state quantization of constraint systems," *Annals of Physics*, vol. 254, no. 2, pp. 419–453, 1997.

[36] J. R. Klauder, "Coherent state path integrals at (nearly) 40," *Path integrals from peV to TeV*, vol. 50, pp. 65–70, 1999.

[37] T. R. Ramadas, I. M. Singer, and J. Weitsman, "Some comments on chern-simons gauge theory," *Communications in mathematical physics*, vol. 126, no. 2, pp. 409–420, 1989.

[38] P. Woit, "Topological quantum theories and representation theory," in *Differential Geometric Methods in Theoretical Physics: Physics and Geometry*, Springer, 1990, pp. 533–545.

[39] J. Govaerts and O. Mattelaer, "A deformation of quantum dynamics through the phase space path integral," *arXiv preprint arXiv:0812.0596*, 2008.

[40] J. Govaerts, C. M. Bwayi, and O. Mattelaer, "The klauder–daubechies construction of the phase-space path integral and the harmonic oscillator," *Journal of Physics A: Mathematical and Theoretical*, vol. 42, no. 44, p. 445 304, 2009.

[41] M. Blau, "Symplectic geometry and geometric quantization," *Lecture notes*, 1992.

[42] B. B.-S. (https://math.stackexchange.com/users/13120/ben-blum-smith), *How to show cotangent bundles are not compact manifolds?* Mathematics Stack Exchange, URL:https://math.stackexchange.com/q/1251948 (version: 2015-04-26).

[43] nLab authors, *Geometric quantization of the 2-sphere*, ncatlab, URL:https://ncatlab.org/nlab/revision/geometric+quantization+of+the+2-sphere/15 (Revision 15).

[44] P. Woit, *Quantum Theory, Groups and Representations: An Introduction*. Springer International Publishing, 2017, ISBN: 9783319646107. DOI: 10.1007/978-3-319-64612-1.

[45] N. Wheeler, *Weyl transform and the phase space formalism*, Reed College, 2017.

[46] A. M. Perelomov, "Coherent states for arbitrary lie group," *Communications in Mathematical Physics*, vol. 26, pp. 222–236, 1972.

[47] J. E. Moyal, "Quantum mechanics as a statistical theory," in *Mathematical Proceedings of the Cambridge Philosophical Society*, Cambridge University Press, vol. 45, 1949, pp. 99–124.

[48] D. Skinner, *Qft in one dimension (= qm)*, Department of Applied Mathematics and Theoretical Physics, University of Cambridge, 2015.

[49] J. Glimm and A. Jaffe, *Quantum physics: a functional integral point of view*. Springer Science & Business Media, 2012.

[50] N. Wiener, "Differential-space," *Journal of Mathematics and Physics*, vol. 2, no. 1-4, pp. 131–174, 1923.

[51] R. E. A. C. Paley, N. Wiener, and A. Zygmund, "Notes on random functions," *Mathematische Zeitschrift*, vol. 37, no. 1, pp. 647–668, 1933.

[52] W. F. Trench, "Conditional convergence of infinite products," *The American mathematical monthly*, vol. 106, no. 7, pp. 646–651, 1999.

[53] R. J. Glauber, "Coherent and incoherent states of the radiation field," *Physical Review*, vol. 131, no. 6, p. 2766, 1963.

[54] L. Sieberer, S. D. Huber, E. Altman, and S. Diehl, "Nonequilibrium functional renormalization for driven-dissipative bose-einstein condensation," *Physical Review B*, vol. 89, no. 13, p. 134 310, 2014.

[55] T. Prosen and T. H. Seligman, "Quantization over boson operator spaces," *Journal of Physics A: Mathematical and Theoretical*, vol. 43, no. 39, p. 392 004, 2010.

[56] H.-P. Breuer and F. Petruccione, *The theory of open quantum systems*. Oxford University Press, USA, 2002.

[57] W. R. Inc., *Mathematica, Version 14.1*, Champaign, IL, 2024.

[58] F. Iachello, C. V. Coane, and J. Venkatraman, "Symmetries of liouvillians of squeeze-driven parametric oscillators," *Journal of Physics A: Mathematical and Theoretical*, vol. 57, no. 41, p. 415 302, 2024.

[59] W. Casteels, R. Fazio, and C. Ciuti, "Critical dynamical properties of a first-order dissipative phase transition," *Physical Review A*, vol. 95, no. 1, p. 012 128, 2017.

[60] I. M. Gel'fand and A. M. Yaglom, "Integration in functional spaces and its applications in quantum physics," *Journal of Mathematical Physics*, vol. 1, no. 1, pp. 48–69, 1960.

[61] G. V. Dunne and K. Kirsten, "Functional determinants for radial operators," *Journal of Physics A: Mathematical and General*, vol. 39, no. 38, p. 11 915, 2006.

[62] A. Ossipov, "Gelfand–yaglom formula for functional determinants in higher dimensions," *Journal of Physics A: Mathematical and Theoretical*, vol. 51, no. 49, p. 495 201, 2018.

[63] E. Witten, "Analytic continuation of chern-simons theory," *AMS/IP Stud. Adv. Math*, vol. 50, p. 347, 2011.

[64] M. Fedoryuk, "The steepest descent method," *Nauka, Moscow*, 1977.

[65] D. Kaminski, "Exponentially improved stationary phase approximations for double integrals," *Methods and Applications of Analysis*, vol. 1, no. 1, pp. 44–56, 1994.

[66] S. Lojasiewicz, "Ensembles semi-analytiques," *Lectures Notes IHES (Bures-sur-Yvette)*, 1965.

[67] S. Lojasiewicz, "Sur les trajectoires du gradient d'une fonction analytique," *Seminari di geometria*, vol. 1983, pp. 115–117, 1982.

[68] Y. Tanizaki and T. Koike, "Real-time feynman path integral with picard–lefschetz theory and its applications to quantum tunneling," *Annals of Physics*, vol. 351, pp. 250–274, 2014.

[69] F. Pham, "Vanishing homologies and the n variables saddlepoint method," in *Proc. Symp. Pure Math.*, vol. 40, 1983, pp. 310–333.

Part III

Stochastic Truncated Wigner for Spin Systems

Chapter 20

The Wigner-Moyal Formalism and Stratonovich Postulates

In Part II we saw that the space of square-integrable functions on the phase space of a system is typically too large to serve as the Hilbert space we wish to work with. While the definition of a suitable polarisation and subsequent quantisation in geometric quantisation can often produce an appropriate smaller subspace, this conceptually amounts to artificially carving out an effective configuration space and makes clear that quantum mechanical wave functions are not the natural objects of study on the phase space.

Stepping back to classical mechanics, this is not entirely surprising. Loosely associating pure, localized quantum states to classical states of the system, the latter correspond to individual points of phase space rather than functions defined on it. Yet classical mechanics does involve objects that are precisely such functions: they are the observables and phase space distribution of the system [1]. Unlike states, for which the Schrödinger equation is a quantized analogue of the classical energy-momentum relation[1], these objects obey classical dynamical equations expressed through phase space coordinates via the Poisson bracket, and so we might expect the possibility of building a quantum theory of these objects on the phase space with dynamical equations reducing to the classical ones in the $\hbar \to 0$ limit. That the quantum analogues of these objects exist in spaces larger than the Hilbert space of the system[2] is promising.

This point of view takes us away from geometric quantisation, arriving instead at what is known as deformation quantisation [2]. The goal of this formal-

[1] Because classical mechanics does not distinguish between state and a fixed set of values for a complete set of observables (the coordinates in a chart on a symplectic manifold), the Hamilton equations for the evolution of a state are indistinguishable from equations for the evolution of observables. Yet upon quantisation these become equations for the evolution of operators (or their expectations via the Ehrenfest theorem), showing that from a quantum point of view they are the latter. One is thus forced to construct the Schrödinger equation as the actual dynamical equation for the state.

[2] Namely the space of linear operators on that Hilbert space, which for finite Hilbert spaces is the tensor product of the Hilbert space with its dual.

ism is to construct an algebra of functions on the phase space symplectic manifold (corresponding to linear operators of the quantum theory) equipped with a non-commutative star product (since the product of quantum mechanical operators is non-commutative) expressed as a series in $\hbar$. In the $\hbar \to 0$ limit this product is to become the ordinary commutative product of functions, while at linear order in $\hbar$ the commutator expressed in terms of it should reduce to the appropriate Poisson bracket. From a purely mathematical point of view the series expression of the star product need not be convergent, giving what is known as 'formal deformation quantisation'. If the theory is to describe real physics, however, it should converge, leading to the more constrained 'strict deformation quantisation'.

The most well known result in this direction is the Wigner-Moyal formalism[3]. Originally formulated for particles on flat phase space, it constructs a representation of operator quantum mechanics that fits the scheme outlined above, giving the following set of correspondences:

Representations of Quantum Mechanics		
Classical Physics	Matrix Quantum Mechanics	Wigner-Moyal Formalism
Phase point	Quantum state	Pure Wigner function
Phase space distribution	Density matrix	Wigner function
Classical observables	Linear operators	Functions on the phase-space manifold
Scalar product	Operator product	Star ($\star$) product
Energy-momentum relation[4]	Schrödinger equation	von Neumann equation for a pure Wigner function
Classical equations of motion	Heisenberg equations	Heisenberg equations
Liouville equation	von Neumann equation	von Neumann equation

In this formalism one maps linear operators A to functions $W_A(\boldsymbol{x}, \boldsymbol{p})$ (known as the symbols of the operator) on the flat phase space and vice versa via an operator

[3]The formalism predates the deformation quantisation program by a good 40 years [3], [4], so it would be unfair to view it as a product of the latter. Nevertheless, it fits neatly into that framework.

[4]Alternatively, the Hamilton-Jacobi equation.

kernel $\Delta(\boldsymbol{x},\boldsymbol{p})$ [5]:

$$\Delta(\boldsymbol{x},\boldsymbol{p}) = \int d\boldsymbol{x}'\, e^{i\boldsymbol{p}\cdot\boldsymbol{x}'/\hbar} |\boldsymbol{x}+\boldsymbol{x}'/2\rangle\langle\boldsymbol{x}-\boldsymbol{x}'/2|, \tag{20.1}$$

$$W_A(\boldsymbol{x},\boldsymbol{p}) = \mathrm{Tr}\left[A\Delta(\boldsymbol{x},\boldsymbol{p})\right], \tag{20.2}$$

$$A = \int d\boldsymbol{x} \int \frac{d\boldsymbol{p}}{(2\pi\hbar)^n} W_A(\boldsymbol{x},\boldsymbol{p})\Delta(\boldsymbol{x},\boldsymbol{p}), \tag{20.3}$$

where n is the number of particles in the system. This mapping is evidently linear, and it is easy to see that Hermitian operators are mapped to real functions and that $W_I = 1$. Combined with an associative star product known as the Moyal product

$$W_A(\boldsymbol{x},\boldsymbol{p}) \star W_B(\boldsymbol{x},\boldsymbol{p}) = W_A(\boldsymbol{x},\boldsymbol{p}) \exp\left[\frac{i}{2}\hbar\left(\overleftarrow{\partial}_{\boldsymbol{x}}\cdot\overrightarrow{\partial}_{\boldsymbol{p}} - \overleftarrow{\partial}_{\boldsymbol{p}}\cdot\overrightarrow{\partial}_{\boldsymbol{x}}\right)\right] W_B(\boldsymbol{x},\boldsymbol{p}), \tag{20.4}$$

and the standardization and traciality properties

$$\mathrm{Tr}\, A = \int d\boldsymbol{x} \int \frac{d\boldsymbol{p}}{(2\pi\hbar)^n} W_A(\boldsymbol{x},\boldsymbol{p}), \tag{20.5}$$

$$\mathrm{Tr}\left[AB\right] = \int d\boldsymbol{x} \int \frac{d\boldsymbol{p}}{(2\pi\hbar)^n} W_A(\boldsymbol{x},\boldsymbol{p}) W_B(\boldsymbol{x},\boldsymbol{p}), \tag{20.6}$$

this provides all the tools needed to perform quantum mechanical calculations in terms of these symbols. The density matrix is mapped to a symbol known as the Wigner function and in the Schrödinger picture this is evolved in time by a suitable dynamical equation, while in the Heisenberg picture it is the symbols of other operators that are evolved. Expectations are taken by tracing symbols of observables against the Wigner function, relying on the traciality property.

Our interest in this construction lies in the following fact: at order $O(\hbar^2)$ the Moyal product is a second order bilinear differential operator. Moreover, the $\hbar^0$ and $\hbar^2$ terms are symmetric in the symbols while the $\hbar$ term is antisymmetric. This means that if one writes down a non-driven dissipative von Neumann equation in terms of the Wigner function accurate up to $O(\hbar^2)$, one obtains a partial differential equation that is first order in both time and phase variables, while a Lindbladian master equation will yield one that is first order in time but second order in phase variables. Since the trace of the density matrix must be conserved so must the total mass of the Wigner function by the standardization property, meaning these will be continuity equations. In particular, the partial differential equation will generally take the form of a Fokker-Planck equation.

Truncating at this order in $\hbar$ thus endows the evolution with a classic stochastic interpretation via the mapping from Fokker-Planck equations to stochastic differential equations (with no noise in the von Neumann case). This means that operator expectations in the theory may be computed by sampling trajectories

from an initial Wigner distribution, evolving them to the time at which the expectation is to be taken, and then averaging the operator symbol over them. While the Wigner function may, unlike a real probability distribution, have regions of negative density, one may still make progress by restricting to initially positive Wigner distributions[5] and, in the case of a Fokker-Planck equation with a steady state, relying on the independence of the steady state from the initial distribution. This stochastic approximation is the Truncated Wigner approximation we met in Part Ib, now phrased in terms of the Wigner-Moyal formalism rather than the path integral.

The Truncated Wigner formalism is well established for particles with a flat phase space, and there are several related approaches to spin degrees of freedom. These include various flavours of bosonizing the spins and using the flat space variant on the resulting quasiparticles [6], the discrete Truncated Wigner method for spin [7], [8] that uses Wooters' discrete phase space [9], [10], and approaches that use the fact that the algebra $\mathrm{su}(2^n)$ together with the identity matrix spans the Hilbert space of a cluster of n spin-$\frac{1}{2}$ particles [11], [12][6].

These are all valuable methods, but all somewhat deviate from the prototypical Truncated Wigner approximation described above:

- The use of bosonization typically leads to a flat phase space with a constraint, so one is in effect doing constraint quantisation [13]. The case of Schwinger bosons for a single spin, for instance, corresponds to the quantisation of $\mathbb{R}^4$ constrained to S^3, the latter being diffeomorphic to and carrying a transitive action of SU(2) and furnishing a quantum theory of spin (see section 5.2 of the cited article). This is entirely valid, but is a very 'extrinsic' approach to something I feel could be more elegantly described by constructing the theory on the appropriate manifold from the start.

- Methods based on a discrete phase space evidently do not produce a Fokker-Planck equation meaning that if one wishes to obtain classical equations with noise, the latter must be added via external considerations rather than appearing intrinsically. The truncation involved in the approximation is also not in $\hbar$, breaking the connection to deformation quantisation. Finally, from an aesthetic point of view, this approach de-emphasizes the connection to the Lie group action on the phase space, which we will see is an important part of the flat space theory.

- Finally, approaches based on spanning spin Hilbert spaces by appropriate bases also lack $\hbar$ as a truncation parameter, and must find an alternative

[5] We will see that it is actually sometimes possible to sample from a non-positive distribution.

[6] The two cited works are quite different in their specifics, one considering a mapping of single spins onto an S^2 phase space and the other of clusters onto a flat phase space. The second work also considers other bases for the Hilbert space. Nevertheless, there is a distinct similarity between the approaches.

justification for the truncation. These approaches are also constructed for a specific magnitude of the spin and size of cluster, as opposed to an approach where the spin magnitude may be continuously varied (indeed, since dimensionless spin magnitude is proportional to $\hbar^{-1}$, it is a natural expansion parameter for the star product).

What we will thus pursue in this part is a Truncated Wigner approach that is formulated on the spin phase space S^2 from the start, respects the deformation quantisation structure by admitting an expansion in $\hbar$, exhibits the same structure for any spin number, and is covariant under the action of the Lie group associated to the system (SU(2) for spin). This approach was begun with the construction of the Wigner-Moyal correspondence for spin [14] and development of the Truncated Wigner approach to $O(\hbar)$ [15]–[17]. Our aim here will be to extend it to $O(\hbar^2)$ and thus to stochastic dynamics.

It is useful to begin by understanding the general structure of constructing a Wigner-Moyal correspondence for a symplectic manifold, known in this context as the Stratonovich-Weyl correspondence, which we will then specialise to S^2 in the next chapter. Specifically, will demand that the classical phase space and corresponding Hilbert space share a transitive action by a Lie group, namely that the classical phase space is a symplectic manifold $\mathcal{M}$, $\mathcal{G}$ is a group that acts transitively on $\mathcal{M}$, and $\mathcal{H}$ is a Hilbert space realizing a unitary irreducible representation π_g of $g \in \mathcal{G}$. For the flat phase space G is typically the Heisenberg group, while for spin it will be SU(2)[7]. With this established, we will seek a mapping $A \in L(\mathcal{H}) \leftrightarrow W_A \in F^\infty(\mathcal{M})$ from linear operators on $\mathcal{H}$ to (generalized) functions on $\mathcal{M}$ satisfying the following "Stratonovich Postulates" [18]:

1. Linearity: $A \mapsto W_A$ is a one-to-one linear map;
2. Reality: $W_{A^\dagger} = W_A$;
3. Standardization: $\int_{\mathcal{M}} d\mu(\zeta)\, W_A(\zeta) = \mathrm{Tr}\, A$;
4. Traciality: $\int_{\mathcal{M}} d\mu(\zeta)\, W_A(\zeta) W_B(\zeta) = \mathrm{Tr}(AB)$;
5. Covariance: $W_{g\cdot A}(\zeta) = W_A(g^{-1} \circ \zeta)$, where $g \cdot A = \pi_g A \pi_g^{-1}$.

Here $\mu(\zeta)$ is an invariant measure (under $\mathcal{G}$) on $\mathcal{M}$. The first four conditions are familiar from the flat phase space example earlier, with the linearity condition preserves the linear structure of the quantum theory, while the traciality condition preserves the statistical properties of the theory when one of the symbols is of a density matrix. The final postulate is not mandatory to preserving the structure of the quantum theory, though we will see the motivation for it in the

[7] Note that, unlike the Heisenberg group and its Stone-von Neumann theorem, SU(2) will have multiple different irreducible representations corresponding to different spin numbers.

next section, and could be replaced by another. This may lead to a different phase space and a de-emphasis of the transitive action of the Lie group, as occurs in Wooters' discrete phase space construction [9], [10]. As we are interested in preserving the geometric structure of the theory, we will retain the covariance postulate.

The most direct way to achieve this correspondence is through the construction of a kernel similar to the flat space kernel $\Delta(\boldsymbol{x}, \boldsymbol{p})$ by which operators may be mapped to functions and vice versa. In the context of the above postulates this is known as the Stratonovich-Weyl kernel, and is described in the next section.

20.1 Stratonovich-Weyl Operator Kernel

The mapping above can be realised by means of an operator kernel $\Delta(\zeta)$. Specifically, we implement the mapping via

$$W_A(\zeta) = \mathrm{Tr}(A\,\Delta(\zeta)). \tag{20.7}$$

The traciality property suggests that this mapping can be inverted via

$$A = \int_{\mathcal{M}} d\mu(\zeta)\, W_A(\zeta)\Delta(\zeta), \tag{20.8}$$

showing that the kernel is self-dual.

The Stratonovich postulates translate to the following properties of the kernel:

1. $\Delta(\zeta)^\dagger = \Delta(\zeta)$ for all $\zeta \in \mathcal{M}$;
2. $\int_{\mathcal{M}} d\mu(\zeta)\,\Delta(\zeta) = I$;
3. $\int_{\mathcal{M}} d\mu(\zeta)\,\mathrm{Tr}(\Delta(\zeta')\Delta(\zeta))\Delta(\zeta) = \Delta(\zeta')$;
4. $\Delta(g \circ \zeta) = \pi_g\,\Delta(\zeta)\,\pi_g^{-1}$.

Note that the last kernel property is true for the flat space Wigner-Moyal kernel [5]:

$$\Delta(\boldsymbol{x}+\boldsymbol{x}', \boldsymbol{p}+\boldsymbol{p}') = e^{\frac{i}{\hbar}(\boldsymbol{p}'\cdot\hat{\boldsymbol{x}}-\boldsymbol{x}'\cdot\hat{\boldsymbol{p}})}\Delta(\boldsymbol{x},\boldsymbol{p})\left(e^{\frac{i}{\hbar}(\boldsymbol{p}'\cdot\hat{\boldsymbol{x}}-\boldsymbol{x}'\cdot\hat{\boldsymbol{p}})}\right)^\dagger \tag{20.9}$$

where $e^{\frac{i}{\hbar}(\boldsymbol{p}'\cdot\hat{\boldsymbol{x}}-\boldsymbol{x}'\cdot\hat{\boldsymbol{p}})}$ is an element of the unitary irreducible representation of the Heisenberg group we saw in Part II with $\hbar$ reinserted. Thus the covariance postulate generalizes what is true for flat space, stating that the action of the associated Lie group must always be respected.

If the kernel is successfully constructed for a given system, the task of constructing the correspondence is largely accomplished. We shall see in Chap. 22

that an expression for a star product respecting the correspondence

$$W_{AB} = W_A \star W_B \tag{20.10}$$

may be constructed directly from the Stratonovich-Weyl kernel via an integral trikernel. The derivation of a differential form of the product, however, is typically a more difficult task. I will present this derivation only for the case of spin.

In the next chapter we will review the construction of this kernel for the case of spin, wherein $\mathcal{M} = S^2$ and $\mathcal{G} = SU(2)$.

Chapter 21

The Spin Kernel

In the case of a spin-j system, the objects considered in the previous chapter take on the values $\mathcal{M} = S^2$, $\mathcal{G} = \mathrm{SU}(2)$, and the Hilbert space $\mathcal{H}$ is $2j+1$-dimensional. The SU(2)-invariant measure on S^2 is, up to normalization, simply the area measure:

$$\mu_j(\mathbf{n}) = \frac{2j+1}{4\pi} \sin\theta d\theta d\phi, \tag{21.1}$$

where $\boldsymbol{n}$ denotes the unit vector of the sphere, and we shall denote this spin-j kernel by $\Delta^{(j)}(\mathbf{n})$.

The explicit form of the spin-j kernel was found in [14] by starting from a general matrix element representation and progressively restricting it by applying the Stratonovich postulates. Since this kernel is the foundation of all the work performed in this part, I devote the present chapter to an exposition of its derivation. We will also see how it is used to work out the symbols of some standard operators and density matrices that we will need in subsequent parts.

21.1 SU(2) Tensor Conventions

Throughout this part we will follow the conventions for SU(2) tensors set out in [19]. In particular, for the spin-j representation, we will have the following important tensors:

- The epsilon tensor $\epsilon^{(j)mn}$, which is the coordinate vector of the rotationally invariant combination of two equal spins:

$$(J^{(1)} + J^{(2)})^2 \sum_{m,n} \epsilon^{(j)mn} |jm\rangle |jn\rangle = 0. \tag{21.2}$$

  It obeys

$$\epsilon^{(j)}_{nm} = (-1)^{2j} \epsilon^{(j)}_{mn}, \quad \sum_{m'} \epsilon^{(j)}_{mm'} \epsilon^{(j)m'n} = (-1)^{2j} \delta^n_m, \tag{21.3}$$

and is also used to raise and lower indices:

$$v^m = \sum_n \epsilon^{(j)mn} v_n, \quad v_m = \sum_n v^n \epsilon^{(j)}_{nm}; \tag{21.4}$$

- The Wigner D-matrices $D^{(j)m}{}_n = \langle jm|\pi^{(j)}_g|jn\rangle$, which are the j-dimensional representation matrices of SU(2). They respect the inversion relation

$$D^{(j)m}{}_n(g^{-1}) = (-1)^{2j} D^{(j)}{}_n{}^m(g); \tag{21.5}$$

- The Clebsch–Gordan coefficients $C^{(j_1 j_2 j)}{}_{m_1 m_2}{}^m$, which are the coordinate vectors of spin combinations in different bases:

$$|j_1 m_1\rangle|j_2 m_2\rangle = \sum_{j,m} C^{(j_1 j_2 j)}{}_{m_1 m_2}{}^m |j_1 j_2; jm\rangle, \tag{21.6}$$

$$|j_1 j_2; jm\rangle = \sum_{m_1, m_2} C^{(j_1 j_2 j) m_1 m_2}{}_m |j_1 m_1\rangle|j_2 m_2\rangle. \tag{21.7}$$

Because of how they couple two spin-j_1 and spin-j_2 representations to a spin-j representation, they have specific behaviour under SU(2) transformations:

$$D^{(j_1)n_1}{}_{m_1}(g) D^{(j_2)n_2}{}_{m_2}(g) C^{(j_1 j_2 j)}{}_{n_1 n_2}{}^m = C^{(j_1 j_2 j)}{}_{m_1 m_2}{}^n D^{(j)m}{}_n(g). \tag{21.8}$$

We will use the Condon–Shortley phase convention for these;

- The Wigner $3j$ symbols

$$\begin{pmatrix} j_1 & j_2 & j_3 \\ m_1 & m_2 & m_3 \end{pmatrix} = \frac{1}{\sqrt{d_{j_3}}} (-1)^{j_1 - j_2 + j_3} C^{(j_1 j_2 j_3)}{}_{m_1 m_2}{}^n \epsilon^{(j_3)}_{nm_3}, \tag{21.9}$$

where $d_j = 2j + 1$. These inherit modified SU(2) transformation properties from the Clebsch-Gordan coefficients:

$$D^{(j_1)m_1}{}_{n_1}(g) D^{(j_1)m_2}{}_{n_2}(g) D^{(j_1)m_3}{}_{n_3}(g) \begin{pmatrix} j_1 & j_2 & j_3 \\ m_1 & m_2 & m_3 \end{pmatrix} = \begin{pmatrix} j_1 & j_2 & j_3 \\ n_1 & n_2 & n_3 \end{pmatrix}, \tag{21.10}$$

meaning they are the invariant tensors, or intertwiners, of the SU(2) representation theory.

Throughout the derivation we will need various other properties of these tensors, which will be quoted without reference. Essentially all of these may be found in [19]. We will also unfortunately not use the repeated index summation convention since, while the theory is tensorial, we will have cause to sum over indices that appear more than two times and the notation would become confusing.

21.2 Constructing the Kernel

With the basics of SU(2) tensors out of the way, we may turn to the derivation of the SU(2) kernel [14]. The core of the method is to write $\Delta^{(j)}(\mathbf{n})$ in terms of the standard spin basis as

$$\Delta^{(j)}(\mathbf{n}) = \sum_{r,s} Z^{(j)r}{}_s(\mathbf{n})|jr\rangle\langle js|. \tag{21.11}$$

and then gradually constrain this representation via application of the Stratonovich postulates. Beginning with the covariance condition

$$\Delta^{(j)}(g \circ \boldsymbol{n}) = \pi_g^{(j)} \Delta(\boldsymbol{n}) (\pi_g^{(j)})^{-1}, \tag{21.12}$$

this gives the relation

$$\begin{aligned} Z^{(j)r}{}_s(g \circ \mathbf{n}) &= \langle jr|\Delta^{(j)}(g \circ \mathbf{n})|js\rangle = \langle jr|\pi_g^{(j)}\Delta^{(j)}(\mathbf{n})\pi_g^{(j)\dagger}|js\rangle \\ &= \sum_{p,q} \langle jr|\pi_g^{(j)}|jp\rangle Z^{(j)p}{}_q(\mathbf{n})\langle jq|\pi_g^{(j)\dagger}|js\rangle \\ &= \sum_{p,q} D^{(j)r}{}_p(g) D^{(j)q}{}_s(g^{-1}) Z^{(j)p}{}_q(\mathbf{n}). \end{aligned} \tag{21.13}$$

Using the Clebsch-Gordan series

$$D^{(j_1)m_1}{}_{n_1}(g) D^{(j_2)m_2}{}_{n_2}(g) = \sum_{j,m,n} C^{(j_1 j_2 j)m_1 m_2}{}_m C^{(j_1 j_2 j)}{}_{n_1 n_2}{}^n D^{(j)m}{}_n(g) \tag{21.14}$$

one obtains

$$\begin{aligned} D^{(j_1)m_1}{}_{n_1}(g) D^{(j_2)m_2}{}_{n_2}(g) &= \sum_{j,m,n} C^{(j_1 j_2 j)m_1 m_2 m} C^{(j_1 j_2 j)}{}_{n_1 n_2 n} D^{(j)}{}_m{}^n(g) \\ &= \sum_{j,m,n} (-1)^{2j}(2j+1) \begin{pmatrix} j_1 & j_2 & j \\ m_1 & m_2 & m \end{pmatrix} \begin{pmatrix} j_1 & j_2 & j \\ n_1 & n_2 & n \end{pmatrix} D^{(j)}{}_m{}^n(g) \\ &= \sum_{j,m,n} (-1)^{2j}(2j+1) \begin{pmatrix} j_1 & j & j_2 \\ m_1 & m & m_2 \end{pmatrix} \begin{pmatrix} j_1 & j & j_2 \\ n_1 & n & n_2 \end{pmatrix} D^{(j)}{}_m{}^n(g) \\ &= \sum_{j,m,n} (-1)^{2(j-j_2)} \frac{2j+1}{2j_2+1} C^{(j_1 j j_2)m_1 m m_2} C^{(j_1 j j_2)}{}_{n_1 n n_2} D^{(j)}{}_m{}^n(g), \end{aligned} \tag{21.15}$$

which, combined with the inversion relation

$$D^{(j)m}{}_n(g^{-1}) = (-1)^{2j} D^{(j)}{}_n{}^m(g), \tag{21.16}$$

yields

$$D^{(j)m_1}{}_{n_1}(g)D^{(j)n_2}{}_{m_2}(g^{-1}) = \sum_{l,m,n} \frac{2l+1}{2j+1} C^{(jlj)m_1 m}{}_{m_2} C^{(jlj)}{}_{n_1 n}{}^{n_2} D^{(l)n}{}_{m}(g^{-1}). \tag{21.17}$$

Substituting this result into (21.13), we obtain

$$Z^{(j)r}{}_{s}(g\circ\mathbf{n}) = \sum_{\substack{l,m,n\\p,q}} \frac{2l+1}{2j+1} C^{(jlj)rm}{}_{s} C^{(jlj)}{}_{pn}{}^{q} D^{(l)n}{}_{m}(g^{-1}) Z^{(j)p}{}_{q}(\mathbf{n}). \tag{21.18}$$

We now define

$$\tilde{Y}^{(l)}_m(\mathbf{n}) = \sum_{p,q} \frac{\sqrt{2l+1}}{\sqrt{2j+1}} C^{(jlj)}{}_{pm}{}^{q} Z^{(j)p}{}_{q}(\mathbf{n}) \tag{21.19}$$

and observe that the orthogonality relation for $3j$-symbols yields

$$\begin{aligned}
\tilde{Y}^{(l)}_m(g\circ\mathbf{n}) &= \sum_{p,q} \frac{\sqrt{2l+1}}{\sqrt{2j+1}} C^{(jlj)}{}_{pm}{}^{q} Z^{(j)p}{}_{q}(g\circ\mathbf{n}) \\
&= \sum_{\substack{k,t,u\\p,q}} \frac{\sqrt{2l+1}\sqrt{2k+1}}{2j+1} C^{(jlj)}{}_{pm}{}^{q} C^{(jkj)pt}{}_{q} D^{(k)u}{}_{t}(g^{-1})\tilde{Y}^{(k)}_u(\mathbf{n}) \\
&= \sum_{\substack{k,t,u\\p,q}} \sqrt{2l+1}\sqrt{2k+1} \begin{pmatrix} j & l & j \\ p & m & q \end{pmatrix} \begin{pmatrix} j & k & j \\ p & t & q \end{pmatrix} D^{(k)u}{}_{t}(g^{-1})\tilde{Y}^{(k)}_u(\mathbf{n}) \\
&= \sum_{k,t,u} \frac{\sqrt{2l+1}\sqrt{2k+1}}{2l+1} \delta_{lk}\delta^t_m D^{(k)u}{}_{t}(g^{-1})\tilde{Y}^{(k)}_u(\mathbf{n}) \\
&= \sum_{u} D^{(l)u}{}_{m}(g^{-1})\tilde{Y}^{(l)}_u(\mathbf{n}).
\end{aligned} \tag{21.20}$$

In the process, we obtain the intermediate result

$$\sum_{p,q} \frac{1}{2j+1} C^{(jlj)}{}_{pm}{}^{q} C^{(jkj)pt}{}_{q} = \frac{1}{2l+1}\delta_{lk}\delta^t_m \tag{21.21}$$

(21.20) is the correct covariance relation for normal spherical harmonics $Y^{(l)}_m$, and we now aim to show that $\tilde{Y}^{(l)}_m \sim Y^{(l)}_m$ up to a constant. To this end, consider the tensor

$$c^{(lk)m}{}_{n} = \int_{S^2} d\mu_l(\mathbf{n})\, \tilde{Y}^{(l)}_n(\mathbf{n}) Y^{(k)*}_m(\mathbf{n}) \tag{21.22}$$

and observe that it intertwines the representations π_k and π_l:

$$\begin{aligned}
D^{(l)s}{}_{m}(g) c^{(lk)m}{}_{n} D^{(l)n}{}_{t}(g^{-1}) &= \int_{S^2} d\mu_l(\mathbf{n})\, \tilde{Y}^{(l)}_t(g\circ\mathbf{n}) Y^{(k)*}_s(g\circ\mathbf{n}) \\
&= \int_{S^2} d\mu_l(\mathbf{n})\, \tilde{Y}^{(l)}_t(\mathbf{n}) Y^{(k)*}_s(\mathbf{n}) = c^{(lk)s}{}_{t},
\end{aligned} \tag{21.23}$$

the integral equality holding by the SU(2) invariance of $\mu_l(\mathbf{n})$.

By Schur's lemma, ${c^{(lk)m}}_n = \lambda^{(jl)}\delta^{lk}\delta^m_n$ for some constants $\lambda^{(jl)}$. Since the spherical harmonics form an orthogonal basis for $L^2(S^2)$ with (we use Racah's normalisation, contrary to the normalisation in Ref. [14])

$$\int_{S^2} d\mu_l(\mathbf{n})\, Y^{(l)}_n(\mathbf{n}) Y^{(k)*}_m(\mathbf{n}) = \delta^{lk}\delta_{nm}, \tag{21.24}$$

we conclude that $\tilde{Y}^{(l)}_m = \lambda^{(jl)} Y^{(l)}_m$.

Thus,

$${Z^{(j)r}}_s(\mathbf{n}) = \sum_{l,m} \frac{\sqrt{2l+1}}{\sqrt{2j+1}} {C^{(jlj)rm}}_s \tilde{Y}^{(l)}_m(\mathbf{n}) = \sum_{l,m} \lambda^{(jl)} \frac{\sqrt{2l+1}}{\sqrt{2j+1}} {C^{(jlj)rm}}_s Y^{(l)}_m(\mathbf{n}). \tag{21.25}$$

The requirement that $\Delta^{(j)}(\mathbf{n})^* = \Delta^{(j)}(\mathbf{n})$ necessitates that ${Z^{(j)r}}_s(\mathbf{n})^* = {Z^{(j)s}}_r(\mathbf{n})$. Using the fact that $Y^{(l)}_m(\mathbf{n})^* = (-1)^m Y^{(l)}_{-m}(\mathbf{n})$,

$$\begin{aligned}
\sum_m {C^{(jlj)rm}}_s Y^{(l)}_m(\mathbf{n})^* &= \sum_m \sqrt{2j+1}(-1)^{-j+l-s} \underbrace{\left(\frac{1}{\sqrt{2j+1}}(-1)^{j-l+s} {C^{(jlj)rm}}_s\right)}_{\begin{pmatrix} j & l & j \\ r & m & -s \end{pmatrix}} (-1)^m Y^{(l)}_{-m}(\mathbf{n}) \\
&= \sum_m \sqrt{2j+1}(-1)^{-j+l-s} \begin{pmatrix} j & l & j \\ s & -m & -r \end{pmatrix} (-1)^m Y^{(l)}_{-m}(\mathbf{n}) \\
&= \sum_m (-1)^{-j+l-s}(-1)^{j-l+r} {C^{(jlj)s-m}}_r (-1)^m Y^{(l)}_{-m}(\mathbf{n}) \\
&= \sum_m {C^{(jlj)s-m}}_r Y^{(l)}_{-m}(\mathbf{n}) \\
&= \sum_m {C^{(jlj)sm}}_r Y^{(l)}_m(\mathbf{n}),
\end{aligned} \tag{21.26}$$

which shows that

$${Z^{(j)r}}_s(\mathbf{n})^* = \sum_{l,m} \lambda^{(jl)*} \frac{\sqrt{2l+1}}{\sqrt{2j+1}} {C^{(jlj)rm}}_s Y^{(l)}_m(\mathbf{n})^* = \sum_{l,m} \lambda^{(jl)*} \frac{\sqrt{2l+1}}{\sqrt{2j+1}} {C^{(jlj)sm}}_r Y^{(l)}_m(\mathbf{n}). \tag{21.27}$$

Since

$${Z^{(j)s}}_r(\mathbf{n}) = \sum_{l,m} \lambda^{(jl)} \frac{\sqrt{2l+1}}{\sqrt{2j+1}} {C^{(jlj)sm}}_r Y^{(l)}_m(\mathbf{n}), \tag{21.28}$$

this shows that $\lambda^{(jl)*} = \lambda^{(jl)}$ and thus that the constants are real.

So far we have used only the covariance and reality postulates (or rather the corresponding properties of Δ^j). To maximally restrict the possible values of the

constants, we now consider the other two properties of the kernel, stemming from the standardization and traciality postulates:

$$\int_{S^2} d\mu_j(\mathbf{n})\,\Delta^j(\mathbf{n}) = I, \tag{21.29}$$

$$\int_{S^2} d\mu_j(\mathbf{n})\,\mathrm{tr}(\Delta^j(\mathbf{m})\Delta^j(\mathbf{n}))\Delta^j(\mathbf{n}) = \Delta^j(\mathbf{m}). \tag{21.30}$$

Because the matrix elements of the kernel Δ^j lie in the Hilbert space of spherical harmonics of order $\leq 2j$, the property (21.30) requires that the integral kernel $\mathrm{tr}(\Delta^j(\mathbf{m})\Delta^j(\mathbf{n}))$ be the identity operator on this space. Substituting our expression for the kernel, we find

$$\begin{aligned}
\mathrm{tr}(\Delta^j(\mathbf{m})\Delta^j(\mathbf{n})) &= \sum_{r,s} Z^{(j)r}{}_s(\mathbf{m}) Z^{(j)s}{}_r(\mathbf{n}) \\
&= \sum_{\substack{r,s \\ l,m,k,p}} \lambda^{(jl)}\lambda^{(jk)} \frac{\sqrt{2l+1}\sqrt{2k+1}}{2j+1} C^{(jlj)rm}{}_s C^{(jkj)sp}{}_r\, Y_m^{(l)}(\mathbf{m}) Y_p^{(k)}(\mathbf{n}) \\
&\overset{(21.27)}{=} \sum_{\substack{r,s \\ l,m,k,p}} \lambda^{(jl)}\lambda^{(jk)} \frac{\sqrt{2l+1}\sqrt{2k+1}}{2j+1} C^{(jlj)rm}{}_s C^{(jkj)}{}_{rp}{}^s\, Y_m^{(l)}(\mathbf{m}) Y_p^{(k)}(\mathbf{n})^* \\
&\overset{(21.21)}{=} \sum_{\substack{r,s \\ l,m,k,p}} \lambda^{(jl)}\lambda^{(jk)} \frac{\sqrt{2l+1}\sqrt{2k+1}}{2l+1} \delta_{lk}\delta_p^m\, Y_m^{(l)}(\mathbf{m}) Y_p^{(k)}(\mathbf{n})^* \\
&= \sum_{lm} (\lambda^{(jl)})^2\, Y_m^{(l)}(\mathbf{m}) Y_m^{(l)}(\mathbf{n})^*.
\end{aligned} \tag{21.31}$$

With Racah's normalization, $\sum_{lm} Y_m^{(l)}(\mathbf{m}) Y_m^{(l)}(\mathbf{n})^*$ is the identity operator on the Hilbert space up to a factor of $\frac{2j+1}{2l+1}$, so we conclude that $(\lambda^{(jl)})^2 = \frac{2l+1}{2j+1}$. Because

$$\int d\mu_j(\mathbf{n})\, Y_m^{(l)}(\mathbf{n}) = \frac{2j+1}{\sqrt{2l+1}} \int d\mu_l(\mathbf{n})\, Y_m^{(l)}(\mathbf{n}) Y_0^{(0)}(\mathbf{n}) = \frac{2j+1}{\sqrt{2l+1}} \delta_{l0}\delta_{m0}, \tag{21.32}$$

property (21.29) together with the expression (21.25) requires that $\lambda^{(j0)}$ be positive. The other $\lambda^{(jl)}$, $0 < l \leq 2j$, have unconstrained signs.

Generally, the choice made is that $\lambda^{(jl)}$ be positive for all l. This choice is related to how this self-dual kernel fits between the non-self dual P and Q kernels (which are frequently used but do not satisfy the traciality postulate, being dual to each-other). The final result is that the kernel is given by

$$Z^{(j)r}{}_s(\mathbf{n}) = \sum_{l,m} \frac{2l+1}{2j+1} C^{(jlj)rm}{}_s\, Y_m^{(l)}(\mathbf{n}). \tag{21.33}$$

Before moving on to tackle the star product, we note the symbols associated to some standard operators and density matrices. In particular, the symbols of the elements of the SU(2) algebra are given by [14]

$$W_{S_x} = \sqrt{j(j+1)}\sin(\theta)\cos(\phi), \tag{21.34}$$

$$W_{S_y} = \sqrt{j(j+1)}\sin(\theta)\sin(\phi), \tag{21.35}$$

$$W_{S_z} = \sqrt{j(j+1)}\cos(\theta), \tag{21.36}$$

which intuitively are just the polar representations of the x, y, z coordinates on a sphere with radius $\sqrt{j(j+1)}$. It will also be invaluable to know the symbols of the pure states of maximum and minimum weight, $|j,j\rangle\langle j,j|$ and $|j,-j\rangle\langle j,-j|$. These may be read off directly from the kernel since the spin basis is orthogonal (for Racah's normalisation, $Y_0^{(l)}(\boldsymbol{n}) = P_l(\cos(\theta))$, where P_l are the Legendre polynomials):

$$\mathrm{Tr}[\Delta^{(j)}(\boldsymbol{n})|j,j\rangle\langle j,j|] = Z^{(j)j}{}_j(\mathbf{n}) = \sum_{l=0}^{2j} \frac{2l+1}{2j+1} C^{(jlj)j0}{}_j P_l(\cos(\theta)), \tag{21.37}$$

$$\mathrm{Tr}[\Delta^{(j)}(\boldsymbol{n})|j,-j\rangle\langle j,-j|] = Z^{(j)-j}{}_{-j}(\mathbf{n}) = \sum_{l=0}^{2j} \frac{2l+1}{2j+1} C^{(jlj)-j0}{}_{-j} P_l(\cos(\theta)). \tag{21.38}$$

Chapter 22

Spin Star Product

22.1 Integral versus Differential Form

With the spin-j kernel in hand, there is a simple representation of the star product in terms of the integral trikernel [14]

$$L^{(j)}(\boldsymbol{n},\boldsymbol{m},\boldsymbol{k}) = \left(\frac{2j+1}{4\pi}\right)^2 \mathrm{Tr}\left[\Delta^{(j)}(\boldsymbol{n})\Delta^{(j)}(\boldsymbol{m})\Delta^{(j)}(\boldsymbol{k})\right] \tag{22.1}$$

in terms of which

$$(W_A \star W_B)(\boldsymbol{n}) = \int_{S^2} d\mu(\boldsymbol{m}) \int_{S^2} d\mu(\boldsymbol{k})\, L^{(j)}(\boldsymbol{n},\boldsymbol{m},\boldsymbol{k}) W_A(\boldsymbol{m}) W_B(\boldsymbol{k}). \tag{22.2}$$

As we are interested in constructing a Fokker-Planck equation, however, what we are after is a differential form for the product. Its construction amounts to defining a bilinear differential operator $L[x,y]$ such that

$$W_{AB} = W_A \star W_B = L[W_A, W_B]. \tag{22.3}$$

The general procedure for constructing this product in the case of SU(2) was given in [15], [16]. The derivation is a comparatively heavy SU(2) tensor calculation, using somewhat obscure properties of 6-j symbols, and I will not present it. The resulting expression

$$W_A \star W_B = N_S \sum_{j=0}^{\infty} a_j \int \frac{d\psi}{2\pi} \tilde{F}^{-1}(\mathcal{J}^2)\Big[((S^+)^j \tilde{F}(\mathcal{J}^2) W_A) \times ((S^-)^j \tilde{F}(\mathcal{J}^2) W_B)\Big] \tag{22.4}$$

is exact, but difficult to use given it is written in terms of fairly abstract differential operators (we will define them below). In the spirit of deformation quantisation, however, it possesses a formal power expansion in a small parameter proportional to $\hbar$. This expansion was worked out to first order in [15], and the corresponding first order Bopp operators were worked out in [17]. The second

work used these to write down a classical Fokker-Planck equation corresponding to the Lindbladian master equation.

Because the resulting Fokker-Planck equation contains terms second order in the small expansion parameter, however, for the derivation to be consistent the star product and Bopp operators[1] [20], [21] used should also be to second order in the parameter. To my knowledge this result is not present in the literature, and so this chapter is devoted to the derivation of an explicit form for the star product that is accurate to second order in the parameter. For completeness I also present Bopp operators to second order.

22.2 Second Order Operator

22.2.1 General Expression and Definitions

We start from equation (39) of [15] for a spin-S system (we use S rather than j in this section to free up the latter for product indices), with $s = s_1 = s_2 = 0$ as we're working with the self-dual representation:

$$W_A \star W_B = N_S \sum_{j=0}^{\infty} a_j \int \frac{d\psi}{2\pi} \tilde{F}^{-1}(\mathcal{J}^2)\Big[((S^+)^j \tilde{F}(\mathcal{J}^2) W_A) \times ((S^-)^j \tilde{F}(\mathcal{J}^2) W_B)\Big] \tag{22.5}$$

where

$$\mathcal{J}^2 = -\left[\frac{\partial^2}{\partial\theta^2} + \cot\theta\frac{\partial}{\partial\theta} + \frac{1}{\sin^2\theta}\left(\frac{\partial^2}{\partial\phi^2} - 2\cos\theta\frac{\partial^2}{\partial\phi\partial\psi} + \frac{\partial^2}{\partial\psi^2}\right)\right], \tag{22.6}$$

$$S^{\pm} = ie^{\mp i\psi}\left(\pm\cot\theta\frac{\partial}{\partial\psi} + i\frac{\partial}{\partial\theta} \mp \frac{1}{\sin\theta}\frac{\partial}{\partial\phi}\right), \tag{22.7}$$

$$a_j = \frac{(-1)^j}{j!(2S+j+1)!}, \tag{22.8}$$

$$N_S = \sqrt{2S+1}, \tag{22.9}$$

$$F(L) = \sqrt{(2S+L+1)!(2S-L)!}, \tag{22.10}$$

$$\tilde{F}(\mathcal{J}^2) D^L{}_{MM'} = F(L) D^L{}_{MM'}. \tag{22.11}$$

The operators $\mathcal{J}^2$ and $S^{\pm}$ possess the property that $[\mathcal{J}^2, S^{\pm}]f(\theta,\phi) = 0$ (note that they do not commute when applied to functions also dependent on ψ). Moreover,

$$\begin{aligned}\mathcal{J}^2(f(\theta,\phi)g(\theta,\phi)) =& g(\theta,\phi)\mathcal{J}^2 f(\theta,\phi) + f(\theta,\phi)\mathcal{J}^2 g(\theta,\phi) \\ &- (S^+ f(\theta,\phi))(S^- g(\theta,\phi)) - (S^+ g(\theta,\phi))(S^- f(\theta,\phi)).\end{aligned} \tag{22.12}$$

[1] Bopp operators replicate the star product action on the Wigner function by some set of quantum operators out of which observables of interest are built out of. For bosonic particles these are typically the creation and annihilation operators, while for spins they are S_z, S_+, and S_-. Bopp operators are a useful shorthand compared to explicitly using the star product.

Before proceeding, we also define some ψ-independent operators via

$$\mathcal{L}^2 = -\left[\frac{\partial^2}{\partial\theta^2} + \cot\theta\frac{\partial}{\partial\theta} + \frac{1}{\sin^2\theta}\frac{\partial^2}{\partial\phi^2}\right], \tag{22.13}$$

$$S^{\pm(j)} = \prod_{k=0}^{j-1}\left(k\cot\theta - \frac{\partial}{\partial\theta} \mp \frac{i}{\sin\theta}\frac{\partial}{\partial\phi}\right), \tag{22.14}$$

such that

$$\mathcal{J}^2 f(\theta,\phi) = \mathcal{L}^2 f(\theta,\phi), \tag{22.15}$$

$$(S^{\pm})^j f(\theta,\phi) = e^{\mp ij\psi} S^{\pm(j)} f(\theta,\phi). \tag{22.16}$$

22.2.2 Order Expansion

We shall carry out the expansion in the parameter $\epsilon = \frac{1}{2S+1}$. If we view S as a physical spin measured in units of $\hbar$, we see that $\epsilon \sim \hbar$ and that this is nothing but the semiclassical approximation. Of course, in most cases the physical spin will not be much greater than $\hbar$, making this approximation a particularly poor fit for spin systems. Nevertheless, this means that we perform the same approximation for both bosons and spins and thus spin truncated Wigner may be seamlessly combined with boson truncated Wigner.

We begin with an expansion of $\tilde{F}(\mathcal{J}^2)$. Note that

$$\begin{aligned} F(L) &= \sqrt{(2S+L+1)!(2S-L)!} \\ &= \sqrt{\left[\frac{(2S+1)!}{2S+1}\prod_{k=0}^{L}(2S+1+k)\right]\left[(2S+1)!\prod_{k=0}^{L}(2S+1-k)^{-1}\right]} \\ &= \frac{(2S+1)!}{\sqrt{2S+1}}\sqrt{\prod_{k=0}^{L}\frac{\frac{1}{\epsilon}+k}{\frac{1}{\epsilon}+k}} = \frac{(2S+1)!}{\sqrt{2S+1}}\sqrt{\prod_{k=0}^{L}\frac{1+\epsilon k}{1+\epsilon k}} \\ &= \frac{(2S+1)!}{\sqrt{2S+1}}\exp\left[\frac{1}{2}\sum_{k=0}^{L}\ln\frac{1+\epsilon k}{1-\epsilon k}\right]. \end{aligned} \tag{22.17}$$

To second order in ϵ,

$$\begin{aligned} \ln\frac{1+\epsilon k}{1-\epsilon k} &= \ln\left[(1+\epsilon k)(1+\epsilon k+\epsilon^2 k^2)\right] \\ &= \ln\left[1+2\epsilon k+2\epsilon^2 k^2+o(\epsilon^2)\right] \\ &= 2\epsilon k + o(\epsilon^2). \end{aligned} \tag{22.18}$$

Thus, substituting this result back into (22.17), we find

$$\begin{aligned} F(L) &= \frac{(2S+1)!}{\sqrt{2S+1}} \exp\left[\frac{1}{2}\epsilon L(L+1) + o(\epsilon^2)\right] \\ &= \frac{(2S+1)!}{\sqrt{2S+1}}\left[1 + \frac{1}{2}\epsilon L(L+1) + \frac{1}{8}\epsilon^2 L^2(L+1)^2 + o(\epsilon^2)\right], \end{aligned} \tag{22.19}$$

from which we conclude that

$$\tilde{F}(\mathcal{J}^2) = \frac{(2S+1)!}{\sqrt{2S+1}} \underbrace{\left[1 + \frac{1}{2}\epsilon\mathcal{J}^2 + \frac{1}{8}\epsilon^2\mathcal{J}^4 + o(\epsilon^2)\right]}_{\tilde{G}(\mathcal{J}^2)}, \tag{22.20}$$

$$\tilde{F}^{-1}(\mathcal{J}^2) = \frac{\sqrt{2S+1}}{(2S+1)!} \underbrace{\left[1 - \frac{1}{2}\epsilon\mathcal{J}^2 + \frac{1}{8}\epsilon^2\mathcal{J}^4 + o(\epsilon^2)\right]}_{\tilde{G}^{-1}(\mathcal{J}^2)}. \tag{22.21}$$

The terms $\frac{(2S+1)!}{\sqrt{2S+1}}$ from $\tilde{F}(\mathcal{J})$ and $\tilde{F}^{-1}(\mathcal{J})$ in (22.5) along with N_S may be combined to rewrite (22.5) as:

$$W_A \star W_B = (2S+1)! \sum_{j=0}^{\infty} a_j \int \frac{d\psi}{2\pi}\, \tilde{G}^{-1}(\mathcal{J}^2)\Big[((S^+)^j \tilde{G}(\mathcal{J}^2) W_A) \times ((S^-)^j \tilde{G}(\mathcal{J}^2) W_B)\Big]. \tag{22.22}$$

This allows us to express $(2S+1)!a_j$ in terms of ϵ:

$$\begin{aligned} (2S+1)!a_j &= \frac{(-1)^j}{j!}\frac{(2S+1)!}{(2S+j+1)!} = \frac{(-1)^j}{j!}\prod_{k=1}^{j}\frac{1}{(2S+k+1)} \\ &= \frac{(-1)^j}{j!}\prod_{k=1}^{j}\frac{\epsilon}{(1+\epsilon k)} = \frac{(-1)^j}{j!}\prod_{k=1}^{j}\Big(\epsilon - \epsilon^2 k + o(\epsilon^2)\Big). \end{aligned} \tag{22.23}$$

To second order in ϵ, therefore, only the $j = 0, 1, 2$ coefficients are relevant and these are

$$c_0 = (2S+1)!a_0 = 1, \tag{22.24}$$

$$c_1 = (2S+1)!a_1 = \epsilon^2 - \epsilon + o(\epsilon^2), \tag{22.25}$$

$$c_2 = (2S+1)!a_2 = \frac{1}{2}\epsilon^2 + o(\epsilon^2), \tag{22.26}$$

through which we may once again rewrite (22.22) as

$$W_A \star W_B = \sum_{j=0}^{2} c_j \int \frac{d\psi}{2\pi}\, \tilde{G}^{-1}(\mathcal{J}^2)\Big[((S^+)^j \tilde{G}(\mathcal{J}^2) W_A) \times ((S^-)^j \tilde{G}(\mathcal{J}^2) W_B)\Big] + o(\epsilon^2). \tag{22.27}$$

We now work out the summand for each j, going by order in ϵ. In each case, it

will be found that the integrand is independent of ψ when simplified (recall that the W-symbols do not depend on ψ, and that we may switch to ψ-independent operators $\mathcal{L}^2$ and $S^{\pm(j)}$ when the expression being acted on is ψ-independent and we can cancel the $e^{ij\psi}$ terms coming from the $S^{\pm}$ operators) and thus the $\int \frac{d\psi}{2\pi}$ integral simply multiplies the integrand by 1 and may be ignored. Since the calculation is heavy on cancelling terms, I denote terms that are about to be cancelled against each-other in the same colour. The final result for each calculation is given a border.

j = 0:

$$\left(1-\frac{1}{2}\epsilon\mathcal{J}^2+\frac{1}{8}\epsilon^2\mathcal{J}^4\right)\left[\left(\left(1+\frac{1}{2}\epsilon\mathcal{J}^2+\frac{1}{8}\epsilon^2\mathcal{J}^4\right)W_A\right)\left(\left(1+\frac{1}{2}\epsilon\mathcal{J}^2+\frac{1}{8}\epsilon^2\mathcal{J}^4\right)W_B\right)\right] \tag{22.28}$$

ϵ^0**:**

$$= \boxed{W_A W_B} \tag{22.29}$$

ϵ^1**:**

$$\begin{aligned} &= \frac{1}{2}W_B\mathcal{J}^2W_A+\frac{1}{2}W_A\mathcal{J}^2W_B-\frac{1}{2}\mathcal{J}^2(W_AW_B) \\ &\overset{(22.12)}{=} \frac{1}{2}\left[(S^+W_A)(S^-W_B)+(S^-W_A)(S^+W_B)\right] \\ &= \boxed{\frac{1}{2}\left[(S^{+(1)}W_A)(S^{-(1)}W_B)+(S^{-(1)}W_A)(S^{+(1)}W_B)\right]} \end{aligned} \tag{22.30}$$

ϵ^2:

$$
\begin{aligned}
&= \frac{1}{4}(\mathcal{J}^2 W_A)(\mathcal{J}^2 W_B) + \frac{1}{8}(W_B \mathcal{J}^4 W_A + W_A \mathcal{J}^4 W_B) \\
&\quad + \frac{1}{8}\mathcal{J}^4 (W_A W_B) - \frac{1}{4}\mathcal{J}^2 (W_B \mathcal{L}^2 W_A + W_A \mathcal{L}^2 W_B) \qquad (22.31)\\
&= \frac{1}{4}(\mathcal{L}^2 W_A)(\mathcal{L}^2 W_B) + \frac{1}{8}(W_B \mathcal{L}^4 W_A + W_A \mathcal{L}^4 W_B) \\
&\quad + \frac{1}{8}\mathcal{J}^2 \Big[W_B \mathcal{L}^2 W_A + W_A \mathcal{L}^2 W_B - (S^{+(1)} W_A)(S^{-(1)} W_B) - (S^{-(1)} W_A)(S^{+(1)} W_B) \Big] \\
&\quad - \frac{1}{4}\mathcal{J}^2 (W_B \mathcal{L}^2 W_A + W_A \mathcal{L}^2 W_B) \qquad (22.32)\\
&= \frac{1}{4}(\mathcal{L}^2 W_A)(\mathcal{L}^2 W_B) + \frac{1}{8}(W_B \mathcal{L}^4 W_A + W_A \mathcal{L}^4 W_B) \qquad (22.33)\\
&\quad - \frac{1}{8}\Big[(\mathcal{L}^2 S^{+(1)} W_A)(S^{-(1)} W_B) + (S^{+(1)} W_A)(\mathcal{L}^2 S^{-(1)} W_B) \\
&\qquad - (S^{+(1)} S^{+(1)} W_A)(S^{-(1)} S^{-(1)} W_B) - (S^{-(1)} S^{+(1)} W_A)(S^{+(1)} S^{-(1)} W_B) \\
&\qquad + (\mathcal{L}^2 S^{-(1)} W_A)(S^{+(1)} W_B) + (S^{-(1)} W_A)(\mathcal{L}^2 S^{+(1)} W_B) \\
&\qquad - (S^{+(1)} S^{-(1)} W_A)(S^{-(1)} S^{+(1)} W_B) - (S^{-(1)} S^{-(1)} W_A)(S^{+(1)} S^{+(1)} W_B) \Big] \\
&\quad - \frac{1}{8}\Big[2(\mathcal{L}^2 W_A)(\mathcal{L}^2 W_B) + W_B \mathcal{L}^4 W_A + W_A \mathcal{L}^4 W_B \\
&\qquad - (S^{+(1)} \mathcal{L}^2 W_A)(S^{-(1)} W_B) - (S^{-(1)} \mathcal{L}^2 W_A)(S^{+(1)} W_B) \\
&\qquad - (S^{+(1)} W_A)(S^{-(1)} \mathcal{L}^2 W_B) - (S^{-(1)} W_A)(S^{+(1)} \mathcal{L}^2 W_B) \Big] \\
&= \boxed{\begin{aligned}
&\frac{1}{8}\Big[(S^{+(1)} S^{+(1)} W_A)(S^{-(1)} S^{-(1)} W_B) + (S^{-(1)} S^{+(1)} W_A)(S^{+(1)} S^{-(1)} W_B) \\
&\quad + (S^{+(1)} S^{-(1)} W_A)(S^{-(1)} S^{+(1)} W_B) + (S^{-(1)} S^{-(1)} W_A)(S^{+(1)} S^{+(1)} W_B) \\
&\quad - (\mathcal{Q} W_A)(S^{-(1)} W_B) - (S^{+(1)} W_A)(\mathcal{R} W_B) \\
&\quad - (\mathcal{R} W_A)(S^{+(1)} W_B) - (S^{-(1)} W_A)(\mathcal{Q} W_B) \Big]
\end{aligned}} \qquad (22.34)
\end{aligned}
$$

where we have defined

$$\mathcal{Q} = [\mathcal{L}^2, S^{+(1)}], \qquad (22.35)$$

$$\mathcal{R} = [\mathcal{L}^2, S^{-(1)}]. \qquad (22.36)$$

j = 1:

$$
\begin{aligned}
&(\epsilon^2 - \epsilon)\Big(1 - \frac{1}{2}\epsilon\mathcal{J}^2 + \frac{1}{8}\epsilon^2\mathcal{J}^4\Big) \\
&\quad \cdot \Big[\Big(S^+\Big(1 + \frac{1}{2}\epsilon\mathcal{J}^2 + \frac{1}{8}\epsilon^2\mathcal{J}^4\Big) W_A\Big)\Big(S^-\Big(1 + \frac{1}{2}\epsilon\mathcal{J}^2 + \frac{1}{8}\epsilon^2\mathcal{J}^4\Big) W_B\Big)\Big]
\end{aligned} \qquad (22.37)
$$

ϵ^0:

$$= \boxed{0} \qquad (22.38)$$

ϵ^1:

$$= \boxed{-(S^{+(1)}W_A)(S^{-(1)}W_B)} \tag{22.39}$$

ϵ^2:

$$= (S^{+(1)}W_A)(S^{-(1)}W_B) + \frac{1}{2}\mathcal{J}^2((S^{+(1)}W_A)(S^{-(1)}W_B)) \tag{22.40}$$
$$- \frac{1}{2}(S^{+(1)}\mathcal{J}^2W_A)(S^{-(1)}W_B) - \frac{1}{2}(S^{+(1)}W_A)(S^{-(1)}\mathcal{J}^2W_B)$$
$$= (S^{+(1)}W_A)(S^{-(1)}W_B) \tag{22.41}$$
$$+ \frac{1}{2}(\mathcal{J}^2S^{+(1)}W_A)(S^{-(1)}W_B) + \frac{1}{2}(S^{+(1)}W_A)(\mathcal{J}^2S^{-(1)}W_B)$$
$$- \frac{1}{2}(S^{+(1)}S^{+(1)}W_A)(S^{-(1)}S^{-(1)}W_B) - \frac{1}{2}(S^{-(1)}S^{+(1)}W_A)(S^{+(1)}S^{-(1)}W_B)$$
$$- \frac{1}{2}(S^{+(1)}\mathcal{J}^2W_A)(S^{-(1)}W_B) - \frac{1}{2}(S^{+(1)}W_A)(S^{-(1)}\mathcal{J}^2W_B)$$
$$= \boxed{\begin{aligned}&(S^{+(1)}W_A)(S^{-(1)}W_B) \\ &+ \frac{1}{2}(\mathcal{Q}W_A)(S^{-(1)}W_B) + \frac{1}{2}(S^{+(1)}W_A)(\mathcal{R}W_B) \\ &- \frac{1}{2}(S^{+(1)}S^{+(1)}W_A)(S^{-(1)}S^{-(1)}W_B) - \frac{1}{2}(S^{-(1)}S^{+(1)}W_A)(S^{+(1)}S^{-(1)}W_B)\end{aligned}} \tag{22.42}$$

j = 2:

$$\frac{1}{2}\epsilon^2\left(1 - \frac{1}{2}\epsilon\mathcal{J}^2 + \frac{1}{8}\epsilon^2\mathcal{J}^4\right) \cdot \left[\left((S^+)^2\left(1 + \frac{1}{2}\epsilon\mathcal{J}^2 + \frac{1}{8}\epsilon^2\mathcal{J}^4\right)W_A\right)\left((S^-)^2\left(1 + \frac{1}{2}\epsilon\mathcal{J}^2 + \frac{1}{8}\epsilon^2\mathcal{J}^4\right)W_B\right)\right] \tag{22.43}$$

ϵ^0:

$$= \boxed{0} \tag{22.44}$$

ϵ^1:

$$= \boxed{0} \tag{22.45}$$

ϵ^2:

$$= \boxed{\frac{1}{2}(S^{+(2)}W_A)(S^{-(2)}W_B)} \tag{22.46}$$

Overall ($\sum_j$):

ϵ^0:

$$= \boxed{W_AW_B} \tag{22.47}$$

ϵ^1:

$$= \frac{1}{2}\left[(S^{+(1)}W_A)(S^{-(1)}W_B) + (S^{-(1)}W_A)(S^{+(1)}W_B)\right] - (S^{+(1)}W_A)(S^{-(1)}W_B) \tag{22.48}$$
$$= \boxed{\frac{1}{2}\left[(S^{-(1)}W_A)(S^{+(1)}W_B) - (S^{+(1)}W_A)(S^{-(1)}W_B)\right]} \tag{22.49}$$

ϵ^2:

$$
\begin{aligned}
&= \frac{1}{8}\Big[(S^{+(1)}S^{+(1)}W_A)(S^{-(1)}S^{-(1)}W_B) + (S^{-(1)}S^{+(1)}W_A)(S^{+(1)}S^{-(1)}W_B) \\
&\quad + (S^{+(1)}S^{-(1)}W_A)(S^{-(1)}S^{+(1)}W_B) + (S^{-(1)}S^{-(1)}W_A)(S^{+(1)}S^{+(1)}W_B) \\
&\quad - (\mathcal{Q}\,W_A)(S^{-(1)}W_B) - (S^{+(1)}W_A)(\mathcal{R}\,W_B) \\
&\quad - (\mathcal{R}\,W_A)(S^{+(1)}W_B) - (S^{-(1)}W_A)(\mathcal{Q}\,W_B)\Big] \\
&\quad + (S^{+(1)}W_A)(S^{-(1)}W_B) \\
&\quad + \frac{1}{2}(\mathcal{Q}\,W_A)(S^{-(1)}W_B) + \frac{1}{2}(S^{+(1)}W_A)(\mathcal{R}\,W_B) \\
&\quad - \frac{1}{2}(S^{+(1)}S^{+(1)}W_A)(S^{-(1)}S^{-(1)}W_B) - \frac{1}{2}(S^{-(1)}S^{+(1)}W_A)(S^{+(1)}S^{-(1)}W_B) \\
&\quad + \frac{1}{2}(S^{+(2)}W_A)(S^{-(2)}W_B)
\end{aligned}
\tag{22.50}
$$

$$
\begin{aligned}
= \boxed{
&-\frac{3}{8}(S^{+(1)}S^{+(1)}W_A)(S^{-(1)}S^{-(1)}W_B) - \frac{3}{8}(S^{-(1)}S^{+(1)}W_A)(S^{+(1)}S^{-(1)}W_B) \\
&+ \frac{1}{8}(S^{+(1)}S^{-(1)}W_A)(S^{-(1)}S^{+(1)}W_B) + \frac{1}{8}(S^{-(1)}S^{-(1)}W_A)(S^{+(1)}S^{+(1)}W_B) \\
&+ \frac{3}{8}(\mathcal{Q}\,W_A)(S^{-(1)}W_B) + \frac{3}{8}(S^{+(1)}W_A)(\mathcal{R}\,W_B) \\
&- \frac{1}{8}(\mathcal{R}\,W_A)(S^{+(1)}W_B) - \frac{1}{8}(S^{-(1)}W_A)(\mathcal{Q}\,W_B)\Big] \\
&+ (S^{+(1)}W_A)(S^{-(1)}W_B) \\
&+ \frac{1}{2}(S^{+(2)}W_A)(S^{-(2)}W_B)
}
\end{aligned}
\tag{22.51}
$$

22.2.3 Simplifying the Operator

The star product for spin is thus given to second order in ϵ by

$$
\begin{aligned}
\star^s &= \mathbb{I}\otimes\mathbb{I} && (22.52)\\
&\quad + \frac{\epsilon}{2}\Big[\, S^{-(1)}\otimes S^{+(1)} - S^{+(1)}\otimes S^{-(1)}\Big] && (22.53)\\
&\quad + \epsilon^2\Big[S^{+(1)}\otimes S^{-(1)} + \frac{1}{2}S^{+(2)}\otimes S^{-(2)} && (22.54)\\
&\qquad + \frac{1}{8}S^{+(1)}S^{-(1)}\otimes S^{-(1)}S^{+(1)} + \frac{1}{8}S^{-(1)}S^{-(1)}\otimes S^{+(1)}S^{+(1)} && (22.55)\\
&\qquad - \frac{3}{8}S^{-(1)}S^{+(1)}\otimes S^{+(1)}S^{-(1)} - \frac{3}{8}S^{+(1)}S^{+(1)}\otimes S^{-(1)}S^{-(1)} && (22.56)\\
&\qquad + \frac{3}{8}F\otimes S^{-(1)} + \frac{3}{8}S^{+(1)}\otimes G - \frac{1}{8}G\otimes S^{+(1)} - \frac{1}{8}S^{-(1)}\otimes F\Big] && (22.57)
\end{aligned}
$$

where

$$S^{+(1)} = -\partial_\theta - i\csc(\theta)\partial_\phi, \tag{22.58}$$

$$S^{-(1)} = -\partial_\theta + i\csc(\theta)\partial_\phi, \tag{22.59}$$

$$S^{+(2)} = \partial_\theta^2 - \cot(\theta)\partial_\theta - \csc^2(\theta)\partial_\phi^2 + 2i\csc(\theta)\partial_\theta\partial_\phi - 2i\cot(\theta)\csc(\theta)\partial_\phi, \tag{22.60}$$

$$S^{-(2)} = \partial_\theta^2 - \cot(\theta)\partial_\theta - \csc^2(\theta)\partial_\phi^2 - 2i\csc(\theta)\partial_\theta\partial_\phi + 2i\cot(\theta)\csc(\theta)\partial_\phi, \tag{22.61}$$

$$F = \csc^2(\theta)\Big(2\cot(\theta)\partial_\phi^2 - 2i\cos(\theta)\partial_\theta\partial_\phi + i\csc(\theta)\partial_\phi + \partial_\theta\Big), \tag{22.62}$$

$$G = \csc^2(\theta)\Big(2\cot(\theta)\partial_\phi^2 + 2i\cos(\theta)\partial_\theta\partial_\phi - i\csc(\theta)\partial_\phi + \partial_\theta\Big). \tag{22.63}$$

It is useful to notice that $\frac{\epsilon}{2}\Big[S^{-(1)}\otimes S^{+(1)} - S^{+(1)}\otimes S^{-(1)}\Big]$ may be rewritten as

$$i\epsilon\left(\overleftarrow{\partial}_\phi\overrightarrow{\partial}_{\cos(\theta)} - \overleftarrow{\partial}_{\cos(\theta)}\overrightarrow{\partial}_\phi\right) = i\epsilon\,{}_s\{\leftarrow,\rightarrow\} \tag{22.64}$$

where ${}_s\{\leftarrow,\rightarrow\}$ is the Poisson bracket on the sphere (with ϕ and $\cos(\theta)$ as conjugate position and momentum). This allows the above cumbersome expression to be rewritten as

$$\star^s = 1 + i\epsilon\,{}_s\{\leftarrow,\rightarrow\} + \epsilon^2\mathcal{B}(\leftarrow,\rightarrow) \tag{22.65}$$

where we have compressed everything multiplying ϵ^2 into $\mathcal{B}(,)$. For completeness, the simplified explicit expression for $\mathcal{B}$ is given by

$$\begin{aligned}\mathcal{B}(W_A,W_B) =& \frac{1}{2}\partial_\theta W_A(\theta,\phi)\partial_\theta W_B(\theta,\phi) - \frac{1}{2}\cot(\theta)\partial_\theta^2 W_A(\theta,\phi)\partial_\theta W_B(\theta,\phi)\\ &- \frac{1}{2}\cot(\theta)\partial_\theta W_A(\theta,\phi)\partial_\theta^2 W_B(\theta,\phi) + \frac{3}{4}\csc^4(\theta)\partial_\phi W_A(\theta,\phi)\partial_\phi W_B(\theta,\phi)\\ &+ \csc^2(\theta)\partial_\theta\partial_\phi W_A(\theta,\phi)\partial_\theta\partial_\phi W_B(\theta,\phi)\\ &- \frac{1}{2}\csc^2(\theta)\partial_\theta^2 W_A(\theta,\phi)\partial_\phi^2 W_B(\theta,\phi)\\ &- \frac{1}{2}\csc^2(\theta)\partial_\phi^2 W_A(\theta,\phi)\partial_\theta^2 W_B(\theta,\phi)\\ &+ \frac{1}{4}\cos(2\theta)\csc^4(\theta)\partial_\phi W_A(\theta,\phi)\partial_\phi W_B(\theta,\phi)\\ &- \cot(\theta)\csc^2(\theta)\partial_\theta\partial_\phi W_A(\theta,\phi)\partial_\phi W_B(\theta,\phi)\\ &- \frac{1}{2}\sin(2\theta)\csc^4(\theta)\partial_\phi W_A(\theta,\phi)\partial_\theta\partial_\phi W_B(\theta,\phi).\end{aligned} \tag{22.66}$$

Finally, we also have the explicit Bopp operators $\mathcal{S} = \sqrt{S(S+1)}$:

$$\begin{aligned}
S_+ \star \circ =& \mathcal{S}e^{i\phi}\sin(\theta)\circ + \mathcal{S}\epsilon e^{i\phi}\Big(\partial_\theta \circ + i\cot(\theta)\partial_\phi \circ\Big) \\
&+ \frac{1}{2}\mathcal{S}\epsilon^2 e^{i\phi}\Big(\sin(\theta)\partial_\theta^2 \circ + 2\cos(\theta)\partial_\theta \circ + i\csc(\theta)\partial_\phi \circ + \csc(\theta)\partial_\phi^2 \circ\Big), \\
S_- \star \circ =& \mathcal{S}e^{-i\phi}\sin(\theta)\circ + \mathcal{S}\epsilon e^{-i\phi}\Big(-\partial_\theta \circ + i\cot(\theta)\partial_\phi \circ\Big) \\
&+ \frac{1}{2}\mathcal{S}\epsilon^2 e^{-i\phi}\Big(\sin(\theta)\partial_\theta^2 \circ + 2\cos(\theta)\partial_\theta \circ - i\csc(\theta)\partial_\phi \circ + \csc(\theta)\partial_\phi^2 \circ\Big), \\
S_z \star \circ =& \mathcal{S}\cos(\theta)\circ - i\mathcal{S}\epsilon\partial_\phi \circ \\
&+ \frac{1}{2}\mathcal{S}\epsilon^2\Big(\cos(\theta)\partial_\theta^2 \circ + \csc(\theta)\Big(\cos(2\theta)\partial_\theta \circ + \cot(\theta)\partial_\phi^2 \circ\Big)\Big), \\
\circ \star S_+ =& \mathcal{S}e^{i\phi}\sin(\theta)\circ + \mathcal{S}\epsilon e^{i\phi}\Big(-\partial_\theta \circ - i\cot(\theta)\partial_\phi \circ\Big) \\
&+ \frac{1}{2}\mathcal{S}\epsilon^2 e^{i\phi}\Big(\sin(\theta)\partial_\theta^2 \circ + 2\cos(\theta)\partial_\theta \circ + i\csc(\theta)\partial_\phi \circ + \csc(\theta)\partial_\phi^2 \circ\Big), \\
\circ \star S_- =& \mathcal{S}e^{-i\phi}\sin(\theta)\circ + \mathcal{S}\epsilon e^{-i\phi}\Big(\partial_\theta \circ - i\cot(\theta)\partial_\phi \circ\Big) \\
&+ \frac{1}{2}\mathcal{S}\epsilon^2 e^{-i\phi}\Big(\sin(\theta)\partial_\theta^2 \circ + 2\cos(\theta)\partial_\theta \circ - i\csc(\theta)\partial_\phi \circ + \csc(\theta)\partial_\phi^2 \circ\Big), \\
\circ \star S_z =& \mathcal{S}\cos(\theta)\circ + i\mathcal{S}\epsilon\partial_\phi \circ \\
&+ \frac{1}{2}\mathcal{S}\epsilon^2\Big(\cos(\theta)\partial_\theta^2 \circ + \csc(\theta)\Big(\cos(2\theta)\partial_\theta \circ + \cot(\theta)\partial_\phi^2 \circ\Big)\Big).
\end{aligned} \tag{22.67}$$

22.3 Tensor Product of Star Products

Compound systems in quantum mechanics are constructed via tensor products of their Hilbert spaces and the operators acting on them. In the Moyal representation, this corresponds to a product of the phase spaces and symbols. To combine symbols, however, the tensor product of the individual star products is also required (if one is using Bopp operators, one simply applies them one at a time as usual).

As an initial example, consider the star product for a free bosonic particle

$$\star^b = e^{i\lambda\{\leftarrow,\rightarrow\}}, \tag{22.68}$$

where $\{,\}$ denotes the Poisson bracket and the arrows denote whether the left or right symbol is to be used (the star product is an infix operator). If we are interested in the expansion to order $O(\lambda^2)$, this becomes

$$\star^b = 1 + i\lambda\{\leftarrow,\rightarrow\} - \frac{\lambda^2}{2}\underbrace{\{\leftarrow,\rightarrow\}^2}_{\left(\overleftarrow{\partial}_{xx}\overrightarrow{\partial}_{pp} - 2\overleftarrow{\partial}_{xp}\overrightarrow{\partial}_{px} + \overleftarrow{\partial}_{pp}\overrightarrow{\partial}_{xx}\right)} + O(\lambda^3) \tag{22.69}$$

Now suppose we consider a compound system involving two such particles (we shall denote them 1 and 2). The symbols now depend on the coordinates of the

product of the two $\mathbb{R}^2$ phase spaces (x_1, p_1, x_2, p_2), and they are combined via the tensor product of the original star products. The tensor product is by definition bilinear and for a pair of bi-differential operators consisting of products of partial derivatives (e.g. $\overleftarrow{\partial}_{x_1}\overrightarrow{\partial}_{p_1}$ and $\overleftarrow{\partial}_{p_2}\overrightarrow{\partial}_{x_2}$) amounts to simply "multiplying them together" while keeping track of which side of the infix expression each operator acts on (thus $\overleftarrow{\partial}_{x_1}\overrightarrow{\partial}_{p_1} \otimes \overleftarrow{\partial}_{p_2}\overrightarrow{\partial}_{x_2} = \overleftarrow{\partial}_{x_1 p_2}\overrightarrow{\partial}_{p_1 x_2}$).

Denoting the Poisson bracket acting on the coordinates of system i by $\{,\}_i$, we see how this occurs for the two-particle system:

$$\begin{aligned}\star_1^b \otimes \star_2^b =& 1 + i\lambda\{\leftarrow,\rightarrow\}_1 \otimes 1 + 1 \otimes i\lambda\{\leftarrow,\rightarrow\}_2 \\ &- \frac{\lambda^2}{2}\{\leftarrow,\rightarrow\}_1^2 \otimes 1 - 1 \otimes \frac{\lambda^2}{2}\{\leftarrow,\rightarrow\}_2^2 \\ &- \lambda^2 \underbrace{\{\leftarrow,\rightarrow\}_1 \otimes \{\leftarrow,\rightarrow\}_2}_{\overleftarrow{\partial}_{x_1 x_2}\overrightarrow{\partial}_{p_1 p_2} - \overleftarrow{\partial}_{x_1 p_2}\overrightarrow{\partial}_{p_1 x_2} - \overleftarrow{\partial}_{p_1 x_2}\overrightarrow{\partial}_{x_1 p_2} + \overleftarrow{\partial}_{p_1 p_2}\overrightarrow{\partial}_{x_1 x_2}} + O(\lambda^3).\end{aligned} \tag{22.70}$$

Rewriting this in terms of the Poisson bracket for the combined system

$$\{\leftarrow,\rightarrow\} = \sum_i \{\leftarrow,\rightarrow\}_i \tag{22.71}$$

we obtain

$$\star_1^b \otimes \star_2^b = 1 + i\lambda\{\leftarrow,\rightarrow\} - \frac{\lambda^2}{2}\{\leftarrow,\rightarrow\}^2 + O(\lambda^3), \tag{22.72}$$

which agrees with the well-known result for a many-particle system with overall Poisson bracket $\{,\}$:

$$\star_{\mathrm{mp}}^b = e^{i\lambda\{\leftarrow,\rightarrow\}}. \tag{22.73}$$

For a system comprising both bosons and spins, we may again construct the appropriate star product by tensoring together $\star^b$ and $\star^s$ appropriately. We begin by constructing it for a system comprising multiple spins, indexed by $j \in J$. Denoting the individual Poisson brackets and $\mathcal{B}$ by ${}_s\{\leftarrow,\rightarrow\}_j$ and $\mathcal{B}_j$, and the overall spin Poisson bracket by ${}_s\{\leftarrow,\rightarrow\}$, it is easy to show that

$$\star^s = \bigotimes_{j\in J} \star_j^s = 1 + i\epsilon\,{}_s\{\leftarrow,\rightarrow\} - \frac{\epsilon^2}{2}\sum_{\substack{j,k\in J \\ j\neq k}} {}_s\{\leftarrow,\rightarrow\}_j \otimes {}_s\{\leftarrow,\rightarrow\}_k + \epsilon^2 \sum_{j\in J} \mathcal{B}_j(\leftarrow,\rightarrow) + O(\epsilon^3). \tag{22.74}$$

Finally, indexing the bosonic particles by $i \in I$, denoting the corresponding Poisson brackets by $\{\leftarrow,\rightarrow\}_i$ and the overall bosonic Poisson bracket by $\{\leftarrow,\rightarrow\}$,

$$\begin{aligned}\star = \star^b \otimes \star^s =& 1 + i\lambda\{\leftarrow,\rightarrow\} + i\epsilon_s\{\leftarrow,\rightarrow\} \\ &- \frac{1}{2}\sum_{\substack{i,j\in I\oplus J \\ i\neq j}} p_i(\leftarrow,\rightarrow)\otimes p_j(\leftarrow,\rightarrow) \\ &- \frac{\lambda^2}{2}\sum_{i\in I}\{\leftarrow,\rightarrow\}_i^2 + \epsilon^2\sum_{j\in J}\mathcal{B}_j(\leftarrow,\rightarrow) + O(3),\end{aligned} \tag{22.75}$$

$$p_i(\leftarrow,\rightarrow) = \begin{cases}\epsilon_s\{\leftarrow,\rightarrow\}_i, & \text{if } i\in J,\\ \lambda\{\leftarrow,\rightarrow\}_i, & \text{if } i\in I.\end{cases} \tag{22.76}$$

Here $O(3)$ indicates expressions of degree > 2 over ϵ and λ. We truncate at this order because both λ and ϵ are physically of order $\hbar$ (indeed λ is essentially $\hbar$), so $O(3)$ is effectively $O(\hbar^3)$ and we have the star product to second order in $\hbar$.

With this, we may now construct the semiclassical equations governing spin-boson dynamics. In this part we will restrict to purely spin systems, since it is the spin part of the formalism that is novel. In the next chapter I will analyse the behaviour of a single spin, showing that the results given by this formalism are almost exact for large spin numbers as expected, but systematically deviate for small spins and discuss this. In the process we will review the behaviour of the Fokker-Planck equation on a sphere and its mapping to a stochastic differential equation in this context.

Chapter 23

Truncated Wigner and the LMG Model

A very simple model to test our formalism on is a restricted form of the Lipkin-Meshkov-Glick (LMG) Hamiltonian [22], describing a single quantum spin, with dissipation (we have reinserted factors of $\hbar$):

$$\partial_t \rho = \mathcal{L}_1[\rho], \tag{23.1}$$

$$\mathcal{L}_1[\rho] = -\frac{i}{\hbar}[H_1, \rho] + \frac{\Gamma}{\hbar}(\hbar^2 S^- \rho S^+ - \frac{\hbar^2}{2}\{S^+S^-, \rho\}), \tag{23.2}$$

$$H_1 = -J\hbar^2 S_x^2 + \Delta\hbar S_z. \tag{23.3}$$

We see that $\Gamma\hbar$ is a frequency, meaning that we can define a a dimensionless time variable $\tau = t\Gamma\hbar$. Then, making the dimensionless definitions

$$\tilde{J} = \frac{J}{\Gamma}, \quad \tilde{\Delta} = \frac{\Delta}{\Gamma\hbar}, \tag{23.4}$$

we obtain the dimensionless equation

$$\partial_\tau \rho = -i[-\tilde{J}S_x^2 + \tilde{\Delta}S_z, \rho] + (S^-\rho S^+ - \frac{1}{2}\{S^+S^-, \rho\}). \tag{23.5}$$

From Refs [23], [24] we know to consider not the symbol $\rho(\theta, \phi)$ but rather the measure-weighted symbol $\bar{\rho}(\theta, \phi) = \sin(\theta)\rho(\theta, \phi)$ when constructing our Fokker-Planck equation (this has to do with our how our area element interacts with the generalised Stokes theorem when formulating the continuity equation), so we consider

$$\begin{aligned}\partial_\tau \bar{\rho}(\theta, \phi) = \sin(\theta)\Big(&- i[[-\tilde{J}S_x(\theta, \phi) \star S_x(\theta, \phi) + \tilde{\Delta}S_z(\theta, \phi), \rho(\theta, \phi)]] \\ &+ \Big(S^-(\theta, \phi) \star \rho \star S^+(\theta, \phi) \\ &- \frac{1}{2}[[[S^+(\theta, \phi) \star S^-(\theta, \phi), \rho(\theta, \phi)]]]\Big)\Big).\end{aligned} \tag{23.6}$$

where

$$[[W_A, W_B]] = W_A \star W_B - W_B \star W_A, \tag{23.7}$$

$$[[[W_A, W_B]]] = W_A \star W_B + W_B \star W_A. \tag{23.8}$$

23.1 Fokker-Planck Equation and Ito SDE

The right hand side can be shown to be an exact differential of a smooth one-form, so this is a continuity equation on the sphere. This confirms that the normalisation of the quasi-distribution is preserved. Moreover, it is not too difficult to show that this is in fact a Fokker-Planck equation in $\bar{\rho}(\theta, \phi)$. Taking 1 to be θ and 2 to be ϕ in index notation, we find that

$$\dot{\bar{\rho}}(\theta, \phi) = -\partial_i[\mu_i(\theta, \phi)\bar{\rho}(\theta, \phi)] + \frac{1}{2}\partial_i\partial_j[D_{ij}(\theta, \phi)\bar{\rho}(\theta, \phi)], \tag{23.9}$$

where

$$D = \begin{pmatrix} \lambda^2 & 0 \\ 0 & \lambda^2 \cot^2(\theta) \end{pmatrix}, \tag{23.10}$$

$$\mu = \lambda \begin{pmatrix} \frac{1}{2}\lambda \cot(\theta) + \mathcal{S}\sin(\theta)(1 + \tilde{J}\sin(2\phi)) \\ \tilde{\Delta} + 2\tilde{J}\mathcal{S}\cos(\theta)\cos^2(\phi) \end{pmatrix}, \tag{23.11}$$

$$\mathcal{S} = \sqrt{j(j+1)}, \tag{23.12}$$

$$\lambda = 2\mathcal{S}\epsilon. \tag{23.13}$$

D is clearly positive-semidefinite on $\theta \in [0, \pi]$ so the Fokker-Planck equation is well-posed and should represent a stochastic process.

Since the sphere cannot be covered by a single coordinate chart and the chart we are presently working has singular points at $\theta = 0, \pi$, some care is called for when converting the Fokker-Planck equation to an SDE. In any interior neighbourhood of the chart the Fokker-Planck equation should describe an Ito stochastic process governed by

$$\begin{pmatrix} d\theta \\ d\phi \end{pmatrix} = \lambda \begin{pmatrix} \frac{1}{2}\lambda \cot(\theta) + \mathcal{S}\sin(\theta)(1 + \tilde{J}\sin(2\phi)) \\ \tilde{\Delta} + 2\tilde{J}\mathcal{S}\cos(\theta)\cos^2(\phi) \end{pmatrix} dt + \begin{pmatrix} \lambda & 0 \\ 0 & \lambda\cot(\theta) \end{pmatrix} \begin{pmatrix} dW_1 \\ dW_2 \end{pmatrix} \tag{23.14}$$

so the question is mainly one of what occurs at the singular points at the boundary of the chart. One approach would be to consider the sphere extrinsically, embedding it in $\mathbb{R}^3$ and lifting the Fokker-Planck equation to one in that space and possessing radius as a conserved quantity. This approach is sketched in Appendix E as a mathematical curiosity and confirmation that our local chart reasoning about the form of the SDE is correct. There is, however, a more direct way

to understand this boundary behaviour.

Writing out the equation for $d\theta$,

$$d\theta = \left(\frac{1}{2}\lambda^2 \cot(\theta) + \lambda \mathcal{S} \sin(\theta)(1 + \tilde{J}\sin(2\phi))\right)dt + \lambda dW_1, \tag{23.15}$$

we notice that the $\frac{1}{2}\lambda^2 \cot(\theta)$ term is highly singular and repulsive at the points $\theta = 0, \pi$. Rescaling the time by $dt\lambda^2 = d\tau$, we obtain (the Wiener term rescales as just λ)

$$d\theta = \Big(\underbrace{\frac{1}{2}\cot(\theta) + \frac{\mathcal{S}}{\lambda}\sin(\theta)(1 + \tilde{J}\sin(2\phi))}_{m(\theta)} \Big)d\tau + dW_1. \tag{23.16}$$

It is then true that

$$\exists c_1 < \infty \; s.t. \left| m(\theta) - \frac{1}{2\theta} \right| \leq c_1 \theta \text{ and } \left| \partial_\theta m(\theta) + \frac{1}{2\theta^2} \right| \leq c_1 \theta \text{ for } \theta \in [0, \pi/2], \tag{23.17}$$

$$\exists c_2 < \infty \; s.t. \left| m(\pi - \theta) - \frac{1}{2\theta} \right| \leq c_2 \theta \text{ and } \left| \partial_\theta m(\pi - \theta) + \frac{1}{2\theta^2} \right| \leq c_2 \theta \text{ for } \theta \in [0, \pi/2], \tag{23.18}$$

which means that the process is asymptotically Bessel-$\frac{1}{2}$ at $\theta = 0, \pi$. This in turn means that it almost surely does not reach these points in finite time if started from any point $\theta \in (0, \pi)$ [25], so the singular nature of the chart at these points poses no problems for defining the SDE so long as we do not initialize trajectories starting from them; since our initial probability density will always assign zero measure to these points, we will have no need to do so.

The only difficulty in this regard arises in simulations, since numerical error may lead a trajectory to overshoot these boundary points even if the abstract process should not reach them. Given that the main feature of the Bessel process is the incredibly strong repulsive term, it seems reasonable to fix this numerical issue by setting $\theta = 0, \pi$ as hard reflecting boundaries in simulations.

23.2 Initial Distribution

With the SDE corresponding to the spherical Fokker-Planck equation identified, we must now identify how we intend to sample from $\bar{\rho}(\theta, \phi)$.

It was argued in Ref. [11] that, since all pure spin states have non-positive symbols, the latter are not valid probability distributions and hence cannot be sampled from. While the first part of this statement is true, the second is erroneous. The positive and negative restrictions[1] $\bar{\rho}_+(\theta, \phi)$, $\bar{\rho}_-(\theta, \phi)$ of the measure-weighted symbol are both positive and, since they have the same boundary conditions and the Fokker-Planck equation is linear, are evolved independently. One

[1] $\bar{\rho}_+(\theta, \phi) \geq 0$, $\bar{\rho}_-(\theta, \phi) \geq 0$, $\bar{\rho}_+(\theta, \phi) - \bar{\rho}_-(\theta, \phi) = \bar{\rho}_(\theta, \phi)$

may thus sample $|\bar{\rho}(\theta,\phi)|$, including samples for which the trajectory originated from the domain of the positive restriction with a positive sign and those for which it originated from the domain of the negative restriction with a negative one when averaging. Since the mass of $|\bar{\rho}(\theta,\phi)|$ may not be equal to 1, we will also need to multiply the final average by this value since averaging over samples assumes the original distribution was normalised.

For the simulations in this chapter, we will initialize the spin in a maximum weight state $|j,j\rangle\langle j,j|$ and consider $j = \frac{1}{2}, 10$. This is so we may observe how large and small spin numbers affect our approximation, which is based on a truncation ideally suited for large spin numbers. From (21.37), (21.38) we know these to be

$$\bar{\rho}_{10}(\theta,\phi) = \sin(\theta)\sum_{l=0}^{20}\frac{2l+1}{21}C^{(10\,l\,10)10\,0}{}_{10}P_l(\cos(\theta)), \tag{23.19}$$

$$\bar{\rho}_{\frac{1}{2}}(\theta,\phi) = \sin(\theta)\sum_{l=0}^{1}\frac{2l+1}{2}C^{(\frac{1}{2}\,l\,\frac{1}{2})\frac{1}{2}\,0}{}_{\frac{1}{2}}P_l(\cos(\theta)). \tag{23.20}$$

The total mass of the norm of the first is numerically found to be 0.0952381, while for the second it is 1.1547.

23.3 Observables

Given that we have only a single spin at our disposal and that the purpose of the present simulations is to get an overall sense of the method's behaviour, we will restrict ourselves to observing the evolution of $\langle S_z\rangle$ over time. As mentioned above, we will initialize in the maximum weight states for two different spin magnitudes and then compare to dynamics obtained by directly integrating the master equation using the QuantumOptics.jl library[2] [26].

This is also a good place to comment on time-correlation functions, specifically why they are difficult to compute. This was touched upon in Part Ib but, with the language of the star product in hand, we may now elaborate. Specifically, consider a conventional time-correlation function of random variables $O_1(x)$ and $O_2(x)$ for a stationary process:

$$\langle O_1(t_1)O_2(t_2)\rangle = \int dx_1 dx_2 dx_3\, O_1(x_1)P(x_1,x_2;t_1-t_2)O_2(x_2)P(x_2,x_3;t_2)P(x_3). \tag{23.21}$$

Here $P(x,t;x',t')$ is the transition probability and $P(x)$ is the initial distribution. Here the transition probability acts as a propagation kernel for the initial distribution, evolving it forward in time. It is this object that is represented by a set of

[2]QuantumOptics.jl is a numerical library for simulating open quantum systems, written in and for the Julia programming language. It is developed by the CQED group at the Institute for Theoretical Physics of the University of Innsbruck.

SDE trajectories starting at x' and finishing at x.

Analogously to the transition probability, there exists an integral kernel for evolving the density matrix symbol. Using the star product integral trikernel one could construct an exact expression for it in terms of symbols of Kraus operators, but from the perspective of Truncated Wigner it is again simply given by sets of trajectories with fixed initial and final points. Denoting this kernel by K, we may write an analogous expression for the time-correlation function of two operators:

$$\begin{aligned}&\langle O_1(t_1)O_2(t_2)\rangle \\ &= \int d\mu_j(\boldsymbol{m})d\mu_j(\boldsymbol{n})d\mu_j(\boldsymbol{k})\, O_1(\boldsymbol{n})\star[K(\boldsymbol{n},\boldsymbol{m};t_1-t_2)O_2(\boldsymbol{m})\star[K(\boldsymbol{m},\boldsymbol{k};t_2)P(\boldsymbol{k})]].\end{aligned} \tag{23.22}$$

Here the product between operators and all preceding terms is now a star product, and therein lies the problem. Expanding the star product in a series will give the normal probabilistic expression as the classical limit, but will now contain extra terms at higher orders. These arise from the 'back action' of quantum measurements on the quantum state, and may be modelled by introducing jumps to the trajectories at the times of measurement [27]. The time symmetric ordering we encountered in Part Ib is in fact a special ordering for bosonic theories that cancels out these back action terms, leaving only the classical expression, and thus allowing for conventional averaging over trajectories. Because the observables of the spin theory are not the canonical position and momentum of the spin Poisson bracket, the time symmetric ordering does not trivially carry over and I do not currently know if an analogous ordering exists. Due to these difficulties, in this part we will restrict ourselves to spatial-correlation functions once we move onto lattice models in the next chapter.

23.4 Spin-10 Simulation

The simulation for spin-10 was run with $\tilde{\Delta} = \tilde{J} = 10$, initialized in the $|10,10\rangle\langle 10,10|$ pure state. The attached plots demonstrate the evolution of the system obtained with the stochastic method compared to direct integration using QuantumOptics.jl [26].

For the stochastic method, 30 instances of the average S_z are calculated, each over n trajectories with $n = 100$, 500, 1000, 2000, 4000, 8000 to show stochastic convergence. The plots on the left show the average of these means together with the maximum and minimum deviations of them from it as compared to the directly integrated solution labelled E.S..

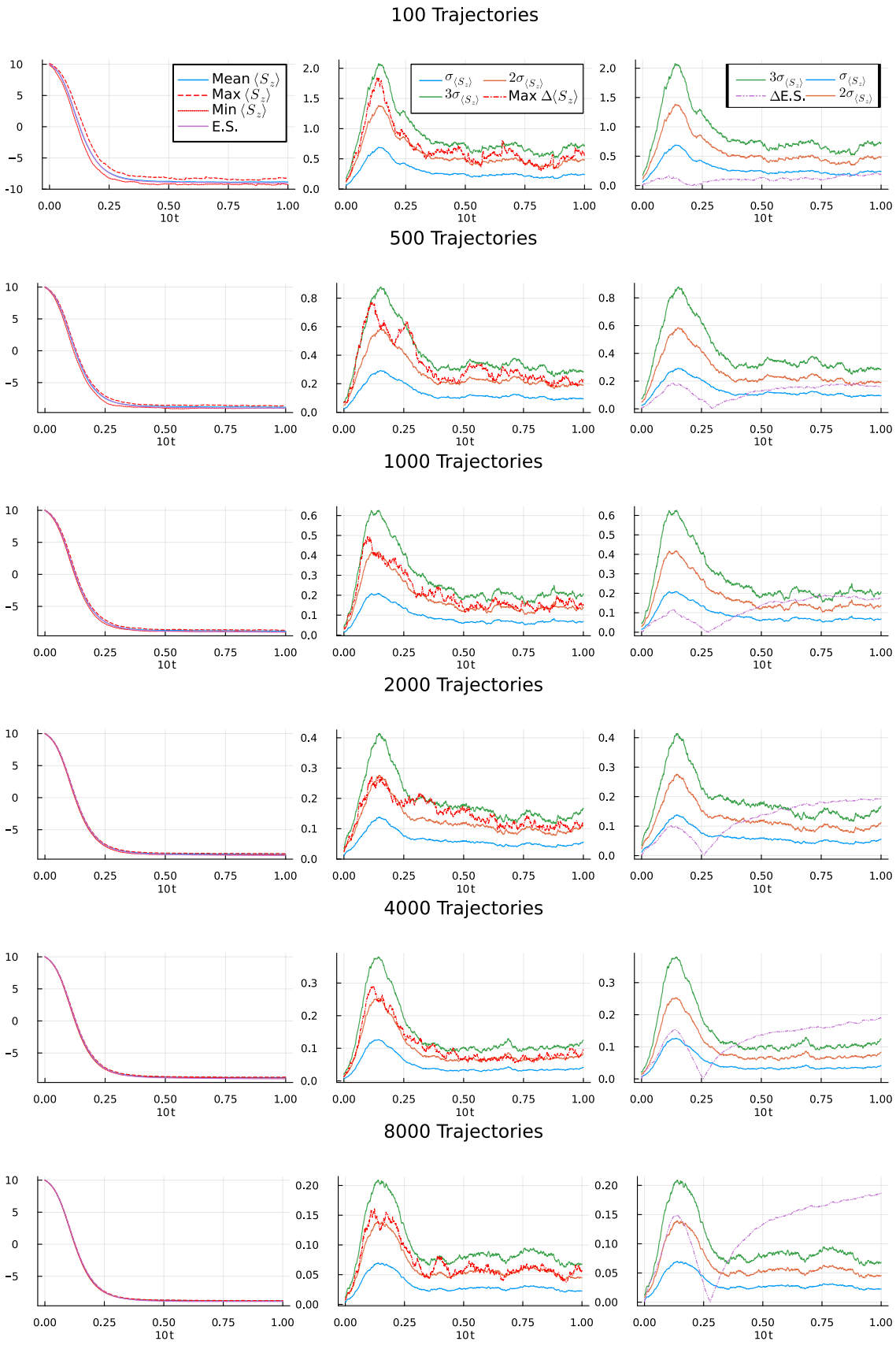

Figure 23.1: Evolution of the spin-10 LMG model using the stochastic Truncated Wigner method and QuantumOptics.jl, the latter labelled E.S. for exact solution. The time axis has been normalized to final time 1 for plotting, with the actual final time being 0.1.

We see that at the initial time the method is exact, meaning the sign-weighted sampling from the non-positive function works correctly (though for $j = 10$ the function is almost positive, so a better demonstration will be the case of $j = \frac{1}{2}$). Furthermore, as the number of trajectories increases, the overall mean and its maximum deviations tightly converge to the directly integrated solution.

This may be seen in more detail in the middle and rightmost plots: the middle show the empirical standard deviations of the mean and that its maximum deviation remains within two or three standard deviations, while the rightmost compare the deviation of the directly integrated solution from the mean against the standard deviations. From the plots on the right we see that at long times there is clearly a systematic difference between the stochastic solution and the directly integrated one. For spin-10, however, this deviation is on the order of 2–3% of the final equilibrium value of the observable, suggesting the method is comparatively accurate for high spin values as expected.

There are two ways to understand this good behaviour for large spins besides the obviously improved accuracy of the series truncation. One is that the correct function space for all symbols in the spin-j theory is spanned by spherical harmonics of order up to $2j$, a constraint the Fokker-Planck equation does not respect. Thus the larger this function space, the less serious the error introduced by the stochastic evolution. The other is that the Fokker-Planck equation is generally only able to produce entirely positive equilibrium distributions[3]. For large spins the pure spin states are almost entirely positive and so this does not pose too much of an issue. The situation is rather different for smaller spins, as we are about to see.

23.5 Spin-$\frac{1}{2}$ Simulation

We repeat the simulation of the previous section for the same parameters, number of trajectories, and so on but with $j = \frac{1}{2}$ and initial state $|\frac{1}{2},\frac{1}{2}\rangle\langle\frac{1}{2},\frac{1}{2}|$. For this spin we have $S_x^2 \propto I$ and so it is easy to see that minimum weight state $|\frac{1}{2},-\frac{1}{2}\rangle\langle\frac{1}{2},-\frac{1}{2}|$ is the steady state (this was not so for spin-10).

Inspecting the corresponding plots, stochastic convergence occurs at the same rate as for spin-10 with the standard deviation of the mean decaying by a factor of 10 between 100 and 8000 trajectories. In this case, however, the mean given by the stochastic method does not converge onto its directly integrated counterpart, with a clear systematic error of approximately 16%. The reason for this is easy to see if one plots the minimum weight pure state symbols for spin-10 and spin-$\frac{1}{2}$ side by side:

[3]One could in principle engineer an equation with multiple steady states and then construct the positive and negative restrictions of a density symbol to converge to different ones, but this would be rather artificial.

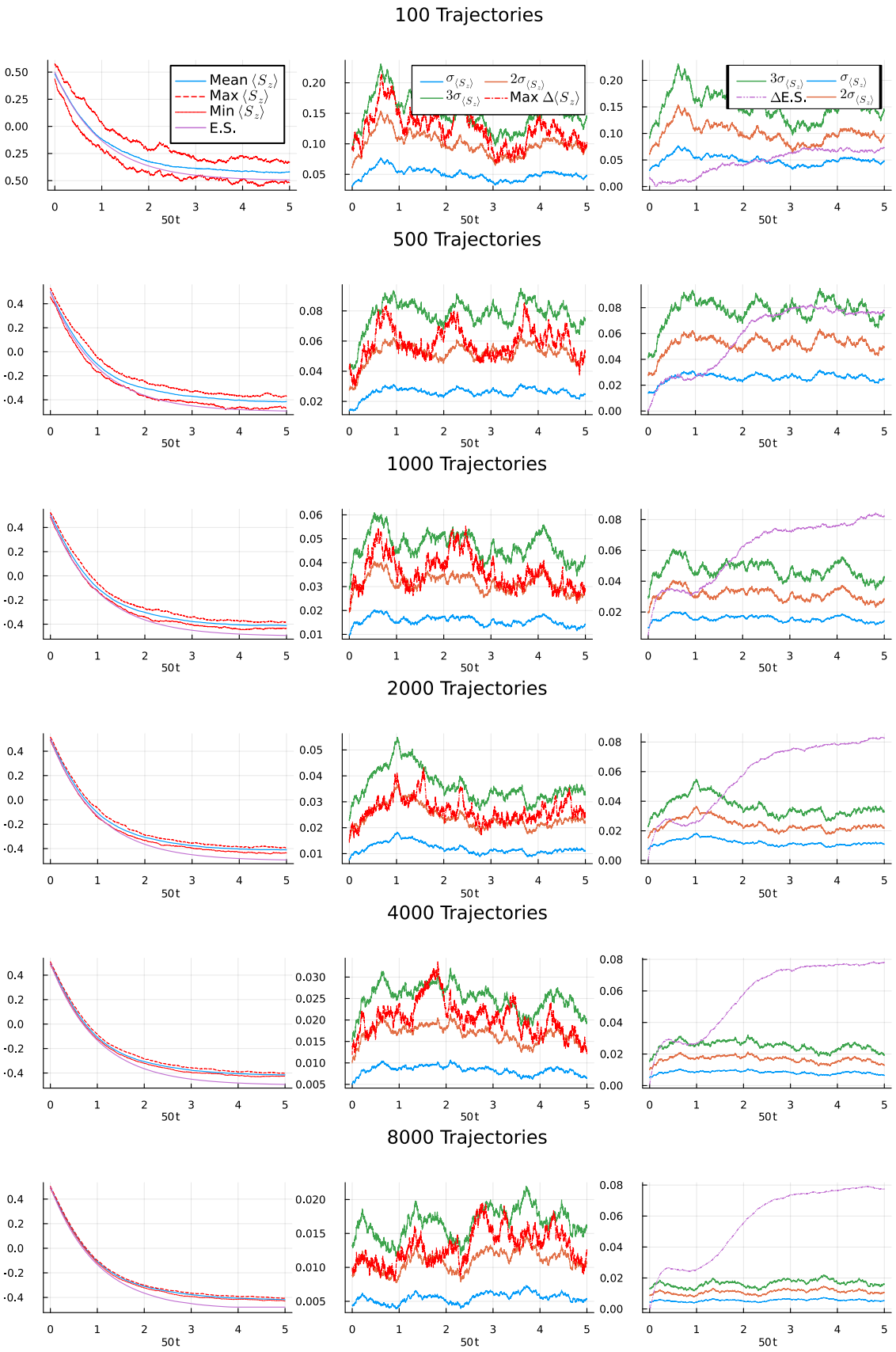

Figure 23.2: Evolution of the spin-$\frac{1}{2}$ LMG model using the stochastic Truncated Wigner method and QuantumOptics.jl, the latter labelled E.S. for exact solution. The time axis has been normalized to final time 1 for plotting, with the actual final time being 0.1.

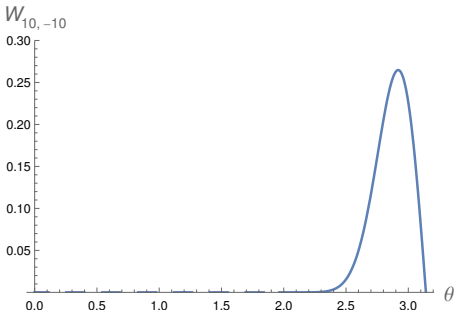

Figure 23.3: Symbol of the pure state $|10,-10\rangle\langle 10,-10|$.

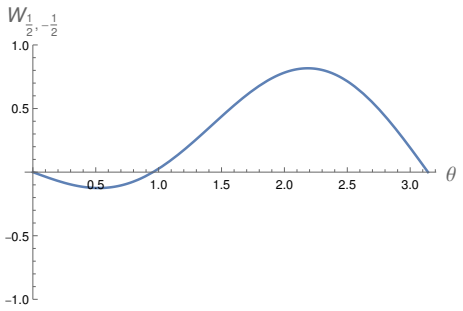

Figure 23.4: Symbol of the pure state $|\frac{1}{2},-\frac{1}{2}\rangle\langle\frac{1}{2},-\frac{1}{2}|$.

While the spin-10 symbol is essentially entirely positive and could be easily reproduced as the stationary distribution of a Fokker-Planck equation (though it is not the stationary distribution in our case), the spin-$\frac{1}{2}$ symbol has a substantial negative portion for small θ. The effect of this is to push the expectation of S_z to be even smaller than a purely positive distribution concentrated at large θ, and this is exactly the effect we see in our plots: the stochastic simulation, which can only produce a positive distribution, does not achieve a sufficiently negative value of $\langle S_z\rangle$ in equilibrium.

Nevertheless, despite this systematic error, the simulation has captured the correct phenomenological behaviour even for a small spin, despite the truncation of the star product expansion being strictly valid in the high spin limit. In the next chapter we will see that this trend continues for significantly more complicated spin lattice models: despite the spin-$\frac{1}{2}$ being seemingly incompatible with the truncation, broadly correct results are obtained regardless for both macro observables and correlation functions.

Chapter 24

Driven-Dissipative Anisotropic XY Model

In this chapter we will apply the stochastic Truncated Wigner method to spin lattice models. Certain considerations relating to convergence rates and the possibility of sampling from non-negative initial distributions must be taken into account when transitioning from a single spin to a large lattice, and these are discussed in Appendix F. For the simulations performed in this chapter I acknowledge the use of the UCL Kathleen High Performance Computing Facility (Kathleen@UCL), and associated support services.

For our purposes the driven-dissipative anisotropic XY model is the spin-$\frac{1}{2}$ lattice model with cyclic boundary conditions defined by

$$H_{XY} = \frac{\hbar^2}{z}\sum_{j,k} J(j,k)\left(S_j^+ S_k^+ + S_j^- S_k^-\right), \tag{24.1}$$

$$\mathcal{L}\rho = -i[H_{XY},\rho] + \Gamma\hbar^2\sum_j\left(S_j^-\rho S_j^+ - \frac{1}{2}\{S_j^+ S_j^-,\rho\}\right), \tag{24.2}$$

$$\partial_t\rho = \frac{1}{\hbar}\mathcal{L}\rho. \tag{24.3}$$

once again we wish to work with a dimensionless equation, so observe that $\Gamma\hbar$ is a frequency and define the dimensionless time $\tau = t\Gamma\hbar$. Then, defining $\tilde{J}(j,k) = \frac{J(j,k)}{\Gamma}$,

$$\partial_\tau\rho = -\frac{i}{z}\left[\sum_{j,k}\tilde{J}(j,k)\left(S_j^+ S_k^+ + S_j^- S_k^-\right),\rho\right] + \sum_j\left(S_j^-\rho S_j^+ - \frac{1}{2}\{S_j^+ S_j^-,\rho\}\right). \tag{24.4}$$

Supposing that there are $N = n^2$ spins arranged in a square lattice according to

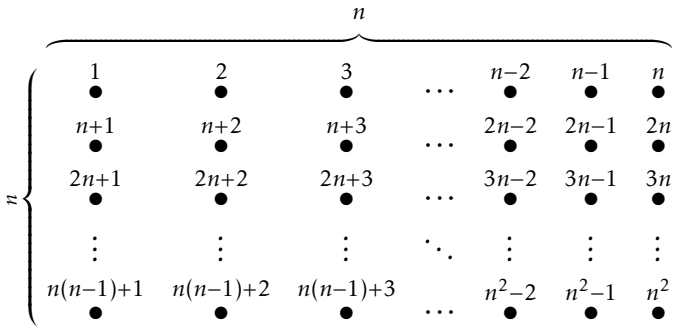

(24.5)

with the corresponding vector of coordinates ordered as $(\theta_1, \phi_1, \theta_2, \phi_2, \ldots, \theta_{n^2}, \phi_{n^2})$, and defining

$$\mathcal{S} = \sqrt{j(j+1)}, \tag{24.6}$$

$$\lambda = 2\mathcal{S}\epsilon, \tag{24.7}$$

as before, we find the following block-diagonal diffusion matrix:

$$D = \frac{\lambda^2}{2}\begin{pmatrix} \boxed{\begin{matrix} 1 & 0 \\ 0 & \cot^2\theta_1 \end{matrix}} & 0 & 0 & 0 \\ 0 & \boxed{\begin{matrix} 1 & 0 \\ 0 & \cot^2\theta_2 \end{matrix}} & 0 & 0 \\ 0 & 0 & \ddots & 0 \\ 0 & 0 & 0 & \boxed{\begin{matrix} 1 & 0 \\ 0 & \cot^2\theta_{n^2} \end{matrix}} \end{pmatrix}. \tag{24.8}$$

We also the drift vector, which may be represented as the sum of a vector μ_D coming from the dissipator and a vector μ_H coming from the Hamiltonian:

$$\mu_D = \lambda\begin{pmatrix} \frac{\lambda}{2}\cot\theta_1 + \mathcal{S}\sin\theta_1 \\ 0 \\ \vdots \\ \frac{\lambda}{2}\cot\theta_i + \mathcal{S}\sin\theta_i \\ 0 \\ \vdots \end{pmatrix}, \quad \mu_H = -\frac{2}{z}\mathcal{S}\lambda\begin{pmatrix} \sum_{j\neq 1}\tilde{J}(1,j)\sin\theta_j\sin(\phi_1+\phi_j) \\ \sum_{j\neq 1}\tilde{J}(1,j)\cot\theta_1\sin\theta_j\cos(\phi_1+\phi_j) \\ \vdots \\ \sum_{j\neq i}\tilde{J}(i,j)\sin\theta_j\sin(\phi_i+\phi_j) \\ \sum_{j\neq i}\tilde{J}(i,j)\cot\theta_i\sin\theta_j\cos(\phi_i+\phi_j) \\ \vdots \end{pmatrix} \tag{24.9}$$

We observe that, as before, the dissipation μ_D vector serves to yield Bessel Process dynamics near the singular points of the coordinate chart, preventing trajectories

from reaching these points.

Here z is a normalizing constant associated with the range of the interaction $\tilde{J}(j,k)$. If we split up $\tilde{J}(j,k)$ as a constant $\tilde{J}$ and range function $r(j,k)$ such that $\tilde{J}(j,k) = \tilde{J} \cdot r(j,k)$, taking a spin i in the middle of the lattice and defining z as

$$z = \frac{1}{2} \sum_{j \neq i} r(i,j) \tag{24.10}$$

allows the mean field phase transition points of this model (to be described momentarily) to depend only on $\tilde{J}$ and not the range function of the interaction in the thermodynamic limit. For nearest-neighbour interactions the above definition gives z as simply the coordination number divided by two.

The mean field equations of this model are given by (extended to ranged interactions from Ref. [28]):

$$\frac{d\langle S_i^x \rangle}{dt} = -\frac{1}{2}\langle S_i^x \rangle - \frac{2\tilde{J}}{z} \sum_{j \neq i} r(i,j) \langle S_i^z \rangle \langle S_j^y \rangle, \tag{24.11}$$

$$\frac{d\langle S_i^y \rangle}{dt} = -\frac{1}{2}\langle S_i^y \rangle - \frac{2\tilde{J}}{z} \sum_{j \neq i} r(i,j) \langle S_i^z \rangle \langle S_j^x \rangle, \tag{24.12}$$

$$\frac{d\langle S_i^z \rangle}{dt} = -(\langle S_i^z \rangle + \frac{1}{2}) + \frac{\tilde{J}}{z} \sum_{j \neq i} r(i,j) \Big(\langle S_i^x \rangle \langle S_j^y \rangle + \langle S_i^y \rangle \langle S_j^x \rangle \Big). \tag{24.13}$$

For small $\tilde{J}$ the equations have a single stationary point at $\langle S_i^x \rangle = \langle S_i^y \rangle = 0$ and $\langle S_i^z \rangle = -\frac{1}{2}$. This is referred to in [28] as the paramagnetic phase. If for every i we consider a solution $\langle S_i^x \rangle = \langle S_j^y \rangle$, $\langle S_j^x \rangle = \langle S_i^y \rangle$ for $r(i,j) \neq 0$, we see that solutions of this form appear at $\tilde{J} = \frac{1}{4}$ while the paramagnetic solution becomes unstable. Thus, in the thermodynamic limit there is a phase transition at $\tilde{J} = \frac{1}{4}$ if no other solutions appear. This is the case for nearest neighbour interactions [28] and 'infinite range' interactions ($r(i,j) = \text{const}$ on a finite lattice, since the thermodynamic limit is not defined in this case) [29]. Between these extremes detailed analysis of the mean field unfortunately appears to not exist in the literature, but it is evident that once destabilised the paramagnetic phase should remain unstable in favour of either the phase described above or some other phase for all $\tilde{J} \geq \frac{1}{4}$.

The invaluable feature of the anisotropic XY model is that the true behaviour disagrees with the mean field. For nearest neighbour interactions one finds that no ordered phase and thus no phase transition at all [30], [31], while for an algebraically decaying interaction the phase diagram is more complicated than the mean field prediction [32]. This presents an opportunity to demonstrate that my method goes beyond the mean field, correctly identifying these phase diagrams and giving phenomenologically correct correlation functions in disordered and ordered phases.

24.1 Nearest Neighbour Interactions

In this case $r(i,j) = 1$ if $|i-j| = 1$ and $= 0$ otherwise. For this system the mean field phase diagram consists of the paramagnetic phase below $\tilde{J} = \frac{1}{4}$ and a 'staggered XY' phase [28] above that. The latter fits our categorization in the previous section, consisting of two chequerboard sub-lattices A and B such that $S_A^x = S_B^y$ and $S_A^y = S_B^x$. This means that spins on the A sub-lattice will form some angle θ with the $x = y$ direction while those on the B sub-lattice will form $-\theta$. This corresponds to a breaking of the global U(1) symmetry of the system given by $S_i^+ \to e^{i\theta}$, $S_i^- \to e^{-i\theta}$, $S_j^+ \to e^{-i\theta}$,$S_j^- \to e^{i\theta}$ for $i \in A$, $j \in B$.

Since in finite spin systems spontaneous symmetry breaking cannot occur [33], we expect the steady state to have $S^x = \sum_i S_i^x = 0$ and $S^y = \sum_i S_i^y = 0$ in the absence of an external symmetry breaking field. Indeed, when modelled by a Fokker-Planck equation, the steady state is expected to correspond to a uniform probabilistic mixture of the symmetry broken states. We will thus focus on observables that are predicted to be non-zero even in this mixture, starting with the macroscopic $S^z = \sum_i S_i^z$ magnetization and the macroscopic product $S^x S^y$. The latter is, as I will momentarily demonstrate, predicted to exhibit fairly large values in the mixture steady state despite not being U(1) invariant.

24.1.1 Macroscopic S^z Magnetization

Throughout this section a 20×20 lattice of spin-$\frac{1}{2}$ particles is simulated for time $\tau = [0, 30]$ (except when stated otherwise). Due to an error in the code describing the initial distribution, its form does not admit a simple description (the code generating it is preserved). Nevertheless, the simulation is run for long enough for convergence to be observed in the expectations under investigation, and the system converges to a state with $S^x = S^y \approx 0$ as expected[1]. Values for $\langle S^z \rangle$ in the thermodynamic limit were calculated in [34] for a range of $\tilde{J}$, and these literature values were reproduced for me using tensor network code inherited from that work by group member Jack Dunham. Fig. 24.1 is a plot of the stochastic method result in blue, the tensor network one in red, and the mean field in green. The exact equation for the mean field is worked out below, and I have normalized the plot to magnetization per spin (with $N = 400$ spins). The blue stochastic plot has errors bars, estimated by empirically calculating the standard deviation of the mean over 80 trajectories from 100 such batches and then extrapolating to 8000 trajectories, but they are so small so as to be invisible.

[1] Since we are interested exclusively in the unique steady state, the precise nature of the initial distribution, and thus the coding error, are irrelevant.

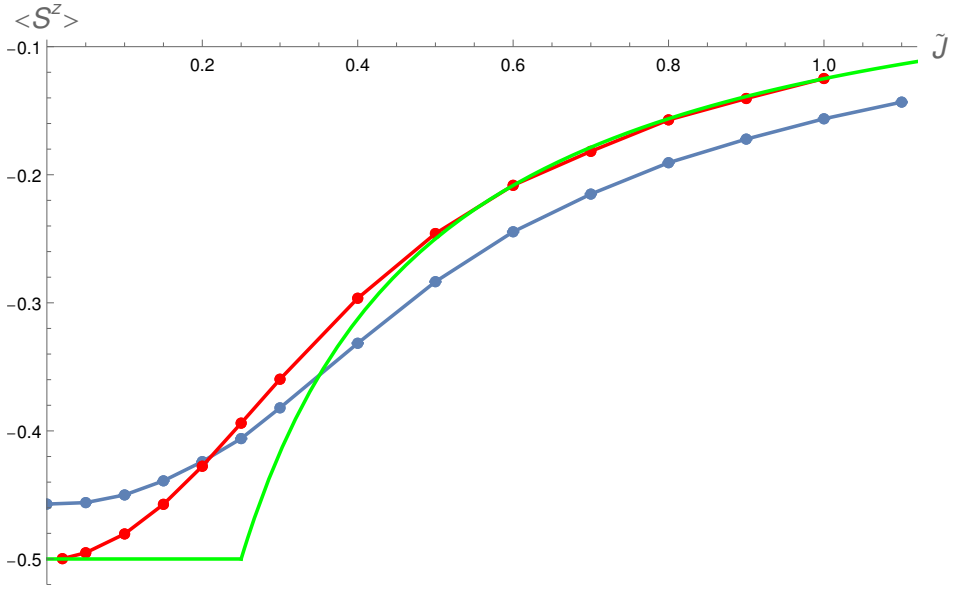

Figure 24.1: $\frac{1}{N}\langle S^z\rangle$ for the nearest neighbour anisotropic XY model with 8000 trajectories[2]in blue, tensor networks results based on [31] in red, MF in green.

Near to the paramagnetic phase we observe an expected overshoot of the true value by the stochastic method due to the inability of the Fokker-Planck equation to accurately represent a pure spin down state that we saw in the previous chapter (or a tensor product of such states). It is less clear what causes the reversal of the trend and undershoot for higher $\tilde{J}$ but, outside of the reversal region, the systematic error appears roughly constant at 0.04–0.05. While this error evidently becomes quite large as a relative error as S^z decreases for larger $\tilde{J}$, it remains on the order of 20% or less up to $\tilde{J} = 0.6$, well past the mean field transition point, and the curves are visually quite close. It is interesting that the method appears to under-perform the mean field for higher $\tilde{J}$ due to the systematic error but does better for lower $\tilde{J}$, correctly capturing the smooth increase in $\langle J^z\rangle$ below the transition point compared to the sharp behaviour of the mean field.

24.1.2 Macroscopic S^xS^y Magnetization

Next, the observable $\langle S^xS^y\rangle$ is a good measure of whether the staggered XY phase exists. To see this, we work out the mean field values for the macroscopic observables in a given symmetry broken state parametrised by the deflection of its A sub-lattice spins from $S^x = S^y$ by angle θ (here N is the number of spins in the

[2]During these simulations, difficulties with the cluster file system meant that some data files were corrupted. As such, in some cases there are up to 20% fewer trajectories than stated. The error bars in the plot account for this.

lattice):

$$\langle S^z\rangle = -\frac{N}{8\tilde{J}}, \quad s = \sqrt{\langle S_A^x\rangle^2 + \langle S_A^y\rangle^2} = \sqrt{\langle S_B^x\rangle^2 + \langle S_B^y\rangle^2} = \frac{N}{2}\sqrt{\frac{1}{4\tilde{J}} - \frac{1}{16\tilde{J}^2}}, \tag{24.14}$$

$$\begin{pmatrix}\langle S_A^x\rangle & \langle S_A^y\rangle\end{pmatrix} = \begin{pmatrix}s\cos\left(\frac{\pi}{4}+\theta\right) & s\sin\left(\frac{\pi}{4}+\theta\right)\end{pmatrix}, \tag{24.15}$$

$$\begin{pmatrix}\langle S_B^x\rangle & \langle S_B^y\rangle\end{pmatrix} = \begin{pmatrix}s\sin\left(\frac{\pi}{4}+\theta\right) & s\cos\left(\frac{\pi}{4}+\theta\right)\end{pmatrix}. \tag{24.16}$$

If we assume the system to be in a uniform classical probabilistic mixture over the symmetry broken states (the approximate expected behaviour of the FP equation in the steady state if the staggered phase exists), then $\langle S^x S^y\rangle$ should be given by

$$\langle S^x S^y\rangle = \frac{s^2}{\pi}\int_0^\pi d\theta \left(\cos\left(\frac{\pi}{4}+\theta\right) + \sin\left(\frac{\pi}{4}+\theta\right)\right)^2 = s^2. \tag{24.17}$$

Plotting s^2 against results obtained via the Truncated Wigner simulations, the fit is fairly poor. While the functional form of s^2 matches the data well, the magnitude of the values obtained via simulation is suppressed by approximately 80 times relative to the s^2 values.

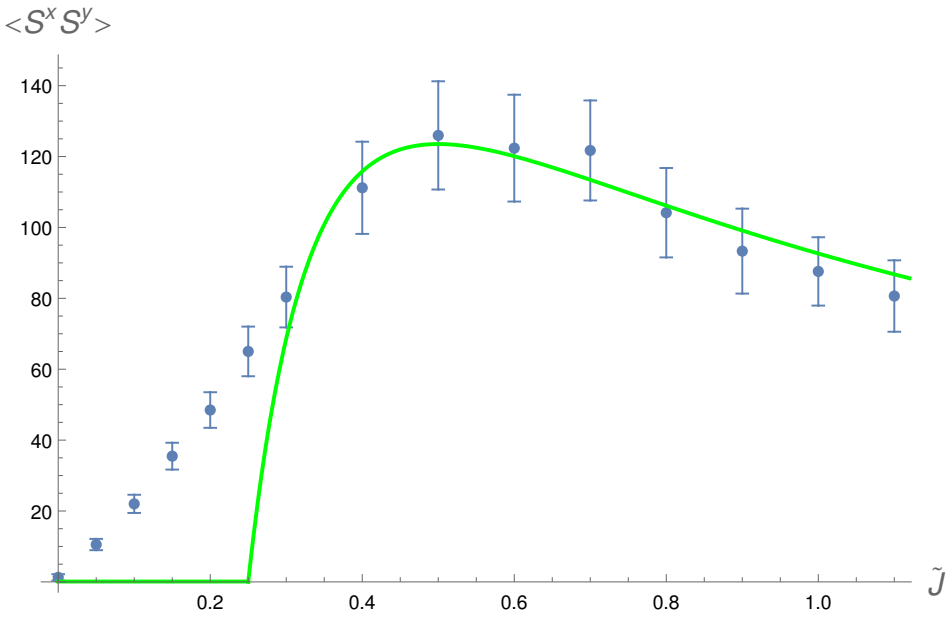

Figure 24.2: Plot of stochastic expectation of $\langle S^x S^y\rangle$ in blue against $\frac{s^2}{80.957}$ for $N = 400$ and 8000 trajectories[3], showing a roughly 98% suppression in the expectation (fitted numerically) relative to the mean field result.

The staggered XY phase is thus clearly heavily suppressed, as predicted by [30], [31].

[3]During these simulations, difficulties with the cluster file system meant that some data files were corrupted. As such, in some cases there are up to 20% fewer trajectories than stated. The error bars in the plot account for this.

24.1.3 $S_i^x S_j^x$, $S_i^y S_j^y$, and $S_i^z S_j^z$ Correlations

We may confirm the suppression of the staggered XY phase by considering the correlation functions of the system. The mean-field prediction for these (symmetric in i, j) quantities in the uniform probabilistic mixture over symmetry-broken states is

$$\langle S_i^x S_j^x \rangle = \langle S_i^y S_j^y \rangle = \begin{cases} \frac{1}{\pi}\int_0^\pi d\theta\, \frac{4s^2}{N^2}\cos^2\left(\frac{\pi}{4}+\theta\right) = \frac{2s^2}{N^2} & \text{if } i,j \in A \text{ or } i,j \in B, \\ \frac{1}{\pi}\int_0^\pi d\theta\, \frac{4s^2}{N^2}\sin\left(\frac{\pi}{4}+\theta\right)\cos\left(\frac{\pi}{4}+\theta\right) = 0 & \text{if } i \in A, j \in B, \end{cases} \tag{24.18}$$

$$\langle S_i^z S_j^z \rangle = \frac{1}{64\tilde{J}^2}. \tag{24.19}$$

This indicates a chequerboard pattern in the $\langle S_i^x S_j^x \rangle$ and $\langle S_i^y S_j^y \rangle$ functions, with sites totally uncorrelated if they are on different lattices and possessing positive correlation independent of distance between them if they share a lattice. The function $\langle S_i^y S_j^y \rangle$ is simpler, exhibiting a simple constant correlation independent of distance.

Computing these functions for $\tilde{J} = 0.3$, a value inside the mean field staggered XY phase, yields the diagrams

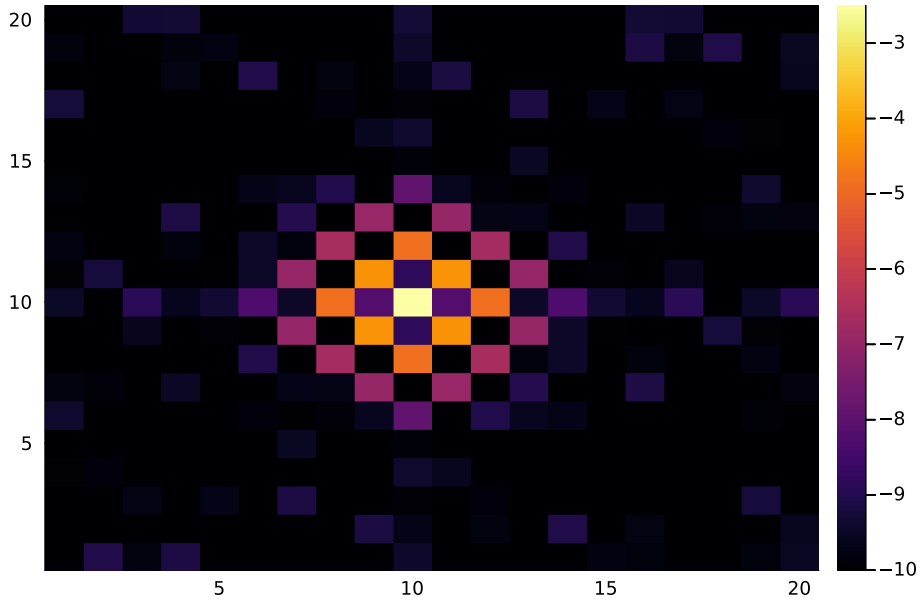

Figure 24.3: $\log\langle S_i^x S_j^x \rangle$ of the nearest neighbour anisotropic XY model for $N = 400$, $\tilde{J} = 0.3$, and 50560 trajectories (also averaged over the lattice), displaying a distinctive chequerboard pattern and exponential decay.

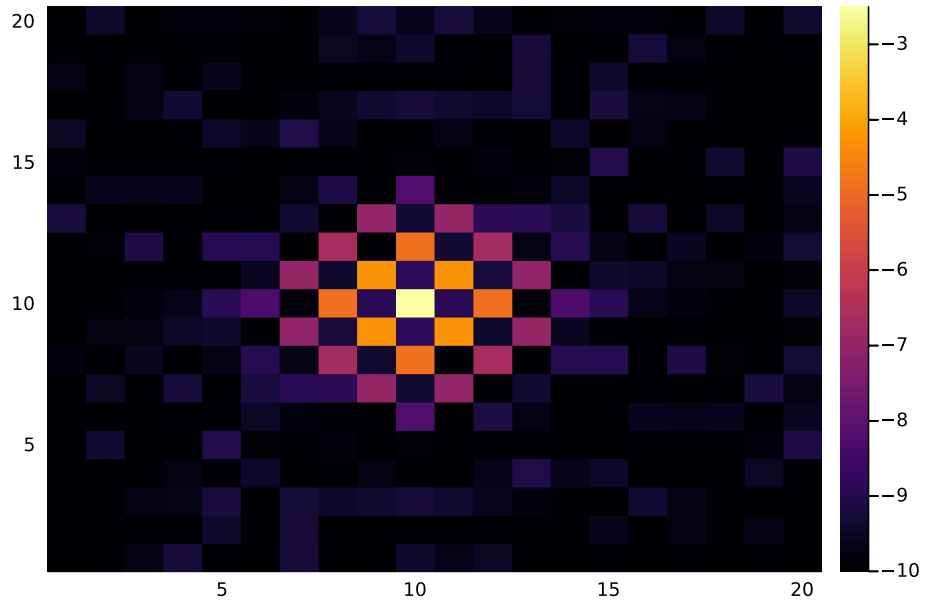

Figure 24.4: $\log\langle S_i^y S_j^y\rangle$ of the nearest neighbour anisotropic XY model for $N = 400$, $\tilde{J} = 0.3$, and 50560 trajectories (also averaged over the lattice), displaying a distinctive chequerboard pattern and exponential decay.

for $\langle S_i^x S_j^x\rangle$ and $\langle S_i^y S_j^y\rangle$. While these clearly display the predicted chequerboard pattern, the correlation function is highly dependent on distance between sites. Indeed, plotting it for i, j in the same sub-lattice (for different sub-lattices it is effectively zero, as predicted by the mean field) and only those points where it exceeds its empirically estimated standard deviation, we find an exponential decay law $\langle S_i^x S_j^x\rangle \approx 0.21 e^{-r/0.57}$ for $r = \sqrt{i^2 + j^2}$ the Euclidean distance on the lattice.

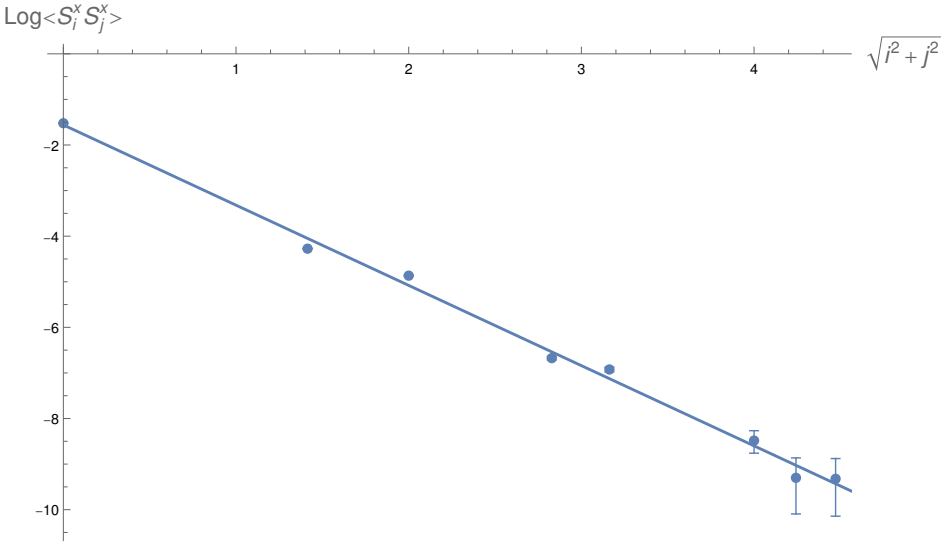

Figure 24.5: $\log\langle S_i^x S_j^x\rangle$ of the nearest neighbour anisotropic XY model for $N = 400$, $\tilde{J} = 0.3$, and 50560 trajectories (also averaged over the lattice), plotted for i, j in the same sub-lattice as a function of Euclidean distance $r = \sqrt{i^2 + j^2}$. The data is well-fitted by an exponential decay law $\langle S_i^x S_j^x\rangle \approx 0.21 e^{-r/0.57}$.

By rotational symmetry the same scaling should hold for $\langle S_i^y S_j^y\rangle$ (and this is

clear from the plots). It is not immediately clear why some points deviate from the fitted line by significantly more than their standard deviations. This could be due to values of the function in the exponential tail being so small[4] as to be affected by the system being almost but still not entirely converged to the steady state in finite time, but this requires further investigation. Furthermore, while the method recovers the correct form for the correlation function, its estimate for the Euclidean correlation distance of $\xi = 0.57$ differs from the estimate of $\xi = 0.93$ obtained for the same parameters in Ref. [31] via tensor network methods. Likely this is again a consequence of the true steady state not being an everywhere positive probability density, and thus approximation of it by the latter introducing errors to its correlation structure.

Since $\langle S_i^z \rangle$ is non-zero and in good agreement with the mean field (see Fig. 24.1), the $\langle S_i^z S_j^z \rangle$ correlation function will also be in good agreement with the mean field. We may instead explore $\langle S_i^z S_j^z \rangle - \langle S_i^z \rangle \langle S_j^z \rangle$, the correlation function of fluctuations around the mean of S_i^z, which displays no particular structure beyond also decaying exponentially with Euclidean distance (faster, in fact, than $\langle S_i^x S_j^x \rangle$ and $\langle S_i^y S_j^y \rangle$, with $\xi \approx 0.27$, which makes sense since its mean field value is 0).

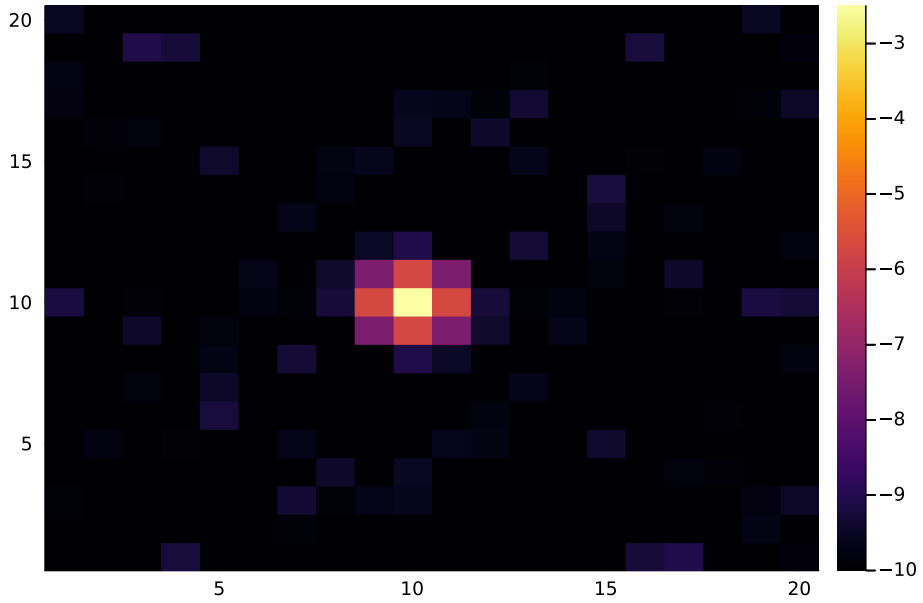

Figure 24.6: $\log(\langle S_i^z S_j^z \rangle - \langle S_i^z \rangle \langle S_j^z \rangle)$ of the nearest neighbour anisotropic XY model for $N = 400$, $\tilde{J} = 0.3$, and 50560 trajectories (also averaged over the lattice), displaying faster exponential decay than $\log\langle S_i^x S_j^x \rangle$ and $\log\langle S_i^y S_j^y \rangle$.

[4] Indeed, to achieve sufficient resolution to resolve the exponential tail over 8 times the number of trajectories were required compared to macroscopic observables, and the function then had to also be averaged over the lattice. The exceptionally rapid decay of the exponential tail generally makes it a challenge to estimate using Monte Carlo methods, since the latter only polynomially improves in accuracy with trajectory number.

24.1.4 Vortex Formation

Finally, we can analyse the mechanism by which the staggered XY phase is suppressed. As noted earlier, the system exhibits a continuous U(1) symmetry, with the symmetry-broken phases parametrized by the angle 2θ, $\theta \in [0, \pi]$ between spin vectors of the two sub-lattices in the S^x-S^y plane. The topological defects supported by a field theory exhibiting symmetry-breaking are fixed by the non-trivial homotopy groups of the vacuum manifold, which is the quotient of the broken symmetry group by the symmetry group under which the symmetry-broken states are still invariant [35]. In this case the vacuum manifold is simply U(1)/1 and is homeomorphic to S^1, meaning its non-trivial homotopy group is $\pi_1(S^1) = (\mathbb{Z}, +)$: a field theory with such a vacuum manifold should support vortex defects. In [30] the universality class of the field theory corresponding to the bosonized form of the nearest neighbour interaction anisotropic XY model was identified via a renormalization group analysis to be that of the classical XY model. Systems in this universality class exhibit a vortex-induced BKT transition [36]–[38] at some effective critical temperature, with long range order below it and a disordered phase above.

Importantly, a mean field analysis in Ref. [30] also found that the effective temperature of the field theory was always higher than the critical temperature of the associated BKT transition, meaning that the long range order of the staggered XY phase is expected to be destroyed by vortex formation. Because my stochastic method has direct access to the ϕ variable associated with orientation in the S^x-S^y plane and is capable of producing single-shot trajectories, it is fairly easy to observe these vortices . For a given trajectory at every moment in time one constructs the lattice of edge midpoints of the original lattice (from now on referred to as the midpoint lattice), assigns to each site of this lattice the difference between the ϕ of B and A sub-lattice vertices of that edge, and then calculates winding numbers around the plaquettes of this lattice. The final result is a lattice of plaquettes with associated winding numbers (the plaquette lattice). This way of identifying vortices will only find those with winding number ± 1[5], but these are the only ones expected to contribute to the BKT transition [39].

The axes of the plaquette lattice are unfortunately not aligned with those of the spin lattice, being offset by $\pi/4$. Performing this rotation, however, causes the finite lattice to no longer be a square, necessitating its embedding in a larger square for the purposes of plotting. Adjusting for this, it is possible to plot the plaquette lattice for trajectories initialized with no vortices after a time greater than is required for the system to converge to the steady state. Plots of the lattice for four such trajectories are provided below.

[5] On a square lattice it is difficult to distinguish between higher winding number vortices and clusters of the ± 1 ones [39].

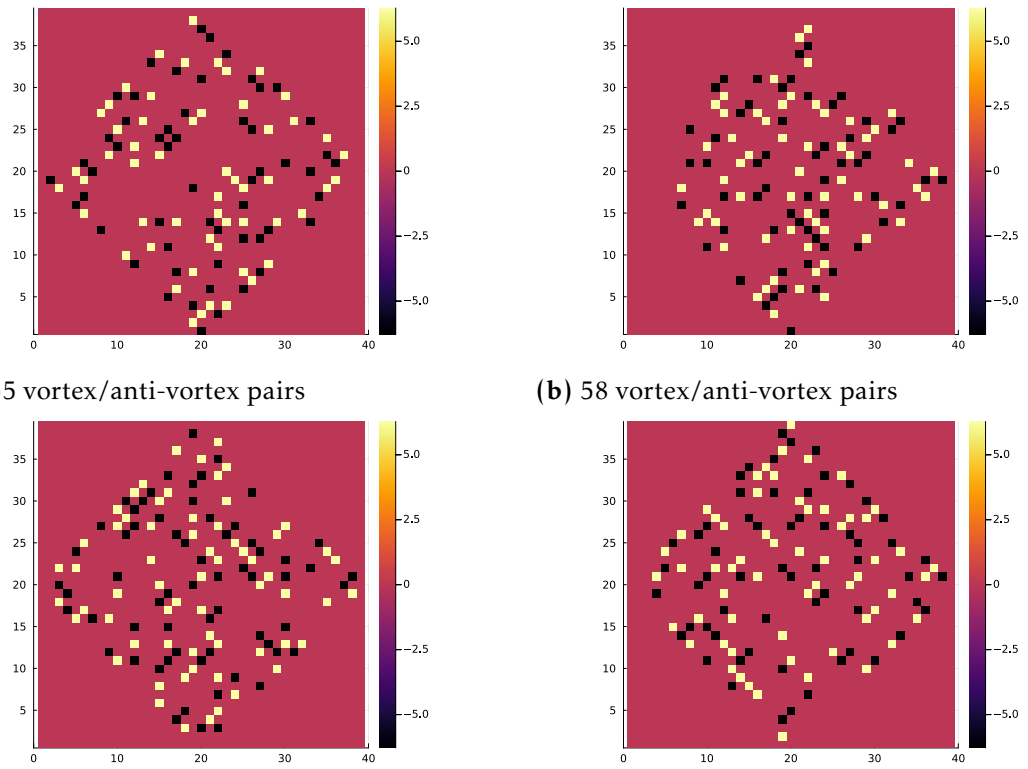

(a) 55 vortex/anti-vortex pairs

(b) 58 vortex/anti-vortex pairs

(c) 64 vortex/anti-vortex pairs

(d) 60 vortex/anti-vortex pairs

Figure 24.7: Vortex lattices (rotated by $\pi/4$ anticlockwise relative to the spin lattice) of single shot trajectories for $\tilde{J} = 0.5$, initialized with no vortices and evolved for $\tau = 30$. The lattices are labelled by the vortex (in yellow)/antivortex (in black) pairs present.

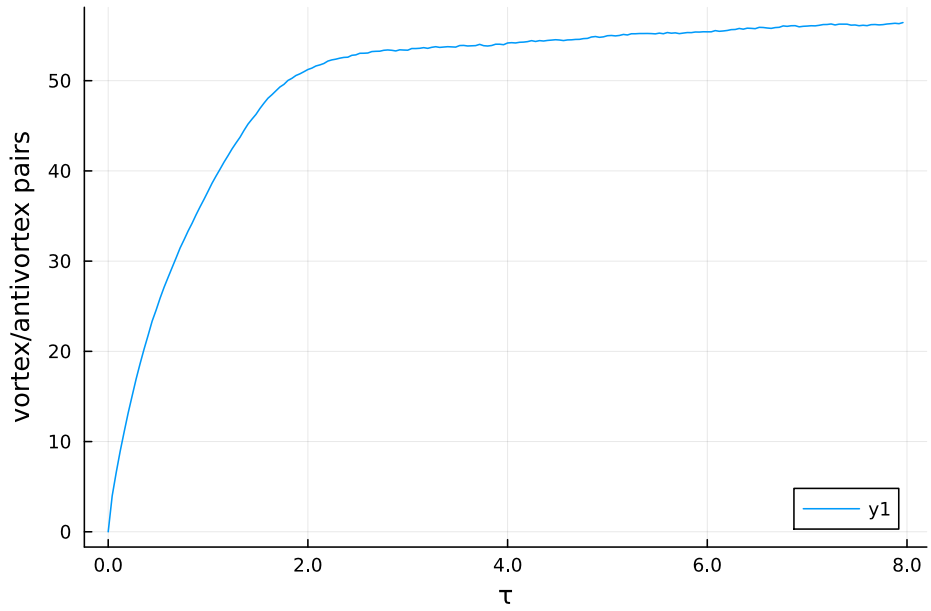

Figure 24.8: Average number of vortex/antivortex pairs for 5600 trajectories and $\tilde{J} = 0.5$. Vortex formation appears to occur on two different time scales, with an initial rapid increase followed by slower saturation.

Vortex proliferation is clearly observed, with an average (over 400 trajectories) of 57 vortex pairs, which is roughly 15% of the available plaquettes. We

may also observe the evolution of vortex pair number with time in Fig. 24.8, noting that this appears to exhibit two different time-scales: there is rapid initial increase in number, followed by a slower saturation. This appears to confirm the argument of [30] for vortex formation as the mechanism for staggered XY phase suppression.

This concludes the present analysis of the nearest neighbour interaction model, confirming that the method gives reasonably accurate estimates for macroscopic expectation values, identifies the suppression of the staggered XY phase through the former and the system correlation functions (thus going beyond the mean field) and is also capable of studying the associated vortices.

We now move onto algebraically decaying long range interactions, for which phases with algebraic long range order do appear to exist.

24.2 Algebraically Decaying Interactions

We consider now a range function of the form

$$r(i,j) = \frac{1}{|i-j|^{\alpha}}, \tag{24.20}$$

which we refer to as algebraically decaying interactions. In 2 dimensions, $\alpha \leq d$ yields what are known as strong long range interactions, meaning that interaction energies of subsystems with the bulk are no longer negligible with respect to their internal energies [40]. This leads to difficulties with conventional definitions of thermodynamic quantities like internal energy and entropy becoming non-extensive, and also means the system is acutely sensitive to its boundary conditions [41]. Such systems may be regularized by means of what is known as the Kac prescription [42], which in our case amounts to z scaling as $O((N^{\frac{1}{d}})^{d-\alpha})$. This preserves the non-extensive properties of the system while ensuring that various quantities remain finite.

Due to the significant sensitivity of this regime to the system's boundary conditions and because in this case $\frac{\tilde{J}}{z} \to 0$ as $N \to \infty$, meaning the mean field disordered phase essentially vanishes in thermodynamic limit, I will not extensively explore it here. Much of the focus will be instead be on $\alpha > 2$, for which z converges to a finite value as $N \to \infty$.

As before, the mean field equations predict a second order phase transition at $\tilde{J} = \frac{1}{4}$ from a paramagnetic phase to one exhibiting order in the S^x-S^y plane. For the present interactions the system no longer possesses an obvious U(1) symmetry associated with the sub-lattices, but still retains a $\mathbb{Z}_2$ symmetry associated with inverting the signs of all S_i^x, S_i^y. For $\alpha = 0$ in finite systems this corresponds to classical bistability between states with $S^x = S^y > 0$ and $S^x = S^y < 0$, referred to

as the ferromagnetic phase [29], and the mean field predicts this basic structure for all α, though I am unaware of specific mean field results in the literature for $0 < \alpha$; Nevertheless, the basic prediction is that of a single phase transition.

In contrast to this, numerical investigations [32] using the discrete Truncated Wigner method have identified a second phase transition for $\alpha > 2$: for sufficiently large $\tilde{J}$ it is possible to transition out of the ferromagnetic phases back into the paramagnetic regime. Moreover, the above mean field description says very little about the actual structure of the ferromagnetic phase compared to the nearest neighbour interaction case where a detailed description in terms of oriented sub-lattices was available. This system is thus an interesting candidate for further investigation with my method, especially since long range interactions are easy to encode using Truncated Wigner in particular.

To study the ferromagnetic phase boundary we may consider the macroscopic magnetization $\langle S^x S^y \rangle$, which we expect to be non-zero for a uniform probabilistic mixture of the ferromagnetic states since it is invariant under $\mathbb{Z}_2$. Plotting the value of this observable over a grid of $(\tilde{J}^{-1}, \alpha)$ allows the creation of a heatmap akin to the one presented in [32].

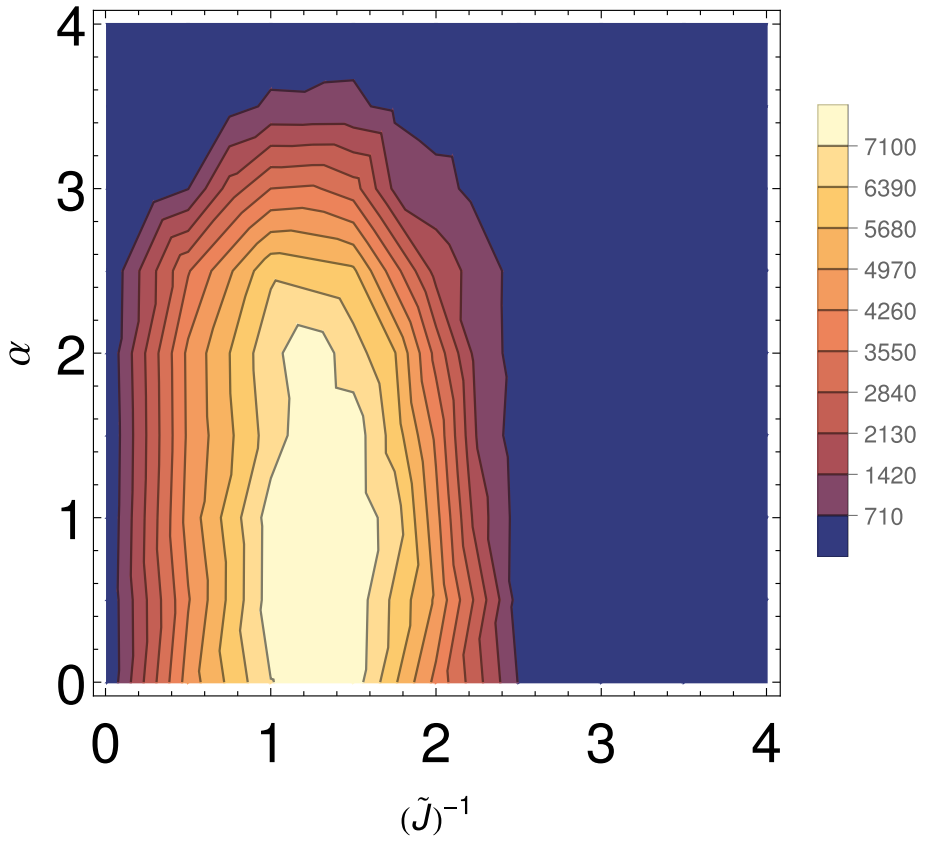

Figure 24.9: $\langle S^x S^y \rangle$ for the algebraically decaying interaction anisotropic XY model, $N = 400$, $\tau = 40$, and 109 parameter combinations using 30 trajectories each. The observable takes on macroscopic value in a significant portion of the phase diagram, indicating the presence of an ordered phase.

We may investigate further by restricting to the $\alpha = 1$ and $\alpha = 3$ cross-sections of this plot and using larger numbers of trajectories for greater precision. Since we do not have the precise form of the mean field solution for arbitrary α, we cannot make the same type of comparison that we did in Fig. 24.2. Nevertheless, we find that inside the ferromagnetic phase $\langle S^x S^y \rangle$ is on the order of the nearest neighbour mean field prediction inside the staggered phase, suggesting order is not suppressed.

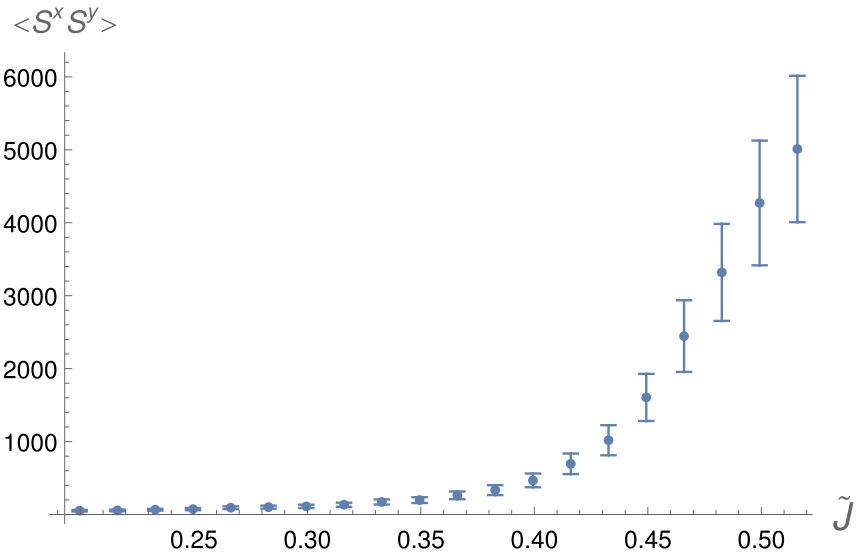

Figure 24.10: $\langle S^x S^y \rangle$ for the algebraically decaying interaction anisotropic XY model, $N = 400$, $\tau = 40$, $\alpha = 1$, and 2000 trajectories. The observable exhibits significant growth after the thermodynamic limit phase transition point $\tilde{J} = 1/4$, clearly being unsuppressed.

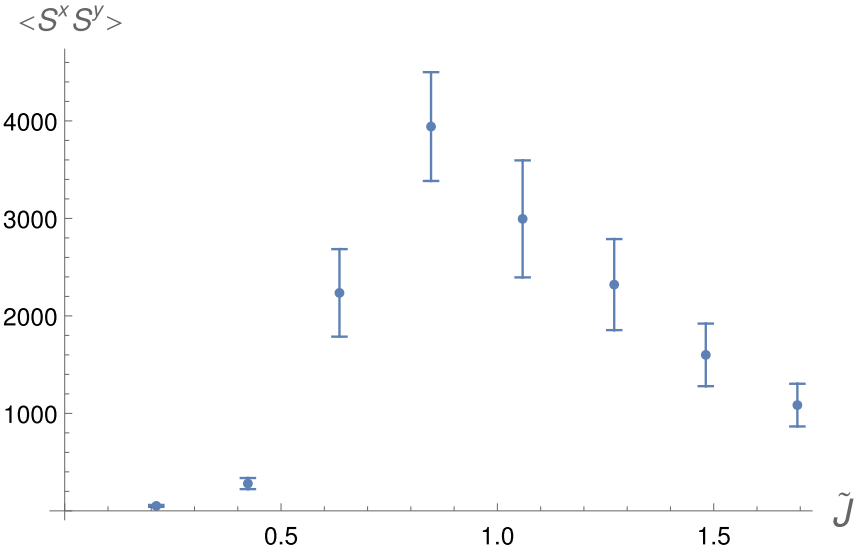

Figure 24.11: $\langle S^x S^y \rangle$ for the algebraically decaying interaction anisotropic XY model, $N = 400$, $\tau = 40$, $\alpha = 3$, and 2000 trajectories. The observable exhibits significant growth after the thermodynamic limit phase transition point $\tilde{J} = 1/4$, clearly being unsuppressed. Moreover, above $\tilde{J} = 0.847$ it begins to decay, agreeing with the appearance of a second phase transition in Ref. [32] for $\alpha > 2$.

Focusing on $\alpha = 3$, we may verify the presence of long range order in the ferromagnetic phase by again considering the correlation functions of the system[6]

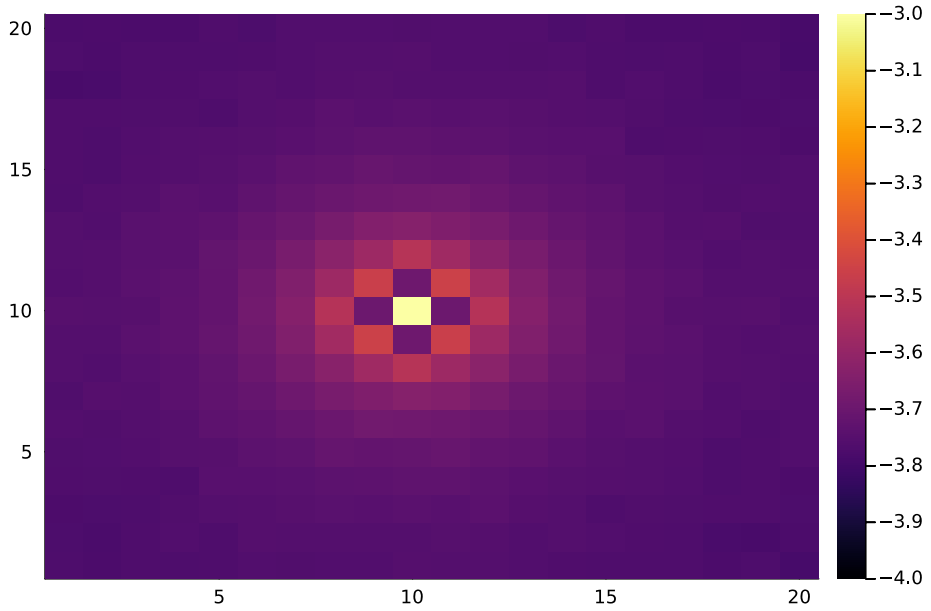

Figure 24.12: $\log\langle S_i^x S_j^x \rangle$ for the algebraically decaying interaction anisotropic XY model, $N = 400$, $\tau = 80$, $\tilde{J} = 0.847$, and 16k trajectories, displaying slow algebraic decay.

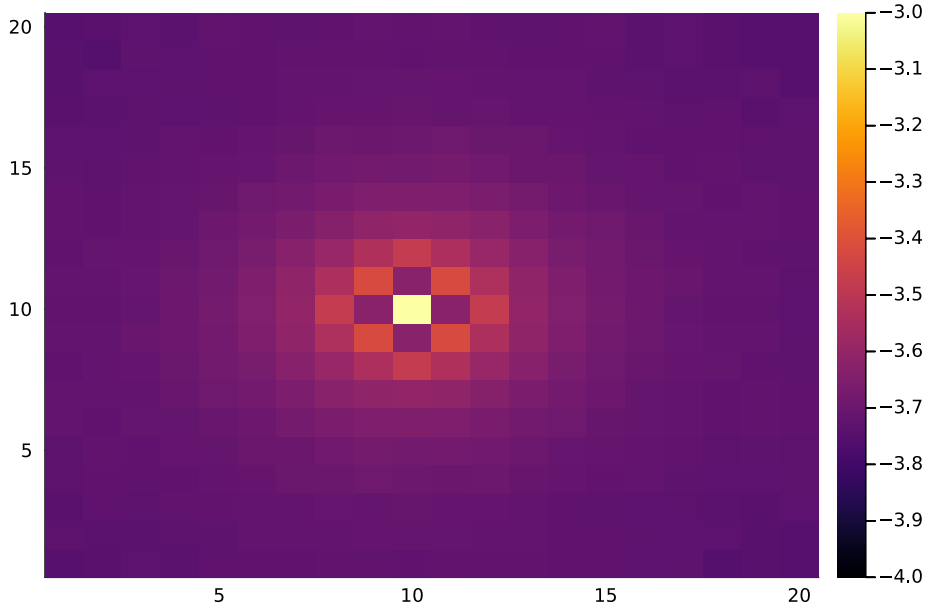

Figure 24.13: $\log\langle S_i^y S_j^y \rangle$ for the algebraically decaying interaction anisotropic XY model, $N = 400$,$\tau = 80$, $\tilde{J} = 0.847$, and 16k trajectories, displaying slow algebraic decay.

[6]The central point in each plot should be ignored since the colour scheme has been truncated to better show the rest of the scaling.

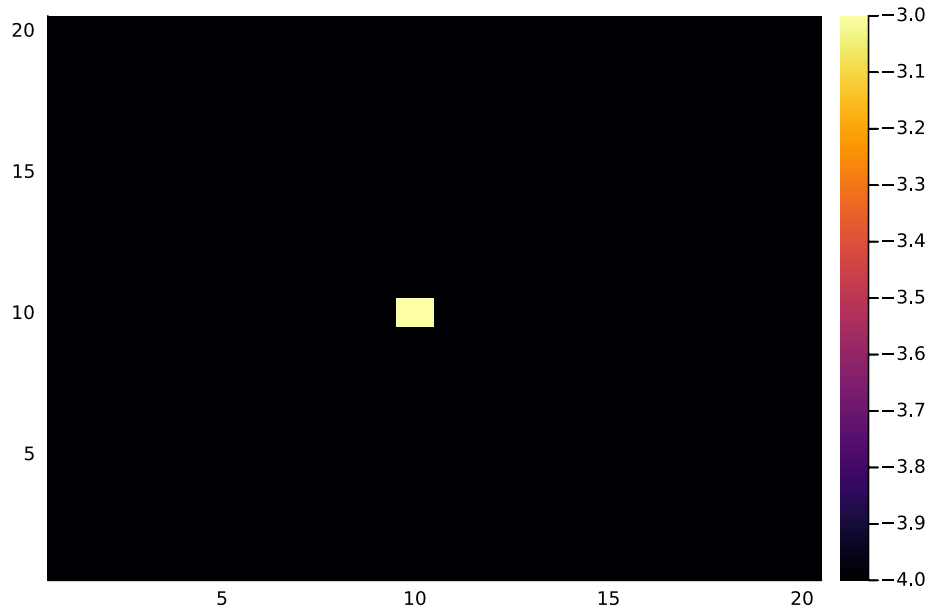

Figure 24.14: $\log(\langle S_i^z S_j^z\rangle - \langle S_i^z\rangle\langle S_j^z\rangle)$ for the algebraically decaying interaction anisotropic XY model, $N = 400$, $\tau = 80$, $\tilde{J} = 0.847$, and 16k trajectories, displaying exponential decay.

Fewer trajectories are currently available for these than for the nearest neighbour interactions model, and it appears that the convergence time increases significantly inside the ferromagnetic phase: I have had to use $\tau = 80$ compared to $\tau = 40$ for the previous plots to achieve comparatively satisfactory convergence. These considerations likely account for the small difference between the $\log\langle S_i^x S_j^x\rangle$ and $\log\langle S_i^y S_j^y\rangle$ plots. As before, $\log(\langle S_i^z S_j^z\rangle - \langle S_i^z\rangle\langle S_j^z\rangle)$ displays exponential decay. Fitting $\log\langle S_i^x S_j^x\rangle$, however, now gives a good with power law decay:

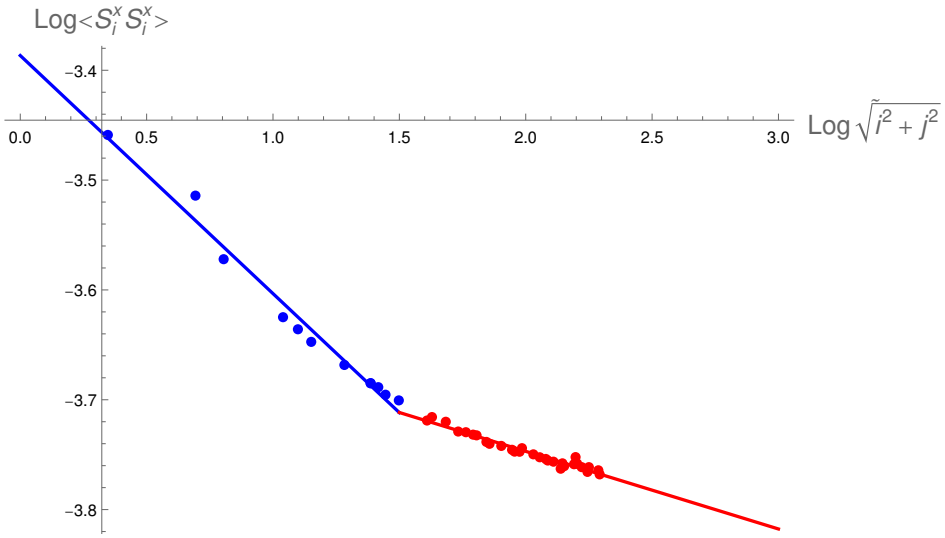

Figure 24.15: $\log\langle S_i^x S_j^x\rangle$ for the algebraically decaying interaction anisotropic XY model, $N = 400$, $\tau = 80$, $\tilde{J} = 0.847$, and 16k trajectories (also averaged over the lattice), plotted as a function of Euclidean distance $r = \sqrt{i^2 + j^2}$. The data is well-fitted by two different power laws, $\sim r^{-0.217}$ and $\sim r^{-0.0707}$.

Curiously there appear to be two different power law regimes. This is possibly

a finite size effect[7] or alternatively the decay obeys a more complicated functional form (from the plots we see a depletion in the correlation functions at short distances). This is a direction requiring further investigation, with more trajectories required for better resolution and longer running times to ensure convergence is sufficient to extract very accurate functional forms. Larger lattice sizes should also be considered to confirm or the refute the presence of finite size effects. Nevertheless, this is indicative of long range order.

Thus, the stochastic method agrees with [32] about the existence of an ordered ferromagnetic phase for the long range interaction anisotropic XY model, and we have been able to calculate macroscopic magnetizations and correlation functions indicating its existence and some of its properties. Since second order phase transitions are present in this model, and interesting further direction would be to probe the system in their vicinity, potentially again using single shot trajectories to probe their mechanisms.

[7] A power law subject to an infrared cut-off (the truncation of its low frequency Fourier modes or, equivalently, the introduction of a finite volume) transforms into a slower exponential decay. The cross-over to a slower decay near the system boundary could thus plausibly be related to this.

Chapter 25

Conclusion

In this part I have developed a stochastic Truncated Wigner method for spin systems based on a consistent truncation in $\hbar$ of the Stratonovich-Weyl correspondence for the latter. The method may be applied to particles of spin other than $\frac{1}{2}$ simply by varying a continuous parameter j, and is truncated in the same parameter as conventional bosonic Truncated Wigner, meaning the two methods may be easily integrated at the same order of semiclassical accuracy. Finally, the method utilises a continuous phase space, meaning it preserves the geometric structure of the theory and gives an easy way to extract quantities like phase winding numbers.

The method has been tested on a single Lipkin-Meshkov-Glick spin to study its behaviour for large and small spin numbers. This was achieved via an approach allowing for the sampling from a non-positive initial Wigner function so long as the dimension of the phase space is not too great. Results confirmed that the method is highly accurate for large spin numbers (consistent with this yielding a small truncation parameter) but experiences increasing systematic error for smaller ones. Nevertheless, the observable under consideration, S^z, still exhibited correct overall behaviour for spin-$\frac{1}{2}$, the worst case scenario, and the systematic was on the order of 16%.

Moving to larger lattice models, the nearest neighbour and algebraically decaying interactions anisotropic XY models were considered: the method was able to efficiently simulate both types of interactions for a comparatively large square lattice of $N = 400$ spins. For the nearest neighbour interactions model, strong suppression of the mean field-predicted staggered XY phase was confirmed, with the observable $\langle S^x S^y \rangle$ exhibiting its mean field functional form but with significantly reduced magnitude, and $\langle S_i^x S_j^x \rangle$ and $\langle S_i^y S_j^y \rangle$ correlation functions exhibiting exponential decay rather than long ranger order. Furthermore, the use of single shot trajectories allowed for the observation of vortices in the staggered XY phase, and the rate of vortex formation was also found. This gives support to the suggestion of [30] that the staggered phase is suppressed by vortex prolif-

eration associated to the BKT transition, and to my knowledge is the first direct simulation observation of this occurring.

In the case of long range interactions, the ferromagnetic phase identified in [32] was found, with the observables $\langle S^x S^y \rangle$, $\langle S_i^x S_j^x \rangle$, and $\langle S_i^y S_j^y \rangle$ now indicating order. The first now exhibited an unsuppressed magnitude (while also confirming the appearance of a second phase transition, agreeing with [32]), while the latter appear to decay according to a power law (albeit with two distinct regimes). This system appears well suited to study via both discrete Truncated Wigner and my method, and offers a good avenue for further exploration. In particular, improved estimates for the correlation functions in the ordered phase and observation of the mechanism associated with the second order phase transitions in this system would be of great interest.

Overall, the method is clearly capable of capturing phenomena beyond the mean field, appears to remain relatively accurate even for small spin values, and is exhibits great flexibility with respect to the forms of interactions it can accommodate (indeed, I am unaware of any restrictions on the latter) and its ability to directly integrate with bosonic Truncated Wigner. As such it is hoped that it will be a valuable addition to the tools available for the study of non-equilibrium spin-boson systems going forwards.

Appendix E

Fokker-Planck on the Sphere via Conserved Quantities

E.1 Fokker-Planck in Different Coordinates [43]

Suppose we want to rewrite the Fokker-Planck equation

$$\frac{\partial}{\partial t}P = -\frac{\partial}{\partial x^i}(\mu^i P) + \frac{1}{2}\frac{\partial^2}{\partial x^i \partial x^j}(D^{ij}P) \tag{E.1}$$

in new coordinates $\bar{x}$ (we shall restrict ourselves to time-independent coordinate transformations). We know from basic probability that the density will transform as

$$J = \left|\det \frac{\partial x^i}{\partial \bar{x}^j}\right|, \tag{E.2}$$

$$\bar{P} = JP. \tag{E.3}$$

Further, from Jacobi's formula, we have

$$\begin{aligned} -\frac{1}{J}\frac{\partial J}{\partial x^i} &= -\frac{\partial \bar{x}^j}{\partial x^l}\frac{\partial}{\partial x^i}\frac{\partial x^l}{\partial \bar{x}^j} = \frac{\partial x^l}{\partial \bar{x}^j}\frac{\partial}{\partial x^i}\frac{\partial \bar{x}^j}{\partial x^l} \\ &= \frac{\partial x^l}{\partial \bar{x}^j}\frac{\partial}{\partial x^l}\frac{\partial \bar{x}^j}{\partial x^i} = \frac{\partial}{\partial \bar{x}^j}\frac{\partial \bar{x}^j}{\partial x^i}. \end{aligned} \tag{E.4}$$

We may use this to rewrite partial derivatives as

$$\frac{\partial}{\partial x^i} = \frac{\partial \bar{x}^j}{\partial x^i}\frac{\partial}{\partial \bar{x}^j} = \frac{\partial}{\partial \bar{x}^j}\frac{\partial \bar{x}^j}{\partial x^i} - \left(\frac{\partial}{\partial \bar{x}^j}\frac{\partial \bar{x}^j}{\partial x^i}\right) = \frac{\partial}{\partial \bar{x}^j}\frac{\partial \bar{x}^j}{\partial x^i} + \frac{1}{J}\frac{\partial J}{\partial x^i} = \frac{1}{J}\frac{\partial}{\partial \bar{x}^j}\frac{\partial \bar{x}^j}{\partial x^i}J, \tag{E.5}$$

which also allows us to obtain a simple expression for repeated derivatives:

$$\begin{aligned}\frac{\partial^2}{\partial x^i \partial x^j} &= \frac{1}{J}\frac{\partial}{\partial \bar{x}^k}\frac{\partial \bar{x}^k}{\partial x^i} J \frac{1}{J}\frac{\partial}{\partial \bar{x}^l}\frac{\partial \bar{x}^l}{\partial x^j} J \\ &= \frac{1}{J}\frac{\partial^2}{\partial \bar{x}^k \partial \bar{x}^l}\frac{\partial \bar{x}^k}{\partial x^i}\frac{\partial \bar{x}^l}{\partial x^j} J - \frac{1}{J}\frac{\partial}{\partial \bar{x}^k}\left(\frac{\partial}{\partial \bar{x}^l}\frac{\partial \bar{x}^k}{\partial x^i}\right)\frac{\partial \bar{x}^l}{\partial x^j} J \\ &= \frac{1}{J}\frac{\partial^2}{\partial \bar{x}^k \partial \bar{x}^l}\frac{\partial \bar{x}^k}{\partial x^i}\frac{\partial \bar{x}^l}{\partial x^j} J - \frac{1}{J}\frac{\partial}{\partial \bar{x}^k}\frac{\partial^2 \bar{x}^k}{\partial x^i \partial x^j} J.\end{aligned} \tag{E.6}$$

Combining these results, this yields the following Fokker-Planck equation:

$$\frac{\partial}{\partial t}\bar{P} = -\frac{\partial}{\partial \bar{x}^i}(\bar{\mu}^i \bar{P}) + \frac{1}{2}\frac{\partial^2}{\partial \bar{x}^i \partial \bar{x}^j}(\bar{D}^{ij}\bar{P}), \tag{E.7}$$

$$\bar{\mu}^i = \frac{\partial \bar{x}^i}{\partial x^j}\mu^j + \frac{1}{2}\frac{\partial^2 \bar{x}^i}{\partial x^j \partial x^k} D^{jk}, \tag{E.8}$$

$$\bar{D}^{ij} = \frac{\partial \bar{x}^i}{\partial x^k}\frac{\partial \bar{x}^j}{\partial x^l} D^{kl}. \tag{E.9}$$

E.2 Fokker-Planck Conserved Quantities [23]

E.2.1 General Theory

For a function Φ to be a conserved quantity, all of its moments must be zero (we assume that P is zero on the boundary of the space):

$$\begin{aligned}\frac{d}{dt}\int dx\, f(\Phi) P &= \int dx\, f(\Phi)\frac{\partial}{\partial t} P \\ &= \int dx\, P\left(\mu^i \frac{\partial \Phi}{\partial x^i} f'(\Phi) + \frac{1}{2} D^{ij}\left[\frac{\Phi}{\partial x^i \partial x^j} f'(\Phi) + \frac{\partial \Phi}{\partial x^i}\frac{\partial \Phi}{\partial x^j} f''(\Phi)\right]\right)\end{aligned} \tag{E.10}$$

The coefficients of f' and f'' must vanish independently, so that (recall that B^{ij} is positive semi-definite):

$$D^{ij}\frac{\partial \Phi}{\partial x^i}\frac{\partial \Phi}{\partial x^j} = 0 \implies D^{ij}\frac{\partial \Phi}{\partial x^j} = 0, \tag{E.11}$$

$$\mu^i \frac{\partial \Phi}{\partial x^i} + \frac{1}{2} D^{ij}\frac{\Phi}{\partial x^i \partial x^j} = 0. \tag{E.12}$$

E.2.2 Radius as a Conserved Quantity

If $\Phi = r$ and we work in $x^i = (r, \theta, \phi)$, the conserved quantity equations reduce to

$$D^{ir} = 0, \tag{E.13}$$

$$\mu^r = 0. \tag{E.14}$$

Because no derivatives with respect to r are now present in the Fokker-Planck equation, there exist solutions of the form $P(r,\theta,\phi) = S(\theta,\phi)\delta(r-c)$, so that the equation reduces down to the Fokker-Planck equation on the sphere very directly.

This means that, to write a Fokker-Planck equation on the sphere "extrinsically", it is sufficient to augment the drift vector and diffusion matrix with some zero entries as above to obtain the corresponding 3D Fokker-Planck equation with radius as a conserved quantity.

E.3 Fokker-Planck → Ito Mapping on a Sphere

Suppose one is supplied with a Fokker-Planck equation on a sphere

$$\frac{\partial}{\partial t}P = -\frac{\partial}{\partial x^i}(\mu^i P) + \frac{1}{2}\frac{\partial^2}{\partial x^i \partial x^j}(D^{ij}P) \tag{E.15}$$

with $x^i = (\theta,\phi)$. As discussed in the previous section, this can be augmented to a 3D equation with $x^i = (r,\theta,\phi)$ by extending D and μ via

$$D^{ir} = 0, \tag{E.16}$$

$$\mu^r = 0. \tag{E.17}$$

Denoting the 3D Cartesian coordinates by $\bar{x}^i$, we may use section E.1 to rewrite the equation as

$$\frac{\partial}{\partial t}\bar{P} = -\frac{\partial}{\partial \bar{x}^i}(\bar{\mu}^i \bar{P}) + \frac{1}{2}\frac{\partial^2}{\partial \bar{x}^i \partial \bar{x}^j}(\bar{D}^{ij}\bar{P}), \tag{E.18}$$

$$\bar{\mu}^i = \frac{\partial \bar{x}^i}{\partial x^j}\mu^j + \frac{1}{2}\frac{\partial^2 \bar{x}^i}{\partial x^j \partial x^k}D^{jk}, \tag{E.19}$$

$$\bar{D}^{ij} = \frac{\partial \bar{x}^i}{\partial x^k}\frac{\partial \bar{x}^j}{\partial x^l}D^{kl}. \tag{E.20}$$

From here we may construct the corresponding Ito process, denoting $\bar{D}^{ij} = \bar{\sigma}^i{}_k\,\bar{\sigma}^j{}_l\,\delta^{kl}$,

$$d\bar{x}^i = \bar{\mu}^i dt + \bar{\sigma}^i{}_j\, dW^j \tag{E.21}$$

in Cartesian coordinates. To return to polar coordinates, we may employ Ito's lemma:

$$\begin{aligned} dx^i &= \frac{\partial x^i}{\partial \bar{x}^j} d\bar{x}^j + \frac{1}{2}\frac{\partial^2 x^i}{\partial \bar{x}^j \partial \bar{x}^k} d\bar{x}^j d\bar{x}^k \\ &= \left(\frac{\partial x^i}{\partial \bar{x}^j} \bar{\mu}^j + \frac{1}{2}\frac{\partial^2 x^i}{\partial \bar{x}^j \partial \bar{x}^k} \bar{\sigma}^j{}_l \, \bar{\sigma}^k{}_m \, \delta^{lm} \right) dt + \frac{\partial x^i}{\partial \bar{x}^j} \bar{\sigma}^j{}_k \, dW^k \\ &= \left(\mu^i + \frac{1}{2}\Big(\frac{\partial x^i}{\partial \bar{x}^j} \frac{\partial^2 \bar{x}^j}{\partial x^k \partial x^l} D^{kl} + \frac{\partial^2 x^i}{\partial \bar{x}^k \partial \bar{x}^l} \bar{D}^{kl} \Big) \right) dt + \sigma^i{}_j \frac{\partial x^j}{\partial \bar{x}^k} dW^k \\ &= \left(\mu^i + \frac{1}{2}\Big(\frac{\partial x^i}{\partial \bar{x}^j} \frac{\partial^2 \bar{x}^j}{\partial x^k \partial x^l} + \frac{\partial^2 x^i}{\partial \bar{x}^m \partial \bar{x}^n} \frac{\partial \bar{x}^m}{\partial x^k} \frac{\partial \bar{x}^n}{\partial x^l} \Big) D^{mn} \right) dt + \sigma^i{}_j \frac{\partial x^j}{\partial \bar{x}^k} dW^k. \end{aligned} \tag{E.22}$$

Here $\sigma^i{}_j = \frac{\partial x^i}{\partial \bar{x}^k} \bar{\sigma}^k{}_l \frac{\partial \bar{x}^l}{\partial x^j}$. Observing that

$$\frac{\partial^2 x^i}{\partial x^k \partial x^l} = 0 = \frac{\partial}{\partial x^k}\left(\frac{\partial x^i}{\partial \bar{x}^j} \frac{\partial \bar{x}^j}{\partial x^l} \right) = \frac{\partial x^i}{\partial \bar{x}^j} \frac{\partial^2 \bar{x}^j}{\partial x^k \partial x^l} + \frac{\partial^2 x^i}{\partial \bar{x}^m \partial \bar{x}^n} \frac{\partial \bar{x}^m}{\partial x^k} \frac{\partial \bar{x}^n}{\partial x^l}, \tag{E.23}$$

we find that

$$dx^i = \mu^i dt + \sigma^i{}_j \frac{\partial x^j}{\partial \bar{x}^k} dW^k. \tag{E.24}$$

Appendix F

Lattice Simulation Considerations

F.1 Monte Carlo Scaling in Higher Dimensions

In moving from a single or small group of spins to large lattice models, the question of how the increase in phase space dimension affects the method arises. While mapping from a Fokker-Planck equation to the associated SDE saves us from the exponential explosion in simulation degrees of freedom, we are instead faced with the requirement to compute integrals by Monte Carlo sampling with stochastic trajectories. This has consequences for what can and cannot be done as the dimension number grows.

It is not true, in general, that Monte Carlo is insensitive to dimension d because a random variable X's variance may exhibit some scaling $C(d)$ with it[1] [44], meaning that the standard deviation of the stochastic average computed with n trajectories scales as (we are assuming X is sufficiently well behaved for the central limit theorem to hold)

$$\sigma_X \asymp \sqrt{\frac{C(d)}{n}}. \tag{F.1}$$

If $C(d)$ grows sufficiently quickly with dimension, the number of trajectories n required to obtain a given absolute accuracy may rapidly become untenable. For spin observables, however, $C(d)$ has a simple upper bound. Since the symbol of a tensor product of m elements of su(2), regardless of which lattice site each is associated to, is bounded by $\mathcal{S}^m$ independent of dimension, its standard deviation will always scale no worse than $\asymp \sqrt{\mathcal{S}^m/n}$. This means that, as the lattice is enlarged, the number of trajectories required to achieve a given absolute accuracy for an m-point correlation function will scale no worse than this dimension-independent bound.

From the previous result, the worst case scaling for a macroscopic magnetization composed of m total spin operators, such as $\langle S^z \rangle$, $\langle S^x S^y \rangle$ and so on, will be

[1] Here we should think of 'physical' random variables, such as position, total spin, or energy, the form of which also changes with dimension and thus leads to the change in variance.

$\sigma \sim \sqrt{(N\mathcal{S})^m/n}$, where N is the lattice size. Here, then, the dimension does enter, and for a fixed absolute error n must increase with it. Nevertheless, for extensive quantities like $\langle S^z \rangle$ the expectation (if it is non-zero) will scale as $\asymp N$, so that the relative error will be

$$\frac{\sigma_{S^z}}{\langle S^z \rangle} \asymp \sqrt{\frac{\mathcal{S}}{Nn}}. \tag{F.2}$$

Thus a larger lattice actually improves the relative error of extensive quantities, explaining why the empirical error bars we find for $\frac{1}{N}S^z$ of the anisotropic XY model are so small: for spin-$\frac{1}{2}$, $N = 400$, and 8000 trajectories, this estimate gives a relative error of 0.05%, which is precisely the order of magnitude of those bars.

For $m = 2$, the scaling of quantities with N depends on the system correlation functions. For very short range correlations, for instance, $\langle S^x S^y \rangle$ will scale roughly as $\asymp N$, in the case of true long range order this could go up to $\asymp N^2$, and algebraic long range order will give some power $1 < \gamma < 2$, $\langle S^x S^y \rangle \asymp N^\gamma$ in between. In the first case,

$$\frac{\sigma_{S^x S^y}}{\langle S^x S^y \rangle} \asymp \sqrt{\frac{\mathcal{S}^2}{n}}, \tag{F.3}$$

so that the relative error is independent of dimension, while for algebraic long range order, we have

$$\frac{\sigma_{S^x S^y}}{\langle S^x S^y \rangle} \asymp \sqrt{\frac{\mathcal{S}^2}{N^{\gamma-1}n}}, \tag{F.4}$$

which improves with dimension but generally slower than for truly extensive quantities. This agrees with the comparatively larger empirical error bars we see for this observable for the anisotropic XY model.

We do not calculate any quantities with $m > 2$, but for those the scaling would depend on m-point correlation functions, and for very short range interactions could be as bad as

$$\frac{\sigma_{(S^\circ)^m}}{\langle (S^\circ)^m \rangle} \asymp \sqrt{\frac{N^{m-2}\mathcal{S}^m}{n}}, \tag{F.5}$$

making them very difficult to calculate with Monte Carlo.

The asymptotic behaviour of simulation times is comparatively simpler, being evidently linear in the time for which the system is to be evolved and either scaling as $\asymp N$ (for interactions involving a finite number of lattice sites) or as $\asymp N^2$ (for long range interactions that cannot be effectively truncated, such as those exhibiting algebraic decay). The latter scaling may be challenging for very large lattices, but is nevertheless still polynomial with a not excessively high power. There may of course be practical issues that are not covered by this analysis, such as the finite memory (further graded by varying access times) available to clusters used for simulation.

F.2 Integrals of Powers of the Wigner Function

In this part we have been predominantly concerned with the calculation of operator expectations wherein the operator and its symbol are known in advance. Quantities such as the von Neumann entropy

$$S = -\operatorname{Tr}[\rho \log \rho], \tag{F.6}$$

however, do not fit this characterisation because the operator $\log \rho$ depends on the density matrix itself, and must be considered separately.

For a function $f(\rho)$ with a series expansion

$$f(\rho) = \sum_n c_n \rho^n, \tag{F.7}$$

the corresponding symbol will be given by a series expansion featuring the star product:

$$W_{f(\rho)} = \sum_n c_n \underbrace{W_\rho \star \ldots \star W_\rho}_{n}. \tag{F.8}$$

Since only a single star product may be omitted via the traciality postulate, expectations of terms in this series for $n > 2$ have unwieldy interpretations as stochastic averages. Using the star product trikernel it is in principle possible to write a term such as

$$\underbrace{W_\rho \star \ldots \star W_\rho}_{n} \tag{F.9}$$

as a string of trikernel integrals averaged over n i.i.d. random variables distributed according to the stochastic approximation of W_ρ. As I will now argue, however, in high phase space dimensions this procedure is so unwieldy even for $n = 2$ that in general the Truncated Wigner approximation is a very poor fit for finding such quantities in lattice systems[2].

For $n = 2$ we may, instead of omitting the star product, use our trikernel idea above:

$$\langle \rho^2 \rangle = \int d\mu(\boldsymbol{n}) d\mu(\boldsymbol{m}) d\mu(\boldsymbol{k})\, L(\boldsymbol{n}, \boldsymbol{m}, \boldsymbol{k}) W_\rho(\boldsymbol{m}) W_\rho(\boldsymbol{k}). \tag{F.10}$$

The structure of the trikernel and the standardization postulate mean that this is equivalent to

$$\langle \rho^2 \rangle = \int d\mu(\boldsymbol{m}) d\mu(\boldsymbol{k})\, \operatorname{Tr}\left[\Delta^{(j)}(\boldsymbol{m}) \Delta^{(j)}(\boldsymbol{k})\right] W_\rho(\boldsymbol{m}) W_\rho(\boldsymbol{k}), \tag{F.11}$$

connecting it to the expression for fidelity in [45]. Thus the stochastic average of

[2] Nevertheless, it is viable for single and small spin systems.

this quantity corresponds to the average of $\mathrm{Tr}\left[\Delta^{(j)}(\boldsymbol{m})\Delta^{(j)}(\boldsymbol{k})\right]$ over two independent random variables distributed according to W_ρ.

The problem is that for high phase space dimension this quantity becomes extremely peaked around $\boldsymbol{m} = \boldsymbol{k}$. For large j this occurs already for a small number of spins (indeed for $j = \infty$ it becomes the Dirac delta function), so let us consider spin-$\frac{1}{2}$. We will consider a simple numerical experiment to illustrate the issue. Taking 1024 uniformly distributed samples from the phase space of a 400 spin system, we find the following statistics for

$$\mathrm{Tr}\left[\Delta^{(j)}(\boldsymbol{m})\Delta^{(j)}(\boldsymbol{k})\right]: \tag{F.12}$$

The sample mean is found to be $9.8 * 10^{-313}$. Eliminating the largest value from the sample, however, reduces the sample mean to $9.6 * 10^{-316}$, a change of three orders of magnitude from one value. This instability of the sample mean is confirmed by the very large sample excess kurtosis value of 1019 (itself also unstable). In effect, the distribution of $\mathrm{Tr}\left[\Delta^{(j)}(\boldsymbol{m})\Delta^{(j)}(\boldsymbol{k})\right]$ in high dimensions becomes fat-tailed[3]. This has severely detrimental implications for the convergence rate of its average with the number of trajectories and the effect evidently becomes worse with dimension (for $N = 400$ it is clearly already very bad). Thus, in general, it is not expected that quantities of this type can be effectively calculated with Truncated Wigner for large lattice systems. Obviously the situation would be even worse for $n > 2$ and thus multiple trikernels.

This difficulty is not surprising given that, were we to remove the star product using the traciality postulate rather than using the trikernel, we would find ourselves calculating the collision entropy of the distribution. For distributions on $\mathbb{R}^d$ with bounded support its estimation in high dimensions is known to be difficult: the upper bound convergence rate given in [46] for their method, for instance, is $O(n^{-\frac{2}{3d}})$, which for even moderately large d is exceptionally slow. While in our case for small j we have the advantage of the distribution being constrained to a specific function subspace, the above arguments suggest this is not enough to overcome the curse of dimensionality.

F.3 Sampling Non-positive Distributions

Large phase space dimensions also have negative implications for our ability to sample from non-positive distributions. Recall that the basic idea amounts to sampling from the absolute value of the distribution and then taking into account whether a trajectory came from the positive or negative portion when averaging, including each with the associated sign. Suppose that, for a single spin

[3] Our numerical experiment demonstrates this for a uniform W_ρ, but it is clear how this will generally be the case due to how peaked the function is.

distribution, the probability of a trajectory originating from the positive region is p and from the negative $1-p$. Then, for N spins in a product state of that distribution, these probabilities become [47] $\frac{1}{2}+\frac{1}{2}(2p-1)^N$ and $\frac{1}{2}-\frac{1}{2}(2p-1)^N$. For non-negligible p (so especially for small j) and large N these become almost equal. For the spin-$\frac{1}{2}$ spin up state and $N=400$, for instance,

$$\bar{\rho}_{\frac{1}{2}}\theta,\phi) = \sin(\theta)\sum_{l=0}^{1}\frac{2l+1}{2}C^{(\frac{1}{2}\ l\ \frac{1}{2})\frac{1}{2}\ 0}{}_{\frac{1}{2}}P_l(\cos(\theta)), \tag{F.13}$$

$p\approx 0.93$, and the difference between these probabilities becomes $\approx 6{\cdot}10^{-27}$. Then, as the trajectories gradually converge to the same stationary distribution it would take on the order of 10^{27} trajectories to accurately resolve this difference in probabilities, which is evidently impractical.

The possibility of sampling from non-positive distributions thus appears restricted to smaller collections of spins: for $N=50$, for instance, the difference is now around 10^{-3}, and so can be resolved with thousands of trajectories. It may thus be a better fit for spin chains than spin lattices.

Bibliography

[1] R. Geroch, *Geometrical Quantum Mechanics: 1974 Lecture Notes*. Minkowski Institute Press, 2013, vol. 3.

[2] nLab authors, *Deformation quantization*, ncatlab, URL:https://ncatlab.org/nlab/revision/deformation+quantization/3 (Revision 3).

[3] E. Wigner, "On the quantum correction for thermodynamic equilibrium," *Physical review*, vol. 40, no. 5, p. 749, 1932.

[4] G. Dito and D. Sternheimer, "Deformation quantization: Genesis, developments and metamorphoses," *Deformation quantization*, vol. 1, pp. 9–54, 2002.

[5] C. Gneiting, T. Fischer, and K. Hornberger, "Quantum phase-space representation for curved configuration spaces," *Physical Review A*, vol. 88, no. 6, p. 062 117, 2013.

[6] J. Huber, P. Kirton, and P. Rabl, "Phase-space methods for simulating the dissipative many-body dynamics of collective spin systems," *SciPost Physics*, vol. 10, no. 2, p. 045, 2021.

[7] J. Schachenmayer, A. Pikovski, and A. M. Rey, "Many-body quantum spin dynamics with monte carlo trajectories on a discrete phase space," *Physical Review X*, vol. 5, no. 1, p. 011 022, 2015.

[8] J. Huber, A. M. Rey, and P. Rabl, "Realistic simulations of spin squeezing and cooperative coupling effects in large ensembles of interacting two-level systems," *Physical Review A*, vol. 105, no. 1, p. 013 716, 2022.

[9] W. K. Wootters, "A wigner-function formulation of finite-state quantum mechanics," *Annals of Physics*, vol. 176, no. 1, pp. 1–21, 1987.

[10] W. K. Wootters, "Picturing qubits in phase space," *IBM Journal of Research and Development*, vol. 48, no. 1, pp. 99–110, 2004.

[11] C. D. Mink, D. Petrosyan, and M. Fleischhauer, "Hybrid discrete-continuous truncated wigner approximation for driven, dissipative spin systems," *Physical Review Research*, vol. 4, no. 4, p. 043 136, 2022.

[12] J. Wurtz, A. Polkovnikov, and D. Sels, "Cluster truncated wigner approximation in strongly interacting systems," *Annals of Physics*, vol. 395, pp. 341–365, 2018.

[13] J. R. Klauder, "Quantization of constrained systems," in *Methods of Quantization: Lectures Held at the 39. Universitätswochen für Kern-und Teilchenphysik, Schladming, Austria*, Springer, 2001, pp. 143–182.

[14] J. C. Várilly and J. Gracia-Bondía, "The moyal representation for spin," *Annals of physics*, vol. 190, no. 1, pp. 107–148, 1989.

[15] A. Klimov and P. Espinoza, "Moyal-like form of the star product for generalized su (2) stratonovich-weyl symbols," *Journal of Physics A: Mathematical and General*, vol. 35, no. 40, p. 8435, 2002.

[16] A. B. Klimov and S. M. Chumakov, *A group-theoretical approach to quantum optics: models of atom-field interactions*. John Wiley & Sons, 2009.

[17] D. Zueco and I. Calvo, "Bopp operators and phase-space spin dynamics: Application to rotational quantum brownian motion," *Journal of Physics A: Mathematical and Theoretical*, vol. 40, no. 17, p. 4635, 2007.

[18] J. M. Gracía-Bondía, "On homogeneous symplectic spaces," in *Deformation Theory and Quantum Groups with Applications to Mathematical Physics: Proceedings of a AMS-IMS-SIAM 1990 Joint Summer Research Conference Held June 14-20 at the University of Massachusetts, Amherst, with Support from the National Science Foundation*, American Mathematical Soc., vol. 134, 1992, p. 93.

[19] I. Mäkinen, "Introduction to su (2) recoupling theory and graphical methods for loop quantum gravity," *arXiv preprint arXiv:1910.06821*, 2019.

[20] F. Bopp, *Werner Heisenberg und die Physik unserer Zeit*. Springer-Verlag, 2013.

[21] C. Zachos, D. Fairlie, and T. Curtright, "Quantum mechanics in phase space: An overview with selected papers," 2005.

[22] D. A. Paz and M. F. Maghrebi, "Driven-dissipative ising model: An exact field-theoretical analysis," *Physical Review A*, vol. 104, no. 2, p. 023 713, 2021.

[23] N. Van Kampen, "Brownian motion on a manifold," *Journal of statistical physics*, vol. 44, pp. 1–24, 1986.

[24] A. V. Gómez and F. J. Sevilla, "A geometrical method for the smoluchowski equation on the sphere," *Journal of Statistical Mechanics: Theory and Experiment*, vol. 2021, no. 8, p. 083 210, 2021.

[25] G. F. Lawler, "Notes on the bessel process," *Lecture notes. Available on the webpage of the author*, pp. 523–531, 2018.

[26] S. Krämer, D. Plankensteiner, L. Ostermann, and H. Ritsch, "Quantumoptics. jl: A julia framework for simulating open quantum systems," *Computer Physics Communications*, vol. 227, pp. 109–116, 2018.

[27] A. Polkovnikov, "Quantum corrections to the dynamics of interacting bosons: Beyond the truncated wigner approximation," *Physical Review A*, vol. 68, no. 5, p. 053 604, 2003.

[28] T. E. Lee, S. Gopalakrishnan, and M. D. Lukin, "Unconventional magnetism via optical pumping of interacting spin systems," *Physical review letters*, vol. 110, no. 25, p. 257 204, 2013.

[29] T. E. Lee, C.-K. Chan, and S. F. Yelin, "Dissipative phase transitions: Independent versus collective decay and spin squeezing," *Physical Review A*, vol. 90, no. 5, p. 052 109, 2014.

[30] M. F. Maghrebi and A. V. Gorshkov, "Nonequilibrium many-body steady states via keldysh formalism," *Physical Review B*, vol. 93, no. 1, p. 014 307, 2016.

[31] C. Mc Keever and M. Szymańska, "Stable ipepo tensor-network algorithm for dynamics of two-dimensional open quantum lattice models," *Physical Review X*, vol. 11, no. 2, p. 021 035, 2021.

[32] P. Rabl, "Stochastic Simulations of Dissipative Spin Systems," in *Spin Phenomena Interdisciplinary Center (SPICE) Workshops, SPICE Workshop on Quantum Spinoptics, June 13th - 15th 2023*, 2023.

[33] F. Strocchi, *Symmetry breaking in the standard model: a non-perturbative outlook*. Springer, 2019, vol. 19.

[34] C. P. Mc Keever, "Tensor network simulation methods for open quantum lattice models," Ph.D. dissertation, UCL (University College London), 2022.

[35] A. Vilenkin, A. Vilenkin, and E. Shellard, *Cosmic strings and other topological defects*. Cambridge University Press, 1994.

[36] V. Berezinskii, "Destruction of long-range order in one-dimensional and two-dimensional systems having a continuous symmetry group i. classical systems," *Sov. Phys. JETP*, vol. 32, no. 3, pp. 493–500, 1971.

[37] V. Berezinskii, "Destruction of long-range order in one-dimensional and two-dimensional systems possessing a continuous symmetry group. ii. quantum systems," *Sov. Phys. JETP*, vol. 34, no. 3, pp. 610–616, 1972.

[38] J. M. Kosterlitz and D. J. Thouless, "Ordering, metastability and phase transitions in two-dimensional systems," in *Basic Notions Of Condensed Matter Physics*, CRC Press, 2018, pp. 493–515.

[39] T. Chern, "Vortex operator and bkt transition in abelian duality," *Physica C: Superconductivity and its Applications*, vol. 523, pp. 55–59, 2016.

[40] F. Bouchet and J. Barre, "Statistical mechanics of systems with long range interactions," in *Journal of Physics: Conference Series*, IOP Publishing, vol. 31, 2006, p. 18.

[41] N. Defenu, T. Donner, T. Macri, G. Pagano, S. Ruffo, and A. Trombettoni, "Long-range interacting quantum systems," *Reviews of Modern Physics*, vol. 95, no. 3, p. 035 002, 2023.

[42] M. Kac, G. Uhlenbeck, and P. Hemmer, "On the van der waals theory of the vapor-liquid equilibrium. i. discussion of a one-dimensional model," *Journal of Mathematical Physics*, vol. 4, no. 2, pp. 216–228, 1963.

[43] H. Risken, *The Fokker-Planck Equation: Methods of Solution and Applications*. Springer, 1996.

[44] N. Branchini, "Simple monte carlo is independent of dimension. or is it?" *https://www.branchini.fun*, 2022.

[45] P. Deuar, "First-principles quantum simulations of many-mode open interacting bose gases using stochastic gauge methods," *arXiv preprint cond-mat/0507023*, 2005.

[46] D. Pál, B. Póczos, and C. Szepesvári, "Estimation of rényi entropy and mutual information based on generalized nearest-neighbor graphs," *Advances in neural information processing systems*, vol. 23, 2010.

[47] D. S. (https://math.stackexchange.com/users/15941/dilip-sarwate), *Probability that a* $(n, \frac{1}{2})$*-binomial random variable is even*, Mathematics Stack Exchange, URL:https://math.stackexchange.com/q/83066 (version: 2011-11-17).